Imaginary- and Real-Frequency Correlation Functions in Condensed Matter Physics: General Properties and Applications

Johannes Josef Halbinger

Munich 2024

Imaginary- and Real-Frequency Correlation Functions in Condensed Matter Physics: General Properties and Applications

Johannes Josef Halbinger

A dissertation submitted

to the Faculty of Physics at the

Ludwig–Maximilians–Universität München

for the degree of

DOCTOR RERUM NATURALIUM

Munich, February 1, 2024

First referee: Prof. Dr. Jan von Delft
Second referee: Prof. Dr. Alessandro Toschi
Day of submission: February 1, 2024
Day of the oral examination: March 22, 2024

Zusammenfassung (Summary in German)

Multipunktkorrelationsfunktionen, auch ℓp-Korrelationsfunktionen genannt, sind als zeit- oder konturgeordnete Erwartungswerte von ℓ quantenmechanischen Operatoren definiert. Zwei häufig benutzte Formalismen zur Berechnung von ℓp-Korrelatoren in der Physik der kondensierten Materie sind der Matsubara-Formalismus (MF) mit imaginären Frequenzen und der Keldysh-Formalimus (KF) mit reellen Frequenzen. Im ersten Formalismus, der nur auf Systeme im thermischen Gleichgewicht anwendbar ist, besitzt jeder ℓp-Korrelator nur eine Komponente. Um Informationen über physikalische Observablen zu erhalten, müssen die Korrelatoren von imaginären zu reellen Frequenzen analytisch fortgesetzt werden, was ein numerisch schlecht konditioniertes Problem ist. Im Gegensatz dazu hat im KF jeder Korrelator 2^ℓ Komponenten, allerdings zu dem Vorteil, dass physikalische Observablen direkt auf der reellen Frequenzachse berechnet werden können.

Vor Kurzem haben Kugler, Lee und von Delft (KLD) unser Verständis zu ℓp-Korrelatoren im MF, KF und auch im Nulltemperaturformalismus (NF) signifikant erweitert. Die Autoren führten eine Spektraldarstellung in Form von formalismusunabhängigen, aber systemabhängigen partiellen Spektralfunktionen (PSFs) und formalismusabhängigen, aber systemunabhängigen Kernels ein. Zudem entwickelten sie ein Multipunktschema der numerischen Renormierungsgruppe (NRG), um PSFs und somit auch Multipunktkorrelatoren und die zugehörigen Vertizes in allen Formalismen für $\ell = 3, 4$ zu berechnen.

Im ersten Teil dieser Arbeit vervollständigen wir die KLD-Spektraldarstellung von ℓp-Korrelatoren im MF, indem wir uns mit den MF-Kernels befassen. Während ihre allgemeine Form für imaginäre Zeiten geläufig ist, waren explizite Ausdrücke für ihre Fouriertransformationen nur für wenige Fälle bekannt. Deren Berechnung wird durch sogenannte anomale Terme erschwert, die für verschwindende bosonische Frequenzen und verschwindende Eigenenergiedifferenzen in der entsprechenden Lehmanndarstellung auftreten können. Wir leiten einen geschlossenen Ausdruck für die MF Kernels her, der für alle ℓ und für eine beliebige Anzahl an anomalen Termen gilt. Anschließend verwenden wir diese Kernels im Kontext der analytischen Fortsetzung von MF-Korrelatoren zu ihren Gegenstücken im KF für Systeme im thermischen Gleichgewicht. Während dieses Verfahren im 2p-Fall wohlbekannt ist, wurde bisher noch kein Rezept ausgearbeitet, das für beliebige ℓ gilt. Basierend auf den Arbeiten von KLD entwickeln wir eine Strategie für die analytische Fortsetzung von ℓp-MF-Korrelatoren, einschließlich anomaler Terme, zu allen 2^ℓ Komponenten des entsprechenden KF-Korrelators. Zusätzlich stellen wir MF-zu-KF-Fortsetzungsformeln und Relationen zwischen den 2^ℓ KF-Komponenten für allgemeine 2p- und 3p- sowie fermionische 4p-Korrelatoren bereit.

Im zweiten Teil dieser Arbeit fokussieren wir uns auf die direkte Anwendung von Korrelationsfunktionsmethoden in zwei verschiedenen Fällen. Als Erstes leiten wir einen symmetrisch verbesserten Schätzer für die numerisch akkurate Berechnung des 4p-Vertizes im MF, KF und NF her. Wir demonstrieren dessen Nützlichkeit und Genauigkeit, indem wir das NRG-Schema von KLD auf das Anderson'sche Störstellenmodell bei verschiedenen Temperaturen und Interaktionen anwenden. Danach untersuchen wir die Auswirkungen von zeitlich eingefrorener („gequenchter") Unordnung auf antiferromagnetische quantenkritische Punkte (QKPs) in zweidimensionalen Metallen mithilfe von feldtheoretischen Methoden. Metallische QKPs haben über die letzten Jahrzehnte immer mehr an Aufmerksamkeit gewonnen, da sie in enger Verbindung zu Hochtemperatursupraleitern und zu seltsam-metallischen Regionen stehen. Mithilfe der ϵ-Entwicklung im KF finden wir, dass gequenchte Unordnung einen zuvor gefundenen stabilen, reinen, seltsam-metallischen Fixpunkt zerstört, da die Renormierungsgruppengleichungen zu starker Unordnung fließen.

Summary **(Summary in English)**

Multipoint, or ℓp, correlation functions are defined as the time- or contour-ordered expectation values of ℓ quantum mechanical operators. In condensed matter physics, two frequently used formalisms for computing ℓp correlators are the imaginary-frequency Matsubara formalism (MF) and the real-frequency Keldysh formalism (KF). In the former, which is only applicable to systems in thermal equilibrium, each ℓp correlator has only one component. To extract information on physical observables, correlators have to be analytically continued from imaginary to real frequencies, which is numerically ill-conditioned. By contrast, in the KF each correlator has 2^{ℓ} components, but it has the merit that physical observables can be directly computed on the real-frequency axis.

Recently, Kugler, Lee, and von Delft (KLD) significantly advanced our understanding of ℓp correlators in the MF, KF, and the zero-temperature formalism (ZF). They introduced spectral representations in terms of formalism-independent but system-dependent partial spectral functions (PSFs) and formalism-dependent but system-independent kernels. Additionally, they developed a multipoint numerical renormalization group (NRG) scheme to evaluate the PSFs and, thus, multipoint correlators and the related vertices in all formalisms for $\ell = 3, 4$.

In the first part of this thesis, we complete the KLD spectral representation of ℓp MF correlators by addressing the MF kernels. While their general form is known in the imaginary-time domain, explicit expressions for their Fourier transforms had been given only for a few cases. The evaluation is complicated by so-called anomalous terms which can occur for vanishing bosonic Matsubara frequencies and vanishing eigenenergy differences in the corresponding Lehmann representation. We derive a closed expression for the MF kernels applicable for all ℓ and an arbitrary number of anomalous terms. Subsequently, we apply these kernels in the context of the analytic continuation of MF correlators to their counterparts in the KF for systems in thermal equilibrium. While this procedure is well-known in the 2p case, a recipe for arbitrary ℓ had not been formulated yet. Based on the works of KLD, we develop a strategy for the analytic continuation of ℓp MF correlators, including anomalous parts, to all 2^{ℓ} components of the corresponding KF correlators. Additionally, we provide MF-to-KF continuation formulas and relations among the 2^{ℓ} KF components for arbitrary 2p and 3p as well as fermionic 4p correlators.

In the second part of this thesis, we focus on direct applications of correlation function methods in two different cases. First, we derive a symmetric improved estimator for the numerically accurate computation of the 4p vertex in the MF, KF, and ZF. We demonstrate its utility and accuracy by applying the NRG scheme of KLD to the single-impurity Anderson model at various temperatures and interactions. Second, we study the effects of quenched disorder on antiferromagnetic quantum critical points (QCPs) in two-dimensional metals via field-theoretical methods. Metallic QCPs have gained increasing attention over the last decades due to their close connection to high-temperature superconductivity and the strange metal region in various compounds. Using the ϵ-expansion in the KF, we find that quenched disorder destroys a previously found stable, clean, strange metal fixed point as the renormalization group equations flow to strong disorder.

Publications

This dissertation is based on the following journal articles, listed in chronological order:

P1 *Quenched disorder at antiferromagnetic quantum critical points in two-dimensional metals*
Johannes Halbinger and Matthias Punk
Sec. 7 / arXiv:2103.06295   Phys. Rev. B **103**, 235157 (2021)

P2 *Spectral representation of Matsubara n-point functions: Exact kernel functions and applications*
Johannes Halbinger, Benedikt Schneider, and Björn Sbierski
Sec. 4 / arXiv:2304.03774   SciPost Phys. 15, 183 (2023)

P3 *Symmetric improved estimators for multipoint vertex functions*
Jae-Mo Lihm, **Johannes Halbinger**, Jeongmin Shim, Jan von Delft, Fabian B. Kugler, and Seung-Sup B. Lee
Sec. 6 / arXiv:2310.12098   submitted to Physical Review B

P4 *Analytic continuation of multipoint correlation functions*
Anxiang Ge*, **Johannes Halbinger***, Seung-Sup B. Lee, Jan von Delft, and Fabian B. Kugler
Sec. 5 / arXiv:2311.11389   accepted by Annalen der Physik

With the approval of all authors, **P4** is reproduced with minor modifications to put it into the context of this thesis in the following parts: Secs. 3.3, 3.4, Ch. 5, App. C, and partially in Sec. 2.3.

Parts of **P4** are based on results derived by Anxiang Ge in his Master's thesis [Ge20]. In order to guarantee a self-contained discussion, they are reproduced in this thesis, with the corresponding Sec. 5.6 and Apps. C.3.3, C.5, and C.6 explicitly marked as such. Nevertheless, the author of this thesis contributed to writing these parts, too, and complemented some of the results of Ref. [Ge20] with additional, explanatory calculations.

---

* These authors contributed equally.

Acknowledgements

First and foremost, I would like to express my deepest gratitude to my supervisors, Matthias Punk and Jan von Delft.

Matthias was the first to introduce me to the field of condensed matter physics, and I learned most of its basics through his great lectures. I am very thankful for his guidance during my master's thesis and the first almost two years of my PhD, for always having time for discussions, and for his continued support even after his departure from academia.

Further, I cannot thank Jan enough for taking me over as his PhD student without hesitation, for proposing such exciting research topics, for always having an open door for discussions, and for nudging me in the right direction whenever I got stuck during a project. I highly value his constant support in all respects during the last almost three years.

I want to thank Alessandro Toschi for corefereeing this thesis.

I am deeply indebted to my collaborators Anxiang Ge, Fabian Kugler, Seung-Sup Lee, Jae-Mo Lihm, Michael Meixner, Björn Sbierski, Thomas Schäfer, Benedikt Schneider, Jeongmin Shim, and Alessandro Toschi. I am thankful to Björn for giving me the opportunity to contribute to the Matsubara kernel project and to Fabian and Seung-Sup for constantly providing input, answers, and constructive feedback for our various projects.

Further, I gratefully acknowledge funding from the IMPRS-QST and thank for the various opportunities to participate in summer schools, workshops, and the APS March Meeting. In particular, I would like to thank Sonya Gzyl as the IMPRS-QST coordinator and Lode Pollet as a member of my thesis advisory board.

I am grateful to all members of the von Delft chair for providing such a pleasant working environment. A special thank you goes to my fellow PhD students Andreas, Anxiang, Benedikt, Chankai, Elias, Jheng-Wei, Julian, Marc, my long-term office mate Marcel, Matthias, Ming, Nepomuk, and Sasha (my apologies if I forgot someone). May the fun lunch breaks at Mensa continue even without me.

I want to thank Andreas, Anxiang, Baris, Fabian, Kevin, Nepomuk, and Rolf for proofreading parts of the thesis.

I am fortunate to have found my good friends Baris and Andreas at the beginning of our bachelor's studies. Over the last ten years, our learning and chilling sessions have helped me to enjoy the highs and get through the lows of being a bachelor's, master's, and PhD student, and I am forever thankful for our time at university.

Last but not least, I am eternally grateful to my family, my parents Monika and Hans, and my brother Stephan, for their never-ending support and to my girlfriend Becky, whose unconditional love and support have helped me even through the toughest times.

Conventions and notation

Here, we summarize conventions and notation (mostly adapted from Refs. [KLvD21, P4]) used throughout this thesis, with focus on Chs. 2, 3, and 5. The conventions in [P1, P2, P3] may differ from those presented here.

Units:

Reduced Planck constant: $\hbar = 1$,   Boltzmann constant: $k_B = 1$

General symbols:

Imaginary unit: i

Ordering symbols: $\mathcal{T}$ (time-ordering), $\overline{\mathcal{T}}$ (anti-time-ordering),

$\mathcal{T}_{\mathcal{C}}$ (contour-ordering)

Operators: $\mathcal{O}^i$, $\boldsymbol{\mathcal{O}} = (\mathcal{O}^1, \ldots, \mathcal{O}^\ell)$, $\boldsymbol{\mathcal{O}}_p = (\mathcal{O}^{\bar{1}}, \ldots, \mathcal{O}^{\bar{\ell}})$

Hamiltonian: H

Energy eigenstates: $\{|\underline{i}\rangle\}$ denotes a complete set of energy eigenstates for a single integer i.

Eigenenergies: $H|\underline{i}\rangle = E_{\underline{i}}|\underline{i}\rangle$, $E_{\underline{i}\,\underline{j}} = E_{\underline{i}} - E_{\underline{j}}$

Inverse temperature: $\beta = 1/T$

Partition function: $Z = \mathrm{Tr}\left[e^{-\beta H}\right]$

Density matrix: $\rho = e^{-\beta H}/Z$

Operator matrix element: $\mathcal{O}^i_{\underline{m}\,\underline{n}} = \langle \underline{m}|\mathcal{O}^i|\underline{n}\rangle$, $\rho_{\underline{m}\,\underline{n}} = \delta_{\underline{m},\underline{n}}\rho_{\underline{m}}$, $\rho_{\underline{m}} = e^{-\beta E_{\underline{m}}}/Z$

Thermal expectation value: $\langle \ldots \rangle = \mathrm{Tr}[\rho \ldots]$

Case distinction for imaginary-time integrals: $\Delta_x = \begin{cases} 0 & \text{if } x = 0 \\ \frac{1}{x} & \text{if } x \neq 0 \end{cases}$

Permutations and signs:

Permutations: $p = (\bar{1} \ldots \bar{\ell})$, $p(i) = \bar{i}$

Sign of permutation: $\zeta_p = \pm 1$ for even (odd) number of transpositions of fermionic operators

Single sign factor: $\zeta^i = \pm 1$ if operator $\mathcal{O}^i$ is bosonic (fermionic)

Product of sign factors: $\zeta^{1\ldots i} = \zeta^1 \zeta^2 \ldots \zeta^i$

Contour/Keldysh indices, times, and frequencies:

Contour indices: $c_i = \pm$, $\boldsymbol{c} = c_1 \ldots c_\ell$, $\boldsymbol{c}_p = c_{\bar{1}} \ldots c_{\bar{\ell}}$

Keldysh indices:	$k_i \in \{1, 2\}$,	$\boldsymbol{k} = k_1 \ldots k_\ell$,	$\boldsymbol{k}_p = k_{\bar{1}} \ldots k_{\bar{\ell}}$
Imaginary times:	τ_i,	$\boldsymbol{\tau} = (\tau_1, \ldots, \tau_\ell)$,	$\boldsymbol{\tau}_p = (\tau_{\bar{1}}, \ldots, \tau_{\bar{\ell}})$
Real times:	t_i,	$\boldsymbol{t} = (t_1, \ldots, t_\ell)$,	$\boldsymbol{t}_p = (t_{\bar{1}}, \ldots, t_{\bar{\ell}})$
Matsubara frequencies:	$\mathrm{i}\omega_i$,	$\mathrm{i}\boldsymbol{\omega} = (\mathrm{i}\omega_1, \ldots, \mathrm{i}\omega_\ell)$,	$\mathrm{i}\boldsymbol{\omega}_p = (\mathrm{i}\omega_{\bar{1}}, \ldots, \mathrm{i}\omega_{\bar{\ell}})$
Real frequencies:	ω_i,	$\boldsymbol{\omega} = (\omega_1, \ldots, \omega_\ell)$,	$\boldsymbol{\omega}_p = (\omega_{\bar{1}}, \ldots, \omega_{\bar{\ell}})$
	ε_i,	$\boldsymbol{\varepsilon} = (\varepsilon_1, \ldots, \varepsilon_\ell)$,	$\boldsymbol{\varepsilon}_p = (\varepsilon_{\bar{1}}, \ldots, \varepsilon_{\bar{\ell}})$

Frequency arguments of

Matsubara kernels: $\quad \Omega_i = \mathrm{i}\omega_i - \varepsilon_i, \quad \boldsymbol{\Omega} = (\Omega_1, \ldots, \Omega_\ell), \quad \boldsymbol{\Omega}_p = (\Omega_{\bar{1}}, \ldots, \Omega_{\bar{\ell}})$

In Ch. 5 and App. C, we also use $\Omega_i = \mathrm{i}\omega_i - \mathrm{i}\omega_i'$ for imaginary frequency convolutions, with $\mathrm{i}\omega_i'$ a Matsubara frequency.

Imaginary shifts of frequencies:

Imaginary shifts:	$\gamma_{i \neq \eta}^{[\eta]} = -\gamma_0, \qquad \gamma_\eta^{[\eta]} = (\ell - 1)\gamma_0, \qquad \gamma_0 > 0$
Shifted frequencies:	$\omega_i^{[\eta]} = \omega_i + \mathrm{i}\gamma_i^{[\eta]}, \qquad \boldsymbol{\omega}^{[\eta]} = (\omega_1^{[\eta]}, \ldots, \omega_\ell^{[\eta]})$,
	$\boldsymbol{\omega}_p^{[\eta]} = (\omega_{\bar{1}}^{[\eta]}, \ldots, \omega_{\bar{\ell}}^{[\eta]})$
Infinitesimal shifts:	$\omega_i^{\pm} = \omega_i \pm \mathrm{i}0^+$

Sums, Matsubara weighting function, and statistical factor:

Sums:
$$\omega_{1\ldots j} = \sum_{i=1}^{j} \omega_i \qquad \text{(same for } \mathrm{i}\omega_{1\ldots i},\ \varepsilon_{1\ldots i},\ \text{and } k_{1\ldots i})$$

Matsubara weighting function:
$$n_{\omega_{1\ldots i}} = n_{1\ldots i} = \frac{\zeta^{1\ldots i}}{e^{-\beta\omega_{1\ldots i}} - \zeta^{1\ldots i}}$$

Statistical factor:
$$N_{\omega_{1\ldots i}} = N_{1\ldots i} = \coth[\beta\omega_{1\ldots i}/2]^{\zeta^{1\ldots i}}$$

Partial spectral functions:

Definition:
$$\mathcal{S}_p(\boldsymbol{t}_p) = \zeta_p \mathrm{Tr}\left[\rho\, \mathcal{O}^{\bar{1}}(t_{\bar{1}}) \ldots \mathcal{O}^{\bar{\ell}}(t_{\bar{\ell}})\right], \qquad \mathcal{O}^i(t_i) = e^{\mathrm{i}Ht_i}\mathcal{O}^i e^{-\mathrm{i}Ht_i}$$

Fourier transform:
$$\mathcal{S}_p(\boldsymbol{\varepsilon}_p) = \int_{-\infty}^{\infty} \frac{\mathrm{d}^\ell t_p}{(2\pi)^\ell} e^{\mathrm{i}\boldsymbol{\varepsilon}_p \cdot \boldsymbol{t}_p} \mathcal{S}_p(\boldsymbol{t}_p) = 2\pi\delta(\varepsilon_{\bar{1}\ldots\bar{\ell}}) S_p(\boldsymbol{\varepsilon}_p)$$

Regular part: $\quad \tilde{S}_p(\boldsymbol{\varepsilon}_p)$

Anomalous part: $\quad \hat{S}_p(\boldsymbol{\varepsilon}_p) \quad$ (see App. C.2 for further decompositions)

Matsubara formalism:

MF kernel:
$$\mathcal{K}(\boldsymbol{\tau}_p) = \prod_{i=1}^{\ell-1}\left[-\theta(\tau_{\bar{i}} - \tau_{\overline{i+1}})\right]$$

$$\mathcal{K}(\mathrm{i}\boldsymbol{\omega}_p) = \int_0^\beta \mathrm{d}^\ell\tau_p \, e^{\mathrm{i}\boldsymbol{\omega}_p \cdot \boldsymbol{\tau}_p} \mathcal{K}(\boldsymbol{\tau}_p) = \beta\delta_{\mathrm{i}\omega_{\overline{1}\ldots\overline{\ell}}} K(\mathrm{i}\boldsymbol{\omega}_p) + \mathcal{R}(\mathrm{i}\boldsymbol{\omega}_p)$$

Primary MF kernel: $K(\mathrm{i}\boldsymbol{\omega}_p)$ (also referred to as the MF kernel)

Residual MF kernel: $\mathcal{R}(\mathrm{i}\boldsymbol{\omega}_p)$

Regular MF kernel: $\displaystyle \tilde{K}(\mathrm{i}\boldsymbol{\omega}_p) = \prod_{i=1}^{\ell-1} \frac{1}{\mathrm{i}\omega_{\overline{1}\ldots\overline{i}}}$

Anomalous MF kernel: $\hat{K}(\mathrm{i}\boldsymbol{\omega}_p)$

MF correlator: $\displaystyle \mathcal{G}(\boldsymbol{\tau}) = \sum_p \mathcal{K}(\boldsymbol{\tau}_p)\mathcal{S}_p(-\mathrm{i}\boldsymbol{\tau}_p)$

$$\mathcal{G}(\mathrm{i}\boldsymbol{\omega}) = \int_0^\beta \mathrm{d}^\ell\tau \, e^{\mathrm{i}\boldsymbol{\omega}\cdot\boldsymbol{\tau}} \mathcal{G}(\boldsymbol{\tau}) = \beta\delta_{\mathrm{i}\omega_{1\ldots\ell}} G(\mathrm{i}\boldsymbol{\omega})$$

$$G(\mathrm{i}\boldsymbol{\omega}) = \sum_p \int_{-\infty}^\infty \mathrm{d}^\ell\varepsilon_p \, \delta(\varepsilon_{\overline{1}\ldots\overline{\ell}}) \, K(\mathrm{i}\boldsymbol{\omega}_p - \boldsymbol{\varepsilon}_p) \, S_p(\boldsymbol{\varepsilon}_p)$$

$$= \sum_p [K * S_p](\mathrm{i}\boldsymbol{\omega}_p)$$

$$\tilde{G}(\mathrm{i}\boldsymbol{\omega}) = \sum_p [\tilde{K} * S_p](\mathrm{i}\boldsymbol{\omega}_p) \qquad \text{(regular part)}$$

$$\hat{G}(\mathrm{i}\boldsymbol{\omega}) = \sum_p [\hat{K} * S_p](\mathrm{i}\boldsymbol{\omega}_p) \qquad \text{(anomalous part)}$$

Partial MF corr.: $G_p(\mathrm{i}\boldsymbol{\omega}_p) = [K * S_p](\mathrm{i}\boldsymbol{\omega}_p)$

(analogously for $\tilde{G}_p$ and $\hat{G}_p$ using $\tilde{K}$ and $\hat{K}$, respectively)

Keldysh formalism:

Keldysh rotation: $D^{k_i c_i} = (-1)^{k_i \delta_{c_i,+}}$

Fully retarded kernel: $\displaystyle \mathcal{K}^{[\lambda]}(\boldsymbol{t}_p) = \prod_{i=1}^{\lambda-1}\left[\mathrm{i}\,\theta(t_{\overline{i+1}} - t_{\overline{i}})\right]\prod_{i=\lambda}^{\ell-1}\left[-\mathrm{i}\,\theta(t_{\overline{i}} - t_{\overline{i+1}})\right]$

$$\mathcal{K}^{[\lambda]}(\boldsymbol{\omega}_p) = \int_{-\infty}^\infty \mathrm{d}^\ell t_p \, e^{\mathrm{i}\boldsymbol{\omega}_p \cdot t_p} \mathcal{K}^{[\lambda]}(\boldsymbol{t}_p) = 2\pi\delta(\omega_{\overline{1}\ldots\overline{\ell}}) K^{[\lambda]}(\boldsymbol{\omega}_p)$$

$$K^{[\lambda]}(\boldsymbol{\omega}_p) = \prod_{i=1}^{\ell-1} \frac{1}{\omega^{[\lambda]}_{\overline{1}\ldots\overline{i}}}$$

Kernel contour basis: $\mathcal{K}^{\boldsymbol{c}_p}(\boldsymbol{t}_p) = (-1)^{\lambda-1}\left(\mathcal{K}^{[\lambda]}(\boldsymbol{t}_p) - \mathcal{K}^{[\lambda+1]}(\boldsymbol{t}_p)\right)$

(only if $\boldsymbol{c}_p = +\cdots+ -\cdots-$, with λ the number of $+$ entries).

$\mathcal{K}^{\boldsymbol{c}_p}(\boldsymbol{\omega}_p)$ and $K^{\boldsymbol{c}_p}(\boldsymbol{\omega}_p)$ follow from Fourier transforming $\mathcal{K}^{[\lambda]}(\boldsymbol{t}_p)$.

Kernel Keldysh basis: $\displaystyle \mathcal{K}^{\boldsymbol{k}_p}(\boldsymbol{t}_p) = \sum_{\lambda=1}^{\ell}(-1)^{\lambda-1}(-1)^{k_{\overline{1}\ldots\overline{\lambda-1}}}\frac{1+(-1)^{k_{\overline{\lambda}}}}{2}\mathcal{K}^{[\lambda]}(\boldsymbol{t}_p)$

$$\mathcal{K}^{[\hat{\eta}_1\ldots\hat{\eta}_\alpha]}(\boldsymbol{t}_p) = \sum_{j=1}^{\alpha}(-1)^{j-1}\mathcal{K}^{[\hat{\eta}_j]}(\boldsymbol{t}_p)$$

See discussion after Eqs. (3.66) for definitions of $[\eta_1 \ldots \eta_\alpha]$ and $[\hat{\eta}_1 \ldots \hat{\eta}_\alpha]$. The kernels in the frequency domain follow from the Fourier transform of $\mathcal{K}^{[\lambda]}(\boldsymbol{t}_p)$.

KF correlator:
$$\mathcal{G}^{\boldsymbol{k}}(\boldsymbol{t}) = \sum_p \mathcal{K}^{\boldsymbol{k}_p}(\boldsymbol{t}_p) \mathcal{S}_p(\boldsymbol{t}_p)$$

$$\mathcal{G}^{\boldsymbol{k}}(\boldsymbol{\omega}) = \int_{-\infty}^{\infty} \mathrm{d}^\ell t \, e^{\mathrm{i}\boldsymbol{\omega}\cdot\boldsymbol{t}} \mathcal{G}^{\boldsymbol{k}}(\boldsymbol{t}) = 2\pi\delta(\omega_{1\ldots\ell}) \, G^{\boldsymbol{k}}(\boldsymbol{\omega})$$

$$G^{\boldsymbol{k}}(\boldsymbol{\omega}) = \sum_p [K^{\boldsymbol{k}_p} * S_p](\boldsymbol{\omega}_p)$$

$$G'^{\boldsymbol{k}}(\boldsymbol{\omega}) = \sum_p [(K^{\boldsymbol{k}_p})^* * S_p](\boldsymbol{\omega}_p)$$

Corresponding expressions for $G^{\boldsymbol{c}}$ and $G^{[\eta_1 \ldots \eta_\alpha]}$ are obtained by replacing $K^{\boldsymbol{k}_p}$ with $K^{\boldsymbol{c}_p}$ and $K^{[\hat{\eta}_1 \ldots \hat{\eta}_\alpha]}$, respectively.

Additional symbols for analytic continuation:

$\hat{G}_i, \ \hat{G}_{i,j}, \ \hat{G}_i^\Delta, \ \hat{G}_i^{\blacktriangle}$:   Further decomposition of anomalous parts of MF correlators (see Eqs. (5.46), (5.47), and (C.5b)).

$\tilde{G}_{\check{\boldsymbol{z}}}, \ \hat{G}_{i;\check{\boldsymbol{z}}}$:   Analytic continuations of regular/anomalous parts of MF correlators (see Sec. 5.4.1).

$\tilde{G}_{\check{\boldsymbol{z}}^r}^\omega, \ \hat{G}_{i;\check{\boldsymbol{z}}^r}^\omega$:   Discontinuities of regular/anomalous parts of MF correlators (see Eq. (5.41)).

$\tilde{K}_{\bar{I}^1|\ldots|\bar{I}^\alpha}\left(\boldsymbol{\omega}_{\bar{I}^1|\ldots|\bar{I}^\alpha}^{[\eta_1]\ldots[\eta_\alpha]}\right)$:   Retarded product kernel (see Eq. (5.64a)). General notation involving subtuples $\bar{I}^i$ is introduced in Sec. 5.6.2.

$S_{[\bar{I}^1,\bar{I}^2]_\pm}(\boldsymbol{\varepsilon})$:   PSF (anti)commutator (see Eq. (5.66)).

Additional definitions for analytic continuation:

Modified Dirac delta : $\hat{\delta}(x) = -2\pi\mathrm{i}\,\delta(x)$

Imaginary-frequ. convolution : $[K \star G](\mathrm{i}\boldsymbol{\omega}_p) = \frac{1}{(-\beta)^{\ell-1}} \sum_{\mathrm{i}\boldsymbol{\omega}'_p} \delta_{\mathrm{i}\omega'_{\bar{1}\ldots\bar{\ell}}} K(\mathrm{i}\boldsymbol{\omega}_p - \mathrm{i}\boldsymbol{\omega}'_p) G(\mathrm{i}\boldsymbol{\omega}')$

(Anti)commutator convolution: $\left(\tilde{K}_{\bar{I}^1|\bar{I}^2} \diamond S_{[\bar{I}^1,\bar{I}^2]_\pm}\right)\left(\boldsymbol{\omega}_{\bar{I}^1|\bar{I}^2}^{[\eta_1][\eta_2]}\right)$

$= \int \mathrm{d}^\ell \varepsilon \, \delta(\varepsilon_{1\ldots\ell}) \tilde{K}_{\bar{I}^1|\bar{I}^2}\left(\boldsymbol{\omega}_{\bar{I}^1|\bar{I}^2}^{[\eta_1][\eta_2]} - \boldsymbol{\varepsilon}_{\bar{I}^1|\bar{I}^2}\right) S_{[\bar{I}^1,\bar{I}^2]_\pm}(\boldsymbol{\varepsilon})$

Acronyms:

aIE: Asymmetric improved estimator,

DMFT: Dynamical mean-field theory,

EOM: Equation of motion,

HA: Hubbard atom,

IE: Improved estimator,

KF: Keldysh formalism,

LEEA: Low-energy effective action,

MF: Matsubara formalism,

MWF: Matsubara weighting function,

NRG: Numerical renormalization group,

PSF: Partial spectral function,

QCP: Quantum critical point,

QPT: Quantum phase transition,

RG: Renormalization group,

SDW: Spin-density wave,

sIE: Symmetric improved estimator,

ZF: Zero-temperature formalism.

Contents

1 Introduction

General motivation

The interplay between theory and experiment in physics lies at the core of extending our understanding of nature. While theories have to be capable of describing experimental observations, experiments are conducted to (in)validate predictions of theoretical models.

A prime example of the latter case (theory before experiment) is the experimental observation of the Higgs particle. In gauge theories, the Higgs mechanism generates the masses of gauge bosons by using the concept of spontaneous symmetry breaking without explicitly breaking local gauge invariance [PS16]. In high-energy physics, it predicted an additional particle for the Standard Model as the excitation of the underlying Higgs field [Tho13]. This Higgs boson was indeed detected at the Large Hadron Collider [ATL12, CMS12] 48 years after the original works by Englert, Brout, and Higgs [EB64, Hig64a, Hig64b].

The discovery of superconductivity by Onnes in 1911 [Onn11] is an example of the inverse scenario (experiment before theory). Only 46 years after its first observation, Bardeen, Cooper, and Schrieffer developed their theory of superconductivity [BCS57a, BCS57b], nowadays known as BCS theory. It explains the effect as the condensation of Cooper pairs, with phonon-mediated attractive interactions acting as the pairing glue between two electrons [AS10]. Interestingly, a variant of the Higgs mechanism (often called Anderson-Higgs-mechanism in this context) explains the Meissner effect, i.e., the expulsion of magnetic fields in superconductors [AS10].

An experimental observation that, to this date, defies a concise understanding in terms of a microscopic theory is the discovery of high-temperature superconductivity in 1986 by Bednorz and Müller [BM86]. Over the last decades, it has been observed in various compounds such as the quasi-two-dimensional cuprates [GMPS20] and iron pnictides [SCM14]. In these materials, the emergence of a non-Fermi liquid (or strange metal) region above the superconducting phase is equally puzzling [SCM14, GMPS20]. It is commonly attributed to an antiferromagnetic quantum critical point hidden beneath the superconducting dome, such that strong interactions between critical fluctuations and electrons destroy the Fermi-liquid-like quasiparticle character of electronic excitations [LRVW07, Sac11]. In theoretical models, the strong coupling of electrons to order parameter fluctuations is incorporated in low-energy effective actions [AC00, ACS03, Sac11], and substantial field-theoretical and numerical progress has been made toward describing the quantum critical points in two-dimensional metals [Lee18, BLST19]. However, the concise theoretical description of non-Fermi liquid hallmarks, such as the linear-in-temperature resistivity, still remains an open challenge.

The constructive interplay between theory and experiment requires that theory can compute experimentally measurable quantities. Due to the statistical nature of quantum mechanics, this is achieved by multipoint correlation functions (or correlators for short), i.e., time- or contour-ordered expectation values of one or multiple quantum mechanical operators [AS10]. For instance, they can yield the conductivity of a system due to an externally applied electric field [Kub57] or determine the single-particle spectral function, which is directly measurable using angle-resolved photoemission spectroscopy [SHS21].

In condensed matter physics, two frequently used frameworks for computing correlators are the Matsubara formalism (MF) [Mat55, ADG75] and the Keldysh formalism (KF) [Sch61, Kel65]. In the latter, multipoint correlators are evaluated directly on the real-time/real-frequency axis, and the KF is hence tailored to compute experimentally observable quantities directly. However, for a number of ℓ operators, the corresponding ℓ-point (ℓp) correlator has 2^ℓ components, drastically increasing the complexity for large ℓ [Kam23]. Conversely, the MF

employs a Wick rotation from real to imaginary times, reducing the number of components for any ℓp correlator to only one [SvL13]. In contrast to the KF, the MF is only applicable for systems in thermal equilibrium, and the final computation of physical observables requires the analytic continuation from imaginary to real frequencies. Conceptually, the analytic continuation is well-known for 2p correlators [BM61, NO98, AS10, WFHT22], and various works made significant progress for larger ℓ [Eli62, Eva90, Kob90, Kob91, Eva92, Tay93, Gue94a, Gue94b, Wel05a, Wel05b]. However, the numerical analytic continuation is ill-conditioned [GJSS91, SOOY17, Kau21], such that numerical real-frequency methods have gained traction over the last years [TCL19, KLvD21, LKvD21, GRW$^+$23].

Recently, Ref. [KLvD21] significantly advanced our understanding of multipoint correlators in the MF and KF. The authors introduced a new spectral representation where correlators are split into system-dependent but formalism-independent partial spectral functions (PSFs) and system-independent but formalism-dependent kernels. In the accompanying Ref. [LKvD21], the authors developed a computation scheme for PSFs up to $\ell = 4$ utilizing the numerical renormalization group (NRG), allowing the study of various impurity systems down to lowest temperatures on the imaginary- and real-frequency axis [KLvD21, LKvD21].

Problem statements and outline of this thesis

In this thesis, we further advance our understanding of multipoint correlators in the MF and KF on a conceptual level building upon Ref. [KLvD21], and apply correlation function methods in two different cases. The specific problems and questions addressed in this thesis are listed below; additional detailed motivations and overviews of previous literature are provided in the respective sections. The remainder of this thesis is organized as follows:

- In Ch. 2, we present a thorough introduction to the mathematical structure of expectation values (Sec. 2.1), correlation functions (Sec. 2.2), and PSFs (Sec. 2.3).

- In Ch. 3, we review properties and spectral representations of 2p MF (Sec. 3.1) and KF (Sec. 3.2) correlators as well as general ℓp MF (Sec. 3.3) and KF (Sec. 3.4) correlators. In Secs. 3.1 and 3.2, we additionally discuss the analytic continuation of 2p correlators. There, we pay special attention to the role of so-called anomalous terms, which may occur for vanishing bosonic Matsubara frequencies and vanishing eigenenergy differences in the corresponding Lehmann representation [KLvD21, WFHT22]. We conclude the chapter by defining the self-energy and the 4p vertex in Sec. 3.5.

- In the spectral representation of ℓp MF correlators, the analytically known MF kernels enforce imaginary-time ordering [KLvD21]. On the other hand, expressions for its Fourier transform were limited to small numbers of anomalous terms [Shv06, HJB$^+$09, KLvD21]. In Ch. 4, we compute the ℓp MF kernels in full generality, including all possible anomalous terms. After a brief overview of previous works, further motivation of the problem, and an outline of our approach in Sec. 4.1, [P2] is reprinted in Sec. 4.2.

- The analytic continuation of 2p MF correlators to its KF counterparts is well-known. However, a general strategy for the analytic continuation of ℓp MF correlators to all 2^ℓ Keldysh components was still missing. We develop such a general recipe, including anomalous terms, in Ch. 5, and apply it to general 2p and 3p as well as fermionic 4p correlators. Chapter 5 reproduces most of the main part of [P4], complemented with App. C reproducing the appendices of [P4]. A detailed overview of the structure of Ch. 5 and App. C is provided at the end of the introduction in Sec. 5.1.

- Improved estimators (IEs) are a viable tool for numerically computing self-energies and vertices more accurately [BHP98, HPW12, KGK$^+$19, Kug22]. However, as pointed out in Refs. [KLvD21, LKvD21], previously existing IEs only improve certain components of the 4p KF vertex. In Ch. 6, we derive a new symmetric IE applicable to all Keldysh components of the 4p vertex and demonstrate its accuracy for the Anderson impurity model [And61] using the multipoint NRG of Ref. [LKvD21]. After a short overview and motivation of our approach as well as a summary of our main results in Sec. 6.1, [P3] is reprinted in Sec. 6.2.

- Quantum critical models for two-dimensional metals are often formulated in the clean limit [Lee18], while realistic materials usually contain some degree of imperfection such as impurities. Additionally, disorder is one of the momentum-relaxing mechanisms that might play a central role in understanding the linear-in-temperature resistivity in the strange metal phase. In Ch. 7, we investigate the effects of quenched disorder at antiferromagnetic quantum critical points in two-dimensional metals. First, we provide a brief introduction to quantum criticality and disorder in Sec. 7.1. After an overview of previous results concerning disordered antiferromagnetic quantum critical models, differences to our approach, and a summary of our main results in Sec. 7.2.1, [P1] is reprinted in Sec. 7.2.2.

- Finally, we conclude this thesis in Ch. 8 with summaries and outlooks of the various projects covered in this thesis.

2 Expectation values and correlators

As stated in the introduction, experimentally measurable quantities of many-body systems are encoded in correlation functions, which are defined in terms of expectation values of one or multiple operators. In Sec. 2.1, we elucidate the mathematical structure of expectation values of single operators. This naturally establishes the time-contour idea which constitutes the underlying principle of the MF, KF, and also the zero-temperature formalism (ZF). The contour idea is then applied to multiple operators in the MF and KF in Sec. 2.2, for which the definitions of ℓp correlators for systems in thermal equilibrium are obtained. Therein, PSFs are identified as the basic building blocks in both formalisms [KLvD21]; their properties in the time and frequency domain are presented in Sec. 2.3. Though parts of this chapter are textbook knowledge, it is presented in a unified notation and in a manner that will facilitate reading the later sections and publications [P2, P3].

2.1 Expectation values

The definition of an expectation value in a quantum mechanical system relies on the following question: Is the physical system of interest completely isolated from its environment, or does a non-vanishing coupling to the environment affect intrinsic properties of the system such as the total energy or particle number? The former setup of an isolated system is a rather crude idealization of reality; nevertheless, it proves useful to motivate the contour idea in Sec. 2.1.1. The effects of the system being in thermal contact with its environment are then discussed in Sec. 2.1.2. The ensuing presentation closely follows Chapters 3–5 of Ref. [SvL13].

2.1.1 Time evolution in expectation values of an isolated system

Consider a quantum mechanical system prepared in some initial state $|\psi_\mathrm{i}\rangle$ at some initial time t_i. Its time evolution is determined by the hermitian, possibly time-dependent Hamiltonian $H(t)$[1] via the Schrödinger equation ($\hbar = 1$)

$$\mathrm{i}\frac{\mathrm{d}}{\mathrm{d}t}|\psi(t)\rangle = H(t)|\psi(t)\rangle, \qquad |\psi(t_\mathrm{i})\rangle = |\psi_\mathrm{i}\rangle, \qquad t > t_\mathrm{i}. \tag{2.1}$$

The expectation value $O(t)$ of a possibly time-dependent operator $\mathcal{O}(t)$ in a system described by the state $|\psi(t)\rangle$ at time t is then defined as

$$O(t) = \langle\psi(t)|\mathcal{O}(t)|\psi(t)\rangle. \tag{2.2}$$

The Schrödinger equation can be formally solved in terms of a unitary operator $U(t, t_\mathrm{i})$ that describes the time evolution of the initial state $|\psi_\mathrm{i}\rangle$ to the state $|\psi(t)\rangle$:

$$|\psi(t)\rangle = U(t, t_\mathrm{i})|\psi_\mathrm{i}\rangle, \qquad U(t_\mathrm{i}, t_\mathrm{i}) = \mathbb{1}, \tag{2.3}$$

with $\mathbb{1}$ the identity operator. To obtain an explicit expression for $U(t, t_\mathrm{i})$, the ansatz (2.3) is inserted into the Schrödinger equation (2.1), leading to

$$\mathrm{i}\frac{\mathrm{d}}{\mathrm{d}t}U(t, t_\mathrm{i}) = H(t)U(t, t_\mathrm{i}), \qquad U(t_\mathrm{i}, t_\mathrm{i}) = \mathbb{1}. \tag{2.4}$$

---

1 Despite considering time-independent Hamiltonians $H(t) = H$ and operators $\mathcal{O}(t) = \mathcal{O}$ for most of this thesis, we include a possible time-dependence in this section for the sake of generality.

Being a linear differential equation for $U(t, t_\mathrm{i})$ with a given initial condition, it can be converted to an integral equation by integrating both sides from the initial time t_i to the final time t:

$$U(t, t_\mathrm{i}) = \mathbb{1} - \mathrm{i} \int_{t_\mathrm{i}}^t \mathrm{d}t_1\, H(t_1) U(t_1, t_\mathrm{i}). \tag{2.5}$$

This equation can be understood as an iterative definition for $U(t, t_\mathrm{i})$: Inserting $U(t_1, t_\mathrm{i}) = \mathbb{1} - \mathrm{i} \int_{t_\mathrm{i}}^{t_1} \mathrm{d}t_2\, H(t_2) U(t_2, t_\mathrm{i})$ on the r.h.s. and repeating this step iteratively, it yields

$$
\begin{aligned}
U(t, t_\mathrm{i}) &= \mathbb{1} - \mathrm{i} \int_{t_\mathrm{i}}^t \mathrm{d}t_1\, H(t_1) + (-\mathrm{i})^2 \int_{t_\mathrm{i}}^t \mathrm{d}t_1\, H(t_1) \int_{t_\mathrm{i}}^{t_1} \mathrm{d}t_2\, H(t_2) U(t_2, t_\mathrm{i}) \\
&= \cdots = \sum_{n=0}^{\infty} (-\mathrm{i})^n \int_{t_\mathrm{i}}^t \mathrm{d}t_1 \int_{t_\mathrm{i}}^{t_1} \mathrm{d}t_2 \ldots \int_{t_\mathrm{i}}^{t_{n-1}} \mathrm{d}t_n\, H(t_1) H(t_2) \ldots H(t_n) \\
&= \sum_{n=0}^{\infty} \frac{(-\mathrm{i})^n}{n!} \int_{t_\mathrm{i}}^t \mathrm{d}t_1 \int_{t_\mathrm{i}}^t \mathrm{d}t_2 \ldots \int_{t_\mathrm{i}}^t \mathrm{d}t_n\, \mathcal{T} \{H(t_1) H(t_2) \ldots H(t_n)\} \\
&= \mathcal{T} \left\{ e^{-\mathrm{i} \int_{t_\mathrm{i}}^t \mathrm{d}t'\, H(t')} \right\}.
\end{aligned}
\tag{2.6}
$$

In the second line, the Hamiltonians, which do not necessarily commute for unequal times, appear with larger time arguments to the left, since $t_1 > t_2 > \cdots > t_n$ in the integration boundaries. In the third line, this time-ordering is made explicit by the time-ordering operator $\mathcal{T}$. In general, for n operators $\mathcal{O}^i(t_i)$, it is defined as

$$\mathcal{T} \left\{ \mathcal{O}^1(t_1) \mathcal{O}^2(t_2) \ldots \mathcal{O}^n(t_n) \right\} = \zeta_p\, \mathcal{O}^{\bar{1}}(t_{\bar{1}}) \mathcal{O}^{\bar{2}}(t_{\bar{2}}) \ldots \mathcal{O}^{\bar{n}}(t_{\bar{n}}), \qquad t_{\bar{1}} > t_{\bar{2}} > \cdots > t_{\bar{n}}. \tag{2.7}$$

Here, the permutation $p = (\bar{1} \ldots \bar{n})$ replaces indices i by their permuted values $p(i) = \bar{i}$. The sign factor ζ_p equals $+1$ (or -1) if the permuted product of operators differs from the unpermuted product by an even (or odd) number of transpositions of fermionic operators. For instance, consider $n = 3$ fermionic operators and the times chosen as $t_3 > t_2 > t_1$. We then have $p = (\overline{123}) = (321)$ with $\zeta_p = -1$ and therefore

$$\mathcal{T} \left\{ \mathcal{O}^1(t_1) \mathcal{O}^2(t_2) \mathcal{O}^3(t_3) \right\} = -\mathcal{O}^3(t_3) \mathcal{O}^2(t_2) \mathcal{O}^1(t_1). \tag{2.8}$$

Note that the time-ordering operator does not impose (anti)commutation relations on the operators upon reordering. Since every integral variable t_i in the third line of Eq. (2.6) takes values $t_i \in [t_\mathrm{i}, t]$, all possible $n!$ orderings of the Hamiltonians contribute to the time-ordering operation; the factor $1/n!$ avoids overcounting of these $n!$ equivalent terms.[2] In the last step of Eq. (2.6) we then identified the infinite sum as the Taylor expansion of an exponential.[3]

   Equation (2.6) solves the Schrödinger equation (2.1) via Eq. (2.3) for a propagation forward in time. An equivalent expression for the evolution backward in time can be obtained

---

2 Consider the contribution from $t_2 > t_1 > t_3 > \cdots > t_n$. Then we find

$$\int_{t_\mathrm{i}}^t \mathrm{d}t_2 \int_{t_\mathrm{i}}^{t_2} \mathrm{d}t_1 \ldots \int_{t_\mathrm{i}}^{t_{n-1}} \mathrm{d}t_n\, H(t_2) H(t_1) \ldots H(t_n) \overset{t_1 \leftrightarrow t_2}{=} \int_{t_\mathrm{i}}^t \mathrm{d}t_1 \int_{t_\mathrm{i}}^{t_1} \mathrm{d}t_2 \ldots \int_{t_\mathrm{i}}^{t_{n-1}} \mathrm{d}t_n\, H(t_1) H(t_2) \ldots H(t_n),$$

   i.e., it is equal to the contribution from the time-ordering $t_1 > t_2 > t_3 > \cdots > t_n$. Similarly, all $n!$ contributions are found to be equivalent. Note that $\zeta_p = +1$ for all permutations of the Hamiltonians as they are hermitian operators.

3 The time-ordering symbol only acts on operators and therefore commutes with the integrals and the sum.

from the Schrödinger equation for a given final state,

$$\mathrm{i}\frac{\mathrm{d}}{\mathrm{d}t}|\psi(t)\rangle = H(t)|\psi(t)\rangle, \qquad |\psi(t_{\mathrm{f}})\rangle = |\psi_{\mathrm{f}}\rangle, \qquad t < t_{\mathrm{f}}, \tag{2.9}$$

which is solved by the operator

$$|\psi(t)\rangle = U(t, t_{\mathrm{f}})|\psi_{\mathrm{f}}\rangle, \qquad U(t, t_{\mathrm{f}}) = \overline{\mathcal{T}}\left\{e^{-\mathrm{i}\int_{t_{\mathrm{f}}}^{t}\mathrm{d}t'\,H(t')}\right\}, \qquad U(t_{\mathrm{f}}, t_{\mathrm{f}}) = \mathbb{1}. \tag{2.10}$$

In contrast to $\mathcal{T}$, the anti-time-ordering operator $\overline{\mathcal{T}}$ places operators with larger time arguments to the right:

$$\overline{\mathcal{T}}\left\{\mathcal{O}^1(t_1)\mathcal{O}^2(t_2)\dots\mathcal{O}^n(t_n)\right\} = \zeta_p\,\mathcal{O}^{\overline{1}}(t_{\overline{1}})\mathcal{O}^{\overline{2}}(t_{\overline{2}})\dots\mathcal{O}^{\overline{n}}(t_{\overline{n}}), \qquad t_{\overline{1}} < t_{\overline{2}} < \cdots < t_{\overline{n}}. \tag{2.11}$$

The definition of the time-evolution operator for general time arguments then follows from Eqs. (2.6) and (2.10),

$$U(t_2, t_1) = \begin{cases} \mathcal{T}\left\{e^{-\mathrm{i}\int_{t_1}^{t_2}\mathrm{d}t'\,H(t')}\right\} & \text{for } t_2 > t_1, \\ \overline{\mathcal{T}}\left\{e^{-\mathrm{i}\int_{t_1}^{t_2}\mathrm{d}t'\,H(t')}\right\} & \text{for } t_1 > t_2, \end{cases} \tag{2.12}$$

with the properties[4]

$$U(t, t) = \mathbb{1}, \qquad U(t_3, t_2)U(t_2, t_1) = U(t_3, t_1), \qquad U^\dagger(t_1, t_2) = U(t_2, t_1). \tag{2.13}$$

According to the last identity the time evolution of $\langle\psi(t)|$ can be inferred from the hermitian conjugation of $|\psi(t)\rangle = U(t, t_{\mathrm{i}})|\psi_{\mathrm{i}}\rangle$ and therefore reads $\langle\psi(t)| = \langle\psi_{\mathrm{i}}|U^\dagger(t, t_{\mathrm{i}}) = \langle\psi_{\mathrm{i}}|U(t_{\mathrm{i}}, t)$. Note that the (anti-)time-ordering operators are redundant for time-independent Hamiltonians $H(t) = H$, and the time-evolution operator is given by the simple form $U(t_2, t_1) = e^{-\mathrm{i}H(t_2-t_1)}$ in this case.

We now return to our primary object of interest: the expectation value in Eq. (2.2). In terms of the time-evolution operator, it takes the form

$$O(t) = \langle\psi_{\mathrm{i}}|U(t_{\mathrm{i}}, t)\mathcal{O}(t)U(t, t_{\mathrm{i}})|\psi_{\mathrm{i}}\rangle. \tag{2.14}$$

Reading this equation from right to left, it describes the evolution of an initially prepared state $|\psi_{\mathrm{i}}\rangle$ to time t, where the operator $\mathcal{O}(t)$ is inserted, and a subsequent evolution back to the initial time, where the overlap with the initial state is calculated. In Fig. 2.1(a), the forward and backward time propagation is represented graphically by a contour consisting of a forward branch and a backward branch, with the largest time given by t.

For later convenience, Eq. (2.14) is further manipulated by inserting the identity operator $\mathbb{1} = U(t, t) = U(t, \infty)U(\infty, t)$. This extends the contour to infinity, with the freedom of inserting $\mathcal{O}(t)$ during either the forward or backward evolution without changing the expectation value:

$$\begin{aligned} O(t) &= \langle\psi_{\mathrm{i}}|U(t_{\mathrm{i}}, \infty)U(\infty, t)\mathcal{O}(t)U(t, t_{\mathrm{i}})|\psi_{\mathrm{i}}\rangle \\ &= \langle\psi_{\mathrm{i}}|U(t_{\mathrm{i}}, t)\mathcal{O}(t)U(t, \infty)U(\infty, t_{\mathrm{i}})|\psi_{\mathrm{i}}\rangle. \end{aligned} \tag{2.15}$$

---

[4] The last equality holds since hermitian conjugation changes $\mathcal{T}$ to $\overline{\mathcal{T}}$, which can be seen by the hermitian conjugation of the second line in Eq. (2.6).

In the first line, $U(\infty, t)\mathcal{O}(t)U(t, t_i)$ can be identified with a time-ordered product of $\mathcal{O}(t)$ and the exponential operator $\exp\{-i \int_{t_i}^{\infty} dt' H(t')\}$, since by definition of the time-ordering operator (2.7) it holds that

$$\mathcal{T}\left\{e^{-i \int_{t_i}^{\infty} dt' H(t')}\mathcal{O}(t)\right\} = \mathcal{T}\left\{e^{-i \int_{t}^{\infty} dt' H(t')}\right\}\mathcal{O}(t)\mathcal{T}\left\{e^{-i \int_{t_i}^{t} dt' H(t')}\right\}$$
$$= U(\infty, t)\mathcal{O}(t)U(t, t_i). \tag{2.16}$$

In terms of $\mathcal{T}$ and $\overline{\mathcal{T}}$, $O(t)$ can then be expressed as

$$O(t) = \langle\psi_i|\overline{\mathcal{T}}\left\{e^{-i \int_{\infty}^{t_i} dt' H(t')}\right\}\mathcal{T}\left\{e^{-i \int_{t_i}^{\infty} dt' H(t')}\mathcal{O}(t)\right\}|\psi_i\rangle$$
$$= \langle\psi_i|\overline{\mathcal{T}}\left\{e^{-i \int_{\infty}^{t_i} dt' H(t')}\mathcal{O}(t)\right\}\mathcal{T}\left\{e^{-i \int_{t_i}^{\infty} dt' H(t')}\right\}|\psi_i\rangle, \tag{2.17}$$

where we similarly identified $U(t_i, t)\mathcal{O}(t)U(t, \infty)$ in the second line of Eq. (2.15) with an anti-time-ordered product.

We are now in the position to mathematically formalize the contour idea by simplifying the structure arising in Eq. (2.17). Let us define the contour $\mathcal{C}_{t_i} = \mathcal{C}_{-;t_i} \oplus \mathcal{C}_{+;t_i}$, with the forward and backward branch $\mathcal{C}_{-;t_i} = [t_i, \infty)$ and $\mathcal{C}_{+;t_i} = (\infty, t_i]$, respectively. For a point $z = t^{\pm} \in \mathcal{C}_{t_i}$ lying on $\mathcal{C}_{t_i}$, the superscript $\pm$ specifies the branch $\mathcal{C}_{\pm;t_i}$ the point resides on, and t is the explicit time on that specified branch.

Being equipped with a contour, it seems convenient to define a contour-ordering operator $\mathcal{T}_{\mathcal{C}}$ that places, in the spirit of $\mathcal{T}$, operators with larger contour arguments $z \in \mathcal{C}_{t_i}$ to the left. But how exactly is "larger" defined on $\mathcal{C}_{t_i}$? This question is answered in Fig. 2.1(b), which serves as a graphical representation of Eq. (2.17) (see also Eq. (2.20) and the discussion thereafter). The orientation of the contour $\mathcal{C}_{t_i}$ is indicated by the arrows. Then, the further along the oriented contour the argument z is located, the larger it is considered to be. This defines the following ordering rules for $\mathcal{T}_{\mathcal{C}}$ for two contour arguments $z_i = t_i^{\pm}$ and $z_j = t_j^{\pm}$:

$$z_i = t_i^- > t_j^- = z_j, \qquad t_i > t_j,$$
$$z_i = t_i^+ > t_j^+ = z_j, \qquad t_i < t_j,$$
$$z_i = t_i^+ > t_j^- = z_j, \qquad \forall\, t_i, t_j. \tag{2.18}$$

These rules impose time-ordering ($\mathcal{T}$) on $\mathcal{C}_{-;t_i}$, anti-time-ordering ($\overline{\mathcal{T}}$) on $\mathcal{C}_{+;t_i}$, and contour arguments on $\mathcal{C}_{+;t_i}$ are later than those on $\mathcal{C}_{-;t_i}$. This exactly coincides with the mathematical structure in Eq. (2.17). Consequently, given n operators $\mathcal{O}^i(z_i)$ with $z_i = t_i^{c_i}$ and $c_i = \pm$, the contour-ordering operator $\mathcal{T}_{\mathcal{C}}$ is defined as

$$\mathcal{T}_{\mathcal{C}}\left\{\mathcal{O}^1(z_1 = t_1^{c_1})\ldots\mathcal{O}^n(z_n = t_n^{c_n})\right\} = \zeta_p\left[\mathcal{O}^{\overline{1}}(t_{\overline{1}}^{c_{\overline{1}}})\ldots\mathcal{O}^{\overline{\lambda}}(t_{\overline{\lambda}}^{c_{\overline{\lambda}}})\right]\left[\mathcal{O}^{\overline{\lambda+1}}(t_{\overline{\lambda+1}}^{c_{\overline{\lambda+1}}})\ldots\mathcal{O}^{\overline{n}}(t_{\overline{n}}^{c_{\overline{n}}})\right]$$
$$\text{with} \quad c_{\overline{1}}, \ldots, c_{\overline{\lambda}} = +, \quad c_{\overline{\lambda+1}}, \ldots, c_{\overline{n}} = -, \quad t_{\overline{1}} < \cdots < t_{\overline{\lambda}}, \quad t_{\overline{\lambda+1}} > \cdots > t_{\overline{n}}. \tag{2.19}$$

It time-orders those operators $\mathcal{O}^{\overline{i}}$ with $c_{\overline{i}} = -$, $i \in \{\lambda+1, \ldots, \ell\}$, and places them to the right of the anti-time-ordered operators $\mathcal{O}^{\overline{j}}$ with $c_{\overline{j}} = +$, $j \in \{1, \ldots, \lambda\}$. In this thesis, operators with contour arguments are defined to be identical on both branches, $\mathcal{O}(z) = \mathcal{O}(t^c) = \mathcal{O}(t)$ and $H(z) = H(t^c) = H(t)$.[5] However, the contour indices c may only be neglected after the contour-ordering was imposed. This is especially important for time-independent operators and Hamiltonians, $\mathcal{O}(t) = \mathcal{O}$ and $H(t) = H$: They still carry a contour argument in order to

---

5 This is generally not the case, see for example the source terms in the generating functional in the KF [Kam23].
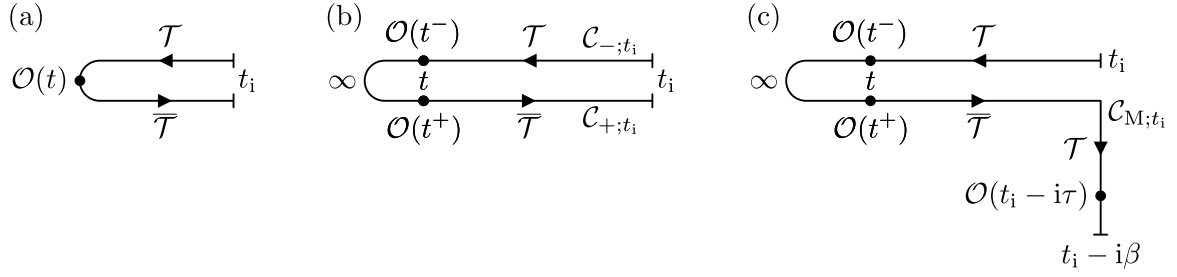
Figure 2.1 Evolution of the contours for evaluating expectation values from (a) Eq. (2.14) to (b) Eq. (2.20) for isolated system and then to (c) Eq. (2.25) for systems in thermal contact with their environment. Lines represent the contour and the time-evolution operator U, arrows indicate the orientation of the contour, and $\mathcal{T}$ ($\overline{\mathcal{T}}$) denote the (anti-)time-ordering prescription on each branch. Operators on the forward ($\mathcal{C}_{-;t_i}$) or backward ($\mathcal{C}_{+;t_i}$) branch yield time-dependent expectation values, while operators on the imaginary-time branch $\mathcal{C}_{M;t_i}$ correspond to thermal expectation values in the initial configuration of the system (see Eq. (2.28)).

have a unique contour-ordering prescription, and only afterward the time-dependence may be dropped.

With these definitions, together with $O(z) = O(t^{\pm}) = O(t)$, the expectation value in Eq. (2.17) takes the form

$$O(z) = \langle \psi_i | \mathcal{T}_\mathcal{C} \left\{ e^{-i \int_{\mathcal{C}_{t_i}} dz' H(z')} \mathcal{O}(z) \right\} |\psi_i\rangle, \tag{2.20}$$

with $z = t^-$ and $z = t^+$ recovering the first and second line therein, respectively. The integral over the contour variable z' is defined as[6]

$$\int_{\mathcal{C}_{t_i}} dz' H(z') = \int_{\mathcal{C}_{-;t_i}} dz' H(z') + \int_{\mathcal{C}_{+;t_i}} dz' H(z') = \int_{t_i}^{\infty} dt' H(t'^-) + \int_{\infty}^{t_i} dt' H(t'^+). \tag{2.21}$$

Equation (2.20) is the central result of this section and is represented graphically in Fig. 2.1(b). It may seem unnecessary to express the simple equation (2.2) in this way, especially since $\mathcal{O}(t^c)$ can be placed on either branch to recover the same time-dependent expectation value via Eq. (2.17). However, when considering expectation values of multiple operators, the contour indices will make a difference, which lies at the heart of the complexity of the KF. Additionally, when considering systems in thermal contact with its environment in the next section, the contour idea inherent in Eq. (2.20) not only applies to real times, but naturally extends to imaginary-time expectation values arising in the MF.

2.1.2 Thermal expectation values

In experiments, the system on which measurements are performed cannot be isolated perfectly from its environment. Therefore, interactions with the environment are expected to influence the system non-trivially, and one cannot assume that the system is always prepared in a single specific initial state $|\psi_i\rangle$. Additionally, one is usually interested in the measurement of macroscopic observables, for which it is not necessary to know the exact microscopic state

---

6 A general integral between two points $z_2 > z_1$ on the contour is defined as

$$\int_{z_1}^{z_2} dz\, \mathcal{O}(z) = \begin{cases} \int_{t_1}^{t_2} dt\, \mathcal{O}(t^{\pm}) & \text{for } z_1, z_2 \in \mathcal{C}_{\pm;t_i}, \\ \int_{t_1}^{\infty} dt\, \mathcal{O}(t^-) + \int_{\infty}^{t_2} dt\, \mathcal{O}(t^+) & \text{for } z_1 \in \mathcal{C}_{-;t_i},\ z_2 \in \mathcal{C}_{+;t_i}. \end{cases}$$

describing the system. Then, one step closer to reality is to consider an ensemble: infinitely many copies of macroscopically identical systems, each of which is initially prepared, with a probability p_n, in one of the states $|\psi_i^{(n)}\rangle$ compatible with the macroscopic properties [BFK+15]. The information about this statistical distribution of initial states is encoded in the density matrix $\rho = \sum_n p_n |\psi_i^{(n)}\rangle\langle\psi_i^{(n)}|$, and expectation values are then defined as

$$O(t) = \langle U(t_i, t)\mathcal{O}(t)U(t, t_i)\rangle = \text{Tr}[\rho\, U(t_i, t)\mathcal{O}(t)U(t, t_i)]. \tag{2.22}$$

For the rest of this thesis, we assume the initial system to be in thermal equilibrium with its environment at a temperature T, implying $\rho = e^{-\beta H}/Z$ with the partition function $Z = \text{Tr}[\rho]$, inverse temperature $\beta = 1/T$ ($k_B = 1$), and H the initial, time-independent Hamiltonian $H = H(t_i)$.[7] In terms of the contour used in Eq. (2.20), the thermal expectation value then reads[8]

$$O(z) = \frac{1}{Z}\text{Tr}\left[e^{-\beta H}\,\mathcal{T}_\mathcal{C}\left\{e^{-i\int_{\mathcal{C}_{t_i}} dz'\, H(z')}\mathcal{O}(z)\right\}\right]. \tag{2.23}$$

Now, a key observation that forms the basis of the MF [Mat55] is that the exponential $e^{-\beta H}$ can be interpreted as the time-evolution operator in imaginary time, since

$$e^{-\beta H} = e^{-i\int_{t_i}^{t_i - i\beta} d\tau\, H} = e^{-i\int_{\mathcal{C}_{M;t_i}} dz'\, H} = U(t_i - i\beta, t_i). \tag{2.24}$$

The imaginary-time contour $\mathcal{C}_{M;t_i} = [t_i, t_i - i\beta]$ can be directly attached to $\mathcal{C}_{t_i}$, defining the new contour $\mathcal{C} = \mathcal{C}_{M;t_i} \oplus \mathcal{C}_{t_i}$ (see Fig. 2.1(c)). Then, the thermal expectation value in Eq. (2.23) takes the alternative form

$$O(z) = \frac{1}{Z}\text{Tr}\left[\mathcal{T}_\mathcal{C}\left\{e^{-i\int_\mathcal{C} dz'\, H(z')}\mathcal{O}(z)\right\}\right]. \tag{2.25}$$

The Hamiltonian with a contour argument $z \in \mathcal{C}$ corresponds to the initial Hamiltonian on the imaginary, vertical branch of the contour and to the time-dependent Hamiltonian on the horizontal (forward and backward) branches:

$$H(z) = \begin{cases} H(t_i) = H & \text{for } z \in \mathcal{C}_{M;t_i}, \\ H(t^\pm) = H(t) & \text{for } z \in \mathcal{C}_{\pm;t_i}. \end{cases} \tag{2.26}$$

Points on $\mathcal{C}_{M;t_i}$ are parameterized as $z_i = t_i - i\tau_i \in \mathcal{C}_{M;t_i}$. The τ_i are often referred to as imaginary times even though they are restricted to real values $\tau_i \in [0, \beta]$. The contour-ordering operator $\mathcal{T}_\mathcal{C}$ is still defined as placing larger contour arguments to left, with the ordering rules in Eq. (2.18) complemented with

$$\begin{aligned} z_i = t_i - i\tau_i > t_j^\pm = z_j, & \qquad \forall \tau_i, t_j, \\ z_i = t_i - i\tau_i > t_i - i\tau_j = z_j, & \qquad \tau_i > \tau_j. \end{aligned} \tag{2.27}$$

This places contour arguments on $\mathcal{C}_{M;t_i}$ to the left of those on $\mathcal{C}_{\pm;t_i}$ and enforces time-ordering on $\mathcal{C}_{M;t_i}$ (see orientation of contour in Fig. 2.1(c)).

---

7 Despite using the notation for canonical ensembles, grand-canonical descriptions are included by assuming that μN is already absorbed in the Hamiltonian H.

8 Of course, this formula does not describe reality in its full glory. For instance, the effect of the environment is solely included in the statistical description of the initial states. However, each initial state $|\psi_i^{(n)}\rangle$ is then assumed to evolve isolated from its environment, yielding Eq. (2.23) [SvL13].

Equation (2.25) extends the domain of definition of $O(z)$ from $z \in \mathcal{C}_{t_\mathrm{i}}$ to $z \in \mathcal{C}$ by allowing z to reside on $\mathcal{C}_{\mathrm{M};t_\mathrm{i}}$, $z = t_\mathrm{i} - \mathrm{i}\tau$. Consistent with the definition of $H(z)$ in Eq. (2.26), operators with contour argument $z \in \mathcal{C}_{\mathrm{M};t_\mathrm{i}}$ are defined to equal the operator at initial times, $\mathcal{O}(z \in \mathcal{C}_{\mathrm{M};t_\mathrm{i}}) = \mathcal{O}(t_\mathrm{i}) = \mathcal{O}$. For imaginary times, Eq. (2.25) then evaluates to

$$
\begin{aligned}
O(t_\mathrm{i} - \mathrm{i}\tau) &= \frac{1}{Z} \operatorname{Tr}\left[\mathcal{T}\left\{ e^{-\mathrm{i}\int_{\mathcal{C}_{\mathrm{M};t_\mathrm{i}}} \mathrm{d}z'\, H} \mathcal{O}(t_\mathrm{i} - \mathrm{i}\tau) \right\} \overline{\mathcal{T}}\left\{ e^{-\mathrm{i}\int_{\mathcal{C}_{+;t_\mathrm{i}}} \mathrm{d}z'\, H(z')} \right\} \mathcal{T}\left\{ e^{-\mathrm{i}\int_{\mathcal{C}_{-;t_\mathrm{i}}} \mathrm{d}z'\, H(z')} \right\} \right] \\
&= \frac{1}{Z} \operatorname{Tr}[\, U(t_\mathrm{i} - \mathrm{i}\beta, t_\mathrm{i} - \mathrm{i}\tau)\, \mathcal{O}\, U(t_\mathrm{i} - \mathrm{i}\tau, t_\mathrm{i})\, U(t_\mathrm{i}, \infty)\, U(\infty, t_\mathrm{i})\,] \\
&= \frac{\operatorname{Tr}\left[e^{-(\beta-\tau)H} \mathcal{O}\, e^{-\tau H} \right]}{\operatorname{Tr}[e^{-\beta H}]} = \operatorname{Tr}[\rho\, \mathcal{O}] = \langle \mathcal{O} \rangle\,,
\end{aligned} \tag{2.28}
$$

where we used the cyclicity of the trace in the last line. Note again that $\mathcal{O}(t_\mathrm{i} - \mathrm{i}\tau) = \mathcal{O}$ must not be inserted before contour-ordering was imposed. Hence, for $z = t_\mathrm{i} - \mathrm{i}\tau \in \mathcal{C}_{\mathrm{M};t_\mathrm{i}}$, Eq. (2.25) corresponds to the thermal expectation value of $\mathcal{O}$ in the initial, equilibrium ensemble of the system, i.e., to Eq. (2.22) with $t = t_\mathrm{i}$. Note that the explicit dependence on t_i in Eq. (2.28) is cancelled; it enters the expectation value only implicitly via the initial density matrix and the initial operator.

2.2 Correlation functions

With Eq. (2.25), an expression for the thermal expectation value of a single operator expressed via the contour $\mathcal{C}$ was derived. In this section, we extend the analysis to the physically most relevant case: Multipoint correlators defined in terms of thermal expectation values of ℓ operators $\boldsymbol{\mathcal{O}} = (\mathcal{O}^1, \ldots, \mathcal{O}^\ell)$ with contour arguments $\boldsymbol{z} = (z_1, \ldots, z_\ell)$, where $\boldsymbol{\mathcal{O}}$ can contain any number of bosonic but only an even number of fermionic operators. To be precise, ℓp correlators are defined as the direct generalization of Eq. (2.25) (with a conventional prefactor $(-\mathrm{i})^{\ell-1}$) [SvL13]:

$$
\mathcal{G}[\boldsymbol{\mathcal{O}}](\boldsymbol{z}) = (-\mathrm{i})^{\ell-1} \frac{1}{Z} \operatorname{Tr}\left[\mathcal{T}_{\mathcal{C}}\left\{ e^{-\mathrm{i}\int_{\mathcal{C}} \mathrm{d}z'\, H(z')} \mathcal{O}^1(z_1) \ldots \mathcal{O}^\ell(z_\ell) \right\} \right]. \tag{2.29}
$$

Remarkably, as mentioned in the beginning of the chapter and discussed in Ref. [SvL13], this definition unifies the MF, KF, and ZF. In particular, the formalisms only differ by the contour $\mathcal{C}$ and contour-ordering operator $\mathcal{T}_{\mathcal{C}}$ under consideration (plus a few additional assumptions, e.g., the adiabatic assumption discussed in Sec. 2.2.2). A thorough analysis of the emergence of the MF and KF correlators will be conducted in the following sections; for a discussion of the ZF correlators, we refer the reader to Ref. [SvL13].

Recently, Ref. [KLvD21] elucidated the structure of ℓp correlators in the different formalisms by separating the contour-ordering operation from thermal expectation values. Since [P2] and [P4] build upon this reference, the ensuing sections additionally serve the purpose of introducing (part of) the notation and results of Ref. [KLvD21] in the time domain and, to some extent, in the frequency domain; Ch. 3 then complements this discussion.

2.2.1 Matsubara formalism

The MF (or imaginary-time formalism) was originally introduced in Ref. [Mat55] as a method to calculate the partition function of interacting many-body systems assuming the systems are in thermal equilibrium. It originates from the observation in Eq. (2.24) that the exponential in the density matrix can be interpreted as a time evolution in imaginary time. Then, correlators with imaginary-time arguments naturally arise, e.g., by treating the interacting part of the

Hamiltonian perturbatively. Nowadays, the MF is established as one of the main formalisms for computing ℓp correlators especially in numerical studies, since it circumvents the increased complexity of the doubled real-time contour used in the KF.

To connect Eq. (2.29) to MF correlators, we restrict all contour arguments to the vertical branch of the contour, $z_i \in \mathcal{C}_{\mathrm{M};t_\mathrm{i}} = [t_\mathrm{i}, t_\mathrm{i} - \mathrm{i}\beta]$. As t_i enters only implicitly via the initial Hamiltonian and operators (see Eq. (2.28) and discussion thereafter), we set $t_\mathrm{i} = 0$ and define the Matsubara contour $\mathcal{C}_\mathrm{M} = [0, -\mathrm{i}\beta]$. Parameterizing $\boldsymbol{z} = -\mathrm{i}\boldsymbol{\tau} = (-\mathrm{i}\tau_1, \ldots, -\mathrm{i}\tau_\ell)$ with $\tau_i \in [0, \beta]$ and using $\mathcal{O}^i(-\mathrm{i}\tau_i) = \mathcal{O}^i$, Eq. (2.29) thus takes the form (for fixed $\tau_{\overline{1}} > \cdots > \tau_{\overline{\ell}}$)

$$
\begin{aligned}
\mathcal{G}[\boldsymbol{\mathcal{O}}](-\mathrm{i}\boldsymbol{\tau}) &= (-\mathrm{i})^{\ell-1} \frac{1}{Z} \mathrm{Tr}\Big[\mathcal{T}\Big\{e^{-\mathrm{i}\int_{\mathcal{C}_\mathrm{M}}\mathrm{d}z'H}\mathcal{O}^1(-\mathrm{i}\tau_1)\ldots\mathcal{O}^\ell(-\mathrm{i}\tau_\ell)\Big\}U(0,\infty)U(\infty,0)\Big] \\
&= (-\mathrm{i})^{\ell-1}\frac{\zeta_p}{Z}\mathrm{Tr}\Big[U(-\mathrm{i}\beta,-\mathrm{i}\tau_{\overline{1}})\,\mathcal{O}^{\overline{1}}\,U(-\mathrm{i}\tau_{\overline{1}},-\mathrm{i}\tau_{\overline{2}})\,\mathcal{O}^{\overline{2}}\ldots U(-\mathrm{i}\tau_{\overline{\ell-1}},-\mathrm{i}\tau_{\overline{\ell}})\,\mathcal{O}^{\overline{\ell}}\,U(-\mathrm{i}\tau_{\overline{\ell}},0)\Big] \\
&= (-\mathrm{i})^{\ell-1}\mathrm{Tr}\Big[\rho\,\mathcal{T}\Big\{\mathcal{O}_H^1(-\mathrm{i}\tau_1)\ldots\mathcal{O}_H^\ell(-\mathrm{i}\tau_\ell)\Big\}\Big] \\
&= (-\mathrm{i})^{\ell-1}\Big\langle\mathcal{T}\Big\{\mathcal{O}_H^1(-\mathrm{i}\tau_1)\ldots\mathcal{O}_H^\ell(-\mathrm{i}\tau_\ell)\Big\}\Big\rangle, \quad\quad\quad (2.30)
\end{aligned}
$$

with $\mathcal{O}_H^i(-\mathrm{i}\tau_i) = e^{H\tau_i}\mathcal{O}^i e^{-H\tau_i}$ an operator in the imaginary-time Heisenberg picture.

As the definition of a general ℓp MF correlator, we use

$$
\mathcal{G}(\boldsymbol{\tau}) = (-\mathrm{i})^{\ell-1}\mathcal{G}[\boldsymbol{\mathcal{O}}](-\mathrm{i}\boldsymbol{\tau}) = (-1)^{\ell-1}\Big\langle\mathcal{T}\Big\{\mathcal{O}^1(-\mathrm{i}\tau_1)\ldots\mathcal{O}^\ell(-\mathrm{i}\tau_\ell)\Big\}\Big\rangle, \quad\quad (2.31)
$$

i.e., a thermal expectation value of ℓ operators time-ordered on the imaginary-time axis $\mathcal{C}_\mathrm{M}$ (see Fig. 2.2(a)). For systems in thermal equilibrium, we suppress the subscripts of the operators, $\mathcal{O}_H^i(-\mathrm{i}\tau_i) \to \mathcal{O}^i(-\mathrm{i}\tau_i) := e^{H\tau_i}\mathcal{O}^i e^{-H\tau_i}$, since the only time-dependence for a time-independent Hamiltonian H is generated by the Heisenberg time evolution. Equation (2.31) coincides with the standard textbook definition of an ℓp MF correlator (up to a conventional prefactor) [BF04].

Following Ref. [KLvD21], the time-ordering operation can be cleanly separated from system-specific properties encoded in the thermal expectation values by summing over all possible $\ell!$ orderings of the operators (for variable τ_i without restrictions)

$$
\mathcal{G}(\boldsymbol{\tau}) = \sum_p \mathcal{K}(\boldsymbol{\tau}_p)\mathcal{S}[\boldsymbol{\mathcal{O}}_p](-\mathrm{i}\boldsymbol{\tau}_p),
$$

$$
\mathcal{K}(\boldsymbol{\tau}_p) = \prod_{i=1}^{\ell-1}\Big[-\theta(\tau_{\overline{i}} - \tau_{\overline{i+1}})\Big],
$$

$$
\mathcal{S}[\boldsymbol{\mathcal{O}}_p](-\mathrm{i}\boldsymbol{\tau}_p) = \zeta_p\Big\langle\mathcal{O}^{\overline{1}}(-\mathrm{i}\tau_{\overline{1}})\ldots\mathcal{O}^{\overline{\ell}}(-\mathrm{i}\tau_{\overline{\ell}})\Big\rangle. \quad\quad (2.32)
$$

Given a tuple $\boldsymbol{\tau}$, the so-called MF kernel $\mathcal{K}(\boldsymbol{\tau}_p)$, with $\boldsymbol{\tau}_p = (\tau_{\overline{1}}, \ldots, \tau_{\overline{\ell}})$ the permuted tuple, guarantees that only the time-ordered expectation value with $\tau_{\overline{1}} > \tau_{\overline{2}} > \cdots > \tau_{\overline{\ell}}$ survives the sum over all permutations p. The information about the operators and the physical system is solely encoded in the PSFs $\mathcal{S}[\boldsymbol{\mathcal{O}}_p](-\mathrm{i}\boldsymbol{\tau}_p)$ depending on imaginary times in the MF, with $\boldsymbol{\mathcal{O}}_p = (\mathcal{O}^{\overline{1}}, \ldots, \mathcal{O}^{\overline{\ell}})$ (see Sec. 2.3 for a detailed discussion).[9]

---

9 The term "spectral function" is mostly used for frequency-dependent objects, for instance, the Fourier transform of $\mathcal{S}[\boldsymbol{\mathcal{O}}_p](-\mathrm{i}\boldsymbol{\tau}_p)$ (or rather its real-time counterpart, see Sec. 2.3). For convenience, we refer to the imaginary- and real-time objects as partial spectral functions, too.

(a)

$$\mathcal{O}^{\overline{1}}(-\mathrm{i}\tau_{\overline{1}}) \quad \ldots \quad \mathcal{O}^{\overline{\ell}}(-\mathrm{i}\tau_{\overline{\ell}})$$

$$-\mathrm{i}\beta \qquad\qquad\qquad\qquad 0$$

$$\left\langle \mathcal{T}\left\{\mathcal{O}^{1}(-\mathrm{i}\tau_{1})\ldots\mathcal{O}^{\ell}(-\mathrm{i}\tau_{\ell})\right\}\right\rangle$$

(b)

$$\mathcal{O}^{\overline{\lambda+1}}(t_{\overline{\lambda+1}}^{-}) \quad \ldots \qquad \mathcal{O}^{\overline{\ell}}(t_{\overline{\ell}}^{-})$$

$$\infty \qquad\qquad\qquad\qquad\qquad -\infty$$

$$\mathcal{O}^{\overline{\lambda}}(t_{\overline{\lambda}}^{+}) \quad \ldots \quad \mathcal{O}^{\overline{1}}(t_{\overline{1}}^{+})$$

$$\left\langle \mathcal{T}_{\mathcal{C}}\left\{\mathcal{O}^{1}(t_{1}^{c_{1}})\ldots\mathcal{O}^{\lambda}(t_{\lambda}^{c_{\lambda}})\mathcal{O}^{\lambda+1}(t_{\lambda+1}^{c_{\lambda+1}})\ldots\mathcal{O}^{\ell}(t_{\ell}^{c_{\ell}})\right\}\right\rangle$$
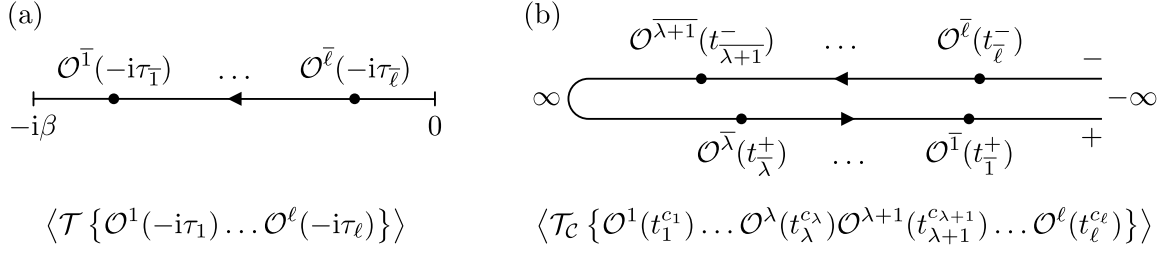
Figure 2.2 Contours considered for MF and KF correlators. (a) MF correlators are defined via time-ordered expectation values on the imaginary-time axis $\mathcal{C}_{\mathrm{M}} = (0, -\mathrm{i}\beta)$, with the times fulfilling $\tau_{\overline{1}} > \cdots > \tau_{\overline{\ell}}$. (b) KF correlators are defined as contour-ordered expectation values on the doubled real-time contour extending to $\pm\infty$. Operators on the backward $(+)$ branch are anti-time-ordered and placed to the right of the time-ordered operators on the forward $(-)$ branch. (Figure adapted from Refs. [KLvD21, P4].)

2.2.2 Keldysh formalism

The Keldysh formalism is formulated on the real-time forward $(\mathcal{C}_{-;t_{\mathrm{i}}})$ and backward $(\mathcal{C}_{+;t_{\mathrm{i}}})$ branch of $\mathcal{C}$, with the contour arguments in Eq. (2.29) given by $z_i = t_i^{c_i}$, $c_i = \pm$. It was introduced in Ref. [Kel65][10] to describe systems out of equilibrium, utilizing the adiabatic assumption: Assuming that the system was initially non-interacting, the interactions (as well as time-dependent perturbations driving the system out of equilibrium) are switched on adiabatically only at later times such that eigenstates of the non-interacting system evolve into eigenstates of the interacting system. This approach has the merit of formulating many-body perturbation theory on the real-time axis only, as the interaction is assumed to vanish on the vertical branch of the contour, i.e., $H(t_{\mathrm{i}}) \stackrel{\mathrm{adia.}}{=} H_0$ with H_0 the non-interacting Hamiltonian [SvL13].

In this section, we focus on real-time equilibrium correlation functions, i.e., time-independent Hamiltonians and operators, $H(t) = H$ and $\mathcal{O}(t) = \mathcal{O}$, consistent with the MF in the previous section. Since the adiabatic assumption was not utilized therein, we will not impose it for the real-time equilibrium correlators either. Then, for contour arguments $\boldsymbol{z} = \boldsymbol{t^c} = (t_1^{c_1}, \ldots, t_\ell^{c_\ell})$, Eq. (2.29) takes the form (for fixed contour indices and times fulfilling the conditions in Eq. (2.19))

$$\begin{aligned}
\mathcal{G}[\boldsymbol{\mathcal{O}}](\boldsymbol{t^c}) &= (-\mathrm{i})^{\ell-1}\frac{1}{Z}\mathrm{Tr}\Big[\mathcal{T}_{\mathcal{C}}\left\{e^{-\mathrm{i}\int_{\mathcal{C}}\mathrm{d}z'H(z')}\mathcal{O}^1(t_1^{c_1})\ldots\mathcal{O}^\ell(t_\ell^{c_\ell})\right\}\Big] \\
&= (-\mathrm{i})^{\ell-1}\frac{\zeta_p}{Z}\mathrm{Tr}\Big[U(t_{\mathrm{i}}-\mathrm{i}\beta, t_{\mathrm{i}})\,U(t_{\mathrm{i}}, t_{\overline{1}})\,\mathcal{O}^{\overline{1}}\ldots U(t_{\overline{\lambda-1}}, t_{\overline{\lambda}})\,\mathcal{O}^{\overline{\lambda}}\,U(t_{\overline{\lambda}}, t_{\overline{\lambda+1}}) \\
&\qquad\qquad\qquad \times\,\mathcal{O}^{\overline{\lambda+1}}\ldots U(t_{\overline{\ell-1}}, t_{\overline{\ell}})\,\mathcal{O}^{\overline{\ell}}\,U(t_{\overline{\ell}}, t_{\mathrm{i}})\Big] \\
&= (-\mathrm{i})^{\ell-1}\,\zeta_p\,\mathrm{Tr}\Big[\rho\,\mathcal{O}_H^{\overline{1}}(t_{\overline{1}})\ldots\mathcal{O}_H^{\overline{\lambda}}(t_{\overline{\lambda}})\,\mathcal{O}_H^{\overline{\lambda+1}}(t_{\overline{\lambda+1}})\ldots\mathcal{O}_H^{\overline{\ell}}(t_{\overline{\ell}})\Big] \\
&= (-\mathrm{i})^{\ell-1}\mathrm{Tr}\Big[\rho\,\mathcal{T}_{\mathcal{C}}\left\{\mathcal{O}_H^1(t_1^{c_1})\ldots\mathcal{O}_H^\ell(t_\ell^{c_\ell})\right\}\Big] \\
&= (-\mathrm{i})^{\ell-1}\left\langle\mathcal{T}_{\mathcal{C}}\left\{\mathcal{O}_H^1(t_1^{c_1})\ldots\mathcal{O}_H^\ell(t_\ell^{c_\ell})\right\}\right\rangle,
\end{aligned} \tag{2.33}$$

with $\mathcal{O}_H^i(t_i) = e^{\mathrm{i}Ht_i}\,\mathcal{O}^i\,e^{-\mathrm{i}Ht_i}$ the operator in the real-time Heisenberg picture. As in the MF, we will suppress the subscripts of the operators, $\mathcal{O}_H^i(t_i) \to \mathcal{O}^i(t_i) := e^{\mathrm{i}Ht_i}\,\mathcal{O}^i\,e^{-\mathrm{i}Ht_i}$.

---

10 For a discussion of previous works with similar contour ideas such as Ref. [Sch61], we refer the reader to Ref. [Kam23]. Further, we refer to general formalisms formulated on the doubled real-time contour as the KF; this nomenclature might differ throughout the literature [SvL13, Kam23].

Equation (2.33) serves as the definition of ℓp KF correlators in the so-called contour basis and, from now on, is denoted by the symbol

$$\mathcal{G}^{\boldsymbol{c}}(\boldsymbol{t}) = \mathcal{G}[\boldsymbol{\mathcal{O}}](\boldsymbol{t^c}) = (-\mathrm{i})^{\ell-1} \left\langle \mathcal{T}_\mathcal{C} \left\{ \mathcal{O}^1(t_1^{c_1}) \dots \mathcal{O}^\ell(t_\ell^{c_\ell}) \right\} \right\rangle. \tag{2.34}$$

Similarly to the MF, the explicit dependence of the real-time equilibrium correlators $\mathcal{G}^{\boldsymbol{c}}(\boldsymbol{t})$ on t_i is cancelled in Eq. (2.33); this is used to extend the domain of definition of $\mathcal{G}^{\boldsymbol{c}}(\boldsymbol{t})$ from $t_i \in [t_\mathrm{i}, \infty)$ to $t_i \in (-\infty, \infty)$ (see Fig. 2.2(b)) [P3].

The effect of the contour-ordering operation in Eq. (2.34) can be separated from the thermal expectation values by summing over all $\ell!$ orderings of the operators [KLvD21] (for variable contour indices and times without restrictions)

$$\mathcal{G}^{\boldsymbol{c}}(\boldsymbol{t}) = \sum_p \mathcal{K}^{\boldsymbol{c}_p}(\boldsymbol{t}_p) \mathcal{S}[\boldsymbol{\mathcal{O}}_p](\boldsymbol{t}_p),$$

$$\mathcal{S}[\boldsymbol{\mathcal{O}}_p](\boldsymbol{t}_p) = \zeta_p \left\langle \mathcal{O}^{\bar{1}}(t_{\bar{1}}) \dots \mathcal{O}^{\bar{\ell}}(t_{\bar{\ell}}) \right\rangle. \tag{2.35}$$

Importantly, it employs the same PSFs $\mathcal{S}[\boldsymbol{\mathcal{O}}_p](\boldsymbol{t}_p)$ as in the MF, but here depending on real times $\boldsymbol{t}_p = (t_{\bar{1}}, \dots, t_{\bar{\ell}})$.

An explicit expression for the kernel $\mathcal{K}^{\boldsymbol{c}_p}(\boldsymbol{t}_p)$ can be directly inferred from the definition of $\mathcal{T}_\mathcal{C}$ (2.19): Given a tuple of times with contour indices $\boldsymbol{t^c}$, it is nonzero only if the permuted tuple of contour indices is of the form $\boldsymbol{c}_p = c_{\bar{1}} \dots c_{\bar{\lambda}} c_{\overline{\lambda+1}} \dots c_{\bar{\ell}} = + \dots + - \dots - = [\lambda, \ell - \lambda]$, with the first entry in the square brackets comprising the λ times $t_{\bar{1}}, \dots, t_{\bar{\lambda}}$ anti-time-ordered $(t_{\bar{1}} < \dots < t_{\bar{\lambda}})$ on the backward $(+)$ branch, and the second entry denoting the $\ell - \lambda$ times $t_{\overline{\lambda+1}}, \dots, t_{\bar{\ell}}$ time-ordered $(t_{\overline{\lambda+1}} > \dots > t_{\bar{\ell}})$ on the forward $(-)$ branch. These requirements are exactly fulfilled by [KLvD21]

$$\mathcal{K}^{\boldsymbol{c}_p}(\boldsymbol{t}_p) = \mathcal{K}^{[\lambda, \ell-\lambda]}(\boldsymbol{t}_p) = (-\mathrm{i})^{\ell-1} \prod_{i=1}^{\lambda-1} \left[\theta(t_{\overline{i+1}} - t_{\bar{i}}) \right] \prod_{i=\lambda+1}^{\ell-1} \left[\theta(t_{\bar{i}} - t_{\overline{i+1}}) \right]. \tag{2.36}$$

Inserting a factor $1 = \theta(t_{\bar{\lambda}} - t_{\overline{\lambda+1}}) + \theta(t_{\overline{\lambda+1}} - t_{\bar{\lambda}})$, it can be expressed through so-called fully retarded kernels $\mathcal{K}^{[\lambda]}(\boldsymbol{t}_p)$, which are nonzero only if $t_{\bar{\lambda}} > t_{\bar{i}}$ for all $i \neq \lambda$ [KLvD21]:

$$\mathcal{K}^{[\lambda, \ell-\lambda]}(\boldsymbol{t}_p) = (-1)^{\lambda-1} \left(\mathcal{K}^{[\lambda]}(\boldsymbol{t}_p) - \mathcal{K}^{[\lambda+1]}(\boldsymbol{t}_p) \right),$$

$$\mathcal{K}^{[\lambda]}(\boldsymbol{t}_p) = \prod_{i=1}^{\lambda-1} \left[\mathrm{i}\,\theta(t_{\overline{i+1}} - t_{\bar{i}}) \right] \prod_{i=\lambda}^{\ell-1} \left[-\mathrm{i}\,\theta(t_{\bar{i}} - t_{\overline{i+1}}) \right]. \tag{2.37}$$

They will play the central role in our approach to the analytic continuation of ℓp correlators (see Sec. 5).

The KF, although being derived in the contour basis with indices $c_i = \pm$, is usually formulated in the so-called Keldysh basis by applying a linear transformation $D^{k_i c_i} = (-1)^{k_i \delta_{c_i,+}}$ to each c_i of $\mathcal{G}^{\boldsymbol{c}}$ (times a global conventional prefactor $\frac{1}{2}$) [P4], where $k_i \in \{1, 2\}$. It has the merit of automatically exploiting redundancy relations of the correlators in the contour basis (see Eq. (3.30) for an $\ell = 2$ example), and was already used in Ref. [Kel65]. Then, the KF correlators in the Keldysh basis, from now on usually referred to as *the* KF correlators, are expressed as [KLvD21]

$$\mathcal{G}^{\boldsymbol{k}}(\boldsymbol{t}) = \sum_p \mathcal{K}^{\boldsymbol{k}_p}(\boldsymbol{t}_p) \mathcal{S}[\boldsymbol{\mathcal{O}}_p](\boldsymbol{t}_p),$$

$$\mathcal{K}^{\boldsymbol{k}_p}(\boldsymbol{t}_p) = \sum_{\lambda=1}^{\ell} (-1)^{\lambda-1} (-1)^{k_{\overline{1}\dots\overline{\lambda-1}}} \frac{1+(-1)^{k_{\overline{\lambda}}}}{2} \mathcal{K}^{[\lambda]}(\boldsymbol{t}_p), \tag{2.38}$$

where $\boldsymbol{k} = k_1 \dots k_\ell$ are the external Keldsyh indices and $\boldsymbol{k}_p = k_{\overline{1}} \dots k_{\overline{\ell}}$ their permuted version. Note that our definition of the KF correlator in Eq. (2.38) differs by a factor $2^{1-\ell/2}$ from Ref. [KLvD21] to avoid a proliferation of these factors in Ch. 5.

2.3 Partial spectral functions

This section reproduces parts of Sec. 2.1 of [P4] *with minor modifications to put it into the context of this thesis and complements it with additional details of PSF properties in the frequency domain as well as a thorough discussion of properties in the time domain.*

In Eqs. (2.32), (2.35), and (2.38), the PSFs $\mathcal{S}[\boldsymbol{\mathcal{O}}_p]$ are identified as the basic building blocks of both the imaginary-time MF ($\mathcal{S}[\boldsymbol{\mathcal{O}}_p](-\mathrm{i}\boldsymbol{\tau}_p)$) and real-time KF ($\mathcal{S}[\boldsymbol{\mathcal{O}}_p](\boldsymbol{t}_p)$) correlators [KLvD21]. As shown below, they are, in fact, two different manifestations of the same analytic functions $\mathcal{S}[\boldsymbol{\mathcal{O}}_p](\boldsymbol{z}_p)$, with $z_{\overline{i}} = t_{\overline{i}} - \mathrm{i}\tau_{\overline{i}}$ being complex times [Eva92]. This observation lies at the heart of favoring the MF over the KF for computing correlators: The information about the physical system of interest is entirely encoded in the PSFs, and therefore both formalisms have to yield physically equivalent results for observables in thermal equilibrium; the information is only stored differently in the correlators due to the different imaginary- and real-time contours [KLvD21, P4]. However, to obtain physical observables from MF correlators, one has to revert to real times (or frequencies) by a suitable analytic continuation. This complication will be addressed in Ch. 5. Below, we derive various properties of the PSFs in the time and frequency domain following Refs. [Eva92, Roh13, KLvD21] and further introduce notation, results, and conventions of Refs. [KLvD21, P4].

2.3.1 Properties in the time domain

As introduced in the previous sections, and repeated here for clarity, the PSFs are defined as thermal expectation values of permuted tuples $\boldsymbol{\mathcal{O}}_p = (\mathcal{O}^{\overline{1}}, \dots, \mathcal{O}^{\overline{\ell}})$ at (for now) real times $\boldsymbol{t}_p = (t_{\overline{1}}, \dots, t_{\overline{\ell}})$, obeying Heisenberg time evolution $\mathcal{O}^i(t_i) = e^{\mathrm{i}Ht_i}\mathcal{O}^i e^{-\mathrm{i}Ht_i}$ for a given time-independent Hamiltonian H:

$$\mathcal{S}_p(\boldsymbol{t}_p) = \zeta_p \Big\langle \prod_{i=1}^{\ell} \mathcal{O}^{\overline{i}}(t_{\overline{i}}) \Big\rangle = \zeta_p \mathrm{Tr}\Big[\rho\, \mathcal{O}^{\overline{1}}(t_{\overline{1}}) \dots \mathcal{O}^{\overline{\ell}}(t_{\overline{\ell}})\Big]. \tag{2.39}$$

Here and in the following, we suppress the operator arguments $[\boldsymbol{\mathcal{O}}_p]$ for brevity, since the subscript on $\mathcal{S}_p$ specifies their order. Note that the following properties in the real-time domain are equally valid for complex times $\boldsymbol{t}_p \to -\mathrm{i}\boldsymbol{\tau}_p$.

In thermal equilibrium, the density matrix ρ and exponentials $e^{\pm\mathrm{i}Ht_i}$ arising from the Heisenberg time evolution commute, yielding[11]

$$\begin{aligned}
\mathcal{S}_p(\boldsymbol{t}_p) &= \mathcal{S}_p(t_{\overline{1}}, \dots, t_{\overline{\ell-1}}, t_{\overline{\ell}}) \\
&= \zeta_p \mathrm{Tr}\Big[\rho\, e^{\mathrm{i}Ht_{\overline{1}}}\mathcal{O}^{\overline{1}} e^{-\mathrm{i}Ht_{\overline{1}}} \dots e^{\mathrm{i}Ht_{\overline{\ell-1}}}\mathcal{O}^{\overline{\ell-1}} e^{-\mathrm{i}Ht_{\overline{\ell-1}}}\, e^{\mathrm{i}Ht_{\overline{\ell}}}\mathcal{O}^{\overline{\ell}} e^{-\mathrm{i}Ht_{\overline{\ell}}}\Big]
\end{aligned}$$

---

11 Generally, it holds that

$$\mathcal{S}_p(\boldsymbol{t}_p) = \mathcal{S}_p(t_{\overline{1}} - t_{\overline{i}}, \dots, t_{\overline{i-1}} - t_{\overline{i}}, 0, t_{\overline{i+1}} - t_{\overline{i}}, \dots, t_{\overline{\ell}} - t_{\overline{i}}) \qquad \forall i \in \{1, \dots, \ell\},$$

and setting $i = \ell$ is just a conventional choice. In the frequency domain, a notation unbiased toward the choice of i is introduced.

$$\begin{aligned}
&= \zeta_p \mathrm{Tr}\Big[\rho\, e^{\mathrm{i}H(t_{\overline{1}}-t_{\overline{\ell}})}\mathcal{O}^{\overline{1}}e^{-\mathrm{i}H(t_{\overline{1}}-t_{\overline{\ell}})}\dots e^{\mathrm{i}H(t_{\overline{\ell-1}}-t_{\overline{\ell}})}\mathcal{O}^{\overline{\ell-1}}e^{-\mathrm{i}H(t_{\overline{\ell-1}}-t_{\overline{\ell}})}\,\mathcal{O}^{\overline{\ell}}\Big] \\
&= \mathcal{S}_p(t_{\overline{1}}-t_{\overline{\ell}},\dots,t_{\overline{\ell-1}}-t_{\overline{\ell}},0).
\end{aligned} \tag{2.40}$$

Consequently, the PSFs are time-translational invariant.

PSFs whose arguments are cyclically related are not independent of each other. For two cyclically related permutations, say $p=(\overline{1}\dots\overline{\lambda-1}\,\overline{\lambda}\dots\overline{\ell})$ and $p_\lambda=(\overline{\lambda}\dots\overline{\ell}\,\overline{1}\dots\overline{\lambda-1})$, the cyclicity of the trace of operator products implies

$$\begin{aligned}
&\mathcal{S}_p(t_{\overline{1}},\dots,t_{\overline{\lambda-1}},t_{\overline{\lambda}},\dots,t_{\overline{\ell}}) \\
&= \frac{\zeta_p}{Z}\mathrm{Tr}\Big[e^{-\beta H}e^{\mathrm{i}Ht_{\overline{1}}}\mathcal{O}^{\overline{1}}e^{-\mathrm{i}Ht_{\overline{1}}}\dots e^{\mathrm{i}Ht_{\overline{\lambda-1}}}\mathcal{O}^{\overline{\lambda-1}}e^{-\mathrm{i}Ht_{\overline{\lambda-1}}}\,e^{\mathrm{i}Ht_{\overline{\lambda}}}\mathcal{O}^{\overline{\lambda}}e^{-\mathrm{i}Ht_{\overline{\lambda}}}\dots e^{\mathrm{i}Ht_{\overline{\ell}}}\mathcal{O}^{\overline{\ell}}e^{-\mathrm{i}Ht_{\overline{\ell}}}\Big] \\
&= \frac{\zeta_p}{Z}\mathrm{Tr}\Big[e^{-\beta H}e^{\mathrm{i}H(t_{\overline{\lambda}}-\mathrm{i}\beta)}\mathcal{O}^{\overline{\lambda}}e^{-\mathrm{i}H(t_{\overline{\lambda}}-\mathrm{i}\beta)}\dots e^{\mathrm{i}H(t_{\overline{\ell}}-\mathrm{i}\beta)}\mathcal{O}^{\overline{\ell}}e^{-\mathrm{i}H(t_{\overline{\ell}}-\mathrm{i}\beta)} \\
&\qquad\qquad \times\, e^{\mathrm{i}Ht_{\overline{1}}}\mathcal{O}^{\overline{1}}e^{-\mathrm{i}Ht_{\overline{1}}}\dots e^{\mathrm{i}Ht_{\overline{\lambda-1}}}\mathcal{O}^{\overline{\lambda-1}}e^{-\mathrm{i}Ht_{\overline{\lambda-1}}}\Big] \\
&= \zeta_p\zeta_{p_\lambda}\mathcal{S}_{p_\lambda}(t_{\overline{\lambda}}-\mathrm{i}\beta,\dots,t_{\overline{\ell}}-\mathrm{i}\beta,t_{\overline{1}},\dots,t_{\overline{\lambda-1}}) \\
&= \zeta_p\zeta_{p_\lambda}\mathcal{S}_{p_\lambda}(t_{\overline{\lambda}},\dots,t_{\overline{\ell}},t_{\overline{1}}+\mathrm{i}\beta,\dots,t_{\overline{\lambda-1}}+\mathrm{i}\beta).
\end{aligned} \tag{2.41}$$

Thus, PSFs with cyclically related arguments are connected by imaginary-time shifts $\pm\mathrm{i}\beta$.

Lehmann representations for PSFs can be obtained by inserting complete sets of eigenstates of the Hamiltonian, denoted by $\{|\underline{i}\rangle\}$ ($i\in\mathbb{N}_+$), with the eigenenergies given by $H|\underline{i}\rangle=E_{\underline{i}}|\underline{i}\rangle$ [KLvD21]. Then, Eq. (2.39) takes the form [Eva92]

$$\begin{aligned}
\mathcal{S}_p(\boldsymbol{t}_p) &= \zeta_p\sum_{\underline{1},\dots,\underline{\ell}}\rho_{\underline{1}}\,e^{\mathrm{i}E_{\underline{1}}t_{\overline{1}}}\,\mathcal{O}^{\overline{1}}_{\underline{1}\,\underline{2}}\,e^{-\mathrm{i}E_{\underline{2}}t_{\overline{1}}}\dots e^{\mathrm{i}E_{\underline{\ell-1}}t_{\overline{\ell-1}}}\,\mathcal{O}^{\overline{\ell-1}}_{\underline{\ell-1}\,\underline{\ell}}\,e^{-\mathrm{i}E_{\underline{\ell}}t_{\overline{\ell-1}}}\,e^{\mathrm{i}E_{\underline{\ell}}t_{\overline{\ell}}}\,\mathcal{O}^{\overline{\ell}}_{\underline{\ell}\,\underline{1}}\,e^{-\mathrm{i}E_{\underline{1}}t_{\overline{\ell}}} \\
&= \zeta_p\sum_{\underline{1},\dots,\underline{\ell}}\rho_{\underline{1}}\prod_{i=1}^{\ell}\Big[e^{\mathrm{i}E_{\underline{i+1}}(t_{\overline{i+1}}-t_{\overline{i}})}\mathcal{O}^{\overline{i}}_{\underline{i}\,\underline{i+1}}\Big],
\end{aligned} \tag{2.42}$$

where $t_{\overline{\ell+1}}=t_{\overline{1}}$, $E_{\underline{\ell+1}}=E_{\underline{1}}$, and $\mathcal{O}^{\overline{i}}_{\underline{\ell}\,\underline{\ell+1}}=\mathcal{O}^{\overline{i}}_{\underline{\ell}\,\underline{1}}$. The matrix elements of the density matrix and operators in the eigenbasis of the Hamiltonian are denoted by $\rho_{\underline{1}}=e^{-\beta E_{\underline{1}}}/Z$ and $\mathcal{O}^{\overline{i}}_{\underline{i}\,\underline{i+1}}=\langle\underline{i}|\mathcal{O}^{\overline{i}}|\underline{i+1}\rangle$, respectively.

As functions of complex times $t_{\overline{i}}\to t_{\overline{i}}-\mathrm{i}\tau_{\overline{i}}$, with $\tau_{\overline{i}}\in\mathbb{R}$ (for now), the PSFs in the Lehmann representation read [Eva92]

$$\mathcal{S}_p(\boldsymbol{t}_p-\mathrm{i}\boldsymbol{\tau}_p)=\frac{\zeta_p}{Z}\sum_{\underline{1},\dots,\underline{\ell}}e^{-E_{\underline{1}}(\beta-\tau_{\overline{1}}+\tau_{\overline{\ell}})}\left[\prod_{i=1}^{\ell-1}e^{-E_{\underline{i+1}}(\tau_{\overline{i}}-\tau_{\overline{i+1}})}\right]\left[\prod_{i=1}^{\ell}e^{\mathrm{i}E_{\underline{i+1}}(t_{\overline{i+1}}-t_{\overline{i}})}\mathcal{O}^{\overline{i}}_{\underline{i}\,\underline{i+1}}\right]. \tag{2.43}$$

Since the energy levels are bounded from below, but can become arbitrarily large for infinitely large systems [Roh13], the exponentials require

$$\beta-\tau_{\overline{1}}+\tau_{\overline{\ell}}\geq 0,\quad \tau_{\overline{i}}-\tau_{\overline{i+1}}\geq 0\quad\text{for }i<\ell\qquad\Leftrightarrow\qquad \beta+\tau_{\overline{\ell}}\geq\tau_{\overline{1}}\geq\tau_{\overline{2}}\geq\dots\geq\tau_{\overline{\ell}} \tag{2.44}$$

for the sums over energy eigenstates to converge [Eva92, Roh13]. Thus, the imaginary times $\tau_{\overline{i}}$ need to be restricted to a compact interval of length β on which they have to be time-ordered. Both conditions are met by the definition of MF correlators, where the imaginary times are restricted to the interval $\tau_{\overline{i}}\in[0,\beta]$, and the time-ordering is ensured by $\mathcal{K}(\boldsymbol{\tau}_p)$ in Eq. (2.32).

2.3.2 Properties in the frequency domain

The real-frequency Fourier transform of $\mathcal{S}_p(\boldsymbol{t}_p)$ is defined as

$$\mathcal{S}_p(\boldsymbol{\varepsilon}_p) = \int_{-\infty}^{\infty} \frac{\mathrm{d}^\ell t_p}{(2\pi)^\ell} \, e^{\mathrm{i}\boldsymbol{\varepsilon}_p \cdot \boldsymbol{t}_p} \mathcal{S}_p(\boldsymbol{t}_p). \tag{2.45}$$

Here, $\boldsymbol{\varepsilon}_p = (\varepsilon_{\bar{1}}, \ldots, \varepsilon_{\bar{\ell}})$ is a permuted version of $\boldsymbol{\varepsilon} = (\varepsilon_1, \ldots, \varepsilon_\ell)$, a tuple of continuous, real-frequency variables. We strictly associate each (integration) variable, such as t_i, ε_i, with the operator $\mathcal{O}^i$ carrying the same index. By using Eq. (2.40) and introducing new integration variables $t'_{\bar{j}} = t_{\bar{j}} - t_{\bar{\ell}}$ for $j \neq \ell$ and $t'_{\bar{\ell}} = t_{\bar{\ell}}$, the definition of the Fourier transform yields [KLvD21]

$$\begin{aligned}
\mathcal{S}_p(\boldsymbol{\varepsilon}_p) &= \int_{-\infty}^{\infty} \frac{\mathrm{d}^\ell t_p}{(2\pi)^\ell} \, e^{\mathrm{i}\boldsymbol{\varepsilon}_p \cdot \boldsymbol{t}_p} \mathcal{S}_p(t_{\bar{1}} - t_{\bar{\ell}}, \ldots, t_{\overline{\ell-1}} - t_{\bar{\ell}}, 0) \\
&= \int_{-\infty}^{\infty} \frac{\mathrm{d}t'_{\bar{\ell}}}{2\pi} e^{\mathrm{i}\varepsilon_{\bar{1}\ldots\bar{\ell}} t'_{\bar{\ell}}} \left[\prod_{j=1}^{\ell-1} \int_{-\infty}^{\infty} \frac{\mathrm{d}t'_{\bar{j}}}{(2\pi)^{\ell-1}} \, e^{\mathrm{i}\varepsilon_{\bar{j}} t'_{\bar{j}}} \right] S_p(t'_{\bar{1}}, \ldots, t'_{\overline{\ell-1}}, 0) \\
&= \delta(\varepsilon_{\bar{1}\ldots\bar{\ell}}) S_p(\boldsymbol{\varepsilon}_p), \tag{2.46}
\end{aligned}$$

i.e., time-translational invariance of $\mathcal{S}_p(\boldsymbol{t}_p)$ implies energy conservation for $\mathcal{S}_p(\boldsymbol{\varepsilon}_p)$ via the Dirac $\delta(\varepsilon_{\bar{1}\ldots\bar{\ell}})$. Here, $\varepsilon_{\bar{1}\ldots\bar{i}} = \varepsilon_{\bar{1}} + \cdots + \varepsilon_{\bar{i}}$ is a shorthand for a frequency sum. We call it bosonic/fermionic if the frequencies $(\varepsilon_{\bar{1}}, \ldots, \varepsilon_{\bar{i}})$ are associated with an even/odd number of fermionic operators, i.e., if the sign $\zeta^{\bar{1}\ldots\bar{i}} = \zeta^{\bar{1}}\ldots\zeta^{\bar{i}}$ equals ± 1 (with $\zeta^j = \pm 1$ for bosonic/fermionic operators $\mathcal{O}^j$). The function $\mathcal{S}_p$ (calligraphic type) on the left of Eq. (2.46) is nonzero only if its arguments satisfy "energy conservation", $\varepsilon_{\bar{1}\ldots\bar{\ell}} = 0$; for S_p (italic type) in the last line, displayed as a function of the complete tuple $\boldsymbol{\varepsilon}_p$, this condition on $\boldsymbol{\varepsilon}_p$ is understood to hold by definition, e.g., by setting $\varepsilon_{\bar{\ell}} = -\varepsilon_{\bar{1}\ldots\overline{\ell-1}}$. This convention for frequency arguments of functions typeset in calligraphics or italics also holds for the correlators, $\mathcal{G}$ vs. G, and kernels, $\mathcal{K}$ vs. K, defined in the following chapter.

The definition of the Fourier transform together with Eq. (2.41) yields the equilibrium condition [KLvD21][12]

$$S_p(\boldsymbol{\varepsilon}_p) = \zeta_p \zeta_{p_\lambda} e^{\beta \varepsilon_{\bar{1}\ldots\overline{\lambda-1}}} S_{p_\lambda}(\boldsymbol{\varepsilon}_{p_\lambda}), \quad \zeta_p \zeta_{p_\lambda} = \zeta^{\bar{1}\ldots\overline{\lambda-1}}. \tag{2.47}$$

Thus, PSFs with cyclically related arguments are proportional to each other in the frequency domain.

For the Lehmann representation in Eq. (2.42), the Fourier transform leads to [KLvD21]

$$S_p(\boldsymbol{\varepsilon}_p) = \zeta_p \sum_{\underline{1},\ldots,\underline{\ell}} \rho_{\underline{1}} \prod_{i=1}^{\ell-1} \left[\mathcal{O}^{\bar{i}}_{\underline{i}\,\underline{i+1}} \delta(\varepsilon_{\bar{1}\ldots\bar{i}} - E_{\underline{i+1}\,\underline{1}}) \right] \mathcal{O}^{\bar{\ell}}_{\underline{\ell}\,\underline{1}}, \tag{2.48}$$

where $E_{\underline{i}\,\underline{j}} = E_{\underline{i}} - E_{\underline{j}}$. As mentioned in the introduction, Ref. [LKvD21] extended the standard NRG to compute these PSFs even for $\ell = 3, 4$. In this method, a complete set of (approximate) eigenstates is constructed for, e.g., impurity models coupled to a (discretized) bath such as the Anderson impurity model (see, e.g., Ref. [BCP08] for a review of the NRG).

In general, we need not require the PSFs to be given by Eq. (2.48), which, in this form, assumes discrete energy levels. To include systems with continuous spectra in the ensuing analysis, it suffices to assume that $S_p(\boldsymbol{\varepsilon}_p)$ may contain sums over Dirac delta functions and a

---

12 In Ref. [KLvD21], it is called cyclicity relation.

part that is (piece-wise) continuous in its arguments. For future reference, we split it into *regular* and *anomalous* parts,[13]

$$S_p(\boldsymbol{\varepsilon}_p) = \tilde{S}_p(\boldsymbol{\varepsilon}_p) + \hat{S}_p(\boldsymbol{\varepsilon}_p), \tag{2.49}$$

where the anomalous part, $\hat{S}_p$, comprises all terms containing *bosonic* Dirac $\delta(\varepsilon_{\bar{1}...\bar{i}})$ factors (i.e., having bosonic $\varepsilon_{\bar{1}...\bar{i}}$ as arguments) setting $\varepsilon_{\bar{1}...\bar{i}} = 0$, while $\tilde{S}_p$ contains everything else (including fermionic Dirac deltas). We will see later that $\hat{S}_p$ gives rise to anomalous contributions to MF correlators, whereas $\tilde{S}_p$ does not (see, e.g., Sec. 3.1.4).

---

13 The nomenclature of "regular" and "anomalous" will be discussed in greater detail throughout Ch. 3.

3 Properties and spectral representations of MF and KF correlators

The interplay between the PSFs, discussed in the previous section, and the MF and KF kernels, given in Eqs. (2.32), (2.36), and (2.38), imply a rich variety of properties for the corresponding MF and KF correlators. They serve the purpose of simplifying the computation of correlators by, e.g., reducing the number of time/frequency arguments or identifying the independent Keldysh components in the real-time formalism, circumventing the need to calculate all 2^ℓ components separately. These properties are particularly important for numerical considerations, where limited computational resources are a crucial bottleneck. For a given Hamiltonian, further physical symmetries such as SU(2)-spin symmetry, particle-hole symmetry, or time-reversal symmetry (to name but a few) can tremendously reduce the computational cost. However, special symmetries of the underlying physical system will not be discussed here; for a detailed summary of their implications, we refer to the literature, e.g., Ref. [Roh13].

In the following, we will derive properties solely arising from the system being in thermal equilibrium. As many of these are common to correlators of an arbitrary number of operators, we will concentrate on the $\ell = 2$ case in Secs. 3.1 and 3.2 for the MF and KF, respectively. In Secs. 3.3 and 3.4 we further summarize key results of Ref. [KLvD21], where parts of the 2p results are generalized to arbitrary ℓ. At last, the self-energy and 4p vertex, defined via 2p and 4p single-particle correlators, are discussed in Sec. 3.5. Throughout all sections, we will introduce additional notation and nomenclature used in Refs. [KLvD21, P2, P4].

3.1 2p MF correlators

General MF correlators were defined in Eq. (2.32) in terms of MF kernels and PSFs. For $\ell = 2$, the permutations $p = (12), (21)$ then yield the 2p MF correlator

$$\mathcal{G}(\tau_1, \tau_2) = -\sum_p \theta(\tau_{\bar{1}} - \tau_{\bar{2}})\mathcal{S}_p(-i\tau_{\bar{1}}, -i\tau_{\bar{2}})$$
$$= -\theta(\tau_1 - \tau_2)\mathcal{S}_{(12)}(-i\tau_1, -i\tau_2) - \theta(\tau_2 - \tau_1)\mathcal{S}_{(21)}(-i\tau_2, -i\tau_1) \qquad (3.1)$$

with the PSFs

$$\mathcal{S}_{(12)}(-i\tau_1, -i\tau_2) = \left\langle \mathcal{O}^1(-i\tau_1)\mathcal{O}^2(-i\tau_2) \right\rangle, \qquad \mathcal{S}_{(21)}(-i\tau_2, -i\tau_1) = \zeta \left\langle \mathcal{O}^2(-i\tau_2)\mathcal{O}^1(-i\tau_1) \right\rangle. \qquad (3.2)$$

The sign factor ζ equals ± 1 if both operators are bosonic/fermionic. The following properties are a direct consequence of the identities for the PSFs discussed in Sec. 2.3 and the time-ordering due to the Heaviside functions.

3.1.1 Time-translational invariance

From the time-translational invariance of the PSFs (2.40), it follows that

$$\mathcal{S}_{(12)}(-i\tau_1, -i\tau_2) = \mathcal{S}_{(12)}\big(-i(\tau_1 - \tau_2), 0\big), \qquad \mathcal{S}_{(21)}(-i\tau_2, -i\tau_1) = \mathcal{S}_{(21)}\big(0, -i(\tau_1 - \tau_2)\big). \qquad (3.3)$$

Since the Heaviside functions in Eq. (3.1) only depend on the time difference $\tau = \tau_1 - \tau_2$, too, the correlator can be written in time-translational invariant form:

$$\mathcal{G}(\tau_1, \tau_2) = G(\tau_1 - \tau_2) = G(\tau), \qquad G(\tau) = -\theta(\tau)\mathcal{S}_{(12)}(-\mathrm{i}\tau, 0) - \theta(-\tau)\mathcal{S}_{(21)}(0, -\mathrm{i}\tau). \quad (3.4)$$

The roman (calligraphic) symbol G ($\mathcal{G}$) indicates that time-translational invariance is (not) explicitly imposed. Since the imaginary times take values in the interval $\tau_1, \tau_2 \in [0, \beta]$, τ is restricted to $\tau \in [-\beta, \beta]$.

3.1.2 (Anti)periodicity in imaginary time

From Eq. (2.41), it follows that the PSFs for permutations $p = (12), (21)$ are related by time shifts $\pm\beta$:

$$\mathcal{S}_{(12)}(-\mathrm{i}\tau_1, -\mathrm{i}\tau_2) = \zeta\, \mathcal{S}_{(21)}\big(-\mathrm{i}(\tau_2 + \beta), -\mathrm{i}\tau_1\big) = \zeta\, \mathcal{S}_{(21)}\big(-\mathrm{i}\tau_2, -\mathrm{i}(\tau_1 - \beta)\big). \quad (3.5)$$

Assuming, for instance, $\tau_1 > \tau_2$, the correlators then fulfill [Roh13]

$$\begin{aligned}
\mathcal{G}(\tau_1, \tau_2 < \tau_1) = -\mathcal{S}_{(12)}(-\mathrm{i}\tau_1, -\mathrm{i}\tau_2) &= -\zeta\, \mathcal{S}_{(21)}\big(-\mathrm{i}(\tau_2 + \beta), -\mathrm{i}\tau_1\big) = \zeta\, \mathcal{G}(\tau_1, \tau_2 + \beta) \\
&= -\zeta\, \mathcal{S}_{(21)}\big(-\mathrm{i}\tau_2, -\mathrm{i}(\tau_1 - \beta)\big) = \zeta\, \mathcal{G}(\tau_1 - \beta, \tau_2). \quad (3.6)
\end{aligned}$$

The last equalities in the first and second line follow from $\tau_2 + \beta > \tau_1$ and the time-ordering operator implicit in $\mathcal{G}$. Imposing time-translational invariance, it then follows that [BF04]

$$G(\tau) = \begin{cases} \zeta G(\tau - \beta) & \text{for } \tau > 0, \\ \zeta G(\tau + \beta) & \text{for } \tau < 0, \end{cases} \quad (3.7)$$

i.e., $G(\tau)$ is a (anti)periodic function in its argument with period β. The first case in Eq. (3.7) corresponds to the result in Eq. (3.6), the second case can be derived analogously for $\tau_1 < \tau_2$.

3.1.3 Fourier transformation

Here, we investigate the consequences of time-translation invariance and (anti)periodicity of the 2p MF correlator for its Fourier transform. To this end, we first consider $G(\tau)$ defined for $\tau \in [-\beta, \beta]$ on an interval of length $L = 2\beta$. It can be Fourier transformed by periodically extending its domain of definition to general $\tau \in \mathbb{R}$.[1]

For simplicity, the normalization factor $1/L$ inherent in the Fourier transformation is split into two parts: a factor $1/2$ for the τ-to-ω transformation, and a factor $1/\beta$ for the ω-to-τ transformation, where $\omega = 2\pi n/L$ with $n \in \mathbb{Z}$ is a discrete frequency. The Fourier transform, denoted by $G(\mathrm{i}\omega)$, then reads [BF04]

$$\begin{aligned}
G(\mathrm{i}\omega) &= \frac{1}{2}\int_{-\beta}^{\beta} \mathrm{d}\tau\, e^{\mathrm{i}\omega\tau} G(\tau) \\
&= \frac{1}{2}\int_{0}^{\beta} \mathrm{d}\tau\, e^{\frac{\pi\mathrm{i}n}{\beta}\tau} G(\tau) + \frac{1}{2}\int_{-\beta}^{0} \mathrm{d}\tau\, e^{\frac{\pi\mathrm{i}n}{\beta}\tau} G(\tau) \\
&= \frac{1}{2}\int_{0}^{\beta} \mathrm{d}\tau\, e^{\frac{\pi\mathrm{i}n}{\beta}\tau} G(\tau) + \frac{1}{2}\int_{0}^{\beta} \mathrm{d}\tau\, e^{\frac{\pi\mathrm{i}n}{\beta}(\tau-\beta)} G(\tau - \beta)
\end{aligned}$$

---

[1] To be precise, we should use the term "Fourier series" rather than "Fourier transformation" for functions defined on a finite interval. However, we still refer to it as a Fourier transformation for later convenience.

$$= \frac{1 + \zeta e^{-\pi \mathrm{i} n}}{2} \int_0^\beta \mathrm{d}\tau \, e^{\frac{\pi \mathrm{i} n}{\beta} \tau} G(\tau). \tag{3.8}$$

In the third step, we substituted $\tau \to \tau - \beta$ in the second integral, and we inserted Eq. (3.7) in the last step. Thus, the Fourier transform vanishes for $\zeta = +1$ ($\zeta = -1$) if n is odd (even). This motivates the definition of the Fourier transformation in terms of bosonic and fermionic Matsubara frequencies $\mathrm{i}\omega$ [BF04]:

$$G(\mathrm{i}\omega) = \int_0^\beta \mathrm{d}\tau e^{\mathrm{i}\omega\tau} G(\tau), \qquad G(\tau) = \frac{1}{\beta} \sum_{\mathrm{i}\omega} e^{-\mathrm{i}\omega\tau} G(\mathrm{i}\omega),$$

$$\mathrm{i}\omega = \begin{cases} 2n\pi \mathrm{i}/\beta & \text{for bosons } (\zeta = +1), \\ (2n+1)\pi \mathrm{i}/\beta & \text{for fermions } (\zeta = -1). \end{cases} \tag{3.9}$$

Here, $\sum_{\mathrm{i}\omega}$, which is symbolic for $\sum_{n \in \mathbb{Z}}$, sums over all possible Matsubara frequencies. Throughout this thesis, we display Matsubara frequencies $\mathrm{i}\omega$ with the imaginary unit to avoid confusion when discussing real, continuous frequencies denoted by ω without the imaginary unit.

For a straightforward generalization to arbitrary ℓp correlators, it is convenient to address the Fourier transform of $\mathcal{G}(\tau_1, \tau_2)$ as well. It is defined as separately Fourier transforming w.r.t. τ_1 and τ_2, introducing two Matsubara frequencies $\mathrm{i}\omega_1$ and $\mathrm{i}\omega_2$. They are both either fermionic or bosonic, depending on the fermionic or bosonic nature of $\mathcal{O}^1$ and $\mathcal{O}^2$. The Fourier transform is then reads [Roh13, KLvD21]

$$\mathcal{G}(\mathrm{i}\omega_1, \mathrm{i}\omega_2) = \int_0^\beta \mathrm{d}\tau_1 \mathrm{d}\tau_2 \, e^{\mathrm{i}\omega_1\tau_1 + \mathrm{i}\omega_2\tau_2} \mathcal{G}(\tau_1, \tau_2) = \int_0^\beta \mathrm{d}\tau_1 \mathrm{d}\tau_2 \, e^{\mathrm{i}\omega_1\tau_1 + \mathrm{i}\omega_2\tau_2} G(\tau_1 - \tau_2)$$

$$= \int_0^\beta \mathrm{d}\tau_2 \, e^{\mathrm{i}\omega_{12}\tau_2} \int_{-\tau_2}^{\beta - \tau_2} \mathrm{d}\tau \, e^{\mathrm{i}\omega_1\tau} G(\tau), \tag{3.10}$$

where we substituted $\tau = \tau_1 - \tau_2$ in the last step. The integrand $e^{\mathrm{i}\omega_1\tau} G(\tau)$ can be identified as a β-periodic function due to Eq. (3.7) and $e^{\pm \mathrm{i}\omega_1 \beta} = \zeta$. Thus, the result of the τ integral remains unchanged when integrating between $0 < \tau < \beta$,[2] and Eq. (3.10) evaluates to

$$\mathcal{G}(\mathrm{i}\omega_1, \mathrm{i}\omega_2) = \int_0^\beta \mathrm{d}\tau_2 \, e^{\mathrm{i}\omega_{12}\tau_2} \int_0^\beta \mathrm{d}\tau \, e^{\mathrm{i}\omega_1\tau} G(\tau) = \int_0^\beta \mathrm{d}\tau_2 \, e^{\mathrm{i}\omega_{12}\tau_2} G(\mathrm{i}\omega_1)$$

$$= \beta \delta_{\mathrm{i}\omega_{12}} G(\mathrm{i}\omega_1). \tag{3.11}$$

Consequently, time-translational invariance implies energy conservation due to the factor $\delta_{\mathrm{i}\omega_{12}}$, the Kronecker symbol for Matsubara frequencies ($\delta_{\mathrm{i}\omega_i = 0} = 1$, $\delta_{\mathrm{i}\omega_i \neq 0} = 0$). In the following, $G(\mathrm{i}\omega_1)$ will usually be displayed as a function of the complete tuple $\mathrm{i}\boldsymbol{\omega} = (\mathrm{i}\omega_1, \mathrm{i}\omega_2)$, $G(\mathrm{i}\omega_1) \to G(\mathrm{i}\boldsymbol{\omega})$, with the condition $\mathrm{i}\omega_{12} = 0$ understood for its arguments.

---

2 We can also show this explicitly by computing

$$\int_{-\tau_2}^{\beta - \tau_2} \mathrm{d}\tau \, e^{\mathrm{i}\omega_1\tau} G(\tau) = \int_{-\tau_2}^0 \mathrm{d}\tau \, e^{\mathrm{i}\omega_1\tau} G(\tau) + \int_0^{\beta - \tau_2} \mathrm{d}\tau \, e^{\mathrm{i}\omega_1\tau} G(\tau)$$

$$= \int_{\beta - \tau_2}^\beta \mathrm{d}\tau \, e^{\mathrm{i}\omega_1\tau} e^{-\mathrm{i}\omega_1\beta} G(\tau - \beta) + \int_0^{\beta - \tau_2} \mathrm{d}\tau \, e^{\mathrm{i}\omega_1\tau} G(\tau) = \int_0^\beta \mathrm{d}\tau \, e^{\mathrm{i}\omega_1\tau} G(\tau),$$

where we substituted $\tau \to \tau - \beta$ in the first integral and used $e^{-\mathrm{i}\omega_1\beta} G(\tau - \beta) = \zeta G(\tau - \beta) = G(\tau)$ in the last step.

3.1.4 Spectral representation

Equation (3.1) expresses the correlator in imaginary time as a sum over products of PSFs and MF kernels. In the frequency domain, the Fourier transform $G(i\boldsymbol{\omega})$ is then computed via convolutions of the Fourier transforms of the PSFs and MF kernels, as shown in Ref. [KLvD21] and repeated in the following.

Inserting Eq. (3.1) into the definition of the Fourier transform (3.10), it follows that

$$
\begin{aligned}
\beta \delta_{i\omega_{12}} G(i\boldsymbol{\omega}) &= \int_0^\beta d\tau_1 d\tau_2 \, e^{i\omega_1 \tau_1 + i\omega_2 \tau_2} \, \mathcal{G}(\tau_1, \tau_2) \\
&= \sum_p \int_0^\beta d\tau_{\bar{1}} \, d\tau_{\bar{2}} \, e^{i\omega_{\bar{1}} \tau_{\bar{1}} + i\omega_{\bar{2}} \tau_{\bar{2}}} \, \mathcal{K}(\boldsymbol{\tau}_p) \, \mathcal{S}_p(-i\tau_{\bar{1}}, -i\tau_{\bar{2}}) \\
&= \sum_p \int d^2\varepsilon_p \, \delta(\varepsilon_{\overline{12}}) \, \mathcal{K}(i\boldsymbol{\omega}_p - \boldsymbol{\varepsilon}_p) \, S_p(\boldsymbol{\varepsilon}_p),
\end{aligned}
\tag{3.12}
$$

with $\int d^2\varepsilon_p = \int_{-\infty}^\infty d\varepsilon_{\bar{1}} d\varepsilon_{\bar{2}}$. In the last step, $\mathcal{S}_p(-i\tau_{\bar{1}}, -i\tau_{\bar{2}})$ was replaced by the real-time Fourier transform of the PSFs with analytically continued times $t_{\bar{i}} \to -i\tau_{\bar{i}}$ [KLvD21],

$$
\mathcal{S}_p(-i\tau_{\bar{1}}, -i\tau_{\bar{2}}) = \int d^2\varepsilon_p \, e^{-\varepsilon_{\bar{1}} \tau_{\bar{1}} - \varepsilon_{\bar{2}} \tau_{\bar{2}}} \, \mathcal{S}_p(\boldsymbol{\varepsilon}_p),
\tag{3.13}
$$

with $\mathcal{S}_p(\boldsymbol{\varepsilon}_p) = \delta(\varepsilon_{\overline{12}}) S_p(\boldsymbol{\varepsilon}_p)$ (see Eq. (2.46)). Abbreviating $\Omega_{\bar{i}} = i\omega_{\bar{i}} - \varepsilon_{\bar{i}}$, the Fourier transform of the MF kernel $\mathcal{K}(\boldsymbol{\tau}_p)$ is defined as [KLvD21]

$$
\mathcal{K}(\boldsymbol{\Omega}_p) = -\int_0^\beta d\tau_{\bar{1}} d\tau_{\bar{2}} \, e^{\Omega_{\bar{1}} \tau_{\bar{1}} + \Omega_{\bar{2}} \tau_{\bar{2}}} \, \theta(\tau_{\bar{1}} - \tau_{\bar{2}}) = \beta \delta_{\Omega_{\overline{12}}} K(\boldsymbol{\Omega}_p) + \mathcal{R}(\boldsymbol{\Omega}_p).
\tag{3.14}
$$

It is split into two contributions: the energy-conservation factor $\beta \delta_{\Omega_{\overline{12}}} = \beta \delta_{i\omega_{12}}$ (due to $\varepsilon_{\overline{12}} = 0$ and $i\omega_{\overline{12}} = i\omega_{12}$) multiplying a primary part $K(\boldsymbol{\Omega}_p)$, with $\Omega_{\overline{12}} = 0$ understood for its arguments, and a residual part $\mathcal{R}(\boldsymbol{\Omega}_p)$, with its arguments not restricted to $\Omega_{\overline{12}} = 0$ [P4]. Since the l.h.s. of Eq. (3.12) is proportional to $\beta \delta_{i\omega_{12}}$, the residual part $\mathcal{R}(\boldsymbol{\Omega}_p)$ cannot contribute to $G(i\boldsymbol{\omega})$ and is therefore neglected in the ensuing analysis; this is proven explicitly in App. A.2.

For the evaluation of the $\tau_{\bar{i}}$ integrals in Eq. (3.14), the cases of vanishing frequencies, $\Omega_{\bar{i}} = 0$, and non-vanishing frequencies, $\Omega_{\bar{i}} \neq 0$, have to be considered separately. The former is included via a Kronecker-like symbol $\delta_{\Omega_{\bar{i}}}$ (see discussion after Eq. (3.16)), the latter via [P2]

$$
\Delta_{\Omega_i} = \begin{cases} 0 & \text{for } \Omega_i = 0, \\ \frac{1}{\Omega_i} & \text{for } \Omega_i \neq 0. \end{cases}
\tag{3.15}
$$

Then, the primary part of the MF kernel is evaluated to (see Refs. [KLvD21, P2] and App. A.1)

$$
K(\boldsymbol{\Omega}_p) = \Delta_{\Omega_{\bar{1}}} - \frac{\beta}{2} \delta_{\Omega_{\bar{1}}},
\tag{3.16}
$$

and is usually referred to as simply *the* MF kernel (in the frequency domain).

Now the following question might arise: Under what circumstances is the distinction between $\Delta_{\Omega_{\bar{1}}}$ and $\delta_{\Omega_{\bar{1}}}$ even necessary? The latter $\delta_{\Omega_{\bar{1}}}$ is nonzero only if $\Omega_{\bar{1}} = 0$, which can hold only if both $i\omega_{\bar{1}} = 0$ and $\varepsilon_{\bar{1}} = 0$ separately, symbolically represented by $\delta_{\Omega_{\bar{1}}} = \delta_{i\omega_{\bar{1}}} \delta_{\varepsilon_{\bar{1}}}$.

For the first condition to be fulfilled, $i\omega_{\bar{1}}$ has to be bosonic, with $\delta_{i\omega_{\bar{1}}}$ being a true Kronecker symbol for Matsubara frequencies. For the second requirement to be met, it is noted that the point $\varepsilon_{\bar{i}} = 0$ has a finite contribution to the integral only if the PSFs contain terms proportional to a Dirac $\delta(\varepsilon_{\bar{i}})$, with $\varepsilon_{\bar{i}}$ a bosonic frequency [P4]. It is thus convenient to split the PSFs into an anomalous part $\hat{S}_p(\boldsymbol{\varepsilon}_p)$, containing factors of bosonic Dirac $\delta(\varepsilon_{\bar{1}})$, and a regular part $\tilde{S}_p(\boldsymbol{\varepsilon}_p)$ comprising all other contributions (see Eq. (2.49) and App. C.2 for a more general discussion of this point):

$$S_p(\boldsymbol{\varepsilon}_p) = \tilde{S}_p(\boldsymbol{\varepsilon}_p) + \hat{S}_p(\boldsymbol{\varepsilon}_p) = \tilde{S}_p(\boldsymbol{\varepsilon}_p) + \delta(\varepsilon_{\bar{1}})\check{S}_p. \tag{3.17}$$

Here, $\check{S}_p$ is a frequency-independent constant and can be nonzero only for $\zeta = +1$, i.e., bosonic $\varepsilon_{\bar{1}}$.[3] Then, the Kronecker-like $\delta_{\varepsilon_{\bar{1}}}$ with a continuous-frequency subscript is defined to extract all terms in the PSFs proportional to the bosonic $\delta(\varepsilon_{\bar{1}})$ [P4]:

$$\delta_{\varepsilon_{\bar{1}}} S_p(\boldsymbol{\varepsilon}_p) = \delta(\varepsilon_{\bar{1}})\check{S}_p. \tag{3.18}$$

Further, the equilibrium condition (2.47) relates the various PSF constituents for permutations $p = (12), (21)$:

$$S_{(12)}(\boldsymbol{\varepsilon}_{(12)}) = \zeta e^{\beta\varepsilon_1} S_{(21)}(\boldsymbol{\varepsilon}_{(21)}),$$
$$\Downarrow$$
$$\tilde{S}_{(12)}(\boldsymbol{\varepsilon}_{(12)}) + \delta(\varepsilon_1)\check{S}_{(12)} = \zeta e^{\beta\varepsilon_1} \tilde{S}_{(21)}(\boldsymbol{\varepsilon}_{(21)}) + \delta(\varepsilon_2)\check{S}_{(21)},$$
$$\Downarrow$$
$$\tilde{S}_{(12)}(\boldsymbol{\varepsilon}_{(12)}) = \zeta e^{\beta\varepsilon_1} \tilde{S}_{(21)}(\boldsymbol{\varepsilon}_{(21)}), \qquad \check{S}_{(12)} = \check{S}_{(21)}. \tag{3.19}$$

The last equality follows from $\delta(\varepsilon_1) = \delta(\varepsilon_2)$ due to $\varepsilon_2 = -\varepsilon_1$. Finally, the 2p MF correlator is obtained by inserting Eqs. (3.14)–(3.19) into Eq. (3.12):

$$\begin{aligned}
G(i\boldsymbol{\omega}) &= \sum_p \int d^2\varepsilon_p \, \delta(\varepsilon_{\overline{12}}) \, K(i\boldsymbol{\omega}_p - \boldsymbol{\varepsilon}_p) \, S_p(\boldsymbol{\varepsilon}_p) \\
&= \int d^2\varepsilon \, \delta(\varepsilon_{12}) \frac{\tilde{S}_{(12)}(\boldsymbol{\varepsilon}_{(12)})}{i\omega_1 - \varepsilon_1} + \left[\Delta_{i\omega_1} - \frac{\beta}{2}\delta_{i\omega_1}\right]\check{S}_{(12)} \\
&\quad + \int d^2\varepsilon \, \delta(\varepsilon_{12}) \frac{\tilde{S}_{(21)}(\boldsymbol{\varepsilon}_{(21)})}{i\omega_2 - \varepsilon_2} + \left[\Delta_{i\omega_2} - \frac{\beta}{2}\delta_{i\omega_2}\right]\check{S}_{(21)} \\
&= \int d^2\varepsilon \, \delta(\varepsilon_{12}) \frac{\tilde{S}_{(12)}(\boldsymbol{\varepsilon}_{(12)}) - \tilde{S}_{(21)}(\boldsymbol{\varepsilon}_{(21)})}{i\omega_1 - \varepsilon_1} - \beta\delta_{i\omega_1}\check{S}_{(12)}. \tag{3.20}
\end{aligned}$$

In the second step, $\varepsilon_2 = -\varepsilon_1$ and $i\omega_2 = -i\omega_1$ were used together with $\Delta_{-i\omega_1} = -\Delta_{i\omega_1}$ and $\delta_{-i\omega_1} = \delta_{i\omega_1}$. Since the regular $\tilde{S}_p(\boldsymbol{\varepsilon}_p)$ do not contain bosonic $\delta(\varepsilon_{\bar{1}})$ by definition, we inserted $\Delta_{i\omega_{\bar{1}}-\varepsilon_{\bar{1}}} = \frac{1}{i\omega_{\bar{1}}-\varepsilon_{\bar{1}}}$ in the kernel multiplying them; however, for $i\omega_{\bar{1}} = 0$, the real-frequency integrals should be understood as principal-value integrals.

The clear separation between regular and anomalous PSF contributions in Eq. (3.20) motivates an equivalent decomposition of the correlator into a regular part ($\tilde{G}$) and an

---

3 Here, we did not use the notation for the frequency-independent constant of [P4], given by $\check{S}_{p;\bar{1}}$ therein. It is only necessary for a unified discussion of PSFs for arbitrary ℓ (see App. C.2), which is beyond the scope of this section.

anomalous part ($\hat{G}$) via the definitions [KLvD21, P4]

$$G(\mathrm{i}\boldsymbol{\omega}) = \tilde{G}(\mathrm{i}\boldsymbol{\omega}) + \beta \delta_{\mathrm{i}\omega_1} \hat{G}_1, \quad \tilde{G}(\mathrm{i}\boldsymbol{\omega}) = \int \mathrm{d}^2\varepsilon\, \delta(\varepsilon_{12}) \frac{S_{\mathrm{std}}(\boldsymbol{\varepsilon})}{\mathrm{i}\omega_1 - \varepsilon_1}, \quad \hat{G}_1 = -\check{S}_{(12)}. \qquad (3.21)$$

Here, the "standard" spectral function is given by a PSF commutator [KLvD21, P4],

$$\begin{aligned} S_{\mathrm{std}}(\boldsymbol{\varepsilon}) = S_{[1,2]_-}(\boldsymbol{\varepsilon}) &= S_{(12)}(\boldsymbol{\varepsilon}_{(12)}) - S_{(21)}(\boldsymbol{\varepsilon}_{(21)}) \\ &= \left(1 - \zeta e^{-\beta\varepsilon_1}\right) \tilde{S}_{(12)}(\boldsymbol{\varepsilon}_{(12)}) = \left(\zeta e^{\beta\varepsilon_1} - 1\right) \tilde{S}_{(21)}(\boldsymbol{\varepsilon}_{(21)}). \end{aligned} \qquad (3.22)$$

It takes unpermuted frequencies $\boldsymbol{\varepsilon}$ fulfilling $\varepsilon_{12} = 0$ as its arguments; only for individual PSFs, the arguments occur in permuted order. In Eq. (3.22), the anomalous contributions, present only for $\zeta = +1$ and proportional to $\delta(\varepsilon_1)$, cancel, since $\delta(\varepsilon_1)(e^{\pm\beta\varepsilon_1} - 1) = 0$ in this case.

At this point, it is worth mentioning that $\tilde{G}$ can be expressed as the convolution of the PSFs and the so-called regular kernel $\tilde{K}$ [KLvD21, P4]:

$$\tilde{G}(\mathrm{i}\boldsymbol{\omega}) = \sum_p \int \mathrm{d}^2\varepsilon_p\, \delta(\varepsilon_{\overline{12}}) \tilde{K}(\mathrm{i}\boldsymbol{\omega}_p - \boldsymbol{\varepsilon}_p) S_p(\boldsymbol{\varepsilon}_p) = \int \mathrm{d}^2\varepsilon\, \delta(\varepsilon_{12}) \frac{S_{\mathrm{std}}(\boldsymbol{\varepsilon})}{\mathrm{i}\omega_1 - \varepsilon_1},$$

$$\tilde{K}(\mathrm{i}\boldsymbol{\omega}_p - \boldsymbol{\varepsilon}_p) = \frac{1}{\mathrm{i}\omega_{\overline{1}} - \varepsilon_{\overline{1}}}. \qquad (3.23)$$

The second equality in the first line follows similarly to Eq. (3.20) without the $\delta_{\mathrm{i}\omega_{\overline{1}}}$ contribution. $\tilde{K}$ and its generalization to general ℓ (see Eq. (3.62)) will play a central role for the analytic continuation of correlators, see Sec. 3.2.2 for $\ell = 2$.

The separation of the anomalous from the full PSFs in Eq. (3.17) seems to be just a mathematical trick for the evaluation of the convolution in Eq. (3.20). However, one might ask whether relevant information about the physical system is encoded in the anomalous part. To answer this question, we start with the Lehmann representation (2.48) of the full PSFs for $\ell = 2$:

$$S_p(\boldsymbol{\varepsilon}_p) = \zeta_p \sum_{\underline{1},\underline{2}} \rho_{\underline{1}} \mathcal{O}^{\overline{1}}_{\underline{1}\,\underline{2}} \delta(\varepsilon_{\overline{1}} - E_{\underline{2}\,\underline{1}}) \mathcal{O}^{\overline{2}}_{\underline{2}\,\underline{1}}. \qquad (3.24)$$

From this expression, we seek all contributions proportional to $\delta(\varepsilon_{\overline{1}})$, which requires $E_{\underline{2}\,\underline{1}} = 0$. Thus, the Lehmann representation for the coefficients $\check{S}_{(12)} = \check{S}_{(21)}$ reads [KS69, Shv06, WFHT22]:

$$\check{S}_{(12)} = \sum_{\substack{\underline{1},\underline{2} \\ E_{\underline{1}} = E_{\underline{2}}}} \rho_{\underline{1}} \mathcal{O}^1_{\underline{1}\,\underline{2}} \mathcal{O}^2_{\underline{2}\,\underline{1}}. \qquad (3.25)$$

The anomalous terms are nonzero only for degenerate energy levels, $E_{\underline{1}} = E_{\underline{2}}$ for $|\underline{1}\rangle \neq |\underline{2}\rangle$), or one of the operators being conserved, $[\mathcal{O}^i, H] = 0$, such that there exists a basis in which both $\mathcal{O}^i$ and H are diagonal, $\mathcal{O}^i_{\underline{1}\,\underline{2}} = \mathcal{O}^i_{\underline{1}\,\underline{1}} \delta_{\underline{1},\underline{2}}$, enforcing $E_{\underline{1}} = E_{\underline{2}}$ due to $|\underline{1}\rangle = |\underline{2}\rangle$ [P2, WFHT22]. Thus, the presence of a finite anomalous term in the 2p MF correlator (3.21) might help to gain a deeper physical insight into, e.g., the energy spectrum of the physical system under consideration [WFHT22]. This point will be further discussed at the end of Sec. 3.2.3.

3.2 2p KF correlators

The general KF correlators in the contour and Keldysh basis were defined in Eqs. (2.35) and (2.38), respectively. For $\ell = 2$, they are given by

$$\mathcal{G}^{\boldsymbol{c}/\boldsymbol{k}}(\boldsymbol{t}) = \mathcal{K}^{c_1 c_2 / k_1 k_2}(\boldsymbol{t}_{(12)}) \mathcal{S}_{(12)}(\boldsymbol{t}_{(12)}) + \mathcal{K}^{c_2 c_1 / k_2 k_1}(\boldsymbol{t}_{(21)}) \mathcal{S}_{(21)}(\boldsymbol{t}_{(21)}), \tag{3.26}$$

with the real-time PSFs

$$\mathcal{S}_{(12)}(t_1, t_2) = \left\langle \mathcal{O}^1(t_1) \mathcal{O}^2(t_2) \right\rangle, \qquad \mathcal{S}_{(21)}(t_2, t_1) = \zeta \left\langle \mathcal{O}^2(t_2) \mathcal{O}^1(t_1) \right\rangle. \tag{3.27}$$

As in the MF, the PSFs and KF kernels only depend on the time difference $t = t_1 - t_2$; accordingly, all components of the correlators in either basis are time-translational invariant:

$$\mathcal{G}^{\boldsymbol{c}/\boldsymbol{k}}(t_1, t_2) = G^{\boldsymbol{c}/\boldsymbol{k}}(t_1 - t_2) = G^{\boldsymbol{c}/\boldsymbol{k}}(t). \tag{3.28}$$

Again, the roman (calligraphic) symbol G ($\mathcal{G}$) indicates that time-translational invariance is (not) explicitly imposed.

In Sec. 2.2, we already mentioned that the PSFs are the basic building blocks of both MF and KF correlators, without directly discussing the consequences of this statement. Starting from Eq. (3.26), we therefore address two questions in the ensuing sections:

1. How are the various KF correlators related, in particular in the Keldysh basis?

2. Given an imaginary-frequency MF correlator $G(i\boldsymbol{\omega}) = \tilde{G}(i\boldsymbol{\omega}) + \beta \delta_{i\omega_1} \hat{G}_1$, how can the corresponding real-frequency correlators be obtained by a suitable analytic continuation?

Of course, the answers in the absence of anomalous terms are standard textbook knowledge for $\ell = 2$ [NO98, AS10, Kam23]; their presence, on the other hand, is acknowledged only in few works, for instance [ST65, KS69, WFHT22]. They are addressed in detail in the following, as part of the insights can be generalized to arbitrary ℓ.

3.2.1 Correlators in contour and Keldysh basis

In order to tackle the two questions, explicit expressions for the real-time correlators are needed. Despite working mostly in the Keldysh basis, it is instructive to first investigate the 2p correlators in the contour basis:[4]

$$\begin{aligned}
\mathcal{G}^{+-}(\boldsymbol{t}) &= \mathcal{G}^{>}(\boldsymbol{t}) = -\mathrm{i}\, \mathcal{S}_{(12)}(t_1, t_2), \\
\mathcal{G}^{-+}(\boldsymbol{t}) &= \mathcal{G}^{<}(\boldsymbol{t}) = -\mathrm{i}\, \mathcal{S}_{(21)}(t_2, t_1), \\
\mathcal{G}^{--}(\boldsymbol{t}) &= \mathcal{G}^{\mathcal{T}}(\boldsymbol{t}) = -\mathrm{i} \left[\theta(t_1 - t_2) \mathcal{S}_{(12)}(t_1, t_2) + \theta(t_2 - t_1) \mathcal{S}_{(21)}(t_2, t_1) \right] \\
&= -\mathrm{i} \left\langle \mathcal{T}\left\{ \mathcal{O}^1(t_1) \mathcal{O}^2(t_2) \right\} \right\rangle, \\
\mathcal{G}^{++}(\boldsymbol{t}) &= \mathcal{G}^{\overline{\mathcal{T}}}(\boldsymbol{t}) = -\mathrm{i} \left[\theta(t_2 - t_1) \mathcal{S}_{(12)}(t_1, t_2) + \theta(t_1 - t_2) \mathcal{S}_{(21)}(t_2, t_1) \right] \\
&= -\mathrm{i} \left\langle \overline{\mathcal{T}}\left\{ \mathcal{O}^1(t_1) \mathcal{O}^2(t_2) \right\} \right\rangle. \tag{3.29}
\end{aligned}$$

They are also referred to as greater ($>$), lesser ($<$), time-ordered ($\mathcal{T}$), and anti-time-ordered ($\overline{\mathcal{T}}$) correlators. By close investigation, it follows that they are indeed not independent: The

---

4 The kernels in the contour basis defined in Eq. (2.36) are given by

$$\mathcal{K}^{+-}(\boldsymbol{t}_p) = -\mathrm{i}, \qquad \mathcal{K}^{-+}(\boldsymbol{t}_p) = 0, \qquad \mathcal{K}^{--}(\boldsymbol{t}_p) = -\mathrm{i}\,\theta(t_{\overline{1}} - t_{\overline{2}}), \qquad \mathcal{K}^{++}(\boldsymbol{t}_p) = -\mathrm{i}\,\theta(t_{\overline{2}} - t_{\overline{1}}).$$

sum of the latter two equals the sum of the former two, $\mathcal{G}^{++} + \mathcal{G}^{--} = \mathcal{G}^{+-} + \mathcal{G}^{-+}$, yielding the redundancy relation[5]

$$\left(\mathcal{G}^{++} + \mathcal{G}^{--} - \mathcal{G}^{+-} - \mathcal{G}^{-+} \right)(\boldsymbol{t}) = 0. \tag{3.30}$$

This relation is the main motivation for applying the linear basis transformation $D^{k_i c_i} = (-1)^{k_i \delta_{c_i,+}}$ to rotate from the contour to the Keldysh basis [Kel65], as it is directly incorporated in the $\boldsymbol{k} = 11$ component:

$$\mathcal{G}^{11}(\boldsymbol{t}) = \frac{1}{2} \sum_{c_i = \pm} D^{1c_1} D^{2c_2} \mathcal{G}^{c_1 c_2}(\boldsymbol{t}) = \left(\mathcal{G}^{++} + \mathcal{G}^{--} - \mathcal{G}^{+-} - \mathcal{G}^{-+} \right)(\boldsymbol{t}) = 0. \tag{3.31}$$

The remaining three correlators in the Keldysh basis,[6]

$$\begin{aligned}
\mathcal{G}^{21}(\boldsymbol{t}) &= \mathcal{G}^R(\boldsymbol{t}) = -i\,\theta(t_1 - t_2)\,\mathcal{S}_{[1,2]_-}(\boldsymbol{t}), \\
\mathcal{G}^{12}(\boldsymbol{t}) &= \mathcal{G}^A(\boldsymbol{t}) = i\,\theta(t_2 - t_1)\,\mathcal{S}_{[1,2]_-}(\boldsymbol{t}), \\
\mathcal{G}^{22}(\boldsymbol{t}) &= \mathcal{G}^K(\boldsymbol{t}) = -i\,\mathcal{S}_{[1,2]_+}(\boldsymbol{t}),
\end{aligned} \tag{3.32}$$

define the so-called retarded ($\mathcal{G}^R$), advanced ($\mathcal{G}^A$), and Keldysh ($\mathcal{G}^K$) correlators [KLvD21, Kam23], expressed through the PSF (anti)commutators $\mathcal{S}_{[1,2]_\pm}(\boldsymbol{t}) = \mathcal{S}_{(12)}(t_1, t_2) \pm \mathcal{S}_{(21)}(t_2, t_1)$. In the time domain, however, the relations among these components are not as apparent as in the contour basis, where Eq. (3.30) could be immediately inferred; to elucidate their connection, we change to the frequency domain.

3.2.2 Fourier transformation and spectral representation

The Fourier transformation of the KF correlator to real frequencies $\boldsymbol{\omega} = (\omega_1, \omega_2)$ is defined as [KLvD21]

$$\mathcal{G}^{\boldsymbol{k}}(\boldsymbol{\omega}) = \int_{-\infty}^{\infty} dt_1 dt_2\, e^{i\omega_1 t_1 + i\omega_2 t_2} \mathcal{G}^{\boldsymbol{k}}(\boldsymbol{t}) = 2\pi \delta(\omega_{12})\, G^{\boldsymbol{k}}(\boldsymbol{\omega}). \tag{3.33}$$

Note that it differs from the convention in Eq. (2.45) by not including the normalization factor $1/(2\pi)^2$, which avoids an inconvenient proliferation of factors of 2π in later results. The last equality follows from time-translational invariance of $\mathcal{G}^{\boldsymbol{k}}(\boldsymbol{t})$ (3.28) (similarly to Eq. (2.46)), with the energy-conservation factor $2\pi\delta(\omega_{12})$ being the KF analogue to $\beta\delta_{i\omega_{12}}$ in the MF. In the following, however, we will not impose time-translational invariance of the correlators explicitly by considering $G^{\boldsymbol{k}}(\boldsymbol{\omega})$, with $\omega_{12} = 0$ understood for its argument. Rather, we will work with $\mathcal{G}^{\boldsymbol{k}}(\boldsymbol{\omega})$, and the factor $2\pi\delta(\omega_{12})$ will serve as a consistency check for the calculations.

---

5 Strictly speaking, this relation is only true for $t_1 \neq t_2$, since the Heaviside functions are not uniquely defined for $t_1 = t_2$. However, this point is of zero measure and will not influence the computations in this thesis. For a recent discussion where this point has to be treated more carefully, see, for instance, App. E of Ref. [GRW$^+$23].

6 The kernels in the Keldysh basis, defined in Eq. (2.38), read

$$\mathcal{K}^{11}(\boldsymbol{t}_p) = 0, \qquad \mathcal{K}^{21}(\boldsymbol{t}_p) = \mathcal{K}^{[1]}(\boldsymbol{t}_p) = -i\,\theta(t_{\bar{1}} - t_{\bar{2}}), \qquad \mathcal{K}^{12}(\boldsymbol{t}_p) = \mathcal{K}^{[2]}(\boldsymbol{t}_p) = i\,\theta(t_{\bar{2}} - t_{\bar{1}}),$$
$$\mathcal{K}^{22}(\boldsymbol{t}_p) = \mathcal{K}^{[1]}(\boldsymbol{t}_p) - \mathcal{K}^{[2]}(\boldsymbol{t}_p) = -i,$$

with the fully retarded kernels $\mathcal{K}^{[\lambda]}(\boldsymbol{t}_p)$ defined in Eq. (2.37).

We start with the simplest case by inserting $\mathcal{G}^K(\boldsymbol{t})$ in Eq. (3.32) into Eq. (3.33). The r.h.s. then reduces to the definition of the Fourier transform of the PSFs (2.45) up to a prefactor:

$$\mathcal{G}^K(\boldsymbol{\omega}) = 2\pi\delta(\omega_{12})G^K(\boldsymbol{\omega}), \qquad G^K(\boldsymbol{\omega}) = -2\pi\mathrm{i}\, S_{[1,2]_+}(\boldsymbol{\omega}). \tag{3.34}$$

For $\mathcal{G}^R(\boldsymbol{t})$ and $\mathcal{G}^A(\boldsymbol{t})$ in Eq. (3.32), an additional complication is introduced by the Heaviside functions, which originate from the fully retarded kernels $\mathcal{K}^{[1]}(t_1,t_2) = -\mathcal{K}^{[2]}(t_2,t_1) = -\mathrm{i}\theta(t_1-t_2)$ and $\mathcal{K}^{[2]}(t_1,t_2) = -\mathcal{K}^{[1]}(t_2,t_1) = \mathrm{i}\theta(t_2-t_1)$ (see Eq. (2.37)). Inserting $\mathcal{G}^{R/A}(\boldsymbol{t})$ together with Eq. (2.46) into Eq. (3.33) yields

$$\mathcal{G}^{R/A}(\boldsymbol{\omega}) = \int \mathrm{d}^2\varepsilon\, \delta(\varepsilon_{12})\, \mathcal{K}^{[1/2]}(\boldsymbol{\omega} - \boldsymbol{\varepsilon})\, S_{[1,2]_-}(\boldsymbol{\varepsilon}), \tag{3.35}$$

where the Fourier transform of the fully retarded kernels for general permutations p is defined as [KLvD21]

$$\begin{aligned}
\mathcal{K}^{[1/2]}(\boldsymbol{\omega}_p) &= \int_{-\infty}^{\infty} \mathrm{d}t_{\bar{1}}\, \mathrm{d}t_{\bar{2}}\, e^{\mathrm{i}\omega_{\bar{1}}t_{\bar{1}}+\mathrm{i}\omega_{\bar{2}}t_{\bar{2}}}\, \mathcal{K}^{[1/2]}(t_{\bar{1}},t_{\bar{2}}) \\
&= (\mp\mathrm{i}) \int_{-\infty}^{\infty} \mathrm{d}t_{\bar{1}}\mathrm{d}t_{\bar{2}}\, e^{\mathrm{i}\omega_{\bar{1}}t_{\bar{1}}+\mathrm{i}\omega_{\bar{2}}t_{\bar{2}}}\, \theta\big(\pm(t_{\bar{1}}-t_{\bar{2}})\big) \\
&= (\mp\mathrm{i}) \int_{-\infty}^{\infty} \mathrm{d}t_{\bar{2}}\, e^{\mathrm{i}\omega_{\overline{12}}t_{\bar{2}}} \int_0^{\infty} \mathrm{d}t\, e^{\pm\mathrm{i}\omega_{\bar{1}}t}.
\end{aligned} \tag{3.36}$$

In the last step, we substituted $t = \pm(t_{\bar{1}} - t_{\bar{2}})$.

The $t_{\bar{2}}$ integral results in $2\pi\delta(\omega_{\overline{12}})$. The t integral is regularized for the upper boundary by introducing an infinitesimal convergence factor via $\omega_{\bar{1}} \to \omega_{\bar{1}} \pm \mathrm{i}0^+ = \omega_{\bar{1}}^{\pm}$. Consequently, the opposite imaginary shift has to be assigned to $\omega_{\bar{2}} \to \omega_{\bar{2}} \mp \mathrm{i}0^+ = \omega_{\bar{2}}^{\mp}$, for the condition $\omega_{\bar{1}}^{\pm} + \omega_{\bar{2}}^{\mp} = \omega_{\overline{12}} = 0 \in \mathbb{R}$ to hold. Then, Eq. (3.36) evaluates to [KLvD21]

$$\mathcal{K}^{[\lambda]}(\boldsymbol{\omega}_p) = 2\pi\delta(\omega_{\overline{12}})K^{[\lambda]}(\boldsymbol{\omega}_p), \qquad K^{[\lambda]}(\boldsymbol{\omega}_p) = \frac{1}{\omega_{\bar{1}}^{[\bar{\lambda}]}}, \tag{3.37}$$

where $\omega_{\overline{12}} = 0$ is understood for the arguments of $K^{[\lambda]}$.[7] In addition, we defined $\omega_i^{[i]} = \omega_i^+$ and $\omega_{j\neq i}^{[i]} = \omega_j^-$ for later reference, such that the tuples $\boldsymbol{\omega}^{[1]}$ and $\boldsymbol{\omega}^{[2]}$ are given by $\boldsymbol{\omega}^{[1]} = (\omega_1^{[1]}, \omega_2^{[1]}) = (\omega_1^+, \omega_2^-)$ and $\boldsymbol{\omega}^{[2]} = (\omega_1^{[2]}, \omega_2^{[2]}) = (\omega_1^-, \omega_2^+)$, with their elements fulfilling $\omega_1^{\pm} + \omega_2^{\mp} = \omega_{12} = 0$ [KLvD21]. Inserting Eq. (3.37) into Eq. (3.35), where the identity permutation is assumed for the kernel, finally yields [P4]

$$\mathcal{G}^{R/A}(\boldsymbol{\omega}) = 2\pi\delta(\omega_{12})\, G^{R/A}(\boldsymbol{\omega}), \qquad G^{R/A}(\boldsymbol{\omega}) = \int \mathrm{d}^2\varepsilon\, \delta(\varepsilon_{12}) \frac{S_{\mathrm{std}}(\boldsymbol{\varepsilon})}{\omega_1^{\pm} - \varepsilon_1}, \tag{3.38}$$

---

7 Note that Eq. (3.34) is consistent with the Fourier transformed version of Eq. (2.38) using the kernel in Eq. (3.37). For $\boldsymbol{k} = 22$, Eq. (2.38) yields

$$\mathcal{G}^K(\boldsymbol{\omega}) = \sum_p \int \mathrm{d}\varepsilon_{\bar{1}}\, \mathrm{d}\varepsilon_{\bar{2}}\, \delta(\varepsilon_{\overline{12}}) \big[\mathcal{K}^{[1]}(\boldsymbol{\omega}_p - \varepsilon_p) - \mathcal{K}^{[2]}(\boldsymbol{\omega}_p - \varepsilon_p)\big]\, S_p(\boldsymbol{\varepsilon}_p),$$

where the difference of fully retarded kernels can be simplified via Eq. (3.37), $\mathcal{K}^{[1]}(\boldsymbol{\omega}_p) - \mathcal{K}^{[2]}(\boldsymbol{\omega}_p) = 2\pi\delta(\omega_{\overline{12}})\big(K^{[1]}(\boldsymbol{\omega}_p) - K^{[2]}(\boldsymbol{\omega}_p)\big)$, with $K^{[1]}(\boldsymbol{\omega}_p) - K^{[2]}(\boldsymbol{\omega}_p) = 1/\omega_{\bar{1}}^+ - 1/\omega_{\bar{1}}^- = -2\pi\mathrm{i}\,\delta(\omega_{\bar{1}})$. Here, we used the Lorentzian representation of the Dirac delta function. Then, the ε_i integrals can be easily evaluated using $2\pi\delta(\omega_{\overline{12}} - \varepsilon_{\overline{12}})\,\delta(\omega_{\bar{1}} - \varepsilon_{\bar{1}})\,\delta(\varepsilon_{\overline{12}}) = 2\pi\delta(\omega_{\overline{12}})\,\delta(\omega_{\bar{1}} - \varepsilon_{\bar{1}})\,\delta(\omega_{\bar{2}} - \varepsilon_{\bar{2}})$, and Eq. (3.34) follows by summing over the permutations.

with the standard spectral function defined in Eq. (3.22).

At this point, we can address the two questions posed in the beginning of Sec. 3.2 for the first time, at least for G^R and G^A. As a consequence of Eq. (3.38), G^A is related to G^R by the complex conjugation of the imaginary part of ω_1^-, i.e., of the KF kernel. This operation is denoted by a prime on the correlator (see Eqs. (3.72) for a more general discussion), such that [P4]

$$G'^A(\boldsymbol{\omega}) = \int \mathrm{d}^2\varepsilon \, \delta(\varepsilon_{12}) \left(\frac{1}{\omega_1^- - \varepsilon_1} \right)^* S_{\mathrm{std}}(\boldsymbol{\varepsilon}) = G^R(\boldsymbol{\omega}), \qquad G'^R(\boldsymbol{\omega}) = G^A(\boldsymbol{\omega}). \qquad (3.39)$$

Additionally, by comparing Eqs. (3.38) and (3.23), it immediately follows that [KLvD21]

$$G^{R/A}(\boldsymbol{\omega}) = \tilde{G}(\mathrm{i}\boldsymbol{\omega} \to \boldsymbol{\omega}^{[1/2]}) \qquad (3.40)$$

as a direct consequence of

$$K^{[\lambda]}(\boldsymbol{\omega}_p) = \tilde{K}(\mathrm{i}\boldsymbol{\omega}_p \to \boldsymbol{\omega}_p^{[\overline{\lambda}]}), \qquad (3.41)$$

see Eqs. (3.23) and (3.37). Therefore, the retarded and advanced components are solely determined by analytic continuations of the regular parts of the corresponding MF correlator [WFHT22, P4]. Conversely, this implies that the anomalous part of the MF correlator can only enter in the Keldysh component G^K; but how exactly?

3.2.3 Fluctuation-dissipation relation

To derive an answer to this question, we closely follow the discussion in Ref. [WFHT22].[8] The authors provide a detailed summary on differences between the zero-frequency limit of the dynamical Kubo susceptibility, the isentropic, and the isothermal susceptibility, their relation to long-term correlations (see Eq. (3.42) below), and, in turn, the direct connection to the presence of anomalous terms (see Eq. (3.43) below) [Kub57, Wil68, KS69, Suz71]. The approach of Ref. [WFHT22] has the merit of additionally providing a link between G^R, G^A, and G^K by relating PSF commutators (determining G^R and G^A) to anticommutators (determining G^K). As Ref. [WFHT22] is formulated within a linear response setting, bosonic operators are considered therein. In the ensuing analysis, on the other hand, regular PSF contributions are displayed with the sign factor ζ for the final results to hold in both the bosonic and fermionic cases.

Let us assume that $\mathcal{S}_{(21)}(0, t_1 - t_2)$ does not decay in the limits $t = t_1 - t_2 \to \pm\infty$, signalling the presence of long-term correlations in the system [WFHT22]:[9]

$$\lim_{t \to \pm\infty} \mathcal{S}_{(21)}(0, t) = C_{\pm}. \qquad (3.42)$$

Then, the Fourier transformation of $\mathcal{S}_{(21)}(0, t)$ is not guaranteed to converge for vanishing frequencies (which corresponds to an integral of $\mathcal{S}_{(21)}(0, t)$ over the whole t range) unless

---

8 For a translation between Ref. [WFHT22] and this thesis, we provide the following relations in the time domain:

$$\mathcal{S}_{(12)}(t, 0) = -\mathrm{i}\chi_{AB}^{>}(t), \qquad \mathcal{S}_{(21)}(0, t) = -\mathrm{i}\chi_{AB}^{<}(t), \qquad \mathcal{S}_{\mathrm{std}}(t, 0) = \mathcal{S}_{(12)}(t, 0) - \mathcal{S}_{(21)}(0, t) = \chi_{AB}^{c}(t),$$
$$\mathcal{G}^K(t) = -\Psi_{AB}(t), \qquad \mathcal{G}^R(t) = -\chi_{AB}^{\mathcal{R}}(t), \qquad \mathcal{G}^A(t) = -\chi_{AB}^{\mathcal{A}}(t).$$

9 To be precise, long-term correlations are quantified by the large-time limit of connected PSFs, i.e., by subtracting $\langle \mathcal{O}^2 \rangle \langle \mathcal{O}^1 \rangle$ from the l.h.s. of Eq. (3.42) [WFHT22]. These disconnected parts can be included by a redefinition of $C_{\pm}$ and are not considered explicitly here.

the long-term asymptotes are subtracted via $\mathcal{S}_{(21)}(0,t) - \theta(t)C_+ - \theta(-t)C_-$. The Fourier transformation of this object yields [WFHT22][10]

$$S_{(21)}(\boldsymbol{\varepsilon}_{(21)}) = \tilde{S}_{(21)}(\boldsymbol{\varepsilon}_{(21)}) + \delta(\varepsilon_2)\,\check{S}_{(21)} \qquad \text{with} \qquad \check{S}_{(21)} = \frac{C_+ + C_-}{2}, \qquad (3.43)$$

i.e., it recovers the decomposition into regular and anomalous PSFs in accordance with Eq. (3.17). Indeed, information about long-term correlations is encoded in the anomalous part of the PSFs and, thus, also of the MF correlator [WFHT22].

In order to relate PSF commutators to anticommutators, the equation

$$S_{\mathrm{std}}(\boldsymbol{\varepsilon}) = S_{[1,2]_-}(\boldsymbol{\varepsilon}) = (\zeta e^{-\beta\varepsilon_2} - 1)\tilde{S}_{(21)}(\boldsymbol{\varepsilon}_{(21)}) \qquad (3.44)$$

(following from Eq. (3.22)) can be inverted to express $\tilde{S}_{(21)}$ through S_{std} [WFHT22]:

$$\mathrm{P}\,\tilde{S}_{(21)}(\boldsymbol{\varepsilon}_{(21)}) = \mathrm{P}\,n_{\varepsilon_2}S_{\mathrm{std}}(\boldsymbol{\varepsilon}). \qquad (3.45)$$

In the bosonic case and for vanishing frequencies, the principle value P regularizes possible singularities of $\tilde{S}_{(21)}(\boldsymbol{\varepsilon}_{(21)})$ (see footnote below) and of the Matsubara weighting function (MWF)

$$n_{\varepsilon_i} = \frac{\zeta^i}{e^{-\beta\varepsilon_i} - \zeta^i} \qquad (3.46)$$

(see Eqs. (5.9) and (5.10) for the choice of nomenclature). From now on, we take the principal value to be understood implicitly. It then follows from Eqs. (3.43), (3.45), and the 2p equilibrium condition (3.19) that [WFHT22]

$$S_{(21)}(\boldsymbol{\varepsilon}_{(21)}) = n_{\varepsilon_2}S_{\mathrm{std}}(\boldsymbol{\varepsilon}) + \delta(\varepsilon_2)\,\check{S}_{(21)},$$
$$S_{(12)}(\boldsymbol{\varepsilon}_{(12)}) = -n_{\varepsilon_1}S_{\mathrm{std}}(\boldsymbol{\varepsilon}) + \delta(\varepsilon_1)\,\check{S}_{(12)}, \qquad (3.47)$$

where we used $\zeta e^{\beta\varepsilon_1}n_{\varepsilon_2} = \zeta e^{\beta\varepsilon_1}n_{-\varepsilon_1} = -n_{\varepsilon_1}$. It is worth mentioning that these results for the PSFs are consistent in the sense that the PSF commutator,

$$S_{[1,2]_-}(\boldsymbol{\varepsilon}) = S_{(12)}(\boldsymbol{\varepsilon}_{(12)}) - S_{(21)}(\boldsymbol{\varepsilon}_{(21)}) = (-n_{\varepsilon_1} - n_{-\varepsilon_1})S_{\mathrm{std}}(\boldsymbol{\varepsilon}) = S_{\mathrm{std}}(\boldsymbol{\varepsilon}), \qquad (3.48)$$

indeed yields the standard spectral function.

Adding the PSFs in Eq. (3.47) relates the PSF anticommutator to S_{std}, implying [WFHT22]

$$G^K(\boldsymbol{\omega}) = -2\pi\mathrm{i}S_{[1,2]_+}(\boldsymbol{\omega}) = -2\pi\mathrm{i}N_{\omega_1}S_{\mathrm{std}}(\boldsymbol{\omega}) - 4\pi\mathrm{i}\delta(\omega_1)\,\check{S}_{(12)}. \qquad (3.49)$$

Here, the Keldysh component G^K is expressed in terms of S_{std}, $\check{S}_{(12)} = \check{S}_{(21)}$, and the statistical factor

$$N_{\omega_i} = -n_{\omega_i} + n_{-\omega_i} = \coth[\beta\omega_i/2]^{\zeta^i}. \qquad (3.50)$$

---

10 In the notation of Ref. [WFHT22], the regular PSF is given by

$$2\pi\mathrm{i}\,\tilde{S}_{(21)}(\boldsymbol{\varepsilon}_{(21)}) = \tilde{\chi}^<(-\varepsilon_2) + (C_+ - C_-)\mathrm{P}\frac{1}{\varepsilon_2},$$

where P denotes the principal value and $\tilde{\chi}^<(-\varepsilon_2)$ is well-behaved for $\varepsilon_2 = 0$. Due to Eq. (3.44), the standard spectral function S_{std} has the well-defined value $S_{\mathrm{std}}(0,0) = \frac{\mathrm{i}\beta}{2\pi}(C_+ - C_-)$ at vanishing frequencies [WFHT22].

Equation (3.49) is the well-known fluctuation-dissipation relation (FDR), extended by an anomalous contribution arising from long-term correlations [WFHT22]. However, in the KF, the FDR is known to relate G^K to G^R and G^A [Kam23]. How can this statement be reconciled with Eq. (3.49)? The solution lies in the fact that G^R and G^A are determined by S_{std} via Eq. (3.38). Using the Lorentzian representation of the Dirac delta function, Eq. (3.38) can be inverted to express S_{std} in terms of G^R and G^A:

$$-2\pi\mathrm{i}\, S_{\mathrm{std}}(\boldsymbol{\omega}) = G^R(\boldsymbol{\omega}) - G^A(\boldsymbol{\omega}). \qquad (3.51)$$

Then, Eq. (3.49) takes the familiar form [Kam23, P4]

$$G^K(\boldsymbol{\omega}) = N_{\omega_1}\left[G^R(\boldsymbol{\omega}) - G^A(\boldsymbol{\omega})\right] + 4\pi\mathrm{i}\delta(\omega_1)\,\hat{G}_1, \qquad (3.52)$$

with $\hat{G}_1 = -\check{S}_{(12)}$ (see Eq. (3.21)).

Equation (3.52) complements the answers to the questions posed in the beginning of Sec. 3.2:

1. The Kelsyh components G^K, G^R, and G^A are related via Eqs. (3.39) and (3.52).

2. Given a 2p MF correlator $G(\mathrm{i}\boldsymbol{\omega}) = \tilde{G}(\mathrm{i}\boldsymbol{\omega}) + \beta\delta_{\mathrm{i}\omega_1}\hat{G}_1$, the corresponding real-frequency KF correlators are obtained by the analytic continuations in Eqs. (3.40) and (3.52).

Additionally, inserting Eqs. (3.51) and (3.40) into Eq. (3.47) demonstrates that a suitable combination of analytic continuations of $\tilde{G}$ with MWFs also determines the PSFs [P4] (see also Eq. (5.23)):

$$2\pi\mathrm{i}\, S_{(12)}(\boldsymbol{\varepsilon}_{(12)}) = n_{\varepsilon_1}\left[\tilde{G}(\varepsilon_1^+, \varepsilon_2^-) - \tilde{G}(\varepsilon_1^-, \varepsilon_2^+)\right] - 2\pi\mathrm{i}\delta(\varepsilon_1)\hat{G}_1,$$
$$2\pi\mathrm{i}\, S_{(21)}(\boldsymbol{\varepsilon}_{(21)}) = -n_{\varepsilon_2}\left[\tilde{G}(\varepsilon_1^+, \varepsilon_2^-) - \tilde{G}(\varepsilon_1^-, \varepsilon_2^+)\right] - 2\pi\mathrm{i}\delta(\varepsilon_2)\hat{G}_1. \qquad (3.53)$$

The PSFs, in turn, determine all Keldysh components via the spectral representation, and Eq. (3.53) thus provides a central link between both formalisms. This observation constitutes the central idea for the analytic continuation of ℓp correlators presented in Ch. 5 [P4].

At this point, let us further comment on the physical relevance of anomalous contributions. As already stated at the end of Sec. 3.1.4, the presence of a nonzero $\check{S}_{(12)}$ indicates either a conserved quantity or at least one degenerate energy level. In fact, as argued in Ref. [WFHT22], $\check{S}_{(12)} \neq 0$ can be exclusively attributed to the latter scenario under certain circumstances. The authors conducted a thorough analysis of anomalous contributions to the spin-spin susceptibility throughout the phase diagram of the Hubbard model using the dynamical mean-field theory (DMFT), in particular also in the coexistence region of the Mott-Hubbard metal-insulator transition. Among other things, they found a nonzero anomalous contribution in the insulating regime, indicating the presence of so-called long-term memory effects of spin correlations and a degenerate ground state, while a sharp change to a vanishing anomalous term was observed at the transition line. This directly links the anomalous term to the intrinsic properties of the physical system, illustrating that anomalous contributions indeed encapsulate vital physical information. Thus, Ref. [WFHT22] demonstrated that the analysis of these contributions has the potential to yield insights into and perspectives on the underlying many-body system.

This concludes our detailed review of properties of 2p MF und KF correlators and their intricate relation via the analytic continuation of imaginary to real frequencies. In the following two sections, we complement the preceding discussions by summarizing central results of Ref. [KLvD21] in the frequency domain and prepare for a thorough investigation of

the analytic continuation of ℓp correlators in Ch. 5 by further introducing the notation used in Ref. [P4].

3.3 ℓp MF correlators

This section reproduces Sec. 2.2 of [P4], which is a summary of the MF results of [KLvD21], with minor modifications to put it into the context of this thesis.

Many of the previously discussed properties of 2p MF correlators can be generalized to arbitrary ℓ. A general ℓp MF correlator $\mathcal{G}(\boldsymbol{\tau})$, defined in Eq. (2.32), is time-translationally invariant since the PSFs and kernels only depend on the difference of times (generalization of Eq. (3.4)) [Roh13]:

$$\mathcal{G}(\boldsymbol{\tau}) = \mathcal{G}(\tau_1 - \tau_\ell, \ldots, \tau_{\ell-1} - \tau_\ell, 0). \tag{3.54}$$

Under shifts $\tau_i \to \tau_i \mp \beta$ with τ_i the largest/smallest time, it is periodic for bosonic and antiperiodic for fermionic $\mathcal{O}^i$ (generalization of Eq. (3.6)) [Roh13]:

$$\mathcal{G}(\tau_1, \ldots, \tau_i, \ldots, \tau_\ell) = \begin{cases} \zeta^i \, \mathcal{G}(\tau_1, \ldots, \tau_i - \beta, \ldots, \tau_\ell) & \text{for } \tau_i > \tau_{j \neq i}, \\ \zeta^i \, \mathcal{G}(\tau_1, \ldots, \tau_i + \beta, \ldots, \tau_\ell) & \text{for } \tau_i < \tau_{j \neq i}. \end{cases} \tag{3.55}$$

From these properties, it then follows that the Fourier transform can be defined as (generalization of Eqs. (3.10) and (3.11)) [Roh13]

$$\mathcal{G}(\mathrm{i}\boldsymbol{\omega}) = \int_0^\beta \mathrm{d}^\ell \tau \, e^{\mathrm{i}\boldsymbol{\omega} \cdot \boldsymbol{\tau}} \mathcal{G}(\boldsymbol{\tau}) = \beta \delta_{\mathrm{i}\omega_{1 \ldots \ell}} G(\mathrm{i}\boldsymbol{\omega}), \tag{3.56}$$

where $\mathrm{i}\boldsymbol{\omega} = (\mathrm{i}\omega_1, \ldots, \mathrm{i}\omega_\ell)$ is a tuple of discrete Matsubara frequencies, with $\mathrm{i}\omega_i$ bosonic/fermionic if $\mathcal{O}^i$ is bosonic/fermionic. On the right, $\delta_{\mathrm{i}\omega_{1 \ldots \ell}}$ enforces energy conservation, $\mathrm{i}\omega_{1 \ldots \ell} = 0$. This condition originates from time translation invariance of $\mathcal{G}(\boldsymbol{\tau})$ (3.54); it is understood to hold for the argument of $G(\mathrm{i}\boldsymbol{\omega})$ by definition.

In Sec. 2.2.1, we discussed the separation of the analytical properties of correlators from the dynamical properties of the physical system of interest by expressing time-ordered products as a sum over $\ell!$ parts, see Eq. (2.32). Accordingly, we decompose the full correlator in terms of *partial* correlators $\mathcal{G}_p(\boldsymbol{\tau}_p)$,

$$\mathcal{G}(\boldsymbol{\tau}) = \sum_p \mathcal{G}_p(\boldsymbol{\tau}_p), \qquad \mathcal{G}_p(\boldsymbol{\tau}_p) = \mathcal{K}(\boldsymbol{\tau}_p) \mathcal{S}_p(-\mathrm{i}\boldsymbol{\tau}_p), \tag{3.57}$$

defined as the product of the MF kernel and the PSF in imaginary time. Then, for given $\boldsymbol{\tau}$, only that partial correlator $\mathcal{G}_p(\boldsymbol{\tau}_p)$ is nonzero for which the permuted tuple $\boldsymbol{\tau}_p$ is time-ordered. Note that the (anti)periodic properties of $\mathcal{G}(\boldsymbol{\tau})$ (3.55) do not hold for the individual partial correlators $\mathcal{G}_p(\boldsymbol{\tau}_p)$; they emerge only once these are summed over all permutations, Eq. (3.57).

The product form of Eq. (3.57) for $\mathcal{G}_p(\boldsymbol{\tau}_p)$ in the time domain implies that, in the Fourier domain, $\mathcal{G}(\mathrm{i}\boldsymbol{\omega})$ can be expressed as a sum over convolutions (generalization of Eq. (3.12)):

$$\mathcal{G}(\mathrm{i}\boldsymbol{\omega}) = \sum_p \mathcal{G}_p(\mathrm{i}\boldsymbol{\omega}_p), \qquad \mathcal{G}_p(\mathrm{i}\boldsymbol{\omega}_p) = \int_0^\beta \mathrm{d}^\ell \tau_p \, e^{\mathrm{i}\boldsymbol{\omega}_p \cdot \boldsymbol{\tau}_p} \mathcal{G}_p(\boldsymbol{\tau}_p) = [\mathcal{K} * S_p](\mathrm{i}\boldsymbol{\omega}_p). \tag{3.58a}$$

Here, the convolution $*$ is defined as

$$[\mathcal{K} * S_p](i\boldsymbol{\omega}_p) = \int_{-\infty}^{\infty} d^\ell \varepsilon_p \, \delta(\varepsilon_{\bar{1}\dots\bar{\ell}}) \mathcal{K}(i\boldsymbol{\omega}_p - \varepsilon_p) S_p(\varepsilon_p), \qquad (3.58b)$$

where $\boldsymbol{\varepsilon}_p$ satisfies $\varepsilon_{\bar{1}\dots\bar{\ell}} = 0$ (due to Eq. (2.46)), and the transformed kernel is defined as follows, with $\boldsymbol{\Omega}_p = i\boldsymbol{\omega}_p - \boldsymbol{\varepsilon}_p$ (generalization of Eq. (3.14)):

$$\mathcal{K}(\boldsymbol{\Omega}_p) = \int_0^\beta d^\ell \tau_p \, e^{\boldsymbol{\Omega}_p \cdot \boldsymbol{\tau}_p} \mathcal{K}(\boldsymbol{\tau}_p) = \beta \delta_{\Omega_{1\dots\ell}} K(\boldsymbol{\Omega}_p) + \mathcal{R}(\boldsymbol{\Omega}_p). \qquad (3.59)$$

Similarly to Eq. (3.14), $\mathcal{K}$ has been split into two contributions: $\beta\delta_{\Omega_{1\dots\ell}}$ times a *primary part* K, with $\Omega_{1\dots\ell} = 0$ understood for its argument, and a *residual part*, $\mathcal{R}$ not containing $\beta\delta_{\Omega_{1\dots\ell}}$. Using $\delta_{\Omega_{1\dots\ell}} = \delta_{i\omega_{1\dots\ell}}$ (since $\varepsilon_{1\dots\ell} = 0$), each partial correlator $\mathcal{G}_p(i\boldsymbol{\omega}_p)$ can correspondingly be split into primary and residual parts,

$$\mathcal{G}_p(i\boldsymbol{\omega}_p) = \beta\delta_{i\omega_{1\dots\ell}} G_p(i\boldsymbol{\omega}_p) + \mathcal{G}_p^{\mathcal{R}}(i\boldsymbol{\omega}_p), \qquad G_p(i\boldsymbol{\omega}_p) = [K * S_p](i\boldsymbol{\omega}_p), \qquad (3.60)$$

with $i\omega_{1\dots\ell} = 0$ understood for the argument of $G(i\boldsymbol{\omega}_p)$, and $\mathcal{G}_p^{\mathcal{R}} = [\mathcal{R} * S_p]$. Since $\mathcal{K}(\boldsymbol{\tau}_p)$ and $\mathcal{G}_p(\boldsymbol{\tau}_p)$ lack the (anti)periodicity properties of $\mathcal{G}(\boldsymbol{\tau})$, the residual parts $\mathcal{R}(\boldsymbol{\Omega}_p)$ and $\mathcal{G}_p^{\mathcal{R}}(i\boldsymbol{\omega}_p)$ are nonzero *per se*. However, inserting Eq. (3.60) into Eq. (3.58a) and noting from Eq. (3.56) that $\mathcal{G}(i\boldsymbol{\omega})$ is proportional to $\beta\delta_{i\omega_{1\dots\ell}}$, one concludes that (generalization of Eq. (3.20))

$$G(i\boldsymbol{\omega}) = \sum_p G_p(i\boldsymbol{\omega}_p) \qquad (3.61)$$

and $\sum_p \mathcal{G}_p^{\mathcal{R}}(i\boldsymbol{\omega}_p) = 0$. Thus, the *full* (summed over p) MF correlator G involves only primary parts G_p; the residual parts $\mathcal{G}_p^{\mathcal{R}}$ cancel out in the sum over all permutations. In the discussions below, we will therefore focus only on the primary parts K and G_p (as done in Ref. [KLvD21]), ignoring the residual parts $\mathcal{R}$ and $\mathcal{G}_p^{\mathcal{R}}$ for now. They will make a brief reappearance in Sec. 5.2.1, where we establish the connection between MF and KF correlators.

Explicit expressions for the primary kernel K were derived in Refs. [Shv06, Shv16, KLvD21, P2] and are collected in App. C.1 (see also Ch. 4 for its computation in full generality). Here, we just remark that K can be split into a *regular* kernel $\tilde{K}$ and an *anomalous* kernel $\hat{K}$:

$$K(\boldsymbol{\Omega}_p) = \begin{cases} \tilde{K}(\boldsymbol{\Omega}_p) & \text{if } \prod_{i=1}^{\ell-1} \Omega_{\bar{1}\dots\bar{i}} \neq 0, \\ \hat{K}(\boldsymbol{\Omega}_p) & \text{else,} \end{cases} \qquad \tilde{K}(\boldsymbol{\Omega}_p) = \prod_{i=1}^{\ell-1} \frac{1}{\Omega_{\bar{1}\dots\bar{i}}}. \qquad (3.62)$$

The regular kernel $\tilde{K}$ will play a crucial role for the analytic continuation of MF to KF correlators, since the latter can be expressed through kernels having the same structure as $\tilde{K}$ (see Eqs. (3.41) and (3.67d) below). The anomalous kernel $\hat{K}$ is nonzero only if we have $\Omega_{\bar{1}\dots\bar{i}} = 0$ for one or more values of $i < \ell$, requiring both $i\omega_{\bar{1}\dots\bar{i}} = 0$ *and* $\varepsilon_{\bar{1}\dots\bar{i}} = 0$. The first condition requires $i\omega_{\bar{1}\dots\bar{i}}$ to be bosonic (with $\zeta^{\bar{1}\dots\bar{i}} = +1$). The second condition requires the PSF $S_p(\boldsymbol{\varepsilon}_p)$ to have an anomalous contribution $\hat{S}_p(\boldsymbol{\varepsilon}_p)$ containing terms proportional to a bosonic Dirac $\delta(\varepsilon_{\bar{1}\dots\bar{i}})$; then (and only then), the $\boldsymbol{\varepsilon}_p$ integrals in the convolution $K * S_p$ receive a finite contribution from the point $\varepsilon_{\bar{1}\dots\bar{i}} = 0$.[11]

The regular/anomalous distinction made for the kernel implies, via Eqs. (3.60) and (3.61), a corresponding decomposition of the full MF correlator G into regular ($\tilde{G}$) and anomalous

---

[11] See Sec. 3.1.4 for an explicit example for $\ell = 2$ and App. C.2.1 for a further general discussion of this point.

($\hat{G}$) parts:

$$G(i\boldsymbol{\omega}) = \tilde{G}(i\boldsymbol{\omega}) + \hat{G}(i\boldsymbol{\omega}), \qquad \tilde{G}(i\boldsymbol{\omega}) = \sum_p \tilde{G}_p(i\boldsymbol{\omega}_p), \tag{3.63a}$$

$$\tilde{G}_p(i\boldsymbol{\omega}_p) = [\tilde{K} * S_p](i\boldsymbol{\omega}_p) = \int_{-\infty}^{\infty} d^\ell\varepsilon_p\,\delta(\varepsilon_{\bar{1}\ldots\bar{\ell}}) \left[\prod_{i=1}^{\ell-1} \frac{1}{i\omega_{\bar{1}\ldots\bar{i}} - \varepsilon_{\bar{1}\ldots\bar{i}}}\right] S_p(\boldsymbol{\varepsilon}_p). \tag{3.63b}$$

The *regular partial correlators* $\tilde{G}_p$, constructed via the regular kernel $\tilde{K}$, will be the central objects for the analytic continuation from MF to KF correlators, as discussed in Sec. 5.2.1 below. Their sum over all permutations defines the *regular full correlator* $\tilde{G}$. The *anomalous full correlator* $\hat{G}$ collects all other contributions to G; these contain one (or multiple) factors $\beta\delta_{i\omega_{\bar{1}\ldots\bar{i}}}$ with $i < \ell$, i.e. they involve vanishing partial frequency sums (see App. C.1.2 for details). The contribution of $\hat{G}$ to MF-to-KF analytical continuation has been rather poorly understood to date except for the case $\ell = 2$, see discussion in Sec. 3.2. In Ch. 5, following [P4], it is fully clarified how it enters: not directly, but indirectly, in that the central objects $\tilde{G}_p(i\boldsymbol{\omega}_p)$ can be expressed explicitly through the full $G = \tilde{G} + \hat{G}$ via imaginary-frequency convolutions of the form $[K \star G](i\boldsymbol{\omega}_p)$ (see Eq. (5.6)). There, $\hat{G}$ must not be neglected.

3.4 ℓp KF correlators

This section reproduces Sec. 2.3 of [P4], which is a summary of KF results of [KLvD21], with minor modifications to put it into the context of this thesis.

In the following, we will focus on the Keldysh basis only. Since both the PSFs and the Keldysh kernels in Eq. (2.38) depend on the difference of times, time-translational invariance for the KF correlators follows (generalization of Eq. (3.28)):

$$\mathcal{G}^{\boldsymbol{k}}(\boldsymbol{t}) = \mathcal{G}^{\boldsymbol{k}}(t_1 - t_\ell, \ldots, t_{\ell-1} - t_\ell, 0). \tag{3.64}$$

For the Fourier transform, this directly implies that (generalization of Eq. (3.33))

$$\mathcal{G}^{\boldsymbol{k}}(\boldsymbol{\omega}) = \int d^\ell t\, e^{i\boldsymbol{\omega}\cdot\boldsymbol{t}}\, \mathcal{G}^{\boldsymbol{k}}(\boldsymbol{t}) = 2\pi\delta(\omega_{1\ldots\ell})G^{\boldsymbol{k}}(\boldsymbol{\omega}). \tag{3.65}$$

Here, the Dirac $\delta(\omega_{1\ldots\ell})$, enforces energy conservation, $\omega_{1\ldots\ell} = 0$; this condition is understood for the argument of $G^{\boldsymbol{k}}(\boldsymbol{\omega})$ by definition. In terms of the permutation expansion in Eq. (2.38), one thus obtains

$$G^{\boldsymbol{k}}(\boldsymbol{\omega}) = \sum_p G_p^{\boldsymbol{k}_p}(\boldsymbol{\omega}_p), \tag{3.66a}$$

$$G_p^{\boldsymbol{k}_p}(\boldsymbol{\omega}_p) = (K^{\boldsymbol{k}_p} * S_p)(\boldsymbol{\omega}_p) = \int d^\ell\varepsilon_p\,\delta(\varepsilon_{\bar{1}\ldots\bar{\ell}})K^{\boldsymbol{k}_p}(\boldsymbol{\omega}_p - \boldsymbol{\varepsilon}_p)S_p(\boldsymbol{\varepsilon}_p). \tag{3.66b}$$

Remarkably, the same convolution structure emerges as for the MF correlator $G(i\boldsymbol{\omega})$ in Eqs. (3.63), for the same reason (Fourier transforms of products yield convolutions). But now the frequency arguments are real, and the kernel is given by $K^{\boldsymbol{k}_p}(\boldsymbol{\omega}_p)$, the Fourier transform of Eq. (2.38) (with $\omega_{\bar{1}\ldots\bar{\ell}} = 0$ understood).

An explicit expression for this kernel, derived in Ref. [KLvD21], is given in Eqs. (3.67) below. There, an alternative notation for Keldysh indices is employed. Each Keldysh index $\boldsymbol{k}$, being a list with entries 1 or 2, is represented as a list $\boldsymbol{k} = [\eta_1\ldots\eta_\alpha]$, where α is the total number of 2's in $\boldsymbol{k}$ and $\eta_i \in \{1, \ldots, \ell\}$ denotes the position of the ith 2 in $\boldsymbol{k}$ in increasing order;

$$\boldsymbol{\omega}^{[\eta]}:$$

Figure 3.1 Depiction of imaginary shifts of frequencies $\omega_i^{[\eta]} = \omega_i + \mathrm{i}\gamma_i^{[\eta]}$ with $i \in \{1, 2, 3, 4\}$ and $\eta = 4$ according to Eq. (3.68). (Figure adapted from Ref. [KLvD21].)

e.g., $\boldsymbol{k} = 1212 = [24]$. Similarly, permuted Keldysh indices are represented as $\boldsymbol{k}_p = [\hat{\eta}_1...\hat{\eta}_\alpha]$, where $\hat{\eta}_i$ denotes the position of the ith 2 in $\boldsymbol{k}_p$. Its values can be deduced from the old η_j's as follows: a 2 in slot η_j of $\boldsymbol{k}$ is moved by the permutation p to the new slot $\mu_j = p^{-1}(\eta_j)$; denoting the list of new 2-slots by $[\mu_1...\mu_\alpha]$ and arranging it in increasing order yields the desired $[\hat{\eta}_1...\hat{\eta}_\alpha]$. Note also that since $\hat{\eta}_j \in \{p^{-1}(\eta_1), ..., p^{-1}(\eta_\alpha)\}$, we have $\overline{\hat{\eta}}_1 \in \{\eta_1, \ldots, \eta_\alpha\}$; hence, $\overline{\hat{\eta}}_j$ is an element of the list specifying the *external* Keldysh index $\boldsymbol{k} = [\eta_1...\eta_\alpha]$. This will be crucial below. We illustrate these conventions for the permutation $p = (4123)$ and $\boldsymbol{k} = 1212 = [24]$. Then, $\boldsymbol{k}_p = 2121$, $[\mu_1\mu_2] = [31]$ and $\boldsymbol{k}_p = [\hat{\eta}_1\hat{\eta}_2] = [13]$; moreover, $\overline{\hat{\eta}}_1 = \overline{1} = 4$ and $\overline{\hat{\eta}}_2 = \overline{3} = 2$ are both elements of $\boldsymbol{k} = [24]$.

Expressed in this notation, Eqs. (3.66) read

$$G^{[\eta_1...\eta_\alpha]}(\boldsymbol{\omega}) = \sum_p G_p^{[\hat{\eta}_1...\hat{\eta}_\alpha]}(\boldsymbol{\omega}_p), \tag{3.67a}$$

$$G_p^{[\hat{\eta}_1...\hat{\eta}_\alpha]}(\boldsymbol{\omega}_p) = \left[K^{[\hat{\eta}_1...\hat{\eta}_\alpha]} * S_p\right](\boldsymbol{\omega}_p), \tag{3.67b}$$

with the permuted Keldysh kernel $K^{[\hat{\eta}_1...\hat{\eta}_\alpha]}$ given by [KLvD21]

$$K^{[\hat{\eta}_1...\hat{\eta}_\alpha]}(\boldsymbol{\omega}_p) = \sum_{j=1}^{\alpha}(-1)^{j-1}K^{[\hat{\eta}_j]}(\boldsymbol{\omega}_p), \tag{3.67c}$$

$$K^{[\eta]}(\boldsymbol{\omega}_p) = \prod_{i=1}^{\ell-1}\frac{1}{\omega_{1...\bar{i}}^{[\overline{\eta}]}}. \tag{3.67d}$$

Equations (3.67) compactly express all partial correlators $G_p^{\boldsymbol{k}_p} = G_p^{[\hat{\eta}_1...\hat{\eta}_\alpha]}$, and hence also the full KF correlator $G^{\boldsymbol{k}} = G^{[\eta_1...\eta_\alpha]}$, through the set of ℓ fully retarded kernels $K^{[\eta]}(\boldsymbol{\omega}_p)$, the Fourier transform of Eq. (2.37). These are defined by Eq. (3.67d), the generalization of Eq. (3.37) to general ℓ, and depend on just a single index η, which takes the value $\hat{\eta}_j$ in Eq. (3.67c). The superscript on the frequencies occurring therein denotes imaginary shifts $\omega_i \to \omega_i^{[\eta]} = \omega_i + \mathrm{i}\gamma_i^{[\eta]}$, with $\gamma_i^{[\eta]} \in \mathbb{R}$ chosen such that $\gamma_{i\neq\eta}^{[\eta]} < 0$, $\gamma_\eta^{[\eta]} > 0$, and $\omega_{1...\ell} = \omega_{1...\ell}^{[\eta]} = 0$. Shifts of precisely this form are needed to regularize the Fourier integrals expressing $\mathcal{K}^{\boldsymbol{k}_p}(\boldsymbol{\omega}_p)$ through $\mathcal{K}^{\boldsymbol{k}_p}(\boldsymbol{t}_p)$ (see Eqs. (3.36) and (3.37) for $\ell = 2$). We choose the same convention as in Ref. [KLvD21],

$$\gamma_{i\neq\eta}^{[\eta]} = -\gamma_0, \quad \gamma_\eta^{[\eta]} = (\ell-1)\gamma_0, \tag{3.68}$$

see Fig. 3.1, with γ_0 taken to be infinitesimal, $\gamma_0 = 0^+$, for analytical considerations. We also use the shorthand $\omega_{i...j}^{\pm} = \omega_{i...j} \pm \mathrm{i}0^+$ to indicate infinitesimal imaginary shifts for sums of frequencies.

Comparing the fully retarded kernel $K^{[\eta]}$ of Eq. (3.67d) with the regular Matsubara kernel $\tilde{K}$ of Eq. (3.62), we find that the former is the analytic continuation of the latter

(generalization of Eq. (3.41)):

$$K^{[\eta]}(\boldsymbol{\omega}_p) = \tilde{K}\big(\mathrm{i}\boldsymbol{\omega}_p \to \boldsymbol{\omega}_p^{[\overline{\eta}]}\big). \tag{3.69}$$

This remarkable relation between MF and KF kernels constitutes the nucleus from which we will develop our strategy for obtaining KF correlators via analytic continuation of MF correlators in Ch. 5.

Two well-known statements on general ℓp correlators follow immediately from Eqs. (3.67). First, for $\alpha = 0$, they imply $G^{[]} = G^{1\cdots1} = 0$. Second, for $\alpha = 1$, we have $\overline{\hat{\eta}}_1 = \eta_1$. Thus, $K^{[\hat{\eta}]}(\boldsymbol{\omega}_p) = \tilde{K}(\boldsymbol{\omega}_p^{[\eta]})$ by Eq. (3.69), and Eq. (3.67b) yields

$$G_p^{[\hat{\eta}]}(\boldsymbol{\omega}) = [\tilde{K} * S_p](\boldsymbol{\omega}_p^{[\eta]}) = \tilde{G}_p(\mathrm{i}\boldsymbol{\omega}_p \to \boldsymbol{\omega}_p^{[\eta]}). \tag{3.70}$$

For the second step, we evoked Eq. (3.63b). Importantly, the superscript on $\boldsymbol{\omega}_p^{[\eta]}$ on the right, which specifies its imaginary frequency shifts, is fully determined by the external Keldysh index η and *not* dependent on p. It thus remains unchanged throughout the sum on p in Eq. (3.66a) for the full correlator $G^{[\eta]}(\boldsymbol{\omega})$, which hence can be expressed as

$$G^{[\eta]}(\boldsymbol{\omega}) = \tilde{G}(\mathrm{i}\boldsymbol{\omega} \to \boldsymbol{\omega}^{[\eta]}). \tag{3.71}$$

The fully retarded ($\alpha = 1$) components of KF correlators are therefore fully determined, via analytic continuation, by the *regular* parts of MF correlators, in accordance with Eq. (3.40) for $\ell = 2$ (with the identification $G^{R/A} = G^{[1/2]}$). Conversely, anomalous parts of MF correlators can only influence Keldysh components with $\alpha \geq 2$ (see Eq. (3.52) with $G^K = G^{[12]}$).

For later use, we also define primed partial correlators (generalization of Eq. (3.39))

$$G'^{[\eta_1\cdots\eta_\alpha]}(\boldsymbol{\omega}) = \sum_p G_p'^{[\hat{\eta}_1\cdots\hat{\eta}_\alpha]}(\boldsymbol{\omega}_p), \tag{3.72a}$$

$$G_p'^{[\hat{\eta}_1\cdots\hat{\eta}_\alpha]}(\boldsymbol{\omega}_p) = \left[\big(K^{[\hat{\eta}_1\cdots\hat{\eta}_\alpha]}\big)^* * S_p\right](\boldsymbol{\omega}_p). \tag{3.72b}$$

They differ from the unprimed correlators of Eq. (3.67b) by the complex conjugation of the kernel, replacing $\omega_i + \mathrm{i}\gamma_i^{[\eta]}$ by $\omega_i - \mathrm{i}\gamma_i^{[\eta]}$, with $\gamma_i^{[\eta]}$ still determined by the rule Eq. (3.68). For $\alpha = 1$, the corresponding $G'^{[\eta]}$ will be called *fully advanced* correlators.[12] For fully retarded or advanced correlators, $G^{[\eta]}$ or $G'^{[\eta]}$, *all* frequencies $\omega_{i\neq\eta}$ acquire negative or positive imaginary shifts, respectively. Note that primed correlators $G'^{\boldsymbol{k}}$ may differ from complex conjugated correlators $G^{*\boldsymbol{k}}$ as the complex conjugation generally affects the PSFs, too.

This concludes our summary of the results of Ref. [KLvD21] needed for the following chapters, in particular Ch. 5.

3.5 Self-energy and 4p vertex

We complement the introductory part of this thesis by defining the self-energy Σ and the two-particle (4p) vertex Γ, the central objects of interest in [P3] (see Sec. 6.1 for a discussion of their relevance). In the following, we consider bosonic or fermionic single-particle annihilation and creation operators d_1 and $d_2^\dagger$. Depending on the specific Hamiltonian $H = H^0 + H_{\text{int}}$, the multi-indices 1 and 2 denote relevant quantum numbers such as spin or orbitals. The

---

12 This might sound confusing since we identified the advanced component G^A for $\ell = 2$ with a fully retarded correlator, see Eq. (3.71). However, for $\ell = 2$ the nomenclature is ambiguous, since $G^A = G'^R$ (see Eq. (3.39)) is also a fully advanced correlator. Similarly, the $\ell = 2$ retarded component is also fully retarded and fully advanced, $G^R = G'^A$.

(a)

(b)
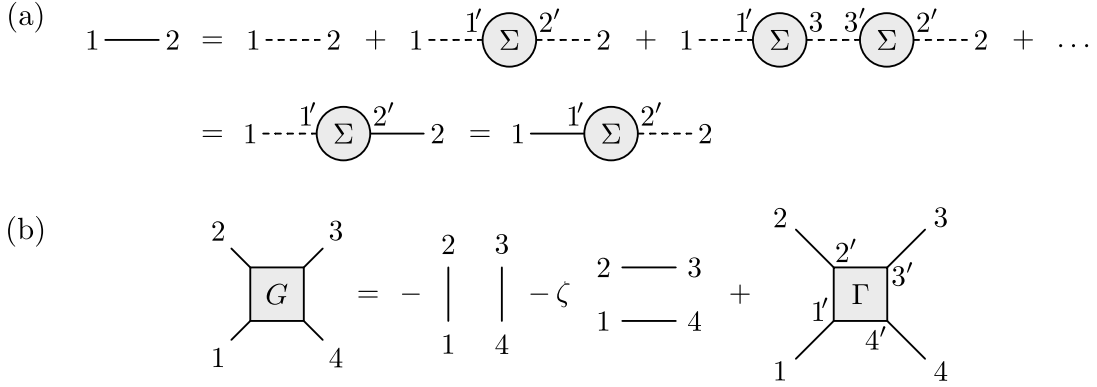
Figure 3.2 Diagrammatic representation of the definition of (a) the self-energy Σ (3.74) and (b) the 4p vertex Γ (3.76a). Summation over internal indices is implied. (a) The solid (dashed) lines represent the full propagator g_{12} (the bare propagator $g_{0;12}$). The last diagram in the first line can be split into two by cutting a bare propagator line; such diagrams are, by definition, not part of Σ, which contains all one-particle irreducible diagrams. (b) Separating the disconnected parts from the 4p correlator G and factoring out external legs defines the 4p vertex Γ.

non-interacting Hamiltonian H^0 comprises all terms at most quadratic in the single-particle operators, and therefore constitutes the exactly solvable part of the model;[13] the interacting part H_{int} contains everything else.

The 2p correlator, or progagator, $g_{12} = G[d_1, d_2^\dagger]$ for two single-particle operators $\mathcal{O} = (d_1, d_2^\dagger)$ is defined as (the Fourier transform of) their time-ordered or contour-ordered expectation value w.r.t. the full Hamiltonian H. For a unified discussion of the MF and the KF, we define

$$g_{12}(z) = \begin{cases} g_{12}(i\omega) & \text{in the MF} \\ g_{12}^{k_1 k_2}(\omega) & \text{in the KF} \end{cases} \qquad \begin{rcases} \Sigma_{12}(i\omega) \\ \Sigma_{12}^{k_1 k_2}(\omega) \end{rcases} = \Sigma_{12}(z), \qquad (3.73)$$

with g and Σ displayed as functions of one frequency (rather than a tuple of two frequencies) throughout this section. Thus, the multi-indices may additionally contain Keldysh indices if $z = \omega$ is a real frequency. The self-energy Σ is defined in terms of the Dyson equation [KBS10] (see Fig. 3.2(a)):

$$\begin{aligned} g_{12}(z) &= g_{12}^0(z) + g_{11'}^0(z)\,\Sigma_{1'2'}(z)\,g_{2'1}(z) \\ &= g_{12}^0(z) + g_{11'}(z)\,\Sigma_{1'2'}(z)\,g_{2'1}^0(z). \end{aligned} \qquad (3.74)$$

Here, a sum over repeated multi-indices is implied, including Keldysh components in the KF. The bare propagator g^0 is defined just as g, but with the inherent expectation value and Heisenberg time evolution evaluated w.r.t. the non-interacting Hamiltonian H^0. Thus, by definition, $\Sigma = 0$ if the interaction vanishes, $H_{\text{int}} = 0$. In diagrammatic language, Σ contains all one-particle irreducible diagrams, i.e., diagrams that cannot be split into two by cutting a bare propagator line [KBS10] (see Fig. 3.2(a)).

The 4p vertex Γ is defined in terms of the 4p correlator G_{1234}, i.e., (the Fourier transform of) the time-ordered or contour-ordered expectation value of the operators $\mathcal{O} = (d_1, d_2^\dagger, d_3, d_4^\dagger)$ w.r.t. the full Hamiltonian H. Again, for a unified discussion of the MF and KF, we define

---

13 It may, in fact, also contain terms depending on other single-particle operators than d_1 or $d_2^\dagger$ as long as they are at most quadratic in these operators (see, e.g., the Anderson impurity model in Eq. (13) of [P3]).

$$G_{1234}(\boldsymbol{z}) = \begin{cases} G_{1234}(\mathrm{i}\boldsymbol{\omega}) & \text{in the MF} & \Gamma_{1234}(\mathrm{i}\boldsymbol{\omega}) \\ G_{1234}^{\boldsymbol{k}}(\boldsymbol{\omega}) & \text{in the KF} & \Gamma_{1234}^{\boldsymbol{k}}(\boldsymbol{\omega}) \end{cases} \Bigg\} = \Gamma_{1234}(\boldsymbol{z}), \qquad (3.75)$$

with $\boldsymbol{k} = k_1 k_2 k_3 k_4$ the Keldysh index and $\boldsymbol{z} = (z_1, z_2, z_3, z_4)$ a tuple of real or complex frequencies fulfilling $z_{1234} = 0$. Γ follows from the connected part of G, denoted by G^{con}, via [KLvD21] (see Fig. 3.2(b)):[14]

$$\begin{aligned} G_{1234}^{\mathrm{con}}(\boldsymbol{z}) &= G_{1234}(\boldsymbol{z}) - G_{1234}^{\mathrm{dis}}(\boldsymbol{z}) \\ &= g_{11'}(z_1)\, g_{33'}(z_3)\, \Gamma_{1'2'3'4'}(\boldsymbol{z})\, g_{2'2}(-z_2)\, g_{4'4}(-z_4), \end{aligned} \qquad (3.76\mathrm{a})$$

$$G_{1234}^{\mathrm{dis}}(\boldsymbol{z}) = -\delta(z_{12})\, g_{12}(z_1)\, g_{34}(z_3) - \zeta\, \delta(z_{14})\, g_{14}(z_1)\, g_{32}(z_3). \qquad (3.76\mathrm{b})$$

Here, $\delta(z_{12})$ is equal to $\beta \delta_{\mathrm{i}\omega_{12}}$ in the MF and to $2\pi \mathrm{i} \delta(\omega_{12})$ in the KF. The sign factor ζ equals ± 1 if the single-particle operators are all bosonic/fermionic. The disconnected part G_{1234}^{dis}, describing the independent propagation of two particles, is subtracted from the full G to obtain G^{con}. Γ then follows by amputating the four external legs g of G^{con}.

Before concluding this section, let us comment on the large-frequency behaviour of Eq. (3.76a). Out of the four frequencies in $\boldsymbol{z}$, only three are independent; let us choose them to be given by z_1, z_3, and $z_{12} = -z_{34}$, yielding the frequency tuple $\boldsymbol{z} = (z_1, z_{12}-z_1, z_3, -z_{12}-z_3)$. Then, in the limit of, say, large z_3, both $g_{33'}$ and $g_{44'}$ scale (at least) like $g_{33'}(z_3), g_{44'}(-z_4 = z_{12}+z_3) \sim 1/z_3$ due to their spectral representation. In [WFHT22], it was additionally derived from diagrammatic arguments that, in the limit of large z_3, Γ approaches a function of z_1 and z_{12} that is independent of z_3. Combining the behaviour of $g_{33'}$, $g_{44'}$, and Γ for large z_3, the leading order term on the r.h.s. of Eq. (3.76a) is at least $1/z_3^2$ in an expansion in powers of $1/z_3$.

This conclusion, however, seems to contradict the spectral representation of G^{con},

$$G_{1234}^{\mathrm{con}}(\mathrm{i}\boldsymbol{\omega}) = \sum_p \left[K * S_p^{\mathrm{con}} \right](\mathrm{i}\boldsymbol{\omega}_p), \qquad G_{1234}^{\mathrm{con};\boldsymbol{k}}(\boldsymbol{\omega}) = \sum_p \left[K^{\boldsymbol{k}_p} * S_p^{\mathrm{con}} \right](\boldsymbol{\omega}_p). \qquad (3.77)$$

Here, the subtraction of disconnected parts is performed on the level of the PSFs [KLvD21], with $S_p^{\mathrm{con}} = S_p - S_p^{\mathrm{dis}}$ (see Eq. (B.4) for an explicit expression of S_p^{dis}). In Eq. (3.77), only the MF and KF kernels depend on the external frequencies $\boldsymbol{z}$ due to $z_{\bar{1}}$, $z_{\overline{12}}$, and $z_{\overline{123}}$ in their denominators. For instance, for the permutation $p = (1234)$, they read z_1, $z_{12} - z_1$, and $z_{12} + z_3$ in terms of the chosen independent frequencies. Consequently, they only contribute a term $\sim 1/z_3$ in the expansion of G^{con} in powers of $1/z_3$, inconsistent with the known expansion of the r.h.s. of Eq. (3.76a). In App. B, we resolve this contradiction by proving an intricate cancellation of these inconsistent $\sim 1/z_3$ contributions for both the MF and KF.

---

14 In Eq. (3.76a), the negative signs in the frequency arguments of the propagators originate from the fact that all operators are Fourier transformed using the same convention, $e^{\mathrm{i}\omega\tau}$ or $e^{\mathrm{i}\omega t}$, see Eqs. (3.56) and (3.65), while one usually uses opposite signs for creation and annihilation operators [KLvD21]. Also note that Eq. (3.76b) only holds if $\langle d_1 \rangle = \langle d_1^\dagger \rangle = 0$.

4 MF kernels

4.1 Overview

The spectral representation of ℓp MF correlators in Eqs. (3.60) and (3.61) consists of PSFs and the primary MF kernel. The latter is implicitly defined via (following from Eqs. (2.32) and (3.59))

$$
\mathcal{K}(\boldsymbol{\Omega}_p) = (-1)^{\ell-1} \left[\int_0^\beta \mathrm{d}\tau_{\overline{1}}\, e^{\Omega_{\overline{1}}\tau_{\overline{1}}} \right] \left[\int_0^{\tau_{\overline{1}}} \mathrm{d}\tau_{\overline{2}}\, e^{\Omega_{\overline{2}}\tau_{\overline{2}}} \right] \dots \left[\int_0^{\tau_{\overline{\ell-2}}} \mathrm{d}\tau_{\overline{\ell-1}}\, e^{\Omega_{\overline{\ell-1}}\tau_{\overline{\ell-1}}} \right] \left[\int_0^{\tau_{\overline{\ell-1}}} \mathrm{d}\tau_{\overline{\ell}}\, e^{\Omega_{\overline{\ell}}\tau_{\overline{\ell}}} \right]
$$
$$
= \beta \delta_{\Omega_{1\dots\ell}} K(\boldsymbol{\Omega}_p) + \mathcal{R}(\boldsymbol{\Omega}_p). \tag{4.1}
$$

The main objective of our publication [P2] is to provide a closed solution for $K(\boldsymbol{\Omega}_p)$ for general ℓ.[1] However, there are two major obstacles: First, it is highly nontrivial to extract $K(\boldsymbol{\Omega}_p)$ from the integrals because of the residual kernel $\mathcal{R}(\boldsymbol{\Omega}_p)$. Second, the incorporation of vanishing partial frequency sums $\Omega_{\overline{j}\dots\overline{\ell}} = 0$ (with $j \geq 2$) requires a case distinction for each of the integrals (see App. A.1 for $\ell = 2$), generating a tremendous number of terms for large ℓ. Contributions containing a vanishing partial frequency sums are referred to as anomalous terms of order a [P2].[2]

To set our publication [P2] into context, we first introduce an alternative spectral representation of ℓp MF correlators that is most frequently employed in the literature for $\ell \leq 4$ [Eli62, Ogu01, Shv06, TKH07, HJB+09, AP15, AP16, Shv16, WFHT22], utilizing the notation in App. B of Ref. [KLvD21]. Due to time-translational invariance (3.54), τ_ℓ can be set to zero, while the remaining time differences can be chosen positive by means of the (anti)periodicity relations (3.55) [Roh13, KLvD21]. Consequently, for the computation of ℓp MF correlators, it suffices to sum over the $(\ell-1)!$ permutations $q = (\overline{1}\dots\overline{\ell-1\ell})$, since $\tau_\ell = 0$ is fixed to be the smallest time [KLvD21]. The Fourier transformation of the corresponding reduced time-ordering kernel $k(\boldsymbol{\tau}_q) = (-1)^{\ell-1} \prod_{i=1}^{\ell-2} \theta(\tau_{\overline{i}} - \tau_{\overline{i+1}})$ then involves only $\ell-1$ time integrals, $k(\boldsymbol{\Omega}_q) = \prod_{i=1}^{\ell-1} \left[\int_0^\beta \mathrm{d}\tau_{\overline{i}}\, e^{\Omega_{\overline{i}}\tau_{\overline{i}}} \right] k(\boldsymbol{\tau}_q)$, and the ℓp MF correlator follows from the alternative spectral representation [KLvD21]

$$
G(\mathrm{i}\boldsymbol{\omega}) = \sum_p \left[K * S_p \right](\mathrm{i}\boldsymbol{\omega}_p) = \sum_q \left[k * S_q \right](\mathrm{i}\boldsymbol{\omega}_q). \tag{4.2}
$$

Due to the equilibrium condition for the PSFs (2.47), the reduced kernels $k(\boldsymbol{\Omega}_q)$ can thus be expressed as linear combinations of the primary kernels,

$$
k(\boldsymbol{\Omega}_q) = \sum_{\lambda=1}^{\ell} e^{\beta\Omega_{\overline{1}\dots\overline{\lambda-1}}} K(\boldsymbol{\Omega}_{(\overline{\lambda}\dots\ell\,\overline{1}\dots\overline{\lambda-1})}), \tag{4.3}
$$

where the sign factor in Eq. (2.47) is absorbed into the exponential function via $\zeta^{\overline{1}\dots\overline{\lambda-1}} = e^{\beta\mathrm{i}\omega_{\overline{1}\dots\overline{\lambda-1}}}$. Note that $k(\boldsymbol{\Omega}_q)$ does not split into a primary kernel multiplying $\beta\delta_{\Omega_{1\dots\ell}}$ and a residual kernel as in Eq. (4.1); the nontrivial (anti)periodic boundary conditions removed all residual parts $\mathcal{R}$, and energy conservation was accounted for by time-translation invariance. Despite these advantages, it is expected that $K(\boldsymbol{\Omega}_p)$ is of much simpler form than $k(\boldsymbol{\Omega}_q)$, as the latter is a sum over ℓ terms depending on the former.

---

1 In [P2], $\mathcal{K}(\boldsymbol{\Omega}_p)$ is defined without the factor $(-1)^{\ell-1}$.

2 For instance, the Kronecker $\delta_{\Omega_{\overline{1}}}$ contribution to the 2p MF kernel in Eq. (3.16), enforcing $\Omega_{\overline{1}} = \Omega_{\overline{2}} = 0$, is an anomalous term of order one.

We are now in the position to discuss previous results for the MF kernel:

1. In most previous works, $k(\mathbf{\Omega}_q)$ is computed for a given $\ell = 2, 3, 4$ without addressing $K(\mathbf{\Omega}_p)$, with varying treatment of anomalous terms [Eli62, Ogu01, Shv06, TKH07, HJB$^+$09, AP15, AP16, Shv16, KLvD21, WFHT22].[3] These references include exact results with the relevant anomalous terms for arbitrary 2p [Shv06, KLvD21, WFHT22] and 3p correlators [Shv06] as well as fermionic 4p correlators [HJB$^+$09, Shv16, KLvD21]. Only Ref. [KLvD21] proceeds to split $k(\mathbf{\Omega}_q)$, including anomalous terms of order one, equally among the $K(\mathbf{\Omega}_p)$ by reversing the step in Eq. (4.2), thus providing expressions for $K(\mathbf{\Omega}_p)$ for arbitrary 2p correlators, 3p correlators with one bosonic operator, and fermionic 4p correlators.

2. Remarkably, Ref. [KLvD21] obtained an expression for $K(\mathbf{\Omega}_p)$ for arbitrary ℓ neglecting anomalous terms. The authors realized that, for a different representation of the integrals in Eq. (4.1) (see Eq. (C.1)), only their lower integration boundaries contribute to $K(\mathbf{\Omega}_p)$, while their upper integration boundaries result in $\mathcal{R}(\mathbf{\Omega}_p)$. However, both boundaries are required for computing anomalous contributions (see footnote after Eq. (C.1)), and a straightforward generalization of their strategy is inapplicable.

Various recent developments motivated extending the above mentioned results for $K(\mathbf{\Omega}_p)$ to anomalous terms of arbitrary order and for general ℓ: (i) The interest in nonlinear response theory expressed through multipoint bosonic correlators [KKWH23], (ii) the development of the spin functional renormalization group (RG) [KK19, GTKK19, GRK20, TK21, TRK$^+$22], where multipoint spin correlators serve as nontrivial initial conditions for the RG flow, and (iii) a new approach to the analytic continuation of multipoint correlators [P4] (see also Ch. 5), where the MF kernel appears in an imaginary-frequency convolution (see Eq. (5.4b)).

In [P2], we extend the insight of Ref. [KLvD21] to our integral representation in Eq. (4.1). Indeed, only the upper integration boundaries of the $\tau_{\bar{i}}$ integrals (with $i > 1$) can contribute to $K(\mathbf{\Omega}_p)$, even to the anomalous terms. This can be easily seen as follows: The integrand of the final $\tau_{\bar{1}}$ integral must contain the exponential factor $e^{\Omega_{\bar{1}\dots\bar{\ell}}\tau_{\bar{1}}}$ in order to produce the energy-conservation factor $\beta\delta_{\Omega_{\bar{1}\dots\bar{\ell}}} = \beta\delta_{\Omega_{1\dots\ell}}$ multiplying $K(\mathbf{\Omega}_p)$. However, this requirement is impeded by the lower integration boundaries of the previous integrals as they reduce the exponential factors to unity; they must therefore contribute to $\mathcal{R}(\mathbf{\Omega}_p)$. Building upon this insight, we develop an iterative procedure to evaluate the integrals in Eq. (4.1) from right to left, resulting in a closed, exact expression for $K(\mathbf{\Omega}_p)$ for general ℓ and anomalous terms of arbitrary order. Subsequently, we apply our formulas to 3p bosonic correlators in the Hubbard atom (see also Sec. 5.7 for a description of the model) and $\ell = 2, 3, 4$ correlators for a free spin of length S.

---

[3] To be precise, Refs. [Shv06, Shv16] compute $k(\mathbf{\Omega}_q)$ via the r.h.s. of Eq. (4.3) by carrying out the integrals in Eq. (4.1) and identifying $\beta\delta_{\Omega_{1\dots\ell}}k(\mathbf{\Omega}_q) = \sum_{\lambda=1}^{\ell} e^{\beta\Omega_{\bar{1}\dots\overline{\lambda-1}}}\mathcal{K}(\mathbf{\Omega}_{(\bar{\lambda}\dots\bar{\ell}\,\bar{1}\dots\overline{\lambda-1})})$. However, the occurrence of the residual terms $\mathcal{R}$ is not discussed, and the analyses proceed with $k(\mathbf{\Omega}_q)$ rather than $K(\mathbf{\Omega}_p)$.

Spectral representation of Matsubara n-point functions: Exact kernel functions and applications

by

J. Halbinger[1], B. Schneider[1], and B. Sbierski[1]

[1]Arnold Sommerfeld Center for Theoretical Physics, Center for NanoScience, and Munich Center for Quantum Science and Technology, Ludwig-Maximilians-Universität München, 80333 Munich, Germany

Spectral representation of Matsubara n-point functions: Exact kernel functions and applications

Johannes Halbinger⋆, Benedikt Schneider and Björn Sbierski

Department of Physics and Arnold Sommerfeld Center for Theoretical Physics (ASC),
Ludwig-Maximilians-Universität München, Theresienstr. 37, München D-80333, Germany
Munich Center for Quantum Science and Technology (MCQST),
Schellingstr. 4, D-80799 München, Germany

⋆ johannes.halbinger@physik.uni-muenchen.de

Abstract

In the field of quantum many-body physics, the spectral (or Lehmann) representation simplifies the calculation of Matsubara n-point correlation functions if the eigensystem of a Hamiltonian is known. It is expressed via a universal kernel function and a system- and correlator-specific product of matrix elements. Here we provide the kernel functions in full generality, for arbitrary n, arbitrary combinations of bosonic or fermionic operators and an arbitrary number of anomalous terms. As an application, we consider bosonic 3- and 4-point correlation functions for the fermionic Hubbard atom and a free spin of length S, respectively.

Contents

1   Introduction

Multi-point correlation functions of n quantum mechanical operators, also known as n-point functions, are a central concept in the study of quantum many-body systems and field theory [1]. They generalize the well-known 2-point functions, which, for the example of electrons in the solid state, are routinely measured by scanning tunneling spectroscopy or angle-resolved photon emission spectroscopy [2]. For magnetic systems, the 2-point spin correlators can be probed in a neutron scattering experiment. Higher order correlation functions with $n = 3, 4, 5...$ can for example be measured in non-linear response settings [3]. In the emerging field of cold atomic quantum simulation, (equal-time) n-point functions are even directly accessible [4].

On the theoretical side the study of higher order correlation functions gains traction as well. One motivation is the existence of exact relations between correlation functions of different order n [5,6]. Although these exact relations can usually not be solved exactly, they form a valuable starting point for further methodological developments like the parquet approximation [7]. Thus even if the 4-point correlator (or, in that context, its essential part, the one-line irreducible vertex [1]) might not be the primary quantity of interest in a calculation, it appears as a building block of the method. Another example is the functional renormalization group method (fRG) in a vertex expansion [8,9]. It expresses the many body problem as a hierarchy of differential equations for the vertices that interpolate between a simple solvable starting point and the full physical theory [10]. Whereas experiments measure correlation functions in real time (or frequency), in theory one often is concerned with the related but conceptually simpler versions depending on imaginary time [1]. In the following, we will focus on these Matsubara correlation functions, which, nevertheless feature an intricate frequency dependence.

Whereas the above theoretical methods usually provide only an approximation for the n-point functions, an important task is to calculate these objects exactly. This should be possible for simple quantum many body systems. We consider systems simple if they are amenable to exact diagonalization (ED), i.e. feature a small enough Hilbert space, like few-site clusters of interacting quantum spins or fermions. Also impurity systems, where interactions only act locally, can be approximately diagonalized using the numerical renormalization group [11].

Knowing the exact n-point functions for simple systems is important for benchmark testing newly developed methods before deploying them to harder problems. Moreover, n-point functions for simple systems often serve as the starting point of further approximations like in the spin-fRG [12–14], or appear intrinsically in a method like in diagrammatic extensions of dynamical mean field theory [15] with its auxiliary impurity problems. Another pursuit enabled by the availability of exact n-point functions is to interpret the wealth of information encoded in these objects, in particular in their rich frequency structure. For example, Ref. [16] studied the fingerprints of local moment formation and Kondo screening in quantum impurity models.

In this work we complete the task to calculate exact n-point functions by generalizing the spectral (or Lehmann) representation [1,17] for Matsubara n-point correlation functions to arbitrary n. We assume that a set of eigenstates and -energies is given. Following pioneering work of Refs. [18–20] and in particular the recent approach by Kugler *et al.* [21], we split the problem of calculating imaginary frequency correlators into the computation of a universal kernel function and a system- and correlator-specific part (called partial spectral function in Ref. [21]). We provide the kernel functions in full generality for an arbitrary number n of bosonic or fermionic frequencies. Previously, these kernel functions were known exactly only up to the 3-point case [18], for the fermionic 4-point case [19–21] or for the general n-point case [21] but disregarding anomalous contributions to the sum that the kernel function con-

(a)
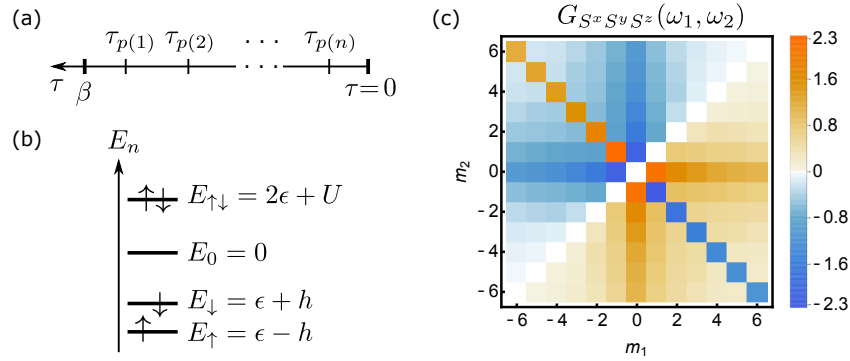
(c) $G_{S^x S^y S^z}(\omega_1, \omega_2)$

Figure 1: (a) Ordering convention for imaginary times in Eq. (9). (b) Eigenstates and energies of the Hubbard atom. (c) Matsubara correlation function $G_{S^x S^y S^z}(\omega_1, \omega_2)$ with $\omega_j = 2\pi m_j/\beta$ ($m_j \in \mathbb{Z}$, $j = 1, 2$) for the Hubbard atom (35) at $\beta = 10$, $h = 0.1$, $\epsilon = -2$, $U = 2$, see Eq. (45). The sharp anti-diagonal ray $\propto \delta_{\omega_1+\omega_2,0}$ represents an anomalous term of order $a = 1$. The other broadened rays become sharp and anomalous for $h \to 0$, see Eq. (49).

sists of. These anomalous contributions are at the heart of the complexity of Matsubara n-point functions. They occur when certain combinations of eigenenergies and external frequencies vanish individually, see the anti-diagonal rays in Fig. 1(c). Physically, they correspond to long-term memory effects, are related to non-ergodicity and, in the case of bosonic two-point functions reflect the difference between static isothermal susceptibilities and the zero-frequency limit of the dynamical Kubo response function [22, 23].

The structure of the paper is as follows: In Sec. 2 we define the Matsubara n-point function $G_{A_1...A_n}(\omega_1, ..., \omega_{n-1})$ and review some of its properties. The spectral representation is derived in Sec. 3 with Eq. (15) being the central equation written in terms of the kernel function $K_n(\Omega_1, ..., \Omega_{n-1})$. Our main result is an exact closed-form expression of this most general kernel function which is given in Sec. 4. Examples for $n = 2, 3, 4, 5$ are given in Sec. 5 where we also discuss simplifications for the purely fermionic case. We continue with applications to two particular systems relevant in the field of condensed matter theory: In Sec. 6, we consider the Hubbard atom and the free spin of length S, for which we compute n-point functions not previously available in the literature. We conclude in Sec. 7.

2 Definition of Matsubara n-point function $G_{A_1...A_n}(\omega_1, ..., \omega_n)$

We consider a set of $n = 2, 3, 4, ...$ operators $\{A_1, A_2, ..., A_n\}$ defined on the Hilbert space of a quantum many-body Hamiltonian H. The operators can be fermionic, bosonic or a combination of both types, with the restriction that there is an even number of fermionic operators. As an example, $A_1 = d^\dagger d \equiv n$, $A_2 = d$, $A_3 = d^\dagger$ where $d^\dagger$ and d are canonical fermionic creation and annihilation operators. A subset of operators is called bosonic if they create a closed algebra under the commutation operation. They are called fermionic if the algebra is closed under anti-commutation, see Sec. 1 of Ref. [24]. Spin operators are thus bosonic.

We define the imaginary time-ordered n-point correlation functions for imaginary times $\tau_k \in [0, \beta]$, [25, 26],

$$G_{A_1 A_2 ... A_n}(\tau_1, \tau_2, ..., \tau_n) \equiv \langle \mathcal{T} A_1(\tau_1) A_2(\tau_2) .. A_n(\tau_n) \rangle, \tag{1}$$

where $A_k(\tau_k) = e^{\tau_k H} A_k e^{-\tau_k H}$ denotes Heisenberg time evolution. Here and in the following, $k = 1, 2, ..., n$. The expectation value is calculated as $\langle ... \rangle = \text{tr}[\rho ...]$ where $\rho = \exp(-\beta H)/Z$

is the thermal density operator at inverse temperature $\beta = 1/T$ and $Z = \operatorname{tr}\exp(-\beta H)$ is the partition function. Note that other conventions for the n-point function differing by a prefactor are also used in the literature, e.g. Ref. [21] multiplies with $(-1)^{n-1}$. In Eq. (1), the imaginary time-ordering operator $\mathcal{T}$ orders the string of Heisenberg operators,

$$\mathcal{T}A_1(\tau_1)A_2(\tau_2)..A_n(\tau_n) \equiv \zeta(p)A_{p(1)}\big(\tau_{p(1)}\big)A_{p(2)}\big(\tau_{p(2)}\big)..A_{p(n)}\big(\tau_{p(n)}\big)\,, \tag{2}$$

where p is the permutation $p \in S_n$ such that $\tau_{p(1)} > \tau_{p(2)} > ... > \tau_{p(n)}$ [see Fig. 1(a)] and the sign $\zeta(p)$ is -1 if the operator string $A_{p(1)}A_{p(2)}..A_{p(n)}$ differs from $A_1A_2..A_n$ by an odd number of transpositions of fermionic operators, otherwise it is $+1$. The special case $n = 2$, with $\zeta(12) = 1$ and $\zeta(21) = \zeta$ ($\zeta = 1$ for $A_{1,2}$ bosonic, $\zeta = -1$ for $A_{1,2}$ fermionic), simplifies to

$$\mathcal{T}A_1(\tau_1)A_2(\tau_2) = \begin{cases} A_1(\tau_1)A_2(\tau_2)\,, & \tau_1 > \tau_2\,, \\ \zeta A_2(\tau_2)A_1(\tau_1)\,, & \tau_2 > \tau_1\,. \end{cases} \tag{3}$$

Imaginary time-ordered correlation functions (1) fulfill certain properties which we review in the following, see e.g. [26] for a more extensive discussion. First, they are invariant under translation of all time arguments,

$$G_{A_1A_2..A_n}(\tau_1, \tau_2, ..., \tau_n) = G_{A_1A_2..A_n}(\tau_1 + \tau, \tau_2 + \tau, ..., \tau_n + \tau)\,, \tag{4}$$

with $\tau \in \mathbb{R}$ such that $\tau_k + \tau \in [0, \beta]$. They also fulfill periodic or anti-periodic boundary conditions for the individual arguments τ_k,

$$G_{A_1..A_n}(\tau_1, ..., \tau_k = 0, ..., \tau_n) = \zeta_k G_{A_1..A_n}(\tau_1, ..., \tau_k = \beta, ..., \tau_n)\,, \tag{5}$$

where $\zeta_k = +1$ or -1 if A_k is from the bosonic or fermionic subset of operators, respectively. This motivates the use of a Fourier transformation,

$$G_{A_1..A_n}(\tau_1, ..., \tau_n) \equiv \beta^{-n} \sum_{\omega_1, ..., \omega_n} e^{-i(\omega_1\tau_1 + ... + \omega_n\tau_n)}G_{A_1..A_n}(\omega_1, ..., \omega_n)\,, \tag{6}$$

$$G_{A_1..A_n}(\omega_1, ..., \omega_n) = \int_0^\beta d\tau_1 \cdots \int_0^\beta d\tau_n\, e^{+i(\omega_1\tau_1 + ... + \omega_n\tau_n)}G_{A_1..A_n}(\tau_1, ..., \tau_n)\,, \tag{7}$$

where $\omega_k = 2\pi m_k/\beta$ or $\omega_k = 2\pi(m_k + 1/2)/\beta$ with $m_k \in \mathbb{Z}$ are bosonic or fermionic Matsubara frequencies, respectively, and $\sum_{\omega_k}$ is shorthand for $\sum_{m_k \in \mathbb{Z}}$. Note that fermionic Matsubara frequencies are necessarily nonzero, a property that will become important later. As we will not discuss the real-frequency formalisms, we will not write the imaginary unit in front of Matsubara frequencies in the arguments of $G_{A_1..A_n}(\omega_1, ..., \omega_n)$. Again, note that in the literature, different conventions for the Fourier transformation of n-point functions are in use. In particular some authors pick different signs in the exponent of Eq. (7) for fermionic creation and annihilation operators, or chose these signs depending on operator positions.

Time translational invariance (4) implies frequency conservation at the left hand side of Eq. (7),

$$G_{A_1..A_n}(\omega_1, ..., \omega_{n-1}, \omega_n) \equiv \beta \delta_{0, \omega_1 + ... + \omega_n} G_{A_1..A_n}(\omega_1, ..., \omega_{n-1})\,, \tag{8}$$

where on the right hand side we skipped the n-th frequency entry in the argument list of G. Note that we do not use a new symbol for the correlation function when we pull out the factor β and the Kronecker delta function.

3 Spectral representation of $G_{A_1...A_n}(\omega_1, ..., \omega_{n-1})$

The integrals involved in the Fourier transformation (7) generate all $n!$ different orderings of the time arguments τ_k. As in Ref. [21] it is thus convenient to use a sum over all $n!$ permutations $p \in S_n$ and employ a product of $n-1$ step-functions θ, with $\theta(x) = 1$ for $x > 0$ and 0 otherwise, to filter out the unique ordering for which $\beta > \tau_{p(1)} > \tau_{p(2)} > ... > \tau_{p(n-1)} > \tau_{p(n)} > 0$, see Fig. 1(a),

$$G_{A_1...A_n}(\tau_1, ..., \tau_n) = \sum_{p \in S_n} \zeta(p) \left[\prod_{i=1}^{n-1} \theta(\tau_{p(i)} - \tau_{p(i+1)}) \right] \langle A_{p(1)}(\tau_{p(1)}) A_{p(2)}(\tau_{p(2)}) ... A_{p(n)}(\tau_{p(n)}) \rangle . \quad (9)$$

To expose explicitly the time dependence of the Heisenberg operators, we insert n times the basis of eigenstates and -energies of the many-body Hamiltonian H. Instead of the familiar notation $|j_1\rangle, |j_2\rangle, ...$ and $E_{j_1}, E_{j_2}, ...$ we employ $|\underline{1}\rangle, |\underline{2}\rangle, ...$ and $E_{\underline{1}}, E_{\underline{2}}, ...$ for compressed notation and denote operator matrix elements as $A^{\underline{1}\,\underline{2}} = \langle \underline{1}|A|\underline{2} \rangle$. We obtain

$$G_{A_1...A_n}(\tau_1, ..., \tau_n) = \sum_{p \in S_n} \zeta(p) \left[\prod_{i=1}^{n-1} \theta(\tau_{p(i)} - \tau_{p(i+1)}) \right] \quad (10)$$

$$\times \frac{1}{Z} \sum_{\underline{1}...\underline{n}} e^{-\beta E_{\underline{1}}} e^{\tau_{p(1)} E_{\underline{1}}} A_{p(1)}^{\underline{1}\,\underline{2}} e^{(-\tau_{p(1)} + \tau_{p(2)}) E_{\underline{2}}} A_{p(2)}^{\underline{2}\,\underline{3}} e^{(-\tau_{p(2)} + \tau_{p(3)}) E_{\underline{3}}} ... e^{(-\tau_{p(n-1)} + \tau_{p(n)}) E_{\underline{n}}} A_{p(n)}^{\underline{n}\,\underline{1}} e^{-\tau_{p(n)} E_{\underline{1}}},$$

and apply the Fourier transform according to the definition (7),

$$G_{A_1...A_n}(\omega_1, ..., \omega_n) = \frac{1}{Z} \sum_{p \in S_n} \zeta(p) \sum_{\underline{1}...\underline{n}} e^{-\beta E_{\underline{1}}} A_{p(1)}^{\underline{1}\,\underline{2}} A_{p(2)}^{\underline{2}\,\underline{3}} ... A_{p(n)}^{\underline{n}\,\underline{1}} \quad (11)$$

$$\times \left[\int_0^\beta d\tau_{p(1)} e^{\Omega_{p(1)}^{\underline{1}\,\underline{2}} \tau_{p(1)}} \right] \left[\int_0^{\tau_{p(1)}} d\tau_{p(2)} e^{\Omega_{p(2)}^{\underline{2}\,\underline{3}} \tau_{p(2)}} \right]$$

$$\times \cdots \times \left[\int_0^{\tau_{p(n-2)}} d\tau_{p(n-1)} e^{\Omega_{p(n-1)}^{\underline{n-1}\,\underline{n}} \tau_{p(n-1)}} \right] \left[\int_0^{\tau_{p(n-1)}} d\tau_{p(n)} e^{\Omega_{p(n)}^{\underline{n}\,\underline{1}} \tau_{p(n)}} \right],$$

where we defined

$$\Omega_k^{\underline{a}\,\underline{b}} \equiv i\omega_k + E_{\underline{a}} - E_{\underline{b}} \in \mathbb{C}. \quad (12)$$

In Eq. (11), the first line carries all the information of the system and the set of operators $\{A_1, A_2, ..., A_n\}$. The remaining terms can be regarded as a universal kernel function defined for general $\{\Omega_1, \Omega_2, ..., \Omega_n\}$ probed at $\Omega_k \in \mathbb{C}$ which depends on the system and correlators via (12). Upon renaming the τ-integration variables $\tau_{p(k)} \to \tau_k$, this kernel function is written as follows:

$$\mathcal{K}_n(\Omega_1, ..., \Omega_n) \equiv \left[\int_0^\beta d\tau_1 e^{\Omega_1 \tau_1} \right] \left[\int_0^{\tau_1} d\tau_2 e^{\Omega_2 \tau_2} \right] ... \left[\int_0^{\tau_{n-2}} d\tau_{n-1} e^{\Omega_{n-1} \tau_{n-1}} \right] \left[\int_0^{\tau_{n-1}} d\tau_n e^{\Omega_n \tau_n} \right]$$

$$(13)$$

$$\equiv \beta \delta_{0, \Omega_1 + \Omega_2 + ... + \Omega_n} K_n(\Omega_1, ..., \Omega_{n-1}) + R_n(\Omega_1, ..., \Omega_n). \quad (14)$$

In the second line we split $\mathcal{K}_n$ into a part K_n proportional to $\beta \delta_{0, \Omega_1 + \Omega_2 + ... + \Omega_n}$ and the rest R_n. We dropped Ω_n from the argument list of K_n which can be reconstructed from $\{\Omega_1, ..., \Omega_{n-1}\}$.

Finally, we express $G_{A_1...A_n}(\omega_1, ..., \omega_n)$ of Eq. (11) using the kernel $\mathcal{K}_n$ so that the general $\Omega_k \in \mathbb{C}$ get replaced by $\Omega_k^{\underline{a}\,\underline{b}}$ of Eq. (12). For these, $\Omega_{p(1)}^{\underline{1}\,\underline{2}} + \Omega_{p(2)}^{\underline{2}\,\underline{3}} + ... + \Omega_{p(n)}^{\underline{n}\,\underline{1}} = i(\omega_1 + \omega_2 + ... + \omega_n)$,

since the E_k cancel pairwise. The structure of Eq. (8) (which followed from time translational invariance) implies that the terms proportional to R_n are guaranteed to cancel when summed over permutations $p \in S_n$, so that only the terms proportional to K_n remain. We drop the $\beta \delta_{0,\omega_1+\omega_2+...+\omega_n}$ from both sides [c.f. Eq. (8)] and find the spectral representation of the n-point correlation function in the Matsubara formalism,

$$G_{A_1...A_n}(\omega_1,...,\omega_{n-1}) = \frac{1}{Z} \sum_{p \in S_n} \zeta(p) \sum_{\underline{1}...\underline{n}} e^{-\beta E_1} A^{12}_{p(1)} A^{23}_{p(2)}...A^{n1}_{p(n)} \times K_n\left(\Omega^{12}_{p(1)}, \Omega^{23}_{p(2)}, ..., \Omega^{n-1\,n}_{p(n-1)}\right). \quad (15)$$

An equivalent expression was derived in the literature before [21], see also Refs. [18–20] for the cases of certain small n. However, kernel functions K_n where previously only known approximately, for situations involving only a low order of anomalous terms, see the discussion in Sec. 5. We define an *anomalous* term of order $a = 1, 2, ... n-1$ as a summand contributing to $K_n(\Omega_1,...,\Omega_{n-1})$ that contains a product of a Kronecker delta functions $\delta_{0,x}$, where x is a sum of a subset of $\{\Omega_1,...,\Omega_{n-1}\}$. As can be seen in Fig. 1(c), these anomalous contributions to $G_{A_1...A_n}(\omega_1,...,\omega_{n-1})$ correspond to qualitatively important sharp features.

In the next section, we present a simple, exact expression for general $K_n(\Omega_1,...,\Omega_{n-1})$. Readers not interested in the derivation can directly skip to the result in Eq. (26) or its explicit form for $n = 2, 3, 4, 5$ in Sec. 5.

4 General kernel function $K_n\left(\Omega_1,...,\Omega_{n-1}\right)$

Assuming the spectrum and matrix elements entering Eq. (15) are known, the remaining task is to find expressions for the kernel function $K_n(\Omega_1,...,\Omega_{n-1})$ defined via Eqns. (13) and (14) as the part of $\mathcal{K}_n(\Omega_1,\Omega_2,...,\Omega_n)$ multiplying $\beta \delta_{0,\Omega_1+\Omega_2+...+\Omega_n}$. To facilitate the presentation in this section, in Eq. (13) we rename the integration variables $\tau_k \to \tau_{n-k+1}$ and define new arguments $z_{n-j+1} = \Omega_j$ for $j = 1, 2, ..., n-1$,

$$\mathcal{K}_n(\Omega_1 = z_n, \Omega_2 = z_{n-1}, ..., \Omega_n = z_1)$$

$$= \left[\int_0^\beta d\tau_n e^{z_n \tau_n}\right]\left[\int_0^{\tau_n} d\tau_{n-1} e^{z_{n-1}\tau_{n-1}}\right]...\left[\int_0^{\tau_3} d\tau_2 e^{z_2 \tau_2}\right]\left[\int_0^{\tau_2} d\tau_1 \underbrace{e^{z_1 \tau_1}}_{\equiv h_1(\tau_1)}\right] \quad (16)$$

$$\underbrace{\phantom{\left[\int_0^{\tau_2} d\tau_1 e^{z_1\tau_1}\right]}}_{\equiv h_2(\tau_2)}$$

$$= \beta \delta_{0,z_1+z_2+...+z_n} K_n(z_n, z_{n-1}, ..., z_2) + R_n(z_n, z_{n-1}, ..., z_1). \quad (17)$$

As indicated in Eq. (16), we call $h_k(\tau_k)$ the integrand for the $\int_0^{\tau_{k+1}} d\tau_k$ integral for $k = 1, 2, ..., n$. At $k = 1$ this integrand is given by $h_1(\tau_1) = e^{z_1 \tau_1}$ and we will find h_k for $k = 2, 3, ..., n$ iteratively. For $z \in \mathbb{C}$, we define the abbreviations $\delta_z \equiv \delta_{0,z}$ and

$$\Delta_z \equiv \begin{cases} 0, & \text{if } z = 0, \\ \frac{1}{z}, & \text{if } z \neq 0, \end{cases} \quad (18)$$

and consider the integral (for $p = 0, 1, 2, ...$ and $\tilde{\tau} \geq 0$, proof by partial integration and induction)

$$\int_0^{\tilde{\tau}} d\tau \, \tau^p e^{z\tau} = \left[\frac{\tilde{\tau}^{p+1}}{p+1}\delta_z + p!(-1)^p \Delta_z^{1+p} \sum_{l=0}^p \frac{(-1)^l}{l!} \Delta_z^{-l} \tilde{\tau}^l\right] e^{z\tilde{\tau}} - p!(-1)^p \Delta_z^{p+1}. \quad (19)$$

Recall that we are only interested in the contribution $K_n(z_n, z_{n-1}, ..., z_2)$ that fulfills frequency conservation, see Eq. (17). The $\delta_{z_1+z_2+...+z_n}$ in front of this term arises from the final τ_n integration of $h_n(\tau_n) \propto e^{(z_1+z_2+...+z_n)\tau_n}$ via the first term in Eq. (19). This however requires

that all z_k (except the vanishing ones, of course) remain in the exponent during the iterative integrations. This requirement is violated by the last term in the general integral (19) (which comes from the lower boundary of the integral). All terms in $\mathcal{K}_n$ that stem from this last term in Eq. (19) thus contribute to R_n and can be dropped in the following [21]. Note however, that it is straightforward to generalize our approach and keep these terms if the full $\mathcal{K}_n$ is required.

To define the iterative procedure to solve the n-fold integral in Eq. (16), we make the ansatz

$$h_k(\tau_k) = \sum_{l=0}^{k-1} f_k(l)\tau_k^l e^{(z_k+z_{k-1}+...+z_1)\tau_k}, \tag{20}$$

which follows from the form of the integral (19) and our decision to disregard the terms contributing to R_n. The ansatz (20) is parameterized by the numbers $f_k(l)$ with $l = 0, 1, ..., k-1$. These numbers have to be determined iteratively, starting from $f_{k=1}(l = 0) = 1$, read off from $h_1(\tau_1) = e^{z_1\tau_1}$, c.f. Eq. (16). Iteration rules to obtain the $f_k(l)$ from $f_{k-1}(l)$ are easily derived from Eqns. (16), (19) and (20). We obtain the recursion relation

$$f_k(l) = \sum_{p=0}^{k-1} \tilde{M}_{k-1}(l,p)f_{k-1}(p). \tag{21}$$

This can be understood as a matrix-vector product of $\mathbf{f}_{k-1} = (f_{k-1}(0), f_{k-1}(1), ..., f_{k-1}(k-2))^{\mathrm{T}}$ with the $k \times (k-1)$-matrix

$$\tilde{M}_{k-1}(l,p) = \frac{p!}{l!}\left[\delta_{l,p+1}\tilde{\delta}_{k-1} + \theta(p-l+1/2)(-1)^{l+p}\tilde{\Delta}_{k-1}^{1+p-l}\right], \tag{22}$$

where $\tilde{\Delta}_k \equiv \Delta_{z_k+...+z_2+z_1}$, $\tilde{\delta}_k \equiv \delta_{z_k+...+z_2+z_1}$. The tilde on top of the $\tilde{\delta}_k$ and $\tilde{\Delta}_k$ signals the presence of a sum of z_j in the arguments (below we will define related quantities without tilde for the sum of Ω_j). Note that the first (second) term in brackets of Eq. (22) comes from the first (second) term in square brackets of Eq. (19).

The next step is to find $K_n(z_n, z_{n-1}, ..., z_2)$. This requires to do the integral $\int_0^\beta d\tau_n h_n(\tau_n)$ which can be again expressed via Eq. (19) but with the replacement $\tilde{\tau} \to \beta$. Only the first term provides a $\beta\delta_{z_1+z_2+...+z_n}$ and is thus identified with K_n. We find:

$$K_n(z_n, z_{n-1}, ..., z_2) = \sum_{l=0}^{n-1} \frac{\beta^l f_n(l)}{l+1}. \tag{23}$$

The argument z_1 that the right hand side of Eq. (23) depends on is to be replaced by $z_1 = -z_2 - z_3 - ... - z_n$, in line with the arguments in $K_n(z_n, z_{n-1}, ..., z_2)$. Then, to conform with Eq. (15), we reinstate $\Omega_j = z_{n-j+1}$ for $j = 1, 2, ..., n-1$. This amounts to replacing the terms $\tilde{\delta}_j$ and $\tilde{\Delta}_j$ that appear in $f_n(l)$ as follows,

$$\tilde{\delta}_j = \delta_{z_j+...+z_2+z_1} = \delta_{\Omega_1+\Omega_2+...+\Omega_{n-j}} \equiv \delta_{n-j}, \tag{24}$$

$$-\tilde{\Delta}_j = -\Delta_{z_j+...+z_2+z_1} = \Delta_{\Omega_1+\Omega_2+...+\Omega_{n-j}} \equiv \Delta_{n-j}, \tag{25}$$

where we used $\Omega_1 + \Omega_2 + ... + \Omega_n = 0 = z_n + ... + z_2 + z_1$. Finally, we can express Eq. (23) using a product of $n-1$ matrices $\tilde{M}$ multiplying the initial length-1 vector with entry $f_1(0) = 1$. Transferring to the Ω-notation by using Eqns. (24) and (25), we obtain

$$\begin{aligned}
&K_n(\Omega_1, ..., \Omega_{n-1}) \\
&= \sum_{i_{n-1}=0}^{n-1}\sum_{i_{n-2}=0}^{n-2}\cdots\sum_{i_2=0}^{2}\sum_{i_1=0}^{1}\frac{\beta^{i_{n-1}}}{i_{n-1}+1}M_1(i_{n-1},i_{n-2})M_2(i_{n-2},i_{n-3})\cdots M_{n-2}(i_2,i_1)M_{n-1}(i_1,0),
\end{aligned} \tag{26}$$

with

$$M_j(l,p) \equiv \frac{p!}{l!}\left[\delta_{l,p+1}\delta_j - \theta\left(p-l+1/2\right)\Delta_j^{1+p-l}\right].$$ (27)

The closed form expression (26) of the universal kernel, to be used in the spectral representation (15), is our main result. By definition it is free of any singularities as the case of vanishing denominators is explicitly excluded in Eq. (18).

5 Explicit kernel functions $K_n(\Omega_1,...,\Omega_{n-1})$ for $n = 2, 3, 4, 5$

While the previous section gives a closed form expression for kernel functions of arbitrary order, we here evaluate the universal kernel functions $K_n(\Omega_1,...,\Omega_{n-1})$ defined in Eq. (14) from Eq. (26) for $n = 2, 3, 4, 5$ and show the results in Tab. 1. In each column, the kernel function in the top row is obtained by first multiplying the entries listed below it in the same column by the common factor in the rightmost column and then taking the sum. The symbols δ_j and Δ_j for $j = 1, 2, ..., n-1$ which appear in Tab. 1 are defined by

$$\delta_j \equiv \delta_{\Omega_1+\Omega_2+...+\Omega_j,0},$$ (28)

$$\Delta_j \equiv \Delta_{\Omega_1+\Omega_2+...+\Omega_j} \equiv \begin{cases} 0, & \text{if } \Omega_1+\Omega_2+...+\Omega_j=0, \\ \frac{1}{\Omega_1+\Omega_2+...+\Omega_j}, & \text{if } \Omega_1+\Omega_2+...+\Omega_j\neq 0, \end{cases}$$ (29)

compare also to the previous section. As an example, for $n = 2$ and $n = 3$ we obtain from Tab. 1

$$K_2(\Omega_1) = -\Delta_{\Omega_1} + \frac{\beta}{2}\delta_{\Omega_1},$$ (30)

$$K_3(\Omega_1,\Omega_2) = +\Delta_{\Omega_1}\Delta_{\Omega_1+\Omega_2} - \frac{\beta}{2}\delta_{\Omega_1}\Delta_{\Omega_2} - \Delta_{\Omega_1}\delta_{\Omega_1+\Omega_2}\left(\frac{\beta}{2}+\Delta_{\Omega_1}\right) + \delta_{\Omega_1}\delta_{\Omega_2}\frac{\beta}{2}\frac{\beta}{3},$$ (31)

respectively. The rows of Tab. 1 are organized with respect to the number a of factors δ_l in the summands. Here, $a = 0$ indicates the regular part and $a = 1, 2, ..., n-1$ indicates anomalous terms. There are $n-1$ *choose* a anomalous terms of order a. Our results are exact and go substantially beyond existing expressions in the literature – these are limited to $n \leq 3$ [18] or to fermionic $n = 4$ [19–21] with $a = 0, 1$ (and $a = 2, 3$ guaranteed to vanish, see below) or arbitrary n with $a = 0$ [21]. Alternative expressions for the $n = 3, 4$ kernel functions with $a \leq 1$ were given in [21], but they are consistent with our kernel functions as they yield the same correlation functions, see the Appendix.

In the case of purely fermionic correlators (all A_k fermionic), individual Matsubara frequencies ω_k cannot be zero and thus the $\Omega_k^{\underline{a}\,\underline{b}} \equiv i\omega_k + E_{\underline{a}} - E_{\underline{b}}$ of Eq. (12) always have a finite imaginary part and are non-zero, regardless of the eigenenergies. In this case, only sums of an even number of frequencies can be zero, and we can simplify $\delta_1 = \delta_3 = \delta_5 = ... = 0$. The expressions for the kernels in Tab. 1, now denoted by $K_n|_F$ for the fermionic case, simplify to

$$K_2(\Omega_1)|_F = -\Delta_1,$$ (32)

$$K_4(\Omega_1,\Omega_2,\Omega_3)|_F = \Delta_1\Delta_3\left[\delta_2\left(\frac{\beta}{2}+\Delta_1\right)-\Delta_2\right],$$ (33)

$$K_6(\Omega_1,...,\Omega_5)|_F = \Delta_1\Delta_3\Delta_5\left\{-\Delta_2\Delta_4 - \delta_2\delta_4\left[\frac{\beta}{2}\frac{\beta}{3}+(\Delta_1+\Delta_3)\left(\frac{\beta}{2}+\Delta_1\right)\right]\right.$$ (34)

$$\left. +\delta_4\Delta_2\left(\frac{\beta}{2}+\Delta_1+\Delta_2+\Delta_3\right)+\delta_2\Delta_4\left(\frac{\beta}{2}+\Delta_1\right)\right\}.$$

Table 1: Universal kernel functions $K_n(\Omega_1, ..., \Omega_{n-1})$ for $n = 2, 3, 4, 5$ defined in Eq. (14) and calculated from Eq. (26) in Sec. 4. In each column, the kernel function in the top row is obtained by first multiplying the entries listed below it in the same column by the common factor in the rightmost column and then taking the sum, see Eqns. (30) and (31) as examples. The symbols δ_j and Δ_j appearing are defined in Eqns. (28) and (29). The rows are organized with respect to the number a of appearances of δ_j, i.e. the order of the anomalous terms.

#anom.	$K_2(\Omega_1)$	$K_3(\Omega_1,\Omega_2)$	$K_4(\Omega_1,\Omega_2,\Omega_3)$	$K_5(\Omega_1,\Omega_2,\Omega_3,\Omega_4)$	factor for entire row
$a=0$	$-\Delta_1$	$+\Delta_1\Delta_2$	$-\Delta_1\Delta_2\Delta_3$	$+\Delta_1\Delta_2\Delta_3\Delta_4$	1
	$+\delta_1$	$-\delta_1\Delta_2$	$+\delta_1\Delta_2\Delta_3$	$-\delta_1\Delta_2\Delta_3\Delta_4$	$\frac{\beta}{2}$
		$-\Delta_1\delta_2$	$+\Delta_1\delta_2\Delta_3$	$-\Delta_1\delta_2\Delta_3\Delta_4$	$\frac{\beta}{2}+\Delta_1$
$a=1$			$+\Delta_1\Delta_2\delta_3$	$-\Delta_1\Delta_2\delta_3\Delta_4$	$\frac{\beta}{2}+\Delta_1+\Delta_2$
				$-\Delta_1\Delta_2\Delta_3\delta_4$	$\frac{\beta}{2}+\Delta_1+\Delta_2+\Delta_3$
		$+\delta_1\delta_2$	$-\delta_1\delta_2\Delta_3$	$+\delta_1\delta_2\Delta_3\Delta_4$	$\frac{\beta}{2}\frac{\beta}{3}$
			$-\delta_1\Delta_2\delta_3$	$+\delta_1\Delta_2\delta_3\Delta_4$	$\frac{\beta}{2}\left(\frac{\beta}{3}+\Delta_2\right)$
$a=2$			$-\Delta_1\delta_2\delta_3$	$+\Delta_1\delta_2\delta_3\Delta_4$	$\frac{\beta}{2}\frac{\beta}{3}+\Delta_1\left(\frac{\beta}{2}+\Delta_1\right)$
				$+\delta_1\Delta_2\Delta_3\delta_4$	$\frac{\beta}{2}\left(\frac{\beta}{3}+\Delta_2+\Delta_3\right)$
				$+\Delta_1\delta_2\Delta_3\delta_4$	$\frac{\beta}{2}\frac{\beta}{3}+(\Delta_1+\Delta_3)\left(\frac{\beta}{2}+\Delta_1\right)$
				$+\Delta_1\Delta_2\delta_3\delta_4$	$\frac{\beta}{2}\frac{\beta}{3}+(\Delta_1+\Delta_2)\left(\frac{\beta}{2}+\Delta_2\right)+\Delta_1^2$
			$+\delta_1\delta_2\delta_3$	$-\delta_1\delta_2\delta_3\Delta_4$	$\frac{\beta}{2}\frac{\beta}{3}\frac{\beta}{4}$
$a=3$				$-\delta_1\delta_2\Delta_3\delta_4$	$\frac{\beta}{2}\frac{\beta}{3}\left(\frac{\beta}{4}+\Delta_3\right)$
				$-\delta_1\Delta_2\delta_3\delta_4$	$\frac{\beta}{2}\left(\frac{\beta}{3}\frac{\beta}{4}+\Delta_2\left(\frac{\beta}{3}+\Delta_2\right)\right)$
				$-\Delta_1\delta_2\delta_3\delta_4$	$\frac{\beta}{2}\frac{\beta}{3}\frac{\beta}{4}+\Delta_1\left(\frac{\beta}{2}\frac{\beta}{3}+\Delta_1\left(\frac{\beta}{2}+\Delta_1\right)\right)$
$a=4$				$+\delta_1\delta_2\delta_3\delta_4$	$\frac{\beta}{2}\frac{\beta}{3}\frac{\beta}{4}\frac{\beta}{5}$

This concludes the general part of this work. Next, we consider two example systems frequently discussed in the condensed matter theory literature. Using our formalism, we provide analytical forms of correlation functions that to the best of our knowledge were not available before.

6 Applications: Hubbard atom and free spin

6.1 Fermionic Hubbard atom

The Hubbard atom (HA) describes an isolated impurity or otherwise localized system with Hamiltonian

$$H = \epsilon\left(n_\uparrow + n_\downarrow\right) + U n_\uparrow n_\downarrow - h\left(n_\uparrow - n_\downarrow\right), \tag{35}$$

see Fig. 1(b) for a sketch. The HA corresponds to the limit of vanishing system-bath coupling of the Anderson impurity model (AIM), or vanishing hopping in the Hubbard model (HM). The particle number operators $n_\sigma = d_\sigma^\dagger d_\sigma$ count the number of fermionic particles with spin $\sigma \in \{\uparrow, \downarrow\}$, each contributing an onsite energy ϵ shifted by an external magnetic field h in z-direction. An interaction energy U is associated to double occupation.

Due to its simplicity and the four-dimensional Hilbert space, the correlation functions for the HA can be found analytically using the spectral representation. It is therefore often used for benchmarking [3, 27, 28]. The presence of the interaction term leads to a non-vanishing $n = 4$ one-line irreducible vertex function. The HA serves as an important reference point to study and interpret properties of the AIM and HM beyond the one-particle level, for example diver-

gences of two-line irreducible vertex functions [29–32] and signatures of the local moment formation in generalized susceptibilities [16, 33]. Using the fermionic kernels in Eqns. (32) and (33), we have checked that our formalism reproduces the results for the 2-point and 4-point correlators given in Refs. [19, 21, 26] for half-filling, $\epsilon = -U/2$ and $h = 0$.

Correlation functions including bosonic operators describe the asymptotic behaviour of the $n = 4$ fermion vertex for large frequencies [34] or the interaction of electrons by the exchange of an effective boson [35, 36]. These relations involve correlation functions of two bosonic operators or of one bosonic and two fermionic operators, giving rise to expressions possibly anomalous in at most one frequency argument, i.e. $a \leq 1$.

For the HA, AIM and HM, bosonic correlation functions for $n > 2$ have not been considered thoroughly so far. Only recently, steps in this direction were taken, particularly in the context of non-linear response theory [3]. The response of a system to first and second order in an external perturbation is described by 2- and 3-point correlation functions, respectively. For the HA, physically motivated perturbations affect the onsite energy via a term $\delta_\epsilon n$ or take the form of a magnetic field $\boldsymbol{\delta}_h \cdot \mathbf{S}$. Here, the parameters δ_ϵ and $\boldsymbol{\delta}_h$ denote the strength of the perturbation and we define

$$n = n_\uparrow + n_\downarrow, \qquad S^x = \frac{1}{2}\left(d_\uparrow^\dagger d_\downarrow + d_\downarrow^\dagger d_\uparrow\right), \quad S^y = \frac{-i}{2}\left(d_\uparrow^\dagger d_\downarrow - d_\downarrow^\dagger d_\uparrow\right), \quad S^z = \frac{1}{2}\left(n_\uparrow - n_\downarrow\right). \tag{36}$$

The resulting changes of the expectation values of the density or magnetization in arbitrary direction are described in second order of the perturbation by the connected parts of the correlation functions $G_{A_1 A_2 A_3}(\tau_1, \tau_2, \tau_3)$, with $A_i \in \{n, S_x, S_y, S_z\}$, where the time-ordered expectation value is evaluated with respect to the unperturbed system (35) and Fourier transformed to the frequencies of interest. These objects have been studied numerically in Ref. [3]. In the following, we give explicit, analytic expressions of the full correlation functions $G_{A_1 A_2 A_3}(\omega_1, \omega_2)$ (i.e. including disconnected parts), for arbitrary parameters ϵ, U and h and for all possible operator combinations using the (bosonic) kernel function K_3, see Eq. (31). To the best of our knowledge, these expressions have not been reported before.

The eigenstates of the HA Hamiltonian (35) [see Fig. 1(b)] describe an empty ($|0\rangle$), singly occupied ($d_\uparrow^\dagger|0\rangle = |\uparrow\rangle$, $d_\downarrow^\dagger|0\rangle = |\downarrow\rangle$) or doubly occupied ($d_\uparrow^\dagger d_\downarrow^\dagger|0\rangle = |\uparrow\downarrow\rangle$) impurity with eigenenergies $E_0 = 0$, $E_\uparrow = \epsilon - h$, $E_\downarrow = \epsilon + h$ and $E_{\uparrow\downarrow} = 2\epsilon + U$, respectively. The partition function is $Z = 1 + e^{-\beta(\epsilon-h)} + e^{-\beta(\epsilon+h)} + e^{-\beta(2\epsilon+U)}$. We define

$$s = \frac{e^{-\beta\epsilon}}{Z}\sinh(\beta h), \qquad c = \frac{e^{-\beta\epsilon}}{Z}\cosh(\beta h), \tag{37}$$

and obtain all non-vanishing bosonic 3-point correlation functions (where $\omega_3 = -\omega_1 - \omega_2$):

$$G_{nnn}(\omega_1, \omega_2) = 2\beta^2 \delta_{\omega_1}\delta_{\omega_2}\left(\frac{4e^{-\beta(2\epsilon+U)}}{Z} + c\right), \tag{38}$$

$$G_{nnS^z}(\omega_1, \omega_2) = \beta^2 \delta_{\omega_1}\delta_{\omega_2}s, \tag{39}$$

$$G_{nS^x S^y}(\omega_1, \omega_2) = -\beta \delta_{\omega_1}s\frac{\omega_2}{\omega_2^2 + 4h^2}, \tag{40}$$

$$G_{nS^x S^x}(\omega_1, \omega_2) = G_{nS^y S^y}(\omega_1, \omega_2) = 2\beta \delta_{\omega_1}\frac{h\,s}{\omega_2^2 + 4h^2}, \tag{41}$$

$$G_{nS^z S^z}(\omega_1, \omega_2) = \frac{\beta^2}{2}\delta_{\omega_1}\delta_{\omega_2}c, \tag{42}$$

$$G_{S^z S^x S^x}(\omega_1, \omega_2) = G_{S^z S^y S^y}(\omega_1, \omega_2) = -s\frac{\omega_2\omega_3 + 4h^2}{(\omega_2^2 + 4h^2)(\omega_3^2 + 4h^2)} + \beta \delta_{\omega_1}\frac{h\,c}{\omega_2^2 + 4h^2}, \tag{43}$$

$$G_{S^z S^z S^z}(\omega_1, \omega_2) = \frac{\beta^2}{4} \delta_{\omega_1} \delta_{\omega_2} s, \tag{44}$$

$$G_{S^x S^y S^z}(\omega_1, \omega_2) = 2h\, s\, \frac{\omega_1 - \omega_2}{(\omega_1^2 + 4h^2)(\omega_2^2 + 4h^2)} - \frac{\beta}{2} \delta_{\omega_3} c \frac{\omega_1}{\omega_1^2 + 4h^2}. \tag{45}$$

We observe that each conserved quantity, in this case n and S_z, contributes an anomalous term $\propto \delta_{\omega_k}$ in its respective frequency argument ω_k. If an operator A_k is conserved $[H, A_k] = 0$, the basis over which we sum in Eq. (15) can be chosen such that both H and A_k are diagonal, $A_k^{12} = A_k^{11} \delta_{1,2}$. If $A_k^{11} \neq 0$ for some state $|\underline{1}\rangle$ the vanishing eigenenergy difference leads to the appearance of an anomalous contribution. If the operators in the correlator additionally commute with each other, in our case for example $[n, S^z] = 0$, there exists a basis in which all operators and the Hamiltonian are diagonal, giving rise to correlation functions anomalous in all frequency arguments.

In the limit of vanishing field $h \to 0$, we introduce an additional degeneracy $E_\uparrow = E_\downarrow = \epsilon$ in the system, potentially resulting in additional anomalous contributions. The corresponding correlation functions can then be obtained in two ways. Either we recompute them using the kernel function K_3 or we take appropriate limits, for example

$$\lim_{h \to 0} \frac{h\, \sinh(\beta h)}{\omega_k^2 + 4h^2} = \frac{\beta}{4} \delta_{\omega_k}, \tag{46}$$

resulting in

$$G_{nnn}(\omega_1, \omega_2) = \beta^2 \delta_{\omega_1} \delta_{\omega_2} \frac{2\left(4e^{-\beta(2\epsilon + U)} + e^{-\beta \epsilon}\right)}{Z}, \tag{47}$$

$$G_{nS^\alpha S^\alpha}(\omega_1, \omega_2) = \beta^2 \delta_{\omega_1} \delta_{\omega_2} \frac{e^{-\beta \epsilon}}{2Z} \quad (\alpha \in \{x, y, z\}), \tag{48}$$

$$G_{S^x S^y S^z}(\omega_1, \omega_2) = \beta \frac{e^{-\beta \epsilon}}{2Z} \left(-\delta_{\omega_1} \Delta_{\omega_2} + \delta_{\omega_2} \Delta_{\omega_1} - \delta_{\omega_1 + \omega_2} \Delta_{\omega_1}\right), \tag{49}$$

with all other correlation functions vanishing. As already pointed out in Ref. [3], only the last correlation function retains a nontrivial frequency dependence due to non-commuting operators.

6.2 Free spin S

We now consider correlation functions of a free spin of length S, without a magnetic field, so that temperature $T = 1/\beta$ is the only energy scale. The operators $\{S^\alpha\}_{\alpha = x,y,z}$ fulfill $S^x S^x + S^y S^y + S^z S^z = S(S+1)$ and the SU(2) algebra $[S^{\alpha_1}, S^{\alpha_2}] = i \sum_{\alpha_3 = \{x,y,z\}} \epsilon^{\alpha_1 \alpha_2 \alpha_3} S^{\alpha_3}$, thus they are bosonic. Since the Hamiltonian vanishes and therefore all eigenenergies are zero, every $\Omega_k^{\underline{a}\,\underline{b}}$ in the spectral representation (15) can vanish and a proper treatment of all anomalous terms is essential. As the Heisenberg time dependence is trivial, $S^\alpha(\tau) = S^\alpha$, the non-trivial frequency dependence of the correlators, which can be non-vanishing at any order $n > 1$, derives solely from the action of imaginary time-ordering.

The correlators are required, for example, as the non-trivial initial condition for the spin-fRG recently suggested by Kopietz et al., Refs. [13, 37–40]. However, for $n > 3$ they are so far only partially available: They are either given for restricted frequency combinations, or for the purely classical case $S^{\alpha_1} = S^{\alpha_2} = ... = S^{\alpha_n}$ where the SU(2) algebra does not matter, or for finite magnetic field via an equation of motion [37] or diagrammatic approach [41, 42].

Table 2: Matsubara correlation functions for a free spin-S up to order $n = 4$. Here, $\omega_4 = -\omega_1 - \omega_2 - \omega_3$.

$n = 2$	$G_{S^+S^-}(\omega) = G_{S^zS^z}(\omega) = \beta\delta_\omega b_1$
$n = 3$	$G_{S^+S^-S^z}(\omega_1, \omega_2) = \beta b_1(-\delta_{\omega_1}\Delta_{i\omega_2} + \delta_{\omega_2}\Delta_{i\omega_1} + \delta_{\omega_1+\omega_2}\Delta_{i\omega_2}) = -iG_{S^xS^yS^z}(\omega_1, \omega_2)$

$n = 4$

$$G_{S^zS^zS^zS^z}(\omega_1, \omega_2, \omega_3) = \delta_{\omega_1}\delta_{\omega_2}\delta_{\omega_3}\beta^3 b_3$$

$$G_{S^+S^+S^-S^-}(\omega_1, \omega_2, \omega_3) = \beta b_1[2 \times \delta_{\omega_1}\delta_{\omega_2}\delta_{\omega_3} \times \tfrac{\beta^2}{5}\left(3b_1 - \tfrac{1}{3}\right) + r]$$

$$G_{S^+S^-S^zS^z}(\omega_1, \omega_2, \omega_3) = \beta b_1[1 \times \delta_{\omega_1}\delta_{\omega_2}\delta_{\omega_3} \times \tfrac{\beta^2}{5}\left(3b_1 - \tfrac{1}{3}\right) - r]$$

$$r = \Delta_{i\omega_1}\Delta_{i\omega_2}\left(\delta_{\omega_1+\omega_3} + \delta_{\omega_2+\omega_3} - \delta_{\omega_3} - \delta_{\omega_4}\right) - \left(\delta_{\omega_1}\Delta^2_{i\omega_2} + \delta_{\omega_2}\Delta^2_{i\omega_1}\right)\left(\delta_{\omega_3} + \delta_{\omega_4}\right)$$

$$- \Delta_{i\omega_3}\Delta_{i\omega_4}\left(\delta_{\omega_1} + \delta_{\omega_2}\right)$$

We define the spin raising and lowering operators,

$$S^\pm = (S^x \pm iS^y)/\sqrt{2}, \tag{50}$$

which have to appear in pairs for a non-vanishing correlator due to spin-rotation symmetry. As for the HA, we do not consider connected correlators in this work for brevity. The classical S^z-correlator can be found from its generating functional with source field h [13],

$$\mathcal{G}(y = \beta h) = \frac{\sinh[y(S + 1/2)]}{(2S + 1)\sinh[y/2]}, \tag{51}$$

$$\langle(S^z)^l\rangle = \lim_{y \to 0}\partial_y^l \mathcal{G}(y) \equiv b_{l-1}, \tag{52}$$

for example $b_1 = \frac{S}{3}(S + 1)$ and $b_3 = \frac{S}{15}\left(3S^3 + 6S^2 + 2S - 1\right)$ and vanishing b_l for even l. For all other correlators involving $\alpha_k = \pm$, we adapt Eq. (15) for the free spin case,

$$G_{S^{\alpha_1}S^{\alpha_2}...S^{\alpha_n}}(\omega_1, ..., \omega_{n-1}) = \sum_{p \in S_n}\langle S^{\alpha_{p(1)}}S^{\alpha_{p(2)}}...S^{\alpha_{p(n)}}\rangle K_n\left(i\omega_{p(1)}, i\omega_{p(2)}, ..., i\omega_{p(n-1)}\right), \tag{53}$$

where we made use of the fact that all eigenenergies are zero and the Heisenberg time evolution is trivial. It is convenient to evaluate the equal-time correlators in Eq. (53) as

$$\langle S^{\alpha_1}S^{\alpha_2}...S^{\alpha_n}\rangle = \frac{1}{2S + 1}\sum_{m=-S}^{S}\langle m|S^{\alpha_1}S^{\alpha_2}...S^{\alpha_n}|m\rangle \equiv \frac{1}{2S + 1}\sum_{m=-S}^{S}\sum_{l=0}^{n}p_l m^l = p_0 + \sum_{l=2}^{n}p_l b_{l-1}, \tag{54}$$

where in the last step we used Eq. (52). We find the real expansion coefficients $\{p_l\}_{l=0,1,...,n}$ iteratively by moving through the string $\alpha_1\alpha_2...\alpha_n$ from the right and start from $p_l = \delta_{0,l}$. Based on the S^z eigenstates $\{|m\rangle\}_{m=-S,...,S-1,S}$ we obtain the iteration rules from $S^z|m\rangle = m|m\rangle$ and $S^\pm|m\rangle = \sqrt{1/2}\sqrt{S(S + 1) - m(m \pm 1)}|m \pm 1\rangle$. We define an auxiliary integer c that keeps track of the intermediate state $|m + c\rangle$, initially $c = 0$. Depending on the α_j that we find in step $j = n, n - 1..., 1$ we take one of the following actions: (i) For $\alpha_j = z$, we update $p_l \leftarrow p_{l-1} + cp_l$ $\forall l$ and leave c unchanged. It is understood that $p_{l<0} = 0$. (ii) For $\alpha_j = +$, we combine the square-root factor brought by the raising operator with the factor that comes from the necessary $\alpha_{j'} = -$ at another place in the string. We replace $p_l \leftarrow -\frac{1}{2}p_{l-2} - \frac{2c+1}{2}p_{l-1} + \left(\frac{3}{2}b_1 - c\frac{c+1}{2}\right)p_l$ $\forall l$ and then let $c \leftarrow c + 1$. (iii) For $\alpha_j = -$, we update $c \leftarrow c - 1$ and keep p_l unchanged, $p_l \leftarrow p_l$ $\forall l$.

Our final results for the free spin correlators are reported in Tab. 2. We reproduce the known spin correlators for $n = 2, 3$ and determine the non-classical correlators $G_{S^+S^+S^-S^-}$ and $G_{S^+S^-S^zS^z}$ at order $n = 4$, which to the best of our knowledge were not available in the

literature.[1] We also confirmed the classical result for $G_{S^z S^z S^z S^z}$, which in our full quantum formalism requires some non-trivial cancellations. To arrive at our results, we used the identity

$$\Delta_{a+b}\left(\Delta_a + \Delta_b\right) - \Delta_a \Delta_b = \delta_a \Delta_b^2 + \delta_b \Delta_a^2 - \delta_{a+b} \Delta_a \Delta_b \, . \tag{55}$$

We finally comment on the relation between the $n = 3$ free spin-S correlator $G_{S^+ S^- S^z}$ from Tab. (2) and the result for $G_{S^x S^y S^z}$ found for the zero-field limit of the HA in Eq. (49). The operators $S^{x,y,z}$ for the Hubbard model [c.f. Eq. (36)] project to the singly-occupied $S = 1/2$ subspace spanned by the states $|\uparrow\rangle, |\downarrow\rangle$. Thus, using $G_{S^x S^y S^z} = i G_{S^+ S^- S^z}$ and specializing the free spin result from Tab. (2) to $S = 1/2$ (where $b_1 = 1/4$) we find agreement with the HA result (49) up to the factor $2e^{-\beta\epsilon}/Z$. This factor represents the expectation value of the projector to the singly-occupied sector in the HA Hilbert space and goes to unity in the local-moment regime.

7 Conclusion

In summary, we have provided exact universal kernel functions for the spectral representation of the n-point Matsubara correlator. Our results are an efficient alternative to equation-of-motion approaches which often have difficulties to capture anomalous terms related to conserved or commuting operators. We expect our results to be useful for various benchmarking applications, as starting points for emerging many-body methods and for unraveling the physical interpretation of n-point functions in various settings. Our results also apply in the limit $T \to 0$ where the formally divergent anomalous contributions are to be understood as $\beta \delta_{\omega,0} \to 2\pi\delta(\omega)$. Some of these Dirac delta-functions will vanish after subtracting the disconnected contributions, others indicate truely divergent susceptibilities like the $1/T$ Curie law for the spin-susceptiblity of the Hubbard atom in the local moment regime [26]. Although our work has focused on imaginary frequency (Matsubara) correlators, with analytical expressions now at hand, it is also interesting to study the intricacies of analytical continuation to real frequencies and thus to further explore the connection of Matsubara and Keldysh correlators [43].

---

[1]We thank Andreas Rückriegel for sharing unpublished results on 4-point free spin correlators and pointing out further simplifications of the analytical expressions.

A Equivalence to convention of Ref. [21]

In Ref. [21] by Kugler, Lee and von Delft (KLD), only regular ($a = 0$) and anomalous terms of order $a = 1$ have been considered for $n = 3, 4$. The corresponding kernel functions were derived from only $(n-1)!$ permutations by setting $\tau_n = 0$ and $\tau_{i \neq n} > 0$, but still applied to all $n!$ permutations to obtain the correlation functions. For $n = 3$, the resulting kernel function (Eq. (46) in Ref. [21]) reads

$$K_{3,\text{KLD}}(\Omega_1, \Omega_2) = \Delta_1 \Delta_2 - \Delta_1 \delta_2 \frac{1}{2}(\beta + \Delta_1) - \delta_1 \Delta_2 \frac{1}{2}(\beta + \Delta_2). \tag{A.1}$$

This can be compared to the corresponding kernel function for $n = 3$ found in our Eq. (31) truncated to $a \leq 1$,

$$K_3^{a \leq 1}(\Omega_1, \Omega_2) = \Delta_1 \Delta_2 - \Delta_1 \delta_2 \left(\frac{\beta}{2} + \Delta_1\right) - \frac{\beta}{2}\delta_1 \Delta_2. \tag{A.2}$$

Both approaches are equally valid and should yield the same correlation functions (consistently discarding terms with $a = 2$), yet the kernel functions are obviously different. To resolve this issue, we define the difference of the kernel functions

$$K_{3,\text{diff}}(\Omega_1, \Omega_2) = K_{3,\text{KLD}}(\Omega_1, \Omega_2) - K_3^{a \leq 1}(\Omega_1, \Omega_2) = \frac{1}{2}\left(\Delta_1^2 \delta_2 - \delta_1 \Delta_2^2\right), \tag{A.3}$$

and show that the corresponding contributions to the correlation function vanishes when summed over cyclically related permutations $p = 123, 231, 312$. These contributions are given by

$$\begin{aligned}
&\frac{1}{Z}\sum_{p=123,231,312} \zeta(p) \sum_{\underline{123}} e^{-\beta E_{\underline{1}}} A_{p(1)}^{12} A_{p(2)}^{23} A_{p(3)}^{31} K_{3,\text{diff}}(\Omega_{p(1)}^{12}, \Omega_{p(2)}^{23}) \\
&= \frac{\zeta(123)}{2Z} \sum_{\underline{123}} e^{-\beta E_{\underline{1}}} A_1^{12} A_2^{23} A_3^{31} \left(\Delta_{\Omega_1^{12}}^2 \delta_{\Omega_1^{12}+\Omega_2^{23}} - \delta_{\Omega_1^{12}} \Delta_{\Omega_1^{12}+\Omega_2^{23}}^2\right) \\
&+ \frac{\zeta(231)}{2Z} \sum_{\underline{123}} e^{-\beta E_{\underline{1}}} A_2^{12} A_3^{23} A_1^{31} \left(\Delta_{\Omega_2^{12}}^2 \delta_{\Omega_2^{12}+\Omega_3^{23}} - \delta_{\Omega_2^{12}} \Delta_{\Omega_2^{12}+\Omega_3^{23}}^2\right) \\
&+ \frac{\zeta(312)}{2Z} \sum_{\underline{123}} e^{-\beta E_{\underline{1}}} A_3^{12} A_1^{23} A_2^{31} \left(\Delta_{\Omega_3^{12}}^2 \delta_{\Omega_3^{12}+\Omega_1^{23}} - \delta_{\Omega_3^{12}} \Delta_{\Omega_3^{12}+\Omega_1^{23}}^2\right).
\end{aligned} \tag{A.4}$$

Considering the second term of permutation $p = 312$ and renaming the summation variables $\underline{2} \to \underline{1}, \underline{3} \to \underline{2}, \underline{1} \to \underline{3}$ yields

$$\begin{aligned}
&-\frac{\zeta(312)}{2Z} \sum_{\underline{123}} e^{-\beta E_{\underline{1}}} A_3^{12} A_1^{23} A_2^{31} \delta_{\Omega_3^{12}} \Delta_{\Omega_3^{12}+\Omega_1^{23}}^2 \\
&= -\frac{\zeta(312)}{2Z} \sum_{\underline{123}} e^{-\beta E_{\underline{3}}} A_1^{12} A_2^{23} A_3^{31} \delta_{\Omega_3^{31}} \Delta_{\Omega_3^{31}+\Omega_1^{12}}^2 \\
&= -\frac{\zeta(123)}{2Z} \sum_{\underline{123}} e^{-\beta E_{\underline{1}}} A_1^{12} A_2^{23} A_3^{31} \delta_{\Omega_1^{12}+\Omega_2^{23}} \Delta_{\Omega_1^{12}}^2,
\end{aligned} \tag{A.5}$$

where we used $\omega_3 = -\omega_1 - \omega_2$ and the fact that $\delta_{\Omega_3^{31}} = \delta_{\omega_3}\delta_{E_{\underline{1}}, E_{\underline{3}}}$ enforces the third operator to be bosonic, such that $\zeta(312) = \zeta(123)$. This term exactly cancels the first contribution of permutation $p = 123$ in (A.4). Repeating similar steps for the remaining terms, we find that

the the second term of $p = 123$ and the first term of $p = 231$ as well as the second term of $p = 231$ and the first term of $p = 312$ cancel, leading to

$$\frac{1}{Z} \sum_{p \in \{123, 231, 312\}} \zeta(p) \sum_{\underline{123}} e^{-\beta E_1} A_{p(1)}^{1\,2} A_{p(2)}^{2\,3} A_{p(3)}^{3\,1} K_{3,\text{diff}} \left(\Omega_{p(1)}^{1\,2}, \Omega_{p(2)}^{2\,3} \right) = 0 \,. \tag{A.6}$$

Similarly, summing over the second set of cyclically related permutations $p = 132, 213, 321$ leads to a vanishing result, leading to the conclusion that

$$\frac{1}{Z} \sum_{p \in S_3} \zeta(p) \sum_{\underline{123}} e^{-\beta E_1} A_{p(1)}^{1\,2} A_{p(2)}^{2\,3} A_{p(3)}^{3\,1} K_{3,\text{diff}} \left(\Omega_{p(1)}^{1\,2}, \Omega_{p(2)}^{2\,3} \right) = 0 \,. \tag{A.7}$$

Thus we have shown that both kernel functions in Eqns. (A.1) and (A.2) are equivalent as they yield the same correlation functions after summing over all permutations. The same statement holds true for case of $n = 4$ and $a = 1$.

References

[1] J. W. Negele and H. Orland, *Quantum many-particle systems*, CRC Press, Boca Raton, USA, ISBN 9780429497926 (1998), doi:10.1201/9780429497926.

[2] H. Bruus and K. Flensberg, *Many-body quantum theory in condensed matter physics*, Oxford University Press, Oxford, UK, ISBN 9780198566335 (2004).

[3] P. Kappl, F. Krien, C. Watzenböck and K. Held, *Nonlinear responses and three-particle correlators in correlated electron systems exemplified by the Anderson impurity model*, Phys. Rev. B **107**, 205108 (2023), doi:10.1103/PhysRevB.107.205108.

[4] G. Semeghini et al., *Probing topological spin liquids on a programmable quantum simulator*, Science **374**, 1242 (2021), doi:10.1126/science.abi8794.

[5] L. Hedin, *New method for calculating the one-particle Green's function with application to the electron-gas problem*, Phys. Rev. **139**, A796 (1965), doi:10.1103/PhysRev.139.A796.

[6] N. E. Bickers, *Self-consistent many-body theory for condensed matter systems*, in *Theoretical methods for strongly correlated electrons*, Springer, New York, USA, ISBN 9780387217178 (2004), doi:10.1007/0-387-21717-7_6.

[7] B. Roulet, J. Gavoret and P. Nozières, *Singularities in the X-ray absorption and emission of metals. I. First-order parquet calculation*, Phys. Rev. **178**, 1072 (1969), doi:10.1103/PhysRev.178.1072.

[8] P. Kopietz, L. Bartosch and F. Schütz, *Introduction to the functional renormalization group*, Springer, Berlin, Heidelberg, Germany, ISBN 9783642050947 (2010), doi:10.1007/978-3-642-05094-7.

[9] W. Metzner, M. Salmhofer, C. Honerkamp, V. Meden and K. Schönhammer, *Functional renormalization group approach to correlated fermion systems*, Rev. Mod. Phys. **84**, 299 (2012), doi:10.1103/RevModPhys.84.299.

[10] C. Wetterich, *Exact evolution equation for the effective potential*, Phys. Lett. B **301**, 90 (1993), doi:10.1016/0370-2693(93)90726-X.

[11] S.-S. B. Lee, F. B. Kugler and J. von Delft, *Computing local multipoint correlators using the numerical renormalization group*, Phys. Rev. X **11**, 041007 (2021), doi:10.1103/PhysRevX.11.041007.

[12] J. Reuther and R. Thomale, *Cluster functional renormalization group*, Phys. Rev. B **89**, 024412 (2014), doi:10.1103/PhysRevB.89.024412.

[13] J. Krieg and P. Kopietz, *Exact renormalization group for quantum spin systems*, Phys. Rev. B **99**, 060403 (2019), doi:10.1103/PhysRevB.99.060403.

[14] A. Rückriegel, J. Arnold, R. Goll and P. Kopietz, *Spin functional renormalization group for dimerized quantum spin systems*, Phys. Rev. B **105**, 224406 (2022), doi:10.1103/PhysRevB.105.224406.

[15] G. Rohringer, H. Hafermann, A. Toschi, A. A. Katanin, A. E. Antipov, M. I. Katsnelson, A. I. Lichtenstein, A. N. Rubtsov and K. Held, *Diagrammatic routes to nonlocal correlations beyond dynamical mean field theory*, Rev. Mod. Phys. **90**, 025003 (2018), doi:10.1103/RevModPhys.90.025003.

[16] P. Chalupa, T. Schäfer, M. Reitner, D. Springer, S. Andergassen and A. Toschi, *Fingerprints of the local moment formation and its Kondo screening in the generalized susceptibilities of many-electron problems*, Phys. Rev. Lett. **126**, 056403 (2021), doi:10.1103/PhysRevLett.126.056403.

[17] H. Lehmann, *Über Eigenschaften von Ausbreitungsfunktionen und Renormierungskonstanten quantisierter Felder*, Nuovo Cimento **11**, 342 (1954), doi:10.1007/BF02783624.

[18] A. Shvaika, *On the spectral relations for multitime correlation functions*, Condens. Matter Phys. **9**, 447 (2006), doi:10.5488/CMP.9.3.447.

[19] H. Hafermann, C. Jung, S. Brener, M. I. Katsnelson, A. N. Rubtsov and A. I. Lichtenstein, *Superperturbation solver for quantum impurity models*, Europhys. Lett. **85**, 27007 (2009), doi:10.1209/0295-5075/85/27007.

[20] A. Shvaika, *Spectral properties of four-time fermionic Green's functions*, Condens. Matter Phys. **19**, 33004 (2016), doi:10.5488/CMP19.33004.

[21] F. B. Kugler, S.-S. B. Lee and J. von Delft, *Multipoint correlation functions: Spectral representation and numerical evaluation*, Phys. Rev. X **11**, 041006 (2021), doi:10.1103/PhysRevX.11.041006.

[22] P. C. Kwok and T. D. Schultz, *Correlation functions and Green functions: Zero-frequency anomalies*, J. Phys. C: Solid State Phys. **2**, 1196 (1969), doi:10.1088/0022-3719/2/7/312.

[23] C. Watzenböck, M. Fellinger, K. Held and A. Toschi, *Long-term memory magnetic correlations in the Hubbard model: A dynamical mean-field theory analysis*, SciPost Phys. **12**, 184 (2022), doi:10.21468/SciPostPhys.12.6.184.

[24] A. Tsvelik, *Quantum field theory in condensed matter physics*, Cambridge University Press, Cambridge, UK, ISBN 9780511615832 (2003), doi:10.1017/CBO9780511615832.

[25] G. Rohringer, A. Valli and A. Toschi, *Local electronic correlation at the two-particle level*, Phys. Rev. B **86**, 125114 (2012), doi:10.1103/PhysRevB.86.125114.

[26] G. Rohringer, *New routes towards a theoretical treatment of nonlocal electronic correlations*, PhD thesis, Technische Universität Wien, Wien, Austria (2013) doi:10.34726/hss.2013.21498.

[27] F. Krien and A. Valli, *Parquetlike equations for the Hedin three-leg vertex*, Phys. Rev. B **100**, 245147 (2019), doi:10.1103/PhysRevB.100.245147.

[28] F. Krien, A. Kauch and K. Held, *Tiling with triangles: Parquet and G W γ methods unified*, Phys. Rev. Res. **3**, 013149 (2021), doi:10.1103/PhysRevResearch.3.013149.

[29] T. Schäfer, S. Ciuchi, M. Wallerberger, P. Thunström, O. Gunnarsson, G. Sangiovanni, G. Rohringer and A. Toschi, *Nonperturbative landscape of the Mott-Hubbard transition: Multiple divergence lines around the critical endpoint*, Phys. Rev. B **94**, 235108 (2016), doi:10.1103/PhysRevB.94.235108.

[30] P. Thunström, O. Gunnarsson, S. Ciuchi and G. Rohringer, *Analytical investigation of singularities in two-particle irreducible vertex functions of the Hubbard atom*, Phys. Rev. B **98**, 235107 (2018), doi:10.1103/PhysRevB.98.235107.

[31] P. Chalupa, P. Gunacker, T. Schäfer, K. Held and A. Toschi, *Divergences of the irreducible vertex functions in correlated metallic systems: Insights from the Anderson impurity model*, Phys. Rev. B **97**, 245136 (2018), doi:10.1103/PhysRevB.97.245136.

[32] M. Pelz, S. Adler, M. Reitner and A. Toschi, *Highly nonperturbative nature of the Mott metal-insulator transition: Two-particle vertex divergences in the coexistence region*, Phys. Rev. B **108**, 155101 (2023), doi:10.1103/PhysRevB.108.155101.

[33] S. Adler, F. Krien, P. Chalupa-Gantner, G. Sangiovanni and A. Toschi, *Non-perturbative intertwining between spin and charge correlations: A "smoking gun" single-boson-exchange result*, (arXiv preprint) doi:10.48550/arXiv.2212.09693.

[34] N. Wentzell, G. Li, A. Tagliavini, C. Taranto, G. Rohringer, K. Held, A. Toschi and S. Andergassen, *High-frequency asymptotics of the vertex function: Diagrammatic parametrization and algorithmic implementation*, Phys. Rev. B **102**, 085106 (2020), doi:10.1103/PhysRevB.102.085106.

[35] F. Krien, A. Valli and M. Capone, *Single-boson exchange decomposition of the vertex function*, Phys. Rev. B **100**, 155149 (2019), doi:10.1103/PhysRevB.100.155149.

[36] M. Gievers, E. Walter, A. Ge, J. von Delft and F. B. Kugler, *Multiloop flow equations for single-boson exchange fRG*, Eur. Phys. J. B **95**, 108 (2022), doi:10.1140/epjb/s10051-022-00353-6.

[37] R. Goll, D. Tarasevych, J. Krieg and P. Kopietz, *Spin functional renormalization group for quantum Heisenberg ferromagnets: Magnetization and magnon damping in two dimensions*, Phys. Rev. B **100**, 174424 (2019), doi:10.1103/PhysRevB.100.174424.

[38] R. Goll, A. Rückriegel and P. Kopietz, *Zero-magnon sound in quantum Heisenberg ferromagnets*, Phys. Rev. B **102**, 224437 (2020), doi:10.1103/PhysRevB.102.224437.

[39] D. Tarasevych and P. Kopietz, *Dissipative spin dynamics in hot quantum paramagnets*, Phys. Rev. B **104**, 024423 (2021), doi:10.1103/PhysRevB.104.024423.

[40] D. Tarasevych, A. Rückriegel, S. Keupert, V. Mitsiioannou and P. Kopietz, *Spin functional renormalization group for the $J_1 J_2 J_3$ quantum Heisenberg model*, Phys. Rev. B **106**, 174412 (2022), doi:10.1103/PhysRevB.106.174412.

[41] V. G. Vaks and S. A. Pikin, *Thermodynamics of an ideal ferromagnetic substance*, Sov. J. Exp. Theor. Phys. **26**, 188 (1968).

[42] V. G. Vaks, A. I. Larkin and S. A. Pikin, *Spin waves and correlation functions in a ferromagnetic*, Sov. J. Exp. Theor. Phys. **26**, 647 (1968).

[43] A. Ge, J. Halbinger, S.-S. B. Lee, J. von Delft and F. B. Kugler, *In preparation*.

5 Analytic continuation of multipoint correlation functions

This chapter reproduces parts of Secs. 1, 7, 9, and all of Secs. 2.4, 2.5, and 3–6 of [P4] *with minor modifications to put these sections into the context of this thesis.*

5.1 Introduction

We now set the stage to turn to the problem of the analytic continuation of general multipoint correlators, covered in [P4]. The connection between the MF and KF by means of analytic continuation is well known for 2p functions, as discussed in Ch. 3.2. For higher-point functions, progress has been made by various authors: Eliashberg discussed the analytic continuation of a specific 4p correlator from the MF to real frequencies [Eli62]. Evans [Eva90] and Kobes [Kob90, Kob91] studied the correspondence between both formalisms for 3p correlators in Refs. [Eva90, Kob90, Kob91]. Evans then considered $\ell \geq 4$ multipoint correlators and showed that fully retarded and fully advanced Keldysh components can be obtained from analytic continuations of MF correlators [Eva92]. Weldon conducted a thorough analysis of real-frequency ℓp functions and proved that these KF components are in fact the only ones that can be identified with an analytically continued MF function [Wel05a, Wel05b]. Taylor extended Evans' results to arbitrary Keldysh components of the fermionic 4p correlator, assuming the absence of anomalous terms in the MF correlator [Tay93]. Guerin derived analogous results from diagrammatic arguments [Gue94a, Gue94b].

We solve the problem of analytic continuation of multipoint functions from the MF to the KF in full generality: We develop a strategy for analytically continuing an arbitrary MF ℓp correlator G (including anomalous terms) to all 2^ℓ components of the corresponding KF correlator $G^{\boldsymbol{k}}$ as functionals of G, i.e. $G^{\boldsymbol{k}} = G^{\boldsymbol{k}}[G]$. We exemplify the procedure for the most relevant cases $\ell \in \{2, 3, 4\}$.

Our analysis not only provides relations between functions in the MF and the KF, but also between different Keldysh components of the KF correlator. As an application of our general results, we derive a complete set of generalized fluctuation-dissipation relations (gFDRs) for 3p and 4p functions. These reproduce the results of Wang and Heinz [WH02] for real fields and the generalization to fermionic ones [JPS10]. Moreover, we give a comprehensive discussion of the role of anomalous terms during analytic continuation and in gFDRs. Regarding the number of independent components in the KF, one observes a general trend, obeyed by the known results for $\ell \in \{2, 3, 4\}$: Due to the doubled time contour, there are 2^ℓ Keldysh components. In the Keldysh basis, $2^\ell - 1$ of them are nonzero, and ℓ are fully retarded components. Now, there are $2^{\ell-1}$ gFDRs $(2, 4, 8$ for $\ell = 2, 3, 4)$. Thus, the number of independent Keldysh components is $2^{\ell-1} - 1$ $(1, 3, 7$ for $\ell = 2, 3, 4)$. It follows that, for $\ell \geq 4$, the fully retarded components do not suffice to encode the entire information of the Keldysh correlator.

The rest of this chapter is organized as follows: In Sec. 5.2, we introduce our general recipe for the analytic continuation of arbitrary ℓp correlators. This recipe is applied to the 2p case in Sec. 5.3 and, after the investigation of analytic properties of regular ℓp MF correlators in Sec. 5.4, also to the 3p and 4p cases in Secs. 5.5 and 5.6. The results also lead to gFDRs between different Keldysh components of the KF correlator. In Sec. 5.7, we perform explicit analytic continuations from MF to KF correlators for the Hubbard atom. The Hubbard atom is a good example for a system with anomalous contributions and, here, serves as a simple,

exactly solvable model with just the right degree of complexity for illustrating our approach. We conclude in Sec. 5.8.

This chapter is complemented with additional discussions and explicit computations in App. C. In App. C.1 and C.2, we give details on the MF kernels and PSFs used in calculations throughout this chapter and App. C. Appendix C.3 is devoted to detailed calculations concerning the analytic continuation of 3p correlators. In App. C.4, we extend insights from 2p and 3p results to deduce the relation between 4p PSFs and analytically continued MF correlators. The spectral representations of various useful combinations of analytically continued MF correlators and anomalous parts are presented in App. C.5. Appendix C.6 expresses the spectral representation of KF correlators in a form especially suited for deriving their connection to MF functions. In App. C.7, we check the consistency of our results for PSFs by using equilibrium properties. Finally, App. C.8 gives details about simplifications used for the analytic continuation of Hubbard atom correlators.

5.2 Recipe for the analytic continuation

5.2.1 The bridge between the MF and KF formalisms

Our strategy builds upon the spectral representation of general ℓp correlators introduced in Ref. [KLvD21] (summarized in Secs. 3.3 and 3.4) and originates from the following observation: Equation (3.70), expressing KF partial correlators through MF partial correlators for $\alpha = 1$, has a counterpart for arbitrary α, obtained via Eqs. (3.67), (3.69), and (3.63b):

$$G_p^{[\hat{\eta}_1...\hat{\eta}_\alpha]}(\boldsymbol{\omega}_p) = \sum_{j=1}^{\alpha}(-1)^{j-1}\big[\tilde{K}*S_p\big]\big(\boldsymbol{\omega}_p^{[\bar{\hat{\eta}}_j]}\big) \tag{5.1a}$$

$$= \sum_{j=1}^{\alpha}(-1)^{j-1}\tilde{G}_p\big(\mathrm{i}\boldsymbol{\omega}_p \to \boldsymbol{\omega}_p^{[\bar{\hat{\eta}}_j]}\big), \tag{5.1b}$$

with $\bar{\hat{\eta}}_j \in \{\eta_1, \ldots, \eta_\alpha\}$. This is already one of our main results: The partial correlators serve as a bridge between the MF and KF. All components of the partial KF correlator $G_p^{\boldsymbol{k}_p} = G_p^{[\hat{\eta}_1...\hat{\eta}_\alpha]}$ can be obtained by taking linear combinations of analytic continuations of partial regular MF correlators, $\tilde{G}_p(\mathrm{i}\boldsymbol{\omega}_p \to \boldsymbol{\omega}_p^{[\bar{\hat{\eta}}_j]})$. The external Keldysh indices $\boldsymbol{k} = [\eta_1...\eta_\alpha]$ and the permutation p together specify the imaginary frequency shifts, encoded in $\boldsymbol{\omega}_p^{[\bar{\hat{\eta}}_j]}$, to be used.

Equation (3.71), expressing the full (p-summed) KF correlators through MF ones for $\alpha = 1$, does not have a counterpart for $\alpha > 1$. Then, the full correlators, given by

$$G^{[\eta_1...\eta_\alpha]}(\boldsymbol{\omega}) = \sum_{p}\big[K^{[\hat{\eta}_1...\hat{\eta}_\alpha]}*S_p\big](\boldsymbol{\omega}_p) \tag{5.2a}$$

$$= \sum_{p}\sum_{j=1}^{\alpha}(-1)^{j-1}\tilde{G}_p\big(\mathrm{i}\boldsymbol{\omega}_p \to \boldsymbol{\omega}_p^{[\bar{\hat{\eta}}_j]}\big), \tag{5.2b}$$

involve a sum $\sum_j$. The $\bar{\hat{\eta}}_j$ indices on the right now depend on p, so that the imaginary frequency shifts vary from one permutation to the next. As a result, the full $G^{[\eta_1...\eta_\alpha]}$, unlike $G^{[\eta]}$, does not depend on a single set of frequency shifts and cannot be directly expressed through a mere analytic continuation of $\tilde{G}(\mathrm{i}\boldsymbol{\omega})$. Instead, Eq. (5.2b) requires separate knowledge of each individual $\tilde{G}_p(\mathrm{i}\boldsymbol{\omega}_p)$. Most computational methods capable of computing the full MF correlator $G(\mathrm{i}\boldsymbol{\omega})$ do not have access to the separate partial MF correlators $\tilde{G}_p(\mathrm{i}\boldsymbol{\omega}_p)$. In the following, we therefore develop a strategy for extracting the

partial MF correlators $\tilde{G}_p(\mathrm{i}\boldsymbol{\omega}_p)$ from a full MF correlator $G(\mathrm{i}\boldsymbol{\omega})$ given as input, assuming the latter to be known analytically. By writing the resulting functions $\tilde{G}_p(\mathrm{i}\boldsymbol{\omega})$ in the form $[\tilde{K} * S_p](\mathrm{i}\boldsymbol{\omega})$, one can deduce explicit expressions for the PSFs $S_p[G]$ as functionals of the input G. By inserting these S_p into Eq. (5.2a), one obtains $G^{[\eta_1...\eta_\alpha]}[G]$ as a functional of G, thereby achieving the desired MF-to-KF analytic continuation.

We start in the MF time domain. There, a specific partial MF correlator $\mathcal{G}_p(\boldsymbol{\tau}_p)$ can be obtained from the full $\mathcal{G}(\boldsymbol{\tau}) = \sum_p \mathcal{G}_p(\boldsymbol{\tau}_p)$ (Eq. (3.57)) using the projector property of MF kernels in the time domain, $\mathcal{K}(\boldsymbol{\tau}_p)\mathcal{K}(\boldsymbol{\tau}_{p'}) = (-1)^{\ell-1}\mathcal{K}(\boldsymbol{\tau}_p)$ if $p = p'$ and 0 otherwise. Hence, we can express the partial correlator as

$$\mathcal{G}_p(\boldsymbol{\tau}_p) = (-1)^{\ell-1}\mathcal{K}(\boldsymbol{\tau}_p)\mathcal{G}(\boldsymbol{\tau}). \tag{5.3}$$

Computing the discrete Fourier transform of Eq. (5.3) according to Eq. (3.58a), we obtain

$$\mathcal{G}_p(\mathrm{i}\boldsymbol{\omega}_p) = [\mathcal{K} \star G](\mathrm{i}\boldsymbol{\omega}_p), \tag{5.4a}$$

with the imaginary-frequency convolution $\star$ defined as

$$[\mathcal{K} \star G](\mathrm{i}\boldsymbol{\omega}_p) = \frac{1}{(-\beta)^{\ell-1}} \sum_{\mathrm{i}\boldsymbol{\omega}'_p} \delta_{\mathrm{i}\omega'_{\bar{1}...\bar{\ell}}}\mathcal{K}(\mathrm{i}\boldsymbol{\omega}_p - \mathrm{i}\boldsymbol{\omega}'_p)G(\mathrm{i}\boldsymbol{\omega}'). \tag{5.4b}$$

We will typically sum over the $\ell - 1$ independent Matsubara frequency variables $\mathrm{i}\omega'_{\bar{1}...\bar{i}}$, with $i \in \{1, \ldots, \ell - 1\}$. Note that the arguments of $G(\mathrm{i}\boldsymbol{\omega}')$ appear in *unpermuted* order, but are to be viewed as functions of the summation variables, i.e., $\mathrm{i}\boldsymbol{\omega}' = \mathrm{i}\boldsymbol{\omega}'(\boldsymbol{\omega}'_p)$. We will often make this explicit using the notation $G_{\mathrm{i}\boldsymbol{\omega}'_p} = G(\mathrm{i}\boldsymbol{\omega}'(\boldsymbol{\omega}'_p))$, where the subscript is a label indicating the $\ell - 1$ independent frequencies chosen to parametrize $\mathrm{i}\boldsymbol{\omega}'$. Consider, e.g., $\ell = 3$ and choose $\mathrm{i}\omega_{\bar{1}}$, $\mathrm{i}\omega_{\overline{12}}$ as summation variables. For the permutation $p = (132)$, the correlator is then represented as $G_{\mathrm{i}\omega_{\bar{1}},\mathrm{i}\omega_{\overline{12}}} = G_{\mathrm{i}\omega_1,\mathrm{i}\omega_{13}} = G(\mathrm{i}\boldsymbol{\omega}(\mathrm{i}\omega_1, \mathrm{i}\omega_{13})) = G(\mathrm{i}\omega_1, -\mathrm{i}\omega_{13}, \mathrm{i}\omega_{13} - \mathrm{i}\omega_1)$.

Using Eq. (3.60) for $\mathcal{G}_p(\mathrm{i}\boldsymbol{\omega}_p)$ and Eq. (3.59) for $\mathcal{K}(\mathrm{i}\boldsymbol{\omega}_p)$ in Eq. (5.4a), we obtain

$$\beta\delta_{\mathrm{i}\omega_{1...\ell}}G_p(\mathrm{i}\boldsymbol{\omega}_p) + G_p^{\mathcal{R}}(\mathrm{i}\boldsymbol{\omega}_p) = \beta\delta_{\mathrm{i}\omega_{1...\ell}}[K \star G](\mathrm{i}\boldsymbol{\omega}_p) + [\mathcal{R} \star G](\mathrm{i}\boldsymbol{\omega}_p). \tag{5.5}$$

By construction, neither $G_p^{\mathcal{R}}$ nor $\mathcal{R}$ contain an overall factor of β; in this sense, they are $\mathcal{O}(\beta^0)$. Likewise, $\mathcal{R} \star G$ is $\mathcal{O}(\beta^0)$, for reasons explained below. Moreover, recall that MF-to-KF continuation via Eq. (5.2b) requires only the regular part $\tilde{G}_p(\mathrm{i}\boldsymbol{\omega}_p)$. We avoid anomalous contributions to $G_p(\mathrm{i}\boldsymbol{\omega}_p)$ in Eq. (5.5) by imposing the condition $\mathrm{i}\omega_{\bar{1}...\bar{i}} \neq 0$ on the external frequencies. Setting $\mathrm{i}\omega_{1...\ell} = 0$, we conclude that

$$\tilde{G}_p(\mathrm{i}\boldsymbol{\omega}_p) + \mathcal{O}(\tfrac{1}{\beta}) = [K \star G](\mathrm{i}\boldsymbol{\omega}_p), \qquad (\mathrm{i}\omega_{\bar{1}...\bar{i}} \neq 0, \ \forall i < \ell)$$

$$= \frac{1}{(-\beta)^{\ell-1}} \sum_{\mathrm{i}\boldsymbol{\omega}'_p} \delta_{\mathrm{i}\omega'_{\bar{1}...\bar{\ell}}}K(\mathrm{i}\boldsymbol{\omega}_p - \mathrm{i}\boldsymbol{\omega}'_p)G_{\mathrm{i}\boldsymbol{\omega}'_p}. \tag{5.6}$$

To find $\tilde{G}_p(\mathrm{i}\boldsymbol{\omega}_p)$, we should thus compute $K \star G$ with $\mathrm{i}\omega_{\bar{1}...\bar{i}} \neq 0$ and retain only the $\mathcal{O}(\beta^0)$ terms, ignoring all $\mathcal{O}(1/\beta^{j\geq 1})$ contributions. Note, however, that the full information on K and G, including both regular and anomalous terms, is needed on the right-hand side to obtain $\tilde{G}_p$ on the left.

Equation (5.6) is an important intermediate result. It provides a recipe for extracting partial regular MF correlators from the full MF correlator by performing Matsubara sums $\sum_{\mathrm{i}\boldsymbol{\omega}'_p}$. After performing the sums, the final results will be analytically continued to yield $\tilde{G}_p(\mathrm{i}\boldsymbol{\omega}_p \to \boldsymbol{\omega}_p^{[\eta]})$ through which all Keldysh correlators can be expressed (Eq. (5.2b)). However, we choose to fully evaluate the Matsubara sums *before* performing this analytic continuation.

The reason is that we will evaluate the sums using contour integration and contour deformation. For the latter step, it is convenient if the arguments of $\tilde{G}_p(\mathrm{i}\boldsymbol{\omega}_p)$ all lie safely on the imaginary axis, where they do not impede contour deformation.

5.2.2 Converting Matsubara sums to contour integrals

Next, we discuss three technical points relevant for performing Matsubara sums explicitly. To be concrete, we illustrate our general statements for the case $\ell = 2$. Other cases are discussed in subsequent sections.

(i) *Singularity-free kernels:* The argument of the kernel $K(\boldsymbol{\Omega}_p)$ in Eq. (5.6) has the form $\boldsymbol{\Omega}_p = \mathrm{i}\boldsymbol{\omega}_p - \mathrm{i}\boldsymbol{\omega}'_p$. This is always bosonic, being the difference of two same-type Matsubara frequencies. The Matsubara sums $\sum_{\mathrm{i}\boldsymbol{\omega}'_p}$ will thus contain terms with $\Omega_{\bar{1}...\bar{i}} = 0$. To facilitate dealing with these, we assume that the kernel has been expressed in "singularity-free" form, where case distinctions ensure that factors of $1/\Omega_{\bar{1}...\bar{i}}$ occur only if $\Omega_{\bar{1}...\bar{i}} \neq 0$. This is possible for the presented correlators, as shown in [P2] and discussed in App. C.1.1. These case distinctions are expressed via the symbol $\Delta_{\Omega_{\bar{1}...\bar{i}}}$ defined in Eq. (3.15). Thus, $K(\boldsymbol{\Omega}_p)$ is assumed to contain $1/\Omega_{\bar{1}...\bar{i}}$ only via $\Delta_{\Omega_{\bar{1}...\bar{i}}}$. A sum over a Δ symbol becomes a restricted sum, lacking the summand for which $\Delta = 0$. For $\ell = 2$, e.g., we have $K(\boldsymbol{\Omega}_p) = \Delta_{\Omega_{\bar{1}}} - \frac{1}{2}\beta\delta_{\Omega_{\bar{1}}}$ (see Eq. (3.16)), so that Eq. (5.6) yields

$$\tilde{G}_p(\mathrm{i}\boldsymbol{\omega}_p) + \mathcal{O}\big(\tfrac{1}{\beta}\big) \overset{\ell=2}{=} \frac{1}{(-\beta)} \sum_{\mathrm{i}\omega'_{\bar{1}}}^{\neq \mathrm{i}\omega_{\bar{1}}} \frac{G_{\mathrm{i}\omega'_{\bar{1}}}}{\mathrm{i}\omega_{\bar{1}} - \mathrm{i}\omega'_{\bar{1}}} + \frac{G_{\mathrm{i}\omega_{\bar{1}}}}{2}. \tag{5.7}$$

with the left subscript $\mathrm{i}\omega_{\bar{1}} \neq 0$.

This involves a restricted sum and an $\mathcal{O}(\beta^0)$ term resulting from $\beta\delta_{\Omega_{\bar{1}}}$ collapsing the sum $\frac{1}{(-\beta)}\sum_{\mathrm{i}\omega'_{\bar{1}}}$ in Eq. (5.6).

(ii) *$\beta\delta$ expansion of G:* To facilitate the identification of the leading-in-β contributions to Eq. (5.6), we assume that the anomalous $\hat{G}$ contribution to $G_{\mathrm{i}\omega'_p} = (\tilde{G} + \hat{G})_{\mathrm{i}\omega'_p}$ has been expressed as an expansion in powers of $\beta\delta_{\mathrm{i}\omega'_{\bar{1}...\bar{i}}}$. Such a $\beta\delta$ expansion is always possible for the correlators under consideration in this work, as discussed in App. C.1.2. Whenever $\beta\delta_{\mathrm{i}\omega'}$ appears in a Matsubara sum $\frac{1}{(-\beta)}\sum_{\mathrm{i}\omega'}$, the sum collapses and their β factors cancel. (This cancellation is why $\mathcal{R} \star G$ in Eq. (5.5) is $\mathcal{O}(\beta^0)$, as stated above, even if G contains anomalous terms.) For $\ell = 2$, e.g., we have $G_{\mathrm{i}\omega'_{\bar{1}}} = \tilde{G}_{\mathrm{i}\omega'_{\bar{1}}} + \beta\delta_{\mathrm{i}\omega'_{\bar{1}}}\hat{G}_{\bar{1}}$, with $\tilde{G}_{\mathrm{i}\omega'_{\bar{1}}}$ singularity-free at all Matsubara frequencies $\mathrm{i}\omega'_{\bar{1}}$ and $\hat{G}_{\bar{1}}$ a constant (see Eqs. (3.21) and (5.14)). Thus, Eq. (5.7) becomes

$$\tilde{G}_p(\mathrm{i}\boldsymbol{\omega}_p) + \mathcal{O}\big(\tfrac{1}{\beta}\big) \overset{\ell=2}{=} \frac{1}{(-\beta)} \sum_{\mathrm{i}\omega'_{\bar{1}}}^{\neq \mathrm{i}\omega_{\bar{1}}} \frac{\tilde{G}_{\mathrm{i}\omega'_{\bar{1}}}}{\mathrm{i}\omega_{\bar{1}} - \mathrm{i}\omega'_{\bar{1}}} + \frac{\tilde{G}_{\mathrm{i}\omega_{\bar{1}}}}{2} - \frac{\hat{G}_{\bar{1}}}{\mathrm{i}\omega_{\bar{1}}}. \tag{5.8}$$

with the left subscript $\mathrm{i}\omega_{\bar{1}} \neq 0$.

Here, the condition $\mathrm{i}\omega_{\bar{1}} \neq 0$ on the left was evoked to replace $\frac{1}{2}G_{\mathrm{i}\omega_{\bar{1}}}$ by $\frac{1}{2}\tilde{G}_{\mathrm{i}\omega_{\bar{1}}}$ on the right.

(iii) *Converting sums to integrals:* By restricting or collapsing Matsubara sums containing Δ or δ factors, one can ensure that the remaining sums are all of the form $\frac{1}{(-\beta)}\sum_{\mathrm{i}\omega'} f(\mathrm{i}\omega')$ or $\frac{1}{(-\beta)}\sum_{\mathrm{i}\omega'}^{\neq \mathrm{i}\omega} f(\mathrm{i}\omega')$, where $f(z)$, viewed as a function of $z \in \mathbb{C}$, is *analytic* at each $\mathrm{i}\omega'$ visited by the sum. (More precisely, for each $\mathrm{i}\omega'$ in the sum, $f(z)$ is analytic in an open domain containing that $\mathrm{i}\omega'$.) We express such sums in standard fashion as contour integrals:

$$\frac{1}{(-\beta)} \sum_{\mathrm{i}\omega'} f(\mathrm{i}\omega') = \oint_z n_z f(z), \tag{5.9a}$$

$$\frac{1}{(-\beta)}\sum_{i\omega'}^{\neq i\omega} f(i\omega') = \oint_z n_z f(z) - \operatorname*{Res}_{z=i\omega}\big(n_z f(z)\big). \tag{5.9b}$$

Here, $\oint_z = \oint \frac{dz}{2\pi i}$ denotes counterclockwise integration around all points $i\omega'$ visited by the sum, and n_z is a MWF chosen as in Eq. (3.46),

$$n_z = \frac{\zeta}{e^{-\beta z} - \zeta} = \frac{1}{(-\beta)}\frac{1}{z - i\omega'} - \frac{1}{2} + \mathcal{O}(z - i\omega'), \tag{5.10}$$

with $\zeta = \pm$ for bosonic/fermionic $i\omega'$. (n_z is related to standard Fermi and Bose distribution functions by $-\zeta(1 + n_z) = 1/(e^{\beta z} - \zeta)$.) The Laurent expansion on the right of Eq. (5.10) shows that n_z has first-order poles with residues $1/(-\beta)$ at all Matsubara frequencies $i\omega'$. Therefore, the integral $\oint_z$ along a contour including all $i\omega'$ frequencies recovers the unrestricted Matsubara sum of Eq. (5.9a) (see left parts of Figs. 5.1(b) and (c)). For the restricted sum of Eq. (5.9b), the first term on the right represents an unrestricted sum, i.e. the restricted sum plus a contribution from $i\omega' = i\omega$, and the residue correction subtracts the latter. For example, consider the case, needed below, that $f(i\omega') = \tilde{f}(i\omega')/(i\omega - i\omega')$, with $\tilde{f}(z)$ analytic at $z = i\omega$. Then, $n_z f(z)$ has a pole of second order at $i\omega$, with

$$\operatorname*{Res}_{z=i\omega}\Big(\frac{n_z \tilde{f}(z)}{i\omega - z}\Big) = \Big(\partial_z\big[(i\omega - z)n_z \tilde{f}(z)\big]\Big)_{z\to i\omega} = \tfrac{1}{2}\tilde{f}(i\omega) + \tfrac{1}{\beta}\Big(\partial_z \tilde{f}(z)\Big)_{z\to i\omega}. \tag{5.11}$$

Note that Eqs. (5.9) remain valid under shifts of the MWF by a constant, $n_z \to n_z + c$. We purposefully exploited this freedom to choose n_z to have $-\frac{1}{2}$ as the second term in the Laurent expansion. The reason is that this leads to a convenient cancellation between terms arising from a δ in K and residue corrections arising from Δ restrictions. For example, when evaluating the Matsubara sum in Eq. (5.8) using Eqs. (5.9b) with $f(i\omega') = \tilde{G}_{i\omega'}/(i\omega - i\omega')$, we obtain:

$$\tilde{G}_p(i\boldsymbol{\omega}_p) + \mathcal{O}\big(\tfrac{1}{\beta}\big) \overset{\ell=2}{\underset{i\omega_{\bar{1}}\neq 0}{=}} \oint_{z_{\bar{1}}} \frac{n_{z_{\bar{1}}}\tilde{G}_{z_{\bar{1}}}}{i\omega_1 - z_{\bar{1}}} - \operatorname*{Res}_{z_{\bar{1}}=i\omega_{\bar{1}}}\Big(\frac{n_{z_{\bar{1}}}\tilde{G}_{z_{\bar{1}}}}{i\omega_{\bar{1}} - z_{\bar{1}}}\Big) + \frac{\tilde{G}_{i\omega_{\bar{1}}}}{2} - \frac{\hat{G}_{\bar{1}}}{i\omega_{\bar{1}}} \tag{5.12a}$$

$$= \oint_{z_{\bar{1}}} \frac{n_{z_{\bar{1}}}\tilde{G}_{z_{\bar{1}}}}{i\omega_1 - z_{\bar{1}}} - \frac{1}{\beta}\Big(\partial_{z_{\bar{1}}}\tilde{G}_{z_{\bar{1}}}\Big)_{z_{\bar{1}}\to i\omega_{\bar{1}}} - \frac{\hat{G}_{\bar{1}}}{i\omega_{\bar{1}}}. \tag{5.12b}$$

The $\frac{1}{2}\tilde{G}_{i\omega_{\bar{1}}}$ term in Eq. (5.12a) conveniently cancels a contribution from the residue correction, evaluated using Eq. (5.11). This cancellation results from our choice of n_z having $-\frac{1}{2}$ in its Laurent expansion. (Similar cancellations occur for $\ell > 2$; see, e.g., App. C.3.2.1.) The $-\frac{1}{\beta}\big(\partial_z \tilde{G}_z\big)_{z\to i\omega}$ term in Eq. (5.12b) is an example of an $\mathcal{O}(\frac{1}{\beta})$ contribution that arises from $K \star G$ but is not part of $\tilde{G}_p$.

Having worked through the example of $\ell = 2$, we conclude this section with some general remarks about Eq. (5.6) for $\tilde{G}_p$. Once the Matsubara sums from the imaginary-frequency convolution $K \star G$ have been expressed through contour integrals, one obtains the general form[1]

$$\tilde{G}_p(i\boldsymbol{\omega}_p) + \mathcal{O}\big(\tfrac{1}{\beta}\big) = \oint_{z_{\bar{1}}} \cdots \oint_{z_{\bar{1}\ldots\overline{\ell-1}}} \tilde{K}(i\boldsymbol{\omega}_p - \boldsymbol{z}_p)\, n_{z_{\bar{1}}}\ldots n_{z_{\bar{1}\ldots\overline{\ell-1}}}\, \tilde{G}_{z_{\bar{1}},\ldots,z_{\bar{1}\ldots\overline{\ell-1}}}$$
$$+ \text{ contributions from } \hat{G}, \tag{5.13}$$

---

[1] We verified this form explicitly for $\ell \leq 7$, using expressions for K derived in [P2], but expect it to hold for arbitrary ℓ.

Here, the $(\ell - 1)$-fold contour integrals involve only the *regular* part, $\tilde{G}$, of the full MF correlator. Its anomalous part, $\hat{G}$, comes with factors $\beta\delta$ that collapse one or multiple sums in Eq. (5.6). Therefore, contributions from $\hat{G}$ to $\tilde{G}_p$ contain at most $\ell - 2$ contour integrals.

The next step, discussed in detail in Sec. 5.3.2, is to deform the integration contour in such a way that it runs infinitesimally above and below the real axis. The anomalous contributions from $\hat{G}$ can then be reincorporated into the real integrals using bosonic Dirac delta functions. As a result, one recovers precisely the form $\tilde{G}_p = \tilde{K} * S_p$ of the spectral representation (3.63b): regular kernels $\tilde{K}$ convolved with other functions, built from MWFs and analytic continuations of the various components of $\tilde{G}$ and $\hat{G}$, the latter multiplied by bosonic Dirac δ functions. These other functions can thus be identified with the PSFs $S_p = \tilde{S}_p + \hat{S}_p$, now expressed through analytic continuations of G. This clarifies, on a conceptual level, how the information contained in the full MF correlator G needs to be repackaged to obtain PSFs, and the explicit formulas for $\ell = 2, 3, 4$ in Eqs. (5.21) (see also Eq. (3.53)), (5.48), and (5.62) constitute the main results of this chapter. These, in turn, can then be used to obtain KF correlators via Eq. (5.2a).

To summarize, the MF-to-KF analytic continuation of arbitrary ℓp correlation functions can be achieved via the following three-step strategy:

- Step 1. *Matsubara summation through contour integration:* Insert the MF kernel K (expressed in singularity-free form) and the MF correlator G (expressed as a $\beta\delta$ expansion), including all regular and anomalous contributions, into Eq. (5.6) for $\tilde{G}_p$. Restrict or collapse Matsubara sums containing Δ or $\beta\delta$ factors and express the remaining sums through contour integrals using Eqs. (5.9), to arrive at Eq. (5.13).

- Step 2. *Extraction of PSFs:* Deform the contours away from the imaginary axis to run along the real axis, while carefully tracking possible singularities of the MF correlators. Reincorporate anomalous contributions via bosonic Dirac delta functions. This results in a spectral representation of the form $\tilde{G}_p = \tilde{K} * S_p$. From this, read off the PSFs $S_p[G]$, expressed through products of MWFs and MF correlators, analytically continued to real frequencies (see, e.g., Eq. (5.21)).

- Step 3. *Construction of KF correlators:* Construct the full KF correlator $G^{[\eta_1 \ldots \eta_\alpha]}$, involving a sum $\sum_p$ over terms of the form $\big[K^{[\hat{\eta}_1 \ldots \hat{\eta}_\alpha]} * S_p\big](\mathrm{i}\boldsymbol{\omega}_p)$ (Eq. (5.2a)). Simplify the kernels $K^{[\hat{\eta}_1 \ldots \hat{\eta}_\alpha]}$ via a set of kernel identities (see, e.g., Eqs. (5.31)) and combine terms with similar structure from the sum $\sum_p$. Insert into the resulting expressions the PSFs from Step 2, and then compute the integrals involved in the $*$ convolution. This leads to equations expressing KF correlators through analytically continued MF correlators, $G^{[\eta_1 \ldots \eta_\alpha]}[G]$.

The result of Step 2 already constitutes an analytic continuation since the PSFs S_p suffice to construct the KF correlators via the spectral representation. Step 3 serves to give direct relations between both formalisms.

In App. C.7.2, we follow an independent approach and use the equilibrium condition to explicitly perform the following consistency check: given an arbitrary set of PSFs S_p as input, compute the MF correlator $G = \sum_p K * S_p$ and verify that the formulas $S_p[G]$ correctly recover the input PSFs from G, giving $S_p[G] = S_p$. This consistency check is presented for general 2p and 3p and for fermionic 4p correlators.

The next sections are devoted to explicitly working out the details of this strategy. To demonstrate its basic ideas, we first revisit the 2p case in the following section. Although we already derived the results by different means in Sec. 3.2.3, we present it in a manner that readily generalizes to the higher-point correlators discussed in subsequent sections: 3p correlators in Sec. 5.5 and 4p correlators in Sec. 5.6.

5.3 Analytic continuation of 2p functions

In this section, we carry through the strategy outlined in Sec. 5.2.2 to obtain the MF-to-KF analytic continuation in the well-known 2p case. While our strategy may seem more cumbersome than the one presented in Sec. 3.2.3 or traditional textbook discussions (see, e.g., Ref. [Wen04]), it has the merit of readily generalizing to $\ell > 2$. We first recapitulate the spectral representation and analytic properties of general 2p MF correlators (Sec. 5.3.1). Then, we express the PSFs in terms of analytically continued MF correlators (Sec. 5.3.2). Finally, we use these to recover familiar expressions for the retarded, advanced, and Keldysh components of the KF 2p correlator (Sec. 5.3.3).

5.3.1 Analytic properties of the 2p MF correlator

We begin by reviewing well-known analytical properties of the 2p MF correlator. This also serves to give concrete examples for our notational conventions.

$G(\mathrm{i}\boldsymbol{\omega}) = G(\mathrm{i}\omega_1, \mathrm{i}\omega_2)$ explicitly depends on one Matsubara frequency, $\mathrm{i}\omega_1$ or $\mathrm{i}\omega_2$, while the other frequency is fixed by energy conservation, $\mathrm{i}\omega_{12} = 0$. Since we want to compute Eq. (5.6) for arbitrary permutations $p = (\overline{12})$, it proves useful to develop an unbiased notation for the frequency dependence. The chosen explicit frequency dependence is indicated by a subscript in $G_{\mathrm{i}\omega_{\overline{1}}}$, such that $G_{\mathrm{i}\omega_1} = G(\mathrm{i}\boldsymbol{\omega}(\omega_1)) = G(\mathrm{i}\omega_1, -\mathrm{i}\omega_1)$ and $G_{\mathrm{i}\omega_2} = G(\mathrm{i}\boldsymbol{\omega}(\omega_2)) = G(-\mathrm{i}\omega_2, \mathrm{i}\omega_2)$. The most general form of $G_{\mathrm{i}\omega_{\overline{1}}}$, covering both fermionic and bosonic cases, reads

$$G(\mathrm{i}\boldsymbol{\omega}(\omega_{\overline{1}})) = G_{\mathrm{i}\omega_{\overline{1}}} = \tilde{G}_{\mathrm{i}\omega_{\overline{1}}} + \beta\delta_{\mathrm{i}\omega_{\overline{1}}}\hat{G}_{\overline{1}}, \tag{5.14}$$

in agreement with the general form Eq. (C.5). The regular part, $\tilde{G}_{\mathrm{i}\omega_{\overline{1}}}$, is singularity-free for all $\mathrm{i}\omega_{\overline{1}}$, including 0. $\hat{G}_{\overline{1}}$ denotes the anomalous part, a constant, contributing only for $\mathrm{i}\omega_{\overline{1}} = 0$. The relation $G_{\mathrm{i}\omega_1} = G_{\mathrm{i}\omega_2}$ enforces $\hat{G}_1 = \hat{G}_2$.

One of the next steps involves the deformation of the integration contour $\oint_{z_{\overline{1}}}$ from the imaginary axis toward the real axis. This requires knowledge of the analytic structure of the MF correlator. It can be made explicit via the spectral representation of G_{z_1} (Eqs. (3.63)), with the PSFs S_p viewed as input. For the regular part, we obtain

$$\tilde{G}_{z_1} = \int \mathrm{d}^2\varepsilon\, \delta(\varepsilon_{12}) \left[\frac{S_{(12)}(\varepsilon_1)}{z_1 - \varepsilon_1} + \frac{S_{(21)}(\varepsilon_2)}{-z_1 - \varepsilon_2} \right] = \int \mathrm{d}\varepsilon_1\, \frac{S_{\mathrm{std}}(\varepsilon_1)}{z_1 - \varepsilon_1}. \tag{5.15}$$

Here, we used the standard spectral function S_{std} defined in Eq. (3.22). In contrast to the previous sections, we will henceforth usually display only the first $\ell - 1$ frequency arguments for individual PSFs to allow for a more compact presentation of our results, in particular for $\ell = 3, 4$. General PSF (anti)commutators, on the other hand, will always take the full, unpermuted tuple $\boldsymbol{\varepsilon}$ as their argument (with $S_{\mathrm{std}}(\varepsilon_1)$ being an exception), implying

$$S_{\mathrm{std}}(\varepsilon_1) = S_{[1,2]_-}(\varepsilon_1, -\varepsilon_1) = S_{(12)}(\varepsilon_1) - S_{(21)}(-\varepsilon_1), \tag{5.16a}$$

$$S_{[1,2]_\pm}(\boldsymbol{\varepsilon}) = S_{(12)}(\varepsilon_1) \pm S_{(21)}(\varepsilon_2). \tag{5.16b}$$

Here, $\varepsilon_{12} = 0$ is understood for the argument of $S_{[1,2]_\pm}(\boldsymbol{\varepsilon})$.

Evidently, $\tilde{G}_{z_1}$ has poles (or branch cuts for continuous spectra) whenever the denominator $z_1 - \varepsilon_1$ in Eq. (5.15) vanishes. This can happen only if $\mathrm{Im}(z_1) = 0$ (or, more generally, $\mathrm{Im}(z_{\overline{1}}) = 0$), indicated in Fig. 5.1 by thick, red lines on the real axis. Hence, the upper and the lower complex half plane are analytic regions of $\tilde{G}_{z_1}$, separated by a branch cut at $\mathrm{Im}(z_1) = 0$.
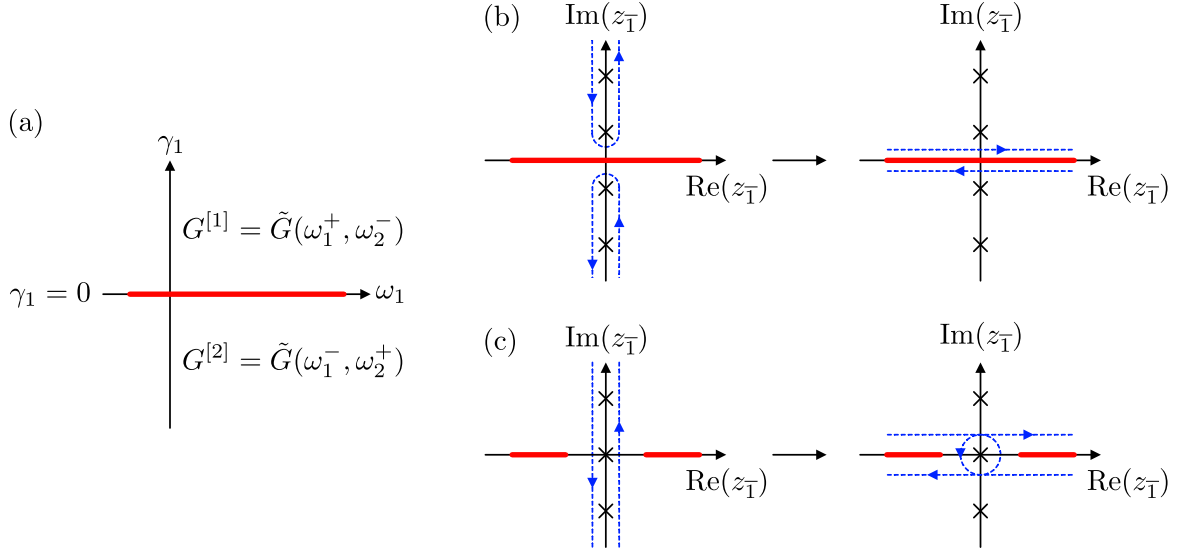
Figure 5.1 (a) Analytic regions of a regular 2p MF correlator as a function of a complex frequency $\omega_1 + \mathrm{i}\gamma_1$ with $\omega_1, \gamma_1 \in \mathbb{R}$. The thick, red line on the real axis depicts a possible branch cut of the correlator. (b,c) Contours to evaluate the Matsubara summation in the (b) fermionic and (c) bosonic case, see Eqs. (5.17) and (5.18), respectively. Crosses indicate the poles of the MWF $n_{z_{\bar{1}}}$ at the Matsubara frequencies on the imaginary axis. The dashed blue contours, initially enclosing all Matsubara frequencies, are deformed away from the imaginary axis to run infinitesimally above and below the real axis. In the bosonic 2p case (c), the branch cut does not extend to $z_{\bar{1}} = 0$ as the correlator, by definition, is free of any singularities at vanishing Matsubara frequencies.

5.3.2 Extraction of PSFs from partial MF correlators

In Sec. 5.2.2, we expressed the regular partial MF correlators $\tilde{G}_p(\mathrm{i}\boldsymbol{\omega}_p)$ for $\ell = 2$ in terms of a contour integral $\oint_{z_{\bar{1}}}$ involving the regular MF correlator $\tilde{G}_{z_{\bar{1}}}$, see Eq. (5.12b). That amounted to Step 1 of our 3-step strategy. Turning to Step 2, we write $\tilde{G}_p(\mathrm{i}\boldsymbol{\omega}_p)$ in the form of a convolution $[\tilde{K} * S_p](\mathrm{i}\boldsymbol{\omega}_p)$, from which we then read out expressions for the PSFs $S_p[G]$.

To this end, we exploit the analyticity of $\tilde{G}_{z_{\bar{1}}}$ in the upper and lower half-plane to deform the contours in $\oint_{z_{\bar{1}}}$ from enclosing the imaginary axis to running infinitesimally above and below the branch cut. We denote the corresponding integration variables along the branch cut by $\varepsilon_{\bar{1}}^{\pm} = \varepsilon_{\bar{1}} \pm \mathrm{i}0^+$, with $\varepsilon_{\bar{1}} = \mathrm{Re}(z_{\bar{1}})$ now being a real variable and $\pm \mathrm{i}0^+$ infinitesimal shifts.

We discuss the cases of fermionic or bosonic frequencies separately. For fermions, the contour deformation of $\oint_{z_{\bar{1}}}$ in Eq. (5.12b) is straightforward and yields (see Fig. 5.1(b))

$$\oint \frac{\mathrm{d}z_{\bar{1}}}{2\pi\mathrm{i}} \frac{n_{z_{\bar{1}}} \tilde{G}_{z_{\bar{1}}}}{\mathrm{i}\omega_{\bar{1}} - z_{\bar{1}}} = \int_{-\infty}^{\infty} \frac{\mathrm{d}\varepsilon_{\bar{1}}}{2\pi\mathrm{i}} \frac{n_{\varepsilon_{\bar{1}}} \tilde{G}^{\varepsilon_{\bar{1}}}}{\mathrm{i}\omega_{\bar{1}} - \varepsilon_{\bar{1}}}. \tag{5.17}$$

Here, we defined $\tilde{G}^{\varepsilon_{\bar{1}}} = \tilde{G}_{\varepsilon_{\bar{1}}^+} - \tilde{G}_{\varepsilon_{\bar{1}}^-}$ as the discontinuity of $\tilde{G}_{z_{\bar{1}}}$ across the branch cut at $\mathrm{Im}(z_{\bar{1}}) = 0$. Moreover, we extended the subscript notation introduced after Eq. (5.4b) to real frequencies with infinitesimal imaginary shifts. (This notation is further discussed after Eq. (5.21).)

In the bosonic case, the pole at $z_{\bar{1}} = 0$ has to be treated separately (see Fig. 5.1(c)):

$$\oint \frac{\mathrm{d}z_{\bar{1}}}{2\pi\mathrm{i}} \frac{n_{z_{\bar{1}}} \tilde{G}_{z_{\bar{1}}}}{\mathrm{i}\omega_{\bar{1}} - z_{\bar{1}}} = \fint_{-\infty}^{\infty} \frac{\mathrm{d}\varepsilon_{\bar{1}}}{2\pi\mathrm{i}} \frac{n_{\varepsilon_{\bar{1}}} \tilde{G}^{\varepsilon_{\bar{1}}}}{\mathrm{i}\omega_{\bar{1}} - \varepsilon_{\bar{1}}} + \operatorname*{Res}_{z_{\bar{1}}=0} \left(\frac{n_{z_{\bar{1}}} \tilde{G}_{z_{\bar{1}}}}{\mathrm{i}\omega_{\bar{1}} - z_{\bar{1}}} \right)$$

$$= \fint_{-\infty}^{\infty} \frac{\mathrm{d}\varepsilon_{\bar{1}}}{2\pi \mathrm{i}} \frac{n_{\varepsilon_{\bar{1}}} \tilde{G}^{\varepsilon_{\bar{1}}}}{\mathrm{i}\omega_{\bar{1}} - \varepsilon_{\bar{1}}} + \mathcal{O}(\tfrac{1}{\beta}). \tag{5.18}$$

Here, $\fint$ indicates a principal-value integral. The residue evaluates to a contribution of order $\mathcal{O}(\tfrac{1}{\beta})$ as the bosonic MWF $n_{z_{\bar{1}}}$ is the only factor having a pole at $z_{\bar{1}} = 0$, with residue $1/(-\beta)$ there (remember that $\mathrm{i}\omega_{\bar{1}} \neq 0$). Combining Eqs. (5.17), (5.18), (5.12b) and omitting $\mathcal{O}(\tfrac{1}{\beta})$ terms, we finally find

$$\tilde{G}_p(\mathrm{i}\boldsymbol{\omega}_p) = \int_{\varepsilon_{\bar{1}}} \frac{n_{\varepsilon_{\bar{1}}} \tilde{G}^{\varepsilon_{\bar{1}}}}{\mathrm{i}\omega_{\bar{1}} - \varepsilon_{\bar{1}}} - \frac{\hat{G}_{\bar{1}}}{\mathrm{i}\omega_{\bar{1}}} = \int_{\varepsilon_{\bar{1}}} \frac{n_{\varepsilon_{\bar{1}}} \tilde{G}^{\varepsilon_{\bar{1}}} + \hat{\delta}(\varepsilon_{\bar{1}}) \hat{G}_{\bar{1}}}{\mathrm{i}\omega_{\bar{1}} - \varepsilon_{\bar{1}}}. \tag{5.19}$$

On the right, we absorbed the anomalous $\hat{G}$ contribution into the integral, defining $\hat{\delta}(\varepsilon_{\bar{1}}) = -2\pi \mathrm{i}\, \delta(\varepsilon_{\bar{1}})$. Moreover, we introduced the symbol $\int_{\varepsilon_i}$ as

$$\int_{\varepsilon_i} \cdots = \begin{cases} \displaystyle\int_{-\infty}^{\infty} \frac{\mathrm{d}\varepsilon_i}{2\pi \mathrm{i}} \cdots & \text{for fermionic } \varepsilon_i \text{ or anomalous frequency,} \\[2ex] \displaystyle\fint_{-\infty}^{\infty} \frac{\mathrm{d}\varepsilon_i}{2\pi \mathrm{i}} \cdots & \text{for bosonic } \varepsilon_i \text{ and regular frequency.} \end{cases} \tag{5.20}$$

We call a frequency ε_i *anomalous* if it is directly set to zero by a Dirac $\hat{\delta}(\varepsilon_i)$ in the integrand, and *regular* otherwise. Since the anomalous contribution arose from a Kronecker $\delta_{\mathrm{i}\omega_{\bar{1}}}$, we arrive at a rule of thumb: when performing Matsubara sums via contour integration and contour deformation to the real axis, Kronecker deltas with Matsubara arguments lead to Dirac deltas with real arguments.

Importantly, Eq. (5.19) has precisely the same form as Eq. (3.63b) for $\ell = 2$, with the correspondence

$$(2\pi \mathrm{i}) S_p(\varepsilon_{\bar{1}}) = n_{\varepsilon_{\bar{1}}} \tilde{G}^{\varepsilon_{\bar{1}}} + \hat{\delta}(\varepsilon_{\bar{1}}) \hat{G}_{\bar{1}}. \tag{5.21}$$

This remarkable formula is the first central result of this section: it shows that a suitable analytic continuation of the MF correlator $G(\mathrm{i}\boldsymbol{\omega})$, combined with a MWF, fully determines the PSF and thus, via the spectral representation Eqs. (5.2a), the KF correlator $G^{\boldsymbol{k}}$. It also clarifies the role of anomalous contributions. In subsequent sections, we will find analogous results for $\ell = 3, 4$.

To conclude this section, we elaborate on the meaning of the super- and supscript notation used above. The discontinuity in Eq. (5.21), $\tilde{G}^{\varepsilon_{\bar{1}}} = \tilde{G}_{\varepsilon_{\bar{1}}^+} - \tilde{G}_{\varepsilon_{\bar{1}}^-}$, consists of analytically continued MF correlators, $\tilde{G}(\mathrm{i}\boldsymbol{\omega}) \to \tilde{G}(\boldsymbol{z})$. Here, the entries of $\boldsymbol{z} = (\varepsilon_1^{\pm}, \varepsilon_2^{\mp})$ are infinitesimally shifted by $+\mathrm{i}0^+$ or $-\mathrm{i}0^+$, but constrained by energy conservation, $\varepsilon_{12} = 0$. The subscript on $\tilde{G}_{\varepsilon_{\bar{1}}^{\pm}}$ has the same meaning as for imaginary frequencies (see paragraph after Eq. (5.4b)): it indicates the chosen explicit (real-)frequency dependence of $\tilde{G}(\boldsymbol{z})$, i.e., $\tilde{G}_{\varepsilon_{\bar{1}}^{\pm}} = \tilde{G}(\boldsymbol{z}(\varepsilon_{\bar{1}}^{\pm}))$, uniquely determining the imaginary shifts in each entry of $\boldsymbol{z}$. To be explicit, we have

$$\tilde{G}^{\varepsilon_1} = \tilde{G}(\varepsilon_1^+, -\varepsilon_1^+) - \tilde{G}(\varepsilon_1^-, -\varepsilon_1^-), \tag{5.22a}$$
$$\tilde{G}^{\varepsilon_2} = \tilde{G}(-\varepsilon_2^+, \varepsilon_2^+) - \tilde{G}(-\varepsilon_2^-, \varepsilon_2^-). \tag{5.22b}$$

Since $\varepsilon_2 = -\varepsilon_1$ (energy conservation) and hence $\varepsilon_2^+ = -\varepsilon_1^-$, we have $\tilde{G}^{\varepsilon_1} = -\tilde{G}^{\varepsilon_2} = \tilde{G}^{-\varepsilon_2}$. (Check for negative superscripts: $\tilde{G}^{-\varepsilon_2} = \tilde{G}_{(-\varepsilon_2)^+} - \tilde{G}_{(-\varepsilon_2)^-} = \tilde{G}_{-\varepsilon_2^-} - \tilde{G}_{-\varepsilon_2^+} = -\tilde{G}^{\varepsilon_2}$.)

For illustration, we give explicit formulas for S_p for the permutations $p = (12)$ and $p = (21)$,

$$(2\pi i)S_{(12)}(\varepsilon_1) = n_{\varepsilon_1}[\tilde{G}(\varepsilon_1^+, -\varepsilon_1^+) - \tilde{G}(\varepsilon_1^-, -\varepsilon_1^-)] + \hat{\delta}(\varepsilon_1)\hat{G}_1.$$
$$(2\pi i)S_{(21)}(\varepsilon_2) = n_{\varepsilon_2}[\tilde{G}(-\varepsilon_2^+, \varepsilon_2^+) - \tilde{G}(-\varepsilon_2^-, \varepsilon_2^-)] + \hat{\delta}(\varepsilon_2)\hat{G}_2, \quad (5.23)$$

where we inserted Eq. (5.22) for the discontinuities. Equation (3.53) then directly follows from these expressions by inserting Eq. (5.28) below. The anomalous contributions satisfy $\hat{G}_1 = \hat{G}_2$ (as explained after Eq. (5.14)) and exist only for bosonic correlators ($\zeta = 1$). Energy conservation $\varepsilon_2 = -\varepsilon_1$ then gives

$$(2\pi i)S_{(21)}(-\varepsilon_1) = n_{-\varepsilon_1}[\tilde{G}(\varepsilon_1^-, -\varepsilon_1^-) - \tilde{G}(\varepsilon_1^+, -\varepsilon_1^+)] + \hat{\delta}(\varepsilon_1)\hat{G}_2$$
$$= \zeta e^{-\beta\varepsilon_1}(2\pi i)S_{(12)}(\varepsilon_1). \quad (5.24)$$

For the last step, we used the identity $-n_{-\varepsilon_1} = \zeta e^{-\beta\varepsilon_1}n_{\varepsilon_1}$. As a useful consistency check, we note that Equation (5.24) corresponds to the equilibrium condition Eq. (2.47) for PSFs (with $p = (21)$, $p_\lambda = (12)$ there, implying $\zeta_p = \zeta$, $\zeta_{p_\lambda} = +1$ and $\varepsilon_{\bar{1}} = \varepsilon_2 = -\varepsilon_1$, $\varepsilon_{p_\lambda(1)} = \varepsilon_1$).

Expressing the standard spectral function $S_{\text{std}}(\varepsilon_1)$ from Eq. (5.16a) in terms of Eq. (5.21), we find

$$(2\pi i)S_{\text{std}}(\varepsilon_1) = n_{\varepsilon_1}\tilde{G}^{\varepsilon_1} + \hat{\delta}(\varepsilon_1)\hat{G}_1 - n_{-\varepsilon_1}\tilde{G}^{-\varepsilon_1} - \hat{\delta}(-\varepsilon_1)\hat{G}_2$$
$$= n_{\varepsilon_1}\tilde{G}^{\varepsilon_1} - n_{-\varepsilon_1}\tilde{G}^{-\varepsilon_1} = (n_{\varepsilon_1} + n_{-\varepsilon_1})\tilde{G}^{\varepsilon_1}$$
$$= -\tilde{G}^{\varepsilon_1}, \quad (5.25)$$

where we used $\tilde{G}^{-\varepsilon_1} = -\tilde{G}^{\varepsilon_1}$.[2] Thus, the discontinuity $\tilde{G}^{\varepsilon_{\bar{1}}}$ in the PSFs (5.21) encodes $S_{\text{std}}(\varepsilon_1)$. Conversely, however, $S_{\text{std}}(\varepsilon_1)$ retains only the discontinuity $\tilde{G}^{\varepsilon_{\bar{1}}}$ in the PSFs (5.21), while the information on the MWF and the anomalous part, both contained in the S_p (5.23), is lost. In App. C.7.2, we use Eq. (5.25) and the equilibrium condition to explicitly perform the following consistency check: given an arbitrary set of PSFs as input, compute the MF correlator $G = \sum_p K * S_p$ and verify that Eq. (5.21) for S_p correctly recovers the input PSFs.

5.3.3 Keldysh correlator

Next, we turn to Step 3 of our 3-step strategy: we use the PSFs obtained above to explicitly construct the Keldysh components $G^{[1]}$, $G^{[2]}$, and $G^{[12]}$, expressed through analytically continued MF correlators. As the structure of KF correlators becomes more intricate with an increasing number of 2's in the Keldysh component, denoted by α in Eqs. (3.67), we discuss the different values of α separately in the following and throughout the rest of this chapter.

5.3.3.1 Keldysh components $G^{[\eta]}$

For $\alpha = 1$, the fully retarded or fully advanced Keldysh components $G^{[\eta]}$ can be deduced from the regular part of MF correlators alone (Eq. (3.71)). Here, we follow the alternative and equivalent strategy of Step 3: we insert the PSFs from Eq. (5.21) into the spectral representation (5.2a):

$$G^{[\eta]}(\boldsymbol{\omega}) = \sum_p [K^{[\hat{\eta}]} * S_p](\boldsymbol{\omega}_p) = \sum_p [\tilde{K} * S_p](\boldsymbol{\omega}_p^{[\eta]}) \quad (5.26a)$$

---

2 Equation (5.25) corresponds to Eq. (3.51) by inserting G^R and G^A using Eq. (5.28).

$$= \int \mathrm{d}^2\varepsilon \, \delta(\varepsilon_{12}) \left(\frac{S_{(12)}(\varepsilon_1)}{\omega_1^{[\eta]} - \varepsilon_1} + \frac{S_{(21)}(\varepsilon_2)}{\omega_2^{[\eta]} - \varepsilon_2} \right) \tag{5.26b}$$

$$= \int \mathrm{d}\varepsilon_1 \, \frac{S_{[1,2]_-}(\varepsilon_1, -\varepsilon_1)}{\omega_1^{[\eta]} - \varepsilon_1}. \tag{5.26c}$$

Here, we used $\omega_2^{[\eta]} = -\omega_1^{[\eta]}$ (Eq. (3.68)) and that the sum over both permutations, $p = (12)$ and (21), leads to the appearance of the PSF commutator $S_{[1,2]_-}$ (equalling S_{std}, cf. Eq. (5.16)).

Before proceeding, a general remark is in order: When the external variables $\boldsymbol{\omega}_p^{[\eta]}$ appear in $*$ convolution integrals such as $\int_{\varepsilon_1}$ in Eqs. (5.26), it is essential to maintain the hierarchy $\gamma_0 \gg 0^+$ for the infinitesimal imaginary shifts $\pm i\gamma_0$ and $\pm i0^\pm$ contained in the external frequencies $\boldsymbol{\omega}_p^{[\eta]}$ and the integration variables $\varepsilon_1^\pm$, respectively. The reason is that the contour deformation from $\oint_{z_1}$ to $\int_{\varepsilon_1}$ has been performed *before* the analytic continuation $i\boldsymbol{\omega}_p \to \boldsymbol{\omega}_p^{[\eta]}$ underlying Eqs. (5.2) and leading to Eq. (5.26) (see Fig. 5.2(a)). This hierarchy is particularly relevant for principle-value integrals $\fint$ (needed below); these exclude an interval $[-0^+, 0^+]$ around the origin, and γ_0 must lie outside this interval.

Inserting $S_{[1,2]_-}(\varepsilon_1, -\varepsilon_1) = S_{\mathrm{std}}(\varepsilon_1) = \tilde{G}^{\varepsilon_1}/(-2\pi i)$ (from Eqs. (5.16a) and (5.25)), we find

$$G^{[\eta]}(\boldsymbol{\omega}) = -\int_{\varepsilon_1} \frac{\tilde{G}^{\varepsilon_1}}{\omega_1^{[\eta]} - \varepsilon_1} = -\int_{\varepsilon_1} \frac{\tilde{G}_{\varepsilon_1^+} - \tilde{G}_{\varepsilon_1^-}}{\omega_1^{[\eta]} - \varepsilon_1} = \tilde{G}_{\omega_1^{[\eta]}}. \tag{5.27}$$

Importantly, no MWFs n_{ε_1} occur in Eq. (5.27). For the last step, we were thus able to close the forward (backward) integration contour involving $\tilde{G}_{\varepsilon_1^+}$ ($\tilde{G}_{\varepsilon_1^-}$) in the upper (lower) half-plane. We then used Cauchy's integral formula for the simple pole at $\omega_1^{[\eta]}$ (see Fig. 5.2(b)). Equation (5.27) expresses the fully retarded Keldysh correlators through analytic continuations of MF correlators, $G^{[\eta]}[G]$, as desired. To make contact with standard notation, we recall that the retarded and advanced 2p components are given by $G^R = G^{21} = G^{[1]}$ and $G^A = G^{12} = G^{[2]}$. Reinstating frequency dependencies, with $\omega_1^{[1]} = \omega_1 + i\gamma_0 \equiv \omega_1^+$ and $\omega_1^{[2]} = \omega_1 - i\gamma_0 \equiv \omega_1^-$, we get (see Eq. (3.40))

$$G^R(\boldsymbol{\omega}) = \tilde{G}(\omega_1^+, \omega_2^-), \quad G^A(\boldsymbol{\omega}) = \tilde{G}(\omega_1^-, \omega_2^+). \tag{5.28}$$

This implies the well-known relation (see Eq. (3.39))

$$G'^R(\boldsymbol{\omega}) = G^A(\boldsymbol{\omega}), \quad G'^A(\boldsymbol{\omega}) = G^R(\boldsymbol{\omega}). \tag{5.29}$$

5.3.3.2 Keldysh component $G^{[12]}$

For $\alpha = 2$, both Keldysh indices equal 2, $G^{22} = G^{[12]}$. Then, the spectral representation in Eq. (5.2a) requires the kernel (Eq. (3.67c))

$$K^{[\hat{\eta}_1 \hat{\eta}_2]}(\boldsymbol{\omega}_p) = \left(K^{[\hat{\eta}_1]} - K^{[\hat{\eta}_2]} \right)(\boldsymbol{\omega}_p) = \tilde{K}(\boldsymbol{\omega}_p^{[\bar{\hat{\eta}}_1]}) - \tilde{K}(\boldsymbol{\omega}_p^{[\bar{\hat{\eta}}_2]}), \tag{5.30}$$

for the case $[\eta_1 \eta_1] = [12] = [\hat{\eta}_1 \hat{\eta}_2]$. Evaluating this for $p = (12)$ and (21), we find

$$K^{[12]}(\boldsymbol{\omega}_{(12)}) = \tilde{K}(\boldsymbol{\omega}_{(12)}^{[1]}) - \tilde{K}(\boldsymbol{\omega}_{(12)}^{[2]}) = \frac{1}{\omega_1^{[1]}} - \frac{1}{\omega_1^{[2]}} = \frac{-2i\gamma_0}{\omega_1^2 + \gamma_0^2} = \hat{\delta}_{\gamma_0}(\omega_1), \tag{5.31a}$$

$$K^{[12]}(\boldsymbol{\omega}_{(21)}) = \tilde{K}(\boldsymbol{\omega}_{(21)}^{[2]}) - \tilde{K}(\boldsymbol{\omega}_{(21)}^{[1]}) = \frac{1}{\omega_2^{[2]}} - \frac{1}{\omega_2^{[1]}} = \frac{-2i\gamma_0}{\omega_2^2 + \gamma_0^2} = \hat{\delta}_{\gamma_0}(\omega_1). \tag{5.31b}$$
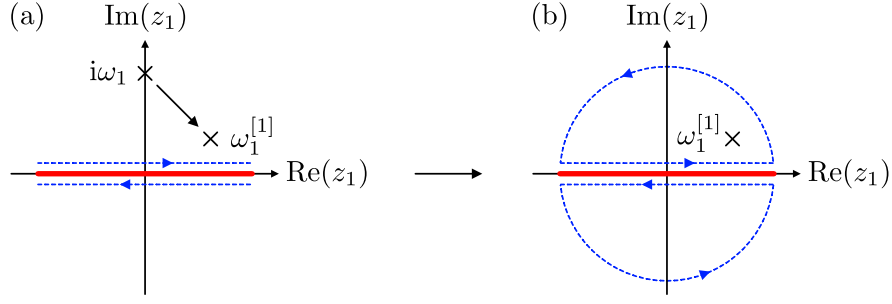
Figure 5.2 (a) Analytic continuation of the Matsubara frequency $i\omega_1 \to \omega_1^{[1]} = \omega_1 + i\gamma_0$ in Eqs. (5.26) for fermionic frequencies. The imaginary part of the external frequency $\omega_1^{[1]}$ has to be larger than the imaginary parts of $\varepsilon_1^\pm$ used to integrate infinitesimally above and below the real axis. The transition from (a) to (b) illustrates the closing of the contour in the upper/lower half-planes to evaluate the integral in Eq. (5.27). As the integrand is independent of the fermionic MWF n_{ε_1}, the only contribution to the integral originates from the simple pole at $z_1 = \omega_1^{[1]}$.

On the right, we introduced a Lorentzian representation of a broadened Dirac delta function:

$$\hat{\delta}_{\gamma_0}(x) = \frac{-2i\gamma_0}{x^2 + \gamma_0^2}, \qquad \lim_{\gamma_0 \to 0^+} \hat{\delta}_{\gamma_0}(x) = -2\pi i\delta(x) = \hat{\delta}(x). \tag{5.32}$$

Finally, we obtain $G^{[12]}$ by convolving the kernels (5.31) with the PSFs (5.21) according to Eq. (5.2a):

$$\begin{aligned} G^{[12]} &= \sum_p \left[K^{[\hat{1}\hat{2}]} * S_p \right](\boldsymbol{\omega}_p) = \int_{\varepsilon_1} (2\pi i) S_{[1,2]_+}(\varepsilon_1, -\varepsilon_1) \, \hat{\delta}_{\gamma_0}(\omega_1 - \varepsilon_1) \\ &= \int_{\varepsilon_1} \left[(1 + 2n_{\varepsilon_1})\tilde{G}^{\varepsilon_1} + 2\hat{\delta}(\varepsilon_1)\hat{G}_1 \right] \hat{\delta}_{\gamma_0}(\omega_1 - \varepsilon_1) \\ &= N_{\omega_1}\tilde{G}^{\omega_1} + 4\pi i\,\delta(\omega_1)\hat{G}_1. \end{aligned} \tag{5.33}$$

For the last step we used (see Eq. (3.50))

$$N_{\omega_i} = -n_{\omega_i} + n_{-\omega_i} = -1 - 2n_{\omega_i} = \coth[\beta\omega_i/2]^{\zeta^i}. \tag{5.34}$$

For bosonic correlators, N_{ω_1} is singular at $\omega_1 = 0$, so that a principle-value integral is implied in Eq. (5.33). Then, the product $N_{\omega_1}\tilde{G}^{\omega_1}$ should be evaluated via the limit $(N_{\omega_1}\tilde{G}^{\omega_1})_{\omega_1 \to 0}$. More precisely, three limits are involved: 0^+, γ_0, and ω_1 should all be sent to zero, while respecting $0^+ \ll \gamma_0 \ll |\omega_1|$ (see discussion after Eq. (5.26)). In the following, we suppress the subscript γ_0 in Eq. (5.32) and always take $\gamma_0 \to 0^+$ after evaluating a principal-value integral (if present).

Summarizing, all Keldysh components can be expressed through analytically continued MF functions. Comparing Eqs. (5.33) and (5.14), we find that the anomalous part, $\hat{G}_1$, enters $G^{[12]}$ with a prefactor of $4\pi i\delta(\omega_1)$, consistent with Eq. (3.52). Using our previous results from Eq. (5.28), yielding $\tilde{G}^{\omega_1} = G^R(\omega_1) - G^A(\omega_1)$, and defining $G^{[12]} = G^K$, the above relation (5.33) can be indeed identified as the FDR (3.52):

$$G^K(\omega_1) = N_{\omega_1}\left[G^R(\omega_1) - G^A(\omega_1) \right] + 4\pi i\,\delta(\omega_1)\hat{G}_1. \tag{5.35}$$

As we found in Secs. 3.2.2 and 3.2.3, the way in which anomalous MF terms appear in KF correlators is via Keldysh correlator G^K.

From now on, we will refer to general relations between components of KF correlators in thermal equilibrium as *generalized fluctuation-dissipation relations* (gFDRs). Equations (5.29) and (5.35) constitute the two gFDRs available for $\ell = 2$. In the absence of anomalous contributions, they reduce the three nonzero KF components to a single independent one (typically chosen as G^R).

5.4 Analytic regions and discontinuities of the MF correlator

Step 2 of our three-step strategy, the extraction of PSFs, requires knowledge of possible singularities of the MF correlators. In the 2p case, for $\tilde{G}_{z_1}$, a branch cut divides the complex z_1 plain into two analytic regions (see Fig. 5.1(a)), and the discontinuity across the branch cut is given by the difference of the analytic continuations $\tilde{G}_{\omega_1^{\pm}}$. In this section, we generalize the concepts of and notations for branch cuts, analytic regions, and discontinuities to general ℓ, enabling a concise discussion of the analytic continuation of 3p and 4p MF correlators in Secs. 5.5 and 5.6, respectively. We focus on the regular parts $\tilde{G}$ of the MF correlators; the anomalous parts will be discussed separately in the sections for $\ell = 3$ and 4.

5.4.1 Analytic regions of $\tilde{G}(\boldsymbol{z})$

Possible singularities of the regular part can be inferred from the spectral representation in Eq. (3.63b)

$$\tilde{G}(\boldsymbol{z}) = \int \mathrm{d}^\ell \varepsilon_p \, \delta(\varepsilon_{\overline{1}\dots\overline{\ell}}) \sum_p \frac{S_p(\boldsymbol{\varepsilon}_p)}{\prod_{i=1}^{\ell-1}(z_{\overline{1}\dots\overline{i}} - \varepsilon_{\overline{1}\dots\overline{i}})}, \tag{5.36}$$

with $z_i = \omega_i + \mathrm{i}\gamma_i$ and $z_{1\dots\ell} = 0$. Singularities can be located at the points where the imaginary part of the denominator vanishes, defining branch cuts by the condition

$$\mathrm{Im}(z_I) = \gamma_I = 0, \tag{5.37}$$

where $z_I = \sum_{i \in I} z_i$ denotes a frequency sum over the elements of a non-empty subset $I \subseteq \{1, \dots, \ell\}$. In total, condition (5.37) defines $2^{\ell-1} - 1$ distinct branch cuts since frequency conservation implies $\mathrm{Im}(z_I) = -\mathrm{Im}(z_{I^c})$ where $I^c = \{1, \dots, \ell\}\backslash I$ is the complement of I, so that $\mathrm{Im}(z_I) = 0$ and $\mathrm{Im}(z_{I^c}) = 0$ describe the same branch cut. The branch cuts divide $\mathbb{C}^\ell$ into regions of analyticity (regions without singularities), each corresponding to one particular analytic continuation of $\tilde{G}$.

We henceforth focus on the case, needed for Eq. (5.2b), that all arguments of $\tilde{G}(\boldsymbol{z})$ are real, up to infinitesimal shifts. To be specific, we take the imaginary shifts of the frequency sums z_I to be infinitesimal, $|\gamma_I| = 0^+$ (with signs determined via conventions described below). Then, $\tilde{G}(\boldsymbol{z})$ is a function of $\ell - 1$ independent real frequencies ω_i, and the analytic region is indicated by including the $2^{\ell-1} - 1$ shift directions $\gamma_I = \pm 0^+$ in the argument of $\tilde{G}(\boldsymbol{z})$. Thus, for 2p, 3p, and 4p correlators, we need 1, 3, and 7 imaginary parts, respectively (see examples below for $\ell = 3, 4$ in Eqs. (5.39) and (5.40)).

For a compact presentation of our results, it is convenient to introduce notation that specifies all imaginary shifts via a $(\ell - 1)$-tuple $\check{\boldsymbol{z}}$ whose components $\check{z}_i = \check{\omega}_i + \mathrm{i}\check{\gamma}_i$ are frequency sums of the form $\check{z}_i = z_I$. Then, the argument of $\tilde{G}(\boldsymbol{z})$ is expressed as $\boldsymbol{z}(\check{\boldsymbol{z}})$, and the imaginary shifts of $\boldsymbol{z}$ are determined by those chosen for $\check{\boldsymbol{z}}$. We will specify the $\ell - 1$ independent frequencies $\check{\boldsymbol{z}}$ chosen to parametrize $\boldsymbol{z}(\check{\boldsymbol{z}})$ using subscripts, $\tilde{G}_{\check{\boldsymbol{z}}} = \tilde{G}(\boldsymbol{z}(\check{\boldsymbol{z}}))$, extending the subscript notation developed in Sec. 5.3.1 for $\ell = 2$ to the regular parts of ℓp correlators. To uniquely determine the imaginary shifts in $z_I(\check{\boldsymbol{z}})$, and hence the analytic region for $\tilde{G}_{\check{\boldsymbol{z}}}$, we

implicitly assign imaginary shifts to all $\check{z}_i$ via the rule

$$2|\check{\gamma}_{i-1}| \leq |\check{\gamma}_i|, \qquad \text{for } 1 < i < \ell. \tag{5.38}$$

It ensures that the imaginary part of any $\text{Im} z_I$ is always nonzero, and that its sign is specified uniquely through the sign choices made for the shifts $\pm|\check{\gamma}_i|$. We specify these sign choices using superscripts on the corresponding real frequencies $\check{\omega}_i$, writing $\check{z}_i = \check{\omega}_i^{\pm} = \check{\omega}_i \pm \mathrm{i}|\check{\gamma}_i|$.

Examples for $\ell = 3$: For $\ell = 3$, the branch cuts are given by $\gamma_1 = 0$, $\gamma_2 = 0$, and $\gamma_3 = 0$, see Fig. 5.3. Therefore, three imaginary parts are required to uniquely identify one analytic region for a regular MF correlator $\tilde{G}(\boldsymbol{z})$, with $\boldsymbol{z} = (z_1, z_2, z_3)$ and $z_i = \omega_i^{\pm}$. Consider, e.g., the set of independent frequencies $\check{\boldsymbol{z}} = (\omega_1^+, \omega_2^-)$ with infinitesimal imaginary shifts fulfilling Eq. (5.38). It yields the analytic continuation (see Fig. 5.3 for the labels of analytic regions):

$$\tilde{G}_{\omega_1^+, \omega_2^-} = \tilde{G}(\omega_1^+, \omega_2^-, -\omega_{12}^-) = \tilde{G}(\omega_1^+, \omega_2^-, \omega_3^+) = G'^{[2]}(\boldsymbol{\omega}). \tag{5.39a}$$

The third argument, $z_3 = -z_{12} = -\check{z}_1 - \check{z}_2 = -\omega_1^+ - \omega_2^-$, has a positive imaginary shift since $\text{Im}(z_3) = -\text{Im}(|\check{\gamma}_1| - |\check{\gamma}_2|) > 0$, by Eq. (5.38). By contrast, for $\check{\boldsymbol{z}} = (\omega_2^-, \omega_1^+)$, we obtain

$$\tilde{G}_{\omega_2^-, \omega_1^+} = \tilde{G}(\omega_1^+, \omega_2^-, -\omega_{12}^+) = \tilde{G}(\omega_1^+, \omega_2^-, \omega_3^-) = G^{[1]}(\boldsymbol{\omega}). \tag{5.39b}$$

Evidently, $\tilde{G}_{\omega_2^-, \omega_1^+} \neq \tilde{G}_{\omega_1^+, \omega_2^-}$, because switching $\omega_1^+ \leftrightarrow \omega_2^-$ in the argument list of $\check{\boldsymbol{z}}$ also switches the relative magnitudes of their imaginary parts, due to Eq. (5.38).

Note that the representation via subscripts is not unique. For instance, $G^{[1]}(\boldsymbol{\omega})$ can also be written as $\tilde{G}_{\omega_{12}^+, \omega_1^+}$, since the subscript $\check{\boldsymbol{z}} = (\omega_{12}^+, \omega_1^+)$ yields $\boldsymbol{z}(\check{\boldsymbol{z}}) = (\omega_1^+, \omega_{12}^+ - \omega_1^+, -\omega_{12}^+) = (\omega_1^+, \omega_2^-, \omega_3^-)$, matching the argments found in Eq. (5.39b). For the last step, the sign of the imaginary shift of the second argument follows from $\text{Im}(z_2) = \text{Im}(\omega_{12}^+ - \omega_1^+) = |\check{\gamma}_1| - |\check{\gamma}_2| < 0$.

Example for $\ell = 4$: For $\ell = 4$, the branch cuts are located at vanishing γ_1, γ_2, γ_3, γ_4, γ_{12}, γ_{13}, and γ_{14}, see Fig. 5.4. Thus, seven imaginary parts are needed to uniquely identify one analytic region for a regular MF correlator $\tilde{G}(\boldsymbol{z})$. We therefore write its argument as $\boldsymbol{z} = (z_1, z_2, z_3, z_4; z_{12}, z_{13}, z_{14})$, with $z_I = \omega_I^{\pm}$, also listing the arguments after the semicolon since the signs of their imaginary parts are needed to fully specify the analytic region. Consider, e.g., $\check{\boldsymbol{z}} = (\omega_{13}^+, \omega_2^-, \omega_3^+)$. Then, $z_4 = -z_{123} = -\check{z}_1 - \check{z}_2 = -\omega_{13}^+ - \omega_2^- = -\omega_{123}^- = \omega_4^+$, $z_{12} = \check{z}_1 + \check{z}_2 - \check{z}_3 = \omega_{13}^+ + \omega_2^- - \omega_3^+ = \omega_{12}^-$, and $z_{14} = -z_{23} = -z_2 - z_3 = -\omega_2^- - \omega_3^+ = -\omega_{23}^+$; the signs of the imaginary shifts on the right sides follow via Eq. (5.38). We thus obtain

$$\begin{aligned} \tilde{G}_{\omega_{13}^+, \omega_2^-, \omega_3^+} &= \tilde{G}(\omega_1^-, \omega_2^-, \omega_3^+, -\omega_{123}^-; \omega_{12}^-, \omega_{13}^+, -\omega_{23}^+) \\ &= \tilde{G}(\omega_1^-, \omega_2^-, \omega_3^+, \omega_4^+; \omega_{12}^-, \omega_{13}^+, \omega_{14}^-) = C_{\text{IV}}^{(34)}. \end{aligned} \tag{5.40}$$

In the last line, the frequency arguments were expressed through those used to label the analytic regions in Fig. 5.4.

5.4.2 Discontinuities of $\tilde{G}(z)$

The discontinuity of $\tilde{G}(\boldsymbol{z})$ across a given branch cut, defined by $\text{Im} z_I = \gamma_I = 0$, quantifies the difference between two neighboring analytic regions, R_+ and R_-, separated by $\gamma_I = 0$. We denote this discontinuity by $\tilde{G}(\boldsymbol{z}^{R_+}) - \tilde{G}(\boldsymbol{z}^{R_-})$. Explicitly, we have opposite imaginary shifts γ_I in the analytic regions, $\gamma_I^{R_+} = 0^+ = -\gamma_I^{R_-}$, and equivalent shifts for all other $\gamma_J^{R_+} = \gamma_J^{R_-}$ with $J \subsetneq \{1, \ldots, \ell\}$ and $J \neq I$. To describe this discontinuity using $\check{\boldsymbol{z}}$ notation, we write

$\check{\boldsymbol{z}}^{R\pm} = (\check{z}_1^{R\pm}, \check{\boldsymbol{z}}^{\mathrm{r}})$, where the first variable is chosen as the one whose imaginary part changes sign across the branch cut, $\check{z}_1^{R\pm} = \omega_I^\pm$, and $\check{\boldsymbol{z}}^{\mathrm{r}}$ denotes a tuple of $\ell - 2$ other, independent frequencies, with imaginary shifts given by the prescription (5.38). Then, extending the superscript notation from Sec. 5.3.1, we can express the discontinuity of $\tilde{G}(\boldsymbol{z})$ across $\mathrm{Im}\,z_I = 0$ as

$$\tilde{G}_{\check{\boldsymbol{z}}^{\mathrm{r}}}^{\omega_I} = \tilde{G}_{\omega_I^+, \check{\boldsymbol{z}}^{\mathrm{r}}} - \tilde{G}_{\omega_I^-, \check{\boldsymbol{z}}^{\mathrm{r}}} = \tilde{G}_{\check{\boldsymbol{z}}^{R+}} - \tilde{G}_{\check{\boldsymbol{z}}^{R-}}. \tag{5.41}$$

Similarly, we define consecutive discontinuities across two branch cuts, $\gamma_I = 0$ and $\gamma_J = 0$, to be evaluated as

$$\tilde{G}_{\check{z}_3,\dots,\check{z}_{\ell-1}}^{\omega_I,\omega_J} = \tilde{G}_{\omega_J^+,\check{z}_3,\dots,\check{z}_{\ell-1}}^{\omega_I} - \tilde{G}_{\omega_J^-,\check{z}_3,\dots,\check{z}_{\ell-1}}^{\omega_I}, \tag{5.42}$$

where we have $\check{z}_1 = \omega_I^\pm$ and $\check{z}_2 = \omega_J^\pm$.

Examples for $\ell = 3$: For a discontinuity across $\gamma_2 = 0$ and $\check{\boldsymbol{z}}^{\mathrm{r}} = \omega_1^+$, we find

$$\begin{aligned}
\tilde{G}_{\omega_1^+}^{\omega_2} &= \tilde{G}_{\omega_2^+,\omega_1^+} - \tilde{G}_{\omega_2^-,\omega_1^+} = \tilde{G}(\omega_1^+,\omega_2^+,-\omega_{12}^+) - \tilde{G}(\omega_1^+,\omega_2^-,-\omega_{12}^+) \\
&= \tilde{G}(\omega_1^+,\omega_2^+,\omega_3^-) - \tilde{G}(\omega_1^+,\omega_2^-,\omega_3^-) = G'^{[3]}(\boldsymbol{\omega}) - G^{[1]}(\boldsymbol{\omega}).
\end{aligned} \tag{5.43}$$

Two consecutive discontinuities across, e.g., $\gamma_1 = 0$ and $\gamma_2 = 0$ yield

$$\begin{aligned}
\tilde{G}^{\omega_1,\omega_2} &= \tilde{G}_{\omega_2^+}^{\omega_1} - \tilde{G}_{\omega_2^-}^{\omega_1} = \tilde{G}_{\omega_1^+,\omega_2^+} - \tilde{G}_{\omega_1^-,\omega_2^+} - \tilde{G}_{\omega_1^+,\omega_2^-} + \tilde{G}_{\omega_1^-,\omega_2^-} \\
&= \tilde{G}(\omega_1^+,\omega_2^+,-\omega_{12}^+) - \tilde{G}(\omega_1^-,\omega_2^+,-\omega_{12}^+) - \tilde{G}(\omega_1^+,\omega_2^-,-\omega_{12}^-) + \tilde{G}(\omega_1^-,\omega_2^-,-\omega_{12}^-) \\
&= G'^{[3]} - G^{[2]} - G'^{[2]} + G^{[3]}.
\end{aligned} \tag{5.44}$$

Example for $\ell = 4$: The discontinuity for, e.g., $\gamma_{123} = 0$ and $\check{\boldsymbol{z}}^{\mathrm{r}} = (\omega_3^+,\omega_1^-)$ evaluates to

$$\begin{aligned}
\tilde{G}_{\omega_3^+,\omega_1^-}^{\omega_{123}} &= \tilde{G}_{\omega_{123}^+,\omega_3^+,\omega_1^-} - \tilde{G}_{\omega_{123}^-,\omega_3^+,\omega_1^-} \\
&= \tilde{G}(\omega_1^-,\omega_2^+,\omega_3^+,-\omega_{123}^+;\omega_{12}^-,\omega_{13}^-,-\omega_{23}^-) - \tilde{G}(\omega_1^-,\omega_2^+,\omega_3^+,-\omega_{123}^-;\omega_{12}^-,\omega_{13}^-,-\omega_{23}^-) \\
&= C_{\mathrm{I}}^{(23)} - C^{(234)}.
\end{aligned} \tag{5.45}$$

5.5 Analytic continuation of 3p correlators

The notation introduced in the previous section enables a concise discussion of the analytic continuation of 3p MF correlators in the following. Section 5.5.1 is devoted to the general structure of these correlators and the connection of their analytical continuations to 3p PSFs. In contrast to the 2p case, the derivation of these PSFs, constituting Steps 1 and 2 of our three-step strategy, is discussed in App. C.3.2; in the main text, we merely state the final result. In Sec. 5.5.2, we show that the PSFs yield all components of the KF correlator as linear combinations of analytically continued MF correlators.

5.5.1 Extraction of PSFs

A general 3p correlator can be decomposed into a regular and various anomalous parts (see Eq. (C.5) and App. C.3.1):

$$G(\mathrm{i}\boldsymbol{\omega}(\omega_{\bar{1}},\omega_{\bar{2}})) = G_{\mathrm{i}\omega_{\bar{1}},\mathrm{i}\omega_{\bar{2}}}$$
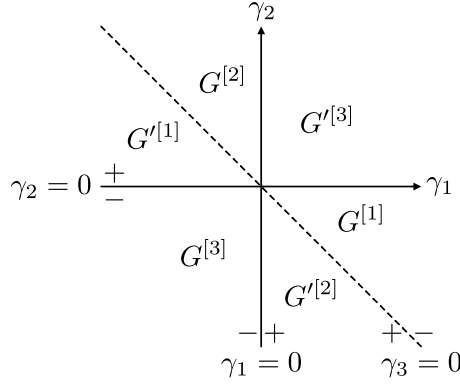
Figure 5.3 Regions of analyticity of regular 3p MF correlators. Lines with $\gamma_i = 0$ denote possible branch cuts of the correlators. (Figure adapted from Ref. [Eva92].) We label each region by that specific Keldysh correlator, $G^{[\eta]}$ or $G'^{[\eta]}$, whose imaginary shifts γ_i lie within that region: For $G^{[1]}$, only ω_1 has a positive imaginary shift, i.e., $\gamma_1 > 0$, $\gamma_2 < 0$, and $\gamma_3 < 0$, implying $G^{[1]}(\boldsymbol{\omega}) = \tilde{G}(\omega_1^+, \omega_2^-, \omega_3^-)$. Primed correlators (Eqs. (3.72)) have inverted imaginary shifts, such that $G'^{[1]}(\boldsymbol{\omega}) = \tilde{G}(\omega_1^-, \omega_2^+, \omega_3^+)$.

$$= \tilde{G}_{i\omega_{\overline{1}}, i\omega_{\overline{2}}} + \beta \delta_{i\omega_{\overline{1}}} \hat{G}_{\overline{1}; i\omega_{\overline{2}}} + \beta \delta_{i\omega_{\overline{2}}} \hat{G}_{\overline{2}; i\omega_{\overline{1}}} + \beta \delta_{i\omega_{\overline{12}}} \hat{G}_{\overline{12}; i\omega_{\overline{1}}} + \beta^2 \, \delta_{i\omega_{\overline{1}}} \delta_{i\omega_{\overline{2}}} \, \hat{G}_{\overline{1}, \overline{2}}. \tag{5.46}$$

Here, $\tilde{G}$ denotes the regular part, whereas $\hat{G}_i$ represents the anomalous part w.r.t. frequency $i\omega_i$, i.e., $\hat{G}_i$ comes with a factor of $\beta\delta_{i\omega_i}$ and is independent of $i\omega_i$. $\hat{G}_{1,2}$ is anomalous w.r.t. all frequencies and is a frequency-independent constant. (Note that, e.g., $\beta\delta_{i\omega_3}\hat{G}_3$ can be written as $\beta\delta_{i\omega_{12}}\hat{G}_{12}$ in the $\beta\delta$ expansion in Eq. (5.46), implying relations like $\hat{G}_{12} = \hat{G}_3$. This unbiased notation allows us to write formulas that hold for any permutation p.)

The full correlator G as well as the components $\tilde{G}$ and $\hat{G}_i$ are, by definition, singularity-free for all Matsubara frequencies. For the anomalous contributions, we further have the decomposition

$$\hat{G}_{3; i\omega_1} = \hat{G}_{3; i\omega_1}^{\boldsymbol{\Delta}} + \Delta_{i\omega_1} \hat{G}_{3; 1}^{\Delta}, \tag{5.47}$$

where $\Delta_{i\omega_i}$ is defined in Eq. (3.15) for a purely imaginary $\Omega_i = i\omega_i$. Here, $\hat{G}_{3;1}^{\Delta}$ comprises all terms proportional to a $\Delta_{i\omega_1}$ symbol, and $\hat{G}_{3; i\omega_1}^{\boldsymbol{\Delta}}$ contains the rest. Analogous definitions hold for all anomalous terms $\hat{G}_i$, see App. C.3.1 for a detailed discussion. The distinction between $\hat{G}_i^{\boldsymbol{\Delta}}$ and $\hat{G}_i^{\Delta}$ is only needed if all three operators are bosonic, in which case all anomalous terms in Eq. (5.46) can occur. For two fermionic and one bosonic operator, all following results equally hold by replacing $\hat{G}_i^{\boldsymbol{\Delta}} \to \hat{G}_i$ and $\hat{G}_i^{\Delta} \to 0$.

In App. C.3.2, we show that the PSFs can be expressed via analytic continuations of the general constituents of the 3p correlator (see Eq. (5.46)):

$$(2\pi i)^2 S_p(\varepsilon_{\overline{1}}, \varepsilon_{\overline{2}}) = n_{\varepsilon_{\overline{1}}} n_{\varepsilon_{\overline{2}}} \tilde{G}^{\varepsilon_{\overline{2}}, \varepsilon_{\overline{1}}} + n_{\varepsilon_{\overline{1}}} n_{\varepsilon_{\overline{12}}} \tilde{G}^{\varepsilon_{\overline{12}}, \varepsilon_{\overline{1}}} + \hat{\delta}(\varepsilon_{\overline{1}}) n_{\varepsilon_{\overline{2}}} \hat{G}_{\overline{1}}^{\boldsymbol{\Delta}; \varepsilon_{\overline{2}}}$$
$$+ \hat{\delta}(\varepsilon_{\overline{2}}) n_{\varepsilon_{\overline{1}}} \hat{G}_{\overline{2}}^{\boldsymbol{\Delta}; \varepsilon_{\overline{1}}} + \hat{\delta}(\varepsilon_{\overline{3}}) n_{\varepsilon_{\overline{1}}} \hat{G}_{\overline{3}}^{\boldsymbol{\Delta}; \varepsilon_{\overline{1}}} + \hat{\delta}(\varepsilon_{\overline{1}}) \hat{\delta}(\varepsilon_{\overline{2}}) \left(\hat{G}_{\overline{1}, \overline{2}} - \tfrac{1}{2} \hat{G}_{\overline{3}; \overline{1}}^{\Delta} \right). \tag{5.48}$$

This is our main result for $\ell = 3$. Explicit expressions of the PSFs for individual permutations are obtained by inserting the permuted indices into the above equation. In Eqs. (C.39), we provide an overview of all possibly occurring discontinuities expressed through the analytic regions in Fig. 5.3. As for 2p PSFs, we provide a consistency check of Eq. (5.48) in App. C.7.

5.5.2 3p Keldysh correlators

In the following two sections, we demonstrate how to construct KF correlators as linear combinations of analytically continued MF correlators using the PSFs in Eq. (5.48), corresponding to Step 3 of our strategy. For $\alpha = 1$, Eq. (3.71) gives the analytic continuation of G to fully retarded components $G^{[\eta]}$ for general ℓ. Therefore, we directly consider the more challenging cases of $\alpha = 2, 3$ in Secs. 5.5.2.1 and 5.5.2.2, respectively. Lastly, in Sec. 5.5.2.3 we provide an overview of all Keldysh components and present gFDRs.

5.5.2.1 Keldysh components $G^{[\eta_1\eta_2]}$

To recapitulate, in Sec. 5.3.3.2 we performed manipulations on the level of the Keldysh kernels for $\ell = 2$ and $\alpha = 2$ by using the identity (5.32), which directly allowed us to evaluate the convolution with the PSFs. Even though the kernels for $\ell = 3$ are more complicated due to an additional factor in the denominator (see Eq. (3.67d)), similar manipulations are presented in App. C.3.3.1 for the Keldysh component $G^{212} = G^{[13]}$. There, it is shown that simplifications of the 3p KF kernel $K^{[\hat{\eta}_1\hat{\eta}_2]}$ (Eq. (3.67c)) yield

$$
G^{[13]}(\boldsymbol{\omega}) = \int_{\varepsilon_1,\varepsilon_2} \hat{\delta}(\omega_1 - \varepsilon_1) \frac{(2\pi\mathrm{i})^2}{\omega_2^- - \varepsilon_2} S_{[1,[2,3]_-]_+}(\varepsilon_1, \varepsilon_2, -\varepsilon_{12})
$$
$$
- \int_{\varepsilon_1,\varepsilon_2} \hat{\delta}(\omega_{12} - \varepsilon_{12}) \frac{(2\pi\mathrm{i})^2}{\omega_2^- - \varepsilon_2} S_{[[1,2]_-,3]_+}(\varepsilon_1, \varepsilon_2, -\varepsilon_{12}). \tag{5.49}
$$

Similarly to the 2p case, we always display the unpermuted $\boldsymbol{\varepsilon}$ for PSF (anti)commutators and insert permuted $\boldsymbol{\varepsilon}_p$ only for individual PSFs, implying, e.g., $S_{2[3,1]_\pm}(\boldsymbol{\varepsilon}) = S_{(231)}(\varepsilon_2, \varepsilon_3) \pm S_{(213)}(\varepsilon_2, \varepsilon_1)$. For the integrations in Eq. (5.49), we fixed the two independent frequencies ε_1 and ε_2 as integration variables. We thus obtain, e.g.,

$$
S_{[1,[2,3]_-]_+}(\boldsymbol{\varepsilon}) = S_{1[2,3]_-}(\boldsymbol{\varepsilon}) + S_{[2,3]_-1}(\boldsymbol{\varepsilon})
$$
$$
= S_{(123)}(\varepsilon_1, \varepsilon_2) - S_{(132)}(\varepsilon_1, \varepsilon_3) + S_{(231)}(\varepsilon_2, \varepsilon_3) - S_{(321)}(\varepsilon_3, \varepsilon_2). \tag{5.50}
$$

with $\varepsilon_3 = -\varepsilon_{12}$ being understood.

To relate the KF to the MF correlator, we insert Eq. (5.48) into the PSF (anti)commutators of Eq. (5.50) and simplify the results using relations for the discontinuities such as $\tilde{G}^{\varepsilon_2,\varepsilon_3} = -\tilde{G}^{\varepsilon_2,\varepsilon_1}$. Such identities follow by explicitly expressing the discontinuities in terms of $G^{[\eta]}$ and $G'^{[\eta]}$ correlators (see Eqs. (C.39)). Then, the PSF (anti)commutator in Eq. (5.50), e.g., reads

$$
(2\pi\mathrm{i})^2 S_{[1,[2,3]_-]_+}(\varepsilon_1, \varepsilon_2, -\varepsilon_{12}) = N_{\varepsilon_1} \tilde{G}^{\varepsilon_1,\varepsilon_2} - 2\hat{\delta}(\varepsilon_1) \hat{G}_1^{\boldsymbol{\Delta};\varepsilon_2} - 2\hat{\delta}(\varepsilon_1)\hat{\delta}(\varepsilon_2)\hat{G}_{1;2}^{\boldsymbol{\Delta}}. \tag{5.51}
$$

Inserting Eq. (5.51) (and a similar expression for $S_{[[1,2]_-,3]_+}$, see Eq. (C.44b)) into Eq. (5.49) and evaluating one of the integrals via the δ-function, we find

$$
G^{[13]}(\boldsymbol{\omega}) = -N_{\omega_1} \int_{\varepsilon_2} \frac{\tilde{G}^{\omega_1,\varepsilon_2}}{\omega_2^- - \varepsilon_2} + 2\hat{\delta}(\omega_1) \left(\int_{\varepsilon_2} \frac{\hat{G}_1^{\boldsymbol{\Delta};\varepsilon_2}}{\omega_2^- - \varepsilon_2} - \frac{\hat{G}_{1;2}^{\boldsymbol{\Delta}}}{\omega_2^-} \right)
$$
$$
- N_{\omega_{12}} \int_{\varepsilon_2} \frac{\tilde{G}^{\omega_{12},\varepsilon_2}}{\omega_2^- - \varepsilon_2} + 2\hat{\delta}(\omega_{12}) \left(\int_{\varepsilon_2} \frac{\hat{G}_3^{\boldsymbol{\Delta};\varepsilon_2}}{\omega_2^- - \varepsilon_2} - \frac{\hat{G}_{3;2}^{\boldsymbol{\Delta}}}{\omega_2^-} \right). \tag{5.52}
$$

Here, it becomes apparent why collecting PSFs in terms of (anti)commutators is beneficial. The integrands in Eq. (5.52) do not contain any MWFs depending on the integration variable ε_2, so that the only pole away from $\mathrm{Im}(z_2) = 0$ comes from the denominators. Consequently,

the integrals over ε_2 can be evaluated by closing the forward/backward integration contours in the upper/lower half-planes. Then, only the pole at $z_2 = \omega_2^-$ contributes (as illustrated in Fig. 5.2 for the integral in Eq. (5.27)), and the final result for the Keldysh correlator $G^{[13]}$ reads

$$
\begin{aligned}
G^{[13]} &= N_{\omega_1} \tilde{G}^{\omega_1}_{\omega_2^-} + N_{\omega_{12}} \tilde{G}^{\omega_{12}}_{\omega_2^-} + 4\pi\mathrm{i}\,\delta(\omega_1)\hat{G}_{1;\omega_2^-} + 4\pi\mathrm{i}\,\delta(\omega_{12})\hat{G}_{3;\omega_2^-} \\
&= N_{\omega_1}\left(G'^{[2]} - G^{[3]} \right) + N_{\omega_3}\left(G'^{[2]} - G^{[1]} \right) + 4\pi\mathrm{i}\,\delta(\omega_1)\hat{G}_1^{[3]} + 4\pi\mathrm{i}\,\delta(\omega_3)\hat{G}_3^{[1]}.
\end{aligned}
\tag{5.53}
$$

Here, we used $N_{\omega_{12}} = -N_{\omega_3}$, expressed $\tilde{G}^{\omega_1}_{\omega_2^-}$ and $\tilde{G}^{\omega_{12}}_{\omega_2^-}$ in terms of the analytic regions in Fig. 5.3, and defined the shorthand

$$
\hat{G}_{i;\omega_j^\pm} = \hat{G}^{\Delta}_{i;\omega_j^\pm} + \frac{\hat{G}^{\Delta}_{i;j}}{\omega_j^\pm}.
\tag{5.54}
$$

We emphasize that Eq. (5.54) should not be interpreted as a direct analytic continuation of Eq. (5.47). Rather, it can be obtained from Eq. (5.47) by replacing $\Delta_{\mathrm{i}\omega_j} \to 1/(\mathrm{i}\omega_j)$ and only afterwards analytically continuing the resulting expression $\mathrm{i}\omega_j \to \omega_j^\pm$. Additionally, we defined the shorthand $\hat{G}_i^{[\eta]} = \hat{G}_i(\boldsymbol{\omega}^{[\eta]})$, such that, e.g., $\hat{G}_{1;\omega_2^-} = \hat{G}_{1;\omega_3^+} = \hat{G}_1^{[3]}$. The other two Keldysh components with $\alpha = 2$, $G^{[12]}$ and $G^{[23]}$, can be derived similarly, and their results are shown in Eqs. (5.58a) and (5.58c), respectively.

5.5.2.2 Keldysh component $G^{[123]}$

In this section, we relate the Keldysh component $G^{[123]}$ to the analytic continued MF correlator. In the derivation of Eq. (5.52), using the identity (5.32) for the $\alpha = 2$ kernel $K^{[\hat{\eta}_1\hat{\eta}_2]}$ was essential. However, the Keldysh kernel for $G^{[123]}$, $K^{[\hat{\eta}_1\hat{\eta}_2\hat{\eta}_3]}$, involves three retarded kernels according to Eq. (3.67c), impeding the direct application of Eq. (5.32).

In App. C.3.3.2, we show that this problem can be circumvented by subtracting a fully retarded component, say, $G^{[3]}$. An analysis of the spectral representation of $G^{[123]} - G^{[3]}$ then leads to

$$
\begin{aligned}
\frac{1}{(2\pi\mathrm{i})^2}(G^{[123]} - G^{[3]})(\boldsymbol{\omega}) &= \int_{\varepsilon_1,\varepsilon_2} \hat{\delta}(\omega_1 - \varepsilon_1)\,\hat{\delta}(\omega_2 - \varepsilon_2)\, S_{[[1,2]_+,3]_+}(\varepsilon_1,\varepsilon_2,-\varepsilon_{12}) \\
&+ \int_{\varepsilon_1,\varepsilon_2} \hat{\delta}(\omega_1 - \varepsilon_1)\,\frac{1}{\omega_2^- - \varepsilon_2}\, S_{[1,[2,3]_-]_-}(\varepsilon_1,\varepsilon_2,-\varepsilon_{12}) \\
&+ \int_{\varepsilon_1,\varepsilon_2} \hat{\delta}(\omega_2 - \varepsilon_2)\,\frac{1}{\omega_1^- - \varepsilon_1}\, S_{[2,[1,3]_-]_-}(\varepsilon_1,\varepsilon_2,-\varepsilon_{12}).
\end{aligned}
\tag{5.55}
$$

Similiar to Eqs. (5.50) and (5.52), we evaluate the PSF (anti)commutators by inserting Eq. (5.48) (see Eq. (C.49)), and subsequently evaluate the integrals either via the δ-functions or via Cauchy's integral formula, yielding

$$
\begin{aligned}
&(G^{[123]} - G^{[3]})(\boldsymbol{\omega}) \\
&= (1 + N_{\omega_1}N_{\omega_2})\tilde{G}^{\omega_2,\omega_1} + N_{\omega_{12}}N_{\omega_1}\tilde{G}^{\omega_{12},\omega_1} + \tilde{G}^{\omega_1}_{\omega_2^-} + \tilde{G}^{\omega_2}_{\omega_1^-} + 4\pi\mathrm{i}\,\delta(\omega_1)N_{\omega_2}\hat{G}_1^{\Delta;\omega_2} \\
&\quad + 4\pi\mathrm{i}\,\delta(\omega_2)N_{\omega_1}\hat{G}_2^{\Delta;\omega_1} + 4\pi\mathrm{i}\,\hat{\delta}(\omega_{12})N_{\omega_1}\hat{G}_3^{\Delta;\omega_1} + (4\pi\mathrm{i})^2\delta(\omega_1)\delta(\omega_2)\hat{G}_{1,2}.
\end{aligned}
\tag{5.56}
$$

A more symmetric form of this result (see Eq. (5.58d)) can be obtained by expressing all discontinuities in terms of the analytic regions in Fig. 5.3 and applying the identity

$$1 + N_{\omega_1} N_{\omega_2} + N_{\omega_1} N_{\omega_3} + N_{\omega_2} N_{\omega_3} = 0, \tag{5.57}$$

which holds for $\ell = 3$ due to frequency conservation.

5.5.2.3 3p generalized fluctuation-dissipation relations

Expressing all Keldysh components with $\alpha \geq 2$ through analytic continuations of MF correlators is equivalent to relating them to fully retarded and advanced components. Indeed, as in the 2p case, knowledge of the fully retarded and advanced components *and* the anomalous terms suffices to obtain all Keldysh components, as brought to bear by the 3p gFDRs (where $N_i = N_{\omega_i}$)

$$G^{[12]} = N_1 \left(\tilde{G}'^{[3]} - \tilde{G}^{[2]} \right) + N_2 \left(\tilde{G}'^{[3]} - \tilde{G}^{[1]} \right) + 4\pi\mathrm{i}\,\delta(\omega_1)\hat{G}_1^{[2]} + 4\pi\mathrm{i}\,\delta(\omega_2)\hat{G}_2^{[1]}, \tag{5.58a}$$

$$G^{[13]} = N_1 \left(\tilde{G}'^{[2]} - \tilde{G}^{[3]} \right) + N_3 \left(\tilde{G}'^{[2]} - \tilde{G}^{[1]} \right) + 4\pi\mathrm{i}\,\delta(\omega_1)\hat{G}_1^{[3]} + 4\pi\mathrm{i}\,\delta(\omega_3)\hat{G}_3^{[1]}, \tag{5.58b}$$

$$G^{[23]} = N_2 \left(\tilde{G}'^{[1]} - \tilde{G}^{[3]} \right) + N_3 \left(\tilde{G}'^{[1]} - \tilde{G}^{[2]} \right) + 4\pi\mathrm{i}\,\delta(\omega_2)\hat{G}_2^{[3]} + 4\pi\mathrm{i}\,\delta(\omega_3)\hat{G}_3^{[2]}, \tag{5.58c}$$

$$G^{[123]} = N_2 N_3 G^{[1]} + N_1 N_3 G^{[2]} + N_1 N_2 G^{[3]} + (1 + N_2 N_3)G'^{[1]} + (1 + N_1 N_3)G'^{[2]}$$

$$+ (1 + N_1 N_2)G'^{[3]} + 4\pi\mathrm{i}\left[\delta(\omega_1)N_2 \left(\hat{G}_1^{\triangle;[2]} - \hat{G}_1^{\triangle;[3]} \right) + \delta(\omega_2)N_3 \left(\hat{G}_2^{\triangle;[3]} - \hat{G}_2^{\triangle;[1]} \right) \right.$$

$$\left. + \delta(\omega_3)N_1 \left(\hat{G}_3^{\triangle;[1]} - \hat{G}_3^{\triangle;[2]} \right) \right] + (4\pi\mathrm{i})^2 \delta(\omega_1)\delta(\omega_2)\hat{G}_{1,2}. \tag{5.58d}$$

These gFDRs agree with the results in Ref. [WH02], and generalize those by also including anomalous contributions. Applications of these formulas to the Hubbard atom are presented in Sec. 5.7.

5.6 Analytic continuation of 4p correlators

Parts of this section are based on results derived by Anxiang Ge in his Master's thesis [Ge20]. For completeness, they are included here, since they are crucial ingredients for the analytic continuation of general multipoint correlators (with emphasis on $\ell = 4$) and the derivation of 4p gFDRs.

In this section, we demonstrate the MF-to-KF analytic continuation of fermionic 4p correlators. In Sec. 5.6.1, we first discuss our convention for labelling analytic regions and provide the expression of PSFs in terms of analytically continued MF correlators. In Sec. 5.6.2, we then generalize the key concept for the construction of 3p KF correlators, namely rewriting the KF spectral representation using kernel identities and PSF (anti)commutators, to arbitrary ℓ, and apply it to the relevant case $\ell = 4$.

5.6.1 Analytic regions and extraction of PSFs

As discussed in Sec. 5.4.1, the possible singularities of a regular 4p MF correlator are located at seven branch cuts, splitting the complex plane into a total of 32 regions (see Fig. 5.4). Importantly, for $\ell \geq 4$, only few of these regions correspond to fully retarded or advanced Keldysh components, in contrast to $\ell = 2, 3$. We label analytic continuations of MF correlators
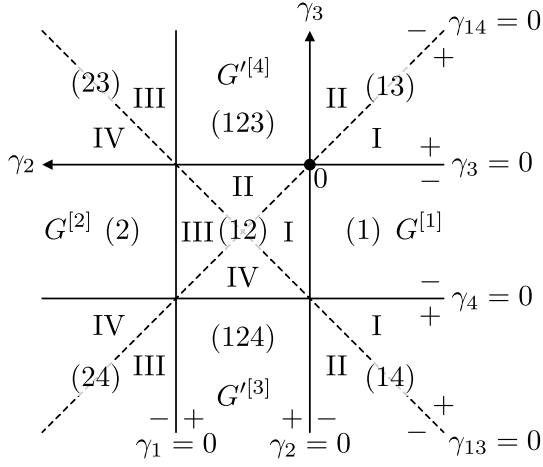
$\gamma_{12} > 0:$ $\gamma_{12} < 0:$
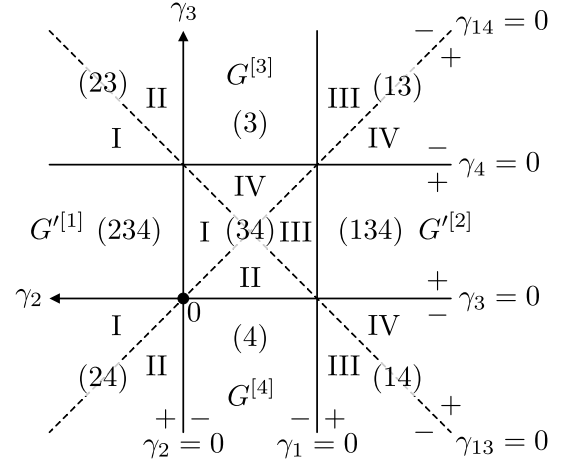
Figure 5.4 Regions of analyticity of regular 4p MF correlators (analogous to Ref. [Eli62]). Lines with $\operatorname{Im} z_i = \gamma_i = 0$ and $\operatorname{Im} z_{ij} = \gamma_{ij} = 0$ denote possible branch cuts. The rectangular regions are labeled by arabic numbers indicating which γ_i are positive; e.g., for region (124), we have $\gamma_1, \gamma_2, \gamma_4 > 0$ but $\gamma_3 < 0$. Consequently, regions composed of one or three arabic numbers correspond to fully retarded or advanced Keldysh components. Regions with two of the γ_i positive, like region (12), are further divided into four subregions by the branch cuts in γ_{ij} and are distinguished by roman numbers $\mathrm{I} - \mathrm{IV}$.

by C, e.g.,

$$\tilde{G}(\omega_1^+, \omega_2^-, \omega_3^+, \omega_4^-; \omega_{12}^-, \omega_{13}^+, \omega_{14}^-) = C_{\mathrm{III}}^{(13)}. \tag{5.59}$$

The superscript of $C_{\mathrm{III}}^{(13)}$ indicates which ω_i (with $1 \leq i \leq 4$) have a positive imaginary shift. Analytic regions with two ω_i's having positive shifts are further divided into four subregions, denoted by roman numbers $\mathrm{I} - \mathrm{IV}$ in the subscripts of C. This is necessary because for $C_{\mathrm{III}}^{(13)}$, e.g., the superscripts do not uniquely determine the imaginary parts of $\omega_1^+ + \omega_2^- = \omega_{12}^\pm$ and $\omega_1^+ + \omega_4^- = \omega_{14}^\pm$. Fully retarded or advanced Keldysh components, on the other hand, are directly related to analytic regions, $G^{[\eta]} = C^{(i)}$ with $i = \eta$ and $G'^{[\eta]} = C^{(ijk)}$ with $i, j, k \neq \eta$, as depicted in Fig. 5.4.

Priming correlators, i.e., complex conjugation of the imaginary parts of frequencies (Eq. (3.72)), is directly applicable to the analytic regions. Consider, e.g., $C^{(1)}$, where only ω_1 has a positive imaginary part; then, priming $C^{(1)}$ yields $(C^{(1)})' = (G^{[1]})' = G'^{[1]} = C^{(234)}$, where only ω_1 has a negative imaginary part. The roman subscripts are chosen such that they are unaffected by complex conjugation of imaginary parts, so that, e.g., $(C_{\mathrm{II}}^{(14)})' = C_{\mathrm{II}}^{(23)}$.

Finally, we note that double bosonic discontinuities, e.g., $\tilde{G}_{\omega_1^+}^{\omega_{13}, \omega_{14}}$, vanish since the fermionic 4p kernel contains only one bosonic frequency, see App. C.5.1.2. This implies that not all analytic regions displayed in Fig. 5.4 are independent, since the following relations hold:

$$C_{\mathrm{I}}^{(ij)} - C_{\mathrm{II}}^{(ij)} + C_{\mathrm{III}}^{(ij)} - C_{\mathrm{IV}}^{(ij)} = 0, \qquad \text{with } 1 \leq i < j \leq 4. \tag{5.60}$$

The identity for $(ij) = (12)$, e.g., follows from $\tilde{G}_{\omega_1^+}^{\omega_{13}, \omega_{14}} = 0$.

After establishing our convention for labelling analytic regions, we now apply our strategy for the analytic continuation to fermionic 4p MF correlators. Anomalous terms, requiring bosonic Matsubara frequencies, only occur for sums of two fermionic Matsubara frequencies,

implying the general form (Eq. (C.5))

$$
\begin{aligned}
G(\mathrm{i}\boldsymbol{\omega}(\omega_{\overline{1}}, \omega_{\overline{2}}, \omega_{\overline{3}})) &= G_{\mathrm{i}\omega_{\overline{1}}, \mathrm{i}\omega_{\overline{2}}, \mathrm{i}\omega_{\overline{3}}} \\
&= \tilde{G}_{\mathrm{i}\omega_{\overline{1}}, \mathrm{i}\omega_{\overline{2}}, \mathrm{i}\omega_{\overline{3}}} + \beta\delta_{\mathrm{i}\omega_{\overline{12}}}\hat{G}_{\overline{12}; \mathrm{i}\omega_{\overline{1}}, \mathrm{i}\omega_{\overline{3}}} + \beta\delta_{\mathrm{i}\omega_{\overline{13}}}\hat{G}_{\overline{13}; \mathrm{i}\omega_{\overline{1}}, \mathrm{i}\omega_{\overline{2}}} + \beta\delta_{\mathrm{i}\omega_{\overline{14}}}\hat{G}_{\overline{14}; \mathrm{i}\omega_{\overline{1}}, \mathrm{i}\omega_{\overline{2}}}.
\end{aligned} \tag{5.61}
$$

The anomalous terms need not be further distinguished by factors of $\Delta_{\mathrm{i}\omega}$ as in Eq. (5.47), since the remaining frequency arguments are fermionic ($\mathrm{i}\omega_i \neq 0$).

Using Eq. (5.61), Steps 1 and 2 of our three-step strategy are discussed in App. C.4; they yield the PSFs

$$
\begin{aligned}
(2\pi\mathrm{i})^3 S_p(\varepsilon_{\overline{1}}, \varepsilon_{\overline{2}}, \varepsilon_{\overline{3}}) &= n_{\varepsilon_{\overline{1}}} n_{\varepsilon_{\overline{2}}} n_{\varepsilon_{\overline{3}}} \tilde{G}^{\varepsilon_{\overline{3}}, \varepsilon_{\overline{2}}, \varepsilon_{\overline{1}}} + n_{\varepsilon_{\overline{1}}} n_{\varepsilon_{\overline{2}}} n_{\varepsilon_{\overline{123}}} \tilde{G}^{\varepsilon_{\overline{123}}, \varepsilon_{\overline{2}}, \varepsilon_{\overline{1}}} + n_{\varepsilon_{\overline{1}}} n_{\varepsilon_{\overline{2}}} n_{\varepsilon_{\overline{13}}} \tilde{G}^{\varepsilon_{\overline{13}}, \varepsilon_{\overline{2}}, \varepsilon_{\overline{1}}} \\
&\quad + n_{\varepsilon_{\overline{1}}} n_{\varepsilon_{\overline{2}}} n_{\varepsilon_{\overline{23}}} \tilde{G}^{\varepsilon_{\overline{23}}, \varepsilon_{\overline{2}}, \varepsilon_{\overline{1}}} n_{\varepsilon_{\overline{1}}} n_{\varepsilon_{\overline{12}}} n_{\varepsilon_{\overline{3}}} \tilde{G}^{\varepsilon_{\overline{3}}, \varepsilon_{\overline{12}}, \varepsilon_{\overline{1}}} + n_{\varepsilon_{\overline{1}}} n_{\varepsilon_{\overline{12}}} n_{\varepsilon_{\overline{123}}} \tilde{G}^{\varepsilon_{\overline{123}}, \varepsilon_{\overline{12}}, \varepsilon_{\overline{1}}} \\
&\quad + n_{\varepsilon_{\overline{1}}} n_{\varepsilon_{\overline{3}}} \hat{\delta}(\varepsilon_{\overline{12}}) \hat{G}^{\varepsilon_{\overline{3}}, \varepsilon_{\overline{1}}}_{\overline{12}} + n_{\varepsilon_{\overline{1}}} n_{\varepsilon_{\overline{2}}} \hat{\delta}(\varepsilon_{\overline{13}}) \hat{G}^{\varepsilon_{\overline{2}}, \varepsilon_{\overline{1}}}_{\overline{13}} + n_{\varepsilon_{\overline{1}}} n_{\varepsilon_{\overline{2}}} \hat{\delta}(\varepsilon_{\overline{14}}) \hat{G}^{\varepsilon_{\overline{2}}, \varepsilon_{\overline{1}}}_{\overline{14}}.
\end{aligned} \tag{5.62}
$$

This is our main result for $\ell = 4$. Equations (C.60) give an overview over all possibly occurring discontinuities expressed through the analytic regions in Fig. 5.4. As for the 2p and 3p cases, we provide a consistency check of Eq. (5.62) in App. C.7.

To conclude this section, we further comment on properties of the anomalous parts. As discussed in App. C.4.2, the anomalous contribution $\hat{G}_{13; \mathrm{i}\omega_1, \mathrm{i}\omega_2}$, e.g., can only depend on the frequencies $\mathrm{i}\omega_1$ and $\mathrm{i}\omega_2$ separately, but not on $\mathrm{i}\omega_{12}$. For anomalos parts, the complex frequency plane is thus divided into only four analytic regions corresponding to the imaginary parts of $\varepsilon_1^{\pm}$ and $\varepsilon_3^{\pm}$, in contrast to the six analytic regions for 3p correlators. This directly implies symmetries for discontinuities, such as $\hat{G}^{\varepsilon_{\overline{2}}, \varepsilon_{\overline{1}}}_{\overline{13}} = \hat{G}^{\varepsilon_{\overline{1}}, \varepsilon_{\overline{2}}}_{\overline{13}}$. Similarly as for the regular parts, we label analytic continuations of anomalous parts with $\hat{C}$, e.g.,

$$
\hat{G}_{12; \omega_1^+, \omega_3^-} = \hat{C}_{12}^{(14)}, \tag{5.63}
$$

with the difference that subscripts indicate the anomalous contributions. Since $\hat{G}_{12; \omega_1^+, \omega_3^-}$ is always multiplied by $\delta(\omega_{12})$, the remaining frequencies must have imaginary parts ω_2^- and ω_4^+. Accordingly, the superscript of $\hat{C}_{12}^{(14)}$ indicates the positive imaginary shifts of ω_1 and ω_4.

5.6.2 4p Keldysh correlators

In this section, we discuss the construction of KF correlators as linear combinations of analytically continued MF correlators. In Eqs. (5.33), (5.49), and (5.55), we expressed various Keldysh components via a convolution of PSF (anti)commutators with modified KF kernels, which originated from kernel identities presented in Eqs. (5.31) and App. C.3.3. To generalize these insights to arbitrary ℓp correlators and to present our results in a concise way, we now introduce further notation. The goal of this notation is to collect terms which are related to discontinuities, each expressible via a sum over restricted permutations, such as the $\sum_{\overline{I}^1 | \overline{I}^2}$ terms in Eq. (5.67).

The set of all indices $L = \{1, \ldots, \ell\}$ can be partitioned into α subsets I^j of length $|I^j|$, such that $L = \bigcup_{j=1}^{\alpha} I^j$ with $I^j \cap I^{j'} = \emptyset$ for $j \neq j'$ and $\ell = \sum_{j=1}^{\alpha} |I^j|$. For a general Keldysh component $[\eta_1 \ldots \eta_\alpha]$, we define the subsets I^j to contain at least the element $\eta_j \in I^j$ for all $j \in \{1, \ldots, \alpha\}$, implying $|I^j| \geq 1$. For example, a possible choice of the subsets for $\ell = 4$ and $[\eta_1 \eta_2] = [12]$ is given by $I^1 = \{1, 3\}$ and $I^2 = \{2, 4\}$. With $\sum_{\overline{I}^1 | \overline{I}^2}$, we denote sums over *restricted* permutations $p = \overline{I}^1 | \overline{I}^2$ for which all indices in subset I^1

appear to the left of those in subset I^2. Then, in the previous example, $\sum_{\overline{I}^1|\overline{I}^2}$ sums over $\overline{I}^1|\overline{I}^2 \in \{(1324),(3124),(1342),(3142)\}$. Consequently, we always find $|\overline{I}^j| = |I^j|$ and $\eta_i \in \overline{I}^j$ for all $j \in \{1, \ldots, \alpha\}$. In the following, we denote the elements of $\overline{I}^j$ by $\overline{I}_i^j$ with $i \in \{1, \ldots, |I^j|\}$.

We further define the *retarded product kernel*

$$\tilde{K}_{\overline{I}^1|\ldots|\overline{I}^\alpha}\left(\boldsymbol{\omega}_{\overline{I}^1|\ldots|\overline{I}^\alpha}^{[\eta_1]\ldots[\eta_\alpha]}\right) = \prod_{j=1}^{\alpha-1}\left[\hat{\delta}(\omega_{\overline{I}^j})\right]\prod_{j=1}^{\alpha}\left[\tilde{K}\left(\boldsymbol{\omega}_{\overline{I}^j}^{[\eta_j]}\right)\right], \tag{5.64a}$$

$$\tilde{K}\left(\boldsymbol{\omega}_{\overline{I}^j}\right) = \prod_{i=1}^{|\overline{I}^j|-1}\frac{1}{\omega_{\overline{I}_1^j\ldots\overline{I}_i^j}}. \tag{5.64b}$$

The regular kernel in the last line is defined according to Eq. (3.67d) but restricted to the subtuple of frequencies $\boldsymbol{\omega}_{\overline{I}^j} = (\omega_{\overline{I}_1^j}, \ldots, \omega_{\overline{I}_{|I^j|}^j})$. Additionally, we defined the shorthand $\hat{\delta}(\omega_{\overline{I}^j}) = -2\pi\mathrm{i}\,\delta(\omega_{\overline{I}^j})$ and $\omega_{\overline{I}^j} = \omega_{I^j} = \sum_{i\in I^j}\omega_i$. The superscript on $\boldsymbol{\omega}_{\overline{I}^1|\ldots|\overline{I}^\alpha}^{[\eta_1]\ldots[\eta_\alpha]}$ indicates that the frequencies carry imaginary parts $\omega_i + \mathrm{i}\gamma_i^{[\eta_j]}$ for $i \in \overline{I}^j$ and $j \in \{1, \ldots, \alpha\}$, such that $\gamma_{\eta_j}^{[\eta_j]} > 0$ and $\gamma_{i\neq\eta_j}^{[\eta_j]} < 0$. The Dirac delta function also ensures conservation of imaginary parts, $\gamma_{I^j} = 0$.

As an example, consider again $\ell = 4$ and $[\eta_1\eta_2] = [12]$ with $\overline{I}^1 = \{3,1\}$ and $\overline{I}^2 = \{2,4\}$. Then, we find

$$\tilde{K}_{\overline{I}^1|\overline{I}^2}\left(\boldsymbol{\omega}_{\overline{I}^1|\overline{I}^2}^{[\eta_1][\eta_2]}\right) = \hat{\delta}(\omega_{\overline{I}^1})\tilde{K}\left(\boldsymbol{\omega}_{\overline{I}^1}^{[\eta_1]}\right)\tilde{K}\left(\boldsymbol{\omega}_{\overline{I}^2}^{[\eta_2]}\right) = \hat{\delta}(\omega_{13})\frac{1}{\omega_3^{[1]}}\frac{1}{\omega_2^{[2]}}. \tag{5.65}$$

The retarded product kernels, together with PSF (anti)commutators, constitute the central objects for expressing Eqs. (3.67) in a form particularly suitable for relating KF components to analytically continued MF correlators.

5.6.2.1 Keldysh components $G^{[\eta_1\eta_2]}$

In Eqs. (5.16b) and (5.50), we introduced PSF (anti)commutators for $\ell = 2$ and $\ell = 3$, respectively. We generalize this notation to arbitrary subsets by defining

$$S_{[\overline{I}^1,\overline{I}^2]_\pm}(\boldsymbol{\varepsilon}) = S_{\overline{I}^1|\overline{I}^2}(\boldsymbol{\varepsilon}_{\overline{I}^1|\overline{I}^2}) \pm S_{\overline{I}^2|\overline{I}^1}(\boldsymbol{\varepsilon}_{\overline{I}^2|\overline{I}^1}), \tag{5.66}$$

where the PSF (anti)commutator takes unpermuted variables $\boldsymbol{\varepsilon}$ as its argument. In App. C.6.2, we then show that Keldysh components with $\alpha = 2$ can be rewritten as

$$G^{[\eta_1\eta_2]}(\boldsymbol{\omega}) = \sum_{(I^1,I^2)\in\mathcal{I}^{12}}\sum_{\overline{I}^1|\overline{I}^2}\left(\tilde{K}_{\overline{I}^1|\overline{I}^2} \diamond S_{[\overline{I}^1,\overline{I}^2]_+}\right)\left(\boldsymbol{\omega}_{\overline{I}^1|\overline{I}^2}^{[\eta_1][\eta_2]}\right). \tag{5.67}$$

Here, $\mathcal{I}^{12} = \{(I^1,I^2)|\,\eta_1 \in I^1, \eta_2 \in I^2, I_1 \cup I^2 = L, I^1 \cap I^2 = \emptyset\}$ is the set of all possibilities to partition $L = \{1,...,\ell\}$ into two non-empty subsets, I^1 and I^2, such that $\eta_1 \in I^1$ and $\eta_2 \in I^2$. The convolution of a kernel with a PSF (anti)commutator is defined as

$$\left(\tilde{K}_{\overline{I}^1|\overline{I}^2} \diamond S_{[\overline{I}^1,\overline{I}^2]_\pm}\right)\left(\boldsymbol{\omega}_{\overline{I}^1|\overline{I}^2}^{[\eta_1][\eta_2]}\right) = \int\mathrm{d}^\ell\varepsilon\,\delta(\varepsilon_{1\ldots\ell})\tilde{K}_{\overline{I}^1|\overline{I}^2}\left(\boldsymbol{\omega}_{\overline{I}^1|\overline{I}^2}^{[\eta_1][\eta_2]} - \boldsymbol{\varepsilon}_{\overline{I}^1|\overline{I}^2}\right)S_{[\overline{I}^1,\overline{I}^2]_\pm}(\boldsymbol{\varepsilon}). \tag{5.68}$$

Further, as shown in Eq. (C.84), Eq. (5.67) can be expressed in terms of analytically continued Matsubara correlators,

$$G^{[\eta_1\eta_2]}(\boldsymbol{\omega}) = \sum_{I^1 \in \mathcal{I}^1} \left[N_{\omega_{I^1}} \tilde{G}^{\omega_{I^1}}_{\boldsymbol{\omega}^*} + 4\pi\mathrm{i}\,\delta(\omega_{I^1})\hat{G}_{I^1;\boldsymbol{\omega}^*} \right], \tag{5.69}$$

with $\mathcal{I}^1 = \{I^1 \subsetneq L | \eta_1 \in I^1, \eta_2 \notin I^1\}$ the set of all subtuples of L containing η_1 but not η_2. The $\ell - 2$ frequencies in $\boldsymbol{\omega}^* = \{\omega_i^- | i \neq \eta_1, i \neq \eta_2\}$ all carry negative imaginary shifts, in accordance with the definition of $\boldsymbol{\omega}^{[\eta_1\eta_2]}$. The anomalous part $\hat{G}_{I^1;\boldsymbol{\omega}^*} = \hat{G}_{I^1}(\boldsymbol{z}(\boldsymbol{\omega}^*))$ for complex $\boldsymbol{z}$, which is independent of the anomalous frequency ω_I and parametrized via $\boldsymbol{\omega}^*$, is defined as

$$\hat{G}_{I^1;\boldsymbol{\omega}^*} = \left[\hat{G}_{I^1}(\mathrm{i}\boldsymbol{\omega}) \right]_{\Delta_{\mathrm{i}\omega} \to \frac{1}{\mathrm{i}\omega}, \mathrm{i}\boldsymbol{\omega} \to z(\boldsymbol{\omega}^*)}. \tag{5.70}$$

We first replaced the symbol $\Delta_{\mathrm{i}\omega}$ by $1/(\mathrm{i}\omega)$ to obtain a functional form that we can analytically continue, and then continue it as $\mathrm{i}\boldsymbol{\omega} \to \boldsymbol{z}(\boldsymbol{\omega}^*)$. Remarkably, Eq. (5.69) holds for arbitrary ℓ, η_1, and η_2, and elucidates how anomalous terms enter the Keldysh components with $\alpha = 2$. Examples are found in Eq. (5.33) for $\ell = 2$, where $[\eta_1\eta_2] = [12]$, $\mathcal{I}^1 = \{1\}$, and $\boldsymbol{\omega}^*$ is an empty set, or in Eq. (5.53) for $\ell = 3$, where $[\eta_1\eta_2] = [13]$, $\mathcal{I}^1 = \{1, 12\}$, and $\boldsymbol{\omega}^* = \omega_2^-$

For $\ell = 4$, consider $[\eta_1\eta_2] = [12]$, implying the set $\mathcal{I}^1 = \{1, 13, 14, 134\}$ and $\boldsymbol{\omega}^* = \omega_3^-, \omega_4^-$. Then, Eq. (5.69) directly yields

$$G^{[12]}(\boldsymbol{\omega}) = N_1 \tilde{G}^{\omega_1}_{\omega_3^-,\omega_4^-} + N_{13} \tilde{G}^{\omega_{13}}_{\omega_3^-,\omega_4^-} + N_{14} \tilde{G}^{\omega_{14}}_{\omega_3^-,\omega_4^-} + N_{134} \tilde{G}^{\omega_{134}}_{\omega_3^-,\omega_4^-}$$
$$+ 4\pi\mathrm{i}\,\delta(\omega_{13})\hat{G}_{13;\omega_3^-,\omega_4^-} + 4\pi\mathrm{i}\,\delta(\omega_{14})\hat{G}_{14;\omega_3^-,\omega_4^-}. \tag{5.71}$$

An expression for $G^{[12]}$ expressed in terms of analytic regions is given in Eq. (5.76). Additionally, a full list of all $G^{[\eta_1\eta_2]}$ is provided in Eqs. (5.75a)–(5.75f) (with relations such as $N_{134}\tilde{G}^{\omega_{134}}_{\omega_3^-,\omega_4^-} = -N_2\tilde{G}^{-\omega_2}_{\omega_3^-,\omega_4^-} = N_2\tilde{G}^{\omega_2}_{\omega_3^-,\omega_4^-}$ used).

5.6.2.2 Other Keldysh components

The derivation of $G^{[123]} - G^{[3]}$ in Sec. 5.5.2.2 can be extended to arbitray ℓ and $[\eta_1\eta_2\eta_3]$ by keeping track of permutations that are cyclically related, generalizing Eq. (5.55) to (see App. C.6.3 for details)

$$(G^{[\eta_1\eta_2\eta_3]} - G^{[\eta_3]})(\boldsymbol{\omega}) = \sum_{(I^1,I^{23})\in\mathcal{I}^{1|23}} \sum_{\bar{I}^1|\bar{I}^{23}} \left[\tilde{K}_{\bar{I}^1|\bar{I}^{23}} \diamond S_{[\bar{I}^1,\bar{I}^{23}]_-} \right]\left(\boldsymbol{\omega}^{[\eta_1][\eta_3]}_{\bar{I}^1|\bar{I}^{23}} \right) \tag{5.72}$$
$$+ \sum_{(I^2,I^{13})\in\mathcal{I}^{2|13}} \sum_{\bar{I}^2|\bar{I}^{13}} \left[\tilde{K}_{\bar{I}^2|\bar{I}^{13}} \diamond S_{[\bar{I}^2,\bar{I}^{13}]_-} \right]\left(\boldsymbol{\omega}^{[\eta_2][\eta_3]}_{\bar{I}^2|\bar{I}^{13}} \right)$$
$$+ \sum_{(I^1,I^2,I^3)\in\mathcal{I}^{123}} \sum_{\bar{I}^1|\bar{I}^2|\bar{I}^3} \left[\tilde{K}_{\bar{I}^1|\bar{I}^2|\bar{I}^3} \diamond S_{[[\bar{I}^1,\bar{I}^2]_+,\bar{I}^3]_+} \right]\left(\boldsymbol{\omega}^{[\eta_1][\eta_2][\eta_3]}_{\bar{I}^1|\bar{I}^2|\bar{I}^3} \right).$$

Here, $\mathcal{I}^{123} = \{(I^1, I^2, I^3) | \eta_1 \in I^1, \eta_2 \in I^2, \eta^3 \in I^3, I^j \cap I^{j'} = \emptyset \text{ for } j \neq j'\}$ is the set of all possibilities to partition $L = \{1, ..., \ell\}$ into three subsets, each of which contains one of the indices $\eta_j \in I^j$. The remaining sets are defined as

$$\mathcal{I}^{1|23} = \{(I^1, I^{23}) | \eta_1 \in I^1, \ \eta_2, \eta_3 \in I^{23}, I^1 \cap I^{23} = \emptyset\}, \tag{5.73a}$$
$$\mathcal{I}^{2|13} = \{(I^2, I^{13}) | \eta_2 \in I^2, \ \eta_1, \eta_3 \in I^{13}, I^2 \cap I^{13} = \emptyset\}. \tag{5.73b}$$

Then, Eq. (5.55) provides an example for $\ell = 3$ and $[\eta_1\eta_2\eta_3] = [123]$, where $\mathcal{I}^{1|23} = \{(1, 23)\}$, $\mathcal{I}^{2|13} = \{(2, 13)\}$ and $\mathcal{I}^{123} = \{(1, 2, 3)\}$.

For $\ell = 4$, consider $[\eta_1\eta_2\eta_3] = [123]$. Compared to the 3p case, the additional index allows for larger sets $\mathcal{I}^{1|23} = \{(1, 234), (14, 23)\}$, $\mathcal{I}^{2|13} = \{(2, 134), (24, 13)\}$, and $\mathcal{I}^{123} = \{(1, 2, 34), (1, 24, 3), (14, 2, 3)\}$, resulting in (suppressing the frequency arguments of PSF (anti)commutators)

$$
(G^{[123]} - G^{[3]})(\boldsymbol{\omega}) = \tilde{G}^{\omega_1}_{\omega_2^-\omega_4^-} + \tilde{G}^{\omega_{14}}_{\omega_2^-\omega_4^-} + \tilde{G}^{\omega_2}_{\omega_1^-\omega_4^-} + \tilde{G}^{\omega_{24}}_{\omega_1^-\omega_4^-}
$$
$$
+ (2\pi i)^3 \int_{\varepsilon_1\varepsilon_2\varepsilon_3} \left[\hat{\delta}(\omega_1 - \varepsilon_1)\hat{\delta}(\omega_2 - \varepsilon_2) \frac{S_{[[1,2]_+,[3,4]_-]_+}}{\omega_3^+ - \varepsilon_3} + \hat{\delta}(\omega_1 - \varepsilon_1)\hat{\delta}(\omega_3 - \varepsilon_3) \frac{S_{[[1,[2,4]_-]_+,3]_+}}{\omega_2^+ - \varepsilon_2} \right.
$$
$$
\left. + \hat{\delta}(\omega_2 - \varepsilon_2)\hat{\delta}(\omega_3 - \varepsilon_3) \frac{S_{[[[1,4]_-,2]_+,3]_+}}{\omega_1^+ - \varepsilon_1} \right]. \tag{5.74}
$$

Here, we identified the terms in the first line of Eq. (5.72) with discontinuities (see App. C.5.1). After inserting the PSFs (see Eqs. (C.89)) and performing the remaining integrations using Cauchy's integral formula, we obtain Eq. (5.75g).

For $\alpha \geq 4$, expressing the spectral representation of $G^{[\eta_1\cdots\eta_\alpha]}$ in terms of retarded product kernels and PSF (anti)commutators becomes increasingly challenging. Nevertheless, we provide a formula for $G^{[1234]}$ and $\ell = 4$ in Eq. (C.90), with a list of all relevant PSF (anti)commutators given in Eq. (C.91). Equation (5.75k) then displays the result after evaluating all convolution integrals.

5.6.2.3 Overview of Keldysh components

To summarize the results of the previous sections, we give an overview of all Keldysh components with $\alpha > 1$:

$$
G^{[12]}(\boldsymbol{\omega}) = N_1 \tilde{G}^{\omega_1}_{\omega_3^-,\omega_4^-} + N_2 \tilde{G}^{\omega_2}_{\omega_3^-,\omega_4^-} + N_{13} \tilde{G}^{\omega_{13}}_{\omega_3^-,\omega_4^-} + N_{14} \tilde{G}^{\omega_{14}}_{\omega_3^-,\omega_4^-}
$$
$$
+ 4\pi i\delta(\omega_{13})\hat{G}_{13;\omega_3^-,\omega_4^-} + 4\pi i\delta(\omega_{14})\hat{G}_{14;\omega_3^-,\omega_4^-}, \tag{5.75a}
$$

$$
G^{[34]}(\boldsymbol{\omega}) = N_3 \tilde{G}^{\omega_3}_{\omega_1^-,\omega_2^-} + N_{13} \tilde{G}^{\omega_{13}}_{\omega_1^-,\omega_2^-} + N_{14} \tilde{G}^{\omega_{14}}_{\omega_1^-,\omega_2^-} + N_4 \tilde{G}^{\omega_4}_{\omega_1^-,\omega_2^-}
$$
$$
+ 4\pi i\delta(\omega_{13})\hat{G}_{13;\omega_1^-,\omega_2^-} + 4\pi i\delta(\omega_{14})\hat{G}_{14;\omega_1^-,\omega_2^-}, \tag{5.75b}
$$

$$
G^{[13]}(\boldsymbol{\omega}) = N_1 \tilde{G}^{\omega_1}_{\omega_2^-,\omega_4^-} + N_{12} \tilde{G}^{\omega_{12}}_{\omega_2^-,\omega_4^-} + N_{14} \tilde{G}^{\omega_{14}}_{\omega_2^-,\omega_4^-} + N_3 \tilde{G}^{\omega_3}_{\omega_2^-,\omega_4^-}
$$
$$
+ 4\pi i\delta(\omega_{12})\hat{G}_{12;\omega_2^-,\omega_4^-} + 4\pi i\delta(\omega_{14})\hat{G}_{14;\omega_2^-,\omega_4^-}, \tag{5.75c}
$$

$$
G^{[24]}(\boldsymbol{\omega}) = N_2 \tilde{G}^{\omega_2}_{\omega_1^-,\omega_3^-} + N_{12} \tilde{G}^{\omega_{12}}_{\omega_1^-,\omega_3^-} + N_{14} \tilde{G}^{\omega_{14}}_{\omega_1^-,\omega_3^-} + N_4 \tilde{G}^{\omega_4}_{\omega_1^-,\omega_3^-}
$$
$$
+ 4\pi i\delta(\omega_{12})\hat{G}_{12;\omega_1^-,\omega_3^-} + 4\pi i\delta(\omega_{14})\hat{G}_{14;\omega_1^-,\omega_3^-}, \tag{5.75d}
$$

$$
G^{[14]}(\boldsymbol{\omega}) = N_1 \tilde{G}^{\omega_1}_{\omega_2^-,\omega_3^-} + N_{12} \tilde{G}^{\omega_{12}}_{\omega_2^-,\omega_3^-} + N_{13} \tilde{G}^{\omega_{13}}_{\omega_2^-,\omega_3^-} + N_4 \tilde{G}^{\omega_4}_{\omega_2^-,\omega_3^-}
$$
$$
+ 4\pi i\delta(\omega_{12})\hat{G}_{12;\omega_2^-,\omega_3^-} + 4\pi i\delta(\omega_{13})\hat{G}_{13;\omega_2^-,\omega_3^-}, \tag{5.75e}
$$

$$
G^{[23]}(\boldsymbol{\omega}) = N_2 \tilde{G}^{\omega_2}_{\omega_1^-,\omega_4^-} + N_{12} \tilde{G}^{\omega_{12}}_{\omega_1^-,\omega_4^-} + N_{13} \tilde{G}^{\omega_{13}}_{\omega_1^-,\omega_4^-} + N_3 \tilde{G}^{\omega_3}_{\omega_1^-,\omega_4^-}
$$
$$
+ 4\pi i\delta(\omega_{12})\hat{G}_{12;\omega_1^-,\omega_4^-} + 4\pi i\delta(\omega_{13})\hat{G}_{13;\omega_1^-,\omega_4^-}, \tag{5.75f}
$$

$$
(G^{[123]} - G^{[3]})(\boldsymbol{\omega}) = (N_1 N_2 + 1) \tilde{G}^{\omega_2,\omega_1}_{\omega_3^+} + (N_1 N_{13} - 1) \tilde{G}^{\omega_{13},\omega_1}_{\omega_2^+} + (N_2 N_{23} - 1) \tilde{G}^{\omega_{23},\omega_2}_{\omega_1^+}
$$
$$
+ N_1 N_{12} \tilde{G}^{\omega_{12},\omega_1}_{\omega_3^+} + N_1 N_3 \tilde{G}^{\omega_3,\omega_1}_{\omega_2^+} + N_2 N_3 \tilde{G}^{\omega_3,\omega_2}_{\omega_1^+} + \tilde{G}^{\omega_1}_{\omega_2^-,\omega_3^+} - \tilde{G}^{\omega_{23}}_{\omega_1^+,\omega_2^-}
$$
$$
+ \tilde{G}^{\omega_2}_{\omega_1^-,\omega_3^+} - \tilde{G}^{\omega_{13}}_{\omega_2^+,\omega_1^-} + 4\pi i\,\delta(\omega_{12})\, N_1\, \hat{G}^{\omega_1}_{12;\omega_3^+} + 4\pi i\,\delta(\omega_{13})\, N_1\, \hat{G}^{\omega_1}_{13;\omega_2^+}
$$

$$+ 4\pi i \, \delta(\omega_{14}) \, N_2 \, \hat{G}^{\omega_2}_{14;\omega_1^+}, \tag{5.75g}$$

$$
\begin{aligned}
(G^{[124]} - G^{[4]})(\boldsymbol{\omega}) &= (N_1 N_2 + 1) \tilde{G}^{\omega_2,\omega_1}_{\omega_4^+} + (N_1 N_{14} - 1) \tilde{G}^{\omega_{14},\omega_1}_{\omega_2^+} + (N_2 N_{24} - 1) \tilde{G}^{\omega_{24},\omega_2}_{\omega_1^+} \\
&+ N_1 N_{12} \tilde{G}^{\omega_{12},\omega_1}_{\omega_4^+} + N_1 N_4 \tilde{G}^{\omega_4,\omega_1}_{\omega_2^+} + N_2 N_4 \tilde{G}^{\omega_4,\omega_2}_{\omega_1^+} + \tilde{G}^{\omega_1}_{\omega_2^-,\omega_4^+} - \tilde{G}^{\omega_{24}}_{\omega_1^+,\omega_2^-} \\
&+ \tilde{G}^{\omega_2}_{\omega_1^-,\omega_4^+} - \tilde{G}^{\omega_{14}}_{\omega_2^+,\omega_1^-} + 4\pi i \, \delta(\omega_{12}) \, N_1 \, \hat{G}^{\omega_1}_{12;\omega_4^+} + 4\pi i \, \delta(\omega_{13}) \, N_2 \, \hat{G}^{\omega_2}_{13;\omega_1^+} \\
&+ 4\pi i \, \delta(\omega_{14}) \, N_1 \, \hat{G}^{\omega_1}_{14;\omega_2^+}, \tag{5.75h}
\end{aligned}
$$

$$
\begin{aligned}
(G^{[134]} - G^{[4]})(\boldsymbol{\omega}) &= (N_1 N_3 + 1) \tilde{G}^{\omega_3,\omega_1}_{\omega_4^+} + (N_1 N_{14} - 1) \tilde{G}^{\omega_{14},\omega_1}_{\omega_3^+} + (N_3 N_{34} - 1) \tilde{G}^{\omega_{34},\omega_3}_{\omega_1^+} \\
&+ N_1 N_{13} \tilde{G}^{\omega_{13},\omega_1}_{\omega_4^+} + N_1 N_4 \tilde{G}^{\omega_4,\omega_1}_{\omega_3^+} + N_3 N_4 \tilde{G}^{\omega_4,\omega_3}_{\omega_1^+} + \tilde{G}^{\omega_1}_{\omega_3^-,\omega_4^+} - \tilde{G}^{\omega_{34}}_{\omega_1^+,\omega_3^-} \\
&+ \tilde{G}^{\omega_3}_{\omega_1^-,\omega_4^+} - \tilde{G}^{\omega_{14}}_{\omega_3^+,\omega_1^-} + 4\pi i \, \delta(\omega_{12}) \, N_3 \, \hat{G}^{\omega_3}_{12;\omega_1^+} + 4\pi i \, \delta(\omega_{13}) \, N_1 \, \hat{G}^{\omega_1}_{13;\omega_4^+} \\
&+ 4\pi i \, \delta(\omega_{14}) \, N_1 \, \hat{G}^{\omega_1}_{14;\omega_3^+}, \tag{5.75i}
\end{aligned}
$$

$$
\begin{aligned}
(G^{[234]} - G^{[4]})(\boldsymbol{\omega}) &= (N_2 N_3 + 1) \tilde{G}^{\omega_3,\omega_2}_{\omega_4^+} + (N_2 N_{24} - 1) \tilde{G}^{\omega_{24},\omega_2}_{\omega_3^+} + (N_3 N_{34} - 1) \tilde{G}^{\omega_{34},\omega_3}_{\omega_2^+} \\
&+ N_2 N_{23} \tilde{G}^{\omega_{23},\omega_2}_{\omega_4^+} + N_2 N_4 \tilde{G}^{\omega_4,\omega_2}_{\omega_3^+} + N_3 N_4 \tilde{G}^{\omega_4,\omega_3}_{\omega_2^+} + \tilde{G}^{\omega_2}_{\omega_3^-,\omega_4^+} - \tilde{G}^{\omega_{34}}_{\omega_2^+,\omega_3^-} \\
&+ \tilde{G}^{\omega_3}_{\omega_2^-,\omega_4^+} - \tilde{G}^{\omega_{24}}_{\omega_3^+,\omega_2^-} + 4\pi i \, \delta(\omega_{12}) \, N_3 \, \hat{G}^{\omega_3}_{12;\omega_2^+} + 4\pi i \, \delta(\omega_{13}) \, N_2 \, \hat{G}^{\omega_2}_{13;\omega_3^+} \\
&+ 4\pi i \, \delta(\omega_{14}) \, N_2 \, \hat{G}^{\omega_2}_{14;\omega_4^+}, \tag{5.75j}
\end{aligned}
$$

$$
\begin{aligned}
G^{[1234]}(\boldsymbol{\omega}) &= (N_1 N_2 N_3 + N_1 + N_3) \tilde{G}^{\omega_3,\omega_2,\omega_1} + (N_1 N_2 N_4 + N_4 + N_2) \tilde{G}^{\omega_4,\omega_2,\omega_1} \\
&+ (N_1 N_2 N_{13} + N_1 - N_2) \tilde{G}^{\omega_{13},\omega_2,\omega_1} + (N_1 N_2 N_{23}) \tilde{G}^{\omega_{23},\omega_2,\omega_1} \\
&+ N_1(1 + N_{12} N_3) \tilde{G}^{\omega_3,\omega_{12},\omega_1} + N_1 N_{12} N_4 \tilde{G}^{\omega_4,\omega_2,\omega_1} + N_1 \tilde{G}^{\omega_1}_{\omega_2^-,\omega_3^-} \\
&+ N_2 \tilde{G}^{\omega_2}_{\omega_3^-,\omega_4^-} + N_3 \tilde{G}^{\omega_3}_{\omega_1^-,\omega_4^-} + N_4 \tilde{G}^{\omega_4}_{\omega_1^-,\omega_2^-} + N_3 \tilde{G}^{\omega_3,\omega_4}_{\omega_2^+} + N_2 \tilde{G}^{\omega_2,\omega_3}_{\omega_1^+} \\
&+ N_4 \tilde{G}^{\omega_4,\omega_1}_{\omega_3^+} + N_1 \tilde{G}^{\omega_1,\omega_2}_{\omega_4^+} + N_2 \tilde{G}^{\omega_2,\omega_4}_{\omega_3^+} + N_4 \tilde{G}^{\omega_4,\omega_2}_{\omega_3^+} + N_1 \tilde{G}^{\omega_1,\omega_3}_{\omega_4^+} \\
&+ N_3 \tilde{G}^{\omega_3,\omega_1}_{\omega_4^+} + 4\pi i N_1 N_3 \delta(\omega_{12}) \hat{G}^{\omega_1,\omega_3}_{12} \\
&+ 4\pi i N_1 N_2 \left[\delta(\omega_{13}) \hat{G}^{\omega_1,\omega_2}_{13} + \delta(\omega_{13}) \hat{G}^{\omega_1,\omega_2}_{14} \right]. \tag{5.75k}
\end{aligned}
$$

These equations constitute the main results of the MF-to-KF analytic continuation: They relate all components of a fermionic KF 4p correlator to linear combinations of analytically continued regular and anomalous parts of the corresponding MF correlator, expressed in terms of discontinuities and statistical factors N_i.

5.6.2.4 4p gFDRs

For 4p correlators, there are several regions of analyticity that cannot be identified with a KF correlator. Therefore, in contrast to $\ell \leq 3$, fully retarded and advanced Keldysh components do not suffice to determine all other Keldysh components. Nevertheless, different Keldysh components can be related to each other. We now present the strategy for deriving these gFDRs for the Keldsyh component $G^{[12]}$.

Since every Keldysh component can be represented as a linear combination of analytically continued MF correlators, the analytic regions can serve as a basis to find relations among different Keldysh components. Expressing the discontinuities in Eq. (5.75a) via analytic regions, the KF correlator $G^{[12]}$ reads

$$G^{[12]} = N_1(C^{(12)}_{\mathrm{III}} - G^{[2]}) + N_{13}(C^{(12)}_{\mathrm{II}} - C^{(12)}_{\mathrm{III}}) + N_{14}(C^{(12)}_{\mathrm{IV}} - C^{(12)}_{\mathrm{III}})$$

$$+ N_2 \big(C_{\text{I}}^{(12)} - G^{[1]}\big) + 4\pi \text{i}\, \delta(\omega_{13})\, \hat{C}_{13}^{(12)} + 4\pi \text{i}\, \delta(\omega_{14})\, \hat{C}_{14}^{(12)}, \tag{5.76}$$

where we inserted $G^{[1]} = C^{(1)}$ and $G^{[2]} = C^{(2)}$. Evidently, $G^{[12]}$ cannot be expressed in terms of fully retarded and advanced components only (modulo anomalous terms) due to the occurrence of $C_{\text{I/III/IV}}^{(12)}$. However, these analytic regions and the same anomalous contributions appear in the primed KF correlator $G'^{[34]}$ as well:

$$
\begin{aligned}
G'^{[34]} = {}& N_3 \big(C_{\text{II}}^{(12)} - G'^{[4]}\big) + N_{13}\big(C_{\text{III}}^{(12)} - C_{\text{II}}^{(12)}\big) + N_{14}\big(C_{\text{III}}^{(12)} - C_{\text{IV}}^{(12)}\big) \\
& + N_4 \big(C_{\text{IV}}^{(12)} - G'^{[3]}\big) - 4\pi \text{i}\, \delta(\omega_{13})\hat{C}_{13}^{(12)} - 4\pi \text{i}\, \delta(\omega_{14})\hat{C}_{14}^{(12)}.
\end{aligned}
\tag{5.77}
$$

Note that priming the $\text{i}\delta(\dots)$ factors amounts to complex conjugation, as these arise from the identity (5.32), i.e., $[\text{i}\delta(\dots)]' = -\text{i}\delta(\dots)$. Therefore, we make the ansatz of expressing $G^{[12]}$ as a linear combination of $G'^{[34]}$, $G^{[1]}$, $G^{[2]}$, $G'^{[3]}$, and $G'^{[4]}$, where the coefficients are determined by comparing terms proportional to the same analytic regions. Even though the resulting set of equations is overdetermined (including anomalous contributions, we have ten equations for five coefficients), we find the gFDR

$$G^{[12]} = -N_1 G^{[2]} - N_2 G^{[1]} + \frac{N_1 + N_2}{N_3 + N_4}\Big[G'^{[34]} + N_3 G'^{[4]} + N_4 G'^{[3]}\Big]. \tag{5.78a}$$

The anomalous terms enter the right-hand side only implicitly via $G'^{[34]}$. However, using $\frac{N_1+N_2}{N_3+N_4}\delta(\omega_{13}) = -\delta(\omega_{13})$ and $\frac{N_1+N_2}{N_3+N_4}\delta(\omega_{14}) = -\delta(\omega_{14})$, it is straightforward to show that the $\hat{C}_{13}^{(12)}$ and $\hat{C}_{14}^{(12)}$ contributions in Eq. (5.76) are recovered by the corresponding terms in Eq. (5.77) via Eq. (5.78a). Conversely, the gFDR for $G^{[34]}$ can be derived from Eq. (5.78a) by solving for $G'^{[34]}$ and priming all correlators.

The gFDRs for all other Keldysh components with $\alpha \geq 2$ follow from the same strategy: Express Keldysh components in terms of linearly independent analytic regions and find relations between different components by solving a set of equations to determine coefficients. In addition to Eq. (5.78a), we then obtain for $\alpha = 2$

$$G^{[13]} = -N_1 G^{[3]} - N_3 G^{[1]} + \frac{N_1 + N_3}{N_2 + N_4}\Big[G'^{[24]} + N_2 G'^{[4]} + N_4 G'^{[2]}\Big], \tag{5.78b}$$

$$G^{[14]} = -N_1 G^{[4]} - N_4 G^{[1]} + \frac{N_1 + N_4}{N_2 + N_3}\Big[G'^{[23]} + N_2 G'^{[3]} + N_3 G'^{[2]}\Big], \tag{5.78c}$$

for $\alpha = 3$

$$
\begin{aligned}
G^{[234]} = {}& (1 + N_2 N_4 + N_2 N_3 + N_3 N_4)G'^{[1]} - N_3 N_4 G^{[2]} - N_2 N_4 G^{[3]} \\
& - N_2 N_3 G^{[4]} - N_4 G^{[23]} - N_3 G^{[24]} - N_2 G^{[34]},
\end{aligned}
\tag{5.78d}
$$

$$
\begin{aligned}
G^{[134]} = {}& (1 + N_1 N_4 + N_1 N_3 + N_3 N_4)G'^{[2]} - N_3 N_4 G^{[1]} - N_1 N_4 G^{[3]} \\
& - N_1 N_3 G^{[4]} - N_4 G^{[13]} - N_3 G^{[14]} - N_1 G^{[34]},
\end{aligned}
\tag{5.78e}
$$

$$
\begin{aligned}
G^{[124]} = {}& (1 + N_1 N_2 + N_1 N_2 + N_2 N_4)G'^{[3]} - N_2 N_4 G^{[1]} - N_1 N_4 G^{[2]} \\
& - N_1 N_2 G^{[4]} - N_4 G^{[12]} - N_2 G^{[14]} - N_1 G^{[24]},
\end{aligned}
\tag{5.78f}
$$

$$
\begin{aligned}
G^{[123]} = {}& (1 + N_1 N_2 + N_1 N_3 + N_2 N_3)G'^{[4]} - N_2 N_3 G^{[1]} - N_1 N_3 G^{[2]} \\
& - N_1 N_2 G^{[3]} - N_1 G^{[23]} - N_2 G^{[13]} - N_3 G^{[12]},
\end{aligned}
\tag{5.78g}
$$

(a)   (b)
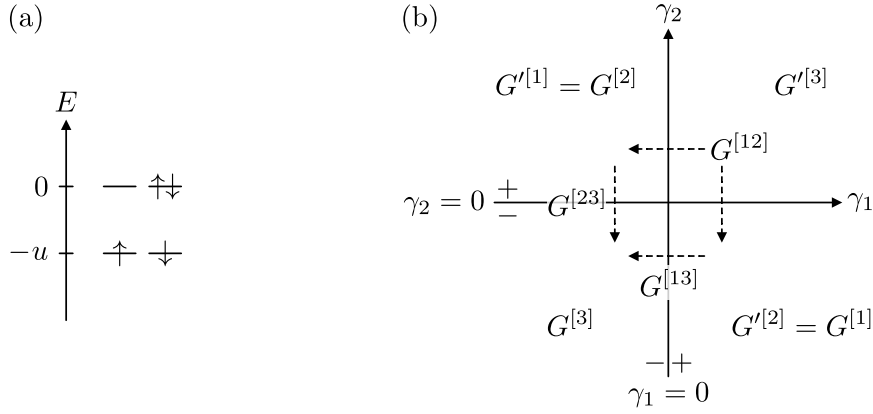
Figure 5.5 (a) Degenerate energy levels of the half-filled Hubbard atom for $u > 0$. (b) Relevant analytic regions of the regular part of the 3p electron-density correlator in Eq. (5.87). As the correlator is independent of $i\omega_3 = -i\omega_{12}$, there are are no poles on the line $\gamma_3 = 0$ in Fig. 5.3, resulting in $G'^{[1]} = G^{[2]}$ and $G'^{[2]} = G^{[1]}$. The dashed arrows indicate the relevant discontinuities for the different Keldysh components with $\alpha = 2$, see Eq. (5.58).

and for $\alpha = 4$

$$G^{[1234]} = (N_2 N_3 N_4 + N_2 + N_3 + N_4)G'^{[1]} + (N_1 N_3 N_4 + N_1 + N_3 + N_4)G'^{[2]} \tag{5.78h}$$
$$+ (N_1 N_2 N_4 + N_1 + N_2 + N_4)G'^{[3]} + (N_1 N_2 N_3 + N_1 + N_2 + N_3)G'^{[4]}$$
$$+ 2N_2 N_3 N_4 G^{[1]} + 2N_1 N_3 N_4 G^{[2]} + 2N_1 N_2 N_4 G^{[3]} + 2N_2 N_3 N_4 G^{[4]}$$
$$+ N_3 N_4 G^{[12]} + N_2 N_4 G^{[13]} + N_2 N_3 G^{[14]} + N_1 N_4 G^{[23]} + N_1 N_3 G^{[24]} + N_1 N_2 G^{[34]}.$$

These results agree with the FDRs found in Ref. [WH02], and therefore provide a consistency check for our approach. Moreover, we checked that the anomalous parts fulfill the same gFDRs. They enter Eqs. (5.78) only implicitly through $G^{[\eta_1 \eta_2]}$ and $G'^{[\eta_1 \eta_2]}$ on the right-hand sides, which contain anomalous parts via Eqs. (5.75a)–(5.75f). This is in contrast to the 2p and 3p cases in Eqs. (5.35) and (5.58), respectively. There, only fully retarded and advanced Keldysh correlators, which solely depend on the regular part $\tilde{G}$ of the corresponding MF correlator (see Eq. (3.71)), occur on the right-hand side, and thus the anomalous parts have to enter the gFDRs explicitly.

5.7 Hubbard atom

To illustrate the use of our analytic continuation formulas, we consider the Hubbard atom (HA) with the Hamiltonian

$$H = U n_\uparrow n_\downarrow - \mu(n_\uparrow + n_\downarrow). \tag{5.79}$$

It describes an interacting system of spin–$\frac{1}{2}$ electrons on a single site, created by $d_\sigma^\dagger$, with $n_\sigma = d_\sigma^\dagger d_\sigma$ the number operator for spin $\sigma \in \{\uparrow, \downarrow\}$. The chemical potential μ is set to the half-filling value $\mu = u = U/2$ for compact results, where U is the interaction parameter. The Hilbert space of the HA is only four-dimensional, with the site being either unoccupied, $|0\rangle$, singly occupied, $|\uparrow\rangle$ or $|\downarrow\rangle$, or doubly occupied, $|\uparrow\downarrow\rangle$. The eigenenergies are (see Fig. 5.5(a))

$$E_0 = E_{\uparrow\downarrow} = 0, \quad E_\uparrow = E_\downarrow = -u. \tag{5.80}$$

The partition sum evaluates to $Z = \text{tr}(e^{-\beta H}) = 2 + 2e^{\beta u}$.

This very simple model is interesting as it is accessible via analytically exact computations. It describes the Hubbard model and the single-impurity Anderson model in the atomic limit (where the interaction U dominates over all other energy scales) and can thus serve as a benchmark for numerical methods [KLvD21, WSK21, KV19, KKH21]. Several correlators of the Hubbard atom were computed in the MF and studied extensively, like fermionic 2p (one-particle) and 4p (two-particle) correlators [HJB$^+$09, PST00, RVT12, Roh13, WLT$^+$20]. The vertex of the Hubbard atom, obtained from the fermionic 4p correlator by dividing out external legs, was used as a starting point for an expansion around strong coupling [Met91, PST00, RVT12, KOBH13]. Additionally, it was found that (despite the simplicity of the model) the two-particle irreducible (2PI) vertices display a complicated frequency dependence, and their divergencies are subject to ongoing research [SCW$^+$16, TGCR18, CGS$^+$18, PART23]. Such divergencies have been related to the breakdown of the perturbative expansion due to the multivaluedness of the Luttinger–Ward functional [SCW$^+$16, GRS$^+$17, KFG15, VWFP18] and to the local moment formation in generalized susceptibilities [CSR$^+$21, AKC$^+$22].

2p and 3p bosonic correlators have gained interest in recent years as well. They describe not only the asymptotic behaviour of the 4p vertex for large frequencies [WLT$^+$20] or the interaction of electrons via the exchange of effective bosons [KVC19, GWG$^+$22], but they are also the central objects of linear and non-linear response theory [Kub57, KKWH23].

KF correlators for the HA (beyond $\ell = 2$) were of smaller interest due to the lack of numerical real-frequency studies. However, substantial progress has been made in this direction [KLvD21, LKvD21, GRW$^+$23, TCL19, P3]. Hence, we exemplify the analytic continuation from MF to KF correlators on the example of the HA for various correlators of interest.

One further comment is in order: The following MF correlators are derived by first computing the PSFs, followed by a convolution with the MF kernels. From our experience, a direct insertion of these PSFs into the spectral representation of KF correlators yields cluttered expressions, cumbersome to simplify due to the infinitesimal imaginary shifts γ_0. With the analytic continuation formulas, on the other hand, terms are conveniently preorganized, collecting those contributions with the same imaginary shifts. Additionally, the discontinuities conveniently yield Dirac delta contributions, as we will show below. In order to derive, e.g., the 3p electron-density correlators in Eqs. (5.88) and (5.89), it is much more convenient to start from the analytic continuation formulas, Eqs. (5.58), than from the original KF Eq. (3.67).

For a compact presentation of our results, we distinguish different correlators with operators in subscripts, e.g., $G[\mathcal{O}^1, \mathcal{O}^2](i\boldsymbol{\omega}) = G_{\mathcal{O}^1\mathcal{O}^2}(i\boldsymbol{\omega})$. Furthermore, we will make use of the identities (proven in App. C.8.1)

$$\frac{\omega^+}{(\omega^+)^2 - u^2} - \frac{\omega^-}{(\omega^-)^2 - u^2} = \frac{\pi}{i}[\delta(\omega + u) + \delta(\omega - u)], \tag{5.81a}$$

$$\frac{1}{(\omega^+)^2 - u^2} - \frac{1}{(\omega^-)^2 - u^2} = \frac{\pi i}{u}[\delta(\omega + u) - \delta(\omega - u)]. \tag{5.81b}$$

All following correlators refer to the connected part.

5.7.1 Examples for $\ell = 2$

5.7.1.1 Fermionic 2p correlator

To begin with, we consider the fermionic 2p correlator (propagator), with $\mathcal{O} = (d_\uparrow, d_\uparrow^\dagger)$. By SU(2) spin symmetry, reversing all spins leaves the correlator invariant. As the nonzero

matrix elements are $\langle\uparrow|d_\uparrow^\dagger|0\rangle = \langle\uparrow\downarrow|d_\uparrow^\dagger|\downarrow\rangle = 1$ and $\langle 0|d_\uparrow|\uparrow\rangle = \langle\downarrow|d_\uparrow|\uparrow\downarrow\rangle = 1$, we can readily compute the PSFs, S_p, via Eq. (2.48). Evaluating the spectral representation yields

$$G_{d_\uparrow d_\uparrow^\dagger}(i\omega) = \frac{i\omega}{(i\omega)^2 - u^2} = \tilde{G}(i\omega). \tag{5.82}$$

By construction, there is no anomalous part $\hat{G}_1 = 0$. The retarded and advanced component are directly obtained from Eq. (5.28):

$$G_{d_\uparrow d_\uparrow^\dagger}^{[1/2]}(\omega) = \frac{\omega^\pm}{(\omega^\pm)^2 - u^2}. \tag{5.83}$$

The Keldysh component involves the difference of the retarded and advanced component. Via Eq. (5.81a), one gets

$$G_{d_\uparrow d_\uparrow^\dagger}^{[12]}(\omega) = \pi i\, t\, [\delta(\omega + u) - \delta(\omega - u)], \tag{5.84}$$

where we used $N_{-\omega} = -N_\omega$ and defined $t = \tanh(\beta u/2)$.

5.7.1.2 Density-density correlator

Our second example is the density-density correlator $\boldsymbol{\mathcal{O}} = (n_\uparrow, n_\downarrow)$. The spectral representation in the MF yields a purely anomalous result

$$G_{n_\uparrow n_\downarrow}(i\omega) = \beta\delta_{i\omega}\tfrac{1}{4}t = \beta\delta_{i\omega}\hat{G}_1. \tag{5.85}$$

Using Eqs. (5.28) and (5.35), the Keldysh components read

$$G_{n_\uparrow n_\downarrow}^{[1]}(\omega) = G_{n_\uparrow n_\downarrow}^{[2]}(\omega) = 0, \qquad G_{n_\uparrow n_\downarrow}^{[12]}(\omega) = 4\pi i\, \delta(\omega)\tfrac{1}{4}t. \tag{5.86}$$

We again emphasize the importance of the anomalous term in the gFDR. If it were discarded, the Keldysh component $G_{n_\uparrow n_\downarrow}^{[12]}$ would falsely vanish entirely.

5.7.2 Examples for $\ell = 3$

5.7.2.1 3p electron-density correlator

Our first example for $\ell = 3$ involves the operators $\boldsymbol{\mathcal{O}} = (d_\uparrow, d_\uparrow^\dagger, n_\uparrow)$. As only the third operator is bosonic, there is at most one anomalous term if $i\omega_3 = -i\omega_{12} = 0$. Indeed, the spectral representation evaluates to

$$\begin{aligned} G_{d_\uparrow d_\uparrow^\dagger n_\uparrow}(i\boldsymbol{\omega}) &= \frac{u^2 - i\omega_1\, i\omega_2}{[(i\omega_1)^2 - u^2]\,[(i\omega_2)^2 - u^2]} + \beta\delta_{i\omega_{12},0}\,\frac{u\, t}{2}\,\frac{1}{(i\omega_1)^2 - u^2} \\ &= \tilde{G}(i\boldsymbol{\omega}) + \beta\delta_{i\omega_{12}}\hat{G}_3(i\omega_1). \end{aligned} \tag{5.87}$$

Since the fully retarded and fully advanced components of the correlator trivially follow from the regular part, we focus on the $\alpha \geq 2$ components in the following. We begin with the Keldysh component $G^{[13]}$ in Eq. (5.58b): The regular part is independent of $i\omega_3 = -i\omega_{12}$, such that the discontinuity across $\gamma_3 = -\gamma_{12} = 0$ vanishes, implying $G'^{[2]} - G^{[1]} = 0$ (see Fig. 5.5(b)). The discontinuity $G'^{[2]} - G^{[3]}$, on the other hand, is nonzero and can be easily

evaluated using Eqs. (5.81), leading to (see App. C.8.2)

$$G^{[13]}_{d_\uparrow d_\uparrow^\dagger n_\uparrow}(\boldsymbol{\omega}) = N_1 \left(\tilde{G}(\omega_1^+, \omega_2^-) - \tilde{G}(\omega_1^-, \omega_2^-) \right) + 4\pi\mathrm{i}\,\delta(\omega_{12})\hat{G}_3(\omega_1^+)$$

$$= \pi\mathrm{i}\,\mathrm{t} \left[\frac{\delta(\omega_1 - u)}{\omega_2^- + u} - \frac{\delta(\omega_1 + u)}{\omega_2^- - u} \right] + 4\pi\mathrm{i}\,\delta(\omega_{12})\frac{u\,\mathrm{t}}{2}\frac{1}{(\omega_1^+)^2 - u^2}. \qquad (5.88)$$

Similarly, the remaining components with $\alpha = 2$, as well as the Keldysh component with $\alpha = 3$, read

$$G^{[23]}_{d_\uparrow d_\uparrow^\dagger n_\uparrow}(\boldsymbol{\omega}) = \pi\mathrm{i}\,\mathrm{t} \left[\frac{\delta(\omega_2 - u)}{\omega_1^- + u} - \frac{\delta(\omega_2 + u)}{\omega_1^- - u} \right] + 4\pi\mathrm{i}\,\delta(\omega_{12})\frac{u\,\mathrm{t}}{2}\frac{1}{(\omega_1^-)^2 - u^2},$$

$$G^{[12]}_{d_\uparrow d_\uparrow^\dagger n_\uparrow}(\boldsymbol{\omega}) = \pi\mathrm{i}\,\mathrm{t} \left[\frac{\delta(\omega_1 - u)}{\omega_2^+ + u} - \frac{\delta(\omega_1 + u)}{\omega_2^+ - u} \right] + \pi\mathrm{i}\,\mathrm{t} \left[\frac{\delta(\omega_2 - u)}{\omega_1^+ + u} - \frac{\delta(\omega_2 + u)}{\omega_1^+ - u} \right],$$

$$G^{[123]}_{d_\uparrow d_\uparrow^\dagger n_\uparrow}(\boldsymbol{\omega}) = \frac{u^2 - \omega_1^+\,\omega_2^+}{\left[(\omega_1^+)^2 - u^2 \right] \left[(\omega_2^+)^2 - u^2 \right]}. \qquad (5.89)$$

Here, $G^{[12]}_{d_\uparrow d_\uparrow^\dagger n_\uparrow}$ includes two discontinuities across $\gamma_1 = 0$ and $\gamma_2 = 0$, but no contribution from $\hat{G}_3$, leading to the different structure compared to the other two Keldysh components with $\alpha = 2$. Surprisingly, $G^{[123]}_{d_\uparrow d_\uparrow^\dagger n_\uparrow}$ is directly determined by $G'^{[3]}$. All other contributions from regular and anomalous parts mutually cancel, see App. C.8.2.

5.7.2.2 Three-spin correlator

3p bosonic correlators are the central objects in non-linear response theory. Here, we consider the correlator for the spin operators $\boldsymbol{\mathcal{O}} = (S_x, S_y, S_z)$, describing second-order changes in the magnetization by applying an external magnetic field. The spin operators are given by

$$S_x = \tfrac{1}{2}\left(d_\uparrow^\dagger d_\downarrow + d_\downarrow^\dagger d_\uparrow \right), \qquad S_y = -\tfrac{\mathrm{i}}{2}\left(d_\uparrow^\dagger d_\downarrow - d_\downarrow^\dagger d_\uparrow \right), \qquad S_z = \tfrac{1}{2}\left(n_\uparrow - n_\downarrow \right). \qquad (5.90)$$

The spectral representation, using the MF kernel in Eq. (C.4b), then yields [P2]

$$G_{S_x S_y S_z}(\mathrm{i}\boldsymbol{\omega}) = -\beta\delta_{\mathrm{i}\omega_1}\tilde{Z}\Delta_{\mathrm{i}\omega_2} + \beta\delta_{\mathrm{i}\omega_2}\tilde{Z}\Delta_{\mathrm{i}\omega_1} - \beta\delta_{\mathrm{i}\omega_{12}}\tilde{Z}\Delta_{\mathrm{i}\omega_1}$$

$$= \beta\delta_{\mathrm{i}\omega_1}\hat{G}_1^\Delta(\mathrm{i}\omega_2) + \beta\delta_{\mathrm{i}\omega_2}\hat{G}_2^\Delta(\mathrm{i}\omega_1) + \beta\delta_{\mathrm{i}\omega_3}\hat{G}_3^\Delta(\mathrm{i}\omega_1), \qquad (5.91)$$

where $\tilde{Z} = \mathrm{i}e^{\beta u}/(2Z)$.

From Eqs. (5.58), we deduce the only nonzero Keldysh components as

$$G^{[12]}_{S_x S_y S_z}(\boldsymbol{\omega}) = -4\pi\mathrm{i}\,\delta(\omega_1)\,\frac{\tilde{Z}}{\omega_2^+} + 4\pi\mathrm{i}\,\delta(\omega_2)\frac{\tilde{Z}}{\mathrm{i}\omega_1^+},$$

$$G^{[13]}_{S_x S_y S_z}(\boldsymbol{\omega}) = -4\pi\mathrm{i}\,\delta(\omega_1)\,\frac{\tilde{Z}}{\omega_2^-} - 4\pi\mathrm{i}\,\delta(\omega_{12})\frac{\tilde{Z}}{\mathrm{i}\omega_1^+},$$

$$G^{[23]}_{S_x S_y S_z}(\boldsymbol{\omega}) = 4\pi\mathrm{i}\,\delta(\omega_1)\,\frac{\tilde{Z}}{\omega_1^-} - 4\pi\mathrm{i}\,\delta(\omega_{12})\frac{\tilde{Z}}{\mathrm{i}\omega_1^-}. \qquad (5.92)$$

Even though anomalous parts contribute to $G^{[123]}$ as well, they solely originate from the $\hat{G}_i^\Delta$ terms, such that $G^{[123]}$ vanishes in this case.

For the application of our 4p analytic continuation formulas to the fermionic 4p correlator in the HA and in the context of vertex corrections to the linear conductance of a specific system, we refer the reader to Secs. 7.3 and 8 as well as Apps. H.3 and H.4 of [P4].

5.8 Conclusion

We showed how to perform the analytic continuation of multipoint correlators in thermal equilibrium from the imaginary-frequency MF to the real-frequency KF. To this end, we used the spectral representation derived in Ref. [KLvD21], separating the correlator into formalism-independent partial spectral functions (PSFs) and formalism-specific kernels. From this analytical starting point, we showed that it is possible to fully recover all 2^ℓ components of the ℓp KF correlator from the one ℓp MF correlator. Our main result is that each of the $(\ell!)$ PSFs can be obtained by linear combinations of analytic continuations of the MF correlator multiplied with combinations of Matsubara weighting functions (MWFs). Explicit formulas are given in Eqs. (5.21) and (5.48) for arbitrary 2p and 3p correlators, respectively, and Eq. (5.62) for fermionic 4p correlators. For these cases, we additionally derived direct MF-to-KF continuation formulas in Eq. (5.35) ($\ell = 2$), Eqs. (5.58) ($\ell = 3$), and Eqs. (5.75) ($\ell = 4$), complementing the general Eq. (3.71) for any ℓ.

We approached the problem of analytic continuation by comparing the spectral representations of general ℓp MF (G) and KF ($G^{[\eta_1 \cdots \eta_\alpha]}$) correlators and by identifying the regular partial MF correlators, $\tilde{G}_p$, as the central link between them. A key insight was that the partial MF correlators can be obtained by an imaginary-frequency convolution of MF kernels with the full MF correlator, $\tilde{G}_p(i\boldsymbol{\omega}_p) + \mathcal{O}(\frac{1}{\beta}) = (K \star G)(i\boldsymbol{\omega}_p)$. Building on this formula, we developed a three-step strategy for the MF-to-KF analytic continuation, applicable to arbitrary ℓp correlators and explicitly presented in the aforementioned cases $\ell \leq 4$. In the first step, we used the kernel representation of [P2] to express the Matsubara sums, inherent in the imaginary-frequency convolution, through contour integrals enclosing the imaginary axis. In the second step, we deformed the contours toward the real axis, carefully tracking possible singularities of the MF correlator. This resulted in a spectral representation $\tilde{G}_p(i\boldsymbol{\omega}_p) = (\tilde{K} * S_p)(i\boldsymbol{\omega}_p)$, which allowed us to extract the PSFs, $S_p[G]$, as functionals of the regular and the various anomalous parts of G multiplied with MWFs. In the third and final step, we simplified the spectral representation for the KF components $G^{[\eta_1 \cdots \eta_\alpha]}$, inserted the PSFs from the second step, and evaluated all real-frequency integrals to express the KF correlators as linear combinations of analytically continued MF correlators.

In our analysis, we explicitly considered so-called anomalous parts of the MF correlator which can occur, e.g., for conserved quantities or in finite systems with degenerate energy eigenstates. These terms do not contribute to fully retarded correlators but are needed to fully recover the other components of the KF correlator.

Exploiting the relations between KF correlators and analytically continued MF functions, we derived generalized fluctuation-dissipation relations (gFDRs) for 3p and 4p correlators, Eqs. (5.58) and (5.78), establishing relations between the different KF components. We thereby reproduced the results of Refs. [WH02, JPS10], while additionally including the anomalous terms.

As an application of our results, we considered various correlators of the Hubbard atom. Starting from their MF expressions, we calculated all components of the corresponding KF correlators using analytic continuation.

6 Symmetric improved estimators

6.1 Overview

The accurate analytical and numerical calculation of the self-energy Σ and 4p vertex Γ (defined in Sec. 3.5) constitutes one of the main challenges in modern many-body physics. While Σ encodes the information about the change of single-particle properties due to the interacting many-body environment [Mah00], Γ describes the effective interaction between two particles and thus signals, for instance, instabilities toward ordered phases [RHT$^+$18]. Their computation is particularly difficult in strongly correlated systems, where often no small expansion parameter is present in the theory.

A significant advance in our understanding of strongly correlated systems was achieved with the development of the DMFT. There, lattice models are mapped onto self-consistent impurity models, which become exact in the limit of infinite dimensions or coordination number [GKKR96]. Nonlocal correlations, which are neglected within DMFT, can then be incorporated by, e.g., diagrammatic extensions, where the local approximations of Σ and Γ serve as a nontrivial starting point [RHT$^+$18]. The accurate numerical computation of these local quantities thus is a key requirement for the study of nonlocal effects and consequently a more realistic treatment of strongly correlated lattice models.

A direct extraction of Σ from the Dyson equation (3.74) and of Γ by amputating the external legs in Eq. (3.76a) is highly prone to numerical errors such as statistical noise in quantum Monte Carlo simulations [HPW12] or discretization artifacts in the NRG [BCP08]. Therefore, it is advisable to utilize IEs for Σ and Γ that are mathematically identical to their definitions in Eqs. (3.74) and (3.76a) but more stable against numerical errors [BHP98, HJB$^+$09, KGK$^+$19, Kug22]. They can be derived using the equation of motion (EOM) approach: Correlators are differentiated w.r.t. one or multiple time arguments, and a subsequent evaluation of the Heisenberg EOMs relate the original correlators to new, auxiliary ones (see, e.g., Eq. (6.3) below). A detailed summary of the history of various IEs resulting from EOMs is given in the introduction of [P3]; here, we only emphasize the key requirements they should fulfill for NRG computations utilized in Refs. [KLvD21, LKvD21, P3]: (i) They should be symmetric w.r.t. all time or frequency arguments, yielding symmetric IEs (sIEs) [KGK$^+$19, LKvD21, Kug22]. (ii) They should not mix non-interacting and interacting correlators [BHP98, LKvD21, Kug22].

IEs for the MF as well as retarded self-energies satisfying both requirements were derived in Ref. [Kug22], considerably improving the numerical accuracy. The need for a counterpart in the multipoint setting is particularly drastic in the KF, where antisymmetric IEs (aIEs) improve only certain components of the 4p KF vertex [LKvD21]. The derivation of multipoint IEs fulfilling requirements (i) and (ii) and the demonstration of their improvement of numerical data is the main objective of [P3].

Let us briefly exemplify our approach for a Hamiltonian $H = H^0 + H_{\text{int}}$, where we assume a non-interacting part $H^0 = H^0_{11'} d_1^\dagger d_{1'}$,[1] with summation over repeated indices implied. For, e.g., a connected 4p MF correlator,[2]

$$\mathcal{G}^{(\cdot,\cdot,\cdot,\cdot)}(\boldsymbol{\tau}) = (-1)^3 \left\langle \mathcal{T} \left\{ d_1(-\mathrm{i}\tau_1)\, d_2^\dagger(-\mathrm{i}\tau_2)\, d_3(-\mathrm{i}\tau_3)\, d_4^\dagger(-\mathrm{i}\tau_4) \right\} \right\rangle^{\text{con}}, \tag{6.1}$$

---

[1] The operators and indices are defined in Sec. 3.5.

[2] The following notations are chosen to match those in [P3]. Therein, however, the standard definition of ℓp MF correlators in the time domain is given by $\mathcal{G}[\mathcal{O}](-\mathrm{i}\boldsymbol{\tau})$ in Eq. (2.30) rather than $\mathcal{G}(\boldsymbol{\tau})$ in Eq. (2.31).

the time derivative $\partial_{\tau_1} = \frac{\partial}{\partial \tau_1}$ acts twofold: on the time-ordering operator, reducing ordering factors $\theta(\pm(\tau_1 - \tau_i))$ to $\pm\delta(\tau_1 - \tau_i)$, and on the operators in the Heisenberg picture. The derivative of the latter can be rewritten as

$$\partial_{\tau_1} d_1(-i\tau_1) = -[d_1, H](-i\tau_1) = -H^0_{11'} d_{1'}(-i\tau_1) - q_1(-i\tau_1), \tag{6.2}$$

with $q_1 = [d_1, H_{int}]$. After a Fourier transformation, the derivative then yields [KGK$^+$19][3]

$$(g^0)^{-1}_{11'}(i\omega_1) \, G^{(\cdot,\cdot,\cdot,\cdot)}_{1'234}(i\boldsymbol{\omega}) = G^{(1,\cdot,\cdot,\cdot)}_{1234}(i\boldsymbol{\omega}), \tag{6.3}$$

with $(g^0)^{-1}_{11'}(i\omega_1) = (i\omega_1 \mathbb{1} - H^0)_{11'}$ the inverse of the bare propagator. The auxiliary correlator $G^{(1,\cdot,\cdot,\cdot)}_{1234}$ is defined as the Fourier transform of the r.h.s. of Eq. (6.1) with d_1 replaced by q_1.

Equation (6.3) resembles amputating the first external leg needed for computing Γ, except for the occurrence of $(g^0)^{-1}$ rather than g^{-1}. However, the former can be expressed through the latter as $(g^0)^{-1}_{11'} = g^{-1}_{11'} + \Sigma_{11'}$ (see Eq. (3.74)), leading to [HPW12, LKvD21][4]

$$g^{-1}_{11'}(i\omega_1) \, G^{(\cdot,\cdot,\cdot,\cdot)}_{1'234}(i\boldsymbol{\omega}) = G^{(1,\cdot,\cdot,\cdot)}_{1234}(i\boldsymbol{\omega}) - \Sigma_{11'}(i\omega_1) \, G^{(\cdot,\cdot,\cdot,\cdot)}_{1'234}(i\boldsymbol{\omega}). \tag{6.4}$$

To extract Γ, the remaining three legs have to be amputated, too. However, with the above expression, we can already address the following question: Why should the r.h.s. yield numerically more accurate results than the l.h.s. if both sides are mathematically identical?

- For large frequencies, the propagator $g^{-1}_{11'}(i\omega_1)$ scales as $\sim i\omega_1$. Hence, numerical errors in computing $G^{(\cdot,\cdot,\cdot,\cdot)}_{1'234}$ are amplified in the vertex by amputating, i.e., dividing $G^{(\cdot,\cdot,\cdot,\cdot)}$ by g [HPW12]; this is avoided on the r.h.s. of Eq. (6.4).

- If $H_{int} = 0$, the connected 4p correlator should vanish, $G^{(\cdot,\cdot,\cdot,\cdot)}_{1234} = 0$, since the total correlator and the disconnected part in the first line of Eq. (3.76a) cancel, implying $\Gamma = 0$. However, due to numerical errors, this cancellation might not be perfect, and $\Gamma \neq 0$ even for $H_{int} = 0$ [LKvD21]. On the r.h.s. of Eq. (6.4), both $G^{(1,\cdot,\cdot,\cdot)}_{1234}$ and $\Sigma_{11'}$ vanish for $H_{int} = 0$ by construction (if Σ is calculated by an IE as well) and directly yield $\Gamma = 0$.

Due to these properties, it is desirable to treat the amputation of the remaining legs for further applications of EOMs via the following simple strategy [P3]: Replace the amputation g^{-1} with $(g^0)^{-1} - \Sigma$ and identify the product of $(g^0)^{-1}$ and a (auxiliary) 4p correlator with the l.h.s. of an EOM (as in Eq. (6.3)). The main results of [P3] can then be summarized as follows:

- We develop a general recipe for deriving IE for general ℓp correlators in the MF, KF, and ZF, building upon the contour formalism introduced in Ch. 2. We use this recipe to extend the results of Ref. [Kug22] to all KF components of the self-energy, and derive sIE for 3p vertices and the 4p vertex in all formalisms fulfilling requirements (i) and (ii). In the 4p case, this naturally recovers the asymptotic decomposition of Ref. [WLT$^+$20]. In our approach, all building blocks of the vertex, in particular also the core part, can be computed independently, with separate sIE estimators for all $\ell \geq 3$ objects.

- For the Anderson impurity model (see Eq. (13) in [P3]) at particle-hole symmetry, we demonstrate the accuracy of our proposed 4p vertex estimator using the multipoint NRG scheme of Ref. [LKvD21] by nontrivial benchmarks against third-order perturbation theory

---

3 Equation (6.3) corresponds to the first-order intermediate result of Ref. [KGK$^+$19].

4 After amputating the remaining legs, Eq. (6.4) corresponds to the aIE of Ref. [HPW12] which is extended to connected correlators on the r.h.s. in Ref. [LKvD21].

at weak coupling, renormalized perturbation theory at strong interactions and temperatures much lower than the Kondo temperature [HOM04, OH18a, OH18b, OTTS22], and the fulfillment of fluctuation-dissipation relations.[5,6]

---

5 The author of this thesis contributed to the calculations in and preparations of the analytical parts of [P3], and thanks the remaining authors for performing the numerical calculations and their analyses.

6 Here, we provide a short list of known typos in [P3] we were kindly made aware of:
- On p. 6 below Eq. (30), it should read "... (e.g. $G^{(1,\cdot)}$ or $G^{(\cdot,2)}$ in Fig. 3)...".
- On p. 10 below Eq. (54), O_n should be replaced by O^n.
- On p. 12 below Eq. (76), the first equation reference should point to Eq. (38).
- On p. 21, D is the half-bandwidth.
- On p. 21, ε_d should be replaced by ε to be consistent with the Hamiltonian in Eq. (13).

Symmetric improved estimators for multipoint vertex functions

by

J.-M. Lihm[1,2,3], **J. Halbinger**[4], J. Shim[4], J. von Delft[4], F. B. Kugler[5], and S.-S. B. Lee[1,3]

[1]Department of Physics and Astronomy, Seoul National University, Seoul 08826, Korea

[2]Center for Correlated Electron Systems, Institute for Basic Science, Seoul 08826, Korea

[3]Center for Theoretical Physics, Seoul National University, Seoul 08826, Korea

[4]Arnold Sommerfeld Center for Theoretical Physics, Center for NanoScience, and Munich

Center for Quantum Science and Technology, Ludwig-Maximilians-Universität München,

80333 Munich, Germany

[5]Center for Computational Quantum Physics, Flatiron Institute, 162 5th Avenue, New York,

NY 10010, USA

Symmetric improved estimators for multipoint vertex functions

Jae-Mo Lihm [●],[1, 2, 3] Johannes Halbinger [●],[4] Jeongmin Shim [●],[4]
Jan von Delft [●],[4] Fabian B. Kugler [●],[5, *] and Seung-Sup B. Lee [●][1, 3, *]

[1]*Department of Physics and Astronomy, Seoul National University, Seoul 08826, Korea*
[2]*Center for Correlated Electron Systems, Institute for Basic Science, Seoul 08826, Korea*
[3]*Center for Theoretical Physics, Seoul National University, Seoul 08826, Korea*
[4]*Arnold Sommerfeld Center for Theoretical Physics, Center for NanoScience, and Munich Center for*
Quantum Science and Technology, Ludwig-Maximilians-Universität München, 80333 Munich, Germany
[5]*Center for Computational Quantum Physics, Flatiron Institute, 162 5th Avenue, New York, NY 10010, USA*
(Dated: October 19, 2023)

Multipoint vertex functions, and the four-point vertex in particular, are crucial ingredients in many-body theory. Recent years have seen significant algorithmic progress toward numerically computing their dependence on multiple frequency arguments. However, such computations remain challenging and are prone to suffer from numerical artifacts, especially in the real-frequency domain. Here, we derive estimators for multipoint vertices that are numerically more robust than those previously available. We show that the two central steps for extracting vertices from correlators, namely the subtraction of disconnected contributions and the amputation of external legs, can be achieved accurately through repeated application of equations of motion, in a manner that is symmetric with respect to all frequency arguments and involves only fully renormalized objects. The symmetric estimators express the core part of the vertex and all asymptotic contributions through separate expressions that can be computed independently, without subtracting the large-frequency limits of various terms with different asymptotic behaviors. Our strategy is general and applies equally to the Matsubara formalism, the real-frequency zero-temperature formalism, and the Keldysh formalism. We demonstrate the advantages of the symmetric improved estimators by computing the Keldysh four-point vertex of the single-impurity Anderson model using the numerical renormalization group.

I. INTRODUCTION

Two-particle correlators and vertices play a crucial role in many-body physics. They encode the effective interaction between two particles, altered from their bare value due to the many-body environment. Understanding and calculating two-particle correlators is essential for studying collective modes, instabilities, and response properties. The two-particle or four-point (4p) vertex is also a key ingredient for extending methods based on quantum impurity models, like dynamical mean-field theory (DMFT) [1, 2], to treat non-local correlations [3]. Owing to the dependence of the 4p vertex on multiple frequency, spin, and orbital degrees of freedom, analytic treatments are limited to only the simplest models [4, 5]. Thus, there has been a longstanding interest in developing efficient and accurate computational methods for evaluating these quantities [6]. Indeed, recent years have brought significant algorithmic progress toward numerically computing the dependence of multipoint functions on their multiple frequency arguments, using, e.g., quantum Monte Carlo (QMC) [7–10] or the numerical renormalization group (NRG) for solving quantum impurity models [11–13].

The present paper addresses the following question: given a reliable numerical method for computing multipoint correlators in the frequency domain, such as QMC or NRG, how can it best be harnessed to extract the cor-

responding vertex? This extraction involves subtracting disconnected parts and amputating external legs. Naive implementations of such subtractions and amputations are prone to numerical artifacts. To minimize their effects, various improved estimators have been proposed. Such estimators are expressions for the quantity of interest (e.g. a self-energy or vertex) that are formally equivalent to the original definition but more robust against numerical artifacts [14–21]. Such artifacts are, e.g., statistical noise in QMC or discretization effects in NRG.

A fruitful approach for deriving improved estimators is to utilize equations of motion (EOMs). In 1998, Bulla, Hewson, and Pruschke [18] used EOMs to derive an improved estimator for the self-energy of quantum impurity models. This estimator is constructed from the usual 2p propagator and an auxiliary 2p correlator involving a certain composite operator generated by the EOM. It is an asymmetric improved estimator (aIE), since it was derived via an EOM acting on only one of the two time arguments of the propagator. The resulting aIE for the self-energy has been widely used for NRG computations ever since.

The EOM strategy of Ref. [18] was generalized to the case of 4p vertices by Hafermann, Patton, and Werner [8]. They derived an aIE for the 4p vertex that contains an additional, 4p auxiliary correlator, again involving a composite operator. The terms are then combined in such a manner that the disconnected parts cancel and one external leg is amputated. Their aIE is asymmetric in the frequency arguments, since it was derived via EOMs act-

	2p self-energy Σ	4p vertex Γ
asymmetric, **full**	Bulla *et al.* [18]	Hafermann *et al.* [8]
symmetric, bare	Kaufmann *et al.* [10]	
symmetric, **full**	Kugler [22]	**this work**

TABLE I. Summary of different improved estimators for self-energies and vertex functions derived using EOMs.

ing on only one of the four time arguments. For some applications, this is a serious limitation. An example is the 4p vertex in the real-frequency Keldysh formalism. The Keldysh vertex of the Anderson impurity model (AIM) was recently computed by three of the present authors using NRG [12, 13]. There, the aIE of Ref. [8] was used, but it was pointed out that this yields improvements for only 4 of the 16 components of the Keldysh vertices. To improve all 16, a *symmetric* improved estimator (sIE) is needed.

A sIE was derived through repeated use of EOMs by Kaufmann, Gunacker, Kowalski, Sangiovanni, and Held [10], and found to be significantly less prone to numerical artifacts than the aIE of Ref. [8]. Yet, their sIE involves not only various full (interacting) multipoint correlators, but also the bare (noninteracting) 2p propagator. It was noted before [13, 18, 22] that this is not ideal for methods where bare and full correlators stem from different numerical settings and would compromise the accuracy of some intended cancellations. NRG is an example of such a method: there, bare and full correlators are typically computed without or with energy discretization, respectively. Consequently, the sIE of Ref. [10] was not used in the NRG computations of Refs. [12, 13]. The occurrence of bare propagators is also unfavorable in scenarios where they qualitatively differ very strongly from the full ones, as, e.g., in a Mott insulating state.

For the self-energy, one of us recently derived an improved estimator for the self-energy that is (i) symmetric in all operators and (ii) involves only fully renormalized correlators. The combination of both properties sets Kugler's sIE [22] apart from previous results ((i) from Ref. [18] and (ii) from Ref. [10]). The aforementioned literature on improved estimators is summarized in Tab. I.

In the present paper, we generalize Kugler's approach to derive sIEs for multipoint vertices. For these, properties (i) and (ii) are particularly useful, since the division by full propagators is required for the amputation of external legs. We also show how the asymptotic and core contributions to the vertex can be isolated and computed separately via estimators of their own, all expressed through combinations of auxiliary correlators involving composite operators. Asymptotic contributions depend on only a subset of all frequency arguments and remain finite if the complementary frequencies are sent to infinity; the core contribution, by contrast, depends on all frequency arguments but decays in all directions. Separate estimators for asymptotic and core contributions are numerically advantageous, as they directly yield the desired quantities, without the need for subtracting
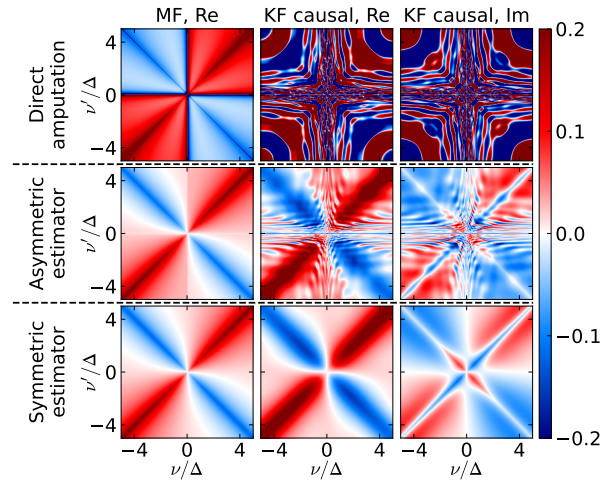
FIG. 1. MF and KF 4p vertices in the AIM at weak interaction ($U = 0.05D$, $\Delta = 2U$, $T = 0.02U$) at $\omega = 0$, normalized by U. The three rows show the results obtained by direct amputation of the correlator, by using an asymmetric improved estimator (aIE) [8, 12, 13], and by using the symmetric improved estimator (sIE) derived in this work. The first, second, and third columns show the MF vertex (which is purely real), the real part of the causal ($\boldsymbol{c} = ----$) component of the KF vertex, and its imaginary part, respectively.

the large-frequency limits of various terms with different asymptotic behaviors.

Our derivation utilizes the framework and notation for multipoint correlators developed in Ref. [12]. There, as here, the overall strategy of the derivation applies equally (modulo some technical differences) in all three of the commonly used many-body frameworks: the imaginary-frequency Matsubara formalism (MF), the real-frequency zero-temperature formalism (ZF), and the real-frequency Keldysh formalism (KF). We illustrate the utility of our sIE for vertices by NRG computations of the 4p vertex of the AIM. We find dramatic improvements relative to results obtained using direct amputation or an aIE. Typical examples of such improvements are shown in Fig. 1, serving as a preview for results presented later on.

The rest of the paper is organized as follows. In Sec. II, we set the scene by concisely recapitulating the derivation of the symmetric self-energy estimator [22] in the MF. In Sec. III, we formulate EOMs for multipoint correlators in the MF, ZF, and KF. In Sec. IV, we use these EOMs to derive sIEs for the self-energy, the 3p and the 4p vertex, and discuss why the proposed estimators are expected to be more robust against numerical artifacts. We present numerical results for the Keldysh 4p vertex of the AIM in Sec. V and conclude with an outlook in Sec. VI.

II. SYMMETRIC SELF-ENERGY ESTIMATOR IN THE MATSUBARA FORMALISM

To provide context, this section reviews the derivation of the symmetric self-energy estimator presented in Ref. [22]. For concreteness, we do so in the MF, for a very simple quantum impurity model, the AIM. We first define 2p correlators (Sec. II A) and derive general EOMs for them (Sec. II B). We then specialize to the AIM, define various auxiliary correlators (Sec. II C), and finally derive a symmetric self-energy estimator (Sec. II D).

A. Definition of 2p correlators

We begin by introducing some notation. We write

$$[\mathcal{O}^1, \mathcal{O}^2]_\zeta = \mathcal{O}^1 \mathcal{O}^2 - \zeta \mathcal{O}^2 \mathcal{O}^1, \tag{1}$$

with $\zeta = 1$ for commutators or $\zeta = -1$ for anticommutators of two operators. Given a Hamiltonian H, thermal expectation values at temperature $1/\beta$ are defined as

$$\langle \mathcal{O}^m \rangle = \frac{\text{Tr}(\mathcal{O}^m e^{-\beta H})}{\text{Tr} \, e^{-\beta H}} \tag{2}$$

and Heisenberg time evolution in imaginary time as

$$\mathcal{O}^m(m) = e^{iHz_m} \mathcal{O}^m e^{-iHz_m}. \tag{3}$$

Here, $(m) = (z_m) = (-i\tau_m)$, with τ_m real, is a shorthand for the MF imaginary time argument (this notation ensures consistency with ZF and KF formulas later, where $z_m = t_m$). A MF 2p correlator of operators $\mathcal{O}^1$ and $\mathcal{O}^2$ at times $(1, 2) = (-i\tau_1, -i\tau_2) = -i\boldsymbol{\tau}$ is defined as

$$\mathcal{G}[\mathcal{O}^1, \mathcal{O}^2](1, 2) = -i \langle \mathcal{T}[\mathcal{O}^1, \mathcal{O}^2](1, 2) \rangle. \tag{4}$$

Here, $\mathcal{T}$ denotes τ ordering,

$$\mathcal{T}[\mathcal{O}^1, \mathcal{O}^2](1, 2) = \theta(\tau_1 - \tau_2) \langle \mathcal{O}^1(1) \mathcal{O}^2(2) \rangle + \zeta_1^2 \theta(\tau_2 - \tau_1) \langle \mathcal{O}^2(2) \mathcal{O}^1(1) \rangle, \tag{5}$$

and $\zeta_1^2 = \zeta_2^1$ is the sign arising when permuting $\mathcal{O}^1$ past $\mathcal{O}^2$: $\zeta_1^2 = -1$ if both are fermionic, $\zeta_1^2 = +1$ otherwise.

The corresponding transformation to the Matsubara frequency domain is

$$\mathcal{G}[\mathcal{O}^1, \mathcal{O}^2](i\boldsymbol{\omega}) = -i \int_0^\beta d^2\tau \, e^{i\boldsymbol{\omega} \cdot \boldsymbol{\tau}} \mathcal{G}[\mathcal{O}^1, \mathcal{O}^2](-i\boldsymbol{\tau}) \tag{6a}$$

$$= \beta \delta_{\omega_{12}, 0} \, G[\mathcal{O}^1, \mathcal{O}^2](i\boldsymbol{\omega}), \tag{6b}$$

with $\omega_{12} = \omega_1 + \omega_2$. Here, time-translational invariance was exploited to factor out a Kronecker delta expressing energy conservation, $\omega_{12} = 0$. We take this constraint to be implicitly understood for the frequency arguments of $G[\mathcal{O}^1, \mathcal{O}^2](i\boldsymbol{\omega})$ and thus omit the second one, writing

$$G[\mathcal{O}^1, \mathcal{O}^2](i\omega, -i\omega) = G[\mathcal{O}^1, \mathcal{O}^2](i\omega). \tag{7}$$

For brevity, we will often omit the operator arguments $[\mathcal{O}^1, \mathcal{O}^2]$ when they can be inferred from the context.

By analogy, an equilibrium expectation value may be viewed as a (constant) 1p function, $\mathcal{G}[\mathcal{O}^1](1) = \langle \mathcal{O}^1 \rangle$. Its Matsubara transform,

$$\mathcal{G}[\mathcal{O}^1](i\omega) = \int_0^\beta d\tau e^{i\omega\tau} \mathcal{G}[\mathcal{O}^1](-i\tau) = \beta \delta_{\omega, 0} \, G[\mathcal{O}^1], \tag{8}$$

is nonzero only for zero frequency, with $G[\mathcal{O}^1] = \langle \mathcal{O}^1 \rangle$ being independent of frequency.

B. General EOMs for 2p correlators

Next, we recall the derivation of EOMs for 2p correlators. We write derivatives as $\partial_m = \partial/\partial z_m = \partial/\partial(-i\tau_m)$, and $\delta(1, 2) = \delta(z_1 - z_2) = i\delta(\tau_1 - \tau_2)$ for delta functions, such that $\partial_1 \theta(\tau_1 - \tau_2) = -\partial_2 \theta(\tau_1 - \tau_2) = \delta(1, 2)$.

The derivatives of a time-ordered product read

$$\partial_1 \mathcal{T}[\mathcal{O}^1, \mathcal{O}^2](1, 2) = \mathcal{T}[\partial_1 \mathcal{O}^1, \mathcal{O}^2](1, 2) + \delta(1, 2) [\mathcal{O}^1, \mathcal{O}^2]_{\zeta_1^2}(2), \tag{9a}$$

$$\partial_2 \mathcal{T}[\mathcal{O}^1, \mathcal{O}^2](1, 2) = \mathcal{T}[\mathcal{O}^1, \partial_2 \mathcal{O}^2](1, 2) + \delta(2, 1) \zeta_1^2 [\mathcal{O}^2, \mathcal{O}^1]_{\zeta_1^2}(1). \tag{9b}$$

Here, $\delta(1, 2)$ arises from differentiating the time ordering step functions. For the last term of Eq. (9b), we used $\mathcal{T}[\mathcal{O}^1(1) \mathcal{O}^2(2)] = \zeta_1^2 \mathcal{T}[\mathcal{O}^2(2) \mathcal{O}^1(1)]$ to move $\mathcal{O}^2(2)$ to the left of $\mathcal{O}^1(1)$ within $\mathcal{T}[\,]$ before differentiating the step functions. As a result, the (anti)commutator obtained from ∂_2 is "flipped" relative to that from ∂_1 and multiplied by an extra ζ_1^2. A similar feature will occur later on in our discussion of multipoint EOMs.

Using the EOM for Heisenberg operators ($m = 1, 2$),

$$i\partial_m \mathcal{O}^m(m) = [\mathcal{O}^m(m), H(m)], \tag{10}$$

we obtain the following EOMs for 2p correlators:

$$i\partial_1 \mathcal{G}[\mathcal{O}^1, \mathcal{O}^2](1, 2) = \mathcal{G}[[\mathcal{O}^1, H], \mathcal{O}^2](1, 2) + \delta(1, 2) \mathcal{G}[[\mathcal{O}^1, \mathcal{O}^2]_{\zeta_1^2}](2), \tag{11a}$$

$$i\partial_2 \mathcal{G}[\mathcal{O}^1, \mathcal{O}^2](1, 2) = \mathcal{G}[\mathcal{O}^1, [\mathcal{O}^2, H]](1, 2) + \delta(2, 1) \zeta_1^2 \mathcal{G}[[\mathcal{O}^2, \mathcal{O}^1]_{\zeta_1^2}](1). \tag{11b}$$

Their Matsubara Fourier transforms read

$$i\omega G[\mathcal{O}^1, \mathcal{O}^2](i\omega) = G[[\mathcal{O}^1, H], \mathcal{O}^2](i\omega) + \langle [\mathcal{O}^1, \mathcal{O}^2]_{\zeta_1^2} \rangle, \tag{12a}$$

$$-i\omega G[\mathcal{O}^1, \mathcal{O}^2](i\omega) = G[\mathcal{O}^1, [\mathcal{O}^2, H]](i\omega) + \zeta_1^2 \langle [\mathcal{O}^2, \mathcal{O}^1]_{\zeta_1^2} \rangle. \tag{12b}$$

These two general EOMs, obtained by differentiating $\mathcal{G}(1, 2)$ using ∂_1 or ∂_2, will be used repeatedly below.

C. Full, bare, and auxiliary correlators of the AIM

For concreteness, we frame the following discussion within the context of an SU(2)-symmetric AIM. Its Hamiltonian has the form $H = H^0 + H_{\text{int}}$, with

$$H^0 = \sum_\sigma \varepsilon d_\sigma^\dagger d_\sigma + \sum_{\sigma b} \varepsilon_b c_{b\sigma}^\dagger c_{b\sigma} + \sum_{\sigma b}(V_b d_\sigma^\dagger c_{b\sigma} + \text{H.c.}),$$

$$H_{\text{int}} = U n_\uparrow n_\downarrow, \quad n_\sigma = d_\sigma^\dagger d_\sigma, \tag{13}$$

with $\sigma \in \{\uparrow, \downarrow\}$. H describes a two-flavor impurity with impurity operators $d_\sigma, d_\sigma^\dagger$ experiencing a local, flavor-off-diagonal interaction U, and hybridizing with a two-flavor bath with bath operators $c_{b\sigma}, c_{b\sigma}^\dagger$ ($b = 1, \ldots, N_{\text{bath}}$). We focus on the conventional AIM where these single-particle operators are all fermionic ($\zeta = -1$) and the flavor corresponds to the spin, but we keep track of the sign factor ζ for generality.

We denote the 2p correlator of d and $d^\dagger$ by

$$g(1,2) = \mathcal{G}[d, d^\dagger](1,2), \quad g(i\omega) = G[d, d^\dagger](i\omega) \tag{14}$$

and call it the "propagator", in distinction to other 2p correlators encountered below. It is flavor-diagonal, hence we omit flavor indices. The full propagator $g(i\omega)$, its bare ($U = 0$) version $g^0(i\omega)$, and the self-energy $\Sigma(i\omega)$ satisfy the Dyson equation

$$g - g^0 = g^0 \Sigma g = g \Sigma g^0. \tag{15}$$

The bare propagator can be obtained by setting up the EOMs for g^0 and $G[d, c_b^\dagger]$ and eliminating the latter ("integrating out the bath"). As shown below, one finds

$$g^0(i\omega) = \frac{1}{i\omega - \varepsilon - \Delta(i\omega)}, \quad \Delta(i\omega) = \sum_b \frac{|V_b|^2}{i\omega - \varepsilon_b}. \tag{16}$$

The hybridization function $\Delta(i\omega)$ fully characterizes the impurity-bath coupling.

Next, we consider the EOMs for the full g. When setting them up using Eq. (12), the equal-time commutators $[d_\sigma, H_{\text{int}}]$ and $[d_\sigma^\dagger, H_{\text{int}}]$ yield "composite operators" which we denote as follows, for short:

$$q_\sigma = [d_\sigma, H_{\text{int}}], \quad q_\sigma^\dagger = [H_{\text{int}}, d_\sigma^\dagger], \tag{17a}$$

$$q_{\sigma\sigma'} = [q_\sigma, d_{\sigma'}^\dagger]_\zeta = [[d_\sigma, H_{\text{int}}], d_{\sigma'}^\dagger]_\zeta \tag{17b}$$

$$= [d_\sigma, q_{\sigma'}^\dagger]_\zeta = [d_\sigma, [H_{\text{int}}, d_{\sigma'}^\dagger]]_\zeta. \tag{17c}$$

Here, Eq. (17c) equals (17b) due to the identity

$$[[\mathcal{O}^1, \mathcal{O}^2], \mathcal{O}^3]_\zeta = [\mathcal{O}^1, [\mathcal{O}^2, \mathcal{O}^3]]_\zeta + [[\mathcal{O}^1, \mathcal{O}^3]_\zeta, \mathcal{O}^2].$$

The composite operator $q_{\sigma\sigma'}$ carries the composite index $\sigma\sigma'$ but has just a single time argument. For the AIM [Eq. (13)], the composite operators take the form

$$q_\sigma^{(\dagger)} = U d_\sigma^{(\dagger)} n_{-\sigma}, \tag{18a}$$
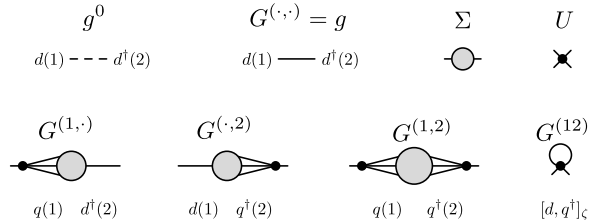
FIG. 2. Diagrammatic representations of the bare and full propagators g^0 and g, the self-energy Σ, the bare vertex U for a quartic interaction, and the auxiliary correlators of Eq. (19) (and Eq. (98) in Sec. IV A). A grey circle with ℓ lines attached represents an ℓp correlator of ℓ elementary d and $d^\dagger$ operators. Long legs represent g's that can be amputated, and short legs indicate completed amputations. An ℓp vertex is obtained from a grey circle with ℓ long legs by subtracting all disconnected parts and amputating all ℓ legs (see Fig. 6).

$$q_{\sigma\sigma'} = U\left(\delta_{\sigma,\sigma'} n_{-\sigma} + \zeta\delta_{\sigma,-\sigma'} d_{-\sigma}^\dagger d_\sigma\right). \tag{18b}$$

When discussing multipoint correlators later on, we will encounter further composite operators, defined via multiple equal-time commutators and labeled by longer composite indices. All correlators involving at least one composite operator will be called "auxiliary correlators".

Below, we need the propagator g, three auxiliary 2p correlators and one auxiliary 1p correlator, defined as follows and depicted diagrammatically in Fig. 2:

$$G^{(\cdot,\cdot)}(i\omega) = G[d_\sigma, d_\sigma^\dagger](i\omega) = g(i\omega), \tag{19a}$$

$$G^{(1,\cdot)}(i\omega) = G[q_\sigma, d_\sigma^\dagger](i\omega), \tag{19b}$$

$$G^{(\cdot,2)}(i\omega) = G[d_\sigma, q_\sigma^\dagger](i\omega), \tag{19c}$$

$$G^{(1,2)}(i\omega) = G[q_\sigma, q_\sigma^\dagger](i\omega), \tag{19d}$$

$$G^{(12)} = G[q_{\sigma\sigma}] = \langle q_{\sigma\sigma}\rangle = U\langle n_{-\sigma}\rangle = \Sigma^{\text{H}}. \tag{19e}$$

The shorthand notation on the left distinguishes them using superscripts, with a single argument, 12, for the 1p correlator and two comma-separated arguments for 2p correlators. For the latter, '·' serves as placeholder for d or $d^\dagger$, while 1 or 2 signal their replacement by q or $q^\dagger$, respectively. The auxiliary correlators $G^{(1,\cdot)}$, $G^{(\cdot,2)}$, and $G^{(1,2)}$ are called F^{L}, F^{R}, and I in Ref. [22]. For correlators diagonal in σ, as here, $G^{(1,\cdot)} = G^{(\cdot,2)}$ [22]; they are denoted F in Refs. [8, 18]. They are 2p correlators of single-particle and composite operators, but involve four single-particle operators since $q \sim dd^\dagger d$. The 1p auxiliary correlator $G^{(12)}$ equals the Hartree self-energy Σ^{H}; its diagrammatic representation in Fig. 2 reflects this fact.

D. Self-energy estimators for the AIM

Finally, we are ready to derive estimators for Σ, exploiting various EOMs. These are obtained using the

general EOMs, Eq. (12), and the commutators

$$\big[d_\sigma, H\big] = \varepsilon d_\sigma + V_b c_{b\sigma} + q_\sigma, \quad \big[c_{b\sigma}, H\big] = \varepsilon_b c_{b\sigma} + V_b^* d_\sigma. \tag{20}$$

We henceforth omit flavor subscripts σ and frequency arguments $(i\omega)$. Setting up the first general EOM, Eq. (12a), for $G^{(\cdot,\cdot)}$ and $G[c_b, d^\dagger]$, we find

$$(i\omega - \varepsilon)G^{(\cdot,\cdot)} = \sum_b V_b G[c_b, d^\dagger] + G^{(1,\cdot)} + 1, \tag{21a}$$

$$(i\omega - \varepsilon_b)G[c_b, d^\dagger] = V_b^* G^{(\cdot,\cdot)}. \tag{21b}$$

By using Eq. (21b) to eliminate $G[c_b, d^\dagger]$ from Eq. (21a), we obtain an EOM involving only impurity correlators,

$$\big(i\omega - \varepsilon - \Delta(i\omega)\big)G^{(\cdot,\cdot)} = G^{(1,\cdot)} + 1, \tag{22a}$$

$$G^{(\cdot,\cdot)}\big(i\omega - \varepsilon - \Delta(i\omega)\big) = G^{(\cdot,2)} + 1. \tag{22b}$$

The second equation can be found analogously to the first, starting from the second general EOM, (12b). The bare $g^0 = G^{(\cdot,\cdot)}|_{U=0}$ follows by setting $G^{(1,\cdot)} = G^{(\cdot,2)} = 0$ in Eq. (22), yielding Eq. (16). Hence, the factors multiplying $G^{(\cdot,\cdot)}$ on the left of Eq. (22) equal $(g^0(i\omega))^{-1}$, implying

$$g = G^{(\cdot,\cdot)} = g^0\,(G^{(1,\cdot)} + 1) = (G^{(\cdot,2)} + 1)g^0. \tag{23}$$

One may also derive Eq. (23) by writing Eq. (21) in the matrix form

$$\begin{pmatrix} i\omega - \varepsilon & -V_1 & -V_2 & \cdots \\ -V_1^* & i\omega - \varepsilon_1 & 0 & \cdots \\ -V_2^* & 0 & i\omega - \varepsilon_2 & \cdots \\ \vdots & \vdots & \vdots & \ddots \end{pmatrix} \begin{pmatrix} G^{(\cdot,\cdot)} \\ G[c_1, d^\dagger] \\ G[c_2, d^\dagger] \\ \vdots \end{pmatrix} = \begin{pmatrix} G^{(1,\cdot)} + 1 \\ 0 \\ 0 \\ \vdots \end{pmatrix}. \tag{24}$$

The matrix on the left is the inverse bare propagator $i\omega - H^0$. By inverting it using the block-matrix identity

$$\begin{pmatrix} A & B \\ C & D \end{pmatrix}^{-1} = \begin{pmatrix} (A - BD^{-1}C)^{-1} & \cdots \\ \cdots & \cdots \end{pmatrix} \tag{25}$$

and solving for the first element $G^{(\cdot,\cdot)}$, we find

$$G^{(\cdot,\cdot)} = \big(i\omega - \varepsilon - \sum_b V_b \frac{1}{i\omega - \varepsilon_b} V_b^*\big)^{-1}(G^{(1,\cdot)} + 1)$$

$$= \big(i\omega - \varepsilon - \Delta(i\omega)\big)^{-1}(G^{(1,\cdot)} + 1), \tag{26}$$

which equals Eq. (23). Equating Eq. (23) to the Dyson equation (15) and solving for Σ, we find the aIE for the self-energy first proposed in Ref. [18]:

$$\Sigma = G^{(1,\cdot)}g^{-1} = g^{-1}G^{(\cdot,2)}. \tag{27}$$

This result corresponds to the Schwinger–Dyson equation for the self-energy.

Next, we follow Ref. [22] to obtain a sIE for Σ. We use the second general EOM, Eq. (12b), to obtain two more EOMs involving $G^{(1,\cdot)}$:

$$G^{(1,\cdot)}\,(i\omega - \varepsilon) = \sum_b G[q, c_b^\dagger]\,V_b^* + G^{(1,2)} + G^{(12)}, \tag{28a}$$
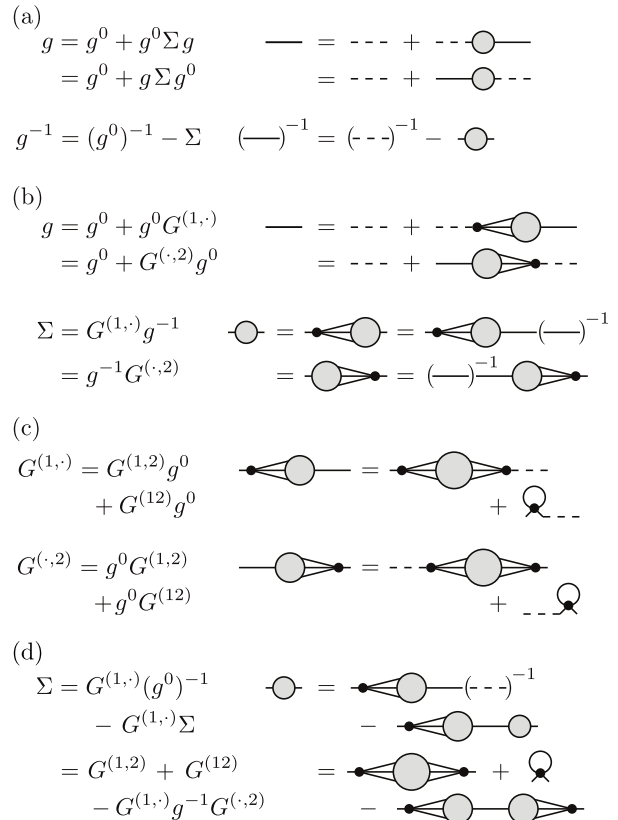
FIG. 3. Diagrammatic derivation of asymmetric and symmetric self-energy estimators. (a) Inversion of the Dyson equation yields $g^{-1} = (g^0)^{-1} - \Sigma$. (b) EOMs for g lead to two aIEs for Σ, involving g-amputated auxiliary correlators, $G^{(1,\cdot)}g^{-1}$ or $g^{-1}G^{(\cdot,2)}$. (c) $G^{(1,\cdot)}$ and $G^{(\cdot,2)}$ satisfy EOMs themselves, involving the auxiliary correlators $G^{(1,2)}$ and $G^{(12)}$. (d) Performing the g-amputation for $G^{(1,\cdot)}g^{-1}$ in (b) by using (a) for g^{-1}, one obtains terms containing $G^{(1,\cdot)}(g^0)^{-1}$; these are known from the EOMs from (c). The last line gives the desired sIE for Σ. Its first and third terms both contain one-particle-reducible contributions. In their difference, however, such contributions cancel, ensuring that Σ is one-particle irreducible (see Fig. 4 for an example at order $\mathcal{O}(U^2)$).

$$G[q, c_b^\dagger]\,(i\omega - \varepsilon_b) = G^{(1,\cdot)}V_b. \tag{28b}$$

The $G^{(12)}$ term, which is independent of ω, comes from the last term of Eq. (12b), involving an equal-time (anti)commutator that yields an expectation value, $\langle [d_\sigma^\dagger, q_\sigma]_\zeta \rangle = \langle q_{\sigma\sigma} \rangle$. We eliminate $G[q, c_b^\dagger]$ to obtain

$$G^{(1,\cdot)} = (G^{(1,2)} + G^{(12)})g^0. \tag{29a}$$

In a similar manner, we obtain

$$G^{(\cdot,2)} = g^0(G^{(1,2)} + G^{(12)}). \tag{29b}$$

Substituting $g^{-1} = (g^0)^{-1} - \Sigma$ in Eq. (27), we find

$$\Sigma = G^{(1,\cdot)}[(g^0)^{-1} - \Sigma]$$

FIG. 4. Expansion of the symmetric self-energy estimator to second order in the interaction U. The one-particle-reducible contributions to the diagrams on the right of the first line cancel, guaranteeing the one-particle irreducibility of Σ.

$$
\begin{aligned}
&= G^{(1,2)} + G^{(12)} - G^{(1,\cdot)}\Sigma \\
&= G^{(1,2)} + \Sigma^{\mathrm{H}} - G^{(1,\cdot)}g^{-1}G^{(\cdot,2)}. \quad (30)
\end{aligned}
$$

For the second equality, we used Eq. (29a) to eliminate $G^{(1,\cdot)}(g^0)^{-1}$. For the third, we replaced Σ by its aIE (27) and used $G^{(12)} = \Sigma^{\mathrm{H}}$ [Eq. (19e)]. Equation (30) is the sIE of Ref. [22]. It has the desirable properties of being (i) symmetric w.r.t. both frequency arguments and (ii) expressed purely through full correlators.

Figure 3 diagrammatically summarizes the derivation of the sIE (30) for the self-energy. It rests on two key insights. First, the external g legs of any $G^{(\cdots)}$ (e.g. $G^{(1,\cdot)}$ or $G^{(1,\cdot)}$ in Fig. 3) can be amputated through multiplication by $g^{-1} = (g^0)^{-1} - \Sigma$; this yields terms of the form $G^{(\cdots)}(g^0)^{-1}$ or $(g^0)^{-1}G^{(\cdots)}$. Second, each such product corresponds to the left side of an EOM; the right side of that EOM contains other auxiliary correlators and frequency-indepedent constants arising from (anti)commutators, thus $(g^0)^{-1}$ can be eliminated altogether. Moreover, this can be done in a fashion symmetric w.r.t. frequency arguments by combining EOMs derived using either ∂_1 or ∂_2.

In the following sections, our goal is to use a similar strategy to derive similar sIEs for general ℓp functions, for arbitrary flavor indices and in any of the MF, ZF, and KF. For the above discussion in the MF, we worked directly in the frequency domain. In the KF, one cannot use the same strategy as the bare propagator is matrix-valued and not simply given by $i\omega - \varepsilon - \Delta$ as in Eq. (22). A more fundamental reason is that, in the KF, the EOM does not fully determine the correlator. For example, the $\boldsymbol{k} = (1,1)$ and $(2,2)$ components of the bare KF propagator obey the same EOM (see Eq. (71)), while the former is zero and the latter is not. In the KF, the boundary condition of the correlators (see Eq. (A2) in App. A) needs to be explicitly used, whereas in the MF it was implicitly imposed through the structure of Matsubara frequencies. We will henceforth work in the time domain, where this boundary condition is formulated. To that end, we need a general, compact notation of multipoint correlators, which we introduce next.
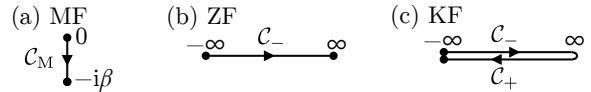
FIG. 5. Time contour for each many-body formalism considered.

III. EOMS FOR MULTIPOINT CORRELATORS

In this section, we generalize the discussion of the previous section from 2p to ℓp correlators. We define them in Sec. III A and derive their general EOMs in Sec. III B. We then write the Hamiltonian as the sum of non-interacting and interacting parts and derive EOMs for full (interacting) ℓp correlators involving bare (non-interacting) propagators and auxiliary ℓp correlators in Sec. III C. We discuss how the non-interacting bath degrees of freedom can be integrated out if needed in Sec. III D. In Sec. III E, we adopt specific formalisms (MF, ZF, KF) and derive EOMs in the frequency domain. In Sec. III F, we show that the obtained EOMs also hold for the connected part of the correlator. Finally, in Sec. III G, we derive an EOM that involves full propagators instead of the bare ones.

A. Definition of ℓp functions

In the MF, ZF, and KF, ℓp correlators of the list of operators $[\boldsymbol{\mathcal{O}}] = [\mathcal{O}^1, \cdots, \mathcal{O}^\ell]$ are defined as

$$
\mathcal{G}_{\mathrm{M}}[\boldsymbol{\mathcal{O}}](-i\boldsymbol{\tau}) = (-i)^{\ell-1}\left\langle \mathcal{T}[\boldsymbol{\mathcal{O}}](-i\boldsymbol{\tau})\right\rangle, \quad (31a)
$$

$$
\mathcal{G}_{\mathrm{Z}}[\boldsymbol{\mathcal{O}}](\boldsymbol{t}) = (-i)^{\ell-1}\left\langle \mathcal{T}[\boldsymbol{\mathcal{O}}](\boldsymbol{t})\right\rangle, \quad (31b)
$$

$$
\mathcal{G}_{\mathrm{K}}^{\boldsymbol{c}}[\boldsymbol{\mathcal{O}}](\boldsymbol{t}) = (-i)^{\ell-1}\left\langle \mathcal{T}[\boldsymbol{\mathcal{O}}](\boldsymbol{t}^{\boldsymbol{c}})\right\rangle, \quad (31c)
$$

respectively. Here, $(-i\boldsymbol{\tau}) = (-i\tau_1, \cdots, -i\tau_\ell)$, and analogously for $\boldsymbol{c}$, $\boldsymbol{t}$ and $\boldsymbol{t}^{\boldsymbol{c}}$; $\langle A\rangle$ denotes thermal averaging w.r.t. the full Hamiltonian H according to Eq. (2); $\mathcal{O}(z) = e^{iHz}\mathcal{O}e^{-iHz}$ as in Eq. (3), and $\mathcal{T}$ denotes time ordering along one of the contours

$$
\mathrm{MF}: \quad -i\tau_m \in \mathcal{C}_{\mathrm{M}} = [0, -i\beta], \quad (32a)
$$

$$
\mathrm{ZF}: \quad t_m \in \mathcal{C}_-, \quad (32b)
$$

$$
\mathrm{KF}: \quad t_m^{c_m} \in \mathcal{C}_- \oplus \mathcal{C}_+, \quad (32c)
$$

shown in Fig. 5. Here, $\mathcal{C}_- = [-\infty, \infty]$ and $\mathcal{C}_+ = [\infty, -\infty]$ are the forward and backward branches of the Keldysh contour. In the KF, each contour variable is specified by a real-valued time argument and a contour index, i.e., $z = t^c$ with $c = -$ ($c = +$) for the forward (backward) branch, and contour variables follow time ordering (anti-time ordering) on the forward (backward) branch. In this work, we focus only on systems in the ground state (ZF) or thermal equilibrium (MF, KF), and do not consider the nonequilibrium KF. We generically denote ℓp correlators by $\mathcal{G}^{\ell\mathrm{p}}$, but suppress the superscript if the number of

(a) $\mathcal{G}^{\ell\mathrm{p}}$ 1 ⟨diagram⟩ 2 ... ℓ (b) $\Gamma^{\ell\mathrm{p}}$ 1 ⟨con⟩ 2 ... ℓ
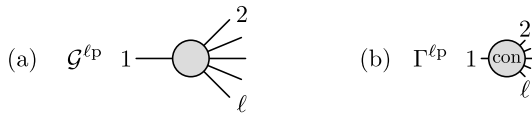
FIG. 6. Diagrammatic representations of (a) the ℓp correlator $\mathcal{G}^{\ell\mathrm{p}}$ and (b) the ℓp vertex $\Gamma^{\ell\mathrm{p}}$, identified as the connected part of an ℓp correlator after amputation of external legs.

	z	∂_z	$\int dz$	$\delta(z,z')$	$\theta(z,z')$
MF	$-i\tau$	$\frac{\partial}{\partial(-i\tau)}$	$-i\int_0^\beta d\tau$	$i\delta(\tau-\tau')$	$\theta(\tau-\tau')$
ZK	t	$\frac{\partial}{\partial t}$	$\int_{-\infty}^{\infty} dt$	$\delta(t-t')$	$\theta(t-t')$
KF	t^c	$\frac{\partial}{\partial t}$	$\sum_c \int_{-\infty}^{\infty} dt\, Z^{cc}$	$Z^{cc'}\delta(t-t')$	$\theta_{cc'}(t-t')$

TABLE II. Definition of contour variables, differentiation, integration, delta functions and step functions, in the Matsubara, zero-temperature and Keldysh formalisms. In the KF, the matrix Z has elements $Z^{cc'} = \delta_{cc'}(-1)^{\delta_{c,+}} = \left(\begin{smallmatrix} 1 & 0 \\ 0 & -1 \end{smallmatrix}\right)$, and the contour-ordering step function $\theta_{cc'}(t-t')$ by definition equals $\theta(t-t')$, 0, 1, or $\theta(t'-t)$ for $cc' = --, -+, +-$ or $++$, respectively. These definitions readily lead to Eq. (34).

arguments is clear from the context. For a diagrammatic depiction, see Fig. 6(a).

To analyze the boundary conditions of the correlators, one must attach a vertical branch to the ZF and KF contours. The only step where the boundary condition affects the results is when deducing the EOM in integral form from its differential form via integration by parts [Eq. (52)]. This derivation is carried out in App. A.

As in the 2p case, Fourier-transformed ℓp correlators are defined by factoring out a delta function arising from time-translational invariance. For the MF, ZF, and KF, we have

$$\mathcal{G}_\mathrm{M}(i\boldsymbol{\omega}) = i(-i)^\ell \int_0^\beta d^\ell\tau\, e^{i\boldsymbol{\omega}\cdot\boldsymbol{\tau}} \mathcal{G}_\mathrm{M}(-i\boldsymbol{\tau}) = \beta\delta_{\omega_{1\cdots\ell},0} G_\mathrm{M}(i\boldsymbol{\omega}),$$

$$\mathcal{G}_\mathrm{Z}(\boldsymbol{\omega}) = \int d^\ell t\, e^{i\boldsymbol{\omega}\cdot\boldsymbol{t}} \mathcal{G}_\mathrm{Z}(\boldsymbol{t}) = 2\pi\delta(\omega_{1\cdots\ell}) G_\mathrm{Z}(\boldsymbol{\omega}),$$

$$\mathcal{G}_\mathrm{K}^{\boldsymbol{c}}(\boldsymbol{\omega}) = \int d^\ell t\, e^{i\boldsymbol{\omega}\cdot\boldsymbol{t}} \mathcal{G}_\mathrm{K}^{\boldsymbol{c}}(\boldsymbol{t}) = 2\pi\delta(\omega_{1\cdots\ell}) G_\mathrm{K}^{\boldsymbol{c}}(\boldsymbol{\omega}), \qquad (33)$$

respectively, where $\omega_{1\cdots\ell} = \omega_1 + \cdots + \omega_\ell$. We omitted the operator arguments $[\boldsymbol{\mathcal{O}}]$ for brevity. Combining the MF prefactors in Eqs. (31) and (33) yields $i(-i)^\ell(-i)^{\ell-1} = (-1)^{\ell-1}$, matching the choice in Ref. [12]. The analytic properties of correlators G in the frequency domain, such as the position of the poles in the complex plane, are determined by the causal structure of the corresponding correlators $\mathcal{G}$ in the time domain (see, e.g., Ref. [12]).

B. General EOMs for ℓp correlators

In this subsection, we derive general EOMs for ℓp correlators in the time domain, employing a unified notation equally applicable to the MF, ZF, and KF.

We begin by introducing the contour variable $z = -i\tau$ for MF, $z = t$ for ZF, and $z = t^c$ for KF. Corresponding definitions for ∂_z, $\int dz$, $\delta(z,z')$ and $\theta(z,z')$ are given in Table II. We further write $(m) = (z_m)$, $\partial_m = \partial_{z_m}$, and $\int_m = \int dz_m$, for short. In all three formalisms, we have

$$\int_m f(m)\delta(m,n) = f(n), \qquad \left.\begin{array}{c}\partial_m \\ \partial_n\end{array}\right\} \theta(m,n) = \pm\delta(m,n). \quad (34)$$

In this unified notation, Eqs. (31) are expressed as [23]

$$\mathcal{G}[\boldsymbol{\mathcal{O}}](\boldsymbol{z}) = (-i)^{\ell-1}\langle \mathcal{T}[\boldsymbol{\mathcal{O}}](\boldsymbol{z})\rangle. \quad (35)$$

Here, $\mathcal{T}[\boldsymbol{\mathcal{O}}](\boldsymbol{z}) = \mathcal{T}\prod_{m=1}^\ell \mathcal{O}^m(m)$ denotes contour ordering: it reorders the product such that "larger" times sit

to the left (if $\theta(m,n) = 1$ (or 0), it puts $\mathcal{O}^m(m)$ to the left (or right) of $\mathcal{O}^n(n)$), and yields an overall sign of $+1$ (-1) if this reordering involves an even (odd) number of exchanges of fermionic operators. To track such signs, we write $\zeta_m^n = \zeta_m^n$ or $\zeta_m^{i_1\cdots i_n} = \zeta_m^{i_1}\cdots\zeta_m^{i_n}$ for the sign arising when moving $\mathcal{O}^m$ past $\mathcal{O}^n$ or $\mathcal{O}^{i_1}\cdots\mathcal{O}^{i_n}$, respectively.

Below, we set up EOMs for $i\partial_m\mathcal{G}^{\ell\mathrm{p}}$, generalizing the procedure of Sec. II B. Just as there, the EOMs for $i\partial_m\mathcal{G}^{\ell\mathrm{p}}$ contain further correlators of two types: auxiliary ℓp correlators that differ from $\mathcal{G}^{\ell\mathrm{p}}$ through the replacement of $\mathcal{O}^m$ by $i\partial_m\mathcal{O}^m = [\mathcal{O}^m, H]$, and $(\ell{-}1)$p correlators that differ from $\mathcal{G}^{\ell\mathrm{p}}$ through the removal of $\mathcal{O}^m$ from the argument list and the replacement of another operator, say $\mathcal{O}^{n(\neq m)}$, by the (anti)commutator $[\mathcal{O}^m, \mathcal{O}^n]_{\zeta_m^n}$. To describe such objects, we introduce some shorthands: we define two lists derived from $(\cdot) = (\boldsymbol{z}) = (z_1, \cdots, z_\ell)$,

$$(\not{m}) = (\boldsymbol{z}^{\not{m}}) = (\cdots, \cancel{z_m}, \cdots) = (\cdots, z_{m-1}, z_{m+1}, \cdots),$$
$$(m', \not{m}) = (\boldsymbol{z}'^m) = (z_m', \boldsymbol{z}^{\not{m}}) = (\cdots, z_{m-1}, z_m', z_{m+1}, \cdots), \quad (36)$$

obtained from the list $(\boldsymbol{z})$ by removing slot m entirely, or by replacing z_m by z_m' in slot m. For example, if $\ell = 4$, then $(\not{2}) = (z_1, z_3, z_4)$ and $(3', \not{3}) = (z_1, z_2, z_3', z_4)$. (Note that m' is a shorthand for z_m', not $z_{m'}$.) Likewise, we define two lists derived from $[\boldsymbol{\mathcal{O}}] = [\mathcal{O}^1, \cdots, \mathcal{O}^\ell]$,

$$[\mathcal{O}'^m, \boldsymbol{\mathcal{O}}^{\not{m}}] = [\cdots, \mathcal{O}^{m-1}, \mathcal{O}'^m, \mathcal{O}^{m+1}, \cdots], \quad (37)$$
$$[\boldsymbol{\mathcal{O}}^{\not{m}n}] = [\cdots, \cancel{\mathcal{O}^m}, \cdots, \mathcal{O}^{n-1}, [\mathcal{O}^m, \mathcal{O}^n]_{\zeta_m^n}, \mathcal{O}^{n+1}, \cdots].$$

The superscript on $\boldsymbol{\mathcal{O}}^{\not{m}n}$ indicates that $\mathcal{O}^m$ has been removed and slot n "altered" by replacing $\mathcal{O}^n$ by the (anti)commutator $[\mathcal{O}^m, \mathcal{O}^n]_{\zeta_m^n}$. A related list, derived from $\boldsymbol{\omega} = (\omega_1, \cdots, \omega_\ell)$, is defined as

$$(\boldsymbol{\omega}^{\not{m}n}) = (\cdots, \cancel{\omega_m}, \cdots, \omega_{n-1}, \omega_{mn}, \omega_{n+1}, \cdots), \quad (38)$$

with ω_m removed and slot n altered by replacing ω_n by $\omega_{mn} = \omega_m + \omega_n$. $(\boldsymbol{\omega}^{\not{m}n})$ appears in Fourier transforms involving $\delta(m,n)$, e.g. $\int_m e^{i(\omega_m t_m + \omega_n t_n)}\delta(m,n) = e^{i\omega_{mn}t_n}$.

A trivial identity is $\mathcal{T}[\mathcal{O}](\boldsymbol{z}) = \mathcal{T}[O^m, \mathcal{O}^{\eta\!\!\!/\!h}](m, \eta\!\!\!/\!h)$, useful when evaluating the action of ∂_m, where O^m plays a special role. In the following, we omit arguments such as $(\boldsymbol{z})$ and $[\mathcal{O}]$ when they can be inferred from context.

The action of ∂_m on a contour-ordered product $\mathcal{T}[\mathcal{O}](\boldsymbol{z})$ of ℓ operators can be compactly expressed as

$$\partial_m \mathcal{T}[\mathcal{O}] = \mathcal{T}[\partial_m \mathcal{O}^m, \mathcal{O}^{\eta\!\!\!/\!h}] + \sum_n^{\eta\!\!\!/\!h} \delta(m, n) \mathcal{T}[\mathcal{O}^{\eta\!\!\!/\!hn}](\eta\!\!\!/\!h),$$

$$\sum_n^{\eta\!\!\!/\!h} \cdot = \sum_{n=1}^{m-1} \zeta_m^{n \cdots m-1} \cdot + \sum_{n=m+1}^{m+1} \cdot + \sum_{n=m+2}^{\ell} \zeta_m^{m+1 \cdots n-1} \cdot . \tag{39}$$

Here, the signs in $\sum_n^{\eta\!\!\!/\!h}$ arise from permuting $\mathcal{O}^m$ leftward if $n < m$ (first term) or rightward if $n > m+1$ (third term) to sit next to $\mathcal{O}^n$ as either $\theta(m, n) \mathcal{O}^m \mathcal{O}^n$ or $\theta(n, m) \zeta_n^m \mathcal{O}^n \mathcal{O}^m$, as required by contour time ordering. The action of ∂_m on these step functions then yields $\delta(m, n)$ times $[\mathcal{O}^m, \mathcal{O}^n]_{\zeta_m^n}$ in the altered slot n, as encoded in $\mathcal{T}[\mathcal{O}^{\eta\!\!\!/\!hn}]$.

Finally, general EOMs for the ℓp correlator of Eq. (35) follow using Eqs. (39) and the operator EOM (10):

$$i\partial_m \mathcal{G}[\mathcal{O}] = \mathcal{G}\big[[\mathcal{O}^m, H], \mathcal{O}^{\eta\!\!\!/\!h}\big] + \sum_n^{\eta\!\!\!/\!h} \delta(m, n) \mathcal{G}[\mathcal{O}^{\eta\!\!\!/\!hn}](\eta\!\!\!/\!h). \tag{40}$$

These generalize the 2p equations (11) to arbitrarily ℓ, expressing $i\partial_m G^{\ell p}$ through $G^{\ell p}$ and $G^{(\ell-1)p}$ functions.

C. Single-particle differentiated EOMs

We henceforth focus on "single-particle differentiated" EOMs, i.e., EOMs in which the operator O^m being time-differentiated in $i\partial_m O^m$ is a single-particle operator. More general EOMs, involving time derivatives of composite operators, are not needed in this work.

We consider a Hamiltonian of the form

$$H = H^0 + H_{\text{int}} = H^0_{aa'} \psi_a^\dagger \psi_{a'} + H_{\text{int}}, \tag{41}$$

with summation over repeated indices implied. Here, ψ_a, $\psi_a^\dagger$ $(a = 1, \cdots, N_{\text{tot}})$ are single-particle operators, such as the d_σ, $d_\sigma^\dagger$ and $c_{\sigma b}$, $c_{\sigma b}^\dagger$ of Sec. II C. We will call a an "orbital" index, though it may include spin. In this section, we do not assume a specific form of interaction. Later in Sec. IV, we apply the EOM to a quartic interaction. The single-particle operators may be either bosonic ($\zeta = 1$) or fermionic ($\zeta = -1$), but they should all have the same type, so that

$$[\psi_a, \psi_{a'}^\dagger]_\zeta = \mathbb{1}_{aa'}, \qquad [\psi_a^\dagger, \psi_{a'}]_\zeta = -\zeta \mathbb{1}_{aa'}. \tag{42}$$

However, the correlators considered below can be of mixed type, i.e., involve both single-particle operators and composite ones, such as $n_a = \psi_a^\dagger \psi_a$.

For the bare propagator, defined for $H_{\text{int}} = 0$, we write

$$g^0_{aa'}(m, m') = g^0[\psi_a, \psi_{a'}^\dagger](z_m, z'_m). \tag{43}$$

Using the general EOM (40) and the equal-time relations

$$[\psi_a, H^0] = H^0_{aa'} \psi_{a'}, \quad [\psi_a, \psi_{a'}^\dagger]_\zeta = \mathbb{1}_{aa'}, \tag{44}$$

one finds two bare-propagator EOMs,

$$(i\partial_m \mathbb{1} - H^0)_{a\bar{a}} g^0_{\bar{a}a'}(m, m') = \delta(m, m') \mathbb{1}_{aa'}, \tag{45a}$$

$$g^0_{a\bar{a}}(m, m')(i\overleftarrow{\partial}_m \mathbb{1} + H^0)_{\bar{a}a'} = -\delta(m, m') \mathbb{1}_{aa'}. \tag{45b}$$

$\overleftarrow{\partial}_m$ denotes a derivative w.r.t. z'_m, acting to the left. According to Eqs. (45), g^0 serves as inverse for the "bare time evolution" expressions $(i\partial_m \mathbb{1} - H^0)$ and $(i\overleftarrow{\partial}_m \mathbb{1} + H^0)$. Below, this will be exploited to remove such expressions from EOMs for general correlators.

Now, consider ℓp correlators involving at least one single-particle operator, say $\mathcal{O}^m = \psi_a^{(\dagger)}$. Corresponding single-particle differentiated EOMs follow via Eq. (40):

$$(i\partial_m \mathbb{1} - H^0)_{aa'} \mathcal{G}[\psi_{a'}, \mathcal{O}^{\eta\!\!\!/\!h}] = \mathcal{F}^m[\psi_a, \mathcal{O}^{\eta\!\!\!/\!h}], \tag{46a}$$

$$\mathcal{G}[\psi_{a'}^\dagger, \mathcal{O}^{\eta\!\!\!/\!h}](i\overleftarrow{\partial}_m \mathbb{1} + H^0)_{a'a} = \mathcal{F}^m[\psi_a^\dagger, \mathcal{O}^{\eta\!\!\!/\!h}]. \tag{46b}$$

For the correlators on the right, containing all contributions not involving g^0, we used the shorthand

$$\mathcal{F}^m[\mathcal{O}] = \mathcal{G}\big[[\mathcal{O}^m, H_{\text{int}}], \mathcal{O}^{\eta\!\!\!/\!h}\big] + \sum_n^{\eta\!\!\!/\!h} \delta(m, n) \mathcal{G}[\mathcal{O}^{\eta\!\!\!/\!hn}](\eta\!\!\!/\!h), \tag{47}$$

where the superscript on $\mathcal{F}^m$ singles out m for special treatment. The first term on the right involves single-index composite operators, to be denoted (cf. Eq. (17a))

$$q_a = [\psi_a, H_{\text{int}}], \quad q_a^\dagger = -[\psi_a^\dagger, H_{\text{int}}]. \tag{48}$$

Figure 7(a) gives a diagrammatic representation of $\mathcal{F}^m$.

Let us exemplify Eq. (47) for the case that *all* operators in $[\mathcal{O}]$ are single-particle operators, $\mathcal{O}^n = \psi_a^{(\dagger)}$. Then, the (anti)commutator in the altered slot n of $[\mathcal{O}^{\eta\!\!\!/\!hn}]$ is nonzero only for the cases listed in Eqs. (42). For $\mathcal{O} = [\psi_1, \psi_2^\dagger]$, e.g., we obtain

$$\mathcal{F}^1[\psi_1, \psi_2^\dagger] = \quad \mathcal{G}[q_1, \psi_2^\dagger] + \delta(1, 2) \mathbb{1}_{12},$$

$$\mathcal{F}^2[\psi_1, \psi_2^\dagger] = -\mathcal{G}[\psi_1, q_2^\dagger] - \delta(2, 1) \mathbb{1}_{21}. \tag{49}$$

The second terms on the right were simplified using $\mathcal{G}\big[[\psi_1, \psi_2^\dagger]_\zeta\big] = \mathcal{G}[\mathbb{1}_{12}] = \mathbb{1}_{12}$. We will call the resulting combinations $\delta(1, 2) \mathbb{1}_{12}$ "identity contractions" and diagrammatically depict them using dotted lines (see Fig. 7). Similarly, for $\mathcal{O} = [\psi_1, \psi_2^\dagger, \psi_3, \psi_4^\dagger]$, we have

$$\mathcal{F}^1[\mathcal{O}] = \quad \mathcal{G}[q_1, \psi_2^\dagger, \psi_3, \psi_4^\dagger] - i\delta(1, 2) \mathbb{1}_{12} \mathcal{G}[\psi_3, \psi_4^\dagger](3, 4)$$

$$- i\delta(1, 4) \mathbb{1}_{14} \mathcal{G}[\psi_2^\dagger, \psi_3](2, 3),$$
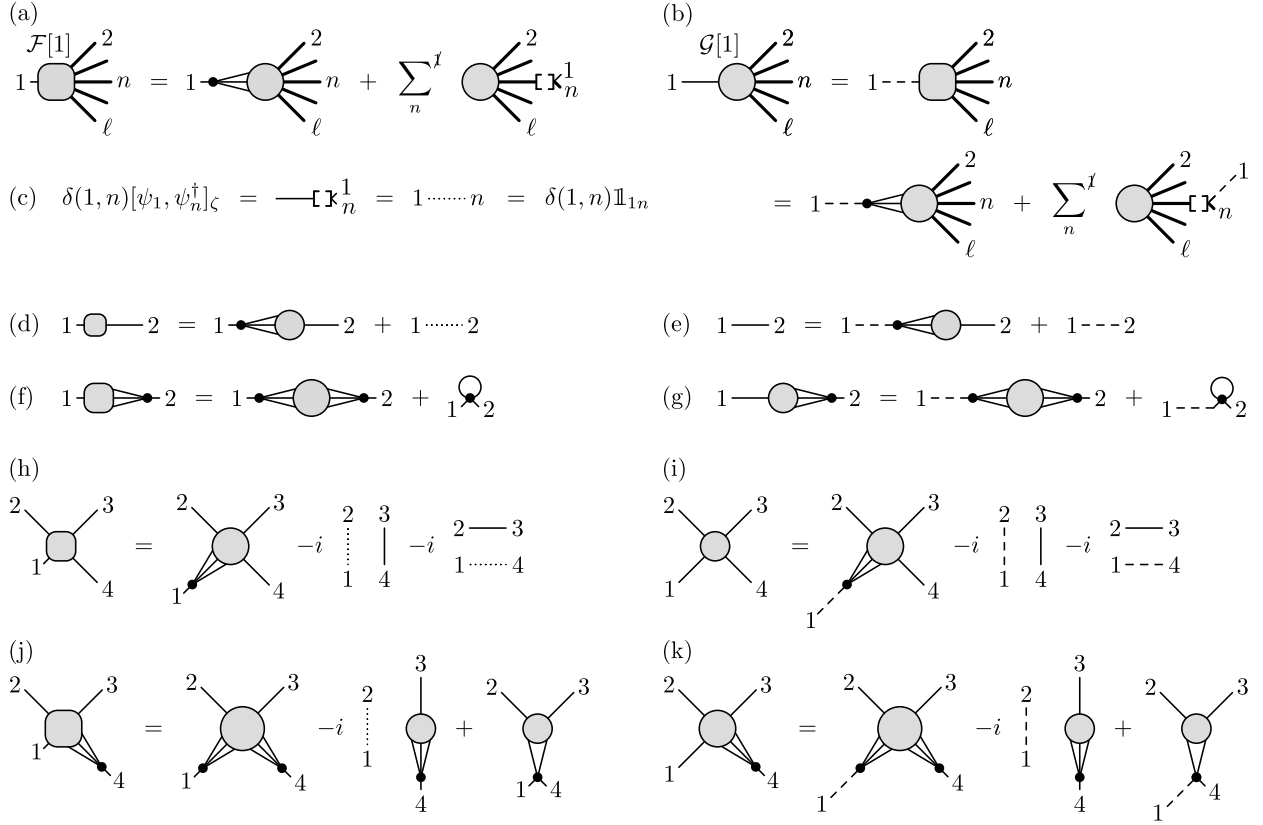
FIG. 7. Diagrammatic depiction of $\mathcal{F}[1] = \mathcal{F}^1[\psi_1, \boldsymbol{\mathcal{O}}^I]$ [Eq. (47)] and $\mathcal{G}[1] = \mathcal{G}[\psi_1, \boldsymbol{\mathcal{O}}^I]$ [Eq. (54)]. Operators from the argument list $\boldsymbol{\mathcal{O}}^I$ are represented by long lines, drawn thin for single-particle operators or thick for operators of unspecified type (single-particle or composite). (a,b) General case. In the $\sum_n^I$ sums, leg n is decorated by tiny [ ] brackets and two endpoints labeled 1 and n, representing the replacement of $\mathcal{O}^n$ by $\delta(1,n)[\psi_1, \mathcal{O}^n]_{\varsigma_1^n}$ [cf. Eqs. (47) and (37)]. (c) For $\mathcal{O}^n = \psi_n^\dagger$, the latter reduces to the identity contraction $\delta(1,n)\mathbb{1}_{1n}$, depicted as a dotted line. (d-k) Examples illustrating (a,b) for various choices of $[\psi_1, \boldsymbol{\mathcal{O}}^I]$, with (d-g) $\ell = 2$ and (h-k) $\ell = 4$: (d,e) $[\psi_1, \psi_2^\dagger]$, (f,g) $[\psi_1, q_2^\dagger]$, (h,i) $[\psi_1, \psi_2^\dagger, \psi_3, \psi_4^\dagger]$, and (j,k) $[\psi_1, \psi_2^\dagger, \psi_3, q_4^\dagger]$. The 2p diagrams (d-g) illustrate how cases encountered in Sec. II D on the self-energy (cf. Fig. 3) arise in the present formulation. (h) represents the first equation of Eqs. (50). The last diagram of (j) depicts the 3p correlator $\mathcal{G}[\psi_2^\dagger, \psi_3, [\psi_1, q_4^\dagger]_\varsigma]$.

$$\mathcal{F}^2[\boldsymbol{\mathcal{O}}] = -\mathcal{G}[\psi_1, q_2^\dagger, \psi_3, \psi_4^\dagger] + i\delta(2,1)\mathbb{1}_{21}\mathcal{G}[\psi_3, \psi_4^\dagger](3,4)$$
$$+ i\varsigma\delta(2,3)\mathbb{1}_{23}\mathcal{G}[\psi_1, \psi_4^\dagger](1,4),$$
$$\mathcal{F}^3[\boldsymbol{\mathcal{O}}] = \mathcal{G}[\psi_1, \psi_2^\dagger, q_3, \psi_4^\dagger] - i\varsigma\delta(3,2)\mathbb{1}_{32}\mathcal{G}[\psi_1, \psi_4^\dagger](1,4)$$
$$- i\delta(3,4)\mathbb{1}_{34}\mathcal{G}[\psi_1, \psi_2^\dagger](1,2),$$
$$\mathcal{F}^4[\boldsymbol{\mathcal{O}}] = -\mathcal{G}[\psi_1, \psi_2^\dagger, \psi_3, q_4^\dagger] + i\delta(4,1)\mathbb{1}_{41}\mathcal{G}[\psi_2^\dagger, \psi_3](2,3)$$
$$+ i\delta(4,3)\mathbb{1}_{43}\mathcal{G}[\psi_1, \psi_2^\dagger](1,2). \tag{50}$$

Again, identity contractions arise on the right from, e.g., $\mathcal{G}\big[[\psi_1, \psi_2^\dagger]_\varsigma, \psi_3, \psi_4^\dagger\big](2,3,4) = (-i)\mathbb{1}_{12}\,\mathcal{G}[\psi_3, \psi_4^\dagger](3,4)$. The first lines of Eqs. (49) and (50) are illustrated in Figs. 7(d) and 7(h), respectively.

We now eliminate the bare time evolution expressions

from the EOMs (46) for $\mathcal{G}[\psi_a, \boldsymbol{\mathcal{O}}^{\eta_h}]$. We begin with

$$\mathcal{G}[\psi_a, \boldsymbol{\mathcal{O}}^{\eta_h}] = \int_{m'} \delta(m,m')\mathbb{1}_{aa'}\mathcal{G}[\psi_{a'}, \boldsymbol{\mathcal{O}}^{\eta_h}](m', \eta_h), \tag{51}$$

an identity which trivially follows from the definition of the delta function and the identity matrix $\mathbb{1}$. By inserting the EOM (45b) for the bare propagator, we find

$$\mathcal{G}[\psi_a, \boldsymbol{\mathcal{O}}^{\eta_h}]$$
$$= \int_{m'} g_{a\bar{a}}^0(m,m')(-i\overleftarrow{\partial'_m}\mathbb{1} - H^0)_{\bar{a}a'}\mathcal{G}[\psi_{a'}, \boldsymbol{\mathcal{O}}^{\eta_h}](m', \eta_h)$$
$$= \int_{m'} g_{aa'}^0(m,m')\mathcal{F}^m[\psi_{a'}, \boldsymbol{\mathcal{O}}^{\eta_h}](m', \eta_h). \tag{52}$$

In the second step, we used integration by parts to convert the partial derivative from acting to the left to acting to the right, i.e., from $-\overleftarrow{\partial'_m}$ to ∂'_m, and then used the ℓp

EOM (46a). Importantly, the boundary term in the integration by parts can be shown to vanish, see App. A or App. B. This procedure is analogous to solving Eq. (24) by multiplying $(i\omega - H^0)^{-1}$ on both sides in Sec. II, but now in the time domain.

Finally, let us express Eq. (52) in a concise form hiding orbital indices. To this end, we define

$$(g_m^0)_{aa'}(m, m') = g_{aa'}^0(m, m'),$$
$$\left(\mathcal{G}[m^{(\dagger)}]\right)_a(\cdot) = \mathcal{G}[\psi_a^{(\dagger)}, \boldsymbol{\mathcal{O}}^{\slashed{m}}](\cdot),$$
$$\left(\mathcal{F}[m^{(\dagger)}]\right)_{a'}(m', \slashed{m}) = \mathcal{F}^m[\psi_{a'}^{(\dagger)}, \boldsymbol{\mathcal{O}}^{\slashed{m}}](m', \slashed{m}). \quad (53)$$

Viewing g_m^0 as an $N_{\text{tot}} \times N_{\text{tot}}$ matrix and $\mathcal{G}[m^{(\dagger)}]$ and $\mathcal{F}[m^{(\dagger)}]$ as vectors of length N_{tot} w.r.t. to their orbital indices, the implicit sum $\sum_{a'}$ in Eq. (52) amounts to matrix-vector multiplication. We thus obtain

$$\mathcal{G}[m](\boldsymbol{z}) = \int_{m'} g_m^0(m, m') \mathcal{F}[m](m', \slashed{m}), \quad (54a)$$

$$\mathcal{G}[m^\dagger](\boldsymbol{z}) = -\int_{m'} \mathcal{F}[m^\dagger](m', \slashed{m}) g_m^0(m', m). \quad (54b)$$

Equation (54b) follows similarly from Eq. (46b), where $\mathcal{O}^m = \psi_a^\dagger$. The extra minus sign reflects the sign difference in the H^0 terms in Eqs. (46a) and (46b).

Figure 7(b) diagrammatically depicts the EOM (54a) for $\mathcal{G}[m]$ with $O^m = d_1$, for the case that the interaction is quartic. The differentiation $i\partial_1$ generates two types of diagrams, both involving a bare propagator: it is either connected to the bare interaction vertex associated with a composite operator $q_1 = [\psi_1, H_{\text{int}}]$ or to the "(anti)commutator leg" representing $[\psi_1, O^n]_\zeta$. If O_n equals the single-particle operator ψ_n, the (anti)commutator reduces to $\mathbb{1}_{1n}$, thus disconnecting the bare propagator, as exemplified in Figs. (7)(e,i,k).

The main upshot of this section is as follows: those external legs of a correlator $\mathcal{G}$ that represent full single-particle propagators g can be converted, via EOMs, to bare single-particle propagators g_0 connected to various other correlators (schematically, $\mathcal{G} = g^0 \mathcal{F}$). This sets the stage for Sec. IV. There, we will remove bare propagators through multiplication by $(g^0)^{-1} = g^{-1} + \Sigma$ (schematically, $\mathcal{F} = (g^0)^{-1}\mathcal{G}$, hence $g^{-1}\mathcal{G} = \mathcal{F} - \Sigma\mathcal{G}$). In this way, we arrive at a strategy for amputating legs (computing $g^{-1}\mathcal{G}$) without explicitly dividing by g.

D. Some remarks on quantum impurity models

We briefly pause the development of our general formalism to make some remarks about quantum impurity models. There, an interacting impurity is coupled to a *non*interacting bath. Typically, the correlators of interest are "impurity correlators", involving only impurity operators. Here, we show that impurity correlators satisfy a suitably modified version of EOM (54), involving only impurity operators and indices.

Let us consider a quantum impurity model where the noninteracting Hamiltonian consists of both impurity operators $d_i, d_i^\dagger$ ($i = 1, \cdots, N_{\text{imp}}$) and bath operators $c_b, c_b^\dagger$ ($b = 1, \cdots, N_{\text{bath}}$), while only impurity operators appear in the interacting Hamiltonian:

$$H_{\text{int}} = H_{\text{int}}[d_i, d_{i'}^\dagger]. \quad (55)$$

The subscripts enumerate both the spin and orbital indices. We let ψ_a ($a = 1, \cdots, N_{\text{tot}} = N_{\text{imp}} + N_{\text{bath}}$) enumerate all annihilation operators:

$$\psi_a = \begin{cases} d_i & \text{for } i = a = 1, \cdots, N_{\text{imp}} \\ c_b & \text{for } b = a - N_{\text{imp}} = 1, \cdots, N_{\text{bath}}. \end{cases} \quad (56)$$

It will henceforth be understood that the indices i and b are used exclusively for impurity or bath operators, respectively, while a encompasses both.

The bare propagator $g_{aa'}^0 = g^0[\psi_a, \psi_{a'}^\dagger]$ of Eq. (43), defined as the propagator with $H_{\text{int}} = 0$, can be obtained by solving the bare EOMs (45) (e.g., by transforming to the Fourier domain). The $aa' = ii'$ components of the resulting bare propagator, $g_{ii'}^0 = g^0[d_i, d_{i'}^\dagger]$, comprise the "bare impurity propagator". It encodes information about the bath via the hybridization function (see, e.g., Eq. (16), or the $H_{\text{int}} = 0$ version of Eqs. (24)–(26)). Together with H_{int}, it *fully* specifies the impurity dynamics. In this sense, once $g_{ii'}^0$ has been found, the bath has in effect been integrated out and needs no further consideration.

The inverse of the bare impurity propagator, $(g^0)_{ii'}^{-1}$, is defined as the inverse of the $N_{\text{imp}} \times N_{\text{imp}}$ matrix $g_{ii'}^0$, *not* the $N_{\text{imp}} \times N_{\text{imp}}$ block of the inverse of the $N_{\text{tot}} \times N_{\text{tot}}$ matrix $g_{aa'}^0$. Thus, in the Fourier domain we have

$$(g^0)_{ii'}^{-1} g_{i'i''}^0 = \mathbb{1}_{ii''}. \quad (57)$$

Now, we turn our attention to full correlators of ℓ impurity operators. We assume that at least one, say $\mathcal{O}^m = d_i^{(\dagger)}$, is a single-particle operator; all others may be general (single-particle or composite) operators, $\mathcal{O}^{n(\neq m)} = \mathcal{O}^n[d_i, d_{i'}^\dagger]$. The EOM for this correlator has the form of the general EOM (52), but now containing only impurity operators on both sides, either elementary or composite ones. To see this, notice that $\mathcal{F}^m[c_b, \boldsymbol{\mathcal{O}}^{\slashed{m}}] = \mathcal{F}^m[c_b^\dagger, \boldsymbol{\mathcal{O}}^{\slashed{m}}] = 0$, since the bath operators (anti)commute with H_{int} and $\boldsymbol{\mathcal{O}}^{\slashed{m}}$. Therefore, the dummy orbital index a' in Eq. (52) can be limited to impurity orbitals. The same is true for all implicit orbital indices in Eq. (54), where we now have

$$(g_m^0)_{ii'}(m, m') = g_{ii'}^0(m, m'),$$
$$\left(\mathcal{G}[m^{(\dagger)}]\right)_i(\cdot) = \mathcal{G}[d_i^{(\dagger)}, \boldsymbol{\mathcal{O}}^{\slashed{m}}](\cdot),$$
$$\left(\mathcal{F}[m^{(\dagger)}]\right)_{i'}(m, \slashed{m}) = \mathcal{F}^m[d_{i'}^{(\dagger)}, \boldsymbol{\mathcal{O}}^{\slashed{m}}](m, \slashed{m}). \quad (58)$$

The EOMs of impurity correlators are again represented by the diagrams of Fig. 7, with g^0 now representing the bare impurity propagator in the presence of a bath.

In what follows, we will keep the discussion general, mostly writing d_i. The EOM and improved estimators for a generic many-body Hamiltonian without a bath [Eq. (41)] can be simply obtained by setting $d_i = \psi_a$ and $N_{\text{bath}} = 0$.

E. EOM in the frequency domain

Next, we Fourier transform the EOM (54) from the time domain to the frequency domain for each of the three formalisms (MF, ZF, KF).

1. MF

In the MF, the Fourier transform of the bare-propagator EOM (45a) reads

$$(i\omega\mathbb{1} - H^0)_{a\bar{a}} g^0_{\bar{a}a'}(i\omega) = \mathbb{1}_{aa'}. \tag{59}$$

Similarly, the Fourier transform of Eq. (47) for $\mathcal{F}^m$ reads

$$F_{\text{M}}^m[\mathcal{O}](i\boldsymbol{\omega}) = G_{\text{M}}\big[[\mathcal{O}^m, H_{\text{int}}], \mathcal{O}^{\not{m}}\big](i\boldsymbol{\omega}) \tag{60}$$
$$+ \sum_n^{\not{m}} G_{\text{M}}\big[\mathcal{O}^{\not{m}n}\big](i\boldsymbol{\omega}^{\not{m}n}),$$

where $\boldsymbol{\omega}^{\not{m}n}$ is defined in Eq. (38).

By Fourier transforming the ℓp EOM (54), one finds

$$G_{\text{M}}[m](i\boldsymbol{\omega}) = g^0_{\text{M},m}(i\omega_m) F_{\text{M}}[m](i\boldsymbol{\omega}),$$
$$G_{\text{M}}[m^\dagger](i\boldsymbol{\omega}) = -F_{\text{M}}[m^\dagger](i\boldsymbol{\omega}) g^0_{\text{M},m}(-i\omega_m), \tag{61}$$

or, more compactly, with implicit frequency arguments,

$$G_{\text{M}}[m] = g^0_{\text{M},m} F_{\text{M}}[m],$$
$$G_{\text{M}}[m^\dagger] = -F_{\text{M}}[m^\dagger] g^0_{\text{M},m}. \tag{62}$$

For $\ell = 2$, $m = 1$, and $[d_i, \mathcal{O}^2] = [d_1, d_2^\dagger]$, Eq. (60) gives

$$F_{\text{M}}^1[d_1, d_2^\dagger] = G_{\text{M}}[q_1, d_2^\dagger] + \mathbb{1}_{12}. \tag{63}$$

Substituting this into the first relation of Eq. (62), one recovers the 2p EOM (23) derived in Sec. II.

2. ZF

In the ZF, the Fourier transforms of Eqs. (45a), (47), and (54) read

$$(\omega\mathbb{1} - H^0)_{a\bar{a}} g^0_{\bar{a}a'}(\omega) = \mathbb{1}_{aa'},$$
$$F_{\text{Z}}^m[\mathcal{O}](\boldsymbol{\omega}) = G_{\text{Z}}\big[[\mathcal{O}^m, H_{\text{int}}], \mathcal{O}^{\not{m}}\big](\boldsymbol{\omega})$$
$$+ \sum_n^{\not{m}} G_{\text{Z}}\big[\mathcal{O}^{\not{m}n}\big](\boldsymbol{\omega}^{\not{m}n}),$$
$$G_{\text{Z}}[m](\boldsymbol{\omega}) = g^0_{\text{Z},m}(\omega_m) F_{\text{Z}}[m](\boldsymbol{\omega}),$$
$$G_{\text{Z}}[m^\dagger](\boldsymbol{\omega}) = -F_{\text{Z}}[m^\dagger](\boldsymbol{\omega}) g^0_{\text{Z},m}(-\omega_m). \tag{64}$$

They have the same structure as the MF Eqs. (59), (60), and (62).

3. KF

Finally, let us derive the EOM in the KF. We will first do so in the contour basis and subsequently transform the result to the Keldysh basis. The time-domain EOM for the bare propagator [Eq. (45a)] reads

$$(i\partial_m\mathbb{1} - H^0)_{a\bar{a}} g^{0\,cc'}_{\bar{a}a'}(t, t') = Z^{cc'}\delta(t - t')\mathbb{1}_{aa'}, \tag{65}$$

where we used $\delta(m, n) = Z^{c_m c_n}\delta(t_m - t_n)$, with $Z = \begin{pmatrix} 1 & 0 \\ 0 & -1 \end{pmatrix}$ the Pauli z matrix defined in Table II. Fourier transforming this EOM gives

$$(\omega\mathbb{1} - H^0)_{a\bar{a}} g^{0\,cc'}_{\bar{a}a'}(\omega) = Z^{cc'}\mathbb{1}_{aa'}. \tag{66}$$

The Fourier transformation of Eq. (47) for $\mathcal{F}^m$ reads

$$F_{\text{K}}^{m,\boldsymbol{c}}[\mathcal{O}](\boldsymbol{\omega}) = G_{\text{K}}^{\boldsymbol{c}}\big[[\mathcal{O}^m, H_{\text{int}}], \mathcal{O}^{\not{m}}\big](\boldsymbol{\omega}) \tag{67}$$
$$+ \sum_n^{\not{m}} Z^{c_m c_n} G_{\text{K}}^{\boldsymbol{c}^{\not{m}}}\big[\mathcal{O}^{\not{m}n}\big](\boldsymbol{\omega}^{\not{m}n}).$$

Here, $\boldsymbol{c}^{\not{m}} = (\cdots, c_{m-1}, c_{m+1}, \cdots)$ is defined as in Eq. (36), and, in the last term, $Z^{c_m c_n}$ comes from the KF version of $\delta(m, n)$ in Eq. (47). (Note that in Eq. (67) all c indices, including c_m and c_n, are fixed by the left side.) Similarly, the Fourier-transformed EOMs (54) for $\mathcal{G}[m^{(\dagger)}]$ read

$$G_{\text{K}}^{\boldsymbol{c}}[m](\boldsymbol{\omega}) = g^{0\,c_m c_m''}_{\text{K},m}(\omega_m) Z^{c_m'' c_m'} F_{\text{K}}^{\boldsymbol{c}'m}[m](\boldsymbol{\omega}),$$
$$G_{\text{K}}^{\boldsymbol{c}}[m^\dagger](\boldsymbol{\omega}) = -F_{\text{K}}^{\boldsymbol{c}'m}[m^\dagger](\boldsymbol{\omega}) Z^{c_m' c_m''} g^{0\,c_m'' c_m}_{\text{K},m}(-\omega_m), \tag{68}$$

where $\boldsymbol{c}'^m = (c_m', \boldsymbol{c}^{\not{m}}) = (\cdots, c_{m-1}, c_m', c_{m+1}, \cdots)$ is defined as in Eq. (36), and summations $\sum_{c_m', c_m''}$ are implied.

It is often useful to transform KF correlators from the contour basis $c \in \{-, +\}$ to the Keldysh basis $k \in \{1, 2\}$, by applying the orthogonal transformation

$$D^{kc} = \frac{1}{\sqrt{2}}\begin{pmatrix} 1 & -1 \\ 1 & 1 \end{pmatrix}_{kc} = \frac{1}{\sqrt{2}}(-1)^{k\cdot\delta_{c,+}} \tag{69}$$

to each contour index:

$$G_{\text{K}}^{\boldsymbol{k}}[\mathcal{O}](\boldsymbol{\omega}) = \sum_{c_1,\cdots,c_\ell} \prod_{p=1}^{\ell} D^{k_p c_p} G_{\text{K}}^{\boldsymbol{c}}[\mathcal{O}](\boldsymbol{\omega}). \tag{70}$$

Then, the bare-propagator EOM (66) becomes

$$(\omega\mathbb{1} - H^0)_{a\bar{a}} g^{0\,kk'}_{\bar{a}a'}(\omega) = X^{kk'}\mathbb{1}_{aa'}. \tag{71}$$

Here, we have used the identity

$$D^{kc} D^{k'c'} Z^{cc'} = (DZD^{-1})^{kk'} = X^{kk'}, \tag{72}$$

which transforms the Pauli z matrix in the contour basis to the Pauli x matrix, $X = \begin{pmatrix} 0 & 1 \\ 1 & 0 \end{pmatrix}$, in the Keldysh basis.

For later use, we also define a rank-ℓ tensor

$$P^{k_1\cdots k_\ell} = \sum_{c,c_1,\cdots,c_\ell} \prod_{n=1}^{\ell} Z^{cc_n} D^{k_n c_n} = \sum_c (-1)^{\ell\cdot\delta_{c,+}} \prod_{n=1}^{\ell} D^{k_n c}$$

$$= \frac{1 + (-1)^\ell (-1)^{k_1 + \cdots + k_\ell}}{\sqrt{2^\ell}}$$

$$= \begin{cases} \frac{1}{\sqrt{2^{\ell-2}}} & \text{if } k_1 + \cdots + k_\ell + \ell \text{ is even,} \\ 0 & \text{if } k_1 + \cdots + k_\ell + \ell \text{ is odd.} \end{cases} \quad (73)$$

The rightmost expression in the first line follows since the Z matrices yield a nonzero result only if all their indices are equal, $c = c_1 = \cdots = c_\ell$. For example, $\ell = 3$ gives

$$P^{k_1 k_2 k_3} = \begin{cases} \frac{1}{\sqrt{2}} & \text{if } k_1 + k_2 + k_3 \text{ is odd,} \\ 0 & \text{if } k_1 + k_2 + k_3 \text{ is even.} \end{cases} \quad (74)$$

This tensor appears when transforming EOMs from the contour to the Keldysh basis. It satisfies the identities (sums over repeated indices are implied)

$$X^{k_1 k_1'} X^{k_2 k_2'} P^{k_1' k_2' k_3} = P^{k_1 k_2 k_3}, \quad (75a)$$

$$P^{k_1 k_2 k_3} P^{k_3 k_4 k_5} = P^{k_1 k_2 k_4 k_5}, \quad (75b)$$

which follow directly from its definition.

Next, we transform Eqs. (67) and (68) to the Keldysh basis. First, we multiply Eq. (67) by $\prod_{p=1}^{\ell} D^{k_p c_p}$ and sum over the contour indices. The last term becomes

$$\sum_{c_1, \cdots, c_\ell} \left(\prod_{p=1}^{\ell} D^{k_p c_p} \right) Z^{c_m c_n} G_{\mathrm{K}}^{\boldsymbol{c}^{\eta n}}$$

$$= \sum_{c_m, c_n} D^{k_m c_m} D^{k_n c_n} Z^{c_m c_n} (D^{-1})^{c_n k_{mn}} G_{\mathrm{K}}^{\boldsymbol{k}^{\eta n}}$$

$$= \sum_{c_n} (-1)^{3 \cdot \delta_{c_n, +}} D^{k_m c_m} D^{k_n c_n} D^{k_{mn} c_n} G_{\mathrm{K}}^{\boldsymbol{k}^{\eta n}}$$

$$= P^{k_m k_n k_{mn}} G_{\mathrm{K}}^{\boldsymbol{k}^{\eta n}}. \quad (76)$$

Here, $\boldsymbol{k}^{\eta n} = (\cdots, \cancel{k_m}, \cdots, k_{n-1}, k_{mn}, k_{n+1}, \cdots)$, defined as in Eq. (37), is obtained from $\boldsymbol{k}$ by removing k_m from the list and replacing k_n by a new dummy index k_{mn}, summation over which is implied. To arrive at the third line, we used $Z^{c_m c_n} = \delta_{c_m c_n} (-1)^{\delta_{c_n, +}} = \delta_{c_m c_n} (-1)^{3 \delta_{c_n, +}}$. Then, Eq. (67) transforms to

$$F_{\mathrm{K}}^{m, \boldsymbol{k}}[\boldsymbol{\mathcal{O}}](\boldsymbol{\omega}) = G_{\mathrm{K}}^{\boldsymbol{k}} \big[[\mathcal{O}^m, H_{\mathrm{int}}], \boldsymbol{\mathcal{O}}^{\eta} \big](\boldsymbol{\omega}) \quad (77)$$
$$+ \sum_n^{\eta} P^{k_m k_n k_{mn}} G_{\mathrm{K}}^{\boldsymbol{k}^{\eta n}}[\boldsymbol{\mathcal{O}}^{\eta n}](\boldsymbol{\omega}^{\eta n}).$$

The P tensor maps the $(\ell - 1)$-element list of Keldysh indices, $\boldsymbol{k}^{\eta n}$, to the original ℓ-element list $\boldsymbol{k}$. Similarly, by transforming Eq. (68) to the Keldysh basis, we find

$$G_{\mathrm{K}}[m] = g_{\mathrm{K}, m}^0 X_m F_{\mathrm{K}}[m], \quad (78a)$$

$$G_{\mathrm{K}}[m^\dagger] = -F_{\mathrm{K}}[m^\dagger] X_m \, g_{\mathrm{K}, m}^0. \quad (78b)$$

Here, the subscript on X_m indicates that it acts on the Keldysh index k_m of $F_{\mathrm{K}}[m^{(\dagger)}]$. We extended Eq. (58) and defined $g_{\mathrm{K}, m}^0$, $G_{\mathrm{K}}[m^{(\dagger)}]$, and $F_{\mathrm{K}}[m^{(\dagger)}]$ as a matrix and vectors in the basis of the orbital and Keldysh indices:

$$(g_{\mathrm{K}, m}^0)_{ii'}^{kk'}(\omega) = g_{\mathrm{K}, ii'}^{0, kk'}(\omega),$$

$$\big(G_{\mathrm{K}}[m^{(\dagger)}] \big)_i^{k_m}(\boldsymbol{\omega}) = G_{\mathrm{K}}^{\boldsymbol{k}}[d_i^{(\dagger)}, \boldsymbol{\mathcal{O}}^{\eta}](\boldsymbol{\omega}),$$

$$\big(F_{\mathrm{K}}[m^{(\dagger)}] \big)_i^{k_m}(\boldsymbol{\omega}) = F_{\mathrm{K}}^{m, \boldsymbol{k}}[d_i^{(\dagger)}, \boldsymbol{\mathcal{O}}^{\eta}](\boldsymbol{\omega}). \quad (79)$$

For the KF, we use this compact notation only in the Keldysh basis, not in the contour basis, because the X matrix changes to the Z matrix when transformed to the contour basis.

The KF EOMs (78) have the same structure as the MF EOMs (62) and ZF EOMs (64), except for the factor X_m acting on the Keldysh indices. In the rest of this paper, we write formulas only in the KF, and drop the subscripts on G_{K} and F_{K}. The corresponding MF and ZF formulas can be obtained by dropping the Keldysh indices and replacing X and P by unity.

We conclude this subsection by giving, for future reference, the Fourier-transformed KF versions of the first lines of Eqs. (49) and (50):

$$F^{1, kk'}[d_1, d_2^\dagger](\omega) = G^{kk'}[q_1, d_2^\dagger](\omega) + X^{kk'} \mathbb{1}_{12}, \quad (80)$$

$$F^{1, \boldsymbol{k}}[d_1, d_2^\dagger, d_3, d_4^\dagger](\boldsymbol{\omega}) = G^{\boldsymbol{k}}[q_1, d_2^\dagger, d_3, d_4^\dagger](\boldsymbol{\omega})$$
$$- 2\pi i \delta(\omega_{12}) X^{k_1 k_2} \mathbb{1}_{12} G^{k_3 k_4}[d_3, d_4^\dagger](\omega_3, \omega_4)$$
$$- 2\pi i \delta(\omega_{14}) X^{k_1 k_4} \mathbb{1}_{14} G^{k_2 k_3}[d_2^\dagger, d_3](\omega_2, \omega_3). \quad (81)$$

To arrive at these equations from Eq. (77), we used

$$\sum_{k_{12}} P^{k_1 k_2 k_{12}} G^{k_{12}}[\mathbb{1}_{12}] = \sum_{k_{12}} P^{k_1 k_2 k_{12}} \sqrt{2} \delta_{k_{12}, 2} = X^{k_1, k_2} \quad (82)$$

for Eq. (80), and, for Eq. (81), we used an analogous equation for $G^{k_{12} k_3 k_4}[\mathbb{1}_{12}, d_3, d_4^\dagger]$.

F. EOM for connected correlators

A vertex is defined in terms of the connected part of the corresponding correlator, i.e., the part that cannot be expressed through products of lower-point correlators. It is therefore desirable to have an EOM directly applicable to connected correlators. Here, we show that the EOM (78) holds also if one evaluates only the connected (con) part or only the disconnected (dis) part of the correlators from both sides:

$$G_{\mathrm{con/dis}}[m] = g_m^0 X_m F_{\mathrm{con/dis}}[m],$$
$$G_{\mathrm{con/dis}}[m^\dagger] = -F_{\mathrm{con/dis}}[m^\dagger] X_m g_m^0. \quad (83)$$

When distinguishing between the connected and disconnected parts, we treat a composite operator as a whole, with the single-particle operators comprising it considered to be mutually connected. For instance, in the expansion of $\mathcal{G}[d_1 d_2^\dagger d_3, d_4^\dagger](t, 0)$ based on Wick's theorem, the term $\mathcal{G}[d_1, d_4^\dagger](t, 0)\mathcal{G}[d_2^\dagger, d_3](t, t)$ appears. Even though the two propagators appear disconnected, this term is classified as connected when concerning the correlator of $d_1 d_2^\dagger d_3$ and $d_4^\dagger$, because the two operators $d_2^\dagger$
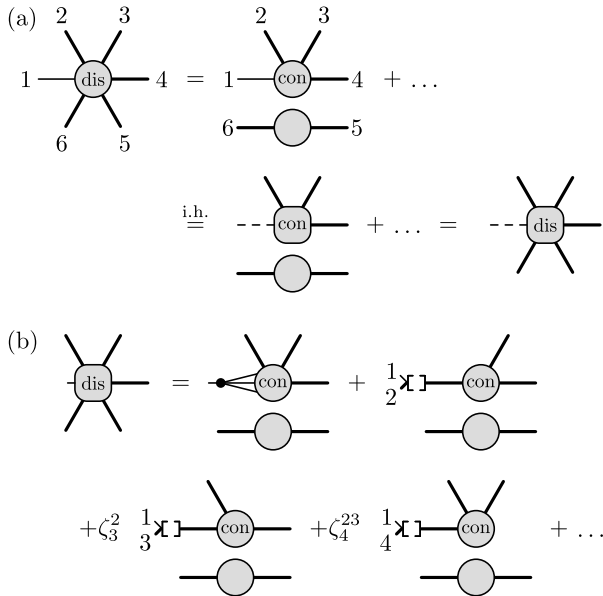
FIG. 8. (a) Diagrammatic representation of the inductive proof, starting from Eq. (85), for a disconnected 6p correlator $G_{\mathrm{dis}}[1]$, for which $\mathcal{O}^1$ is a single-particle operator. We only display diagrams corresponding to $S = \{2,3,4\}$; the dots represent contributions from all other disconnected parts. In the second step, we used the induction hypothesis (i.h.) to obtain Eq. (86). (b) Corresponding diagrammatic representation of $F_{\mathrm{dis}}[1]$, see Eq. (87).

and d_3 from the second correlator are connected to the operator d_1 from the first.

Considering the connected part vastly simplifies the EOM for $\ell \geq 3$. For example, the connected part of the F^1 correlator in Eq. (81) simply reads

$$F_{\mathrm{con}}^{1,\boldsymbol{k}}[d_1, d_2^\dagger, d_3, d_4^\dagger](\boldsymbol{\omega}) = G_{\mathrm{con}}^{\boldsymbol{k}}[q_1, d_2^\dagger, d_3, d_4^\dagger](\boldsymbol{\omega}). \quad (84)$$

For 2p correlators, the EOM for the connected part has the same form as the total EOM because the disconnected part is zero for a 1p correlator.

Equation (83) can be understood inductively. Let us assume that the EOM holds for the connected ℓ'p correlators for all $\ell' < \ell$. Disconnected ℓp correlators involve sums over products of connected and disconnected lower-point correlators. According to the inductive assumption, the connected factors already satisfy the EOMs, while the disconnected factors are spectators regarding the manipulations performed when applying the EOMs. Therefore, their product also satisfies the EOMs. This idea is schematically illustrated in Fig. 8 for $\ell = 6$.

We now develop this idea into a formal proof. For $\ell = 1$, the disconnected part is zero, so the EOM trivially holds for both parts. Now, we assume that the EOM holds for connected ℓ'p correlators with all $\ell' < \ell$ and show that the EOM holds for the disconnected ℓp correlator. Without loss of generality, we set $m = 1$, as the

EOMs for $m \neq 1$ follow from the former by permuting the operators. The disconnected part of the ℓp correlator can be expressed as

$$G_{\mathrm{dis}}[d_1, \mathcal{O}^I] = \sum_{\mathcal{S}} \zeta^{\mathcal{S}} G[\mathcal{O}^{\mathcal{S}'}] G_{\mathrm{con}}[d_1, \mathcal{O}^{\mathcal{S}}] \quad (85)$$

where $\mathcal{O}^{\mathcal{S}}$ and $\mathcal{O}^{\mathcal{S}'}$ are sublists of $\mathcal{O}$ listing the operators connected or not connected to d_1, respectively, indexed by sets $\mathcal{S}$ and $\mathcal{S}'$ with $\mathcal{S} \cup \mathcal{S}' = \{2, \cdots, \ell\}$. $\zeta^{\mathcal{S}}$ is a sign factor and the sum $\sum_{\mathcal{S}}$ enumerates all disconnected contributions. The diagram for $\ell = 6$ and $S = \{2,3,4\}$ is shown in the first line of Fig. 8(a).

By the induction hypothesis, $G_{\mathrm{con}}[d_1, \mathcal{O}^{\mathcal{S}}]$ satisfies Eq. (83). Hence, we can write Eq. (85) as

$$G_{\mathrm{dis}}[d_1, \mathcal{O}^I] = \sum_{\mathcal{S}} \zeta^{\mathcal{S}} G[\mathcal{O}^{\mathcal{S}'}] g_1^0 X_1 F_{\mathrm{con}}[d_1, \mathcal{O}^{\mathcal{S}}]$$
$$= g_1^0 X_1 F_{\mathrm{dis}}[d_1, \mathcal{O}^I], \quad (86)$$

where, in the last step, we identified

$$F_{\mathrm{dis}}^1[\mathcal{O}] = \sum_{\mathcal{S}} \zeta^{\mathcal{S}} G[\mathcal{O}^{\mathcal{S}'}] F_{\mathrm{con}}^1[\mathcal{O}^1, \mathcal{O}^{\mathcal{S}}]. \quad (87)$$

Figure 8(b) shows the corresponding diagrams for $\ell = 6$ operators and $S = \{2,3,4\}$. Equation (86) is the desired ℓp EOM of the disconnected part. The ℓp EOM holds also for the connected part, since $G_{\mathrm{con}} = G - G_{\mathrm{dis}}$, concluding the proof.

G. EOM with full propagators

The EOM derived in the previous sections involves full correlators and bare propagators. For methods where bare and full propagators stem from different numerical settings, it is desirable, as argued before, to exclusively use fully renormalized objects [13, 18, 22, 24]. Here, we derive such an EOM. The idea, inspired by Ref. [22], is to express the bare propagator g^0 through the full propagator g and the self-energy Σ using $(g^0)^{-1} = g^{-1} + \Sigma$. Applying this manipulation to the EOM [Eq. (83)] yields

$$g_m^{-1} G_{\mathrm{con}}[m] = X_m F_{\mathrm{con}}[m] - \Sigma_m G_{\mathrm{con}}[m], \quad (88a)$$
$$G_{\mathrm{con}}[m^\dagger] g_m^{-1} = -F_{\mathrm{con}}[m^\dagger] X_m - G_{\mathrm{con}}[m^\dagger] \Sigma_m. \quad (88b)$$

Equations (88) are the first main result of this paper. They generalize the 4p MF EOM of Hafermann *et al.* [8] for $m = 1$ to an arbitrary ℓp correlator, to any index m, and to the KF and ZF. The g^{-1} term on the left-hand side amputates one external leg of the correlator; the terms on the right achieve this amputation in a manner that conveniently avoids division by g. Repeated use of such manipulations will amputate the connected correlator and thus yield the vertex without the need to explicitly divide out the propagators. Thereby, we obtain improved estimators for multipoint vertices.
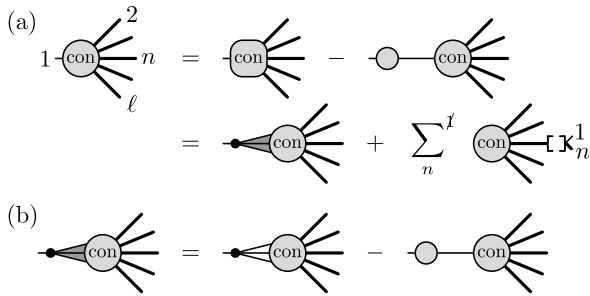
FIG. 9. (a) Depiction of the EOMs (88) (first line) and (90) (second line) for the connected part of a full propagator, $G_{\mathrm{con}}[1]$, for a quartic interaction. (b) Depiction of Eq. (91) for $G_{\mathrm{con}}[1_\bullet]$ (indicated by dark shading between internal legs), involving the subtraction of one-particle-reducible contributions. The short length of the leg labeled 1 indicates that the corresponding external leg has been amputated.

The second terms on the right of Eqs. (88) subtract one-particle-reducible (1PR) contributions from the first terms. To make this explicit, we express $F_{\mathrm{con}}[m^{(\dagger)}]$ as

$$F_{\mathrm{con}}[m^{(\dagger)}] = (-)G_{\mathrm{con}}[q_m^{(\dagger)}, \mathcal{O}^{\not{h}}] + F_{\mathrm{con}}^{[\,]}[m^{(\dagger)}]. \qquad (89)$$

By definition, the first and second terms on the right are obtained from those of Eq. (77) by replacing $\mathcal{O}^m$ there by ψ_m (or $\psi_m^\dagger$). The superscript on $F_{\mathrm{con}}^{[\,]}$ indicates that its operator argument $\mathcal{O}^{\not{h}n}$ involves an (anti)commutator. The $(-)$ sign before G_{con}, applicable for $F_{\mathrm{con}}[m^\dagger]$ but not for $F_{\mathrm{con}}[m]$, reflects the sign difference in definitions (48) for $q_m^\dagger$ and q_m. Then, Eqs. (88) can be expressed as

$$g_m^{-1}G_{\mathrm{con}}[m] = G_{\mathrm{con}}[m_\bullet] + X_m F_{\mathrm{con}}^{[\,]}[m], \qquad (90a)$$

$$G_{\mathrm{con}}[m^\dagger]g_m^{-1} = G_{\mathrm{con}}[m_\bullet^\dagger] - F_{\mathrm{con}}^{[\,]}[m^\dagger]X_m. \qquad (90b)$$

where we defined

$$G_{\mathrm{con}}[m_\bullet] = X_m G_{\mathrm{con}}[q_m, \mathcal{O}^{\not{h}}] - \Sigma_m G_{\mathrm{con}}[m], \qquad (91a)$$

$$G_{\mathrm{con}}[m_\bullet^\dagger] = G_{\mathrm{con}}[q_m^\dagger, \mathcal{O}^{\not{h}}]X_m - G_{\mathrm{con}}[m^\dagger]\Sigma_m. \qquad (91b)$$

The second terms on the right of Eqs. (91) subtract the 1PR contributions from the first terms, completing the amputation of the m-th leg. Figure 9 gives a diagrammatic depiction of Eqs. (88) and (91).

IV. SYMMETRIC IMPROVED ESTIMATORS

In this section, we use the EOM to derive improved estimators for the self-energy, 3p vertex, and 4p vertex. Although we write the formula in the KF, let us emphasize that all results of this section apply also to the MF and ZF when all the Keldysh indices are dropped and the coefficients $X^{kk'}$ and $P^{k_1 \cdots k_n}$ are replaced by unity.

We confine ourselves to Hamiltonians with a quartic interaction:

$$H_{\mathrm{int}} = \sum_{i,i',j,j'} U_{ii'jj'} d_i^\dagger d_{i'} d_j^\dagger d_{j'}. \qquad (92)$$

Due to the sum over orbital indices, different choices of the U tensor can describe the same interaction. The symmetrized interaction tensor

$$U_{1234}^{\mathrm{sym}} = U_{1234} + \zeta U_{3214} + \zeta U_{1432} + U_{3412}, \qquad (93)$$

is unique for a given interaction. For the single-orbital AIM [Eq. (13)], one may choose $U_{\uparrow\uparrow\downarrow\downarrow} = U_0$ and let all other components be zero to get $U_{\sigma\sigma'\sigma'}^{\mathrm{sym}} = \zeta U_{\sigma\sigma'\sigma'\sigma}^{\mathrm{sym}} = U_0 \delta_{\bar\sigma,\sigma'}$, where $\bar\sigma$ denotes the opposite spin to σ. Later, we show that U^{sym} equals the bare vertex (see Eqs. (101b) and (101c)).

For notational convenience, we henceforth focus on ℓp correlators with $\ell \leq 4$ (though the strategy presented below can readily be generalized). We write the 4p connected correlator as

$$G_{1234}^{(\cdot,\cdot,\cdot,\cdot)\boldsymbol{k}}(\boldsymbol{\omega}) = G_{\mathrm{con}}^{\boldsymbol{k}}[d_1, d_2^\dagger, d_3, d_4^\dagger](\boldsymbol{\omega}), \qquad (94)$$

using odd (even) indices for annihilation (creation) operators. The superscript $(\cdot,\cdot,\cdot,\cdot)$ indicates that this correlator is a 4p object and will later serve as a "parent correlator" for the definition of various auxiliary correlators. Hereafter, we omit the subscript 1234 and superscript $\boldsymbol{k}$ for 4p correlators. We primarily work with the connected correlators, as vertices are defined from these by amputating their external legs. Working with the connected part also simplifies the equations after repeated applications of the EOM. The 4p vertex is defined as

$$\Gamma(\boldsymbol{\omega}) = g_1^{-1}(\omega_1)g_3^{-1}(\omega_3)G^{(\cdot,\cdot,\cdot,\cdot)}(\boldsymbol{\omega})g_2^{-1}(-\omega_2)g_4^{-1}(-\omega_4), \qquad (95)$$

where g_m^{-1} is matrix-multipied to the m-th orbital and Keldysh indices of the 4p correlator. This 4p vertex is called F in Refs. [3, 10, 12, 13, 25, 26] and γ in Ref. [8].

A. Auxiliary correlators

As for $G^{2\mathrm{p}}$, the estimators for $G^{4\mathrm{p}}$ will be obtained through multiple applications of EOMs. These will generate various auxiliary correlators, all derived from the same "parent correlator" $G^{4\mathrm{p}}$, containing not only the single-particle operators d_i and $d_i^\dagger$, but also the composite operators $q_i = [d_i, H_{\mathrm{int}}]$ and $q_i^\dagger = [H_{\mathrm{int}}, d_i^\dagger]$, and (possibly nested) (anti)commutators of all of these, arising from the $[\mathcal{O}^n, H_{\mathrm{int}}]$ and $\delta(m,n)$ terms in the EOMs, respectively. For (anti)commutators involving composite operators, we recursively introduce the following compact notation (generalizing Eq. (17b)):

$$q_{i_1 i_2} = [q_{i_1}^{(\dagger)}, d_{i_2}^{(\dagger)}]_{\zeta^1},$$

$$q_{i_1 i_2 i_3} = [q_{i_1 i_2}, d_{i_3}^{(\dagger)}]_{\zeta^2},$$

$$q_{i_1 \cdots i_n} = [q_{i_1 \cdots i_{n-1}}, d_{i_n}^{(\dagger)}]_{\zeta^{n-1}}. \qquad (96)$$

An anticommutator is taken if both operators are fermionic; a commutator is taken otherwise. Daggers are used if the corresponding operators in the parent correlator [Eq. (94)] have daggers. Such indices will be labelled with an even integer, 2 or 4. For example, for a fermionic system, the composite operators derived from Eq. (94) include the following:

$$q_{12} = \{q_1, d_2^{\dagger}\}, \ q_{23} = \{q_2^{\dagger}, d_3\}, \qquad (97)$$

$$q_{123} = [q_{12}, d_3], \ q_{234} = [q_{23}, d_4^{\dagger}], \ q_{1234} = \{q_{123}, d_4^{\dagger}\}.$$

The KF versions of the auxiliary correlators of Eqs. (19) are defined as

$$G_{12}^{(\cdot, \cdot)\boldsymbol{k}}(\omega) = G^{\boldsymbol{k}}[d_1, d_2^{\dagger}](\omega) = g_{12}^{\boldsymbol{k}}(\omega),$$

$$G_{12}^{(1, \cdot)\boldsymbol{k}}(\omega) = G^{\boldsymbol{k}}[q_1, d_2^{\dagger}](\omega),$$

$$G_{12}^{(\cdot, 2)\boldsymbol{k}}(\omega) = G^{\boldsymbol{k}}[d_1, q_2^{\dagger}](\omega),$$

$$G_{12}^{(1,2)\boldsymbol{k}}(\omega) = G^{\boldsymbol{k}}[q_1, q_2^{\dagger}](\omega),$$

$$G_{12}^{(12)\boldsymbol{k}} = P^{k_1 k_2 k_{12}} G^{k_{12}}[[q_1, d_2^{\dagger}]_{\zeta}]. \qquad (98)$$

Hereafter, for 2p auxiliary correlators, we omit the subscript 12 for orbital indices and the superscript $\boldsymbol{k}$ for Keldysh indices. The diagrammatic representations are given in Fig. 2. As in the MF case, $G^{(12)}$ is the Hartree self-energy:

$$G^{(12)} = P^{k_1 k_2 k_{12}} \langle [q_1, d_2^{\dagger}]_{\zeta} \rangle \sqrt{2} \delta_{k_{12}, 2} = \Sigma_{12}^{\mathrm{H}} X^{k_1 k_2}. \quad (99)$$

Here, the $\sqrt{2}\delta_{k_{12}, 2}$ term comes from the transformation of $G^c[q_{12}] = \langle q_{12} \rangle$ to the Keldysh basis as $\sum_c D^{kc} = \sqrt{2}\delta_{k, 2}$. The factor $P^{k_1 k_2 2} = \frac{1}{\sqrt{2}} X^{k_1 k_2}$ [Eq. (74)] maps the single Keldysh index of $G^{k_{12}}$ via a summation on k_{12} to a two-fold Keldysh index $k_1 k_2$.

Next, we consider connected auxiliary correlators derived from the parent $G^{4\mathrm{p}}$ of Eq. (94). We illustrate our notational conventions, described below, with some examples, assuming all $d_i^{(\dagger)}$ to be fermionic:

$$G^{(\cdot, \cdot, \cdot)} = G_{\mathrm{con}}^{\boldsymbol{k}}[d_1, d_2^{\dagger}, d_3, d_4^{\dagger}], \qquad (100)$$

$$G^{(1,2,\cdot,\cdot)} = G_{\mathrm{con}}^{\boldsymbol{k}}[q_1, q_2^{\dagger}, d_3, d_4^{\dagger}],$$

$$G^{(1,\cdot,3,\cdot)} = G_{\mathrm{con}}^{\boldsymbol{k}}[q_1, d_2^{\dagger}, q_3, d_4^{\dagger}],$$

$$G^{(12,\cdot,\cdot)} = P^{k_1 k_2 k_{12}} G_{\mathrm{con}}^{k_{12} k_3 k_4}[\{q_1, d_2^{\dagger}\}, d_3, d_4^{\dagger}],$$

$$G^{(23,\cdot,\cdot)} = P^{k_2 k_3 k_{23}} G_{\mathrm{con}}^{k_{23} k_1 k_4}[\{q_2^{\dagger}, d_3\}, d_1, d_4^{\dagger}],$$

$$G^{(12,3,\cdot)} = P^{k_1 k_2 k_{12}} G_{\mathrm{con}}^{k_{12} k_3 k_4}[\{q_1, d_2^{\dagger}\}, q_3, d_4^{\dagger}],$$

$$G^{(124,3)} = P^{k_1 k_2 k_4 k_{124}} G_{\mathrm{con}}^{k_{124} k_3}[[\{q_1, d_2^{\dagger}\}, d_4^{\dagger}], q_3],$$

$$G^{(12,34)} = P^{k_1 k_2 k_{12}} P^{k_3 k_4 k_{34}} G_{\mathrm{con}}^{k_{12} k_{34}}[\{q_1, d_2^{\dagger}\}, \{q_3, d_4^{\dagger}\}],$$

$$G^{(1234)} = P^{k_1 k_2 k_3 k_4 k_{1234}} G_{\mathrm{con}}^{k_{1234}}[\{[\{q_1, d_2^{\dagger}\}, d_3], d_4^{\dagger}\}].$$

By definition, all correlators $G^{(\cdots)}$ carrying superscripts in round brackets are *connected* correlators. Depend-
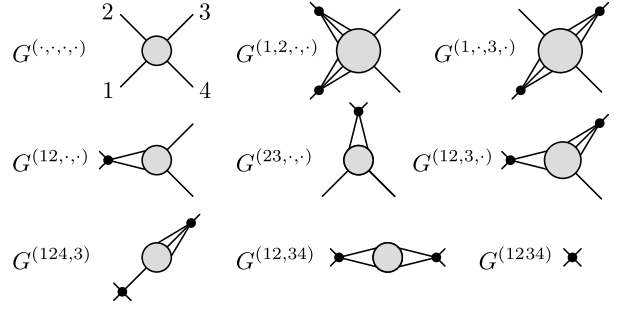
FIG. 10. Diagrammatic representations of the 4p auxiliary correlators of Eq. (100) for a quartic interaction. Only the connected diagrams are evaluated.

ing on the number and type of composite operators involved, they may be 4p, 3p, 2p, and 1p correlators; correspondingly, the superscripts contain 4, 3, 2, or 1 comma-separated arguments. As before, '·' is a placeholder for $d_i^{(\dagger)}$, a solitary numeral i signals its replacement by $q_i^{(\dagger)}$, and $i_1 \cdots i_n$ denotes the replacement of the corresponding operators by the composite operator $q_{i_1 \cdots i_n}$.

All such auxiliary correlators depend on the same number of indices and frequency arguments: 4 orbital indices, 4 Keldysh indices, and 4 frequency arguments. These are inherited from those of parent $G^{4\mathrm{p}}$, either directly for single-particle operators $d_i^{(\dagger)}$ and $q_i^{(\dagger)}$, or indirectly for composite operators, according to the following rules: to $q_{i_1 \cdots i_n}$, assign the frequency $\omega_{i_1 \cdots i_n} = \omega_{i_1} + \cdots + \omega_{i_n}$ and the dummy Keldysh index $k_{i_1 \cdots i_n}$, then map the latter to an n-fold index $k_{i_1} \cdots k_{i_n}$ through multiplication by the rank-$(n+1)$ tensor $P^{k_{i_1} \cdots k_{i_n} k_{i_1 \cdots i_n}}$ [Eq. (73)] and summation over the dummy $k_{i_1 \cdots i_n}$.

Finally, when defining auxiliary correlators, we order the operator arguments according to the following conventions: (i) operators with higher nesting come first, and (ii) non-nested operators (q, d, $q^{\dagger}$, and $d^{\dagger}$) are ordered by their subscripts in increasing order. In Eq. (100), we suppressed frequency arguments, since they can be inferred from the structure of the superscripts. For example, the superscripts $(12, \cdot, \cdot)$ and $k_{12} k_3 k_4$ both indicate a frequency argument $(\omega_{12}, \omega_3, \omega_4)$, while superscripts $(124, 3)$ and $k_{124} k_3$ both indicate (ω_{124}, ω_3), etc.

Figure 10 is a diagrammatic representation of the 4p auxiliary correlators listed in Eqs. (100). Some auxiliary correlators, such as $G^{(12,\cdot,\cdot)}$, $G^{(12,34)}$, and $G^{(1234)}$, contain bosonic operators. Diagrams in which the latter are disconnected from all the other operators should also be subtracted to obtain the connected part. As mentioned before, for composite operators, all the external legs of the constituent single-particle operators are regarded as being connected to each other. As reflected in the diagram, the 1p correlator $G^{(1234)}$ equals the bare vertex up to a sign factor:

$$-G^{(1234)} = \Gamma_{\mathrm{bare}}, \qquad (101\mathrm{a})$$

$$\Gamma_{\text{bare}} = U^{\text{sym}}_{1234} \qquad \text{(MF, ZF)}, \tag{101b}$$

$$\Gamma^{\boldsymbol{k}}_{\text{bare}} = \begin{cases} \frac{1}{2} U^{\text{sym}}_{1234} & \text{if } k_1+k_2+k_3+k_4 \text{ is odd} \\ 0 & \text{otherwise} \end{cases} \tag{101c}$$

with U^{sym} defined in Eq. (93).

We also define auxiliary correlators where some operators are replaced by $q_i^{(\dagger)}$, and the corresponding 1PR contributions are subtracted as in Eq. (91). We denote such correlators using bullets ('•') instead of dots ('·') in the superscript and define them as

$$G^{(\bullet,x_2,x_3,x_4)} = X_1 G^{(1,x_2,x_3,x_4)} - \Sigma_1 G^{(\cdot,x_2,x_3,x_4)},$$
$$G^{(x_1,\bullet,x_3,x_4)} = G^{(x_1,2,x_3,x_4)} X_2 - G^{(x_1,\cdot,x_3,x_4)} \Sigma_2,$$
$$G^{(x_1,x_2,\bullet,x_4)} = X_3 G^{(x_1,x_2,3,x_4)} - \Sigma_3 G^{(x_1,x_2,\cdot,x_4)},$$
$$G^{(x_1,x_2,x_3,\bullet)} = G^{(x_1,x_2,x_3,4)} X_4 - G^{(x_1,x_2,x_3,\cdot)} \Sigma_4, \tag{102}$$

where $x_n \in \{\bullet, \cdot, n\}$. Note that X_n and Σ_n are left (right) multiplied for odd (even) indices, reflecting the absence or presence of a dagger in the corresponding operator of the parent correlator [Eq. (94)]. One can apply this definition recursively to evaluate auxiliary correlators with multiple bullets in the superscript, e.g.,

$$G^{(\bullet,\bullet,\cdot,\cdot)} = G^{(\bullet,2,\cdot,\cdot)} X_2 - G^{(\bullet,\cdot,\cdot,\cdot)} \Sigma_2$$
$$= X_1 G^{(1,2,\cdot,\cdot)} X_2 - \Sigma_1 G^{(\cdot,2,\cdot,\cdot)} X_2$$
$$- X_1 G^{(1,\cdot,\cdot,\cdot)} \Sigma_2 + \Sigma_1 G^{(\cdot,\cdot,\cdot,\cdot)} \Sigma_2. \tag{103}$$

B. Self-energy estimators

We now derive the sIEs, starting with the self-energy. We will reproduce the result of Ref. [22] but will take a slightly different path. Instead of using the EOM with the bare propagator (78), we apply the EOM with the full propagator (88) to $G^{(\cdot,\cdot)}$ twice, once for each external leg. This amputates the legs and yields the self-energy. The same procedure will be used to derive the multipoint vertex estimators.

First, using $g = G^{(\cdot,\cdot)} = G[d_1, d_2^\dagger]$ in Eqs. (88), we find

$$g^{-1}g = X G^{(1,\cdot)} - \Sigma g + \mathbb{1}, \tag{104a}$$
$$g g^{-1} = G^{(\cdot,2)} X - g\Sigma + \mathbb{1}. \tag{104b}$$

Solving for Σ, we find two aIEs for the self-energy, distinguished here by superscripts and illustrated in Fig. 3(b):

$$\Sigma^{\text{L}} = X G^{(1,\cdot)} g^{-1}, \tag{105a}$$
$$\Sigma^{\text{R}} = g^{-1} G^{(\cdot,2)} X. \tag{105b}$$

Next, we employ EOMs for the auxiliary correlators that appear in the aIE by using $G^{(1,\cdot)} = G[q_1, d_2^\dagger]$ in Eq. (88b) or $G^{(\cdot,2)} = G[d_1, q_2^\dagger]$ in Eq. (88a):

$$G^{(1,\cdot)} g^{-1} = \left(G^{(1,2)} + G^{(12)} \right) X - G^{(1,\cdot)} \Sigma^{\text{R}}, \tag{106a}$$

FIG. 11. Depiction of Eq. (109) for the symmetric self-energy estimator Σ^{S}, expressed through 1PR-subtracted correlators (cf. Fig. 9(b)).

$$g^{-1} G^{(\cdot,2)} = X \left(G^{(1,2)} + G^{(12)} \right) - \Sigma^{\text{L}} G^{(\cdot,2)}. \tag{106b}$$

On the right, we used Σ^{R} (or Σ^{L}) in terms containing the self-energy as a factor on the right (or left), because this choice leads to the third, symmetric self-energy estimator discussed in IV B. It is obtained by substituting Eqs. (106) into the aIEs of Eqs. (105). The two expressions obtained this way,

$$\Sigma^{S} = X \left[\left(G^{(1,2)} + G^{(12)} \right) X - G^{(1,\cdot)} \Sigma^{R} \right], \tag{107a}$$
$$\Sigma^{S} = \left[X \left(G^{(1,2)} + G^{(12)} \right) - \Sigma^{L} G^{(\cdot,2)} \right] X, \tag{107b}$$

are equal (hence we denote both by Σ^{S}), as can be seen by inserting the aIEs of Eq. (105) on the right (we also use $X G^{(12)} X = \Sigma^{\text{H}} X$ [Eq. (99)]):

$$\Sigma^{S} = X G^{(1,2)} X + \Sigma^{\text{H}} X - X G^{(1,\cdot)} g^{-1} G^{(\cdot,2)} X. \tag{108}$$

Equation (108) is the Keldysh version of the sIE for the self-energy illustrated in Fig. 3(c). The term involving $G^{(1,\cdot)} g^{-1} G^{(\cdot,2)}$ subtracts all 1PR diagrams from $G^{(1,2)}$ (cf. Fig. 4). Using Eqs. (107), this 1PR subtraction can also be expressed as

$$\Sigma^{\text{S}} = X G^{(1,\bullet)} + X \Sigma^{\text{H}} = G^{(\bullet,2)} X + \Sigma^{\text{H}} X, \tag{109}$$

where we employed notation analogous to that of Eqs. (102). Figure 11 illustrates Eq. (109) using the shaded vertex of Fig. 9(b). The choice of using Σ^{L} or Σ^{R} in subtraction terms containing the self-energy as left or right factors will also be used in later sections when evaluating the multipoint estimators.

C. 3p vertex estimators

The sIE for the 4p vertex turns out to depend, among others, on a number of 3p vertices. In this section, we therefore explain how to obtain sIEs for these. To be concrete, we consider the 3p vertex for the auxiliary correlator $G^{(ab,\cdot,\cdot)}$, defined by amputating the external legs that correspond to d or $d^\dagger$. For example, the vertex for $G^{(12,\cdot,\cdot)}$, called $\Gamma^{(12,\cdot,\cdot)}$, or $\Gamma^{(12)}$ for short, is

$$\Gamma^{(12,\cdot,\cdot)} = g_3^{-1} G^{(12,\cdot,\cdot)} g_4^{-1} = (12) \!\!\!\begin{smallmatrix} 3 \\ \blacktriangleright\!\!-\!\!\bigcirc \\ 4 \end{smallmatrix}. \tag{110}$$

Here, g_3^{-1} and g_4^{-1} matrix-multiply the third and fourth orbital and Keldysh indices of $G^{(12,\cdot,\cdot)}$.

For fermionic systems, these 3p vertices are fermion-boson vertices which are related to the Hedin vertex [27].

They are an important ingredients of, e.g., diagrammatic extensions of dynamical mean-field theory and the calculation of response properties [25, 28–35]. We note that although $\Gamma^{(12)}$ has four Keldysh indices, one can easily convert it to have 3 Keldysh indices to more clearly reveal its 3p nature:

$$\sum_{k_1,k_2} P^{k_1 k_2 k_{12}} \Gamma^{(12)\,\boldsymbol{k}} = \Gamma^{(12)\,k_{12}k_3k_4}. \qquad (111)$$

Our goal is to derive an estimator for $\Gamma^{(12)}$, symmetric with respect to legs 3 and 4, by using EOMs (88) to amputate the external legs of $G^{(12,\cdot,\cdot)}$. We first find the EOM w.r.t. ω_3 for $G^{(12,\cdot,\cdot)} = G_{\mathrm{con}}[q_{12}, d_3, d_4^\dagger](\omega_{12}, \omega_3, \omega_4)$ by using Eq. (88a) with $m = 2$:

$$X_3[g_3^{-1} + \Sigma_3]G^{(12,\cdot,\cdot)}(\boldsymbol{\omega})$$
$$= P^{k_1 k_2 k_{12}} F_{\mathrm{con}}^{2,k_{12}k_3k_4}[q_{12}, d_3, d_4^\dagger](\omega_{12}, \omega_3, \omega_4)$$
$$= P^{k_1 k_2 k_{12}} \Bigg[G_{\mathrm{con}}^{k_{12}k_3k_4}[q_{12}, q_3, d_4^\dagger](\omega_{12}, \omega_3, \omega_4)$$
$$+ P^{k_{12}k_3k_{123}} G_{\mathrm{con}}^{k_{123}k_4}\left[[d_3, q_{12}], d_4^\dagger\right](\omega_{123}, \omega_4)$$
$$+ P^{k_3 k_4 k_{34}} G_{\mathrm{con}}^{k_{12}k_{34}}\left[q_{12}, [d_3, d_4^\dagger]_\zeta\right](\omega_{12}, \omega_{34}) \Bigg]. \quad (112)$$

The first term in the square bracket gives $G^{(12,3,\cdot)}(\boldsymbol{\omega})$ [Eq. (100)]. The second term gives $-G^{(123,\cdot)}(\boldsymbol{\omega})$ when Eq. (75b), the identity $P \cdot P = P$, is used; the minus sign comes from $[d_3, q_{12}] = -q_{123}$ [Eq. (97)]. The third term vanishes because the connected part of $G[q_{12}, [d_3, d_4^\dagger]_\zeta] = G[q_{12}, \mathbb{1}_{34}]$ is zero: the identity operator does not have any external leg and thus cannot be connected with other operators. Therefore, Eq. (112) becomes

$$X_3[g_3^{-1} + \Sigma_3]G^{(12,\cdot,\cdot)} = G^{(12,3,\cdot)} - G^{(123,\cdot)}. \qquad (113)$$

Writing this equation in terms of the 1PR-subtracted auxiliary correlators [Eq. (102)], we find

$$g_3^{-1} G^{(12,\cdot,\cdot)} = G^{(12,\bullet,\cdot)} - X_3 G^{(123,\cdot)}, \qquad (114)$$

Amputating the remaining fourth leg from $g_3^{-1} G^{(12,\cdot,\cdot)}$, one finds the aIE for the 3p vertex:

$$\Gamma^{(12)} = \left[G^{(12,\bullet,\cdot)} - X_3 G^{(123,\cdot)} \right] g_4^{-1}. \qquad (115)$$

Now, consider the EOM w.r.t. ω_4 for each of the auxiliary correlators on the right of Eq. (115):

$$G^{(12,\cdot,\cdot)} g_4^{-1} = G^{(12,\cdot,\bullet)} + \zeta G^{(124,\cdot)} X_4,$$
$$G^{(12,3,\cdot)} g_4^{-1} = G^{(12,3,\bullet)} + \left[G^{(12,34)} + \zeta G^{(124,3)} \right] X_4,$$
$$G^{(123,\cdot)} g_4^{-1} = G^{(123,\bullet)} + G^{(1234)} X_4. \qquad (116)$$

By substituting these equations to Eq. (115), one obtains the sIE for the 3p vertex:

$$\Gamma^{(12)}$$
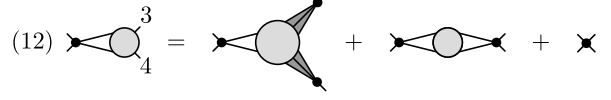
FIG. 12. Diagrammatic representation of the sIE for the 3p vertex $\Gamma^{(12)}$ [Eq. (120)], comprising only connected diagrams.

$$= G^{(12,\bullet,\bullet)} + X_3\left[G^{(12,34)} + \zeta G^{(124,3)} - G^{(1234)} \right] X_4$$
$$\quad - \zeta \Sigma_3 G^{(124,\cdot)} X_4 - X_3 G^{(123,\bullet)}$$
$$= \mathcal{K}^{(12,\cdot,\cdot)} + X_3\left[G^{(12,34)} - G^{(1234)} \right] X_4$$
$$\quad + \zeta G^{(124,\bullet)} X_4 - X_3 G^{(123,\bullet)}. \qquad (117)$$

Here, $\mathcal{K}^{(12,\cdot,\cdot)}$, or $\mathcal{K}^{(12)}$ for short, is defined as

$$\mathcal{K}^{(12,\cdot,\cdot)} = G^{(12,\bullet,\bullet)}$$
$$= X_3 G^{(12,3,4)} X_4 - X_3 G^{(12,3,\cdot)} \Sigma_4$$
$$\quad - \Sigma_3 G^{(12,\cdot,4)} X_4 + \Sigma_3 G^{(12,\cdot,\cdot)} \Sigma_4. \qquad (118)$$

$\mathcal{K}^{(12)}$ is one-particle irreducible (1PI) in the third and fourth legs thanks to the 1PR subtraction shown in Fig. 9(b). It is a sum of four terms, obtained by performing one of the two operations for both $n = 3$ and $n = 4$: (i) multiply by $-\Sigma_n$ ($x_n = \cdot$) or (ii) insert n into the superscript for the auxiliary correlator and multiply by X_n ($x_n = n$). The symbol $\mathcal{K}$ is used as this term is identical (up to a sign) to the $\mathcal{K}_2$ asymptotic class of the 4p vertex [26] (see Sec. IV F).

Next, we note that the last line of Eq. (117) vanishes. Since H_{int} is a 4p interaction, $\left[\{q_a^{(\dagger)}, d_b^{(\dagger)}\}, d_c^{(\dagger)} \right] = x_{abcd}^{(abc)} d_d^{(\dagger)}$ holds for a constant factor $x_{abcd}^{(abc)}$, yielding

$$G^{(123,\bullet)} = x_{123d}^{(123)} (G_{d4}^{(\cdot,2)} X_4 - G_{d4}^{(\cdot,\cdot)} \Sigma_4) = 0,$$
$$G^{(124,\bullet)} = x_{124d}^{(124)} (X_3 G_{3d}^{(1,\cdot)} - \Sigma_3 G_{3d}^{(\cdot,\cdot)}) = 0, \qquad (119)$$

where the cancellations follow from Eq. (105). Using $X_3 G^{(12,34)} X_4 = G^{(12,34)}$ (via Eq. (75a)) and $G^{(1234)} = -\Gamma_{\mathrm{bare}}$ (Eq. (101a)), we find the following compact sIE for $\Gamma^{(12)}$, represented diagrammatically in Fig. 12:

$$\Gamma^{(12)} = \mathcal{K}^{(12)} + G^{(12,34)} + \Gamma_{\mathrm{bare}},$$
$$\Gamma^{(13)} = \mathcal{K}^{(13)} + G^{(13,24)} - \zeta \Gamma_{\mathrm{bare}},$$
$$\Gamma^{(14)} = \mathcal{K}^{(14)} - G^{(14,23)} + \Gamma_{\mathrm{bare}},$$
$$\Gamma^{(23)} = \mathcal{K}^{(23)} + G^{(14,23)} - \Gamma_{\mathrm{bare}},$$
$$\Gamma^{(24)} = \mathcal{K}^{(24)} - G^{(13,24)} + \zeta \Gamma_{\mathrm{bare}},$$
$$\Gamma^{(34)} = \mathcal{K}^{(34)} + G^{(12,34)} + \Gamma_{\mathrm{bare}}. \qquad (120)$$

We also listed analogous sIEs for the other 3p vertices, which can be derived similarly.

D. 4p vertex estimators

Finally, we derive a sIE for the 4p vertex Γ [Eq. (95)]. We use the same strategy of repeatedly applying the

EOM (88) to 4p auxiliary correlators. At the m-th order, we use the EOM w.r.t. ω_m as well as the lower-order estimators.

The EOM of the 4p connected correlator $G^{(\cdot,\cdot,\cdot,\cdot)}$ w.r.t. ω_1 is

$$g_1^{-1} G^{(\cdot,\cdot,\cdot,\cdot)} = G^{(\bullet,\cdot,\cdot,\cdot)}. \tag{121}$$

By amputating the remaining external legs, we find a first-order 4p aIE:

$$\Gamma = g_3^{-1} G^{(\bullet,\cdot,\cdot,\cdot)} g_2^{-1} g_4^{-1}. \tag{122}$$

This equation is the 4p aIE used in Eq. (84) of Ref. [13]. The same formula holds if one takes the correlators themselves instead of their connected parts as the disconnected parts on both sides cancel via the 2p EOM. Then, Eq. (122) becomes Eq. (26) of Ref. [8].

The relevant EOMs w.r.t. ω_2 are

$$G^{(\cdot,\cdot,\cdot,\cdot)} g_2^{-1} = G^{(\cdot,\bullet,\cdot,\cdot)},$$
$$G^{(1,\cdot,\cdot,\cdot)} g_2^{-1} = G^{(1,\bullet,\cdot,\cdot)} + G^{(12,\cdot,\cdot)} X_2. \tag{123}$$

By inserting Eq. (123) into Eq. (122), we find a second-order 4p aIE:

$$\Gamma = g_3^{-1} \Big[G^{(\bullet,\bullet,\cdot,\cdot)} + G^{(12,\cdot,\cdot)} \Big] g_4^{-1}. \tag{124}$$

Inserting the EOMs

$$g_3^{-1} G^{(\cdot,\cdot,\cdot,\cdot)} = G^{(\cdot,\cdot,\bullet,\cdot)}$$
$$g_3^{-1} G^{(1,\cdot,\cdot,\cdot)} = G^{(1,\cdot,\bullet,\cdot)} - X_3 \zeta G^{(13,\cdot,\cdot)}$$
$$g_3^{-1} G^{(\cdot,2,\cdot,\cdot)} = G^{(\cdot,2,\bullet,\cdot)} - X_3 G^{(23,\cdot,\cdot)}$$
$$g_3^{-1} G^{(1,2,\cdot,\cdot)} = G^{(1,2,\bullet,\cdot)} - X_3 \big[\zeta G^{(13,2,\cdot)} + G^{(23,1,\cdot)} \big], \tag{125}$$

into the second-order aIE [Eq. (124)], we obtain a third-order 4p aIE:

$$\begin{aligned}
\Gamma &= \Big[G^{(\bullet,\bullet,\bullet,\cdot)} + g_3^{-1} G^{(12,\cdot,\cdot)} + \zeta G^{(13,\cdot,\cdot)} \Sigma_2 \\
&\quad - \zeta G^{(13,2,\cdot)} X_2 + \Sigma_1 G^{(23,\cdot,\cdot)} - X_1 G^{(23,1,\cdot)} \Big] g_4^{-1} \\
&= \Big[G^{(\bullet,\bullet,\bullet,\cdot)} + g_3^{-1} G^{(12,\cdot,\cdot)} - \zeta G^{(13,\bullet,\cdot)} - G^{(23,\bullet,\cdot)} \Big] g_4^{-1}.
\end{aligned} \tag{126}$$

The second and third rows of this formula can be simplified using the 3p EOMs

$$G^{(13,\cdot,\cdot)} g_2^{-1} = G^{(13,\bullet,\cdot)} + \zeta G^{(123,\cdot)} X_2,$$
$$g_1^{-1} G^{(23,\cdot,\cdot)} = G^{(23,\bullet,\cdot)} + X_1 G^{(123,\cdot)}, \tag{127}$$

which lead to

$$\Gamma = \Big[G^{(\bullet,\bullet,\bullet,\cdot)} + 2 X_1 G^{(123,\cdot)} \Big] g_4^{-1} + \Gamma^{(12)} - \zeta \Gamma^{(13)} - \Gamma^{(23)}. \tag{128}$$

Finally, using the EOM w.r.t. ω_4

$$\begin{aligned}
G^{(\cdot,\cdot,\cdot,\cdot)} g_4^{-1} &= G^{(\cdot,\cdot,\cdot,\bullet)}, \\
G^{(1,\cdot,\cdot,\cdot)} g_4^{-1} &= G^{(1,\cdot,\cdot,\bullet)} + G^{(14,\cdot,\cdot)} X_4, \\
G^{(\cdot,2,\cdot,\cdot)} g_4^{-1} &= G^{(\cdot,2,\cdot,\bullet)} + \zeta G^{(24,\cdot,\cdot)} X_4 \\
G^{(\cdot,\cdot,3,\cdot)} g_4^{-1} &= G^{(\cdot,\cdot,3,\bullet)} + G^{(34,\cdot,\cdot)} X_4, \\
G^{(1,2,\cdot,\cdot)} g_4^{-1} &= G^{(1,2,\cdot,\bullet)} + \big[G^{(14,2,\cdot)} + \zeta G^{(24,1,\cdot)} \big] X_4, \\
G^{(1,\cdot,3,\cdot)} g_4^{-1} &= G^{(1,\cdot,3,\bullet)} + \big[G^{(14,\cdot,3)} + G^{(34,1,\cdot)} \big] X_4, \\
G^{(\cdot,2,3,\cdot)} g_4^{-1} &= G^{(\cdot,2,3,\bullet)} + \big[\zeta G^{(24,\cdot,3)} + G^{(34,\cdot,2)} \big] X_4, \\
G^{(1,2,3,\cdot)} g_4^{-1} &= G^{(1,2,3,\bullet)} + \big[G^{(14,2,3)} + \zeta G^{(24,1,3)} \\
&\qquad + G^{(34,1,2)} \big] X_4,
\end{aligned} \tag{129}$$

we find the desired fourth-order 4p sIE,

$$\begin{aligned}
\Gamma &= \Gamma_{\text{core}} \\
&\quad + \mathcal{K}^{(12)} - \zeta \mathcal{K}^{(13)} - \mathcal{K}^{(23)} + \mathcal{K}^{(34)} + \zeta \mathcal{K}^{(24)} + \mathcal{K}^{(14)} \\
&\quad + G^{(12,34)} - \zeta G^{(13,24)} - G^{(14,23)} \\
&\quad + \Gamma_{\text{bare}},
\end{aligned} \tag{130}$$

fully symmetric in all four frequencies. Here, we used

$$\Gamma_{\text{core}} = G^{(\bullet,\bullet,\bullet,\bullet)}. \tag{131}$$

This term is defined recursively in Eq. (102) and contains $2^4 = 16$ terms that can be evaluated using the same rule as the 3p case [Eq. (118)]: either (i) multiply $-\Sigma_n$ ($x_n = n$) or (ii) add n in the superscript of the auxiliary correlator and multiply X_n ($x_n = \cdot$), for $n = 1, 2, 3, 4$. We also used the definition of $\mathcal{K}^{(ab)}$ [Eq. (118)] to isolate the bosonic 2p correlators $G^{(12,34)}$, $G^{(13,24)}$, and $G^{(14,23)}$, and the bare vertex $G^{(1234)}$. From the top to bottom of Eq. (130), the rows contain 4p, 3p, 2p, and 1p correlators. Equation (130), giving a sIE for the 4p vertex, is our second main result. Figure 13 depicts it diagrammatically.

E. Perturbative behavior of the estimators

One regime where the robustness of sIEs against numerical errors becomes particularly evident is the weak-interaction limit. In this regime, when using diagonalization-based methods like NRG without improved estimators, numerical artifacts may dominate the signal due to the small magnitude of the vertex [13]. We hence discuss the perturbative limit explicitly in the following. However, note that the improved estimators are of course formally exact at all interaction strengths.

First, let us consider the self-energy. In the limit of small U, directly calculating the self-energy from the Dyson equation [Eq. (15)] can lead to an error of order $\mathcal{O}(U^0)$ due to an imperfect cancellation between the bare and full propagators. In the aIE [Eq. (105)], the leading error is $\mathcal{O}(U^1)$ as the auxiliary correlator $G^{(1,\cdot)}$ contains
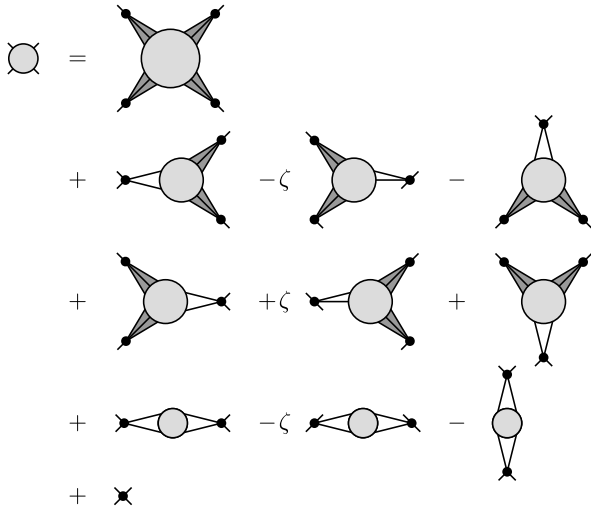
FIG. 13. Diagrammatic representation of the 4p sIE of Eq. (130) (listing the contributions in the same order as there). Only connected diagrams are involved. Indices of the amputated external legs are indicated by their orientation.

H_{int}. Analogously, with the sIE [Eq. (108)], the error in the frequency-dependent part is $\mathcal{O}(U^2)$ because all terms in the estimator (except the Hartree self-energy, which is computed directly via the equilibrium density matrix, using Eq. (99)) include H_{int} at least twice.

Next, for the 3p sIEs in Eq. (120) and Fig. 12, a perturbative expansion of the three terms gives contributions of order $\mathcal{O}(U^3)$, $\mathcal{O}(U^2)$, and $\mathcal{O}(U^1)$, respectively. The third, $\mathcal{O}(U^1)$ term is the exact bare vertex. The second, $\mathcal{O}(U^2)$ term is a bosonic 2p correlator which can be computed much more accurately than the 3p correlators. Only the first, $\mathcal{O}(U^3)$ term $\mathcal{K}^{(12)}$ involves 3p correlators. Finally, the 4p sIE also contains the exact bare vertex at $\mathcal{O}(U)$ and involves only bosonic 2p correlators up to $\mathcal{O}(U^2)$:

$$\Gamma = \Gamma_{\text{bare}} + G^{(12,34)} - \zeta G^{(13,24)} - G^{(14,23)} + \mathcal{O}(U^3). \quad (132)$$

Thus, the 4p sIE is highly accurate in the weak-coupling limit, with errors from multipoint calculations entering only at $\mathcal{O}(U^3)$. In contrast, a direct amputation of the correlator [Eqs. (110) and (95)] or the use of first-order aIEs [Eq. (115) and (122)] introduces errors three and two orders (two and one orders) earlier, respectively, than for the 4p (3p) sIE.

Our estimators for the 3p and 4p vertex are invariant under a shift of H_{int} by a quadratic term:

$$H_0 \to H_0 + \lambda_{ij} d_i^\dagger d_j, \quad H_{\text{int}} \to H_{\text{int}} - \lambda_{ij} d_i^\dagger d_j. \quad (133)$$

The self-energy estimators transform as

$$\Sigma \to \Sigma - \lambda. \quad (134)$$

Since NRG is linear in each argument of the correlator, the choice of λ does not affect the numerical results calculated with the estimators (for a given z shift) [22]. An

interesting choice of the shift is $\lambda = \Sigma^{\text{H}}$. In this case, Σ scales as $\mathcal{O}(U^2)$ in the small-U limit. Then, the first and second terms of the 1PR-subtracted vertex [Fig. 9(b)] scale as $\mathcal{O}(U^1)$, and $\mathcal{O}(U^2)$, respectively. Hence, $\mathcal{K}^{(12)}$ [Eq. (118)] and Γ_{core} [Eq. (131)] can be decomposed into terms that enter at different orders in the perturbative expansion according to the number of occurrences of Σ. For example, in Eq. (118), we have a $\mathcal{O}(U^3)$ term $(X_3 G^{(12,3,4)} X_4)$, two $\mathcal{O}(U^4)$ terms $(\Sigma_3 G^{(12,\cdot,4)} X_4$ and $X_3 G^{(12,3,\cdot)} \Sigma_4)$, and a $\mathcal{O}(U^5)$ term $(\Sigma_3 G^{(12,\cdot,\cdot)} \Sigma_4)$. Similarly, for Γ_{core}, the perturbative order of each term can be classified into orders ranging from $\mathcal{O}(U^4)$ to $\mathcal{O}(U^8)$.

F. Relation to the vertex asymptotics

A similar numerical advantage of the sIEs is also expected in the large frequency limit. When the input frequencies are much larger than any intrinsic energy scales of the system, the propagator g is inversely proportional to the frequency. At high frequencies, numerical results for g become noisy due to the vanishing magnitude and a small signal-to-noise ratio. Direct amputation, i.e. division by g, introduces a large error in the vertex. The sIEs for Γ^{3p} and Γ^{4p} are free from this error because they do not require any amputation.

The 4p sIE of Eq. (129) bears a close connection to the asymptotic behaviors of the 4p vertex. If any of the external frequency arguments is taken to infinity, a diagram carrying this frequency in a (non-amputated) line vanishes [26, 36]. We now use this property to connect the 4p sIE [Eq. (130)] and its diagrammatic representation (Fig. 13) to the asymptotic classes of the 4p vertex.

If all four frequency arguments are taken to infinity without any particular constraint except $\omega_{1234} = 0$, the 4p vertex reduces to the bare interaction. The last term of the 4p sIE (130) is this bare interaction [Eq. (101a)]:

$$\lim_{|\omega_1|, \cdots, |\omega_4| \to \infty} \Gamma(\boldsymbol{\omega}) = \Gamma_{\text{bare}}. \quad (135)$$

Nontrivial asymptotic classes are defined by the limits of some or all frequencies going to infinity while keeping the sum of two frequencies to a fixed, finite value. Concretely, we have [26]

$$\lim_{|\nu_r| \to \infty} \lim_{|\nu'_r| \to \infty} \Gamma(\boldsymbol{\omega_r}) = \Gamma_{\text{bare}} + \mathcal{K}_1^r(\omega_r),$$
$$\lim_{|\nu'_r| \to \infty} \Gamma(\boldsymbol{\omega_r}) = \Gamma_{\text{bare}} + \mathcal{K}_1^r(\omega_r) + \mathcal{K}_2^r(\nu_r, \omega_r),$$
$$\lim_{|\nu_r| \to \infty} \Gamma(\boldsymbol{\omega_r}) = \Gamma_{\text{bare}} + \mathcal{K}_1^r(\omega_r) + \mathcal{K}_{2'}^r(\nu'_r, \omega_r),$$
$$(136)$$

where we parametrize the frequencies as

$$\boldsymbol{\omega_r} = \begin{cases} (\nu_r, -\nu_r - \omega_r, \nu'_r + \omega_r, -\nu'_r) & \text{for } r = t \text{ (ph)}, \\ (\nu_r, -\nu'_r, -\nu_r - \omega_r, \nu'_r + \omega_r) & \text{for } r = p \text{ (pp)} \\ (\nu_r, -\nu'_r, \nu'_r + \omega_r, -\nu_r - \omega_r) & \text{for } r = a \text{ (}\overline{\text{ph}}\text{)}. \end{cases} \quad (137)$$

Here, t, p, and a denote the transverse, parallel, and antiparallel channels, according to, e.g., the conventions of Ref. [37–39].

The first asymptotic class $\mathcal{K}_1$ corresponds to the bosonic 2p correlators [26] in the third line of Eq. (130):

$$
\begin{aligned}
\mathcal{K}_1^t(\omega_t) &= G^{(12,34)}(-\omega_t, \omega_t), \\
\mathcal{K}_1^p(\omega_p) &= -\zeta G^{(13,24)}(-\omega_p, \omega_p), \\
\mathcal{K}_1^a(\omega_a) &= -G^{(14,23)}(-\omega_a, \omega_a).
\end{aligned}
\tag{138}
$$

The second asymptotic class, involving $\mathcal{K}_2$ and $\mathcal{K}_{2'}$, comes from the $\mathcal{K}^{(ab)}$ terms:

$$
\begin{aligned}
\mathcal{K}_2^t(\nu_t, \omega_t) &= \mathcal{K}^{(34)}(\omega_t, \nu_t, -\nu_t - \omega_t), \\
\mathcal{K}_{2'}^t(\nu_t', \omega_t) &= \mathcal{K}^{(12)}(-\omega_t, \nu_t' + \omega_t, -\nu_t'), \\
\mathcal{K}_2^p(\nu_p, \omega_p) &= \zeta \mathcal{K}^{(24)}(\omega_p, \nu_p, -\nu_p - \omega_p), \\
\mathcal{K}_{2'}^p(\nu_p', \omega_p) &= -\zeta \mathcal{K}^{(13)}(-\omega_p, -\nu_p', \nu_p' + \omega_p), \\
\mathcal{K}_2^a(\nu_a, \omega_a) &= -\mathcal{K}^{(23)}(\omega_a, \nu_a, -\nu_a - \omega_a), \\
\mathcal{K}_{2'}^a(\nu_a', \omega_a) &= \mathcal{K}^{(14)}(-\omega_a, -\nu_a', \nu_a' + \omega_a).
\end{aligned}
\tag{139}
$$

The remaining core contribution, which does not contribute to the asymptotics, is Eq. (131):

$$
\Gamma - \left[\Gamma_{\text{bare}} + \sum_r \left(\mathcal{K}_1^r + \mathcal{K}_2^r + \mathcal{K}_{2'}^r \right) \right] = \Gamma_{\text{core}}.
\tag{140}
$$

For computational schemes built on the asymptotics-based parametrization of the 4p vertex, using the 4p sIE is highly advantageous because each asymptotic class is calculated separately. The core contribution, in particular, which decays in all high-frequency limits, can be calculated using Eq. (131). This is expected to be much more accurate than subtracting terms that belong to different asymptotic classes from the full vertex.

G.   Subtracting the disconnected contributions

So far, we presented 3p and 4p sIEs involving *connected* auxiliary correlators. Such estimators are suitable for NRG, where correlators are computed using spectral representations which offer a natural way for obtaining connected correlators by subtracting disconnected parts on the level of partial spectral functions [12, 13]. Yet, other methods, like QMC, only have access to the total correlator. It is then useful to have total correlators instead of their connected parts in the vertex estimators.

Leaving the derivation to App. D, we here present a KF 4p sIE involving only total correlators:

$$
\Gamma = \Gamma_{\text{tot}} - 2\pi\delta(\omega_{12})\Sigma_{12}^{k_1 k_2}\Sigma_{34}^{k_3 k_4} - 2\pi\delta(\omega_{14})\zeta\Sigma_{14}^{k_1 k_4}\Sigma_{32}^{k_3 k_2}.
\tag{141}
$$

Here, the subscript 'tot' indicates that the connected auxiliary correlators in Eq. (130) are replaced by total correlators, i.e. the sum of the connected and disconnected parts. The additional self-energy terms cancel the disconnected diagrams in the total correlator. In the MF, the Dirac delta function $2\pi\delta(\omega)$ is replaced by the Kroneker delta $\beta\delta_{\omega,0}$.

The additional disconnected terms involve the self-energy; hence, they vanish in the noninteracting case, as well as in the perturbative limit up to $\mathcal{O}(U^1)$ (or $\mathcal{O}(U^2)$ if H_{int} is shifted to give $\Sigma^{\text{H}} = 0$, cf. Sec. IV E). Moreover, they are much smaller than those obtained by direct amputation, where disconnected terms involve the square of the inverse propagator. When using sIEs, significant cancellations occur between the disconnected parts of the various auxiliary 4p correlators involved; thus, the disconnected parts surviving these cancellations are much smaller.

In App. D, we also show that the estimators using total correlators share the same perturbative and asymptotic properties as the original estimators expressed through connected correlators discussed in the previous sections.

One remaining choice to be made is which self-energy estimators to use when evaluating the vertex estimators. Possible choices include the aIEs Σ^{L} [Eq. (105a)] and Σ^{R} [Eq. (105b)], and the sIE Σ^{S} [Eq. (108)]. Although these estimators are all equivalent analytically, this choice may affect the results in the presence of numerical noise.

We propose to use the aIE Σ^{L} (Σ^{R}) for the self-energies Σ_1 and Σ_3 (Σ_2 and Σ_4) which left- and right-multiply the auxiliary correlators. This choice maximizes the cancellation of disconnected diagrams: e.g., the disconnected term in the 3p sIE for $\Gamma^{(34)}$ is proportional to

$$
\Sigma^{\text{L}} G^{(\cdot,\cdot)} \Sigma^{\text{R}} - X G^{(1,\cdot)} \Sigma^{\text{R}} - \Sigma^{\text{L}} G^{(\cdot,2)} X + X G^{(1,2)} X + \Sigma^{\text{H}} X.
$$

If Eqs. (105) are used, the first three terms are all equal up to signs. Thus, two of them mutually cancel (even if Σ^{L} and Σ^{R} differ due to numerical noise), so that the expression simplifies to

$$
-X G^{(1,\cdot)} g^{-1} G^{(\cdot,2)} X + X G^{(1,2)} X + \Sigma^{\text{H}} X = \Sigma^{\text{S}}.
\tag{142}
$$

Then, by using Σ^{S} in Eq. (141) to remove the remaining disconnected terms, the cancellation is made exact. Such a cancellation may be particularly beneficial for QMC where the total correlators are computed. For NRG, the disconnected parts are already subtracted on the level of partial spectral functions. Still, we use Σ^{L} (Σ^{R}) for left (right) multiplications in Eq. (130), expecting that this helps with the cancellation of any remnant disconnected terms that might have survived as numerical artifacts.
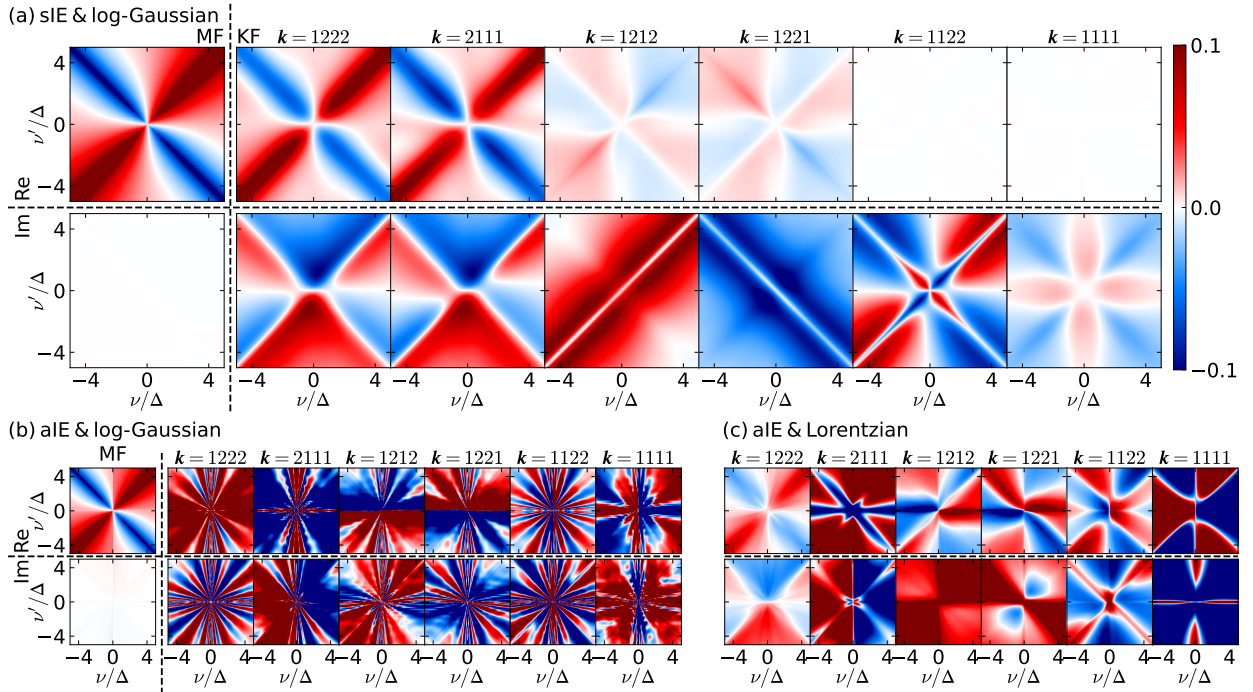
FIG. 14. MF and KF 4p vertices $(\Gamma_{\uparrow\downarrow} - \Gamma_{\text{bare};\uparrow\downarrow})/U$ in the AIM at weak interaction ($\Delta/D = 0.1$, $U/\Delta = 0.5$, and $T/\Delta = 0.01$) at $\omega = 0$. They were computed using (a) the sIE of Eq. (130), and (b,c) the aIE of Eq. (122), with (a,b) log-Gaussian broadening or (c) Lorentzian broadening (see App. E 2 for details). Only the KF vertices are shown for (c) as broadening does not affect MF vertices. For all three panels (a,b,c), the upper (lower) row shows the real (imaginary) part. For the sIE, the MF vertex is purely real, and the KF vertex at $\boldsymbol{k} = 1122$ and $\boldsymbol{k} = 1111$ are purely imaginary. Keldysh components not plotted are related to those plotted by crossing symmetry, complex conjugation, or both (see App. C). The aIE vertex breaks these symmetries. In panels (b) and (c), the KF data is clearly inferior (more noisy, showing spurious features, etc.) than in (a), illustrating that aIEs are not suitable for computing all components of the KF vertex.

V. NUMERICAL RESULTS

In this section, we demonstrate the advantages of sIEs over aIEs for NRG computations of the 4p vertex [12, 13]. To this end, we consider the AIM and compare results from NRG to those of third-order perturbation theory (PT3) and renormalized perturbation theory (RPT) [40–43]. For our purposes, NRG, PT3, and RPT may all be viewed as black-box methods for computing MF and KF vertices, where PT3 and RPT are restricted to weak interaction and asymptotically low energies, respectively. (Reference [13] describes the inner workings of NRG vertex computations and App. E some further refinements needed for present purposes.) We also refrain from discussing the physics of the AIM or analyzing the physical information encoded in its 4p vertex. Instead, we focus on the advantages of sIEs over aIEs.

The Hamiltonian of the AIM was already given in Eq. (13). We here take a rectangular hybridization function $-\text{Im}\Delta^R(\nu) = \pi \sum_b |V_b|^2 \delta(\nu - \varepsilon_b) = \Delta\Theta(D - |\nu|)$ with bandwidth D and hybridization strength Δ. We focus on the particle-hole symmetric case, $\varepsilon_d = -U/2$.

In the following, we represent the 4p vertex in the t-channel parametrization [Eq. (137)] at vanishing transfer frequency,

$$\Gamma_{\sigma\sigma'}(\nu, \nu') = \Gamma_{\sigma\sigma'}(\nu, \nu', \omega = 0)$$
$$= \Gamma[d_\sigma, d_\sigma^\dagger, d_{\sigma'}, d_{\sigma'}^\dagger](\nu, -\nu, \nu', -\nu'). \quad (143)$$

Thus, Γ describes the effective interaction of an electron with energy ν and spin σ and an electron with energy ν' and spin σ'. We will analyze Γ in the MF and the KF. In the KF, we will consider its components in the Keldysh basis as well as the causal component in the contour basis (corresponding to $\boldsymbol{c} = ----$). The latter is a particularly sensitive probe to the numerical accuracy as it involves a sum over all components in the Keldysh basis:

$$\Gamma^{\text{causal}} = \tfrac{1}{4} \sum_{k_1,\cdots,k_4} \Gamma^{k_1 k_2 k_3 k_4}. \quad (144)$$

By crossing and complex conjugation symmetries, one has (see App. C)

$$\text{Re}\,\Gamma^{\text{causal}} = \tfrac{1}{2}\text{Re}\,(\Gamma^{1222} + \Gamma^{2111}) + (\nu \leftrightarrow \nu'), \quad (145a)$$

$$\text{Im}\,\Gamma^{\text{causal}} = \tfrac{1}{4}\text{Im}\,(\Gamma^{1212} + \Gamma^{1221} + \Gamma^{1122} + \tfrac{1}{2}\Gamma^{1111})$$
$$+ (\nu \leftrightarrow \nu'). \quad (145b)$$
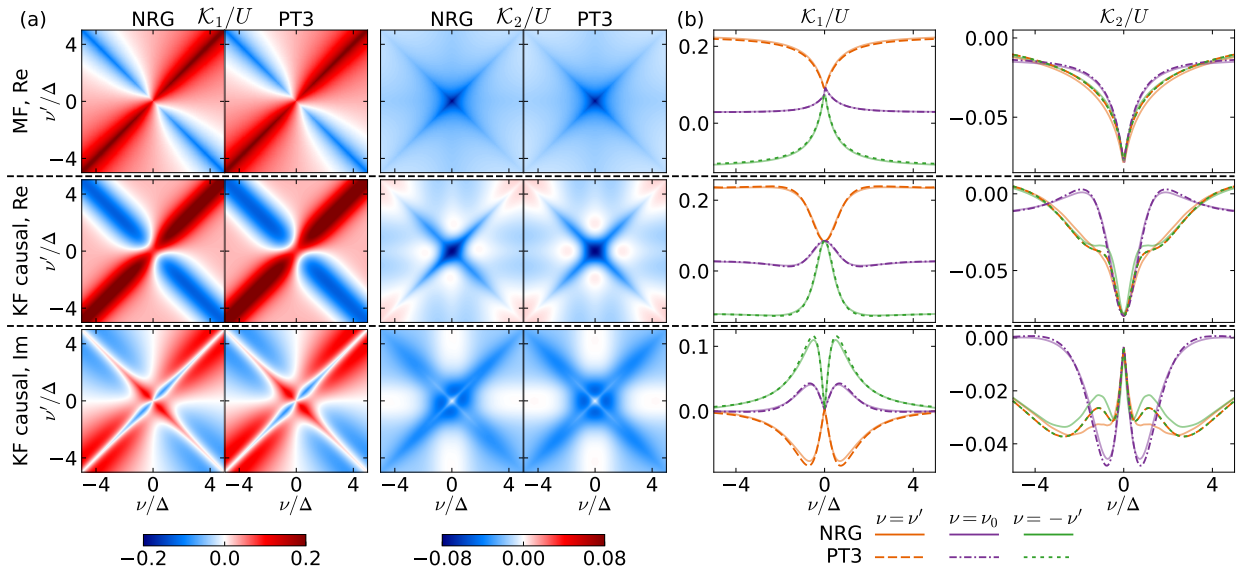
FIG. 15. (a) MF and KF 4p vertices in the first and second asymptotic classes, $\mathcal{K}_1 = \sum_{r=a,p,t} \mathcal{K}_1^r$ and $\mathcal{K}_2 = \sum_{r=a,p,t} \mathcal{K}_2^r + \mathcal{K}_{2'}^r$, normalized by U, in the AIM at weak interaction (parameters: same as for Fig. 14). The first, second, and third rows show the MF vertex (which is purely real), and the real and imaginary parts of the causal component of the KF vertex, respectively, comparing results from NRG (first, third columns) and third-order perturbation theory (PT3) (second, fourth columns). (b) Line cuts of the vertices in (a) along the diagonal (orange), y axis (purple), and anti-diagonal (green). ν_0 is π/β for the MF and 0 for the KF. Overall, the agreement is excellent both qualitatively, see (a), and quantitatively, see (b). For $\mathcal{K}_2$ in the right column of (b), the PT3 and NRG results do not fully agree, because PT3 yields a symmetry between diagonal and anti-diagonal cuts which is lifted by terms beyond third order (for orange and green, dashed PT3 lines coincide, solid NRG ones do not).
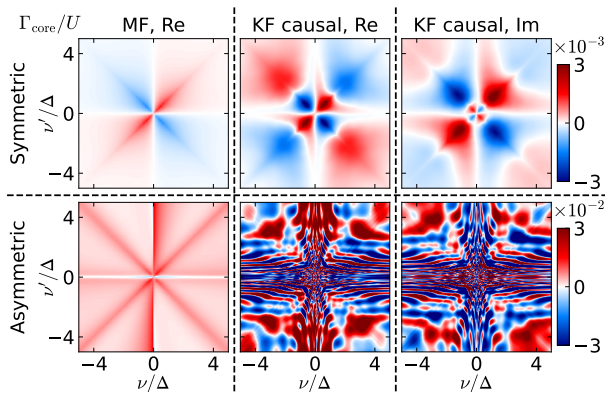
FIG. 16. Core part of the MF and KF 4p vertices $\Gamma_{\rm core}/U$, in the AIM at weak interaction (parameters: same as for Fig. 14). The first, second, and third columns show the MF vertex (which is purely real), and the real part and imaginary parts of the causal component of the KF vertex, respectively, computed using sIEs (top row) or aIEs (bottom row). The latter are dominated by numerical noise, the former not.

A. Weak interaction

As the first benchmark, we study the AIM at weak interaction, $\Delta/D = 0.1$, $U/\Delta = 0.5$, and $T/\Delta = 0.01$, and compare our NRG results against those from PT3. In the weak coupling regime, defined by $U/(\pi\Delta) \ll 1$ [44, 45], PT3 yields fairly accurate results and thus serves as a useful benchmark. For NRG, being a diagonalization-based method, the accuracy of the results does not depend on the strength of the coupling, i.e., weak coupling is as non-trivial a challenge as strong coupling.

Figures 14(a) and 14(b) compare the 4p vertex obtained using the sIE [Eq. (130)] and the aIE [Eq. (122)], respectively, both broadened the same way, using a narrow (log-Gaussian) broadening kernel (see App. E 2 for details). The aIE results are completely dominated by fan-shaped noise, an artifact of NRG discretization. By contrast, the sIE results are almost completely free from such artifacts. This clearly illustrates the advantage of the sIE over the aIE. For comparison, Fig. 14(c) shows aIE results broadened with a much broader (Lorentzian) kernel (in the same way as for the aIE results of Ref. [12], Fig. 12). This hides the discretization artifacts by smearing them out, at the cost of strongly over-broadening the physically meaningful features seen in the sIE results of Fig. 14(a). In addition, Keldysh components of the aIE vertex other than the fully retarded $\boldsymbol{k} = 1222$ component strongly deviate from the corresponding sIE result.

Figure 15 displays the contributions from the $\mathcal{K}_1$ and $\mathcal{K}_2$ asymptotic classes obtained with NRG and PT3. We find an excellent agreement for all asymptotic terms, in
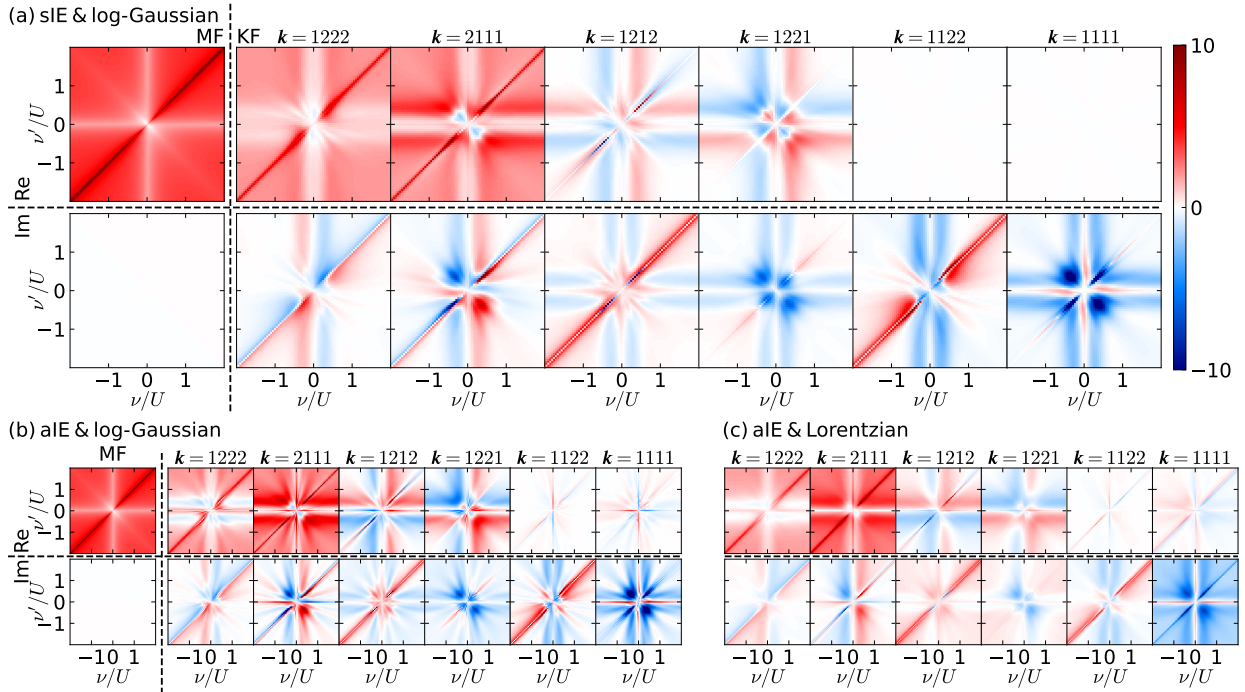
FIG. 17. MF and KF 4p vertices $(\Gamma_{\uparrow\downarrow} - \Gamma_{\mathrm{bare};\uparrow\downarrow})/U$, for the AIM, analogous to Fig. 14, but at a much stronger interaction $(\Delta/D = 0.04$, $U/\Delta = 5$, and $T/\Delta = 0.0025)$, with $\omega = 0$.
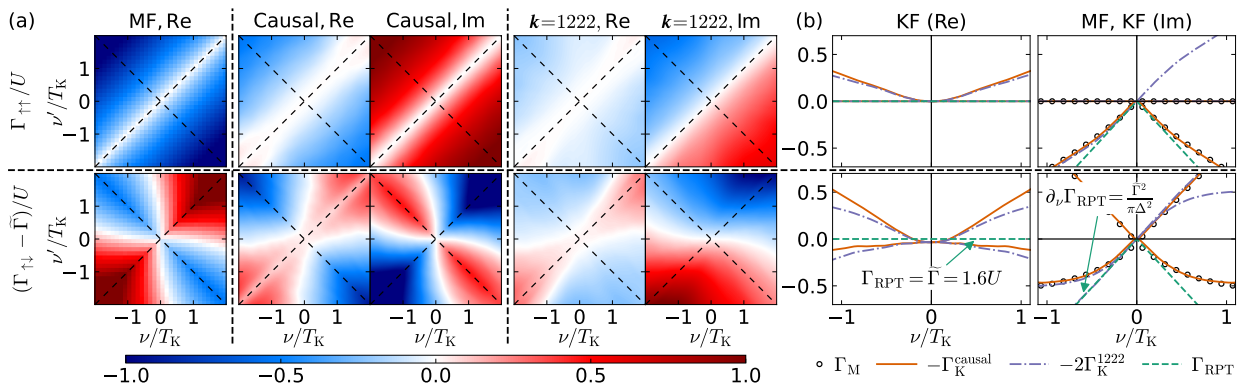
FIG. 18. (a) Low-energy part of the MF and KF 4p vertices $(\Gamma_{\sigma\sigma'} - \widetilde{\Gamma}_{\sigma\sigma'})/U$ in the AIM at strong interaction (parameters: same as for Fig. 17), computed with the sIE. The vertices are an order of magnitude smaller than those shown in Fig. 17. (b) One-dimensional cuts of the vertices along $\nu = \nu'$ and $\nu = -\nu'$ (dashed lines in (a)). The Fermi-liquid predictions for the vertex, obtained by RPT [Eq. (146)], are shown using green dashed lines. In the regime of validity of RPT, $|\nu|, |\nu'|, T \ll T_{\mathrm{K}}$, the agreement between NRG and RPT is remarkably good. The RPT parameters are $\widetilde{U} = 0.20U$, $Z = 0.36$, and $\widetilde{\Gamma} = \widetilde{U}/Z^2 = 1.6U$.

the MF and the KF. The fact that even the line cuts match perfectly is testament to the accurate broadening of the NRG data.

Next, we focus on the core part, which is very challenging to compute from perturbation theory due to the leading-order contribution of the envelope diagram. Figure 16 compares the core vertex obtained using the sIE [Eq. (131)] (top row) and an aIE (bottom row). Since the

aIE [Eq. (122)] does not contain a decomposition into asymptotic classes, one must subtract the asymptotic contributions from the full vertex to get the core part [Eq. (140)]. For the AIM parameters used here, the core vertex is around two orders of magnitude smaller than the full vertex. Hence, the subtraction entails a large numerical error. Indeed, the data in the bottom row of Fig. 16 is completely dominated by numerical noise, ten times
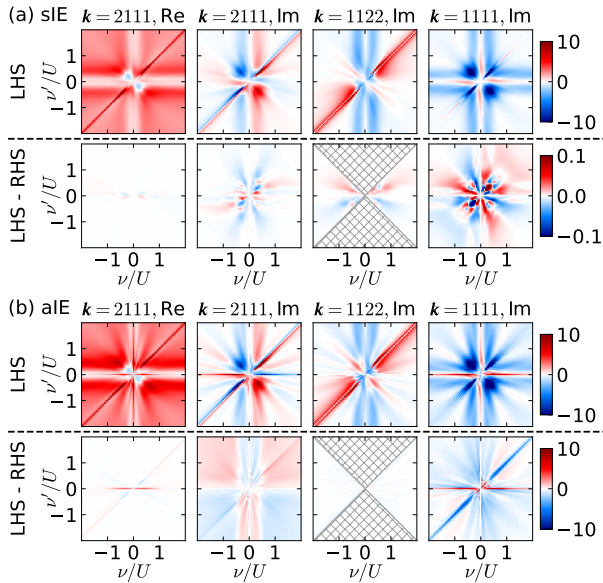
FIG. 19. FDRs of the KF 4p vertices in the AIM at a strong interaction (parameters: same as for Fig. 17), computed using (a) the sIE and (b) an aIE. The four columns show the real and imaginary parts of Eqs. (147a), (147b), and (147c), respectively, normalized by U. Their left sides are shown in the upper rows of (a,b), the difference between the left and right sides (violation of the FDR) in the bottom rows. Remarkably, for the sIE the violations are two orders of magnitude smaller than the vertices, and our 4p sIE NRG results thus satisfy vertex FDRs to within a few percent. By contrast, for the aIE, the violations are not much smaller than the vertices themselves, implying sizeable violations of the FDRs. In the bottom row for $\boldsymbol{k} = 1122$, we do not plot results in the hatched region where $|\nu'| > |\nu| + 4T$, as the right-hand side of Eq. (147b) becomes numerically unstable due to the $\frac{\cosh(\nu'/2T)}{\cosh(\nu/2T)}$ term, which increases exponentially with $|\nu'| - |\nu|$.

larger than the true core vertex (upper row), in both the MF and the KF. By contrast, using the sIE, the core vertex is determined from its own estimator (131), which involves no subtraction of terms with different asymptotics or perturbative order. Thereby, the sIE is much less susceptible to numerical errors than the aIE.

B. Strong interaction

We now turn to the nonperturbative regime with a stronger interaction $\Delta/D = 0.04$, $U/\Delta = 5$, and $T/\Delta = 0.0025$. Figure 17 compares sIE and aIE results for the 4p vertex. The MF and KF vertices differ significantly from the weak-coupling case (Fig. 14). The discretization artifacts observed with the aIE in Fig. 17(b) are less prominent at strong coupling than at weak coupling, but are still noticeable. Yet, being asymmetric, the aIE breaks several symmetries of the vertex, having, e.g., a

nonzero real part in the $\boldsymbol{k} = 1122$ and 1111 components.

In the nonperturbative regime, accurate reference results for the entire 4p vertex are not available. However, in the low-energy Fermi-liquid regime, where the temperature and all frequencies are much lower than the Kondo temperature T_K (here, $T \simeq 0.02T_K$ [12]), RPT predicts a specific behavior of the vertex [40–43]. For an SU(2)-symmetric single-orbital AIM at half filling, the MF, causal KF, and fully retarded KF vertices in the low-temperature, low-frequency limit have the following form [41–43],

$$\Gamma_{M,\sigma\sigma'}(i\nu, i\nu') = \widetilde{\Gamma}\delta_{\sigma\bar{\sigma}'} - \frac{\widetilde{\Gamma}^2}{\pi\Delta^2}(|\nu-\nu'| - \delta_{\sigma\bar{\sigma}'}|\nu+\nu'|),$$
(146a)

$$\Gamma_{K,\sigma\sigma'}^{causal}(\nu, \nu') = \widetilde{\Gamma}\delta_{\sigma\bar{\sigma}'} + i\frac{\widetilde{\Gamma}^2}{\pi\Delta^2}(|\nu-\nu'| - \delta_{\sigma\bar{\sigma}'}|\nu+\nu'|),$$
(146b)

$$2\Gamma_{K,\sigma\sigma'}^{1222}(\nu, \nu') = \widetilde{\Gamma}\delta_{\sigma\bar{\sigma}'} + i\frac{\widetilde{\Gamma}^2}{\pi\Delta^2}[(\nu-\nu') - \delta_{\sigma\bar{\sigma}'}(\nu+\nu')],$$
(146c)

where $\bar{\sigma} = -\sigma$. The last equation for the fully retarded KF vertex is derived using the analytic continuation of the absolute value $f(i\nu) = |\nu|$ to $f^{R/A} = -i(\nu \pm i0^+)$. The effective static interaction $\widetilde{\Gamma}$ is given by $\widetilde{\Gamma}_{\sigma\sigma'} = \delta_{\sigma\bar{\sigma}'}\widetilde{U}/Z^2$, where $\widetilde{U}$ is the quasiparticle interaction and Z the quasiparticle weight. These can be directly extracted from the low-energy eigenspectrum spectrum of NRG [12, 40, 46–48]; for our strong-coupling parameters, we find $\widetilde{U} = 0.20U$, $Z = 0.36$, and $\widetilde{\Gamma} = \widetilde{U}/Z^2 = 1.6U$. These are the same values as in Ref. [12]. While, there, the agreement with RPT in the limit $\nu, \nu' \to 0$ was checked for the MF and fully retarded KF vertices, we here significantly extend this comparison by including the linear order in ν and ν' and all Keldysh components.

Figure 18(a) shows the low-energy part of the sIE vertex, with $|\nu|, |\nu'| \lesssim T_K$. Figure 18(b) compares NRG and RPT results for line cuts of the vertex, showing remarkably good agreement in the low-energy regime $|\nu'| \ll T_K$, for both the MF and KF. This provides strong confirmation of the accuracy of the imaginary- and real-frequency vertices computed from NRG using the sIE. We note that the small undershooting of $\Gamma_{\uparrow\downarrow}(0, 0, 0)$ can be systematically improved by using a denser grid for binning and a smaller broadening parameter, at the expense of increased computational costs (see App. E).

As a final test, we check how well the NRG results for $\Gamma^{\boldsymbol{k}}$ satisfy generalized fluctuation-dissipation relations (FDRs). These FDRs are known from the literature [49–51] and take a particularly simple form at $\omega = 0$:

$$\Gamma^{2111} = \Gamma^{2122} + t_{\nu'}(\Gamma^{2112} - \Gamma^{2121})$$
$$- 2it_\nu t_{\nu'} \operatorname{Im}\Gamma^{2212} + it_\nu \operatorname{Im}\Gamma^{2211},$$
(147a)

$$\operatorname{Im}\Gamma^{1122} = c_{\nu'}^2/c_\nu^2 \operatorname{Im}\Gamma^{2211}$$
$$+ 2t_\nu \operatorname{Im}\Gamma^{1222} - 2t_{\nu'}c_{\nu'}^2/c_\nu^2 \operatorname{Im}\Gamma^{2212},$$
(147b)

$$\mathrm{Im}\,\Gamma^{1111} = [2t_\nu(1+t_{\nu'}^2)\,\mathrm{Im}\,\Gamma^{1222} - t_{\nu'}^2\,\mathrm{Im}\,\Gamma^{1122}$$
$$+\, t_\nu t_{\nu'}(\mathrm{Im}\,\Gamma^{2121}-\mathrm{Im}\,\Gamma^{2112})] + (\nu \leftrightarrow \nu'). \quad (147c)$$

Here, we used $c_\nu = \cosh\frac{\nu}{2T}$ and $t_\nu = \tanh\frac{\nu}{2T}$ (same for ν') for short and omitted the frequency argument $(\nu, \nu', \omega = 0)$ for the vertices. FDRs for the other Keldysh components with one 2 follow from Eq. (147a) by crossing symmetry or complex conjugation (cf. App. C). Figure 19 shows that the FDRs are all satisfied remarkably well for the sIE vertex [Fig. 19(a)], with errors two orders of magnitude smaller than the signal. By contrast, the FDRs are strongly violated for the aIE vertex [Fig. 19(b)].

VI. SUMMARY AND OUTLOOK

We presented a new estimator for the 4p vertex which is symmetric in all indices and involves only full (interacting) correlators. This sIE achieves the amputation of external legs via EOMs, without dividing the correlators by propagators, and also maximizes the cancellation of the disconnected parts between multipoint objects. The asymptotic decomposition of the vertex naturally arises from the sIE, ensuring the accuracy of every term via a separate estimator for each, without any large-frequency limits or numerically unstable subtractions. We demonstrate the utility of the sIE by calculating the 4p vertex of the AIM at weak coupling and strong coupling using multipoint NRG. Both the imaginary-frequency MF and real-frequency KF vertices agree very well with known limits, namely weak-coupling perturbation theory and low-energy Fermi-liquid theory, and the latter accurately satisfies the generalized fluctuation-dissipation relations. We expect that the sIE may also be useful for other computational methods such as QMC. For NRG, it provides a robust way of computing the real-frequency Keldysh vertex, opening up the possiblility for studying real-frequency nonlocal correlations via diagrammatic extensions of DMFT [3].

Appendix A: Boundary conditions of correlators

In this Appendix, we show that the boundary term that arises when integrating by parts in Eq. (52) vanishes. In the MF, this can be easily seen using the boundary condition of the imaginary-time correlator on the contour of Fig. 5(a). However, in the ZF and the KF, correlators defined by Eq. (31) and the contours of Figs. 5(b) and 5(c) do not have simple boundary conditions. We can nevertheless show that the boundary term vanishes, using (i) correlators ordered on a modified (L-shaped) contour (Fig. 20) [23] and (ii) the adiabatic assumption, which is widely adopted (also in the original work of Keldysh [52]) as it simplifies the derivation.

It may be surprising that the adiabatic assumption is evoked in the ZF and KF but not in the MF. After all, in thermal equilibrium (which we assume in this work), the entire information is encoded in MF correlators. Indeed, one can obtain the retarded components of the KF by analytic continuation [12, 50] and all other components by further accounting for the discontinuities of the MF correlator in the complex frequency plane [51]. We resolve this issue in App. B by showing that it is indeed possible (albeit more tedious) to derive the KF EOMs in thermal equilibrium without the adiabatic assumption.

1. Contour formalism for MF, ZF, KF correlators

Using the notation for ℓp correlators from Sec. III, we define a correlator of ℓ operators $\boldsymbol{\mathcal{O}}$ at times $\boldsymbol{z}$ on the contour $\mathcal{C}$ with a (possibly) time-dependent Hamiltonian $H(z)$ as

$$\mathcal{G}[\boldsymbol{\mathcal{O}}](\boldsymbol{z}) = (-i)^{\ell-1}\frac{\mathrm{Tr}\left[\mathcal{T}e^{-i\int d\bar{z}H(\bar{z})}\mathcal{O}_\mathrm{S}^1(1)\cdots\mathcal{O}_\mathrm{S}^\ell(\ell)\right]}{\mathrm{Tr}\left[\mathcal{T}e^{-i\int d\bar{z}H(\bar{z})}\right]}, \quad (A1)$$

where $\mathcal{T}$ denotes the contour ordering of the operators. Here, $\mathcal{O}_\mathrm{S}^m(m)$ denote operators in the Schrödinger picture, in contrast to the Heisenberg operators $\mathcal{O}^m(m)$ of Eq. (3), because time dependence is generated by $e^{-i\int d\bar{z}H(\bar{z})}$. The correlator (A1) satisfies the Kubo–Martin–Schwinger (KMS) boundary condition

$$\mathcal{G}[\boldsymbol{\mathcal{O}}](\boldsymbol{z})\big|_{z_m=z_\mathrm{i}} = \zeta_m \mathcal{G}[\boldsymbol{\mathcal{O}}](\boldsymbol{z})\big|_{z_m=z_\mathrm{f}}, \quad (A2)$$

where z_i and z_f are the endpoints of $\mathcal{C}$, and ζ_m is $+1$ (-1) if $\mathcal{O}^m$ is a bosonic (fermionic) operator. The sign factor arises from commuting $\mathcal{O}^m$ past all other operators. (The correlator is nonzero only for an even number of fermionic operators. Hence, if $\mathcal{O}^m$ is fermionic, the remaining operators include an odd number of fermionic operators, leading to a -1 sign factor.) The KMS boundary condition is easily proven using the cyclicity of the trace [23].

Such a simple boundary condition does not hold for the correlators from Eq. (35), defined as the thermal expectation value of time-ordered operators, because in gen-
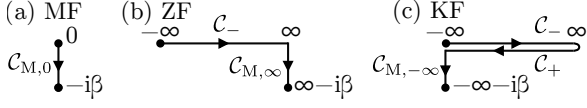
FIG. 20. Time contour for each many-body formalism considered similar to Fig. 5, but with the vertical imaginary-time branches for (b) and (c).

eral $\mathcal{O}^m$ does not commute with the thermal density matrix $\rho = e^{-\beta H}/\operatorname{Tr} e^{-\beta H}$ involved in the thermal average $\langle\ldots\rangle$. In the KF (Fig. 5(c)), e.g., we have $z_\mathrm{i} = -\infty^-$ and $z_\mathrm{f} = -\infty^+$, which leads to

$$
\begin{aligned}
\mathcal{G}[\boldsymbol{\mathcal{O}}](z_\mathrm{i}, z_2, \cdots) &= \operatorname{Tr}\left[\rho\mathcal{O}^1(-\infty)\mathcal{O}^2(2)\cdots\right] \\
&\neq \zeta_1 \mathcal{G}[\boldsymbol{\mathcal{O}}](z_\mathrm{f}, z_2, \cdots) = \operatorname{Tr}\left[\rho\mathcal{O}^2(2)\cdots\mathcal{O}^\ell(\ell)\mathcal{O}^1(-\infty)\right] \\
&= \operatorname{Tr}\left[\mathcal{O}^1(-\infty)\rho\mathcal{O}^2(2)\cdots\right], \quad \text{(A3)}
\end{aligned}
$$

if $\mathcal{O}^1$ does not commute with ρ.

To connect Eq. (A1) with the correlators of the MF, ZF, and KF, we choose the contours

$$
\begin{aligned}
&\text{MF}: \overline{\mathcal{C}} = \mathcal{C}_{\mathrm{M},0} = [0, -i\beta], &&\text{(A4a)} \\
&\text{ZF}: \overline{\mathcal{C}} = \mathcal{C}_- \oplus \mathcal{C}_{\mathrm{M},\infty}, &&\text{(A4b)} \\
&\text{KF}: \overline{\mathcal{C}} = \mathcal{C}_- \oplus \mathcal{C}_+ \oplus \mathcal{C}_{\mathrm{M},-\infty}, &&\text{(A4c)}
\end{aligned}
$$

respectively, as illustrated in Fig. 20, where $\mathcal{C}_{\mathrm{M},a} = [a, a-i\beta]$. The overline distinguishes these contours from those used in the main text (Eq. (32) and Fig. 5). In the MF, we set

$$
\text{MF}: H(z) = H. \quad \text{(A5a)}
$$

The time evolution on the vertical branch $\mathcal{C}_{\mathrm{M},0}$ then generates $e^{-\beta H}$, the interacting thermal state. Thus, we readily find that, in the MF, the contour-ordered correlators are identical to the imaginary-time-ordered correlators [Eq. (31a)].

In the ZF and KF, we instead use

$$
\text{ZF}: H(z) = \begin{cases} H_\eta(t) & \text{if } z \in [-\infty, \infty] \\ H^0 & \text{if } z \in [\infty, \infty - i\beta] \end{cases}, \quad \text{(A5b)}
$$

$$
\text{KF}: H(z) = \begin{cases} H_\eta(t) & \text{if } z = t^\pm, t < 0 \\ H & \text{if } z = t^\pm, t \geq 0 \\ H^0 & \text{if } z \in [-\infty, -\infty - i\beta] \end{cases}, \quad \text{(A5c)}
$$

where

$$
H_\eta(t) = H^0 + e^{-\eta|t|} H_{\mathrm{int}} \quad \text{(A6)}
$$

describes the adiabatic switching of the interaction with an infinitesimal rate $\eta = 0^+$ on the horizontal branches. The interaction is fully switched off on the vertical branch.

In the KF, the time evolution on the vertical branch generates $e^{-\beta H^0}$, the noninteracting thermal state. According to the adiabatic assumption, the adiabatic switching of the interaction on the horizontal branches connects this state to the interacting thermal state [52]:

$$
\frac{e^{-\beta H}}{\operatorname{Tr} e^{-\beta H}} \overset{\text{adia.}}{=} U_\eta(0, -\infty) \frac{e^{-\beta H^0}}{\operatorname{Tr} e^{-\beta H^0}} U_\eta(-\infty, 0), \quad \text{(A7)}
$$

where U_η is the time-evolution operator for H_η. Under this adiabatic assumption, the contour-ordered correlator is identical to the ordinary Keldysh correlators defined as the equilibrium expectation value of contour-time-ordered operators [Eq. (31c)] [23]:

$$
\mathcal{G}_\mathrm{K}^{\boldsymbol{c}}[\boldsymbol{\mathcal{O}}](\boldsymbol{t}) \overset{\text{adia.}}{=} (-i)^{\ell-1}\left\langle \mathcal{T}[\boldsymbol{\mathcal{O}}](\boldsymbol{t^c})\right\rangle. \quad \text{(A8)}
$$

In the ZF, the adiabatic switching connects the noninteracting ground state $\left|\Psi^0\right\rangle$ to the interacting ground state $|\Psi\rangle$ (assuming no level crossing) [53]:

$$
|\Psi\rangle \overset{\text{adia.}}{=} U_\eta(0, -\infty)\left|\Psi^0\right\rangle. \quad \text{(A9)}
$$

Then, again, the ZF contour-ordered correlator equals the ground-state expectation value of time-ordered operators [Eq. (31b)]:

$$
\mathcal{G}_\mathrm{Z}[\boldsymbol{\mathcal{O}}](\boldsymbol{t}) \overset{\text{adia.}, T=0}{=} (-i)^{\ell-1}\left\langle \mathcal{T}[\boldsymbol{\mathcal{O}}](\boldsymbol{t})\right\rangle. \quad \text{(A10)}
$$

2. Derivation of vanishing boundary terms

Let us now prove Eq. (52). The derivation of the EOMs leading up to Eq. (52) [including Eqs. (39), (40), (45), and (46)] holds unchanged for the contour correlators defined by Eq. (A1). The step from Eq. (51) to Eq. (52), with the boundary term made explicit, reads

$$
\begin{aligned}
&\mathcal{G}[\psi_a, \boldsymbol{\mathcal{O}}^{\not{h}}] \\
&= \int_{m'} g_{a\bar{a}}^0(m, m')(-i\overleftarrow{\partial'_m}\mathbb{1} - H^0)_{\bar{a}a'}\mathcal{G}[\psi_{a'}, \boldsymbol{\mathcal{O}}^{\not{h}}](m', \not{h}) \\
&= \int_{m'} g_{a\bar{a}}^0(m, m')(i\partial'_m\mathbb{1} - H^0)_{\bar{a}a'}\mathcal{G}[\psi_{a'}, \boldsymbol{\mathcal{O}}^{\not{h}}](m', \not{h}) \\
&\quad - ig_{aa'}^0(m, m')\mathcal{G}[\psi_{a'}, \boldsymbol{\mathcal{O}}^{\not{h}}](m', \not{h})\big|_{z_\mathrm{i}}^{z_\mathrm{f}}. \quad \text{(A11)}
\end{aligned}
$$

Thanks to the KMS boundary condition [Eq. (A2)], which holds for all three choices of the contour $\overline{\mathcal{C}}$ defined in Eq. (A4), the last line vanishes:

$$
g^0(m, z_\mathrm{i})\mathcal{G}(z_\mathrm{i}, \not{h}) = g^0(m, z_\mathrm{f})\mathcal{G}(z_\mathrm{f}, \not{h}). \quad \text{(A12)}
$$

Here, we omitted the orbital subscript and operator arguments for brevity. The sign factors coming from g^0 and $\mathcal{G}$ are both ζ_m and thus cancel as $\zeta_m^2 = 1$. We emphasize that this logic cannot be used for the ZF and KF contours *without* vertical branches [Eq. (32)] as the KMS boundary condition (A2) then does not hold (Eq. (A3)).

Inserting the EOM (46a) into Eq. (A11), we find the analogue of Eq. (52),

$$
\mathcal{G}[\psi_a, \boldsymbol{\mathcal{O}}^{\not{h}}] = \int_{m'} g_{aa'}^0(m, m')\mathcal{F}^m[\psi_{a'}, \boldsymbol{\mathcal{O}}^{\not{h}}](m', \not{h}), \quad \text{(A13)}
$$

where the integral over z'_m is performed over $\overline{\mathcal{C}}$ [Eq. (A4)]. In the MF, this concludes the proof because $\overline{\mathcal{C}}_\mathrm{M} = \mathcal{C}_\mathrm{M}$. In the ZF and KF, $\overline{\mathcal{C}}$ and $\mathcal{C}$ differ by the vertical branches $\mathcal{C}_{\mathrm{M},\infty}$ and $\mathcal{C}_{\mathrm{M},-\infty}$, respectively. If all the time arguments $\boldsymbol{z}$ are on the horizontal branches $C_\pm$, z'_m on the vertical branch does not contribute to the integral of Eq. (A13), because the interaction is zero on the vertical branch [Eqs. (A5b) and (A5c)]:

$$\mathcal{F}^m(z'_m, \boldsymbol{z}^{\eta_h})\big|_{\mathrm{Im}\, z'_m \neq 0 \text{ and } z_n \in C_\pm} = 0. \tag{A14}$$

Note that the adiabatic assumption is crucial here: if the interaction were nonzero on the vertical branch, Eq. (A14) would not hold. With the vertical branch not contributing, the integration domain in Eq. (A13) becomes $\mathcal{C}$, thus concluding the proof of Eq. (52).

Appendix B: EOM derivation without adiabatic assumption

In this Appendix, we prove the EOM in the integral form [Eq. (54)] in the KF without resorting to the adiabatic assumption. Without the adiabatic assumption, one needs to use a contour with the interaction present on both the horizontal and vertical branches. We will show that the contribution of the vertical branch to the EOM vanishes. We thus recover the EOM with only the horizontal branchs, as used in the main text.

After introducing the relevant contours in Sec. B 1, we prove the EOM in Sec. B 2 by rewriting the correlators in terms of ℓp greater correlators [Eq. (B11)]. We finish in Sec. B 3 by presenting a much simpler proof that applies only to a subset of Keldysh components.

1. Correlators without the adiabatic assumption

We use the contour

$$\mathcal{C}_{t_0} = \mathcal{C}_{-,t_0} \oplus \mathcal{C}_{+,t_0} \oplus \mathcal{C}_{\mathrm{M},t_0}, \tag{B1}$$
$$\mathcal{C}_{-,t_0} = [t_0, \infty], \ \mathcal{C}_{+,t_0} = [\infty, t_0], \ \mathcal{C}_{\mathrm{M},t_0} = [t_0, t_0 - i\beta],$$

as shown in Fig. 21(a), and set

$$H(z) = H. \tag{B2}$$

Since the interaction is present on the vertical branch, the adiabatic assumption [Eq. (A7)] is *not* needed to equate the contour-ordered correlators with the equilibrium expectation values. Instead, Eq. (A1) directly yields

$$\mathcal{G}^{\boldsymbol{c}}_{\mathrm{KF, w/o\, adia.}}[\boldsymbol{\mathcal{O}}](\boldsymbol{t}) = (-i)^{\ell-1} \Big\langle \mathcal{T} \prod_{i=1}^{\ell} [\mathcal{O}](\boldsymbol{t}^{\boldsymbol{c}}) \Big\rangle. \tag{B3}$$

If all time arguments lie on the horizontal branches, i.e., for real valued $t_1, \cdots, t_\ell$, the contour $\mathcal{C}_{t_0}$ itself defines a real-time correlator $\mathcal{G}^{\boldsymbol{c}}(\boldsymbol{t})$ only for $t_i \geq t_0$. Still, we can
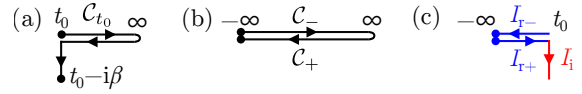
FIG. 21. Time contours for KF (a) without or (b) with the adiabatic assumption (Fig. 5(c)), and (c) the difference between (a) and (b).

extend the definition to $t_i < t_0$ in a manner that yields a time-translation-invariant correlator by construction. We define a time shift $\Delta t = t_0 - \min(t_0, t_1, \cdots, t_\ell)$ so that

$$\boldsymbol{t} + \Delta t = (t_1 + \Delta t, \cdots, t_\ell + \Delta t) \tag{B4}$$

are on the contour $\mathcal{C}_{t_0}$, i.e. $t_i + \Delta t \geq t_0$. Then, we define

$$\mathcal{G}^{\boldsymbol{c}}(\boldsymbol{t}) = \mathcal{G}^{\boldsymbol{c}}(\boldsymbol{t} + \Delta t), \tag{B5}$$

where the left side is given by the right side. This extended definition enlarges the domain of $\mathcal{G}^{\boldsymbol{c}}(\boldsymbol{t})$ to include $\mathcal{C}_- \oplus \mathcal{C}_+$ (Fig. 21(b)), the domain of the correlator of Eq. (31c), as a subset. By construction, the resulting $\mathcal{G}^{\boldsymbol{c}}(\boldsymbol{t})$ satisfies time-translational invariance. We note that one cannot simply set $t_0 = -\infty$ because this limit is ill-defined for the EOM in the integral form (e.g., Eq. (B8b) evaluates to Eq. (B24)).

Let us consider the EOM (54a) with $m = 1$. (Other EOMs easily follow by permutation and complex conjugation.) Our goal is to prove the EOM (54a) with z'_1 integrated over $\mathcal{C}_- \oplus \mathcal{C}_+$ (Fig. 21(b) or Fig. 5(c)):

$$\mathcal{G}[1](\boldsymbol{z}) = \int_{1' \in \mathcal{C}_\pm} g_1^0(1,1')\mathcal{F}[1](1', \not{1}). \tag{B6}$$

A similar equation, but with z'_1 integrated over $\mathcal{C}_{t_0}$ (Fig. 21(a)), can readily be derived as in Sec. A 2:

$$\mathcal{G}[1](\boldsymbol{z}) = \int_{1' \in \mathcal{C}_{t_0}} g_1^0(1,1')\mathcal{F}[1](1', \not{1}). \tag{B7}$$

We will now derive Eq. (B6) from Eq. (B7) by showing that the right sides of the two equations are equal.

The difference between the right sides comes from the integral over the segments shown in Fig. 21(c). This is given by $I_\mathrm{r} + I_\mathrm{i}$, where $I_\mathrm{r} = I_{\mathrm{r}+} + I_{\mathrm{r}-}$, and

$$I_{\mathrm{r}\pm}(\boldsymbol{t}^{\boldsymbol{c}}) = \pm \int_{-\infty}^{t_0} dt' g_{aa'}^0(1, t'^\pm)\mathcal{G}[q_{a'}, \boldsymbol{\mathcal{O}}^{\boldsymbol{I}}](t'^\pm, \not{1}), \tag{B8a}$$

$$I_\mathrm{i}(\boldsymbol{t}^{\boldsymbol{c}}) = -i \int_0^\beta d\tau g_{aa'}^0(1, t_0 - i\tau)\mathcal{G}[q_{a'}, \boldsymbol{\mathcal{O}}^{\boldsymbol{I}}](t_0 - i\tau, \not{1}). \tag{B8b}$$

The right sides contain $\mathcal{G}$, not $\mathcal{F}$, because the equal-time commutators in $\mathcal{F}$ (the last term of Eq. (47)) do not contribute since the domains of $1'$ and $\not{1}$ do not overlap. We used the shorthand $q_{a'} = [\psi_{a'}, H_\mathrm{int}]$ and

$$(1, t') = (t_1^{c_1}, t'), \quad (z, \not{1}) = (z, t_2^{c_2}, \cdots, t_\ell^{c_\ell}) \tag{B9}$$

as in Eq. (36). Henceforth, we drop the superscript 0 on g and abbreviate $\mathcal{G}[q_{a'}, \boldsymbol{\mathcal{O}^I}]$ as $\mathcal{G}_{a'}$. The time arguments $\boldsymbol{t^c}$ are treated as given, fixed points on the contour $C_-^{t_0} \oplus C_+^{t_0}$, so that

$$t_i \geq t_0. \tag{B10}$$

2. General proof of the EOM

To prove $I_{\mathrm{r}} + I_{\mathrm{i}} = 0$, we begin by defining an $\ell\mathrm{p}$ "greater correlator"

$$\mathcal{G}^{>\boldsymbol{c^I}}[\boldsymbol{\mathcal{O}}](z, \boldsymbol{t^I}) = (-i)^{\ell-1} \left\langle \mathcal{O}^1(z)\, \mathcal{T}[\boldsymbol{\mathcal{O}^I}](\boldsymbol{t^I}^{\boldsymbol{c^I}}) \right\rangle, \quad \text{(B11)}$$

where the superscript $>$ denotes that $\mathcal{O}^1(z)$ does not follow the contour ordering and is always ordered as the operator last in time, put at the leftmost site. This correlator is a generalization of the greater component of the 2p correlator $\mathcal{G}^>(t, t') = \mathcal{G}(t^+, t'^-)$. We allow z to be any complex number in Eq. (B11). The Fourier transform of the greater correlator reads

$$\mathcal{G}^{>\boldsymbol{c^I}}(t, \boldsymbol{t^I}) = \int \frac{d^\ell \omega}{(2\pi)^\ell} e^{-i\boldsymbol{\omega}\cdot\boldsymbol{t}} G^{>\boldsymbol{c^I}}(\boldsymbol{\omega}) 2\pi\delta(\omega_{1\cdots\ell}). \tag{B12}$$

We now rewrite the integrands of $I_{\mathrm{r}\pm}$ and I_{i} in terms of greater correlators, starting with I_{i} [Eq. (B8b)]. While $t_0 - i\tau$ is the first argument of $\mathcal{G}[q_{a'}, \boldsymbol{\mathcal{O}^I}](t_0 - i\tau, \boldsymbol{t})$ and thus already in the right place for equating this correlator with a greater correlator, this is not the case for $g_{aa'}(1, t_0 - i\tau)$. However, using the simple relation $G[\mathcal{O}^1, \mathcal{O}^2](z_1, z_2) = \zeta G[\mathcal{O}^2, \mathcal{O}^1](z_2, z_1)$, which holds irrespective of the contour used in Eq. (A1), we can switch the two arguments of g. Thereby, we obtain

$$g_{aa'}(1, t_0 - i\tau) = \zeta g^>[\psi_{a'}^\dagger, \psi_a](t_0 - i\tau, 1),$$
$$\mathcal{G}(t_0 - i\tau, \boldsymbol{t}) = \mathcal{G}^>(t_0 - i\tau, \boldsymbol{t}). \tag{B13}$$

Rewriting $I_{\mathrm{i}}(\boldsymbol{t^c})$ in terms of the greater correlators yields

$$\begin{aligned}
I_{\mathrm{i}}(\boldsymbol{t^c}) &= -i\int_0^\beta d\tau\, g_{aa'}(1, t_0 - i\tau)\mathcal{G}_{a'}(t_0 - i\tau, \boldsymbol{t}) \\
&= -i\int_0^\beta d\tau\, \zeta g^>[\psi_{a'}^\dagger, \psi_a](t_0 - i\tau, 1)\mathcal{G}_{a'}^>(t_0 - i\tau, \boldsymbol{t}) \\
&= -i\int_0^\beta d\tau\, f(t_0 - i\tau, \boldsymbol{t^c}). \tag{B14}
\end{aligned}$$

Here, we defined

$$f(z, \boldsymbol{t^c}) = \zeta g^>[\psi_{a'}^\dagger, \psi_a](z, 1)\mathcal{G}_{a'}^>(z, \boldsymbol{t}), \tag{B15}$$

which appears with $z = t_0 - i\tau$. Below, it will reappear with other complex time arguments.

Similarly, for $I_{\mathrm{r},+}$ [Eq. (B8a)], t'^+ is the last contour argument because $t' \leq t_0$. Applying the same permutation to the arguments of g, we find

$$g_{aa'}(1, t'^+) = \zeta g^>[\psi_{a'}^\dagger, \psi_a](t', 1),$$

$$\mathcal{G}_{a'}(t'^+, \boldsymbol{t}) = \mathcal{G}_{a'}^>(t', \boldsymbol{t}). \tag{B16}$$

Substituting these equations into Eq. (B8a) yields

$$\begin{aligned}
I_{\mathrm{r},+}(\boldsymbol{t^c}) &= \int_{-\infty}^{t_0} dt'\, g_{aa'}(1, t'^+)\mathcal{G}_{a'}(t'^+, \boldsymbol{t}) \\
&= \int_{-\infty}^{t_0} dt'\, \zeta g^>[\psi_{a'}^\dagger, \psi_a](t', 1)\mathcal{G}_{a'}^>(t', \boldsymbol{t}) \\
&= \int_{-\infty}^{t_0} dt'\, f(t', \boldsymbol{t^c}). \tag{B17}
\end{aligned}$$

Finally, for $I_{\mathrm{r},-}$ [Eq. (B8a)], $t' \leq t_0$ is the smallest time argument but is on the forward branch ($c' = -$). Yet, we can still relate the correlators to greater correlators by applying time translation by $t_0 - t'$ and using the KMS boundary condition [Eq. (A2)]:

$$\begin{aligned}
g_{aa'}(1, t'^-) &= g_{aa'}^{c_1 -}(t_1 - t' + t_0, t_0) \\
&= \zeta g_{aa'}^{c_1 \mathrm{M}}(t_1 - t' + t_0, t_0 - i\beta) \\
&= g^>[\psi_{a'}^\dagger, \psi_a](t' - i\beta, 1), \tag{B18} \\
\mathcal{G}_{a'}(t'^-, \boldsymbol{t}) &= \mathcal{G}_{a'}^{-\boldsymbol{c^I}}(t_0, \boldsymbol{t^I} - t' + t_0) \\
&= \zeta \mathcal{G}_{a'}^{\boldsymbol{c^I}}(t_0 - i\beta, \boldsymbol{t^I} - t' + t_0) \\
&= \zeta \mathcal{G}_{a'}^>(t' - i\beta, \boldsymbol{t}). \tag{B19}
\end{aligned}$$

The KMS boundary condition is used in the second equalities of Eqs. (B18) and (B19). For the third equalities, we used Eq. (B13) and the time-translational invariance. Substituting Eqs. (B18) and (B19) into Eq. (B8a) gives

$$\begin{aligned}
I_{\mathrm{r},-}(\boldsymbol{t^c}) &= -\int_{-\infty}^{t_0} dt'\, g_{aa'}(1, t'^-)\mathcal{G}_{a'}(t'^-, \boldsymbol{t}) \\
&= -\int_{-\infty}^{t_0} dt'\, \zeta g^>[\psi_{a'}^\dagger, \psi_a](t' - i\beta, 1)\mathcal{G}_{a'}^>(t' - i\beta, \boldsymbol{t}) \\
&= -\int_{-\infty}^{t_0} dt'\, f(t' - i\beta, \boldsymbol{t^c}). \tag{B20}
\end{aligned}$$

By combining Eqs. (B14), (B17) and (B20), we find

$$I_{\mathrm{i}}(\boldsymbol{t^c}) = \int_{t_0}^{t_0 - i\beta} dz\, f(z, \boldsymbol{t^c}), \tag{B21a}$$

$$I_{\mathrm{r}}(\boldsymbol{t^c}) = \int_{-\infty}^{t_0} dt'\, \big[f(t', \boldsymbol{t^c}) - f(t' - i\beta, \boldsymbol{t^c}) \big]. \tag{B21b}$$

Next, we evoke the Fourier representation of f,

$$f(z, \boldsymbol{t^c}) = \int \frac{d\Omega}{2\pi} \frac{d^\ell \omega}{(2\pi)^\ell} e^{-i\Omega z} e^{-i\boldsymbol{\omega}\cdot\boldsymbol{t}} f^{\boldsymbol{c}}(\Omega, \boldsymbol{\omega}). \tag{B22}$$

Although it is not needed in what follows, one can show

$$\begin{aligned}
f^{\boldsymbol{c}}(\Omega, \boldsymbol{\omega}) &= 2\pi\delta(\Omega + \omega_{1\cdots\ell})f^{\boldsymbol{c}}(\boldsymbol{\omega}), \\
f^{\boldsymbol{c}}(\boldsymbol{\omega}) &= \zeta g^>[\psi_{a'}^\dagger, \psi_a](-\omega_1, \omega_1)G_{a'}^{>\boldsymbol{c^I}}(-\omega_{2\cdots\ell}, \boldsymbol{\omega^I}), \tag{B23}
\end{aligned}$$

since Fourier transforms turn Eq. (B15) into a convolution, and a convolution of two delta functions is a single delta function, $\delta(\Omega + \omega_{1\ldots\ell})$. In evaluating Eqs. (B21) with Eq. (B22), we switch the z (or t') and Ω integrals. For I_i, the z integral reads

$$\int_{t_0}^{t_0 - i\beta} dz\, e^{i\Omega z} = \frac{-i}{\Omega} e^{i\Omega t_0} \left(e^{\Omega\beta} - 1 \right). \tag{B24}$$

For I_r, we use the Fourier transform of the step function,

$$\int_{-\infty}^{t_0} dt' e^{i\Omega t'} = \int_{-\infty}^{\infty} dt' \Theta(t_0 - t') e^{i\Omega t'} = \frac{-i}{\Omega - i0^+} e^{i\Omega t_0},$$

$$\int_{-\infty}^{t_0} dt' e^{i\Omega(t' - i\beta)} = \frac{-i}{\Omega - i0^+} e^{i\Omega t_0} e^{\Omega\beta}. \tag{B25}$$

In total, we get

$$\begin{aligned}
I_\mathrm{i}(\boldsymbol{t^c}) + I_\mathrm{r}(\boldsymbol{t^c}) &= i\int \frac{d\Omega}{2\pi} \frac{d^\ell\omega}{(2\pi)^\ell} e^{i\Omega t_0}(e^{\Omega\beta} - 1) \\
&\quad \times \left(\frac{1}{\Omega - i0^+} - \frac{1}{\Omega} \right) e^{-i\boldsymbol{\omega}\cdot\boldsymbol{t}} f^{\boldsymbol{c}}(\Omega, \boldsymbol{\omega}) \\
&= \int \frac{d\Omega}{2\pi} \frac{d^\ell\omega}{(2\pi)^\ell} e^{i\Omega t_0}(1 - e^{\Omega\beta})\pi\delta(\Omega) e^{-i\boldsymbol{\omega}\cdot\boldsymbol{t}} f^{\boldsymbol{c}}(\Omega, \boldsymbol{\omega}) \\
&= 0. \tag{B26}
\end{aligned}$$

In conclusion, adding the contributions from the horizontal and vertical branches to the difference between the right sides of Eqs. (B6) and (B7) yields $(1 - e^{\Omega\beta})\delta(\Omega) = 0$, thus proving $I_\mathrm{i} + I_\mathrm{r} = 0$ and the EOM.

Note that this derivation applies only to the equilibrium KF as we have set $H(z) = H$. In the nonequilibrium case where $H(z)$ depends on z, correlators that mix horizontal and vertical branches need to be taken into account to close the EOM.

We further note that well-known FDRs in the frequency domain can be derived from the KMS boundary condition using identities similar to those derived in this Appendix [23]. As an illustration, let us derive the 2p FDR. We begin by noting that Eq. (B19) is valid for all t_1 and t_2 if $c_1 = +$. Then, one finds

$$g^<(t_2, t_1) = \zeta g(t_1^+, t_2^-) = \zeta g^>(t_2 - i\beta, t_1), \tag{B27}$$

whose Fourier transformation reads

$$g^<(\omega) = \zeta e^{-\beta\omega} g^>(\omega). \tag{B28}$$

By substituting $g^{>/<} = \frac{1}{2}(\pm g^R \mp g^A + g^K)$, we find the familiar 2p FDR

$$\begin{aligned}
g^K(\omega) &= \frac{1 + \zeta e^{-\beta\omega}}{(1 - \zeta e^{-\beta\omega})} [g^R(\omega) - g^A(\omega)] \\
&= [\coth(\beta\omega/2)]^\zeta [g^R(\omega) - g^A(\omega)]. \tag{B29}
\end{aligned}$$

3. Derivation of the EOMs for fully retarded correlators

Let us finish this Appendix by presenting two cases where I_r and I_i are both trivially zero: correlators whose

Keldysh components satisfy $k_1 = 1$ or $\boldsymbol{k^{\mathcal{I}}} = (1, \cdots, 1)$. EOMs in these two cases suffice to derive the sIEs for the fully retarded correlators, which have only a single 2 in the list of Keldysh indices. For example, for $\boldsymbol{k} = (2111)$, we may use the latter case when deriving the EOM for the first operator, and the former otherwise. The EOMs for these components may as well be derived by the analytic continuation of the MF EOMs.

In the Keldysh basis, the integrals of interest are

$$I_\mathrm{r}^{\boldsymbol{k}}(\boldsymbol{t}) = -\int_{-\infty}^{t_0} dt'\, g_{aa'}^{k_1 k'}(t_1, t') X^{k'k''} \mathcal{G}^{k''\boldsymbol{k^{\mathcal{I}}}}(t', \boldsymbol{t^{\mathcal{I}}}), \tag{B30a}$$

$$I_\mathrm{i}^{\boldsymbol{k}}(\boldsymbol{t}) = -i\int_0^\beta d\tau\, g_{aa'}^{k_1 \mathrm{M}}(t_1, t_0 - i\tau) \mathcal{G}^{\mathrm{M}\boldsymbol{k^{\mathcal{I}}}}(t_0 - i\tau, \boldsymbol{t^{\mathcal{I}}}), \tag{B30b}$$

where the superscript M denotes that $t_0 - i\tau$ is on the vertical branch. For $I_\mathrm{r} = I_\mathrm{r,-} + I_\mathrm{r,+}$, the sum over the forward and backward branches converts to the sum over dummy Keldysh indices k' and k''. The $(-1)^{\delta_{c,+}}$ sign factor converts to $X^{k'k''}$ via Eq. (72).

To show $I_\mathrm{r} = I_\mathrm{i} = 0$, we use a well-known property of the KF correlators: the correlator is zero if the Keldysh index of the largest real-time argument is 1 [54]:

$$\mathcal{G}^{\boldsymbol{k}}(\boldsymbol{z}) = 0 \text{ if } k_n = 1 \text{ and } z_n = t_n \geq \operatorname{Re} z_i \text{ for all } i. \tag{B31}$$

This holds because moving z_n from the forward to the backward branch keeps that operator order and thus the correlator invariant. A subsequent Keldysh rotation with $D^{k=1,c} \propto (-1)^{\delta_{c,+}}$ then yields zero.

Let us begin with the $k_1 = 1$ components. I_r in the Keldysh basis [Eq. (B30a)] contains the propagator $g^{1k'}(t_1, t')$. In the integration domain $t' \in [-\infty, t_0]$, $t' \leq t_0 \leq t_1$ holds [Eq. (B10)], and t_1 is the largest real-time argument. Since $k_1 = 1$, Eq. (B31) yields

$$g^{1k'}(t_1, t') = 0 \quad \Rightarrow \quad I_\mathrm{r} = 0. \tag{B32}$$

Similarly, I_i in the Keldysh basis includes the propagator $g^{1\mathrm{M}}(t_1, t_0 - i\tau)$. This term is again zero because t_1 is the largest real-time argument:

$$g^{1\mathrm{M}}(t_1, t_0 - i\tau) = 0 \quad \Rightarrow \quad I_\mathrm{i} = 0. \tag{B33}$$

Similarly, one can derive $I_\mathrm{r} = I_\mathrm{i} = 0$ for $\boldsymbol{k^{\mathcal{I}}} = 1$, i.e., for a fully retarded correlator. Let n be the index where t_n is the largest among $t_2, \cdots, t_\ell$. Since $t' \in [-\infty, t_0]$, we find $t_n \geq t'$. Then, Eq. (B31) gives (because $k_n = 1$)

$$\mathcal{G}^{k''\boldsymbol{k^{\mathcal{I}}}}(t', \boldsymbol{t^{\mathcal{I}}}) = 0 \quad \Rightarrow \quad I_\mathrm{r} = 0. \tag{B34}$$

Analogously, one has

$$\mathcal{G}^{\mathrm{M}\boldsymbol{k^{\mathcal{I}}}}(t_0 - i\tau, \boldsymbol{t^{\mathcal{I}}}) = 0 \quad \Rightarrow \quad I_\mathrm{i} = 0. \tag{B35}$$

Appendix C: Symmetries of the 4p vertex

In this Appendix, we present symmetries of the 4p vertex $\Gamma_{\sigma\sigma'}(\nu, \nu')$ in the t-channel parametrization at vanishing transfer frequency [Eq. (143)]. A general 4p vertex Γ_{1234} satisfies the crossing symmetry

$$\Gamma_{1234} = -\Gamma_{3214} = -\Gamma_{1432} = \Gamma_{3412} \qquad (C1)$$

and the complex conjugation symmetry

$$\Gamma^*_{1234}(\boldsymbol{\omega}_{1234}) = \zeta_{\boldsymbol{k}} \, \Gamma_{2143}(-\boldsymbol{\omega}_{2143}), \qquad (C2)$$

where $\zeta_{\boldsymbol{k}} = (-1)^{1 + \sum_i k_i}$. Here, the numeric subscripts refer to all the relevant arguments: Keldysh, spin, orbital, and frequency.

For a single-orbital system at zero transfer frequency, we get a chain of identities:

$$\Gamma^{k_1 k_2 k_3 k_4}_{\sigma\sigma\sigma'\sigma'}(\nu, \nu') \qquad = \Gamma^{k_3 k_4 k_1 k_2}_{\sigma'\sigma'\sigma\sigma}(\nu', \nu) \qquad (C3a)$$

$$= \zeta_{\boldsymbol{k}}[\Gamma^{k_2 k_1 k_4 k_3}_{\sigma\sigma\sigma'\sigma'}(\nu, \nu')]^* \quad = \zeta_{\boldsymbol{k}}[\Gamma^{k_4 k_3 k_2 k_1}_{\sigma'\sigma'\sigma\sigma}(\nu', \nu)]^*. \quad (C3b)$$

Since $\Gamma_{\uparrow\uparrow\downarrow\downarrow} = \Gamma_{\downarrow\downarrow\uparrow\uparrow}$ under SU(2) symmetry, assumed in this work, there is no restriction from spin space.

Thereby, we obtain the symmetries

$$\Gamma^{1222}_{\sigma\sigma'}(\nu, \nu') \qquad = \Gamma^{2212}_{\sigma\sigma'}(\nu', \nu)$$
$$= [\Gamma^{2122}_{\sigma\sigma'}(\nu, \nu')]^* \qquad = [\Gamma^{2221}_{\sigma\sigma'}(\nu', \nu)]^*, \qquad (C4a)$$
$$\Gamma^{2111}_{\sigma\sigma'}(\nu, \nu') \qquad = \Gamma^{1121}_{\sigma\sigma'}(\nu', \nu)$$
$$= [\Gamma^{1211}_{\sigma\sigma'}(\nu, \nu')]^* \qquad = [\Gamma^{1112}_{\sigma\sigma'}(\nu', \nu)]^*, \qquad (C4b)$$
$$\Gamma^{1212}_{\sigma\sigma'}(\nu, \nu') \qquad = \Gamma^{1212}_{\sigma\sigma'}(\nu', \nu)$$
$$= -[\Gamma^{2121}_{\sigma\sigma'}(\nu, \nu')]^* \qquad = -[\Gamma^{2121}_{\sigma\sigma'}(\nu', \nu)]^*, \qquad (C4c)$$
$$\Gamma^{1221}_{\sigma\sigma'}(\nu, \nu') \qquad = \Gamma^{2112}_{\sigma\sigma'}(\nu', \nu)$$
$$= -[\Gamma^{2112}_{\sigma\sigma'}(\nu, \nu')]^* \qquad = -[\Gamma^{1221}_{\sigma\sigma'}(\nu', \nu)]^*, \qquad (C4d)$$
$$\Gamma^{1122}_{\sigma\sigma'}(\nu, \nu') \qquad = \Gamma^{2211}_{\sigma\sigma'}(\nu', \nu)$$
$$= -[\Gamma^{1122}_{\sigma\sigma'}(\nu, \nu')]^* \qquad = -[\Gamma^{2211}_{\sigma\sigma'}(\nu', \nu)]^*, \qquad (C4e)$$
$$\Gamma^{1111}_{\sigma\sigma'}(\nu, \nu') \qquad = \Gamma^{1111}_{\sigma\sigma'}(\nu', \nu)$$
$$= -[\Gamma^{1111}_{\sigma\sigma'}(\nu, \nu')]^* \qquad = -[\Gamma^{1111}_{\sigma\sigma'}(\nu', \nu)]^*. \qquad (C4f)$$

We conclude that the independent components are

$$\Gamma^{1222}_{\sigma\sigma'}(\nu, \nu'), \quad \Gamma^{2111}_{\sigma\sigma'}(\nu, \nu'), \quad \Gamma^{1122}_{\sigma\sigma'}(\nu, \nu' \leq \nu),$$
$$\Gamma^{1221}_{\sigma\sigma'}(\nu, \nu' \leq \nu), \quad \mathrm{Im}\,\Gamma^{1212}_{\sigma\sigma'}(\nu, \nu'), \quad \mathrm{Im}\,\Gamma^{1111}_{\sigma\sigma'}(\nu, \nu' \leq \nu).$$
$$(C5)$$

With the arguments $(\nu, \nu' \leq \nu)$, we indicate that there is a symmetry in $(\nu \leftrightarrow \nu')$, so that it in principles suffices to compute only half of the data points in the frequency plane.

By using these symmetries, we find the following identities for the causal vertex:

$$\mathrm{Re}\,\Gamma^{\mathrm{causal}} = \tfrac{1}{2}\,\mathrm{Re}(\Gamma^{1222} + \Gamma^{2212} + \Gamma^{2111} + \Gamma^{1121})$$
$$= \tfrac{1}{2}\,\mathrm{Re}(\Gamma^{1222} + \Gamma^{2111}) + (\nu \leftrightarrow \nu'), \quad (C6a)$$

$$\mathrm{Im}\,\Gamma^{\mathrm{causal}} = \tfrac{1}{4}\,\mathrm{Im}(2\Gamma^{1212} + 2\Gamma^{1221} + \Gamma^{1122}$$
$$+ \Gamma^{2211} + \Gamma^{1111})$$
$$= \tfrac{1}{4}\,\mathrm{Im}(\Gamma^{1212} + \Gamma^{1221} + \Gamma^{1122} + \tfrac{1}{2}\Gamma^{1111})$$
$$+ (\nu \leftrightarrow \nu'). \qquad (C6b)$$

Appendix D: Vertex estimators using the total correlator

In this Appendix, we derive sIEs for 3p and 4p vertices involving only total correlators, useful for methods like QMC, as discussed in Sec. IV G. The main results are Eqs. (D4), (D8), and (D11). These estimators have a form similar to those using the connected correlators and the same perturbative and asymptotic properties (see Secs. IV E and IV F). The estimators of this section have additional terms involving the self-energy to cancel disconnected contributions.

Below, we derive the relations for fermionic systems in normal (non-superconducting) phases preserving the U(1) charge symmetry, ruling out terms like $\langle d^{(\dagger)}_\sigma \rangle$ and $\langle d_\uparrow d_\downarrow \rangle$ in the disconnected parts. We add subscripts to correlators to distinguish the connected part ('con'), the disconnected part ('dis'), and the total ('tot') correlator; $G_{\mathrm{tot}} = G_{\mathrm{con}} + G_{\mathrm{dis}}$. For later use, we define

$$\widetilde{\Sigma} = \Sigma - \Sigma^{\mathrm{H}} X. \qquad (D1)$$

This modified self-energy is $\mathcal{O}(U^2)$ in the perturbative limit and decays to zero in the large-frequency limit.

We begin with the 3p vertex estimator [Eq. (120)]

$$\Gamma^{(34)} = \mathcal{K}^{(34)}_{\mathrm{con}} + G^{(12,34)}_{\mathrm{con}} + \Gamma_{\mathrm{bare}}. \qquad (D2)$$

The second term is an auxiliary correlator defined in terms of a 2p bosonic connected correlator [Eq. (100)]. The corresponding disconnected part is

$$G^{(12,34)}_{\mathrm{dis}} = P^{k_1 k_2 k_{12}} P^{k_3 k_4 k_{34}} G^{k_{12} k_{34}}_{\mathrm{dis}}[q_{12}, q_{34}]$$
$$= 2\pi\delta(\omega_{12}) X^{k_1 k_2} X^{k_3 k_4} \Sigma^{\mathrm{H}}_{12} \Sigma^{\mathrm{H}}_{34}, \qquad (D3)$$

where we used $\langle q_{12} \rangle = \Sigma^{\mathrm{H}}_{12}$ [Eq. (99)]. Note that $\delta(\omega_{12})$ and $\delta(\omega_{34})$ can be used interchangeably because the energy conservation constraint, $\omega_{1234} = 0$, is implicitly understood. In the MF, the Dirac delta function $2\pi\delta(\omega_{12})$ is replaced by the Kronecker delta $\beta\delta_{\omega_{12},0}$. Similarly deriving the disconnected parts for other bosonic 2p correlators and using $q_{23} = -\zeta q_{32}$, we find

$$G^{(12,34)}_{\mathrm{con}} = G^{(12,34)}_{\mathrm{tot}} - 2\pi\delta(\omega_{12}) X^{k_1 k_2} \Sigma^{\mathrm{H}}_{12} X^{k_3 k_4} \Sigma^{\mathrm{H}}_{34},$$
$$G^{(13,24)}_{\mathrm{con}} = G^{(13,24)}_{\mathrm{tot}},$$
$$G^{(14,23)}_{\mathrm{con}} = G^{(14,23)}_{\mathrm{tot}} + 2\pi\delta(\omega_{14}) \zeta X^{k_1 k_4} \Sigma^{\mathrm{H}}_{14} X^{k_3 k_2} \Sigma^{\mathrm{H}}_{32}.$$
$$(D4)$$

For the first term $\mathcal{K}^{34}_{\mathrm{con}}$ in Eq. (D2), which is defined via Eq. (118) and is related to the $\mathcal{K}_2$ asymptotic class

[Eq. (139)], the disconnected part is given by

$$\mathcal{K}_{\mathrm{dis}}^{(34)} = \sum_{\substack{x_n \in \{n,\cdot\} \\ n \in \{1,2\}}} L_{x_1} G_{\mathrm{dis}}^{(x_1,x_2,34)} L_{x_2}$$
$$= \Sigma_1 G_{\mathrm{dis}}^{(\cdot,\cdot,34)} \Sigma_2 - X_1 G_{\mathrm{dis}}^{(1,\cdot,34)} \Sigma_2$$
$$- \Sigma_1 G_{\mathrm{dis}}^{(\cdot,2,34)} X_2 + X_1 G_{\mathrm{dis}}^{(1,2,34)} X_2. \qquad (D5)$$

This result involves diagrams in which the first and second legs are disconnected from the third and fourth legs. For example, the disconnected part of $G^{(\cdot,\cdot,34)}$ reads

$$G_{\mathrm{dis}}^{(\cdot,\cdot,34)} = P^{k_3 k_4 34} G_{\mathrm{dis}}^{k_1 k_2 34}[d_1, d_2^\dagger, q_{34}]$$
$$= 2\pi\delta(\omega_{12}) X^{k_3 k_4} \Sigma_{34}^{\mathrm{H}} G_{12}^{(\cdot,\cdot)}, \qquad (D6)$$

where we again used $\langle q_{34}\rangle = \Sigma_{34}^{\mathrm{H}}$ [Eq. (99)]. By applying the same procedure to all terms in Eq. (D5), we find

$$\mathcal{K}_{\mathrm{dis}}^{(34)} = 2\pi\delta(\omega_{12}) X^{k_3 k_4} \Sigma_{34}^{\mathrm{H}} \big(\Sigma G^{(\cdot,\cdot)}\Sigma - XG^{(1,\cdot)}\Sigma$$
$$- \Sigma G^{(\cdot,2)}X + XG^{(1,2)}X\big)_{12}^{k_1 k_2}$$
$$= 2\pi\delta(\omega_{12}) X^{k_3 k_4} \Sigma_{34}^{\mathrm{H}} \widetilde{\Sigma}_{12}^{k_1 k_2}. \qquad (D7)$$

For the second equality, we employed the self-energy estimators (105) and (108). Using Eqs. (D4) and (D7) to convert the right side of Eq. (D2) to the total correlator, we find the desired 3p vertex estimator. In the following, we also list the sIEs for other 3p vertices which can be derived similarly,

$$\mathcal{K}_{\mathrm{con}}^{(12)} = \mathcal{K}_{\mathrm{tot}}^{(12)} - 2\pi\delta(\omega_{12})\widetilde{\Sigma}_{34}^{k_3 k_4} X^{k_1 k_2} \Sigma_{12}^{\mathrm{H}},$$
$$\mathcal{K}_{\mathrm{con}}^{(13)} = \mathcal{K}_{\mathrm{tot}}^{(13)},$$
$$\mathcal{K}_{\mathrm{con}}^{(14)} = \mathcal{K}_{\mathrm{tot}}^{(14)} - 2\pi\delta(\omega_{14})\zeta\widetilde{\Sigma}_{32}^{k_3 k_2} X^{k_1 k_4} \Sigma_{14}^{\mathrm{H}},$$
$$\mathcal{K}_{\mathrm{con}}^{(23)} = \mathcal{K}_{\mathrm{tot}}^{(23)} + 2\pi\delta(\omega_{14})\zeta\widetilde{\Sigma}_{14}^{k_1 k_4} X^{k_3 k_2} \Sigma_{32}^{\mathrm{H}},$$
$$\mathcal{K}_{\mathrm{con}}^{(24)} = \mathcal{K}_{\mathrm{tot}}^{(24)},$$
$$\mathcal{K}_{\mathrm{con}}^{(34)} = \mathcal{K}_{\mathrm{tot}}^{(34)} - 2\pi\delta(\omega_{12})\widetilde{\Sigma}_{12}^{k_1 k_2} X^{k_3 k_4} \Sigma_{34}^{\mathrm{H}}. \qquad (D8)$$

After replacing the connected auxiliary correlators by the total ones, a disconnected term involving self-energies is subtracted. In Eq. (D8), thanks to $\widetilde{\Sigma}$, the $\mathcal{K}^{(34)}$ estimator is still manifestly $\mathcal{O}(U^3)$ in the perturbative limit and decays in the $|\omega_1| \to \infty$ or $|\omega_2| \to \infty$ limits. Note that by shifting the noninteracting and interacting Hamiltonian by $\Sigma_{ij}^{\mathrm{H}} d_i^\dagger d_j$ and $-\Sigma_{ij}^{\mathrm{H}} d_i^\dagger d_j$, respectively, the Hartree self-energy and the disconnected part of the 3p vertex estimators can be eliminated.

We close with the 4p vertex estimator (130). As most terms already appear in the 3p estimator, it suffices to consider the core vertex Γ_{core} [Eq. (131)]. In the normal (non-superconducting) phase, a disconnected 4p correlator has legs 1 and 2 disconnected from 3 and 4, or legs 1 and 4 disconnected from 2 and 3. The first case gives

$$\Gamma_{\mathrm{core, dis\text{-}12}}$$

$$= 2\pi\delta(\omega_{12}) \sum_{\substack{x_n \in \{n,\cdot\} \\ n \in \{1,2,3,4\}}} L_{x_1} L_{x_3} G_{12}^{(x_1,x_2)} G_{34}^{(x_3,x_4)} L_{x_2} L_{x_4}$$
$$= 2\pi\delta(\omega_{12}) \sum_{\substack{x_n \in \{n,\cdot\} \\ n \in \{1,2\}}} L_{x_1} G_{12}^{(x_1,x_2)} L_{x_2} \sum_{\substack{x_n \in \{n,\cdot\} \\ n \in \{3,4\}}} L_{x_3} G_{34}^{(x_3,x_4)} L_{x_4}$$
$$= 2\pi\delta(\omega_{12})\widetilde{\Sigma}_{12}^{k_1 k_2}\widetilde{\Sigma}_{34}^{k_3 k_4}, \qquad (D9)$$

where $\widetilde{\Sigma}$ appears as in Eq. (D5). Similarly, the second term reads

$$\Gamma_{\mathrm{core, dis\text{-}14}} = 2\pi\delta(\omega_{14})\zeta\widetilde{\Sigma}_{12}^{k_1 k_2}\widetilde{\Sigma}_{34}^{k_3 k_4}. \qquad (D10)$$

Thus, the vertex estimator is

$$\Gamma_{\mathrm{core}} = \Gamma_{\mathrm{core, tot}} - 2\pi\delta(\omega_{12})\widetilde{\Sigma}_{12}^{k_1 k_2}\widetilde{\Sigma}_{34}^{k_3 k_4}$$
$$- 2\pi\delta(\omega_{14})\zeta\widetilde{\Sigma}_{14}^{k_1 k_4}\widetilde{\Sigma}_{32}^{k_3 k_2}. \qquad (D11)$$

Again, disconnected terms involving the self-energy are subtracted. Since $\widetilde{\Sigma}$ is of order $\mathcal{O}(U^2)$ in the perturbative limit and decays in the large-frequency limit, the perturbative and asymptotic behavior of Γ_{core} is preserved. Substituting Eqs. (D4), (D8), and (D11) into Eq. (130), we get the estimator (141) for the total vertex.

Appendix E: Details of the NRG implementation

For quantum impurity models, it is possible to compute local multipoint correlators with NRG using a strategy described in detail in Ref. [13]. In this appendix, we describe some further refinements of this strategy, needed to obtain the results shown in the present paper.

1. Barycentric binning

In essence, the NRG is a scheme iteratively diagonalizing a discretized representation of a quantum impurity model [11]. The states generated during the iterative diagonalization can be used to construct a complete set of approximate eigenstates for the interacting Wilson chain Hamiltonian, $\mathcal{H}|\underline{i}\rangle \approx E_{\underline{i}}|\underline{i}\rangle$. These can be used in Lehmann-type representations for partial spectral functions (PSFs), with matrix elements $\langle\underline{i}|\mathcal{O}|\underline{j}\rangle = \mathcal{O}_{\underline{ij}}$ and energy differences $E_{\underline{i1}} = E_{\underline{i}} - E_{\underline{1}}$. The Lehmann representation for an ℓp PSF has the form of a sum over the transitions between these eigenstates, containing many discrete delta functions [12, 13]:

$$S[\mathcal{O}](\varepsilon_1,\cdots,\varepsilon_{\ell-1}) = \sum_{\underline{1},\cdots,\underline{\ell}} \rho_{\underline{1}} \prod_{i=1}^{\ell-1} [\mathcal{O}_{\underline{i\,i+1}}^i \delta(\varepsilon_i - E_{\underline{i1}})] \mathcal{O}_{\underline{\ell 1}}^\ell. \qquad (E1)$$

These delta functions are collected by "binning" [55–57], which shifts the energy $E_{\underline{i1}}$ to the nearest grid point of a pre-determined grid. The grid is chosen to have logarithmic spacing to capture the logarithmic discretization

of the bath in NRG. For $\ell > 2$, one must be able to capture the dependence of multiple frequencies of different magnitudes. To this end, Ref. [13] introduced a "slicing" scheme, which encodes the frequency binning directly in the tensor representation of $\mathcal{O}$. However, the slicing approach yields a factor $(N_\varepsilon)^{\ell-2}$ to the computational cost, with N_ε the number of bins. Thus, it is desirable to use as few bins as possible to reduce the computational cost. On the other hand, using too coarse a grid leads to large errors from shifting energies for binning.

To minimize the error arising from binning with moderate computational cost, we use a barycentric binning scheme, which attributes the spectral weight to both adjacent bins (instead of the single nearest bin) in order to conserve the barycenter. Hence, to bin a delta function $\delta(\varepsilon - E_{\underline{21}})$, we first find the grid points $\underline{\varepsilon}_n$ and $\underline{\varepsilon}_{n+1}$ just below and above the transition energy: $\underline{\varepsilon}_n < E_{\underline{21}} < \underline{\varepsilon}_{n+1}$. Then, we split the weight of the delta function to these two bins with weights inversely proportional to the distance in the logarithmic scale:

$$\delta(\varepsilon - E_{\underline{21}}) \approx w\delta(\varepsilon - \underline{\varepsilon}_n) + (1-w)\delta(\varepsilon - \underline{\varepsilon}_{n+1}),$$
$$w = \frac{\ln\left|\underline{\varepsilon}_{n+1}\right| - \ln\left|E_{\underline{21}}\right|}{\ln\left|\underline{\varepsilon}_{n+1}\right| - \ln\left|\underline{\varepsilon}_n\right|}. \quad \text{(E2)}$$

Though one needs to consider two bins for a single spectral contribution, the total number of relevant bins does not double, but merely increase by $\sim 30\%$, since the bins are typically clustered [13, 58]. Additionally, with the barycentric scheme, the binning error is largely suppressed, allowing for a much coarser frequency grid (cf. Sec. E 4), decreasing the overall computational cost.

2. Log-Gaussian broadening

To obtain smooth functions, the discrete PSFs obtained from the Lehmann representation need to be broadened. Conversion from a binned, discrete PSF $S(\underline{\varepsilon})$ to a continuous one $\widetilde{S}(\varepsilon)$ can be written as an integration involving a broadening kernel B_i:

$$\widetilde{S}(\boldsymbol{\varepsilon}) = \int d^{\ell-1}\underline{\varepsilon}\, S(\underline{\varepsilon}) \prod_{i=1}^{\ell-1} B_i(\varepsilon_i, \underline{\varepsilon}'_i). \quad \text{(E3)}$$

For 2p calculations, the usual choice of the broadening kernel is a convolution of a log-Gaussian and a Fermi-Dirac function [11, 13, 56, 59]:

$$B_{\mathrm{LG+F}}(\varepsilon, \underline{\varepsilon}) = \int d\varepsilon'\, \delta_{\mathrm{F}}(\varepsilon, \varepsilon')\delta_{\mathrm{LG}}(\varepsilon', \underline{\varepsilon}),$$

$$\delta_{\mathrm{sLG}}(\varepsilon', \underline{\varepsilon}) = \frac{\Theta(\varepsilon'\underline{\varepsilon})}{\sqrt{\pi}\sigma_{\mathrm{LG}}|\underline{\varepsilon}|} \exp\left[-\left(\frac{\ln|\underline{\varepsilon}/\varepsilon'|}{\sigma_{\mathrm{LG}}} - \frac{\sigma_{\mathrm{LG}}}{4}\right)^2\right],$$

$$\delta_{\mathrm{cLG}}(\varepsilon', \underline{\varepsilon}) = \frac{\Theta(\varepsilon'\underline{\varepsilon})}{\sqrt{\pi}\sigma_{\mathrm{LG}}|\underline{\varepsilon}|} \exp\left(-\frac{\ln^2|\underline{\varepsilon}/\varepsilon'|}{\sigma_{\mathrm{LG}}^2} - \frac{\sigma_{\mathrm{LG}}^2}{4}\right),$$

$$\delta_{\mathrm{F}}(\varepsilon, \varepsilon') = \frac{1}{2\gamma_{\mathrm{F}}}\left(1 + \cosh\frac{\varepsilon - \varepsilon'}{\gamma_{\mathrm{F}}}\right)^{-1}. \quad \text{(E4)}$$

In the first line on the right, LG stands for either symmetric log-Gaussian (sLG), used for fermionic operators, or centered log-Gaussian (cLG), used for bosonic operators (following Ref. [13]). The log-Gaussian broadening smooths the logarithmically-spaced discrete data resulting from discretization. The subsequent Fermi broadening removes artifacts at low frequency $\varepsilon \sim T$. The broadening width is proportional to the discrete frequency in the former and fixed in the latter. Correspondingly, the broadening parameter σ_{LG} is dimensionless, while γ_{F} has the dimension of energy.

In Refs. [12, 13], a Lorentzian kernel

$$B_{\mathrm{L}}(\varepsilon, \underline{\varepsilon}) = \frac{1}{\pi}\frac{(\sigma_{\mathrm{L}}|\underline{\varepsilon}| + \gamma_{\mathrm{L}})}{(\varepsilon - \underline{\varepsilon})^2 + (\sigma_{\mathrm{L}}|\underline{\varepsilon}| + \gamma_{\mathrm{L}})^2} \quad \text{(E5)}$$

was used for 3p and 4p calculations because, for the aIE used there, log-Gaussian broadening turned out to yield seemingly under-broadened results.

Here, we find that, using sIEs, log-Gaussian broadening does *not* yield under-broadening. On the contrary, we find that, as in the 2p case, log-Gaussian broadening is preferable to Lorentzian broadening for multipoint correlators because the Lorentzian kernel strongly over-broadens low-frequency features. For example, Fig. 22 shows that the vertex obtained with Lorentzian broadening [Fig. 22(a)] violates the FDT much more strongly than those obtained with log-Gaussian and Fermi broadening [Fig. 22(b)]. Thus, we use the log-Gaussian and Fermi broadening (E4) for all calculations.

In this work, the broadening parameters in Eqs. (E4) were chosen as $\sigma_{\mathrm{LG}} = 0.3$ and $\gamma_{\mathrm{F}} = 0.5T$ throughout; these were the smallest values that remove the wiggles signalling under-broadening. For the Lorentian broadening results, we used $\sigma_{\mathrm{L}} = 0.6$ and $\gamma_{\mathrm{L}} = 3T$ in Figs. 14(c) and 17(c), which are the parameters used in Refs. [12, 13].

3. Diagonalization of the kept density matrix

As discussed in App. B of Ref. [13], the two sources of error in subtracting disconnected parts from the PSFs are (i) finite off-diagonal elements of the density matrices in the kept sectors, and (ii) binning. Effect of the latter is minimized by using the barycentric binning explained in App. E 1. To eliminate the former source of error, we re-diagonalize the kept-sector density matrices that are constructed by the standard full-density-matrix NRG. The re-diagonalizing basis is taken as the kept energy eigenstates (overriding those obtained during the iterative diagonalization), and we identify the corresponding energy eigenvalues as the diagonal elements of the kept-sector Hamiltonian in the re-diagonalizing basis.

4. Computational parameters

In NRG, the bath is discretized on a logarithmic grid with grid points $\pm D\Lambda^{-k-z}$, where $k \geq 0$ is an integer and

(a) Lorentzian

(b) Log-Gaussian + Fermi
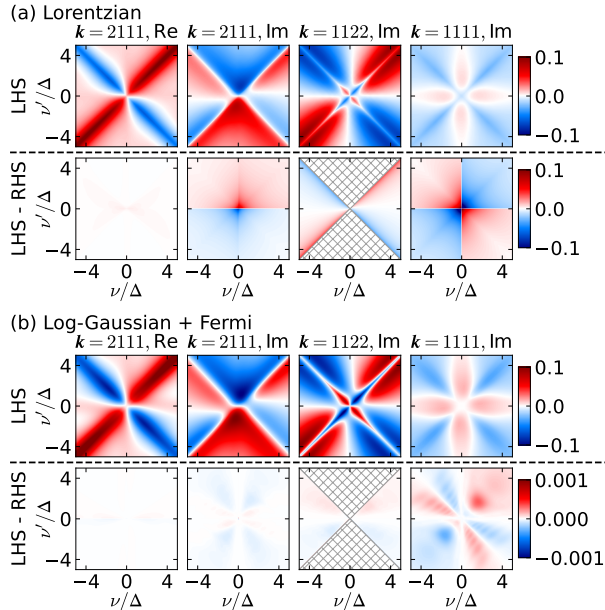
FIG. 22. FDRs of the KF 4p vertex, analogous to Fig. 19 but at weak interaction (parameters: same as for Fig. 14), obtained with sIEs and (a) a Lorentzian broadening (E5) with $\sigma_\mathrm{L} = 0.3$ and $\gamma_\mathrm{L} = 0.5T$, and (b) log-Gaussian and Fermi broadening (E4) with $\sigma_\mathrm{LG} = 0.3$ and $\gamma_\mathrm{F} = 0.5T$. Note that the colorscale for the panels showing FDR violation (lower row, LHS−RHS) is two orders smaller in (b) than in (a).

$z \in (0, 1]$ is a shift parameter [60]. PSFs computed with $z = 1/n_z, 2/n_z, \cdots, 1$ are averaged to reduce discretization artifact. In this work, we used $\Lambda = 4$ and $n_z = 4$, and kept $N_\mathrm{keep} = 200$ multiplets respecting U(1) charge and SU(2) spin symmetries in the iterative diagonalization of the Wilson chain.

The transition energies are collected in logarithmically spaced bins [13]. The bins are located at $\underline{\varepsilon}[\pm m] = \pm 10^{(|m|-1)/n_\mathrm{dec}} \varepsilon_\mathrm{min}$ for nonzero integer m and $\underline{\varepsilon}[0] = 0$. We used $n_\mathrm{dec} = 8$ ($n_\mathrm{dec} = 16$) bins per decade for the AIM with weak interaction Fig. 14 (strong interaction Fig. 17), and set $\varepsilon_\mathrm{min} = T/20$. Using $n_\mathrm{dec} = 16$

was needed to get the low-energy vertices for the AIM at strong interaction in better agreement with RPT as shown in Fig. 18. Figure 23 shows that the agreement of the MF vertex at the lowest fermionic frequencies with the RPT vertex improves for the larger $n_\mathrm{dec} = 16$.

To evaluate an ℓp sIE, one needs to compute 2^ℓ ℓp auxiliary correlators [Eq. (131)], where each correlator involves $\ell!$ PSFs. For the 4p case, this amounts to $2^4 \times 4! = 384$ PSFs in total. In practice, one can utilize symmetries to reduce the number of PSFs evaluated. Here, we use the SU(2) symmetry of the Hamiltonian and the permutation symmetry of the PSFs to reduce the number of independent 4p PSFs to 120. These PSFs can all be computed in parallel. Although we consider the single-orbital AIM only at half-filling, we did not exploit particle-hole symmetry.
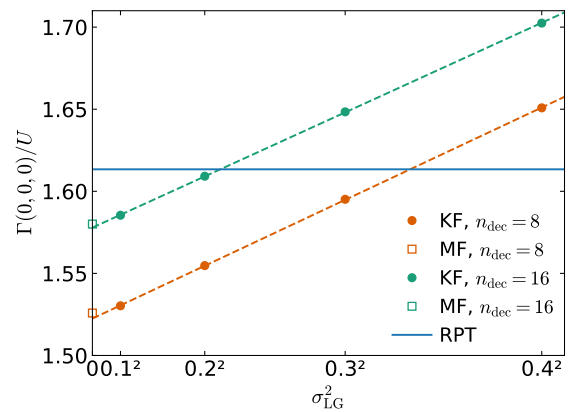
FIG. 23. Dependence of the zero-energy KF vertex $\Gamma^\mathrm{causal}_{\uparrow\downarrow}(0, 0, 0)$ and the average of the MF vertices $\Gamma_{\mathrm{M},\uparrow\downarrow}(\pm i\pi T, \pm i\pi T, 0)$ in the AIM at strong interaction (parameters: same as for Fig. 17) on σ^2_LG and n_dec. Dashed lines are linear fits of the KF results, shown in circles. Larger n_dec gives MF vertices in better agreement with RPT, while the KF vertices are further affected by broadening.

[1] A. Georges, G. Kotliar, W. Krauth, and M. J. Rozenberg, Dynamical mean-field theory of strongly correlated fermion systems and the limit of infinite dimensions, Rev. Mod. Phys. **68**, 13 (1996).

[2] G. Kotliar, S. Y. Savrasov, K. Haule, V. S. Oudovenko, O. Parcollet, and C. A. Marianetti, Electronic structure calculations with dynamical mean-field theory, Rev. Mod. Phys. **78**, 865 (2006).

[3] G. Rohringer, H. Hafermann, A. Toschi, A. A. Katanin, A. E. Antipov, M. I. Katsnelson, A. I. Lichtenstein, A. N. Rubtsov, and K. Held, Diagrammatic routes to nonlocal correlations beyond dynamical mean field theory, Rev.

Mod. Phys. **90**, 025003 (2018).

[4] T. Ribic, G. Rohringer, and K. Held, Nonlocal correlations and spectral properties of the Falicov–Kimball model, Phys. Rev. B **93**, 195105 (2016).

[5] P. Thunström, O. Gunnarsson, S. Ciuchi, and G. Rohringer, Analytical investigation of singularities in two-particle irreducible vertex functions of the hubbard atom, Phys. Rev. B **98**, 235107 (2018).

[6] G. Rohringer, A. Valli, and A. Toschi, Local electronic correlation at the two-particle level, Phys. Rev. B **86**, 125114 (2012).

[7] J. Kuneš, Efficient treatment of two-particle vertices in

dynamical mean-field theory, Phys. Rev. B **83**, 085102 (2011).

[8] H. Hafermann, K. R. Patton, and P. Werner, Improved estimators for the self-energy and vertex function in hybridization-expansion continuous-time quantum Monte Carlo simulations, Phys. Rev. B **85**, 205106 (2012).

[9] T. Schäfer, G. Rohringer, O. Gunnarsson, S. Ciuchi, G. Sangiovanni, and A. Toschi, Divergent precursors of the Mott–Hubbard transition at the two-particle level, Phys. Rev. Lett. **110**, 246405 (2013).

[10] J. Kaufmann, P. Gunacker, A. Kowalski, G. Sangiovanni, and K. Held, Symmetric improved estimators for continuous-time quantum Monte Carlo, Phys. Rev. B **100**, 075119 (2019).

[11] R. Bulla, T. A. Costi, and T. Pruschke, Numerical renormalization group method for quantum impurity systems, Rev. Mod. Phys. **80**, 395 (2008).

[12] F. B. Kugler, S.-S. B. Lee, and J. von Delft, Multipoint correlation functions: Spectral representation and numerical evaluation, Phys. Rev. X **11**, 041006 (2021).

[13] S.-S. B. Lee, F. B. Kugler, and J. von Delft, Computing local multipoint correlators using the numerical renormalization group, Phys. Rev. X **11**, 041007 (2021).

[14] M. Jarrell, Hubbard model in infinite dimensions: A quantum Monte Carlo study, Phys. Rev. Lett. **69**, 168 (1992).

[15] M. Sweeny, Monte Carlo study of weighted percolation clusters relevant to the Potts models, Phys. Rev. B **27**, 4445 (1983).

[16] U. Wolff, Lattice field theory as a percolation process, Phys. Rev. Lett. **60**, 1461 (1988).

[17] W. Bietenholz, A. Pochinsky, and U. J. Wiese, Meron-cluster simulation of the θ vacuum in the 2d $O(3)$ model, Phys. Rev. Lett. **75**, 4524 (1995).

[18] R. Bulla, A. C. Hewson, and T. Pruschke, Numerical renormalization group calculations for the self-energy of the impurity anderson model, J. Phys. Condens. Matter **10**, 8365 (1998).

[19] B. Ammon, H. G. Evertz, N. Kawashima, M. Troyer, and B. Frischmuth, Quantum Monte Carlo loop algorithm for the $t-j$ model, Phys. Rev. B **58**, 4304 (1998).

[20] R. Assaraf and M. Caffarel, Zero-variance principle for Monte Carlo algorithms, Phys. Rev. Lett. **83**, 4682 (1999).

[21] A. S. Mishchenko, N. V. Prokof'ev, A. Sakamoto, and B. V. Svistunov, Diagrammatic quantum Monte Carlo study of the Fröhlich polaron, Phys. Rev. B **62**, 6317 (2000).

[22] F. B. Kugler, Improved estimator for numerical renormalization group calculations of the self-energy, Phys. Rev. B **105**, 245132 (2022).

[23] G. Stefanucci and R. Van Leeuwen, *Nonequilibrium many-body theory of quantum systems: a modern introduction* (Cambridge University Press, 2013).

[24] R. Bulla, T. A. Costi, and D. Vollhardt, Finite-temperature numerical renormalization group study of the Mott transition, Phys. Rev. B **64**, 045103 (2001).

[25] A. Galler, P. Thunström, P. Gunacker, J. M. Tomczak, and K. Held, *Ab initio* dynamical vertex approximation, Phys. Rev. B **95**, 115107 (2017).

[26] N. Wentzell, G. Li, A. Tagliavini, C. Taranto, G. Rohringer, K. Held, A. Toschi, and S. Andergassen, High-frequency asymptotics of the vertex function: Diagrammatic parametrization and algorithmic implementation, Phys. Rev. B **102**, 085106 (2020).

[27] L. Hedin, New method for calculating the one-particle Green's function with application to the electron-gas problem, Phys. Rev. **139**, A796 (1965).

[28] A. A. Katanin, A. Toschi, and K. Held, Comparing pertinent effects of antiferromagnetic fluctuations in the two- and three-dimensional Hubbard model, Phys. Rev. B **80**, 075104 (2009).

[29] A. Rubtsov, M. Katsnelson, and A. Lichtenstein, Dual boson approach to collective excitations in correlated fermionic systems, Ann. Phys. **327**, 1320 (2012).

[30] T. Ayral and O. Parcollet, Mott physics and spin fluctuations: A unified framework, Phys. Rev. B **92**, 115109 (2015).

[31] E. G. C. P. van Loon, F. Krien, H. Hafermann, A. I. Lichtenstein, and M. I. Katsnelson, Fermion-boson vertex within dynamical mean-field theory, Phys. Rev. B **98**, 205148 (2018).

[32] F. Krien, A. Valli, and M. Capone, Single-boson exchange decomposition of the vertex function, Phys. Rev. B **100**, 155149 (2019).

[33] F. Krien and A. Valli, Parquetlike equations for the Hedin three-leg vertex, Phys. Rev. B **100**, 245147 (2019).

[34] F. Krien, A. Valli, P. Chalupa, M. Capone, A. I. Lichtenstein, and A. Toschi, Boson-exchange parquet solver for dual fermions, Phys. Rev. B **102**, 195131 (2020).

[35] F. Krien, A. Kauch, and K. Held, Tiling with triangles: Parquet and $GW\gamma$ methods unified, Phys. Rev. Res. **3**, 013149 (2021).

[36] J. Kaufmann, P. Gunacker, and K. Held, Continuous-time quantum Monte Carlo calculation of multiorbital vertex asymptotics, Phys. Rev. B **96**, 035114 (2017).

[37] F. B. Kugler and J. v. Delft, Multiloop functional renormalization group for general models, Phys. Rev. B **97**, 035162 (2018).

[38] F. B. Kugler and J. v. Delft, Derivation of exact flow equations from the self-consistent parquet relations, New J. Phys. **20**, 123029 (2018).

[39] M. Gievers, E. Walter, A. Ge, J. von Delft, and F. B. Kugler, Multiloop flow equations for single-boson exchange fRG, Eur. Phys. J. B **95**, 108 (2022).

[40] A. Hewson, A. Oguri, and D. Meyer, Renormalized parameters for impurity models, Eur. Phys. J. B **40**, 177 (2004).

[41] A. Oguri and A. C. Hewson, Higher-order Fermi-liquid corrections for an Anderson impurity away from half filling, Phys. Rev. Lett. **120**, 126802 (2018).

[42] A. Oguri and A. C. Hewson, Higher-order Fermi-liquid corrections for an Anderson impurity away from half filling: Equilibrium properties, Phys. Rev. B **97**, 045406 (2018).

[43] A. Oguri, Y. Teratani, K. Tsutsumi, and R. Sakano, Current noise and Keldysh vertex function of an Anderson impurity in the Fermi-liquid regime, Phys. Rev. B **105**, 115409 (2022).

[44] V. Zlatić and B. Horvatić, Series expansion for the symmetric Anderson Hamiltonian, Phys. Rev. B **28**, 6904 (1983).

[45] A. Ge, N. Ritz, E. Walter, S. Aguirre, J. von Delft, and F. B. Kugler, Real-frequency quantum field theory applied to the single-impurity Anderson model, arXiv:2307.10791 (2023).

[46] A. C. Hewson, Renormalized perturbation expansions

and fermi liquid theory, Phys. Rev. Lett. **70**, 4007 (1993).

[47] V. Pandis and A. C. Hewson, Analytic flow equations for the Fermi liquid parameters of the Anderson impurity model, Phys. Rev. Lett. **115**, 076401 (2015).

[48] F. B. Kugler, M. Zingl, H. U. R. Strand, S.-S. B. Lee, J. von Delft, and A. Georges, Strongly correlated materials from a numerical renormalization group perspective: How the Fermi-liquid state of Sr_2RuO_4 emerges, Phys. Rev. Lett. **124**, 016401 (2020).

[49] E. Wang and U. Heinz, Generalized fluctuation-dissipation theorem for nonlinear response functions, Phys. Rev. D **66**, 025008 (2002).

[50] A. Ge, *Analytic Continuation of Correlators from the Matsubara to the Keldysh Formalism*, Ph.D. thesis, Ludwig-Maximilians-Universität München (2020).

[51] A. Ge, J. Halbinger, J. von Delft, S.-S. B. Lee, and F. B. Kugler, Analytic continuation of multi-point functions, unpublished (2023).

[52] L. V. Keldysh, Diagram technique for nonequilibrium processes, Sov. Phys. JETP **20**, 1018 (1965).

[53] M. Gell-Mann and F. Low, Bound states in quantum field theory, Phys. Rev. **84**, 350 (1951).

[54] S. G. Jakobs, M. Pletyukhov, and H. Schoeller, Properties of multi-particle Green's and vertex functions within Keldysh formalism, J. Phys. A **43**, 103001 (2010).

[55] R. Peters, T. Pruschke, and F. B. Anders, Numerical renormalization group approach to Green's functions for quantum impurity models, Phys. Rev. B **74**, 245114 (2006).

[56] A. Weichselbaum and J. von Delft, Sum-rule conserving spectral functions from the numerical renormalization group, Phys. Rev. Lett. **99**, 076402 (2007).

[57] A. Weichselbaum, Tensor networks and the numerical renormalization group, Phys. Rev. B **86**, 245124 (2012).

[58] S.-S. B. Lee and A. Weichselbaum, Adaptive broadening to improve spectral resolution in the numerical renormalization group, Phys. Rev. B **94**, 235127 (2016).

[59] S.-S. B. Lee and A. Weichselbaum, Adaptive broadening to improve spectral resolution in the numerical renormalization group, Phys. Rev. B **94**, 235127 (2016).

[60] R. Žitko and T. Pruschke, Energy resolution and discretization artifacts in the numerical renormalization group, Phys. Rev. B **79**, 085106 (2009).

7 Quantum criticality and disorder in two-dimensional metals

In this chapter, we turn to the study of continuous quantum phase transitions, a rather different topic compared to the previous chapters. The ensuing analysis is based on the field-theoretic path integral formalism rather than the operator-based Hamiltonian formalism of the previous chapters. For a comprehensive introduction to field theories in the context of condensed matter physics, we refer the reader to the literature, e.g., Refs. [AS10, Kam23].

Nevertheless, the recurring theme of this thesis, the application of correlation function methods, carries on; this time, they are used to determine properties of two-dimensional metals near an antiferromagnetic instability at zero temperature in the presence of quenched disorder. The physical relevance of these systems was already motivated in the introduction. However, to facilitate the discussion of our publication [P1], we present a brief review of quantum criticality and disorder in Sec. 7.1.[1] We start by deriving a schematic phase diagram of quantum critical models in Sec. 7.1.1. In Sec. 7.1.2, we then motivate a low-energy effective action to study antiferromagnetic spin-density wave quantum criticality and discuss various approaches to derive physical properties in Sec. 7.1.3. After a short review of quenched disorder in Sec. 7.1.4, we finally present our publication [P1] in Sec. 7.2.

7.1 Basics of quantum criticality and disorder

7.1.1 Generic phase diagram for quantum criticality

To derive the generic phase diagram for models near a continuous quantum phase transition (see Fig. 7.1(a)), we closely follow Ref. [Voj03a]. We will assume a Hamiltonian $H = H_0 + H_{int}$ decomposed into a kinetic (H_0) and interacting, static (H_{int}) part, with $Z = \text{Tr}\left[e^{-\beta H}\right]$ the corresponding partition function.

Here, we are interested in continuous phase transitions separating two phases that are distinguished using a local order parameter $\vec{\phi}$:[2] A disordered phase, where the expectation value of $\vec{\phi}$ vanishes, $\langle \vec{\phi} \rangle = 0$, and an ordered phase, where $\langle \vec{\phi} \rangle \neq 0$. The phase transition is controlled by a parameter, e.g., temperature, that tunes the distance to the critical point, r, with $\langle \vec{\phi} \rangle$ developing a nonzero value at the critical point $r = 0$.

For classical systems, a long-range-ordered phase can emerge below a critical temperature T_c, such that $r \sim |T - T_c|$. In such systems, the partition function factorizes, $Z = Z_0 Z_{int}$, since $[H_0, H_{int}] = 0$. The phase transition is then usually driven by the static, non-Gaussian, interacting part of the theory, implying a static order parameter $\vec{\phi} = \vec{\phi}(\boldsymbol{x})$. Approaching the phase transition $r \to 0$, thermal fluctuations of the order parameter become correlated on an increasing length scale ξ, which is implicitly defined via $\langle \vec{\phi}(\boldsymbol{x})\vec{\phi}(\boldsymbol{0}) \rangle \sim e^{-|\boldsymbol{x}|/\xi}$ [AS10], until ξ diverges close to the critical point as

$$\xi \sim |r|^{-\nu}. \tag{7.1}$$

Here, $\nu > 0$ is a universal critical exponent associated with the divergence of the correlation length ξ.

In quantum mechanical systems, quantum phase transitions (QPTs) at $T = 0$ can occur by driving a non-thermal control parameter $\bar{r}$, e.g., pressure, doping, or the relative strength

---

1 Conceptually, the first three sections of Sec. 7.1 closely follow Ch. 2 of Ref. [Ger17].
2 For consistency with the following sections, we assume the order parameter to be a vector quantity.

of kinetic and interacting parts of the Hamiltonian. Then, order emerges below a critical value $\overline{r}_c$, implying $r \sim |\overline{r} - \overline{r}_c|$. In contrast to classical systems, statics and dynamics remain coupled in quantum systems, as we can generally expect that $[H_0, H_{int}] \neq 0$. Consequently, the order parameter is promoted to a dynamical field, $\vec{\phi} = \vec{\phi}(\tau, \boldsymbol{x})$.[3] Then, not only does the correlation length diverge as the quantum critical point (QCP) is approached, but quantum fluctuations of the order parameter become also correlated on increasing time scales ξ_τ

$$\xi_\tau \sim \xi^z \sim |r|^{-\nu z}, \tag{7.2}$$

with $z > 0$ the dynamical critical exponent.

Now one might ask: Given that quantum fluctuations drive QPTs at $T = 0$, which is experimentally inaccessible, do they influence physical properties at finite temperatures as well? To answer this question, two energy scales have to be compared: the temperature itself, being the typical energy of thermal fluctuations, and $\omega \sim \xi_\tau^{-1} \sim |r|^{\nu z}$, the typical energy of quantum fluctuations. Then, if $\omega \gg T$, quantum fluctuations play the predominant role, while they are negligible compared to temperature-induced fluctuations for $\omega \ll T$. The former case defines the so-called quantum critical region with boundaries $T \sim \omega \sim |r|^{\nu z}$, see Fig. 7.1(a).

In the remainder of this chapter, we are concerned with QPTs in two-dimensional ($2d$) metals. The normal state of metals is typically described by Landau's Fermi liquid theory. Therein, the basic assumption is that, at low T, the excitations of the interacting fermionic system can be described in terms of well-defined quasiparticles with quantum numbers identical to those of the non-interacting fermions [Mah00, Sac11]. The stability of the quasiparticles is justified by their increasing lifetime $\tau_{qp} \sim \varepsilon_{qp}^{-2}$ near the Fermi surface in the presence of interactions, where ε_{qp} is the quasiparticle energy relative to the Fermi surface [LRVW07]. As mentioned in the introduction, various strongly correlated materials, such as cuprates or iron pnictides, feature a strange metal phase [SCM14, GMPS20] with characteristics of physical observables in stark contrast with ordinary Fermi liquid predictions, for instance [Pim19]:

- The low-temperature electrical resistivity in the quantum critical region scales linearly in T, in contrast to the ordinary T^2 behaviour of a standard Fermi liquid [SCM14, GMPS20].

- Under the assumption of well-defined quasiparticles, the Mott-Ioffe-Regel limit constitutes a high-temperature bound for the resistivity if the mean free path ℓ of the quasiparticles becomes of the order of the lattice spacing. This bound is often violated in the quantum critical region [GCH03], indicating the absence of well-defined quasiparticles [EK95].

In the cuprates and iron pnictides, for instance, the strange metal phase appears to be associated with the quantum critical region of a QCP [SCM14, GMPS20]. Therefore, it is generally believed that abovementioned non-Fermi liquid hallmarks originate from strong interactions between electrons and order parameter fluctuations which destroy the well-defined quasiparticle nature of fermionic excitations [ACS03, MS10b].

7.1.2 Low-energy effective action for spin-density wave quantum criticality

A possible instability in $2d$ metals is a QPT to antiferromagnetic spin-density wave (SDW) order with ordering wave vector $\boldsymbol{Q} = (\pi, \pi)$ and has been studied extensively over the last decades [Her76, Mil93, AC00, ACS03, AC04, MS10b, SL15, SLL17, LSL17, SLL18]. To understand the origin of the low-energy effective action (LEEA) assumed in this context, it is

---

3 For simplicity, we work in the MF in most of this introductory section, while [P1] is formulated in the KF.

(a)

(b)
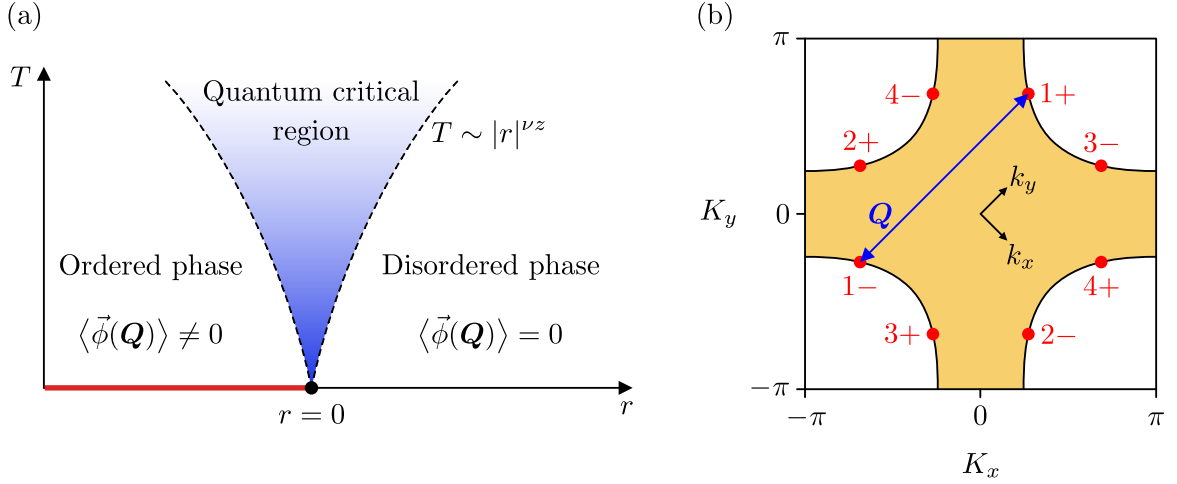
Figure 7.1 (a) Schematic phase diagram close to a quantum critical point at $r = 0$ and $T = 0$. Effects of quantum critical fluctuations are believed to influence observable properties in the quantum critical region. In two dimensions, long-range order at finite T by breaking a continuous symmetry is forbidden by the Mermin-Wagner theorem and therefore only occurs at $T = 0$ (red line). (Figure adapted from Refs. [Voj03a, Pim19].) (b) Fermi surface for the $2d$ Hubbard model on a square lattice including next-nearest-neighbor hopping. The parameters are $(\mu, t, t') = (-0.8, 1, -0.5)$. The orange region denotes the occupied electronic states. The SDW wave vector $\boldsymbol{Q} = (\pi, \pi)$ pairwise connects eight hot spots on the Fermi surface (red dots). The coordinates $\boldsymbol{k} = (k_x, k_y)$ are used to linearize the dispersions around these hot spots, see Eq. (7.8). (Figure adapted from Refs. [SL15, Ger17].)

instructive to motivate it starting from the $2d$ Hubbard model on the square lattice (closely following Ref. [Fra13, Ger17]),[4]

$$H = -\sum_{i,j,\sigma} (t_{ij} + \mu\,\delta_{ij})\, d^\dagger_{i,\sigma} d_{j,\sigma} + U \sum_{i,\sigma} n_{i,\uparrow}\, n_{i,\downarrow} . \tag{7.3}$$

The operator $d^{(\dagger)}_{i,\sigma}$ annihilates (creates) an electron with spin $\sigma = \uparrow, \downarrow$ on lattice site i, with $n_{i,\sigma} = d^\dagger_{i,\sigma} d_{i,\sigma}$ counting their number. We restrict the hopping-matrix element t_{ij} to nearest (t) and next-nearest neighbors (t'). The chemical potential μ controls the total number of particles $N_d = \sum_{i,\sigma} n_{i,\sigma}$, and the on-site interaction $U > 0$ penalizes double occupation.

For antiferromagnetic instabilities, it is instructive to rewrite Eq. (7.3) in terms of the spin operators

$$\vec{S}_i = \frac{1}{2} \sum_{\sigma,\sigma'} d^\dagger_{i,\sigma} \vec{\tau}_{\sigma\sigma'} d_{i,\sigma'}, \qquad \vec{\tau} = (\tau_x, \tau_y, \tau_z)^T, \tag{7.4}$$

with τ_i the ith Pauli matrix acting in spin space. Then, the Hamiltonian takes the form [Fra13]

$$H = -\sum_{i,j,\sigma} (t_{ij} + \mu\,\delta_{ij})\, d^\dagger_{i,\sigma} d_{j,\sigma} - \frac{2}{3} U \sum_i \vec{S}_i^{\,2}, \tag{7.5}$$

where a constant contribution $N_d U/2$ was dropped.

The spin expectation value $\langle \vec{S}_i \rangle$ determines whether the system is in the disordered ($\langle \vec{S}_i \rangle = 0$) or ordered ($\langle \vec{S}_i \rangle \neq 0$) phase. Performing a mean-field decoupling $\vec{S}_i = \langle \vec{S}_i \rangle + \delta \vec{S}_i$ by

---

[4] The Hubbard model is believed to be the simplest model applicable to study the high-T_c superconductivity in cuprates [GMDSV95], thus constituting an optimal starting point for our theoretical considerations.

expanding Eq. (7.5) to linear order in the fluctuations $\delta \vec{S}_i$ yields the mean-field Hamiltonian [Fra13]

$$H_{\text{MF}} = -\sum_{i,j,\sigma} (t_{ij} + \mu\,\delta_{ij})\,d_{i,\sigma}^\dagger d_{j,\sigma} + \frac{2}{3}U\sum_i \langle \vec{S}_i \rangle^2 + \frac{4}{3}U\sum_i \langle \vec{S}_i \rangle\,\vec{S}_i. \tag{7.6}$$

In the Néel state, spins on neighboring sites are aligned antiparallel, implying $\langle \vec{S}_i \rangle = \vec{S}_0(-1)^{-n_{x_i}-n_{y_i}} = \vec{S}_0\,e^{\mathrm{i}\boldsymbol{Q}\boldsymbol{x}_i}$. Here, $\boldsymbol{Q} = (\pi,\pi)^T$ is the ordering wave vector and $\boldsymbol{x}_i = (n_{x_i}, n_{y_i})^T$ with $n_{x_i}, n_{y_i} \in \mathbb{R}$ parameterizes the lattice.[5] The constant vector $\vec{S}_0$ encodes the orientation and magnitude of the spins. Fourier transforming H_{MF} via $d_{i,\sigma}^{(\dagger)} = \frac{1}{\sqrt{N}}\sum_{\boldsymbol{K}} e^{\pm \mathrm{i}\boldsymbol{K}\boldsymbol{x}_i} d_{\boldsymbol{k},\sigma}^{(\dagger)}$,[6] with N the number of lattice sites, it reads [Ger17]

$$H_{\text{MF}} = \sum_{\boldsymbol{K},\sigma} \varepsilon(\boldsymbol{K})\,d_{\boldsymbol{K},\sigma}^\dagger d_{\boldsymbol{K},\sigma} + \frac{2}{3}U\sum_{\boldsymbol{K},\sigma,\sigma'} d_{\boldsymbol{K}+\boldsymbol{Q},\sigma}^\dagger \left[\vec{S}_0 \cdot \vec{\tau} \right]_{\sigma,\sigma'} d_{\boldsymbol{K},\sigma'}. \tag{7.7}$$

In this step, a constant contribution $2NU\vec{S}_0^2/3$ was dropped. The dispersion $\varepsilon(\boldsymbol{K}) = -2t\left[\cos(K_x) + \cos(K_y)\right] - 2t'\left[\cos(K_x + K_y) + \cos(K_x - K_y)\right] - \mu$ [Ger17] determines the Fermi surface via $\varepsilon(\boldsymbol{k}_F) = 0$, with $\boldsymbol{k}_F$ the Fermi momentum. Evidently, the order parameter scatters electrons with a momentum transfer $\boldsymbol{Q}$. However, for a LEEA, both electronic momenta $\boldsymbol{K}$ and $\boldsymbol{K} + \boldsymbol{Q}$ should be located in the vicinity of the Fermi surface; this requirement defines the eight so-called hot spots (see red dots in Fig. 7.1(b)), which we denote by a single mutual symbol $\boldsymbol{k}_F^{\text{hs}}$.

The mean-field analysis suggests the following degrees of freedom for a LEEA amenable to a field-theoretic analysis of antiferromagnetic SDW instabilities. First, the spin operator is promoted to a dynamical order parameter field, $S_i \to \vec{\phi}(\tau, \boldsymbol{x})$ [ACS03].[7] Its Fourier transform $\vec{\phi}(p_0, \boldsymbol{Q}+\boldsymbol{p})$, with the Matsubara frequency p_0, carries momentum $\boldsymbol{Q}+\boldsymbol{p}$ with $|\boldsymbol{p}| \ll |\boldsymbol{Q}| \sim |\boldsymbol{k}_F|$. Then, electrons with momentum $\boldsymbol{K}$ scatter off the order parameter fluctuations into a state with momentum $\boldsymbol{K} + \boldsymbol{Q} + \boldsymbol{p}$. Consequently, if $\boldsymbol{K} = \boldsymbol{k}_F + \boldsymbol{k}$, with $|\boldsymbol{k}| \ll |\boldsymbol{k}_F|$, is in the vicinity of a hot spot ($\boldsymbol{k}_F = \boldsymbol{k}_F^{\text{hs}}$), the same holds true for $\boldsymbol{K} + \boldsymbol{Q} + \boldsymbol{p} = \boldsymbol{k}_F^{\text{hs}} + \boldsymbol{k} + \boldsymbol{q} \approx \boldsymbol{k}_F^{\text{hs}}$. Conversely, if $\boldsymbol{K} = \boldsymbol{k}_F + \boldsymbol{k}$ is not in the vicinity of a hot spot ($\boldsymbol{k}_F \neq \boldsymbol{k}_F^{\text{hs}}$), the electron is scattered into a high-energy state $\boldsymbol{K} + \boldsymbol{Q} + \boldsymbol{p} \approx \boldsymbol{k}_F + \boldsymbol{Q} \neq \boldsymbol{k}_F^{\text{hs}}$. Such processes are excluded from the LEEA by only incorporating hot spot electrons, with their dispersions linearized around these points [MS10b]. This motivates the following LEEA $S = S_\psi + S_\phi + S_Y$ [SL15]:[8]

$$S_\psi = \sum_{n=1}^4 \sum_{m=\pm} \sum_{\sigma=\uparrow,\downarrow} \int_k \psi_{n,\sigma}^{(m)*}(k)\left[\mathrm{i}k_0 + e_n^m(\boldsymbol{k})\right]\psi_{n,\sigma}^{(m)}(k),$$

$$S_\phi = \frac{1}{2}\int_p \left[r + p_0^2 + c^2\,|\boldsymbol{p}|^2\right]\vec{\phi}(-p)\vec{\phi}(p) + \frac{u_0}{4!}\int_{p_1,p_2,p_3}\left[\vec{\phi}(p_1+p_3)\vec{\phi}(p_2-p_3)\right]\left[\vec{\phi}(-p_1)\vec{\phi}(-p_2)\right],$$

$$S_Y = g_0 \sum_{n=1}^4 \sum_{\sigma,\sigma'=\uparrow,\downarrow} \int_{k,p}\left[\vec{\phi}(p)\,\psi_{n,\sigma}^{(+)*}(k+p)\,\vec{\tau}_{\sigma,\sigma'}\,\psi_{n,\sigma'}^{(-)}(k) + \text{c.c.}\right]. \tag{7.8}$$

Here, $\psi(k)$ with $k = (k_0, \boldsymbol{k})$ denotes hot spot electrons with Matsubara frequency k_0 and momentum $\boldsymbol{k} = (k_x, k_y)$; the linearized disperions are given by $e_1^\pm(\boldsymbol{k}) = -e_3^\pm(\boldsymbol{k}) = vk_x \pm k_y$ and $e_2^\pm(\boldsymbol{k}) = -e_4^\pm(\boldsymbol{k}) = \mp k_x + vk_y$ (see Fig. 7.1(b)), with v the Fermi velocity. The integrals

---

5 For simplicity, we set the lattice constant to unity.

6 In contrast to the previous sections, we will use opposite signs for the Fourier convention of creation and annihilation operators.

7 Usually, this step is performed via a Hubbard-Stratonovich transformation (see, e.g., Ref. [Ger17]).

8 For simplicity, the intrinsic scales $\boldsymbol{k}_F$ and $\boldsymbol{Q}$ are usually not written out explicitly.

extend over the complete $\mathbb{R}^3$, $\int_k = \int_{-\infty}^{\infty} \frac{dk_0\, dk_x\, dk_y}{(2\pi)^3}$. The bosonic part of the action S_ϕ takes the form of a Ginzburg-Landau-type action describing phase transitions in terms of the order parameter alone, with c the boson velocity and u_0 the strength of the quartic boson interaction. The mass term r can be identified with the driving parameter for the phase transition; it is usually set to $r = 0$ to directly perform calculations at the QCP. The Yukawa coupling with strength g_0 between the SDW order parameter fluctuations and the hot spot electrons is encoded in S_Y.

Let us illustrate the complexity of the action (7.8) by performing a scaling analysis in the usual Wilsonian RG spirit [Pim19]: Integrate out high energy degrees of freedom, rescale momenta by a scale parameter $b \gtrsim 1$ to reintroduce the original cutoff, and rescale the fields to leave the Gaussian part of the action invariant. For later motivation (see Sec. 7.1.3 and Eq. (7.10) therein), we assume a general number of d momenta (with $d = 2$ being the physically relevant case) to enter the dispersion in S_ψ linearly and the dispersion in S_ϕ quadratically.[9] Then, the Gaussian parts are invariant under the scaling transformations

$$k_0' = b\, k_0, \qquad \boldsymbol{k}' = b\, \boldsymbol{k}, \qquad \psi'(k') = b^{\frac{-d-2}{2}} \psi(k), \qquad \vec{\phi}'(p') = b^{\frac{-d-3}{2}} \vec{\phi}(p),$$
$$r' = b^2 r, \qquad u_0' = b^{3-d} u_0, \qquad g_0' = b^{\frac{3-d}{2}} g_0, \tag{7.9}$$

except for the term containing r, which is (as usual) a relevant parameter. The scaling analysis reveals that the Yukawa coupling as well as the quartic boson interaction are relevant parameters under RG transformations in $d = 2$. Consequently, they grow larger as the theory is scaled toward low energies, and plain perturbation theory in the interactions is not applicable.

7.1.3 Approaches to quantum critical models

The strong coupling nature of Eq. (7.8) in two dimensions renders the theoretical analysis of $2d$ SDW QPTs quite challenging. Over the last decades, various approaches have been proposed in tackling this problem; these are summarized here (closely following Ref. [Pim19]).

- Since ψ enters the action (7.8) at most quadratically, it is tempting to integrate out the fermionic degrees of freedom. This approach was taken within the Hertz-Millis theory [Her76, Mil93], yielding an effective theory for the order parameter $\vec{\phi}$ alone. Within this theory, the only remnant of the fermions is a Landau-damping contribution $|p_0|$ in the quadratic part of the bosonic action, overshadowing the p_0^2 dependence at low energies. Afterward, a new scaling analysis for the order parameter action reveals that all terms $\sim u_{2n}(\vec{\phi}\,\vec{\phi})^n$ with $n > 2$ are irrelevant in $d = 2$. This approach is problematic for at least two reasons:
  - In the scaling analysis, it is assumed that the interactions u_{2n} are constant at low energies. However, in Refs. [ACS03, AC04] it was shown that they are non-analytic functions of frequencies and momenta, and in fact all interactions $(\vec{\phi}\,\vec{\phi})^n$ are marginal in $d = 2$. This observation renders the effective order parameter theory practically useless.
  - The back action of Landau-damped bosons on the fermions is neglected. Indeed, taking this effect into account, non-Fermi liquid exponents in the frequency-dependent part of the self-energy are found in $d = 2$ [Sac11], undermining the basic assumption of well-defined quasiparticle-like excitations.

---

9 The extension of the action Eq. (7.8) to higher dimensions is not unique due to the presence of a Fermi surface [Lee18]. Later, we will keep the dimension of the Fermi surface fixed while increasing its co-dimension.

Consequently, itinerant fermions in $2d$ should not be integrated out, and one has to study the fermionic and bosonic degrees of the SDW model (7.8) on equal footing.

- The strong-coupling nature of the theory can be accepted by enforcing the interactions not to flow under RG transformations (interaction-driven scaling); then, the theory does not naturally possess any small expansion parameter. However, it can be artificially introduced via, e.g., a large number of fermionic flavours N_f (such as spins or hot spots) [ACS03], and an expansion was believed to be controlled in powers $1/N_f$. Physical results are then recovered by extrapolating to the relevant N_f. Unfortunately, as shown in Refs. [Lee09, MS10a, MS10b], this approach fails, too. For an IR-convergent theory, the large N_f expansion has to be performed using dressed fermionic and bosonic propagators, where the self-energies are approximated by their one-loop corrections. This simple fact impedes the expansion as an infinite number of diagrams was found to contribute to the self-energy and vertex corrections to leading order in $1/N_f$.[10]

- Another possible small expansion parameter is the deviation from the upper critical dimension $d_c = 3$, above which the low-energy physics of the theory is governed by the non-interacting, Gaussian fixed point. Then, for dimensions d fulfilling $0 < \epsilon = d_c - d \ll 1$, interactions are assumed to be small, and a perturbative expansion in the couplings is performed. RG flow equations for the parameters of the theory can then be derived in the framework of dimensional regularization and minimal subtraction.[11] In the context of metallic $2d$ QCPs, this idea was first put forward in Ref. [DL13]. The perturbative expansion is justified a posteriori if, at a putative stable fixed point of the flow equations, the interactions are proportional to ϵ. Results in the relevant dimension d are then obtained by extrapolating to the corresponding value of ϵ.

In our publication [P1], the last approach was chosen, based on the work of Ref. [SL15]. There, the co-dimension of the Fermi surface is increased, leaving a one-dimensional Fermi surface embedded in a higher-dimensional space via the fermionic kinetic action

$$S_\psi = \sum_{n=1}^{4} \sum_{\sigma=\uparrow,\downarrow} \int_k \overline{\Psi}_{n,\sigma}(k) \left[\mathrm{i}\sigma_y k_0 + \mathrm{i}\boldsymbol{\sigma_z}\tilde{\boldsymbol{k}} + \mathrm{i}\sigma_y \varepsilon_n(\boldsymbol{k}) \right] \Psi_{n,\sigma}(k). \tag{7.10}$$

The spinors $\Psi_{1,\sigma} = (\psi_{1,\sigma}^{(+)}, \psi_{3,\sigma}^{(+)})^T$, $\Psi_{2,\sigma} = (\psi_{2,\sigma}^{(+)}, \psi_{4,\sigma}^{(+)})^T$, $\Psi_{3,\sigma} = (\psi_{1,\sigma}^{(-)}, -\psi_{3,\sigma}^{(-)})^T$, and $\Psi_{2,\sigma} = (\psi_{2,\sigma}^{(-)}, -\psi_{4,\sigma}^{(-)})^T$ depend on the generalized momentum $k = (k_0, \tilde{\boldsymbol{k}}, \boldsymbol{k})$, with $\tilde{\boldsymbol{k}}$ the artificially introduced $d-2$ momenta. The Pauli matrices σ_i, with $\boldsymbol{\sigma_z} = (\sigma_z, \ldots, \sigma_z)$ a $(d-2)$ dimensional vector, act in spinor space. The dispersions $\varepsilon_1(\boldsymbol{k}) = e_1^+(\boldsymbol{k})$, $\varepsilon_2(\boldsymbol{k}) = e_2^+(\boldsymbol{k})$, $\varepsilon_3(\boldsymbol{k}) = e_1^-(\boldsymbol{k})$, and $\varepsilon_4(\boldsymbol{k}) = e_2^-(\boldsymbol{k})$ encode the information about the original one-dimensional Fermi surface. Indeed, this action describes fermions with energy $E_n(\tilde{\boldsymbol{k}}, \boldsymbol{k}) = \pm\sqrt{\tilde{\boldsymbol{k}}^2 + [\varepsilon_n(\boldsymbol{k})]^2}$, which vanishes if $\tilde{\boldsymbol{k}}^2 = 0$ and $[\varepsilon_n(\boldsymbol{k})]^2 = 0$, corresponding to a one-dimensional Fermi surface in d-dimensional momentum space. The original theory (7.8) is readily obtained by setting $d = 2$ in Eq. (7.10).

Performing an ϵ-expansion, Ref. [SL15] identified a stable non-Fermi liquid fixed point with vanishing fixed point values for all parameters v, c, g, u_0, but finite fixed point values

---

10 For the SDW theory in Eq. (7.8), it should be noted that v dynamically emerges as a small expansion parameter at low energies [SL15], allowing for an exact solution of the theory using the interaction-driven scaling ansatz [SLL17] . However, as we are ultimately interested in the disorder-averaged SDW action, it is not clear a priori whether v remains a small parameter in the presence of disorder, and therefore a different approach should be utilized.

11 For an introduction in the context of the familiar ϕ^4 theory, we refer the reader to Ref. [KSF01].

for the ratios v/c and g^2/v. In [P1] we then addressed the question of the stability of this fixed point in the presence of quenched disorder.

7.1.4 Quenched disorder

Realistic systems usually contain some degree of imperfection, for instance, defects in the lattice or the presence of impurities. Accounting for the effects of such disorder is a rather difficult but necessary task. Indeed, it is one of the momentum-relaxing mechanisms that yield a nonzero dc resistivity and is thus believed to play an important role in explaining the T-linear electrical resistivity in the strange metal phase. In the following, we will consider the case of quenched, i.e., time-independent disorder. Depending on the degrees of freedom, quenched disorder can be incorporated into a theory in various ways. Here, we discuss two possibilities:

- In fermionic theories, electrons can scatter off the impurities. For nonmagnetic disorder, this effect is accounted for by a random, time-independent scattering potential $V(\boldsymbol{x})$ coupling to the fermionic density, $\int \mathrm{d}t\,\mathrm{d}\boldsymbol{x}\,V(\boldsymbol{x})\,\psi^\dagger(t,\boldsymbol{x})\,\psi(t,\boldsymbol{x})$ [Kam23].[12] In the absence of a QCP (and after disorder averaging, see below), the fermionic fields are then typically integrated out to obtain an effective action describing the interactions of diffusive electrons [Fin83, CdCL$^+$84, KA99].

- For theories in the presence of instabilities, disorder generally reduces the tendency toward the ordered phase. Consequently, long-range order with a globally nonzero order parameter develops below a reduced critical value $\bar{r}_c^{\mathrm{d}} < \bar{r}_c$ [Voj13]. In the regime $\bar{r}_c^{\mathrm{d}} < \bar{r} < \bar{r}_c$, however, the order parameter can be locally nonzero in so-called rare regions that do not contain impurities. This effect is incorporated by a random boson mass term $r \to r + \delta r(\boldsymbol{x})$ which locally changes the critical value [Voj03a].[13]

The remaining discussion is formulated in terms of the disorder potential $V(\boldsymbol{x})$; all arguments are equally applicable to the random boson mass $\delta r(\boldsymbol{x})$.

$V(\boldsymbol{x})$ describes one specific realization of disorder in the system, which is usually unknown. It is therefore natural to seek for a probabilistic description of disorder effects, where a single disorder configuration V is realized with a probability $P[V]$, suppressing the $\boldsymbol{x}$-dependence. Physical observables are then calculated via the disorder average [Kam23]

$$\langle\ldots\rangle_{\mathrm{dis}} = \int \mathcal{D}V \ldots P[V], \qquad \int \mathcal{D}V P[V] = 1, \tag{7.11}$$

where $\int \mathcal{D}V$ denotes a functional integral over all possible disorder realizations. In the following, the probability distribution is assumed to be of Gaussian form with zero mean [Kam23],

$$\langle V(\boldsymbol{x})\rangle_{\mathrm{dis}} = 0, \qquad \langle V(\boldsymbol{x})V(\boldsymbol{x}')\rangle_{\mathrm{dis}} = u(\boldsymbol{x} - \boldsymbol{x}'), \tag{7.12}$$

with $u(\boldsymbol{x} - \boldsymbol{x}')$ the disorder correlation function.

In the MF, physical observables are deduced from the logarithm of the now disorder-dependent partition function $\ln Z[V]$. However, the disorder average $\langle \ln Z[V]\rangle_{\mathrm{dis}}$ is hard to

---

12 Here, we change from imaginary- to real-time arguments, as [P1] is formulated in the KF. In the MF, t can be simply replaced with τ.

13 The regime $\bar{r}_c^{\mathrm{d}} < \bar{r} < \bar{r}_c$ is also called Griffiths region [Voj13] after Griffiths [Gri69]. For random Ising ferromagnets, he showed that the magnetization is a nonanalytic function of the external magnetic field even above the critical temperature $\bar{r}_c^{\mathrm{d}} = T_c^{\mathrm{d}}$, but below the clean critical temperature T_c. This nonanalytic behaviour was later attributed to contributions of the rare regions [Voj13].

evaluate, much harder than the disorder average of the partition function itself, $\langle Z[V] \rangle_{\text{dis}}$. This complication can be circumvented by the so-called replica trick, which is based on the identity $\langle \ln Z[V] \rangle_{\text{dis}} = \lim_{n \to 0} \frac{1}{n} \ln \left(\langle Z[V]^n \rangle_{\text{dis}} \right)$ [Dot00]. To be precise, the field theory is replicated n times, with $n \in \mathbb{N}$ assumed first, afterward calculations are performed with $\langle Z[V]^n \rangle_{\text{dis}}$, and finally physical results are obtained by continuing to $n \in \mathbb{R}$ and taking the limit $n \to 0$. The replica trick has the merit of preserving the simplicity of the MF compared to, e.g., the KF. However, it is generally not known whether the continuation to real n is unique and whether approximations at integer n are equally applicable for arbitrary real n [VZ85, Zir99, Dot10].

The complication of the disorder average in the MF can be traced back to the fact that, in Eq. (2.30), the disorder potential not only occurs in the numerator via the time evolution operators but also in the denominator via the normalization factor $1/Z$. This difficulty can be avoided in the KF by making use of the adiabatic assumption (see the discussion at the beginning of Sec. 2.2.2). Assuming that the disorder potential was turned on (and off) some time after (and before) the system was initially prepared, the normalization factor $1/Z$ in Eq. (2.33) only depends on the initial, disorder-independent Hamiltonian [Kam23]. Thus, in the KF, the disorder average can be easily carried out for the numerator only, avoiding the need of the replica trick at the cost of imposing the adiabatic assumption.

7.2 Quenched disorder at antiferromagnetic quantum critical points in two-dimensional metals

7.2.1 Overview

After the discussions of the preceding sections, we can now turn to the effect of quenched disorder at antiferromagnetic QCPs in $2d$ metals. General metallic QCPs in the presence of quenched disorder are a topic of ongoing research with a long history, see, e.g., Refs. [KB96a, KB96b, NVBK99, MMS02, Voj03b, HKV07].

For antiferromagnetic QCPs, Ref. [KB96b] incorporated disorder effects into a Hertz-Millis order parameter theory via a δ-correlated random boson mass ($u(\boldsymbol{x} - \boldsymbol{x}') \sim \delta(\boldsymbol{x} - \boldsymbol{x}')$ in Eq. (7.12) with $V \to \delta r$). The disorder average, performed via the replica trick, then induced a new $\vec{\phi}^4$ interaction term additional to u_0 in Eq. (7.8). Their one-loop flow equations, derived using a standard momentum-shell RG calculation, featured a stable fixed point with finite disorder in $d < 4$, indicative of an antiferromagnetic phase transition with disorder-driven critical exponents. However, they also found a finite basin of attraction for this fixed point; for initial parameter values outside this region, the RG equations experienced a runaway flow to strong disorder, implying a breakdown of their perturbative ansatz.

An extension of this analysis was provided by Ref. [NVBK99]. There, the effect of fluctuations around nonzero saddle-point solutions of the order parameter in the rare regions are taken into account. These led to an additional term in the order parameter theory, and a subsequent one-loop RG analysis revealed a general runaway flow to strong disorder with no stable fixed point for arbitrary initial parameters.

It has to be emphasized that both studies were based on Hertz-Millis order parameter theories, which, as already discussed, are known to break down in $2d$ metals. Therefore, in the publication below, we introduce disorder into the KF version of the SDW action in Eqs. (7.8) and (7.10) without integrating out the fermions. We derive flow equations in the ϵ-expansion framework introduced in Ref. [SL15] for a random potential $V(\boldsymbol{x})$ with δ-correlations and power-law correlations. However, to keep the complexity of the computations manageable, two crucial simplifications are made. First, no random boson mass is considered. Second, it is assumed that the disorder potential only scatters electrons within single hot spots, which

reduces the number of disorder-induced fermionic interactions considerably. Additionally, under this assumption, electrons far away from hot spots cannot be scattered into the vicinity of the hot spots, ensuring the validity of the hot spot theory.

Unfortunately, the flow equations do not allow for a stable disorder-driven fixed point. Instead, we find a runaway flow to strong coupling for all initial values of the parameters of the theory due to a mutual enhancement of interactions and disorder. Since we cannot access a potential fixed point outside the perturbative regime with our approach, we cannot make a certain statement about the fate of the system at low energies. However, following the flow to strong disorder, we find that fermionic and bosonic degrees of freedom effectively decouple at low energies; hence, a potential candidate is an Anderson-localized, insulating ground state.

Quenched disorder at antiferromagnetic quantum critical points in two-dimensional metals

by

J. Halbinger[1] and M. Punk[1]

[1]Arnold Sommerfeld Center for Theoretical Physics, Center for NanoScience, and Munich

Center for Quantum Science and Technology, Ludwig-Maximilians-Universität München,

80333 Munich, Germany

Quenched disorder at antiferromagnetic quantum critical points in two-dimensional metals

Johannes Halbinger and Matthias Punk

Physics Department, Arnold Sommerfeld Center for Theoretical Physics, Center for NanoScience, and Munich Center for Quantum Science and Technology (MCQST), Ludwig-Maximilians University Munich, Theresienstr. 37, 80333 Munich, Germany

We study spin density wave quantum critical points in two-dimensional metals with a quenched disorder potential coupling to the electron density. Adopting an ϵ expansion around three spatial dimensions, where both disorder and the Yukawa-type interaction between electrons and bosonic order parameter fluctuations are marginal, we present a perturbative, one-loop renormalization group analysis of this problem, where the interplay between fermionic and bosonic excitations is fully incorporated. Considering two different Gaussian disorder models restricted to small-angle scattering, we show that the non-Fermi liquid fixed point of the clean spin density wave (SDW) hot spot model is generically unstable and the theory flows to strong coupling due to a mutual enhancement of interactions and disorder. We study properties of the asymptotic flow towards strong coupling, where our perturbative approach eventually breaks down. Our results indicate that disorder dominates at low energies, suggesting that the ground state in two dimensions is Anderson-localized.

I. INTRODUCTION

In the vicinity of a quantum critical point (QCP) in quasi two-dimensional metals, the strong interaction between electrons and order parameter fluctuations destroys the quasiparticle character of electronic excitations, which lies at the heart of Landau's Fermi liquid theory. Indeed, non-Fermi liquids or strange metals are frequently found in the vicinity of magnetic QCPs [1], with heavy fermion materials, iron-pnictides, and cuprates as prominent examples [2–4]. One striking aspect of such non-Fermi liquid behavior is the observed linear temperature dependence of the electrical resistivity, together with the absence of resistivity saturation at the Mott-Ioffe-Regel bound at high temperatures. The latter is often attributed to a breakdown of the quasiparticle picture in such materials [5].

While the theoretical description of metallic quantum critical points has seen substantial progress using both numerical as well as field-theoretical developments [6,7], central questions still remain open. In particular, the computation of dc transport properties and the question if a linear-in-T resistivity is a generic feature of metallic QCPs poses a formidable challenge, as it requires to account for processes which relax the total momentum of a current carrying state, either via disorder or umklapp scattering. Previous analytic works studied dc transport either using the Boltzmann equation [8–10], or perturbatively in the presence of weak disorder, assuming that disorder does not drive the system away from the clean non-Fermi liquid fixed point [11–13]. In this paper, we investigate if the latter assumption is indeed valid and perform a detailed renormalization group (RG) study of spin density wave (SDW) quantum critical points in the presence of quenched disorder.

So far, the fate of metallic QCPs with quenched disorder has been primarily studied using the Hertz approach [14], with few notable exceptions [15]. In the former the fermionic

degrees of freedom are integrated out and one is left with a Ginzburg-Landau-type theory for the overdamped bosonic order parameter fluctuations. Within this approach several possible scenarios about the fate of various quantum critical points in the presence of disorder have been put forward, including the potential for novel fixed points at finite or infinite disorder [16–19]. Interestingly, for the SDW QCP in metals with Ising symmetry, it has been argued that the critical point is washed out and replaced by a smooth crossover due to Griffiths effects, i.e., rare ordered regions in the disorder potential [20]. Even though many questions still remain open, it is important to emphasize that the Hertz approach is invalid for clean two-dimensional systems, because the interaction between electrons and bosonic order parameter fluctuations leads to a loss of electronic quasiparticle coherence and to a singular nature of the bosonic n-point vertices in the Ginzburg-Landau expansion. Accounting for this delicate interplay requires a careful theoretical analysis treating both fermionic and bosonic excitations on equal footing, which is particularly challenging in a renormalization group setting. Early studies of these models without disorder were based on diagrammatic approaches [21–24] and were believed to be justified within a large-N_f expansion, with N_f the number of fermionic flavours [25]. More recent works showed that such expansions are in fact uncontrolled and these theories remain strongly coupled in the $N_f \to \infty$ limit [26–28].

The main goal of this work is to perform a controlled renormalization group study of antiferromagnetic QCPs in two-dimensional metals in the presence of quenched disorder, by reformulating the ϵ expansion for the SDW hot spot model developed by Sur and Lee [29] on the closed-time Schwinger-Keldysh contour. This allows us to directly perform a disorder average of the partition function and to study the interplay between fermionic excitations, bosonic order parameter fluctuations and disorder induced interactions between the fermions in a controlled manner. In contrast to the above
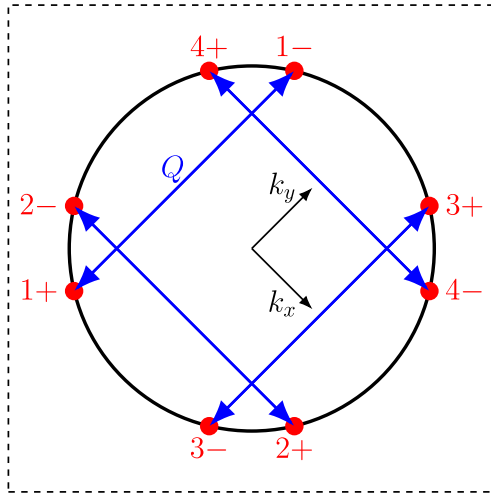
FIG. 1. Fermi surface and scattering geometry of electrons near the eight hot spots connected by the antiferromagnetic ordering wave vector $\mathbf{Q} = (\pi, \pi)$ modulo reciprocal lattice vectors. The dashed line marks the boundary of the first Brillouin zone for the square lattice. The momenta k_x and k_y indicate the local coordinate system at the hot spots which is used in the following.

mentioned Hertz-type theories as well as Finkel'stein-type RG studies of interacting electrons with quenched disorder [15,30–33], the crucial difference in our approach is that electronic degrees of freedom are *not* integrated out and are treated on equal footing with the bosonic excitations.

Importantly, we only consider models of disorder potentials which impart a small momentum transfer $|\mathbf{p}| \ll k_F$ onto the electrons, with k_F the characteristic Fermi momentum, such that electrons stay in the vicinity of a hot spot when scattering off the disorder potential. Besides simplifying the analysis, this restriction also ensures that the hot spot model remains valid, as cold electrons far away from the hot spots cannot become hot by scattering off the disorder potential with a large momentum transfer and end up in the vicinity of a hot spot.

Even though disorder does not lead to backscattering of electrons in our model, we nonetheless expect a nondivergent dc conductivity due to the interplay between disorder and the Yukawa-type interaction of electrons with order parameter fluctuations. Since the latter gives rise to large angle scattering, their combination allows electrons to equilibrate across all hot spots around the Fermi surface. Moreover, disorder localizes the cold electrons in $2d$ [34], which consequently do not participate in transport and cannot short circuit the

contribution of hot electrons as would be the case without disorder [8].

In this work we focus on two Gaussian disorder models, a δ-correlated disorder potential within single hot spots, as well as a power-law correlated disorder potential. A simple tree-level scaling analysis seems to indicate that δ-correlated disorder is irrelevant in $d > 2$ spatial dimensions, but we show that the linearised electron dispersion in the hot spot model leads to UV/IR mixing and the effective disorder coupling is in fact marginal in $d = 3$, as is the Yukawa interaction. For this reason, we can treat both interactions simultaneously in a perturbative ϵ expansion around three spatial dimensions. Lastly, we refrain from a discussion of potentially important Griffiths effects due to a random boson mass term, as this is beyond the scope of this work.

The remainder of this paper is structured as follows: in Sec. II we reformulate the hot spot model of Sur and Lee on the Keldysh contour and discuss our disorder model. Our one-loop RG results for both disorder models are discussed in Sec. III, with technical details shifted to the appendices. We conclude with a brief discussion in Sec. IV.

II. MODEL

A. Keldysh formulation of the Sur-Lee model

We start from a hot spot model of electrons on the square lattice in two dimensions, coupled to fluctuations of an antiferromagnetic order parameter with ordering wave vector $\mathbf{Q} = (\pi, \pi)$. Here electrons interact predominantly in the vicinity of eight hot spots on the Fermi surface, where they can resonantly scatter off antiferromagnetic fluctuations which impart a momentum transfer $\mathbf{Q}$, modulo reciprocal lattice vectors, onto the electrons (see Fig. 1 for a sketch of the hot spot geometry) [25]. In particular we use an extension of this model developed by Sur and Lee, which is amenable to dimensional regularization [29]. In their approach the Fermi surface geometry of the $2d$ model is left unchanged, but the number of dimensions orthogonal to the Fermi surface (i.e., its co-dimension) is increased. A tree-level scaling analysis then shows that a controlled ϵ expansion around $d = 3$ dimensions is possible. Since we are going to study this model in the presence of quenched disorder, we start by reformulating the action of the Sur-Lee model on the closed-time Schwinger-Keldysh contour. As the Keldysh partition function is normalized to unity per construction, we can directly perform a disorder average of the partition function and/or the generating functional later on [32]. After Keldysh rotation of the fields its action takes the form

$$S = S_\Psi + S_\phi + S_Y + S_{\phi^4} \tag{1}$$

with

$$S_\Psi = \sum_{n,j,\sigma} \int_k \left(\overline{\Psi}^{(1)}_{n,j,\sigma}(k) \quad \overline{\Psi}^{(2)}_{n,j,\sigma}(k) \right) \begin{pmatrix} \sigma_y(\omega + i\delta) - i\boldsymbol{\sigma_z}\tilde{\mathbf{k}} - i\sigma_x \varepsilon_n(\mathbf{k}) & \sigma_y \delta_f(\omega) \\ 0 & \sigma_y(\omega - i\delta) - i\boldsymbol{\sigma_z}\tilde{\mathbf{k}} - i\sigma_x \varepsilon_n(\mathbf{k}) \end{pmatrix} \begin{pmatrix} \Psi^{(1)}_{n,j,\sigma}(k) \\ \Psi^{(2)}_{n,j,\sigma}(k) \end{pmatrix}, \tag{2}$$

$$S_\phi = \frac{1}{2} \int_p \left(\vec{\phi}^c(p) \quad \vec{\phi}^q(p) \right) \begin{pmatrix} 0 & 2[(\omega - i\delta)^2 - a^2\tilde{\mathbf{p}}^2 - c^2\mathbf{p}^2] \\ 2[(\omega + i\delta)^2 - a^2\tilde{\mathbf{p}}^2 - c^2\mathbf{p}^2] & \delta_b(\omega) \end{pmatrix} \begin{pmatrix} \vec{\phi}^c(-p) \\ \vec{\phi}^q(-p) \end{pmatrix}, \tag{3}$$

$$S_Y = -i \frac{g}{\sqrt{N_f}} \sum_{n,j,\sigma,\sigma'} \int_{k,p} \overline{\Psi}^{(a)}_{n,j,\sigma}(k+p)\, \Phi^\alpha_{\sigma\sigma'}(p)\gamma^\alpha_{(ab)}\sigma_x\, \Psi^{(b)}_{\bar{n},j,\sigma'}(k), \tag{4}$$

$$S_{\phi^4} = -\frac{u_1}{4}\int_{p_1,p_2,p_3} \mathrm{Tr}\{\Phi^c(p_1+p_3)\Phi^c(p_2-p_3) + \Phi^q(p_1+p_3)\Phi^q(p_2-p_3)\}\mathrm{Tr}\{\Phi^c(-p_1)\Phi^q(-p_2)\}$$

$$-\frac{u_2}{4}\int_{p_1,p_2,p_3} \mathrm{Tr}\{[\Phi^c(p_1+p_3)\Phi^c(p_2-p_3) + \Phi^q(p_1+p_3)\Phi^q(p_2-p_3)]\Phi^c(-p_1)\Phi^q(-p_2)\}. \tag{5}$$

For a detailed discussion of the theory in higher dimensions and a Keldysh formulation of the hot spot model in two dimensions we refer the reader to Refs. [29,35], respectively. Here we follow the notation of Sur and Lee where $\Psi^{(i)}_{1,j,\sigma} = (\psi^{(i)}_{1+,j,\sigma}, \psi^{(i)}_{3+,j,\sigma})^T$, $\Psi^{(i)}_{2,j,\sigma} = (\psi^{(i)}_{2+,j,\sigma}, \psi^{(i)}_{4+,j,\sigma})^T$, $\Psi^{(i)}_{3,j,\sigma} = (\psi^{(i)}_{1-,j,\sigma}, -\psi^{(i)}_{3-,j,\sigma})^T$ and $\Psi^{(i)}_{4,j,\sigma} = (\psi^{(i)}_{2-,j,\sigma}, -\psi^{(i)}_{4-,j,\sigma})^T$ are two component fermionic spinors comprised of fermion fields at antipodal hot spots (see Fig. 1), $\overline{\Psi} = \Psi^\dagger \sigma_y$ with $\sigma_{x,y,z}$ the Pauli matrices, $\boldsymbol{\sigma_z}$ is a $(d-2)$-dimensional vector with entries σ_z and the index n runs over the four distinct hot spot pairs with $\bar{1} = 3$, $\bar{2} = 4$, $\bar{3} = 1$ and $\bar{4} = 2$. The superscript (i) distinguishes the two Keldysh components and the infinitesimal $\delta_f(\omega)$, $\delta_b(\omega) \sim \delta = 0^+$ are needed for convergence. As in Ref. [29], the action is generalised to a SU(N_f) fermion flavour group and to a SU(N_c) spin group, with j and σ as respective indices (the physical model corresponds to $N_f = 1$ and $N_c = 2$). SDW order parameter fluctuations are described by the matrix valued field $\Phi^\alpha = \vec{\phi}^\alpha \cdot \vec{\tau}$, with $\vec{\tau}$ denoting the $N_c^2 - 1$ generators of SU(N_c) and $\alpha \in \{q,c\}$ is the Keldysh index. The Keldysh rotation was performed using the convention

$$\begin{aligned}
\vec{\phi}^+ &= \vec{\phi}^c + \vec{\phi}^q, & \vec{\phi}^- &= \vec{\phi}^c - \vec{\phi}^q, \\
\psi^+ &= \tfrac{1}{\sqrt{2}}(\psi^{(1)} + \psi^{(2)}), & \overline{\psi}^+ &= \tfrac{1}{\sqrt{2}}(\overline{\psi}^{(1)} + \overline{\psi}^{(2)}), \\
\psi^- &= \tfrac{1}{\sqrt{2}}(\psi^{(1)} - \psi^{(2)}), & \overline{\psi}^- &= \tfrac{1}{\sqrt{2}}(\overline{\psi}^{(2)} - \overline{\psi}^{(1)}),
\end{aligned} \tag{6}$$

where the indices $\pm$ denote fields on the forward and backward branch of the closed time contour. Furthermore we defined the linearised fermionic dispersions near the hot spots

$$\begin{aligned}
\varepsilon_1(\mathbf{k}) &= vk_x + k_y, & \varepsilon_3(\mathbf{k}) &= vk_x - k_y, \\
\varepsilon_2(\mathbf{k}) &= -k_x + vk_y, & \varepsilon_4(\mathbf{k}) &= k_x + vk_y.
\end{aligned} \tag{7}$$

The $(d+1)$-dimensional integral $\int_k = \int \frac{d\omega d\tilde{\mathbf{k}} d\mathbf{k}}{(2\pi)^{d+1}}$ runs over real frequency ω, the two-dimensional momentum $\mathbf{k} = (k_x, k_y)$ as well as the $(d-2)$ additional momentum directions $\tilde{\mathbf{k}}$ orthogonal to the Fermi surface in the (k_x, k_y) plane.

The Yukawa coupling term $\sim g$ between fermions and order parameter fluctuations has been written in compact form with the help of the matrices

$$\gamma^c_{(ab)} = \begin{pmatrix} 1 & 0 \\ 0 & 1 \end{pmatrix}, \quad \gamma^q_{(ab)} = \begin{pmatrix} 0 & 1 \\ 1 & 0 \end{pmatrix}. \tag{8}$$

Note that we use the convention of Greek superscripts for the bosonic Keldysh indices and Latin superscripts in brackets for fermionic Keldysh indices, where a sum over repeated indices is implied.

The bare fermion propagators in general dimensions are given by

$$-i\langle \Psi^{(a)}_{n,j,\sigma}(k)\overline{\Psi}^{(b)}_{n,j,\sigma}(k)\rangle = \begin{pmatrix} G^R_n(k) & G^K_n(k) \\ 0 & G^A_n(k) \end{pmatrix}, \tag{9}$$

where the retarded/advanced and Keldysh Green's functions

$$G^{R/A}_n(k) = \frac{\sigma_y(\omega \pm i\delta) - i\boldsymbol{\sigma_z}\tilde{\mathbf{k}} - i\sigma_x \varepsilon_n(\mathbf{k})}{(\omega \pm i\delta)^2 - \tilde{\mathbf{k}}^2 - \varepsilon_n^2(\mathbf{k})}, \tag{10}$$

$$G^K_n(k) = F_f(\omega)[G^R_n(k) - G^A_n(k)] \tag{11}$$

are now matrices in spinor space and $F_f(\omega) = \mathrm{sgn}(\omega)$ in thermal equilibrium and at zero temperature. The retarded and advanced propagators are related via $(\sigma_y G^R_n)^\dagger = \sigma_y G^A_n$ and therefore $(\sigma_y G^K_n)^\dagger = -\sigma_y G^K_n$. Note that these relations hold for the inverse propagators as well.

For the bare boson propagators, we find

$$-i\langle \phi^{\alpha,a}(p)\phi^{\beta,b}(-p)\rangle = \begin{pmatrix} D^K(p) & D^R(p) \\ D^A(p) & 0 \end{pmatrix}\delta_{ab} \tag{12}$$

(a and b labeling the vector component) with

$$D^{R/A}(p) = \frac{1}{2}\frac{1}{(\omega \pm i\delta)^2 - a^2\tilde{\mathbf{p}}^2 - c^2\mathbf{p}^2}, \tag{13}$$

$$D^K(p) = F_b(\omega)[D^R(p) - D^A(p)], \tag{14}$$

and $F_b(\omega) = \mathrm{sgn}(\omega)$ in thermal equilibrium and at zero temperature. The retarded and advanced propagators can be obtained from each other via $[D^R(\omega, \vec{p})]^\dagger = D^A(\omega, \vec{p}) = D^R(-\omega, \vec{p})$, where we used the shorthand notation $\vec{p} = (\tilde{\mathbf{p}}, \mathbf{p})$. Consequently, the Keldysh propagator obeys $[D^K(\omega, \vec{p})]^\dagger = -D^K(\omega, \vec{p}) = -D^K(-\omega, \vec{p})$. Again, these relations hold for the inverse propagators as well.

A simple tree level scaling analysis of the action in Eqs. (2)–(5) in $d+1$ dimensions shows that scaling dimensions of the fields and couplings at the Gaussian fixed point are given by

$$\begin{aligned}
[\Psi] &= -\frac{d+2}{2}, & [\vec{\phi}] &= -\frac{d+3}{2}, \\
[g] &= \frac{3-d}{2}, & [u_{1,2}] &= 3-d,
\end{aligned} \tag{15}$$

which shows that both the Yukawa interaction g as well as the ϕ^4 interactions $u_{1,2}$ are irrelevant in $d > 3$ spatial dimensions and an expansion in $\varepsilon = 3 - d$ is feasible [29].

B. Quenched disorder

The main goal of this work is to study the model in Eqs. (2)–(5) in the presence of a quenched, random disorder

potential V, which couples to the density of fermions via the following term in the action:

$$S_{\text{dis},0} = -\int_{\omega,\vec{k},\vec{p}} V(\vec{p})\, \overline{\Psi}^{(a)}_{n,j,\sigma}(\vec{k}+\vec{p},\omega)\sigma_y \Psi^{(a)}_{n,j,\sigma}(\vec{k},\omega) \quad (16)$$

with $\vec{k} = (\tilde{\mathbf{k}}, \mathbf{k})$ and a sum over repeated indices is implied. To keep the hot spot model valid and the complexity manageable, we assumed here that the disorder potential scatters fermions only within a single hot spot, as can be seen from the presence of the σ_y matrix and the fact that the two spinors carry the same hot spot index n in Eq. (16). Taking an Edwards model with identical, randomly placed impurities as an example for the disorder potential, this would correspond to an impurity scattering potential with a finite range, such that the momentum transfer $\vec{p}$ is much smaller than the characteristic Fermi momentum $|\vec{p}| \ll k_F$. This simplifying assumption also precludes cold electrons from becoming hot by scattering off impurities from cold regions of the Fermi surface to hot spot regions. Only in this case the hot spot model remains valid and cold electrons away from the hot spots can be safely omitted from our analysis.

Even though the assumption of a small momentum transfer precludes backscattering due to disorder, it is important to realize that the Yukawa coupling gives rise to such large-angle scattering processes. As already mentioned in the introduction, the combination of disorder and magnetic scattering is thus expected to lead to a nondiverging dc conductivity in this model. The small-angle scattering assumption implicit in Eq. (16) drastically simplifies the following analysis, because otherwise the disorder averaged interaction would contain a

vast number of different couplings from various hot spot combinations which renormalise differently. In our model, there is only one disorder coupling constant, however.

In this work, we study two different Gaussian disorder models with zero mean $\langle V(\vec{p})\rangle_{\text{dis}} = 0$ and disorder correlation function

$$\langle V(\vec{p})V(-\vec{p})\rangle_{\text{dis}} = 2u(\vec{p}). \quad (17)$$

The first model is a white noise model with δ-correlated disorder in real-space, which is restricted to single hot spots, whereas the second model exhibits power-law correlated disorder in the two physical dimensions and δ correlations in the additional $d-2$ dimensions:

$$\delta\text{-correlated:} \quad u(\vec{p}) = u_0, \quad (18)$$

$$\text{power-law:} \quad u(\vec{p}) = u_0\, |\mathbf{p}|^{\alpha-2} \quad (19)$$

with exponent $\alpha > 0$. Note again that our δ-correlated disorder model is different from a standard white noise model with arbitrary large momentum transfer, as electrons only scatter within the same hot spot in our case.

The Keldysh formalism allows us to directly perform a disorder average of the partition function over all possible realisations of the Gaussian distributed potential $V(\vec{p})$, with this disorder average defined by

$$\langle \cdots \rangle_{\text{dis}} = \int \mathcal{D}[V(\vec{p})] \cdots \exp\left\{-\frac{1}{4}\int_{\vec{p}} \frac{V(\vec{p})V(-\vec{p})}{u(\vec{p})}\right\}. \quad (20)$$

This leads to the following additional, disorder induced four-fermion interaction term in the action

$$S_{\text{dis}} = i\sum_{n,n'}\sum_{j,j'}\sum_{\sigma,\sigma'}\int_{\substack{\vec{k}_1,\vec{k}_2,\vec{k}_3 \\ \omega_1,\omega_2}} \left[\overline{\Psi}^{(a)}_{n,j,\sigma}(\vec{k}_1+\vec{k}_3,\omega_1)\sigma_y\Psi^{(a)}_{n,j,\sigma}(\vec{k}_1,\omega_1)\right]u(\vec{k}_3)\left[\overline{\Psi}^{(b)}_{n',j',\sigma'}(\vec{k}_2-\vec{k}_3,\omega_2)\sigma_y\Psi^{(b)}_{n',j',\sigma'}(\vec{k}_2,\omega_2)\right] \quad (21)$$

with $u(\vec{k}_3)$ given in Eqs. (18) and (19). Note that u_0 is restricted to positive values for the functional integral to be well defined. The tree level scaling dimension of the disorder coupling constant u_0 is given by

$$\delta\text{-correlated:} \quad [u_0] = 2 - d, \quad (22)$$

$$\text{power-law:} \quad [u_0] = 4 - d - \alpha. \quad (23)$$

It is convenient to set $\alpha = 1$ for power-law correlated disorder, because in this case all coupling constants are marginal in $d = 3$ and a systematic ϵ expansion in $\epsilon = 3 - d$ can be carried out. Even though the disorder coupling for δ-correlated disorder is seemingly irrelevant in dimensions $d > 2$, we will show below that the loop expansion is organized in terms of an effective coupling $u_\delta = u_0\Lambda$, with Λ the UV momentum cutoff. Note that this coupling has scaling dimension $[u_\delta] = 3 - d$, such that a systematic expansion in small $\epsilon = 3 - d$ is possible as well.

In the following, we study the action $S + S_{\text{dis}}$ of the SDW critical point with quenched disorder after introducing dimensionless coupling constants by replacing $g \to g\mu^{\epsilon/2}$, $u_{1,2} \to u_{1,2}\mu^\epsilon$ and $u_0 \to u_0\mu^{\epsilon-1}$ for the δ-correlated model or

$u_0 \to u_0\mu^\epsilon$ for power-law correlations with $\alpha = 1$, with μ an arbitrary mass scale.

III. RESULTS

Here we focus on results for the δ-correlated disorder model and discuss differences for power-law correlated disorder at the end of this section.

A. Organization of the perturbation series in $u_0\Lambda$

Due to the fact the fermionic dispersion relations in Eq. (7) are linearised and because quadratic terms are irrelevant in the RG sense, the diagrammatic perturbation series for δ-correlated disorder turns out to be organised in powers of $u_\delta = u_0\Lambda$, with Λ the UV momentum cutoff. Indeed, each loop integral which only contains fermion propagators with the same dispersion relation (i.e., fermions at the same hot spot and/or at antipodal hot spots) as well as disorder vertices, exhibits a trivial linear dependence on the UV momentum cutoff Λ. This can be easily seen by shifting the loop momentum, e.g., via $k_y \to k_y - vk_x$ for loops which only contain propagators with dispersion $\varepsilon_1(\mathbf{k})$, and similarly for loops

with other fermion dispersions. The loop integrand is thus trivially independent of k_x, which leads to a linear dependence on the UV cutoff Λ.

Crucially, such linearly diverging loop integrals cannot involve bosonic propagators or Yukawa vertices, which mix fermions at different hot spots with different dispersion relations. For this reason linearly diverging loops only appear in combination with a disorder interaction vertex u_0 and the linear Λ dependence can be absorbed into the disorder coupling u_δ as defined above, increasing its tree-level scaling dimension to $[u_\delta] = 3 - d$. Importantly, this allows us to study both the Yukawa and the disorder interaction on equal footing in an ϵ expansion around $d = 3$ dimensions.

Note that sub-leading diagrams exist as well, which contain disorder vertices u_0, but no accompanying linear diverging loop integrals, e.g., if these loops contain boson propagators. Such diagrams are irrelevant at low energies and thus do not appear in our analysis.

B. One-loop RG flow equations for δ-correlated disorder

In this section, we present one loop RG flow equations for all dimensionless coupling constants. Detailed calculations of the one-loop diagrams and the renormalization procedure are presented in the Appendix. The flow equations for the velocities and the (effective) dimensionless coupling constants for δ-correlated disorder potentials read

$$\frac{\partial c}{\partial \ell} = -\frac{g^2}{v}\frac{1}{8\pi^2 N_f N_c}\left\{cN_f N_c \pi - 2v(N_c^2 - 1)[h_1(c, v, a) - h_2(c, v, a)]\right\} + \frac{cu_\delta}{\pi^2}, \tag{24}$$

$$\frac{\partial v}{\partial \ell} = -\frac{g^2 v}{c}\frac{N_c^2 - 1}{2\pi^2 N_f N_c}h_2(c, v, a), \tag{25}$$

$$\frac{\partial a}{\partial \ell} = -\frac{g^2}{cva}\frac{1}{8\pi^2 N_f N_c}\left\{(a^2 - 1)c\pi N_f N_c - 2a^2 v(N_c^2 - 1)[h_1(c, v, a) - h_q(c, v, a)]\right\} + \frac{au_\delta}{\pi^2}, \tag{26}$$

$$\frac{\partial g}{\partial \ell} = \frac{\epsilon}{2}g - \frac{g^3}{cv}\frac{1}{8\pi^3 N_f N_c}\left(c\pi^2 N_f N_c - v\{h_3(c, v, a) + \pi(N_c^2 - 1)[h_1(c, v, a) - h_q(c, v, a) - 2h_2(c, v, a)]\}\right) + \frac{gu_\delta}{2\pi^2}, \tag{27}$$

$$\frac{\partial u_1}{\partial \ell} = \epsilon u_1 - \frac{1}{2\pi^2 ac^2}\left[(N_c^2 + 7)u_1^2 + \frac{2(2N_c^2 - 3)}{N_c}u_1 u_2 + \frac{3(N_c^2 + 3)}{N_c^2}u_2^2\right] - \frac{u_1 g^2}{cv}\frac{1}{4\pi^2 N_f N_c}\left\{2\pi cN_f N_c \right.$$
$$\left. + v(N_c^2 - 1)[-3h_1(c, v, a) + h_q(c, v, a) + 2h_2(c, v, a)]\right\} + \frac{3}{\pi^2}u_1 u_\delta, \tag{28}$$

$$\frac{\partial u_2}{\partial \ell} = \epsilon u_2 - \frac{u_2}{c^2 a\pi^2}\left(6u_1 + \frac{N_c^2 - 9}{N_c}u_2\right) - \frac{u_2 g^2}{cv}\frac{1}{4\pi^2 N_f N_c}\left\{2\pi cN_f N_c + v(N_c^2 - 1)[-3h_1(c, v, a) + h_q(c, v, a)\right.$$
$$\left. + 2h_2(c, v, a)]\right\} + \frac{3}{\pi^2}u_2 u_\delta, \tag{29}$$

$$\frac{\partial u_\delta}{\partial \ell} = \epsilon u_\delta + \frac{2u_\delta^2}{\pi^2} + \frac{u_\delta g^2}{c}\frac{N_c^2 - 1}{4\pi^2 N_f N_c}[2h_1(c, v, a) - h_q(c, v, a) - h_2(c, v, a)], \tag{30}$$

where the dimensionless disorder couplings u_δ and u_0 (see Sec. III A) are related via $u_\delta = u_0 \Lambda/\mu$. Moreover, $\ell = \ln(\mu_0/\mu)$ is a logarithmic energy scale, $c, v, a, u_i > 0$ and the functions $h_i(c, v, a)$ are defined in the Appendix. Note that these flow equations reduce to the ones found by Sur and Lee in Ref. [29] for $u_\delta = 0$ and $a = 1$. The boson velocity c does not flow to zero in the presence of disorder, thus the arguments in Ref. [36] that certain two-loop diagrams are important at leading order in ϵ for the clean SDW critical point, do not play a role here.

Unfortunately these flow equations do not feature a stable fixed point at finite u_δ. Rather the RG flow is generically directed to strong coupling, with all parameters apart from the velocity v diverging at low energies, where our perturbative approach eventually breaks down (see Fig. 2). An analysis of the flow equations in the limit of large N_f is performed in Appendix C.

It is worthwhile to emphasise that our flow equations for the Yukawa coupling g and the disorder coupling u_δ are formally similar to the flow equations for the ϕ^4 interaction and the disorder coupling in the Hertz-theory of metallic SDW quantum critical points with quenched disorder, where the fermions are integrated out. This theory was analysed in a double expansion in Ref. [37]. As the latter flow equations do feature novel fixed points at finite disorder and interactions, it will be elucidating to analyze the differences to our case. In order to facilitate an analytic analysis we make a simplifying assumption and set the boson velocity in the additional dimensions a to its value at the clean SDW fixed point, $a = 1$, where $h_q \equiv h_1$. Considering the hyperplane $\beta_c \equiv -\frac{\partial c}{\partial \ell} = 0$, where potential fixed points of the boson velocity c are located, allows us to replace $h_1 - h_2$ in Eq. (30), leading to the flow equation for u_δ

$$\frac{\partial u_\delta}{\partial \ell} = \epsilon u_\delta + \frac{u_\delta^2}{\pi^2} + \frac{u_\delta g^2}{8\pi v} \tag{31}$$

(a)

(b)
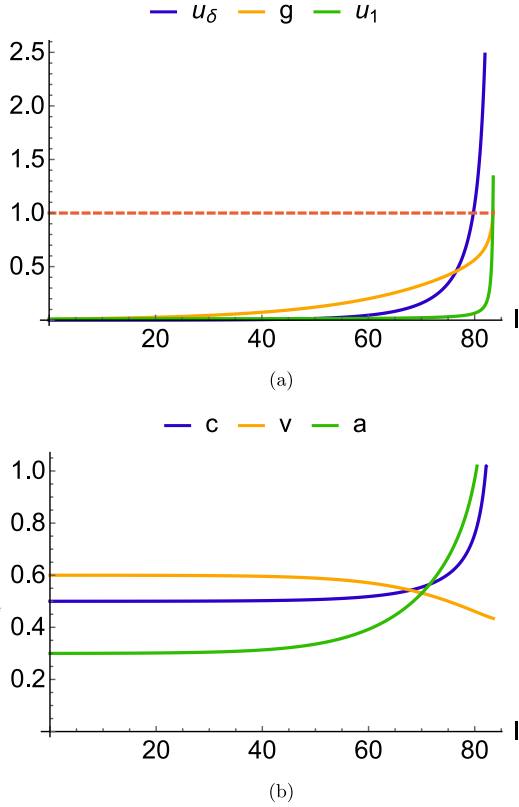
FIG. 2. RG flows as function of the logarithmic energy scale $\ell = \ln(\mu_0/\mu)$. In (a), we plot the flow of the dimensionless disorder coupling u_δ, the Yukawa-coupling g and the ϕ^4 interaction u_1, whereas (b) shows plots of the fermion velocity v and the boson velocities c and a. Initial conditions: $(u_\delta, g, u_1, c, v, a) = (0.01, 0.01, 0.0001, 0.5, 0.6, 0.3)$ and $\epsilon = 0.1$, $N_f = 1$, and $N_c = 2$. For $N_c = 2$, the two ϕ^4 interaction terms are identical up to a factor of two and u_2 can be set to zero for simplicity. The dashed red line in (a) indicates where the perturbation theory formally breaks down.

independent of N_f and N_c. On the other hand, the flow equation for the Yukawa coupling generically reads

$$\frac{\partial g}{\partial \ell} = \frac{\epsilon}{2} g - \kappa\, g^3 + \frac{u_\delta g}{2\pi^2}, \qquad (32)$$

where κ depends on c, v, N_f, and N_c and can be read off from Eq. (27) for $a = 1$. As mentioned above, these flow equations are strikingly similar to the ones found in Ref. [37], which do feature a fixed point at finite u_δ. The main difference in our case is that the last term in Eq. (31) comes with a plus sign, i.e., the Yukawa coupling g antiscreens and thus enhances the disorder interaction at low energies, in contrast to Ref. [37], where the disorder coupling is screened by the ϕ^4 interaction. This antiscreening is the main reason why our theory does not allow for a fixed point at finite disorder and flows to strong coupling at low energies. A secondary reason is the dynamical nesting of the Fermi surface due to the flow of v to smaller values, which enhances the antiscreening and also would lead to a divergence of κ in the limit of $v \to 0$.

Even though we cannot access a potential strong disorder fixed point in our perturbative approach, we can attempt to

extract some information about the behavior of the flow towards strong coupling. Since u_δ diverges at a finite value of the logarithmic flow parameter ℓ and the dimensionless coupling constants are monotonic functions of ℓ in the regime where u_δ diverges, it is convenient to parametrize their flow in terms of $\ln u_\delta$ instead [38]. Corresponding flow equations can be found in Appendix C.

In Fig. 3, we show plots of g^2/u_δ, v, and u_1/u_δ as functions of $\ln u_\delta$. Note that g^2/u_δ vanishes asymptotically along the flow to strong coupling, indicating that disorder dominates the Yukawa coupling at low energies. In contrast to the clean non-Fermi liquid fixed point, the fermion velocity v does not flow to zero, but to a constant value instead, indicating that the hot spots are not perfectly nested at low energies. This can be traced back to the fact that g^2/u_δ vanishes sufficiently fast along the flow to strong coupling, such that the flow of v stops before it vanishes. Lastly, the ϕ^4 interaction u_1 diverges even faster than the disorder interaction u_δ along the flow to strong coupling. This can be interpreted as a tendency towards local moment formation, indicating that the ground state might be in a random singlet phase [39].

Moreover, we can analyze the scaling of the fermion and boson propagators along the flow to strong coupling. In two dimensions, the fermionic and bosonic propagators scale as a function of frequency like (see Appendix C)

$$G(\omega) \sim \omega^{-\frac{1-2\tilde{\eta}_\Psi}{z_\omega}}, \qquad (33)$$

$$D(\omega) \sim \omega^{-\frac{2-2\tilde{\eta}_\phi}{z_\omega}}. \qquad (34)$$

Since the dynamical critical exponent and the effective anomalous dimensions flow to the asymptotic values $z_\omega \simeq u_\delta/\pi^2$, $\tilde{\eta}_\Psi \sim \mathcal{O}(g^2)$, $\tilde{\eta}_\phi \simeq -u_\delta/\pi^2$ for large $u_{\delta/p}$, the frequency exponent of the fermionic propagator approaches zero along the flow to strong coupling, whereas the bosonic propagator keeps its bare frequency dependence $D(\omega) \sim \omega^{-2}$. An example of the flows of the exponents are shown in Fig. 3(c). The fact that $G(\omega) \sim$ const. is reminiscent of a simple constant impurity scattering rate, which overshadows frequency dependent power laws in the electron self-energy due to the interaction with order-parameter fluctuations. It is also worth mentioning that our results for the fermion propagator do not show indications of Sachdev-Ye-Kitaev (SYK) scaling [i.e., $G(\omega) \sim \omega^{-1/2}$] as we approach strong coupling [40].

Together with the flow of g^2/u_δ to zero, these results indicate that disorder effects dominate over the interaction between electrons and order parameter fluctuations at low energies. Since electron interactions seem to play a minor role here, a likely scenario for the fate of the $2d$ SDW QCP with quenched disorder is an Anderson-localized, insulating electronic ground state.

C. Power-law correlated disorder

Here we briefly discuss the power-law correlated disorder model with $\alpha = 1$, where the disorder coupling constant u_0 has the same scaling dimension as the Yukawa coupling g, i.e., $[u_0] = [g] = \epsilon$. In contrast to the discussion in Sec. III A, the linear UV divergences $\sim \Lambda$ in certain loop integrals for δ-correlated disorder turn into additional $\sim \ln \Lambda$ divergences in the power-law correlated case, due to the $|\mathbf{p}|^{-1}$ dependence in
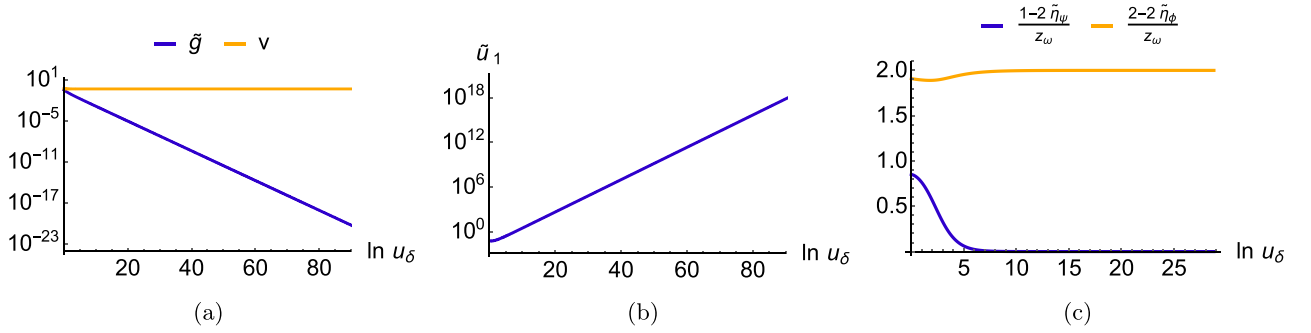
FIG. 3. RG flows as function of $\ln u_\delta$ (see main text for details). (a) Flow of $\tilde{g} = g^2/u_\delta$ and v, (b) $\tilde{u}_1 = u_1/u_\delta$, and (c) the frequency exponents of the fermionic and bosonic propagators. The initial conditions in (a) and (b) are taken from Fig. 2 at $u_\delta = 1$, i.e., $(\tilde{g}, \tilde{u}_1, c, v, a) = (0.3035, 0.0600, 0.7370, 0.4641, 0.9347)$ for which the fermion velocity converges to $v = 0.4325$. The frequency exponents in (c) are plotted for the same initial values as in Fig. 2, but with $\epsilon = 1$. For comparison, at the clean SDW fixed point the exponents are given by $\frac{1-2\tilde{\eta}_\psi}{z_\omega} = 1 - \frac{5}{6}\epsilon$ and $\frac{2-2\tilde{\eta}_\phi}{z_\omega} = 2 - \frac{5}{3}\epsilon$ at leading order in ϵ.

Eq. (19). We absorb these additional logarithmic divergences into the disorder coupling constant by defining $u_p = u_0 \ln \Lambda$. Details of the calculations can be found in the appendices.

The flow equations for the model with power-law correlated disorder with $\alpha = 1$ have the same form as in Eqs. (24)–(30) with the replacement $u_\delta \to \frac{u_p}{\sqrt{1+v^2}}$. In analogy to the δ-correlated case, for any positive, nonzero UV initial condition for the disorder coupling u_p we always observe a flow to strong coupling. Consequently the same conclusions can be drawn as for the δ-correlated case.

IV. DISCUSSION AND CONCLUSION

In this work, we presented a controlled, perturbative RG analysis of antiferromagnetic quantum critical points in two-dimensional metals with quenched disorder. We considered disorder models with small angle scattering only, such that cold electrons far away from the hot spots cannot become hot by scattering off the disorder potential and thus the hot spot model remains valid. Adopting the ϵ expansion by Sur

and Lee, we derived one-loop flow equations and showed that the clean non-Fermi liquid fixed point is unstable in the presence of disorder and the theory flows to strong coupling. Extrapolating the flow to strong coupling and studying its asymptotics, we concluded that the ground state in two dimensions is potentially Anderson-localized and thus nonmetallic. Since the strong coupling fixed point is not accessible in our approach, it would be interesting to see if our results can be tested using sign-problem free determinant quantum Monte Carlo simulations [6,41], where disorder can be included in principle.

APPENDIX A: ONE-LOOP CORRECTIONS WITHOUT DISORDER

In this Appendix, we derive the divergent parts of the self-energies and vertex corrections coming from the Yukawa and the ϕ^4 interaction at one-loop order. Compared to the results in Ref. [29], the ϵ poles are slightly modified due to the additional boson velocity a, which only plays a role as soon as disorder is taken into account. Diagrams are shown in Fig. 4.
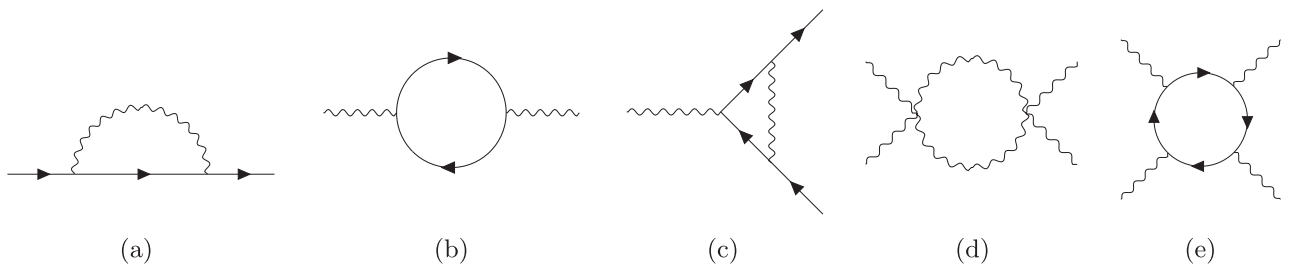
FIG. 4. One-loop contributions from Yukawa and ϕ^4 interactions to (a) fermionic self-energy, (b) bosonic self-energy, (c) Yukawa vertex, and (d) and (e) ϕ^4 vertices. Only diagram (e) does not lead to a pole in $\epsilon = 3 - d$. Solid (wiggly) lines represent fermionic (bosonic) propagators. All propagators are matrices in the Keldysh-index space.

1. Fermion self-energy

The one-loop fermion self-energy due to the Yukawa interaction is given by the integral

$$\Sigma_{Y,n}^{(ab)}(q) = -2ig^2\mu^\epsilon \frac{N_c^2-1}{N_f N_c} \int_k D^{\alpha\beta}(k)\gamma_{(ac)}^\alpha \sigma_x G_{\bar{n}}^{(cd)}(q-k)\sigma_x \gamma_{(db)}^\beta, \tag{A1}$$

and has the same causality structure as the inverse fermion propagator

$$\Sigma_Y^{(ab)} = \begin{pmatrix} \Sigma_{Y,n}^R & \Sigma_{Y,n}^K \\ 0 & \Sigma_{Y,n}^A \end{pmatrix}. \tag{A2}$$

Indeed, the $\Sigma_{Y,n}^{(21)}$ component

$$\Sigma_{Y,n}^{(21)} \sim \int_\omega \left[D^R(k)G_{\bar{n}}^A(q-k) + D^A(k)G_{\bar{n}}^R(q-k) \right] \tag{A3}$$

vanishes by integrating over the frequency since all poles of the propagators lie in the same half plane. For the remaining components, it is sufficient to calculate the retarded self-energy

$$\Sigma_{Y,n}^R(q) = -2ig^2\mu^\epsilon \frac{N_c^2-1}{N_f N_c} \int_k \sigma_x \left[D^K(k)G_{\bar{n}}^R(q-k) + D^R(k)G_{\bar{n}}^K(q-k) \right]\sigma_x, \tag{A4}$$

since $\Sigma_{Y,n}^A$ and $\Sigma_{Y,n}^K$ can be obtained via the relations $\sigma_y \Sigma_{Y,n}^A(q) = [\sigma_y \Sigma_{Y,n}^R(q)]^\dagger$ and $\Sigma_{Y,n}^K(q) = \text{sgn}(q_0)[\Sigma_{Y,n}^R(q) - \Sigma_{Y,n}^A(q)]$, respectively.

Writing the Keldysh propagators in terms of the retarded and advanced propagators, the retarded fermion self-energy can be brought into the form

$$\Sigma_{Y,n}^R(q) = -\frac{2}{\pi}ig^2\mu^\epsilon \frac{N_c^2-1}{N_f N_c} \int_{\tilde{\mathbf{k}},\mathbf{k}} \sigma_x \left[\int_{q_0}^\infty d\omega D^R(k)G_{\bar{n}}^A(q-k) - \int_0^\infty d\omega D^A(k)G_{\bar{n}}^R(q-k) + \int_0^{q_0} d\omega D^R(k)G_{\bar{n}}^R(q-k) \right]\sigma_x. \tag{A5}$$

A pole in $\epsilon = 3 - d$ can be only obtained by sending one integration bound to infinity, whereas finite integration bounds cannot contribute to a divergence of the integral. Thus the last term can be neglected safely and the remaining two terms may be written as

$$\Sigma_{Y,n}^R(q) = -\frac{2}{\pi}ig^2\mu^\epsilon \frac{N_c^2-1}{N_f N_c} \int_{\tilde{\mathbf{k}},\mathbf{k}} \int_0^\infty d\omega\, \sigma_x \left[D^R(k)G_{\bar{n}}^A(q-k) - D^A(k)G_{\bar{n}}^R(q-k) \right]\sigma_x$$

$$= -\frac{2}{\pi}ig^2\mu^\epsilon \frac{N_c^2-1}{N_f N_c} \int_{\tilde{\mathbf{k}},\mathbf{k}} \int_0^\infty d\omega\, \text{Im}\left\{ \frac{1}{(\omega+i\delta)^2 - a^2\tilde{\mathbf{k}}^2 - c^2\mathbf{k}^2} \frac{i\sigma_y(\omega-q_0+i\delta) + \sigma_{\mathbf{z}}(\tilde{\mathbf{k}}-\tilde{\mathbf{q}}) - \sigma_x \varepsilon_{\bar{n}}(\mathbf{k}-\mathbf{q})}{(\omega-q_0+i\delta)^2 - (\tilde{\mathbf{k}}-\tilde{\mathbf{q}})^2 - \varepsilon_{\bar{n}}^2(\mathbf{k}-\mathbf{q})} \right\}. \tag{A6}$$

Introducing a Feynman parameter and completing the squares in the denominator, we find

$$\Sigma_{Y,n}^R(q) = -i\frac{g^2\mu^\epsilon}{c}\frac{N_c^2-1}{N_f N_c}\frac{1}{2^{d-2}\pi^{\frac{d}{2}+1}\Gamma(\frac{d}{2})} \int_0^1 dx \frac{[x+(1-x)a^2]^{\frac{2-d}{2}}}{\sqrt{1-x}\sqrt{c^2+x(1+v^2-c^2)}} \int_0^\infty dr\, r^{d-1} \int_{-xq_0}^\infty d\omega$$

$$\times \text{Im}\left\{ \frac{i\sigma_y[\omega+i\delta-(1-x)q_0] - \sigma_{\mathbf{z}}\frac{(1-x)a^2}{x+(1-x)a^2}\tilde{\mathbf{q}} + \sigma_x \frac{(1-x)c^2}{c^2+x(1+v^2-c^2)}\varepsilon_{\bar{n}}(\mathbf{q})}{[(\omega+i\delta)^2 - r^2 - \bar{q}]^2} \right\}, \tag{A7}$$

where $\bar{q} = \bar{q}(x,c,v,a,q)$ is a real function of the Feynman parameter, the velocities, the external frequency, and the external momenta. Evaluating the remaining integrals and expanding in small ϵ yields the pole

$$\Sigma_{Y,n}^R(q) = -\frac{g^2}{4\pi^2 c\epsilon}\frac{N_c^2-1}{N_f N_c}[\sigma_y h_1(c,v,a)q_0 - i\sigma_{\mathbf{z}}h_q(c,v,a)\tilde{\mathbf{q}} + i\sigma_x h_2(c,v,a)\varepsilon_{\bar{n}}(\mathbf{q})] \tag{A8}$$

with

$$h_1(c,v,a) = \int_0^1 dx \sqrt{\frac{1-x}{[c^2+x(1+v^2-c^2)][x+(1-x)a^2]}}, \tag{A9}$$

$$h_q(c,v,a) = a^2 \int_0^1 dx \sqrt{\frac{1-x}{[c^2+x(1+v^2-c^2)][x+(1-x)a^2]^3}}, \tag{A10}$$

$$h_2(c,v,a) = c^2 \int_0^1 dx \sqrt{\frac{1-x}{[c^2+x(1+v^2-c^2)]^3[x+(1-x)a^2]}}. \tag{A11}$$

Correspondingly, the advanced component of the self-energy takes the same form, such that there is no ϵ pole for the Keldysh self-energy.

2. Boson self-energy

The boson self-energy

$$\Pi^{\alpha\beta}(q) = 2ig^2\mu^\epsilon \sum_n \int_k \mathrm{Tr}\big\{\gamma^\alpha_{(ab)}\sigma_x G^{(bc)}_{\bar{n}}(k)\gamma^\beta_{(cd)}\sigma_x G^{(da)}_n(k-p)\big\} \tag{A12}$$

is independent of the velocity a since the integral only contains fermionic propagators. Thus the divergent parts of the retarded and advanced self-energies can be derived to take the form

$$\Pi^{qc}(q) = \Pi^R(q) = \Pi^A(-q) = -\frac{g^2}{2\pi v\epsilon}\big(q_0^2 - \tilde{\mathbf{q}}^2\big), \tag{A13}$$

whereas the Keldysh component $\Pi^K(q) = \mathrm{sgn}(q_0)[\Pi^R(q) - \Pi^A(q)]$ remains finite again.

3. Yukawa vertex correction

The counter term to the Yukawa vertex coming from corrections due to the Yukawa vertex itself takes the form

$$S_{Y,\mathrm{count}} = -i\frac{g\mu^{\frac{\epsilon}{2}}}{\sqrt{N_f}}\sum_{n,j}\sum_{\sigma_1,\sigma_2}\int_{p,q}\vec{\phi}^\alpha(q)\vec{\tau}_{\sigma_1\sigma_2}\overline{\Psi}^{(a)}_{n,j,\sigma_1}(p+q)V^{\alpha,(ab)}_{Y,n}\Psi^{(b)}_{\bar{n},j,\sigma_2}(p), \tag{A14}$$

where

$$V^{\alpha,(ab)}_{Y,n} = -2i\frac{g^2\mu^\epsilon}{N_fN_c}\int_k \sigma_x\gamma^{\beta_1}_{(ac)}G^{(cd)}_{\bar{n}}(p+q-k)\sigma_x\gamma^\alpha_{(de)}D^{\beta_1\beta_2}(k)G^{(ef)}_n(p-k)\sigma_x\gamma^{\beta_2}_{(fb)} \tag{A15}$$

has eight components corresponding to the different Keldysh indices. In fact, $V^{c,(12)}_n$, $V^{c,(21)}_n$, $V^{q,(11)}_n$ and $V^{q,(22)}_n$ turn out to be zero, whereas the remaining four components lead to the same integral expression. Hence we can write $V^{\alpha,(ab)}_{Y,n} = \gamma^\alpha_{(ab)}V_{Y,n}$ with

$$
\begin{aligned}
V_{Y,n} &= -4i\frac{g^2\mu^\epsilon}{N_fN_c}\int_{\bar{\mathbf{k}},k}\int_0^\infty \frac{d\omega}{2\pi}\big[D^R(k)\sigma_x G^A_{\bar{n}}(p+q-k)\sigma_x G^A_n(p-k)\sigma_x - D^A(k)\sigma_x G^R_{\bar{n}}(p+q-k)\sigma_x G^R_n(p-k)\sigma_x\big] \\
&= -4\frac{g^2\mu^\epsilon}{N_fN_c}\sigma_x \\
&\quad \times \mathrm{Im}\bigg\{\int_{\bar{\mathbf{k}},k}\int_0^\infty \frac{d\omega}{2\pi}\frac{(\omega+i\delta)^2 - (\tilde{\mathbf{k}}-\tilde{\mathbf{p}})^2 + \varepsilon_{\bar{n}}(\mathbf{k})\varepsilon_n(\mathbf{k})}{\big[(\omega+i\delta)^2 - (\tilde{\mathbf{k}}-\tilde{\mathbf{p}})^2 - \varepsilon^2_{\bar{n}}(\mathbf{k})\big]\big[(\omega+i\delta)^2 - (\tilde{\mathbf{k}}-\tilde{\mathbf{p}})^2 - \varepsilon^2_n(\mathbf{k})\big]\big[(\omega+i\delta)^2 - a^2\tilde{\mathbf{k}}^2 - c^2\mathbf{k}^2\big]}\bigg\},
\end{aligned} \tag{A16}
$$

where we set all external frequencies and momenta to zero except for $\tilde{\mathbf{p}}$. Changing integration variables to $\varepsilon_{\bar{n}}(\mathbf{k}) = \sqrt{2v}R\sin\theta$, $\varepsilon_n(\mathbf{k}) = \sqrt{2v}R\cos\theta$ and introducing two Feynman parameters, the divergent part of the integral can be extracted from

$$
\begin{aligned}
V_{Y,n} = &-\frac{1}{2^{d-3}\pi^{\frac{d}{2}+2}\Gamma\big(\frac{d-2}{2}\big)}\frac{g^2\mu^\epsilon}{N_fN_c}\sigma_x \\
&\times \mathrm{Im}\bigg\{\int_0^1 dx\,dy\,(1-y)\int_0^{2\pi}d\theta\int_0^\infty drdR\,r^{d-3}\,R\,\frac{(\omega+i\delta)^2 - r^2 + vR^2\sin(2\theta)}{\{(\omega+i\delta)^2 - [1+x(1-x)a^2]r^2 - cR^2\zeta(c,v,x,y,\theta) - \bar{p}^2\}^3}\bigg\}
\end{aligned} \tag{A17}
$$

with $\zeta(c,v,x,y,\theta) = \frac{2v}{c}(1-y)[x\cos^2\theta + (1-x)\sin^2\theta] + \frac{c}{2v}y(\cos\theta+\sin\theta)^2 + \frac{cv}{2}y(\cos\theta-\sin\theta)^2$ and $\bar{p}^2 = \frac{y(1-y)a^2}{1+(a^2-1)y}\tilde{\mathbf{p}}^2$. Evaluating the remaining integrals and expanding in small ϵ, we obtain the pole

$$V_{Y,n} = -\frac{g^2}{8\pi^3cN_fN_c\epsilon}h_3(c,v,a)\sigma_x \tag{A18}$$

with

$$h_3(c,v,a) = \frac{1}{2}\int_0^1 dx\,dy\,\frac{1-y}{\sqrt{1+(a^2-1)y}}\int_0^{2\pi}d\theta\,\frac{1}{\zeta(c,v,x,y,\theta)}\bigg[\frac{2+(a^2-1)y}{1+(a^2-1)y} - \frac{2v\sin(2\theta)}{c\zeta(c,v,x,y,\theta)}\bigg]. \tag{A19}$$
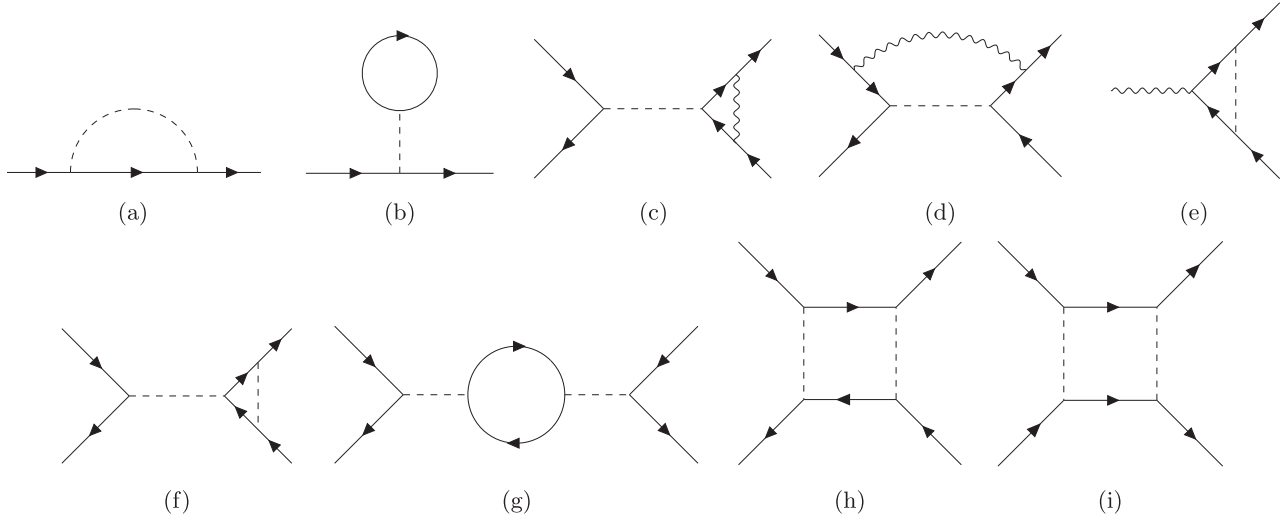
FIG. 5. One-loop contributions including disorder to (a) and (b) fermionic self-energy, (c) and (d) disorder vertex coming from Yukawa interaction, (e) Yukawa vertex coming from disorder interaction, and (f)–(i) disorder vertex from disorder interaction. Dashed lines represent factors of $u(\vec{k})$.

4. $\vec{\phi}^4$ vertex correction

The one-loop diagrams leading to counter terms for the $\vec{\phi}^4$ vertices contain only bosonic propagators. For a general second boson velocity a, we therefore obtain an additional factor of a^{-1} in $d = 3$ by rescaling the integration variable $\tilde{\mathbf{k}} \to a^{-1}\tilde{\mathbf{k}}$ in the boson propagators. Consequently, the counter terms to the $\vec{\phi}^4$ vertices read

$$
S_{\phi^4,\text{count}} = -\frac{u_1\mu^\epsilon}{4} V_{\phi^4,u_1} \int_{p_1,p_2,p_3} \text{Tr}\{\Phi^c(p_1+p_3)\Phi^c(p_2-p_3) + \Phi^q(p_1+p_3)\Phi^q(p_2-p_3)\}\text{Tr}\{\Phi^c(-p_1)\Phi^q(-p_2)\}
$$
$$
- \frac{u_2\mu^\epsilon}{4} V_{\phi^4,u_2} \int_{p_1,p_2,p_3} \text{Tr}\{[\Phi^c(p_1+p_3)\Phi^c(p_2-p_3) + \Phi^q(p_1+p_3)\Phi^q(p_2-p_3)]\Phi^c(-p_1)\Phi^q(-p_2)\} \tag{A20}
$$

with

$$
V_{\phi^4,u_1} = \frac{1}{2\pi^2 c^2 a}\left[\frac{u_1}{\epsilon}(N_c^2+7) + \frac{u_2}{\epsilon}\frac{2(2N_c^2-3)}{N_c} + \frac{u_2^2}{u_1\epsilon}\frac{3(N_c^2+3)}{N_c^2}\right], \tag{A21}
$$

$$
V_{\phi^4,u_2} = \frac{1}{\pi^2 c^2 a}\left[\frac{6u_1}{\epsilon} + \frac{u_2}{\epsilon}\frac{N_c^2-9}{N_c}\right]. \tag{A22}
$$

APPENDIX B: ONE-LOOP CORRECTIONS INCLUDING DISORDER

1. Fermion self-energy

The fermion self-energy obtained from the disorder vertex [Fig. 5(a)] is given by

$$
\Sigma_{\text{dis},n}^{(ab)}(q) = 2 \int_{\vec{k}} \sigma_y G_n^{(ab)}(\vec{k}, q_0)\sigma_y u(\vec{k}-\vec{q}), \tag{B1}
$$

where $u(\vec{k}-\vec{q}) = u_0\mu^{\epsilon-1}$ for δ-correlated disorder and $u(\vec{k}-\vec{q}) = u_0\mu^\epsilon |\mathbf{k}-\mathbf{q}|^{-1}$ for the power-law correlated case with $\alpha = 1$. The second contribution [Fig. 5(b)] only leads to an unimportant renormalization of the chemical potential and will be omitted.

a. δ-correlated disorder

Taking the retarded/advanced component of the self-energy, the matrix product simplifies to

$$
\Sigma_{\text{dis},n}^{R/A}(q) = 2u_0\mu^{\epsilon-1} \int_{\vec{k}} \frac{\sigma_y(q_0 \pm i\delta) + i\sigma_{\mathbf{z}}\tilde{\mathbf{k}} + i\sigma_x\varepsilon_n(\mathbf{k})}{(q_0 \pm i\delta)^2 - \tilde{\mathbf{k}}^2 - \varepsilon_n^2(\mathbf{k})}. \tag{B2}
$$

Since the integrand only depends on a single hot spot via $\varepsilon_n(\mathbf{k})$, it is always possible to shift out one of the integration variables k_x or k_y. Taking, e.g., $n = 1$ with $\varepsilon_1(\mathbf{k}) = vk_x + k_y$ and shifting $k_y \to k_y - vk_x$ leads to

$$\Sigma^{R/A}_{\text{dis},n}(q) = 2u_0\mu^{\epsilon-1}\frac{\Lambda}{\pi} \int_{\tilde{\mathbf{k}},k_y} \frac{\sigma_y(q_0 \pm i\delta) + i\boldsymbol{\sigma_z}\tilde{\mathbf{k}} + i\sigma_x k_y}{(q_0 \pm i\delta)^2 - \tilde{\mathbf{k}}^2 - k_y^2}, \tag{B3}$$

with Λ being the cutoff for the k_x integral. Evaluating the remaining integrals and expanding in small $\epsilon = 3 - d$, we obtain

$$\Sigma^{R/A}_{\text{dis},n}(q) = -\frac{u_\delta}{\pi^2\epsilon}\sigma_y q_0, \tag{B4}$$

where we defined the effective coupling $u_\delta = u_0\Lambda/\mu$. Furthermore we dropped the dependence on $\delta = 0^+$ since it is only needed to make the integrals convergent. Note that the calculation is in fact independent of the hot spot index, such that (B4) holds for any n.

b. Power-law correlated disorder

For the power-law correlated case, the retarded/advanced fermion self-energy can be calculated from

$$\Sigma^{R/A}_{\text{dis},n}(q) = 2u_0\mu^\epsilon \int_{\tilde{\mathbf{k}}} \frac{1}{\sqrt{k_x^2 + k_y^2}}\frac{\sigma_y(q_0 \pm i\delta) + i\boldsymbol{\sigma_z}\tilde{\mathbf{k}} + i\sigma_x\varepsilon_n(\mathbf{k} + \mathbf{q})}{(q_0 \pm i\delta)^2 - \tilde{\mathbf{k}}^2 - \varepsilon_n^2(\mathbf{k} + \mathbf{q})}. \tag{B5}$$

Taking again $n = 1$ as an example, the above integral can be brought into the form

$$\Sigma^{R/A}_{\text{dis},n}(q) = 2u_0\mu^\epsilon \int_{\tilde{\mathbf{k}}} \frac{1}{\sqrt{k_x^2 + k_y^2}}\frac{\sigma_y(q_0 \pm i\delta) + i\boldsymbol{\sigma_z}\tilde{\mathbf{k}} + i\sigma_x[\sqrt{1 + v^2}k_y + \varepsilon_1(\mathbf{q})]}{(q_0 \pm i\delta)^2 - \tilde{\mathbf{k}}^2 - [\sqrt{1 + v^2}k_y + \varepsilon_1(\mathbf{q})]^2}, \tag{B6}$$

where the linear divergence of the k_x integral in the δ-correlated case is now replaced by a logarithmic divergence. Evaluating the remaining integrals thus leads to

$$\Sigma^{R/A}_{\text{dis},n}(q) = -\frac{u_p}{\sqrt{1 + v^2}\pi^2\epsilon}\sigma_y q_0 \tag{B7}$$

with the effective interaction $u_p = u_0 \ln \Lambda$. Again, the calculation is independent of the specific choice of n.

2. Disorder vertex correction coming from disorder vertex

The counter term for the disorder vertex coming from diagram Fig. 5(f) reads

$$S_{\text{dis,count}} = i \sum_{n_1,n_2} \sum_{\sigma_1,\sigma_2} \sum_{j_1,j_2} \int_{\substack{\vec{k}_1,\vec{k}_2,\vec{k}_3 \\ \omega_1,\omega_2}} \left[\overline{\Psi}^{(a)}_{n_1,j_1,\sigma_1}(\vec{k}_1 + \vec{k}_3, \omega_1)\sigma_y\Psi^{(a)}_{n_1,j_1,\sigma_1}(\vec{k}_1, \omega_1)\right]u(\vec{k}_3)$$

$$\times \left[\overline{\Psi}^{(b)}_{n_2,j_2,\sigma_2}(\vec{k}_2 - \vec{k}_3, \omega_2)U^{(bc)}_{\text{dis},n}\Psi^{(c)}_{n_2,j_2,\sigma_2}(\vec{k}_2, \omega_2)\right] \tag{B8}$$

with

$$U^{(bc)}_{\text{dis},n} = -4 \int_{\vec{p}} \sigma_y G^{(bd)}_n(\vec{p} + \vec{k}_2 - \vec{k}_3, \omega_2)\sigma_y G^{(dc)}_n(\vec{p} + \vec{k}_2, \omega_2)\sigma_y u(\vec{p}). \tag{B9}$$

The diagram in Fig. 5(g) trivially vanishes by integrating over the internal frequency of the fermion loop since only combinations $G^{(ab)}G^{(ba)} \sim G^R G^R$, $G^A G^A$ contribute. The other two diagrams do not lead to a renormalization of the disorder vertex as well, which will be explained in the following sections.

In principle, we could set the external frequency to zero implying that the exact nature of the propagators (i.e., retarded or advanced) does not matter for the calculation of the poles, s.t. any expression containing a Keldysh propagator vanishes immediately. Thus, the off-diagonals of the vertex correction $U^{\text{dis},(bc)}_n$ are zero, whereas the diagonals are identical and nonzero. Nevertheless, we keep the external frequency finite in the following to regulate the momentum integrals, but the final expression of the poles will be independent of the frequency of course.

a. δ-correlated disorder

Setting the external momenta to zero and $u(\vec{p}) = u_0\mu^{\epsilon-1}$, the divergent part of the diagonal entries of the vertex correction can be extracted from

$$U^{(11)}_{\text{dis},n} = -4u_0\mu^{\epsilon-1}\sigma_y \int_{\vec{p}} \frac{(\omega_2 + i\delta)^2 + \tilde{\mathbf{p}}^2 + \varepsilon_n^2(\mathbf{p})}{\left[(\omega_2 + i\delta)^2 - \tilde{\mathbf{p}}^2 - \varepsilon_n^2(\mathbf{p})\right]^2}. \tag{B10}$$

As was the case for the fermion self-energy, we can shift out one of the momenta in $\varepsilon_n(\mathbf{k})$, leaving us with a linearly diverging integral, such that we find

$$U_{\text{dis},n}^{(11)} = -4u_0\mu^{\epsilon-1}\sigma_y\frac{\Lambda}{\pi}\int_{\tilde{\mathbf{p}},p_y}\frac{(\omega_2+i\delta)^2+\tilde{\mathbf{p}}^2+p_y^2}{\left[(\omega_2+i\delta)^2-\tilde{\mathbf{p}}^2-p_y^2\right]^2} = -\frac{2u_\delta}{\pi^2\epsilon}\sigma_y = U_{\text{dis},n}^{(22)}. \tag{B11}$$

The hot spot indices of the internal propagators in the two diagrams Figs. 5(h) and 5(i) do not have to be the same in principal. If they have the same index, we indeed find ϵ poles, but the contributions from the two diagrams exactly cancel. If they have different indices, the momentum integrals turn out to be divergent for any $d \geqslant 2$ since we cannot shift out one of the integration variables. In $d = 3$, the divergence is linear in the cutoff Λ (without an ϵ pole) and therefore subleading to terms $\sim \frac{\Lambda}{\epsilon} \sim \Lambda \ln \Lambda$, such that their contribution can be neglected.

b. Power-law correlated disorder

In the power-law correlated case, the linear divergence is again replaced by a logarithmic divergence, leading to the pole

$$U_{\text{dis},n}^{(11)} = U_{\text{dis},n}^{(22)} = -\frac{2u_p}{\sqrt{1+v^2}\pi^2\epsilon}\sigma_y. \tag{B12}$$

The two diagrams Figs. 5(h) and 5(i) turn out to be finite for any $d \leqslant 3$.

3. Disorder vertex correction coming from Yukawa vertex

Similarly to (B8), we need to add a counter term to the disorder vertex coming from corrections via the Yukawa interaction [Fig. 5(c)], which can be calculated via

$$U_{Y,n}^{(bc)} = 4ig^2\mu^\epsilon\frac{N_c^2-1}{N_cN_f}\int_{\omega,\vec{p}}\gamma_{(bd)}^\alpha\sigma_x G_{\tilde{n}}^{(de)}(\vec{k}_2-\vec{k}_3-\vec{p},\omega)\sigma_y D^{\alpha\beta}(\vec{k},\omega_2-\omega)G_{\tilde{n}}^{(ef)}(\vec{k}_2-\vec{p},\omega)\sigma_x\gamma_{(fc)}^\beta \tag{B13}$$

and is identical for both δ-correlated and power-law correlated disorder. In principle three additional diagrams [Fig. 5(d) plus two permutations of the direction of the fermions] could possibly renormalize the disorder vertex, but the integrals are convergent in $d = 3$ due to a missing internal frequency integral.

Again, the off-diagonal contributions vanish, whereas the diagonal contributions are equal and nonzero. Simplifying the sum over Keldysh indices and setting all external momenta and frequencies to zero except for $\tilde{\mathbf{k}}_2$, the integral reduces to

$$U_{Y,n}^{(11)} = 8g^2\mu^\epsilon\frac{N_c^2-1}{N_cN_f}\sigma_y\text{Im}\left\{\int_{\vec{p}}\int_0^\infty\frac{d\omega}{2\pi}\frac{(\omega+i\delta)^2+(\tilde{\mathbf{p}}-\tilde{\mathbf{k}}_2)^2+\varepsilon_{\tilde{n}}^2(\mathbf{p})}{\left[(\omega+i\delta)^2-(\tilde{\mathbf{p}}-\tilde{\mathbf{k}}_2)^2-\varepsilon_{\tilde{n}}^2(\mathbf{p})\right]^2[(\omega+i\delta)^2-a^2\tilde{\mathbf{p}}^2-c^2\mathbf{p}^2]}\right\}. \tag{B14}$$

Introducing a Feynman parameter and completing the squares in the resulting numerator, the divergent part of the integral can be extracted from

$$U_{Y,n}^{(11)} = 8g^2\mu^\epsilon\frac{N_c^2-1}{N_cN_f}\sigma_y$$

$$\times\text{Im}\left\{\int_0^1 dx\,x\int_{\vec{p}}\int_0^\infty\frac{d\omega}{\pi}\frac{(\omega+i\delta)^2+\tilde{\mathbf{p}}^2+v^2p_x^2+\frac{c^4(1-x)^2}{[(1-x)c^2+xv^2]^2}p_y^2}{\left\{(\omega+i\delta)^2-(x+(1-x)a^2)\tilde{\mathbf{p}}^2-[(1-x)c^2+xv^2]p_x^2-\frac{c^2(1-x)[c^2+x(1+v^2-c^2)]}{(1-x)c^2+xv^2}p_y^2-\bar{k}_2^2\right\}^3}\right\} \tag{B15}$$

with $\bar{k}_2^2 = \frac{x(1-x)a^2}{x+(1-x)a^2}\tilde{\mathbf{k}}_2^2$ and evaluates to

$$U_{Y,n}^{(11)} = 8g^2\mu^\epsilon\frac{N_c^2-1}{N_cN_f}\sigma_y$$

$$\times\text{Im}\left\{-\frac{i}{32\pi^2c\epsilon}\int_0^1 dx\frac{x}{\sqrt{1-x}}\frac{1}{\sqrt{c^2+x(1+v^2-c^2)}\sqrt{x+(1-x)a^2}}\left(-1+\frac{1}{x+(1-x)a^2}+\frac{1+v^2}{c^2+x(1+v^2-c^2)}\right)\right\}. \tag{B16}$$

The Feynman parameter integral turns out to be numerically the same as $2h_1(c,v,a)$, such that we obtain

$$U_{Y,n}^{(11)} = U_{Y,n}^{(22)} = 8g^2\frac{N_c^2-1}{N_cN_f}\text{Im}\left\{-\frac{i}{32\pi^2c\epsilon}2h_1(c,v,a)\right\} = -\frac{g^2}{2\pi^2c\epsilon}\frac{N_c^2-1}{N_cN_f}h_1(c,v,a). \tag{B17}$$

Note that the ϵ pole is again independent of the hot spot index n.

4. Yukawa vertex correction coming from disorder vertex

We need to add a similar counter term as in (A14) to cancel possible corrections to the Yukawa vertex coming from the disorder interaction. The divergent part of the one-loop contribution [Fig. 5(e)] can be calculated from the expression

$$V_{\mathrm{dis},n}^{\alpha,(ab)} = -2 \int_{\tilde{k}} \sigma_y G_n^{(ac)}(\vec{k} + \vec{p} + \vec{q}, p_0 + q_0)\gamma_{(cd)}^{\alpha}\sigma_x G_{\bar{n}}^{(db)}(\vec{k} + \vec{p}, p_0)\, u(\vec{k}). \tag{B18}$$

Again, this vertex correction has the Keldysh index structure of the original Yukawa vertex $V_{\mathrm{dis},n}^{\alpha,(ab)} = \gamma_{(ab)}^{\alpha} V_{\mathrm{dis},n}$ with

$$V_{\mathrm{dis},n} = -2\sigma_x \int_{\tilde{k}} \frac{\varepsilon_n(\mathbf{k})\varepsilon_{\bar{n}}(\mathbf{k}) - \tilde{\mathbf{k}}^2}{\left[(p_0 + i\delta)^2 - \tilde{\mathbf{k}}^2 - \varepsilon_n^2(\mathbf{k})\right]\left[(p_0 + i\delta)^2 - \tilde{\mathbf{k}}^2 - \varepsilon_{\bar{n}}^2(\mathbf{k})\right]}u(\vec{k}), \tag{B19}$$

where we set all external frequencies and momenta to zero except for p_0. The final result will be independent of the hot spot index n again, such that we choose $n = 1$ in the following for simplicity.

a. δ-correlated case

For a general finite fermion velocity v, the momentum integral is again divergent for dimensions $d \geqslant 2$, but only with a linear Λ divergence without an ϵ pole in $d = 3$. Only for $v = 0$, the dependence on one of the integration variables drops out and we obtain

$$\lim_{v \to 0} V_{\mathrm{dis},n} = \frac{u_\delta}{\pi^2 \epsilon}\sigma_x. \tag{B20}$$

Since the limit $v \to 0$ can be reached only asymptotically during the RG flow, we will neglect the above contribution in our calculations.

b. Power-law correlated case

In the limit of vanishing fermion velocity, the integral can be computed straightforwardly

$$V_{\mathrm{dis},1} = 2u_0\mu^\epsilon \sigma_x \int_{\tilde{k}} \frac{\tilde{\mathbf{k}}^2 + k_y^2}{\left[(p_0 + i\delta)^2 - \tilde{\mathbf{k}}^2 - k_y^2\right]^2}\frac{1}{\sqrt{k_x^2 + k_y^2}} = \frac{u_p}{\pi^2 \epsilon}\sigma_x. \tag{B21}$$

For general finite v, the integrand (B19) is rewritten by introducing two Feynman parameters

$$\begin{aligned}
V_{\mathrm{dis},1} &= \frac{3}{2}u_0\mu^\epsilon \sigma_x \int_0^1 dx dy \frac{y}{\sqrt{1-y}} \int_{\tilde{k}} \frac{\tilde{\mathbf{k}}^2 + k_y^2 - v^2[1 - (1-2x)^2 y^2]k_x^2}{\left[y\tilde{\mathbf{k}}^2 + k_y^2 + (1 - y\{1 - v^2[1 - (1-2x)^2 y]\})k_x^2 - y(p_0 + i\delta)^2\right]^{\frac{5}{2}}} \\
&= \frac{u_0}{4\pi^2 \epsilon}h_v(v)\sigma_x,
\end{aligned} \tag{B22}$$

where

$$h_v(v) = \int_0^1 dx dy \frac{1 - [1 - 4v^2 x(1-x)]y^2}{\sqrt{y(1-y)}(1 - y\{1 - v^2[1 - (1-2x)^2 y]\})^{\frac{3}{2}}} \tag{B23}$$

is formally convergent for finite v, but divergent in the limit $v \to 0$. Comparing to (B21), we conclude that we need to cut off h_v as soon as it becomes of order $\mathcal{O}(\ln \Lambda)$ via $\lim_{v \to 0} h_v(v) = 4 \ln \Lambda$.

In contrast to the δ-correlated case, we obtain an ϵ pole independent of the choice of v and therefore need to include a counter term in principle. Since v turns out to flow to a constant, finite value in the presence of disorder [see Fig. 3(a)], the contribution from (B22) is suppressed by factors $1/\ln \Lambda$ compared to other terms in the β functions and therefore it can be neglected in the flow equations.

APPENDIX C: RENORMALIZATION

1. β functions and scaling forms

In the following, we use the minimal subtraction scheme, where the divergent parts of the self-energies and vertex corrections are used as counter terms to obtain RG flow equations. Since we used the definition $\overline{\Psi}(G_0^{-1} - \Sigma)\Psi$ and $\frac{1}{2}\vec{\phi}(D_0^{-1} - \Pi)\vec{\phi}$ for the self-energies, we need to add the self-energies and also the counter terms for the interaction vertices to cancel the ϵ poles. This leads to the renormalized action

$$\begin{aligned}
S_{\mathrm{ren}} = \sum_{n,j,\sigma} \int_k &\begin{pmatrix} \overline{\Psi}_{n,j,\sigma}^{(1)}(k) & \overline{\Psi}_{n,j,\sigma}^{(2)}(k) \end{pmatrix} \\
&\times \begin{pmatrix} \sigma_y(Z_1\omega + i\delta) - Z_2 i\boldsymbol{\sigma_z}\tilde{\mathbf{k}} - Z_4 i\sigma_x \varepsilon_n\!\left(\frac{Z_3}{Z_4}v; \mathbf{k}\right) & 2i\,\mathrm{sgn}(\omega)\delta\,\sigma_y \\ 0 & \sigma_y(Z_1\omega - i\delta) - Z_2 i\boldsymbol{\sigma_z}\tilde{\mathbf{k}} - Z_4 i\sigma_x \varepsilon_n\!\left(\frac{Z_3}{Z_4}v; \mathbf{k}\right) \end{pmatrix} \begin{pmatrix} \Psi_{n,j,\sigma}^{(1)}(k) \\ \Psi_{n,j,\sigma}^{(2)}(k) \end{pmatrix}
\end{aligned}$$

$$+ \frac{1}{2} \int_p \begin{pmatrix} \vec{\phi}^c(p) & \vec{\phi}^q(p) \end{pmatrix} \begin{pmatrix} 0 & 2[Z_5(\omega - i\delta)^2 - Z_6 a^2 \tilde{\mathbf{p}}^2 - c^2 \mathbf{p}^2] \\ 2[Z_5(\omega + i\delta)^2 - Z_6 a^2 \tilde{\mathbf{p}}^2 - c^2 \mathbf{p}^2] & 2i\delta \end{pmatrix} \begin{pmatrix} \vec{\phi}^c(-p) \\ \vec{\phi}^q(-p) \end{pmatrix}$$

$$- iZ_7 \frac{g\mu^{\frac{\epsilon}{2}}}{\sqrt{N_f}} \sum_{n,j,\sigma,\sigma'} \int_{k,p} \overline{\Psi}^{(a)}_{n,j,\sigma}(k+p) \, \Phi^\alpha_{\sigma\sigma'}(p) \gamma^\alpha_{(ab)} \sigma_x \, \Psi^{(b)}_{\bar{n},j,\sigma'}(k)$$

$$- Z_8 \frac{u_1 \mu^\epsilon}{4} \int_{p_1,p_2,p_3} \mathrm{Tr}\{\Phi^c(p_1+p_3)\Phi^c(p_2-p_3) + \Phi^q(p_1+p_3)\Phi^q(p_2-p_3)\} \mathrm{Tr}\{\Phi^c(-p_1)\Phi^q(-p_2)\}$$

$$- Z_9 \frac{u_2 \mu^\epsilon}{4} \int_{p_1,p_2,p_3} \mathrm{Tr}\{[\Phi^c(p_1+p_3)\Phi^c(p_2-p_3) + \Phi^q(p_1+p_3)\Phi^q(p_2-p_3)]\Phi^c(-p_1)\Phi^q(-p_2)\}$$

$$+ iZ_{10} \sum_{n,n'} \sum_{j,j'} \sum_{\sigma,\sigma'} \int_{\substack{\vec{k}_1,\vec{k}_2,\vec{k}_3 \\ \omega_1,\omega_2}} \left[\overline{\Psi}^{(a)}_{n,j,\sigma}(\vec{k}_1+\vec{k}_3, \omega_1)\sigma_y \overline{\Psi}^{(a)}_{n,j,\sigma}(\vec{k}_1, \omega_1)\right] u(\vec{k}_3) \left[\overline{\Psi}^{(b)}_{n',j',\sigma'}(\vec{k}_2 - \vec{k}_3, \omega_2)\sigma_y \overline{\Psi}^{(b)}_{n',j',\sigma'}(\vec{k}_2, \omega_2)\right] \tag{C1}$$

with the renormalization constants

$$Z_2 = 1 - \frac{g^2}{\epsilon} \frac{1}{4\pi^2 c} \frac{N_c^2 - 1}{N_f N_c} h_q(c, v, a), \tag{C2}$$

$$Z_3 = 1 + \frac{g^2}{\epsilon} \frac{1}{4\pi^2 c} \frac{N_c^2 - 1}{N_f N_c} h_2(c, v, a), \tag{C3}$$

$$Z_4 = 1 - \frac{g^2}{\epsilon} \frac{1}{4\pi^2 c} \frac{N_c^2 - 1}{N_f N_c} h_2(c, v, a), \tag{C4}$$

$$Z_5 = 1 - \frac{g^2}{\epsilon} \frac{1}{4\pi v}, \tag{C5}$$

$$Z_6 = 1 - \frac{g^2}{\epsilon} \frac{1}{4\pi a^2 v}, \tag{C6}$$

$$Z_8 = 1 + \frac{u_1}{\epsilon} \frac{N_c^2 + 7}{2\pi^2 c^2 a} + \frac{u_2}{\epsilon} \frac{2N_c^2 - 3}{N_c \pi^2 c^2 a} + \frac{u_2^2}{u_1 \epsilon} \frac{3(N_c^2 + 3)}{2N_c^2 \pi^2 c^2 a}, \tag{C7}$$

$$Z_9 = 1 + \frac{u_1}{\epsilon} \frac{6}{\pi^2 c^2 a} + \frac{u_2}{\epsilon} \frac{N_c^2 - 9}{N_c \pi^2 c^2 a} \tag{C8}$$

independent of the choice of the disorder correlation model (i.e., δ-correlated or power-law), as well as

$$Z_1 = 1 - \frac{g^2}{\epsilon} \frac{1}{4\pi^2 c} \frac{N_c^2 - 1}{N_f N_c} h_1(c, v, a) - \frac{u_\delta}{\epsilon} \frac{1}{\pi^2}, \tag{C9}$$

$$Z_7 = 1 - \frac{g^2}{\epsilon} \frac{1}{8\pi^3 c N_f N_c} h_3(c, v, a), \tag{C10}$$

$$Z_{10} = 1 - \frac{g^2}{\epsilon} \frac{1}{2\pi^2 c} \frac{N_c^2 - 1}{N_f N_c} h_1(c, v, a) - \frac{u_\delta}{\epsilon} \frac{2}{\pi^2} \tag{C11}$$

for the δ-correlated case and

$$Z_1 = 1 - \frac{g^2}{\epsilon} \frac{1}{4\pi^2 c} \frac{N_c^2 - 1}{N_f N_c} h_1(c, v, a) - \frac{u_p}{\epsilon} \frac{1}{\sqrt{1 + v^2}\pi^2}, \tag{C12}$$

$$Z_7 = 1 - \frac{g^2}{\epsilon} \frac{1}{8\pi^3 c N_f N_c} h_3(c, v, a) + \frac{u_p}{\epsilon} \frac{1}{4\pi^2 \ln \Lambda} h_v(v), \tag{C13}$$

$$Z_{10} = 1 - \frac{g^2}{\epsilon} \frac{1}{2\pi^2 c} \frac{N_c^2 - 1}{N_c N_f} h_1(c, v, a) - \frac{u_p}{\epsilon} \frac{2}{\sqrt{1 + v^2}\pi^2} \tag{C14}$$

for the power-law correlated case. For the following calculations, we will use the notation $Z_i = 1 + \frac{g^2}{\epsilon} Z_{i1,g} + \frac{u_{\delta/p}}{\epsilon} Z_{i1,u}$ except for Z_8 and Z_9, where we write $Z_i = 1 + \frac{u_1}{\epsilon} Z_{i1,u_1} + \frac{u_2}{\epsilon} Z_{i1,u_2} + \frac{u_2^2}{u_1 \epsilon} Z_{i1,u_1 u_2}$.

Defining the bare momenta and fields as

$$\omega_B = Z_1 Z_4^{-1} \omega, \quad \tilde{\mathbf{k}}_B = Z_2 Z_4^{-1} \tilde{\mathbf{k}}, \quad \mathbf{k}_B = \mathbf{k},$$

$$\Psi_B = Z_1^{-1/2} Z_2^{(2-d)/2} Z_4^{d/2} \Psi, \quad \vec{\phi}_B = Z_1^{-3/2} Z_2^{(2-d)/2} Z_4^{(d+1)/2} Z_5^{1/2} \vec{\phi}, \tag{C15}$$

the action can be brought into its original form by defining the bare velocities and coupling constants via

$$c_B = Z_1 Z_4^{-1} Z_5^{-1/2} c, \quad v_B = Z_3 Z_4^{-1} v, \quad a_B = Z_1 Z_2^{-1} Z_5^{-1/2} Z_6^{1/2} a,$$

$$g_B = \mu^{\epsilon/2} Z_1^{1/2} Z_2^{(2-d)/2} Z_4^{(d-5)/2} Z_5^{-1/2} Z_7 \, g, \quad u_{\delta/p,B} = \mu^{\epsilon} Z_2^{2-d} Z_4^{d-4} Z_{10} \, u_{\delta/p},$$

$$u_{1,B} = \mu^{\epsilon} Z_1^3 Z_2^{2-d} Z_4^{d-5} Z_5^{-2} Z_8 \, u_1, \quad u_{2,B} = \mu^{\epsilon} Z_1^3 Z_2^{2-d} Z_4^{d-5} Z_5^{-2} Z_9 \, u_2. \tag{C16}$$

During the renormalization procedure we absorbed some renormalization factors Z_i into the infinitesimal $\delta = 0^+$ since the Z_i are formally of order $\mathcal{O}(1)$ in the correct order of limits, namely expanding in the interactions first and in small $\epsilon = 3 - d$ second.

The β functions of the parameters $i \in \{c, v, a, g, u_1, u_2, u_{\delta/p}\}$ are obtained from the coupled equations

$$\beta_c = \mu \frac{dc}{d\mu} = c \sum_i \beta_i \left(-\frac{\partial_i Z_1}{Z_1} + \frac{\partial_i Z_4}{Z_4} + \frac{1}{2} \frac{\partial_i Z_5}{Z_5} \right), \tag{C17}$$

$$\beta_v = v \sum_i \beta_i \left(\frac{\partial_i Z_4}{Z_4} - \frac{\partial_i Z_3}{Z_3} \right), \tag{C18}$$

$$\beta_a = a \sum_i \beta_i \left(-\frac{\partial_i Z_1}{Z_1} + \frac{\partial_i Z_2}{Z_2} + \frac{1}{2} \frac{\partial_i Z_5}{Z_5} - \frac{1}{2} \frac{\partial_i Z_6}{Z_6} \right), \tag{C19}$$

$$\beta_g = -\frac{\epsilon}{2} g + g \sum_i \beta_i \left(-\frac{1}{2} \frac{\partial_i Z_1}{Z_1} + \frac{d-2}{2} \frac{\partial_i Z_2}{Z_2} + \frac{5-d}{2} \frac{\partial_i Z_4}{Z_4} + \frac{1}{2} \frac{\partial_i Z_5}{Z_5} - \frac{\partial_i Z_7}{Z_7} \right), \tag{C20}$$

$$\beta_{u_1} = -\epsilon u_1 + u_1 \sum_i \beta_i \left[-3 \frac{\partial_i Z_1}{Z_1} + (d-2) \frac{\partial_i Z_2}{Z_2} + (5-d) \frac{\partial_i Z_4}{Z_4} + 2 \frac{\partial_i Z_5}{Z_5} - \frac{\partial_i Z_8}{Z_8} \right], \tag{C21}$$

$$\beta_{u_2} = -\epsilon u_2 + u_2 \sum_i \beta_i \left[-3 \frac{\partial_i Z_1}{Z_1} + (d-2) \frac{\partial_i Z_2}{Z_2} + (5-d) \frac{\partial_i Z_4}{Z_4} + 2 \frac{\partial_i Z_5}{Z_5} - \frac{\partial_i Z_9}{Z_9} \right], \tag{C22}$$

$$\beta_{u_{\delta/p}} = -\epsilon u_{\delta/p} + u_{\delta/p} \sum_i \beta_i \left[(d-2) \frac{\partial_i Z_2}{Z_2} + (4-d) \frac{\partial_i Z_4}{Z_4} - \frac{\partial_i Z_{10}}{Z_{10}} \right] \tag{C23}$$

and are solved to give

$$\beta_c = \frac{1}{2} g^2 c (2 Z_{11,g} - 2 Z_{41,g} - Z_{51,g}) + c u_{\delta/p} Z_{11,u}, \tag{C24}$$

$$\beta_v = g^2 v (Z_{31,g} - Z_{41,g}), \tag{C25}$$

$$\beta_a = \frac{1}{2} g^2 a (2 Z_{11,g} - 2 Z_{21,g} - Z_{51,g} + Z_{61,g}) + a u_{\delta/p} Z_{11,u}, \tag{C26}$$

$$\beta_g = -\frac{\epsilon}{2} g + \frac{1}{2} g^3 (Z_{11,g} - Z_{21,g} - 2 Z_{41,g} - Z_{51,g} + 2 Z_{71,g}) + \frac{1}{2} g u_{\delta/p} (Z_{11,u} + 2 Z_{71,u}), \tag{C27}$$

$$\beta_{u_1} = -\epsilon u_1 + u_1^2 Z_{81,u_1} + u_1 u_2 Z_{81,u_2} + u_2^2 Z_{81,u_1 u_2} + u_1 g^2 (3 Z_{11,g} - Z_{21,g} - 2 Z_{41,g} - 2 Z_{51,g})$$
$$+ 3 u_1 u_{\delta/p} Z_{11,u}, \tag{C28}$$

$$\beta_{u_2} = -\epsilon u_2 + u_2^2 Z_{91,u_2} + u_1 u_2 Z_{91,u_1} + u_2 g^2 (3 Z_{11,g} - Z_{21,g} - 2 Z_{41,g} - 2 Z_{51,g}) + 3 u_2 u_{\delta/p} Z_{11,u}, \tag{C29}$$

$$\beta_{u_{\delta/p}} = -\epsilon u_{\delta/p} + u_{\delta/p}^2 Z_{101,u} + u_{\delta/p} g^2 (-Z_{21,g} - Z_{41,g} + Z_{101,g}) \tag{C30}$$

to leading order in ϵ.

The general scaling form of the correlation functions

$$G^{(m,m,2n)}(\{k_i\}, \mu, c, v, a, g, u_1, u_2, u_{\delta/p}) = \delta^{(d+1)}(\{k_i\}) \langle \Psi(k_1) \dots \Psi(k_m) \overline{\Psi}(k_{m+1}) \dots \overline{\Psi}(k_{2m}) \phi(k_{2m+1}) \dots \phi(k_{2m+2n}) \rangle, \tag{C31}$$

with the δ function ensuring energy and momentum conservation, can be derived from the RG equation

$$\left\{ \sum_{j=1}^{2m+2n} \left(z_\omega \omega_j \partial_{\omega_j} + z_{\tilde{\mathbf{k}}} \tilde{\mathbf{k}}_j \nabla_{\tilde{\mathbf{k}}_j} + \mathbf{k}_j \nabla_{\mathbf{k}_j} \right) - \sum_i \beta_i \partial_i - 2m \left(\eta_\Psi - \frac{d+2}{2} \right) - 2n \left(\eta_\phi - \frac{d+3}{2} \right) - \left[z_\omega + z_{\tilde{\mathbf{k}}} (d-2) + 2 \right] \right\}$$
$$\times G^{(m,m,2n)}(\{k_i\}, \mu, c, v, a, g, u_1, u_2, u_{\delta/p}) = 0. \tag{C32}$$

Here we defined the dynamical critical exponents

$$z_\omega = 1 + \frac{d \ln(Z_1/Z_4)}{d \ln \mu} = 1 - g^2 (Z_{11,g} - Z_{41,g}) - u_{\delta/p} Z_{11,u}, \tag{C33}$$

$$z_{\tilde{\mathbf{k}}} = 1 + \frac{d \ln(Z_2/Z_4)}{d \ln \mu} = 1 - g^2(Z_{21,g} - Z_{41,g}) \tag{C34}$$

and the anomalous dimensions of the fields

$$\eta_\Psi = \frac{1}{2} \frac{d \ln Z_\Psi}{d \ln \mu} = \frac{g^2}{2}(Z_{11,g} + Z_{21,g} - 3Z_{41,g}) + \frac{u_{\delta/p}}{2} Z_{11,u}, \tag{C35}$$

$$\eta_\phi = \frac{1}{2} \frac{d \ln Z_\phi}{d \ln \mu} = \frac{g^2}{2}(3Z_{11,g} + Z_{21,g} - 4Z_{41,g} - Z_{51,g}) + \frac{3}{2} u_{\delta/p} Z_{11,u}, \tag{C36}$$

where $Z_\Psi = Z_1^{-1} Z_2^{2-d} Z_4^d$ and $Z_\phi = Z_1^{-3} Z_2^{2-d} Z_4^{d+1} Z_5$.

At fixed points, where the β functions vanish, the fermionic and bosonic propagators take the scaling form

$$G(k) = \frac{1}{|k_y|^{1-2\tilde{\eta}_\Psi}} f_\Psi\left(\frac{\omega}{|k_y|^{z_\omega}}, \frac{\tilde{\mathbf{k}}}{|k_y|^{z_{\tilde{\mathbf{k}}}}}, \frac{k_x}{|k_y|}\right), \tag{C37}$$

$$D(k) = \frac{1}{|k_y|^{2-2\tilde{\eta}_\phi}} f_\phi\left(\frac{\omega}{|k_y|^{z_\omega}}, \frac{\tilde{\mathbf{k}}}{|k_y|^{z_{\tilde{\mathbf{k}}}}}, \frac{k_x}{|k_y|}\right), \tag{C38}$$

where $f_{\Psi/\phi}$ are universal scaling functions and

$$\tilde{\eta}_{\Psi/\phi} = \eta_{\Psi/\phi} + \frac{z_\omega + z_{\tilde{\mathbf{k}}}(1-\epsilon) - 2 + \epsilon}{2} \tag{C39}$$

are effective anomalous dimensions.

2. Reparametrization of flow equations

The flow of the parameters is usually parametrized in terms of a logarithmic length scale $\ell = \ln(\mu_0/\mu)$, where, e.g., $\frac{dg}{d\ell} = -\beta_g$ describes the flow to lower energies for increasing ℓ. In the context of this paper, it is convenient to introduce a different flow parameter to be able to follow the flow up to arbitrary strong disorder. Since $\beta_{u_{\delta/p}}$ is positive definite (at least when the flow to strong disorder begins), we choose $\ln u_{\delta/p}$ as an alternative flow parameter. Furthermore, we introduce new coupling constants $\tilde{g} = g^2/u_{\delta/p}$, $\tilde{u}_1 = u_1/u_{\delta/p}$ and $\tilde{u}_2 = u_2/u_{\delta/p}$, whose flow equations can be written down directly, e.g.,

$$\frac{d\tilde{g}}{d \ln u_{\delta/p}} = \frac{dg^2}{du_{\delta/p}} - \frac{g^2}{u_{\delta/p}} = \frac{2g\beta_g}{\beta_{u_{\delta/p}}} - \tilde{g}. \tag{C40}$$

Using the explicit expressions of the β functions in Eqs. (C27) and (C30), we can simplify

$$\frac{2g\beta_g}{\beta_{u_{\delta/p}}} = \tilde{g} \frac{-\frac{\epsilon}{u_{\delta/p}} + \tilde{g}(Z_{11,g} - Z_{21,g} - 2Z_{41,g} - Z_{51,g} + 2Z_{71,g}) + Z_{11,u} + 2Z_{71,u}}{-\frac{\epsilon}{u_{\delta/p}} + Z_{101,u} + \tilde{g}(-Z_{21,g} - Z_{41,g} + Z_{101,g})}, \tag{C41}$$

where we can drop the $\frac{\epsilon}{u_{\delta/p}}$-terms for $u_{\delta/p} \to \infty$. The flow equations of all parameters in terms of the RG scale $\ln u_{\delta/p}$ can then be derived to be

$$\frac{d\tilde{g}}{d \ln u_{\delta/p}} = \tilde{g}\left(\frac{\tilde{g}(Z_{11,g} - Z_{21,g} - 2Z_{41,g} - Z_{51,g} + 2Z_{71,g}) + Z_{11,u} + 2Z_{71,u}}{Z_{101,u} + \tilde{g}(-Z_{21,g} - Z_{41,g} + Z_{101,g})} - 1\right), \tag{C42}$$

$$\frac{d\tilde{u}_1}{d \ln u_{\delta/p}} = \tilde{u}_1\left(\frac{\tilde{u}_1 Z_{81,u_1} + \tilde{u}_2 Z_{81,u_2} + \frac{\tilde{u}_2^2}{\tilde{u}_1} Z_{81,u_1 u_2} + \tilde{g}(3Z_{11,g} - Z_{21,g} - 2Z_{41,g} - 2Z_{51,g}) + 3Z_{11,u}}{Z_{101,u} + \tilde{g}(-Z_{21,g} - Z_{41,g} + Z_{101,g})} - 1\right), \tag{C43}$$

$$\frac{d\tilde{u}_2}{d \ln u_{\delta/p}} = \tilde{u}_2\left(\frac{\tilde{u}_2 Z_{91,u_2} + \tilde{u}_1 Z_{91,u_1} + \tilde{g}(3Z_{11,g} - Z_{21,g} - 2Z_{41,g} - 2Z_{51,g}) + 3Z_{11,u}}{Z_{101,u} + \tilde{g}(-Z_{21,g} - Z_{41,g} + Z_{101,g})} - 1\right), \tag{C44}$$

$$\frac{dc}{d \ln u_{\delta/p}} = c \frac{\frac{1}{2}\tilde{g}(2Z_{11,g} - 2Z_{41,g} - Z_{51,g}) + Z_{11,u}}{Z_{101,u} + \tilde{g}(-Z_{21,g} - Z_{41,g} + Z_{101,g})}, \tag{C45}$$

$$\frac{dv}{d \ln u_{\delta/p}} = v \frac{\tilde{g}(Z_{31,g} - Z_{41,g})}{Z_{101,u} + \tilde{g}(-Z_{21,g} - Z_{41,g} + Z_{101,g})}, \tag{C46}$$

$$\frac{da}{d \ln u_{\delta/p}} = a \frac{\frac{1}{2}\tilde{g}(2Z_{11,g} - 2Z_{21,g} - Z_{51,g} + Z_{61,g}) + Z_{11,u}}{Z_{101,u} + \tilde{g}(-Z_{21,g} - Z_{41,g} + Z_{101,g})}. \tag{C47}$$

3. Large-N_f limit

To perform a systematic analysis of the flow equations presented in the main text in the limit of large N_f, we note that u_0 and therefore $u_{\delta/p}$ have to be rescaled by a factor of $1/N_f$. Then the possible leading order contributions to the fermionic self-energy and the disorder vertex correction in Figs. 5(b) and 5(g) are not of order $\mathcal{O}(N_f)$, but of order $\mathcal{O}(1)$, consistent with the order of corrections coming from the Yukawa coupling. As can be seen in Eqs. (C2) - (C14), only the renormalization constants Z_5 and Z_6 coming from the bosonic self-energy and Z_8 and Z_9 coming from the vertex correction to the ϕ^4 interactions survive the limit of large N_f to leading order $\mathcal{O}(1)$. The flow equations given in the main text hence reduce to

$$\frac{\partial c}{\partial l} = -\frac{g^2}{8\pi v}c, \tag{C48}$$

$$\frac{\partial v}{\partial l} = 0, \tag{C49}$$

$$\frac{\partial a}{\partial l} = -\frac{g^2}{8\pi v}\frac{a^2 - 1}{a}, \tag{C50}$$

$$\frac{\partial g}{\partial l} = \frac{\epsilon}{2}g - \frac{g^3}{8\pi v}, \tag{C51}$$

$$\frac{\partial u_1}{\partial l} = \epsilon u_1 - \frac{11}{2\pi^2 ac^2}u_1^2 - \frac{g^2}{2\pi v}u_1, \tag{C52}$$

$$\frac{\partial u_\delta}{\partial l} = \epsilon u_\delta, \tag{C53}$$

where we set $N_c = 2$. We see that disorder decouples from the other flow equations and trivially diverges due to its scaling dimension. From the remaining flow equations we find a fixed line for the Yukawa coupling $g^* = \sqrt{4\pi v\epsilon}$ parametrized by the fermion velocity v, which does not flow at this order in N_f. The fixed-line values g^* imply that c and u_1 flow to zero, i.e., $c^* = u_1^* = 0$, whereas the second boson velocity a takes the value $a^* = 1$. As discussed in the main text, subleading effects entering at order $\mathcal{O}(1/N_f)$ change the flow drastically due to the antiscreening of the disorder interaction by the Yukawa coupling.

[1] H. V. Löhneysen, A. Rosch, M. Vojta, and P. Wölfle, Rev. Mod. Phys. **79**, 1015 (2007).

[2] G. R. Stewart, Rev. Mod. Phys. **73**, 797 (2001).

[3] T. Shibauchi, A. Carrington, and Y. Matsuda, Annu. Rev. Cond. Mat. Phys. **5**, 113 (2014).

[4] R. L. Greene, P. R. Mandal, N. R. Poniatowski, and T. Sarkar, Annu. Rev. Cond. Mat. Phys. **11**, 213 (2020).

[5] V. J. Emery and S. A. Kivelson, Phys. Rev. Lett. **74**, 3253 (1995).

[6] E. Berg, S. Lederer, Y. Schattner, and S. Trebst, Annu. Rev. Condens. Matter Phys. **10**, 63 (2019).

[7] S.-S. Lee, Annu. Rev. Condens. Matter Phys. **9**, 227 (2018).

[8] R. Hlubina and T. M. Rice, Phys. Rev. B **51**, 9253 (1995).

[9] A. Rosch, Phys. Rev. Lett. **82**, 4280 (1999).

[10] D. L. Maslov, V. I. Yudson, and A. V. Chubukov, Phys. Rev. Lett. **106**, 106403 (2011).

[11] S. A. Hartnoll, R. Mahajan, M. Punk, and S. Sachdev, Phys. Rev. B **89**, 155130 (2014).

[12] A. A. Patel and S. Sachdev, Phys. Rev. B **90**, 165146 (2014).

[13] H. Freire, Ann. Phys. (NY) **384**, 142 (2017).

[14] J. A. Hertz, Phys. Rev. B **14**, 1165 (1976).

[15] P. A. Nosov, I. S. Burmistrov, and S. Raghu, Phys. Rev. Lett. **125**, 256604 (2020).

[16] T. R. Kirkpatrick and D. Belitz, Phys. Rev. B **53**, 14364 (1996).

[17] R. Narayanan, T. Vojta, D. Belitz, and T. R. Kirkpatrick, Phys. Rev. Lett. **82**, 5132 (1999).

[18] A. J. Millis, D. K. Morr, and J. Schmalian, Phys. Rev. B **66**, 174433 (2002).

[19] J. A. Hoyos, C. Kotabage, and T. Vojta, Phys. Rev. Lett. **99**, 230601 (2007).

[20] T. Vojta, Phys. Rev. Lett. **90**, 107202 (2003).

[21] B. L. Altshuler, L. B. Ioffe, and A. J. Millis, Phys. Rev. B **50**, 14048 (1994).

[22] Y. B. Kim, A. Furusaki, X.-G. Wen, and P. A. Lee, Phys. Rev. B **50**, 17917 (1994).

[23] J. Polchinski, Nucl. Phys. B **422**, 617 (1994).

[24] W. Metzner, D. Rohe, and S. Andergassen, Phys. Rev. Lett. **91**, 066402 (2003).

[25] A. Abanov and A. V. Chubukov, Phys. Rev. Lett. **84**, 5608 (2000).

[26] S.-S. Lee, Phys. Rev. B **80**, 165102 (2009).

[27] M. A. Metlitski and S. Sachdev, Phys. Rev. B **82**, 075127 (2010).

[28] M. A. Metlitski and S. Sachdev, Phys. Rev. B **82**, 075128 (2010).

[29] S. Sur and S.-S. Lee, Phys. Rev. B **91**, 125136 (2015).

[30] A. M. Finkel'shtein, Zh. Eksp. Teor. Fiz. **84**, 168 (1983) [Sov. Phys. JETP **57**, 97 (1983)].

[31] C. Castellani, C. Di Castro, P. A. Lee, M. Ma, S. Sorella, and E. Tabet, Phys. Rev. B **30**, 1596 (1984).

[32] A. Kamenev and A. Andreev, Phys. Rev. B **60**, 2218 (1999).

[33] C. Chamon, A. W. W. Ludwig, and C. Nayak, Phys. Rev. B **60**, 2239 (1999).

[34] E. Abrahams, P. W. Anderson, D. C. Licciardello, and T. V. Ramakrishnan, Phys. Rev. Lett. **42**, 673 (1979).

[35] A. A. Patel, P. Strack, and S. Sachdev, Phys. Rev. B **92**, 165105 (2015).

[36] P. Lunts, A. Schlief, and S.-S. Lee, Phys. Rev. B **95**, 245109 (2017).

[37] T. R. Kirkpatrick and D. Belitz, Phys. Rev. Lett. **76**, 2571 (1996).

[38] R. M. Nandkishore and S. A. Parameswaran, Phys. Rev. B **95**, 205106 (2017).

[39] R. N. Bhatt and D. S. Fisher, Phys. Rev. Lett. **68**, 3072 (1992).

[40] S. Sachdev, Phys. Rev. X **5**, 041025 (2015).

[41] E. Berg, M. A. Metlitski, and S. Sachdev, Science **338**, 1606 (2012).

8 Conclusion and outlook

The outlook on possible future investigations of our analytic continuation results reproduces parts of Sec. 9 of [P4].

In this thesis, we focused on the theory of correlation functions and their subsequent applications to accurately computing 4p vertices utilizing the NRG and the effects of quenched disorder on antiferromagnetic QCPs in $2d$ metals. After a detailed introduction to expectation values, PSFs, ℓp MF and KF correlators, and their spectral representations in Secs. 2 and 3, we discussed our publications [P1, P2, P3, P4].

A closed expression for the MF kernels for general ℓ, including anomalous terms of arbitrary order, was derived in Sec. 4 by iteratively evaluating the integrals in Eq. (4.1). We used the MF kernels to compute 3p bosonic correlators in the HA as well as 2p, 3p, and 4p correlators of a free spin of length S. Our results could be beneficial for, e.g., benchmarking against various analytically solvable models such as the HA.

The MF kernels found an immediate application in the analytic continuation of multipoint correlation functions in Ch. 5. They are a vital ingredient for our strategy outlined in Sec. 5.2 as they appear in the imaginary-frequency convolution in Eq. (5.4b), where all possible anomalous terms have to be accounted for. A detailed summary of our results derived throughout Ch. 5 was presented in Sec. 5.8; here, we comment on possible future investigations. It would be interesting to apply our formulas in conjunction with the algorithmic Matsubara integration technique [TCL19]. There, the evaluation of Feynman diagrams yields an exact symbolic expression for $G(i\boldsymbol{\omega})$ that can be readily continued to full Keldysh correlators or to PSFs. If, by contrast, the Matsubara results are only available as numerical data, the numerical analytic continuation is an ill-conditioned problem. Nevertheless, recent advances suggest that it can possibly be tamed to some extent by exploiting further information on mathematical properties of the function [FYG21, FYZG21, HGL23]. Numerically representing multipoint MF correlators is another fruitful direction to explore. References [SOOY17, KCP22] showed that 2p MF functions can be represented compactly by a suitable basis expansion. Yet, for multipoint functions, Ref. [WSK21] found that the overcompleteness of the basis hinders an extraction of the basis coefficients by projection. Here, a numerical counterpart of our method for recovering individual PSFs S_p (or partial correlators G_p) from a full correlator $G(i\boldsymbol{\omega})$ might be helpful. Finally, our formulas might also be useful for evaluating diagrammatic relations typically formulated for correlators while using the PSFs as the main information carriers.

In Sec. 6, we addressed the problem of accurately computing the 4p vertex with numerical techniques via IEs. We first outlined our strategy for deriving sIEs that only involve interacting correlators and provided arguments for their improved numerical accuracy. Explicitly carrying out this strategy yielded a sIE for the 4p vertex that is equivalent to its asymptotic decomposition [WLT$^+$20], with each 3p and 4p constituent having a separate estimator. We demonstrated its improved utility in the MF and KF by applying the multipoint NRG of Ref. [LKvD21] to the Anderson impurity model at various temperatures and interactions. Our scheme paves the way for, e.g., understanding the intricate real-frequency structures of the 4p KF vertex via the physically intuitive single-boson exchange decomposition [KVC19]. Its ingredients are within reach of our sIE as they are closely related to the asymptotic classes [GWG$^+$22]. A single-boson exchange analysis of the local moment formation in the Anderson impurity model or the DMFT solution of the Hubbard model [CSR$^+$21, AKC$^+$22] down to

lowest temperatures could deepen our understanding of impurity physics on the two-particle level not only on the imaginary- but also on the real-frequency axis.

In Sec. 7, after a brief review of the basics of quantum criticality and disorder, we studied the effect of quenched disorder on $2d$ metals near an antiferromagnetic instability at zero temperature. We performed an ϵ-expansion to derive RG flow equations for the parameters of our disordered hot spot theory, which showed a runaway flow to strong disorder. As we only considered disorder scattering among single hot spots, a straightforward extension of our approach could incorporate scattering between all hot spots and, in addition, a random boson mass; this was recently pursued in Ref. [JK23]. At one-loop order, the authors also observed a runaway flow to strong disorder for a nonzero disorder potential coupling to the fermions. They argued that a stable fixed point might occur at two-loop order due to the screening of the disorder scattering by the Yukawa coupling. The enormous number of diagrams, however, impedes a direct two-loop analysis. Further, neglecting electrons away from hot spots is not justified a priori as they might be scattered to the vicinity of a hot spot by the disorder potential. For these reasons, it is advisable to approach the problem of disordered antiferromagnetic quantum critical models differently. A promising new direction are Sachdev-Ye-Kitaev-like disorder averages [EGPS21, GPES22]. Indeed, a fermionic potential and a Yukawa coupling that are random in flavor and real space recovered the experimentally observed strange metal temperature dependencies of the dc resistivity and the specific heat [PGES23]. As the authors focus on order parameters with a vanishing ordering wave vector $\boldsymbol{Q} = 0$, an extension to order parameters with $\boldsymbol{Q} \neq 0$, like in the antiferromagnetic case, would be worthwhile to investigate.

As a final remark, let us comment on the general progress of numerical real-frequency methods provided by the projects presented in this thesis. In the MF, a thorough understanding of the analytic properties of correlators has been pivotal for two (out of many) reasons: deriving numerically robust representations of the self-energy and 4p vertex [HPW12, KGK+19] and compressing numerical data to develop highly efficient algorithms [SOOY17, WSK21]. In the works presented in this thesis, we advanced our understanding of the analytic structure of real-frequency correlators in the KF and applied it to derive a numerically robust sIE for the 4p vertex. Its accurate computation using the NRG scheme of Ref. [LKvD21] is thus feasible for strongly correlated systems in the context of DMFT. In conjunction with newly developing approaches to compress numerical data efficiently [RNFW+24], this opens the door for various new applications. For instance, using the nonperturbative, local DMFT solution as the input to a functional renormalization group flow [TAB+14], nonlocal correlations could be incorporated on the real-frequency axis [GRW+23] while taming the perturbative restrictions imposed by the parquet approximation.

A Additional computations for 2p MF correlators

A.1 Calculation of the 2p MF kernel

In this appendix, we derive the explicit expression for $\mathcal{K}(\boldsymbol{\Omega}_p)$ for $\ell = 2$, defined in Eq. (3.14), including the residual part $\mathcal{R}(\boldsymbol{\Omega}_p)$. Imposing the restriction of the Heaviside function on the upper boundary of the $\tau_{\overline{2}}$ integral, we compute

$$
\begin{aligned}
\mathcal{K}(\boldsymbol{\Omega}_p) &= -\int_0^\beta d\tau_{\overline{1}}\, e^{\Omega_{\overline{1}}\tau_{\overline{1}}} \int_0^{\tau_{\overline{1}}} d\tau_{\overline{2}}\, e^{\Omega_{\overline{2}}\tau_{\overline{2}}} \\
&= -\int_0^\beta d\tau_{\overline{1}}\, e^{\Omega_{\overline{1}}\tau_{\overline{1}}} \left[\Delta_{\Omega_{\overline{2}}} \left(e^{\Omega_{\overline{2}}\tau_{\overline{1}}} - 1 \right) + \delta_{\Omega_{\overline{2}}} \tau_{\overline{1}} \right].
\end{aligned}
\tag{A.1}
$$

Here, we considered the cases $\Omega_{\overline{2}} \neq 0$ and $\Omega_{\overline{2}} = 0$ using $\Delta_{\Omega_{\overline{2}}}$ (see Eq. (3.15)) and $\delta_{\Omega_{\overline{2}}}$, respectively. The $\tau_{\overline{1}}$ integral for the term including the exponential $e^{\Omega_{\overline{2}}\tau_{\overline{1}}}$ readily evaluates to

$$
\int_0^\beta d\tau_{\overline{1}}\, e^{\Omega_{\overline{12}}\tau_{\overline{1}}} = \int_0^\beta d\tau_{\overline{1}}\, e^{i\omega_{\overline{12}}\tau_{\overline{1}}} = \beta \delta_{i\omega_{\overline{12}}} = \beta \delta_{\Omega_{\overline{12}}}.
\tag{A.2}
$$

The first and third equalities follow due to $\varepsilon_{\overline{12}} = 0$ (see Eq. (3.12)), implying $\Omega_{\overline{12}} = i\omega_{\overline{12}} - \varepsilon_{\overline{12}} = i\omega_{\overline{12}}$. The second equality uses that $i\omega_{\overline{12}}$ is a bosonic Matsubara frequency, since it is the sum of either two fermionic or two bosonic Matsubara frequencies. The $\tau_{\overline{1}}$ integral for the remaining terms in Eq. (A.1) can be evaluated by distinguishing the cases $\Omega_{\overline{1}} \neq 0$ and $\Omega_{\overline{1}} = 0$, yielding

$$
\begin{aligned}
\mathcal{K}(\boldsymbol{\Omega}_p) &= -\beta \delta_{i\omega_{\overline{12}}} \Delta_{\Omega_{\overline{2}}} + \Delta_{\Omega_{\overline{2}}} \Delta_{\Omega_{\overline{1}}} \left(e^{\beta\Omega_{\overline{1}}} - 1 \right) + \beta \Delta_{\Omega_{\overline{2}}} \delta_{\Omega_{\overline{1}}} - \delta_{\Omega_{\overline{2}}} \delta_{\Omega_{\overline{1}}} \frac{\beta^2}{2} \\
&\quad + \delta_{\Omega_{\overline{2}}} \Delta_{\Omega_{\overline{1}}} \left[\Delta_{\Omega_{\overline{1}}} \left(e^{\beta\Omega_{\overline{1}}} - 1 \right) - \beta e^{\beta\Omega_{\overline{1}}} \right].
\end{aligned}
\tag{A.3}
$$

This defines the primary and residual parts of the kernel (see Eq. (3.14)) by identifying contributions with factors $\beta \delta_{\Omega_{\overline{12}}}$. Using $\Delta_{\Omega_{\overline{2}}} = -\Delta_{\Omega_{\overline{1}}}$ in the first term on the r.h.s. of Eq. (A.3) and $\delta_{\Omega_{\overline{2}}} \delta_{\Omega_{\overline{1}}} = \delta_{\Omega_{\overline{12}}} \delta_{\Omega_{\overline{1}}}$, we obtain

$$
\begin{aligned}
\mathcal{K}(\boldsymbol{\Omega}_p) &= \beta \delta_{\Omega_{\overline{12}}} K(\boldsymbol{\Omega}_p) + \mathcal{R}(\boldsymbol{\Omega}_p), \\
K(\boldsymbol{\Omega}_p) &= \Delta_{\Omega_{\overline{1}}} - \frac{\beta}{2} \delta_{\Omega_{\overline{1}}}, \\
\mathcal{R}(\boldsymbol{\Omega}_p) &= \Delta_{\Omega_{\overline{2}}} \Delta_{\Omega_{\overline{1}}} \left(e^{\beta\Omega_{\overline{1}}} - 1 \right) + \beta \Delta_{\Omega_{\overline{2}}} \delta_{\Omega_{\overline{1}}} + \delta_{\Omega_{\overline{2}}} \Delta_{\Omega_{\overline{1}}} \left[\Delta_{\Omega_{\overline{1}}} \left(e^{\beta\Omega_{\overline{1}}} - 1 \right) - \beta e^{\beta\Omega_{\overline{1}}} \right] \\
&= \Delta_{\Omega_{\overline{2}}} \Delta_{\Omega_{\overline{1}}} \left(\zeta e^{-\beta\varepsilon_{\overline{1}}} - 1 \right) + \beta \left(\Delta_{\Omega_{\overline{2}}} \delta_{\Omega_{\overline{1}}} - \delta_{\Omega_{\overline{2}}} \Delta_{\Omega_{\overline{1}}} \right).
\end{aligned}
\tag{A.4}
$$

In the last step, we inserted $e^{i\omega_{\overline{1}}\beta} = \zeta$. However, the anomalous terms proportional to $\delta_{\Omega_{\overline{2}}}$ are nonzero only if $i\omega_{\overline{2}}$ and therefore $i\omega_{\overline{1}}$ are bosonic, implying $\zeta = +1$. Additionally, since $\delta_{\Omega_{\overline{2}}}$ enforces $\varepsilon_{\overline{2}} = 0$, it follows from $\varepsilon_{\overline{12}} = 0$ that $e^{\beta\varepsilon_{\overline{1}}} = e^{-\beta\varepsilon_{\overline{2}}} = 1$. Thus, the term proportional to $\delta_{\Omega_{\overline{2}}} \left(e^{\beta\Omega_{\overline{1}}} - 1 \right) = 0$ vanishes.

A.2 Cancellation of residual terms

Here, we explicitly show that the contribution of the residual part $\mathcal{R}(\boldsymbol{\Omega}_p)$ to the correlator in Eq. (3.12) vanishes, i.e.,

$$\mathcal{G}^{\mathcal{R}}(i\boldsymbol{\omega}) = \sum_p \int d^2\varepsilon_p\, \delta(\varepsilon_{\overline{12}})\, \mathcal{R}(i\boldsymbol{\omega}_p - \boldsymbol{\varepsilon}_p)\, S_p(\boldsymbol{\varepsilon}_p) = 0. \tag{A.5}$$

It suffices to consider the product $\mathcal{R}(\boldsymbol{\Omega}_p)\, S_p(\boldsymbol{\varepsilon}_p)$ without the convolution integrals. We use the equilibrium condition $S_{(12)}(\boldsymbol{\varepsilon}_{(12)}) = \zeta e^{\beta\varepsilon_1} S_{(21)}(\boldsymbol{\varepsilon}_{(21)})$ and

$$\delta_{\Omega_{1/2}} S_{(12)}(\boldsymbol{\varepsilon}_{(12)}) = \delta_{i\omega_{1/2}}\delta_{\varepsilon_{1/2}} S_{(12)}(\boldsymbol{\varepsilon}_{(12)}) = \delta_{\Omega_{1/2}} S_{(21)}(\boldsymbol{\varepsilon}_{(21)}), \tag{A.6}$$

which directly follows from Eqs. (3.18) and (3.19) using $\delta(\varepsilon_2) = \delta(\varepsilon_1)$ due to $\varepsilon_{12} = 0$. Then, we find

$$
\begin{aligned}
\sum_p \mathcal{R}(\boldsymbol{\Omega}_p)\, S_p(\boldsymbol{\varepsilon}_p) &= \left[\Delta_{\Omega_2}\Delta_{\Omega_1}\left(\zeta e^{-\beta\varepsilon_1} - 1\right) + \beta\left(\Delta_{\Omega_2}\delta_{\Omega_1} - \delta_{\Omega_2}\Delta_{\Omega_1}\right)\right] S_{(12)}(\boldsymbol{\varepsilon}_{(12)}) \\
&\quad + \left[\Delta_{\Omega_1}\Delta_{\Omega_2}\left(\zeta e^{-\beta\varepsilon_2} - 1\right) + \beta\left(\Delta_{\Omega_1}\delta_{\Omega_2} - \delta_{\Omega_1}\Delta_{\Omega_2}\right)\right] S_{(21)}(\boldsymbol{\varepsilon}_{(21)}) \\
&= \left[\Delta_{\Omega_2}\Delta_{\Omega_1}\left(\zeta e^{-\beta\varepsilon_1} - 1\right) + \beta\left(\Delta_{\Omega_2}\delta_{\Omega_1} - \delta_{\Omega_2}\Delta_{\Omega_1}\right)\right] S_{(12)}(\boldsymbol{\varepsilon}_{(12)}) \\
&\quad + \left[\Delta_{\Omega_1}\Delta_{\Omega_2}\left(1 - \zeta e^{-\beta\varepsilon_1}\right) + \beta\left(\Delta_{\Omega_1}\delta_{\Omega_2} - \delta_{\Omega_1}\Delta_{\Omega_2}\right)\right] S_{(12)}(\boldsymbol{\varepsilon}_{(12)}) \\
&= 0,
\end{aligned}
\tag{A.7}
$$

which concludes the proof of Eq. (A.5).

B Vertex asymptotics in the spectral representation

In this appendix, we demonstrate the consistency of the large-frequency behaviour of Eq. (3.76a) in the MF and KF, where the asymptotics of the 2p correlators and the vertex Γ on the r.h.s. are known [WLT$^+$20]. We will focus on the case presented in Sec. 3.5: The independent frequencies are given by z_1, z_3, and $z_{12} = -z_{34}$, with z_3 and consequently also $z_4 = -z_{12} - z_3$ assumed to be large[1] (with z_i either representing imaginary or real frequencies). Then, Eq. (3.76a) is consistent if $G^{\mathrm{con}} \sim 1/z_3^2$.

For generality, we do not set $\boldsymbol{\mathcal{O}} = (d_1, d_2^\dagger, d_3, d_4^\dagger)$ in the ensuing analysis. Rather, it is assumed that the operators in the tuple $\boldsymbol{\mathcal{O}} = (\mathcal{O}^1, \mathcal{O}^2, \mathcal{O}^3, \mathcal{O}^4)$ are single-particle operators of unspecified creation or annihilation type, and either all bosonic or all fermionic. Further, it is assumed that $\langle \mathcal{O}^i \rangle = 0$ for all i.

Let us further comment on Ref. [WLT$^+$20]: Therein, the independent frequencies (for all operators being fermionic) are two fermionic frequencies ν and ν' and one bosonic frequency ω, which enter the tuple $\boldsymbol{z}$ differently according to the chosen channel parametrization (ph, pp, and $\overline{\mathrm{ph}}$). Then, the so-called asymptotic classes are defined by either taking $|\nu| \to \infty$, or $|\nu'| \to \infty$, or both. The following proof covers the former two cases for all channels in a unified way (up to possible sign factors arising from the permutation of fermionic operators). The channel-specific limits follow by choosing the following operators and frequencies in the convention of [P3].

$$
\begin{aligned}
&\text{ph-channel and } |\nu| \to \infty: &&\boldsymbol{\mathcal{O}} = (d_4^\dagger, d_3, d_1, d_2^\dagger), &&\boldsymbol{\omega} = (-\nu', \nu' + \omega, \nu, -\nu - \omega), \\
&\text{ph-channel and } |\nu'| \to \infty: &&\boldsymbol{\mathcal{O}} = (d_1, d_2^\dagger, d_4^\dagger, d_3), &&\boldsymbol{\omega} = (\nu, -\nu - \omega, -\nu', \nu' + \omega), \\[4pt]
&\text{pp-channel and } |\nu| \to \infty: &&\boldsymbol{\mathcal{O}} = (d_2^\dagger, d_4^\dagger, d_1, d_3), &&\boldsymbol{\omega} = (-\nu', \nu' + \omega, \nu, -\nu - \omega), \\
&\text{pp-channel and } |\nu'| \to \infty: &&\boldsymbol{\mathcal{O}} = (d_1, d_3, d_2^\dagger, d_4^\dagger), &&\boldsymbol{\omega} = (\nu, -\nu - \omega, -\nu', \nu' + \omega), \\[4pt]
&\overline{\mathrm{ph}}\text{-channel and } |\nu| \to \infty: &&\boldsymbol{\mathcal{O}} = (d_2^\dagger, d_3, d_1, d_4^\dagger), &&\boldsymbol{\omega} = (-\nu', \nu' + \omega, \nu, -\nu - \omega), \\
&\overline{\mathrm{ph}}\text{-channel and } |\nu'| \to \infty: &&\boldsymbol{\mathcal{O}} = (d_1, d_4^\dagger, d_2^\dagger, d_3), &&\boldsymbol{\omega} = (\nu, -\nu - \omega, -\nu', \nu' + \omega). &&\text{(B.1)}
\end{aligned}
$$

For imaginary frequencies, the tuple $\boldsymbol{\omega}$ is replaced with $\mathrm{i}\boldsymbol{\omega}$, i.e., with all elements multiplied by the imaginary unit.

The proof proceeds as follows: In Sec. B.1, we derive useful relations for PSFs if one of the real frequencies is integrated out. These are used in Secs. B.2 and B.3 for the MF and KF, respectively, to derive the scaling of G^{con} in the limit of large z_3, leading to the required behaviour $G^{\mathrm{con}} \sim 1/z_3^2$.

B.1 Useful relations for connected PSFs

In the main text, we regard the PSFs S_p as functions of the permuted real frequencies $\boldsymbol{\varepsilon}_p = (\varepsilon_{\overline{1}}, \ldots, \varepsilon_{\overline{\ell}})$, with the condition $\varepsilon_{\overline{1}\ldots\overline{\ell}} = \varepsilon_{1\ldots\ell} = 0$ understood. In this appendix, it is convenient to apply the variable change $\varepsilon_i' = \varepsilon_{\overline{1}\ldots\overline{i}}$ for $i \leq \ell - 1$ [LKvD21]. Then, the arguments of the 4p PSFs are independent of the permutation and are given by $S_p(\boldsymbol{\varepsilon}_p) =$

---

1 The proofs of two or even three independent frequencies being large will not be presented here, as they follow from similar principles.

$S_p(\varepsilon_{\overline{1}}, \ldots, \varepsilon_{\overline{\ell}}) = S_p(\varepsilon'_1, \varepsilon'_2 - \varepsilon'_1, \ldots, \varepsilon'_{\ell-1} - \varepsilon'_{\ell-2}, -\varepsilon'_{\ell-1}) = S_p(\boldsymbol{\varepsilon}')$, where we defined the tuple $\boldsymbol{\varepsilon}' = (\varepsilon'_1, \varepsilon'_2 - \varepsilon'_1, \ldots, \varepsilon'_{\ell-1} - \varepsilon'_{\ell-2}, -\varepsilon'_{\ell-1})$. Then, it follows from Eq. (2.46) that

$$S_p(\boldsymbol{\varepsilon}') = \zeta_p \left[\prod_{i=1}^{\ell-1} \int_{-\infty}^{\infty} \frac{\mathrm{d}t_{\overline{i}}}{(2\pi)^{\ell-1}} \, e^{\mathrm{i}(\varepsilon'_i - \varepsilon'_{i-1})t_{\overline{i}}} \right] \left\langle \mathcal{O}^{\overline{1}}(t_{\overline{1}}) \ldots \mathcal{O}^{\overline{\ell-1}}(t_{\overline{\ell-1}}) \mathcal{O}^{\overline{\ell}} \right\rangle, \tag{B.2}$$

with $\varepsilon'_0 = 0$ for $i = 1$. Additionally, we will use 2p PSFs defined without a permutation sign and displayed with only one frequency argument:

$$S'_{(\overline{ij})}(\varepsilon') = \int_{-\infty}^{\infty} \frac{\mathrm{d}t_{\overline{i}}}{2\pi} \, e^{\mathrm{i}\varepsilon' t_{\overline{i}}} \left\langle \mathcal{O}^{\overline{i}}(t_{\overline{i}}) \mathcal{O}^{\overline{j}} \right\rangle. \tag{B.3}$$

As defined in Eq. (3.76a), the 4p vertex follows from the connected 4p correlator by factoring out the external propagators. The connected 4p correlator, in turn, can be computed by a convolution of the usual MF and KF kernels with connected 4p PSFs, $S_p^{\mathrm{con}}(\boldsymbol{\varepsilon}') = S_p(\boldsymbol{\varepsilon}') - S_p^{\mathrm{dis}}(\boldsymbol{\varepsilon}')$, which follow by subtracting from $S_p(\boldsymbol{\varepsilon}')$ the disconnected PSFs [KLvD21, LKvD21]

$$\zeta_p S_p^{\mathrm{dis}}(\boldsymbol{\varepsilon}') = S'_{(\overline{12})}(\varepsilon'_1) \, S'_{(\overline{34})}(\varepsilon'_3) \, \delta(\varepsilon'_2) + \zeta \, S'_{(\overline{13})}(\varepsilon'_1) \, S'_{(\overline{24})}(\varepsilon'_3) \, \delta(\varepsilon'_1 - \varepsilon'_2 + \varepsilon'_3)$$
$$+ S'_{(\overline{14})}(\varepsilon'_1) \, S'_{(\overline{23})}(\varepsilon'_2 - \varepsilon'_1) \, \delta(\varepsilon'_1 - \varepsilon'_3). \tag{B.4}$$

Here, ζ equals ± 1 if all operators are bosonic/fermionic. Our proofs for the asymptotic behaviour of connected 4p MF and KF correlators in Secs. B.2 and B.3, respectively, rely on relations between different connected PSFs if one of the frequencies ε'_i is integrated out, e.g.,

$$\int_{-\infty}^{\infty} \mathrm{d}\varepsilon'_1 \, S_{(\overline{1234})}^{\mathrm{con}}(\boldsymbol{\varepsilon}') = \int_{-\infty}^{\infty} \mathrm{d}\varepsilon'_1 \, S_{(\overline{1234})}(\boldsymbol{\varepsilon}') - \int_{-\infty}^{\infty} \mathrm{d}\varepsilon'_1 \, S_{(\overline{1234})}^{\mathrm{dis}}(\boldsymbol{\varepsilon}'). \tag{B.5}$$

Here, we inserted the general permutation $p = (\overline{1234})$ into the subscripts of the PSFs. The calculation of the two contributions on the r.h.s. are presented in the following two sections.

B.1.1 Integral over disconnected PSFs

Let us start with $S_{(\overline{1234})}^{\mathrm{dis}}(\boldsymbol{\varepsilon}')$ by inserting Eq. (B.4) into the second term of Eq. (B.5):

$$\zeta_{(\overline{1234})} \int_{-\infty}^{\infty} \mathrm{d}\varepsilon'_1 \, S_{(\overline{1234})}^{\mathrm{dis}}(\boldsymbol{\varepsilon}') = \left[\int_{-\infty}^{\infty} \mathrm{d}\varepsilon'_1 \, S'_{(\overline{12})}(\varepsilon'_1) \right] S'_{(\overline{34})}(\varepsilon'_3) \, \delta(\varepsilon'_2) + \zeta \, S'_{(\overline{13})}(\varepsilon'_2 - \varepsilon'_3) \, S'_{(\overline{24})}(\varepsilon'_3)$$
$$+ S'_{(\overline{14})}(\varepsilon'_3) \, S'_{(\overline{23})}(\varepsilon'_2 - \varepsilon'_3). \tag{B.6}$$

The remaining integral can be evaluated using Eq. (B.3),

$$\int_{-\infty}^{\infty} \mathrm{d}\varepsilon'_1 \, S'_{(\overline{12})}(\varepsilon'_1) = \int_{-\infty}^{\infty} \mathrm{d}\varepsilon'_1 \int_{-\infty}^{\infty} \frac{\mathrm{d}t_{\overline{1}}}{2\pi} \, e^{\mathrm{i}\varepsilon'_1 t_{\overline{1}}} \left\langle \mathcal{O}^{\overline{1}}(t_{\overline{1}}) \mathcal{O}^{\overline{2}} \right\rangle = \left\langle \mathcal{O}^{\overline{1}} \mathcal{O}^{\overline{2}} \right\rangle, \tag{B.7}$$

where the integral over ε'_1 yielded $2\pi\delta(t_{\overline{1}})$. With the definition of $[\mathcal{O}^{\overline{i}}, \mathcal{O}^{\overline{j}}]_{-\zeta} = \delta^{\overline{i},\overline{j}}$, where $[\cdot, \cdot]_{\mp}$ denotes a (anti)commutator and $\delta^{\overline{i},\overline{j}}$ should be understood as a scalar (it either vanishes or enforces quantum numbers of the two single-particle operators $\mathcal{O}^{\overline{i}}$ and $\mathcal{O}^{\overline{j}}$ to be equal), it follows that

$$\int_{-\infty}^{\infty} \mathrm{d}\varepsilon'_1 \, S'_{(\overline{12})}(\varepsilon'_1) = \delta^{\overline{1},\overline{2}} + \zeta \left\langle \mathcal{O}^{\overline{2}} \mathcal{O}^{\overline{1}} \right\rangle = \delta^{\overline{1},\overline{2}} + \zeta \int_{-\infty}^{\infty} \mathrm{d}\varepsilon'_1 \int_{-\infty}^{\infty} \frac{\mathrm{d}t_{\overline{2}}}{2\pi} \, e^{\mathrm{i}\varepsilon'_1 t_{\overline{2}}} \left\langle \mathcal{O}^{\overline{2}}(t_{\overline{2}}) \mathcal{O}^{\overline{1}} \right\rangle$$

$$= \delta^{\overline{1},\overline{2}} + \zeta \int_{-\infty}^{\infty} \mathrm{d}\varepsilon_1' \, S'_{(\overline{21})}(\varepsilon_1'). \tag{B.8}$$

Thus, Eq. (B.6) can be rewritten as

$$\zeta_{(\overline{1234})} \int_{-\infty}^{\infty} \mathrm{d}\varepsilon_1' \, S^{\mathrm{dis}}_{(\overline{1234})}(\boldsymbol{\varepsilon}') = \delta^{\overline{1},\overline{2}} S'_{(\overline{34})}(\varepsilon_3') \, \delta(\varepsilon_2') + \zeta \left[\int_{-\infty}^{\infty} \mathrm{d}\varepsilon_1' \, S'_{(\overline{21})}(\varepsilon_1') \right] S'_{(\overline{34})}(\varepsilon_3') \, \delta(\varepsilon_2')$$
$$+ \zeta \, S'_{(\overline{13})}(\varepsilon_2' - \varepsilon_3') \, S'_{(\overline{24})}(\varepsilon_3') + S'_{(\overline{14})}(\varepsilon_3') \, S'_{(\overline{23})}(\varepsilon_2' - \varepsilon_3')$$
$$= \delta^{\overline{1},\overline{2}} \, S'_{(\overline{34})}(\varepsilon_3') \, \delta(\varepsilon_2') + \zeta \, \zeta_{(\overline{2134})} \int_{-\infty}^{\infty} \mathrm{d}\varepsilon_1' \, S^{\mathrm{dis}}_{(\overline{2134})}(\boldsymbol{\varepsilon}'), \tag{B.9}$$

where we identified the disconnected PSF (B.4) for permutation $p = (\overline{2134})$ in the last step:

$$\zeta_{(\overline{2134})} \int_{-\infty}^{\infty} \mathrm{d}\varepsilon_1' \, S^{\mathrm{dis}}_{(\overline{2134})}(\boldsymbol{\varepsilon}') = \left[\int_{-\infty}^{\infty} \mathrm{d}\varepsilon_1' \, S'_{(\overline{21})}(\varepsilon_1') \right] S'_{(\overline{34})}(\varepsilon_3') \, \delta(\varepsilon_2') + \zeta \, S'_{(\overline{23})}(\varepsilon_2' - \varepsilon_3') \, S'_{(\overline{14})}(\varepsilon_3')$$
$$+ S'_{(\overline{24})}(\varepsilon_3') \, S'_{(\overline{13})}(\varepsilon_2' - \varepsilon_3'). \tag{B.10}$$

Using $\zeta_{(\overline{2134})} = \zeta \, \zeta_{(\overline{1234})}$, since the two permutations $(\overline{1234})$ and $(\overline{2134})$ differ by at most one transposition of fermionic operators, the disconnected PSFs therefore fulfill the relations

$$\int_{-\infty}^{\infty} \mathrm{d}\varepsilon_1' \left[S^{\mathrm{dis}}_{(\overline{1234})}(\boldsymbol{\varepsilon}') - S^{\mathrm{dis}}_{(\overline{2134})}(\boldsymbol{\varepsilon}') \right] = \zeta_{(\overline{1234})} \, \delta^{\overline{1},\overline{2}} \, S'_{(\overline{34})}(\varepsilon_3') \, \delta(\varepsilon_2'),$$
$$\int_{-\infty}^{\infty} \mathrm{d}\varepsilon_2' \left[S^{\mathrm{dis}}_{(\overline{1234})}(\boldsymbol{\varepsilon}') - S^{\mathrm{dis}}_{(\overline{1324})}(\boldsymbol{\varepsilon}') \right] = \zeta_{(\overline{1234})} \, \delta^{\overline{2},\overline{3}} \, S'_{(\overline{14})}(\varepsilon_1') \, \delta(\varepsilon_1' - \varepsilon_3'),$$
$$\int_{-\infty}^{\infty} \mathrm{d}\varepsilon_3' \left[S^{\mathrm{dis}}_{(\overline{1234})}(\boldsymbol{\varepsilon}') - S^{\mathrm{dis}}_{(\overline{1243})}(\boldsymbol{\varepsilon}') \right] = \zeta_{(\overline{1234})} \, \delta^{\overline{3},\overline{4}} \, S'_{(\overline{12})}(\varepsilon_1') \, \delta(\varepsilon_2'). \tag{B.11}$$

The last two equalities follow from an equivalent derivation.

B.1.2 Integral over full PSFs

Next, we focus on the first integral in Eq. (B.5) by inserting Eq. (B.2) for $\ell = 4$:

$$\zeta_{(\overline{1234})} \int_{-\infty}^{\infty} \mathrm{d}\varepsilon_1' \, S_{(\overline{1234})}(\boldsymbol{\varepsilon}')$$
$$= \int_{-\infty}^{\infty} \mathrm{d}\varepsilon_1' \int_{-\infty}^{\infty} \frac{\mathrm{d}t_{\overline{1}} \, \mathrm{d}t_{\overline{2}} \, \mathrm{d}t_{\overline{3}}}{(2\pi)^3} \, e^{\mathrm{i}\varepsilon_1' t_{\overline{1}} + \mathrm{i}(\varepsilon_2' - \varepsilon_1')t_{\overline{2}} + \mathrm{i}(\varepsilon_3' - \varepsilon_2')t_{\overline{3}}} \left\langle \mathcal{O}^{\overline{1}}(t_{\overline{1}}) \mathcal{O}^{\overline{2}}(t_{\overline{2}}) \mathcal{O}^{\overline{3}}(t_{\overline{3}}) \mathcal{O}^{\overline{4}} \right\rangle$$
$$= \int_{-\infty}^{\infty} \frac{\mathrm{d}t_{\overline{2}} \, \mathrm{d}t_{\overline{3}}}{(2\pi)^2} \, e^{\mathrm{i}\varepsilon_2' t_{\overline{2}} + \mathrm{i}(\varepsilon_3' - \varepsilon_2')t_{\overline{3}}} \left\langle \left(\mathcal{O}^{\overline{1}} \mathcal{O}^{\overline{2}} \right)(t_{\overline{2}}) \mathcal{O}^{\overline{3}}(t_{\overline{3}}) \mathcal{O}^{\overline{4}} \right\rangle$$
$$= \delta^{\overline{1},\overline{2}} \int_{-\infty}^{\infty} \frac{\mathrm{d}t_{\overline{2}} \, \mathrm{d}t_{\overline{3}}}{(2\pi)^2} \, e^{\mathrm{i}\varepsilon_2' t_{\overline{2}} + \mathrm{i}(\varepsilon_3' - \varepsilon_2')t_{\overline{3}}} \left\langle \mathcal{O}^{\overline{3}}(t_{\overline{3}}) \mathcal{O}^{\overline{4}} \right\rangle$$
$$+ \zeta \int_{-\infty}^{\infty} \frac{\mathrm{d}t_{\overline{2}} \, \mathrm{d}t_{\overline{3}}}{(2\pi)^2} \, e^{\mathrm{i}\varepsilon_2' t_{\overline{2}} + \mathrm{i}(\varepsilon_3' - \varepsilon_2')t_{\overline{3}}} \left\langle \left(\mathcal{O}^{\overline{2}} \mathcal{O}^{\overline{1}} \right)(t_{\overline{2}}) \mathcal{O}^{\overline{3}}(t_{\overline{3}}) \mathcal{O}^{\overline{4}} \right\rangle. \tag{B.12}$$

In the second step, we used that the ε_1' integral evaluates to $2\pi\delta(t_{\overline{1}} - t_{\overline{2}})$, and in the third step we inserted the (anti)commutator $[\mathcal{O}^{\overline{1}}, \mathcal{O}^{\overline{2}}]_{-\zeta} = \delta^{\overline{1},\overline{2}}$. The first term on the r.h.s. can be identified with a 2p PSF,

$$\delta^{\overline{1},\overline{2}} \int_{-\infty}^{\infty} \frac{\mathrm{d}t_{\overline{2}} \, \mathrm{d}t_{\overline{3}}}{(2\pi)^2} \, e^{\mathrm{i}\varepsilon_2' t_{\overline{2}} + \mathrm{i}(\varepsilon_3' - \varepsilon_2')t_{\overline{3}}} \left\langle \mathcal{O}^{\overline{3}}(t_{\overline{3}}) \mathcal{O}^{\overline{4}} \right\rangle = \delta^{\overline{1},\overline{2}} \, \delta(\varepsilon_2') \, S'_{(\overline{34})}(\varepsilon_3'), \tag{B.13}$$

while the second term equals

$$\zeta\,\zeta_{(\overline{2134})}\int_{-\infty}^{\infty}\mathrm{d}\varepsilon_1'\,S_{(\overline{2134})}(\boldsymbol{\varepsilon}') = \zeta\int_{-\infty}^{\infty}\frac{\mathrm{d}t_{\overline{2}}\,\mathrm{d}t_{\overline{3}}}{(2\pi)^2}\,e^{\mathrm{i}\varepsilon_2' t_{\overline{2}}+\mathrm{i}(\varepsilon_3'-\varepsilon_2')t_{\overline{3}}}\left\langle\left(\mathcal{O}^{\overline{2}}\mathcal{O}^{\overline{1}}\right)(t_{\overline{2}})\mathcal{O}^{\overline{3}}(t_{\overline{3}})\mathcal{O}^{\overline{4}}\right\rangle. \quad \text{(B.14)}$$

Using $\zeta_{(\overline{2134})} = \zeta\,\zeta_{(\overline{1234})}$, we then arrive at

$$\int_{-\infty}^{\infty}\mathrm{d}\varepsilon_1'\,\left[S_{(\overline{1234})}(\boldsymbol{\varepsilon}') - S_{(\overline{2134})}(\boldsymbol{\varepsilon}')\right] = \zeta_{(\overline{1234})}\,\delta^{\overline{1},\overline{2}}\,S_{(\overline{34})}'(\varepsilon_3')\,\delta(\varepsilon_2'),$$

$$\int_{-\infty}^{\infty}\mathrm{d}\varepsilon_2'\,\left[S_{(\overline{1234})}(\boldsymbol{\varepsilon}') - S_{(\overline{1324})}(\boldsymbol{\varepsilon}')\right] = \zeta_{(\overline{1234})}\,\delta^{\overline{2},\overline{3}}\,S_{(\overline{14})}'(\varepsilon_1')\,\delta(\varepsilon_1' - \varepsilon_3'),$$

$$\int_{-\infty}^{\infty}\mathrm{d}\varepsilon_3'\,\left[S_{(\overline{1234})}(\boldsymbol{\varepsilon}') - S_{(\overline{1243})}(\boldsymbol{\varepsilon}')\right] = \zeta_{(\overline{1234})}\,\delta^{\overline{3},\overline{4}}\,S_{(\overline{12})}'(\varepsilon_1')\,\delta(\varepsilon_2'). \quad \text{(B.15)}$$

Again, the last two equalities follow from an equivalent derivation.

B.1.3 Integral over connected PSFs

Subtracting Eq. (B.11) from Eq. (B.15) yields the key identities used in the following sections:

$$\int_{-\infty}^{\infty}\mathrm{d}\varepsilon_1'\,\left[S_{(\overline{1234})}^{\mathrm{con}}(\boldsymbol{\varepsilon}') - S_{(\overline{2134})}^{\mathrm{con}}(\boldsymbol{\varepsilon}')\right] = 0,$$

$$\int_{-\infty}^{\infty}\mathrm{d}\varepsilon_2'\,\left[S_{(\overline{1234})}^{\mathrm{con}}(\boldsymbol{\varepsilon}') - S_{(\overline{1324})}^{\mathrm{con}}(\boldsymbol{\varepsilon}')\right] = 0,$$

$$\int_{-\infty}^{\infty}\mathrm{d}\varepsilon_3'\,\left[S_{(\overline{1234})}^{\mathrm{con}}(\boldsymbol{\varepsilon}') - S_{(\overline{1243})}^{\mathrm{con}}(\boldsymbol{\varepsilon}')\right] = 0. \quad \text{(B.16)}$$

Note again that these relations were derived for single-particle operators, either all bosonic or all fermionic, assuming $\langle\mathcal{O}^i\rangle = 0$ for all i.

B.2 Asymptotics in the MF

The connected 4p correlator in the MF can be obtained via the convolution [KLvD21]

$$G^{\mathrm{con}}(\mathrm{i}\boldsymbol{\omega})$$

$$= \sum_p\int\mathrm{d}^3\varepsilon'\left[\frac{1}{(\mathrm{i}\omega_{\overline{1}} - \varepsilon_1')(\mathrm{i}\omega_{\overline{12}} - \varepsilon_2')(\mathrm{i}\omega_{\overline{123}} - \varepsilon_3')} - \frac{\beta}{2}\delta_{\mathrm{i}\omega_{\overline{12}}-\varepsilon_2'}\frac{1}{(\mathrm{i}\omega_{\overline{1}} - \varepsilon_1')(\mathrm{i}\omega_{\overline{123}} - \varepsilon_3')}\right]S_p^{\mathrm{con}}(\boldsymbol{\varepsilon}'),$$
$$\text{(B.17)}$$

where $\mathrm{d}^3\varepsilon' = \mathrm{d}\varepsilon_1'\mathrm{d}\varepsilon_2'\mathrm{d}\varepsilon_3'$. The permutations yielding inconsistent (i.e., $\sim 1/(\mathrm{i}\omega_3)$) contributions for large $\mathrm{i}\omega_3$ are given by $p = (\overline{12}34)$, $(\overline{12}43)$, $(\overline{1}34\overline{2})$, $(\overline{1}34\overline{2})$, $(34\overline{12})$, and $(43\overline{12})$, where the overlines denote further permutations of indices 1 and 2. For instance, $p = (34\overline{12})$ covers the two permutations $p = (3412)$, (3421). Assuming the additional independent frequencies to be $\mathrm{i}\omega_1$ and $\mathrm{i}\omega_{12} = -\mathrm{i}\omega_{34}$, the leading-order contributions to G^{con} in an expansion in powers of $1/(\mathrm{i}\omega_3)$ then read

$$G^{\mathrm{con}}(\mathrm{i}\omega_1, \mathrm{i}\omega_{12} - \mathrm{i}\omega_1, \mathrm{i}\omega_3, \mathrm{i}\omega_{34} - \mathrm{i}\omega_3)$$

$$= \frac{1}{\mathrm{i}\omega_3}\sum_{\overline{12}}\int\mathrm{d}^3\varepsilon'\left[\frac{1}{(\mathrm{i}\omega_{\overline{1}} - \varepsilon_1')(\mathrm{i}\omega_{\overline{12}} - \varepsilon_2')} - \frac{\beta}{2}\delta_{\mathrm{i}\omega_{\overline{12}}-\varepsilon_2'}\frac{1}{\mathrm{i}\omega_{\overline{1}} - \varepsilon_1'}\right]S_{(\overline{1234})}^{\mathrm{con}}(\boldsymbol{\varepsilon}')$$

$$
-\frac{1}{i\omega_3}\sum_{\overline{12}}\int d^3\varepsilon' \left[\frac{1}{(i\omega_{\overline{1}}-\varepsilon_1')(i\omega_{\overline{12}}-\varepsilon_2')} - \frac{\beta}{2}\delta_{i\omega_{\overline{12}}-\varepsilon_2'}\frac{1}{i\omega_{\overline{1}}-\varepsilon_1'}\right]S^{\mathrm{con}}_{(\overline{12}43)}(\varepsilon')
$$

$$
+\frac{1}{i\omega_3}\sum_{\overline{12}}\int d^3\varepsilon' \ \frac{1}{(i\omega_{\overline{1}}-\varepsilon_1')(i\omega_{\overline{1}}+i\omega_{34}-\varepsilon_3')}\,S^{\mathrm{con}}_{(\overline{1}34\overline{2})}(\varepsilon')
$$

$$
-\frac{1}{i\omega_3}\sum_{\overline{12}}\int d^3\varepsilon' \ \frac{1}{(i\omega_{\overline{1}}-\varepsilon_1')(i\omega_{\overline{1}}+i\omega_{43}-\varepsilon_3')}\,S^{\mathrm{con}}_{(\overline{1}43\overline{2})}(\varepsilon')
$$

$$
+\frac{1}{i\omega_3}\sum_{\overline{12}}\int d^3\varepsilon' \left[\frac{1}{(i\omega_{34}-\varepsilon_2')(i\omega_{34}+i\omega_{\overline{1}}-\varepsilon_3')} - \frac{\beta}{2}\delta_{i\omega_{34}-\varepsilon_2'}\frac{1}{i\omega_{34}+i\omega_{\overline{1}}-\varepsilon_3'}\right]S^{\mathrm{con}}_{(34\overline{12})}(\varepsilon')
$$

$$
-\frac{1}{i\omega_3}\sum_{\overline{12}}\int d^3\varepsilon' \left[\frac{1}{(i\omega_{43}-\varepsilon_2')(i\omega_{43}+i\omega_{\overline{1}}-\varepsilon_3')} - \frac{\beta}{2}\delta_{i\omega_{43}-\varepsilon_2'}\frac{1}{i\omega_{43}+i\omega_{\overline{1}}-\varepsilon_3'}\right]S^{\mathrm{con}}_{(43\overline{12})}(\varepsilon')
$$

$$
+\mathcal{O}\!\left(\frac{1}{(i\omega_3)^2}\right). \tag{B.18}
$$

Here, $\sum_{\overline{12}}$ denotes the sum over permutations of indices 1 and 2. We observe that the expanded kernels are equal for permutations that differ by an exchange of indices 3 and 4, e.g., $p=(\overline{12}34)$ and $p=(\overline{12}43)$. Thus, using $\omega_{43}=\omega_{34}$, the leading-order terms of G^{con} reduce to

$$
G^{\mathrm{con}}(i\omega_1, i\omega_{12}-i\omega_1, i\omega_3, i\omega_{34}-i\omega_3)
$$
$$
=\frac{1}{i\omega_3}\sum_{\overline{12}}\int d\varepsilon_1' d\varepsilon_2'\left[\frac{1}{(i\omega_{\overline{1}}-\varepsilon_1')(i\omega_{\overline{12}}-\varepsilon_2')}-\frac{\beta}{2}\delta_{i\omega_{\overline{12}}-\varepsilon_2'}\frac{1}{i\omega_{\overline{1}}-\varepsilon_1'}\right]
$$
$$
\times\int d\varepsilon_3'\left[S^{\mathrm{con}}_{(\overline{12}34)}(\varepsilon')-S^{\mathrm{con}}_{(\overline{12}43)}(\varepsilon')\right]
$$
$$
+\frac{1}{i\omega_3}\sum_{\overline{12}}\int d\varepsilon_1' d\varepsilon_3'\ \frac{1}{(i\omega_{\overline{1}}-\varepsilon_1')(i\omega_{\overline{1}}+i\omega_{34}-\varepsilon_3')}\int d\varepsilon_2'\left[S^{\mathrm{con}}_{(\overline{1}34\overline{2})}(\varepsilon')-S^{\mathrm{con}}_{(\overline{1}43\overline{2})}(\varepsilon')\right]
$$
$$
+\frac{1}{i\omega_3}\sum_{\overline{12}}\int d\varepsilon_2' d\varepsilon_3'\left[\frac{1}{(i\omega_{34}-\varepsilon_2')(i\omega_{34}+i\omega_{\overline{1}}-\varepsilon_3')}-\frac{\beta}{2}\delta_{i\omega_{34}-\varepsilon_2'}\frac{1}{i\omega_{34}+i\omega_{\overline{1}}-\varepsilon_3'}\right]
$$
$$
\times\int d\varepsilon_1'\left[S^{\mathrm{con}}_{(34\overline{12})}(\varepsilon')-S^{\mathrm{con}}_{(43\overline{12})}(\varepsilon')\right]
$$
$$
+\mathcal{O}\!\left(\frac{1}{(i\omega_3)^2}\right)
$$
$$
=\mathcal{O}\!\left(\frac{1}{(i\omega_3)^2}\right). \tag{B.19}
$$

In the last step, we inserted Eq. (B.16). Therefore, we showed that G^{con} indeed has the correct scaling behaviour $1/(i\omega_3)^2$ for large $i\omega_3$ and, consequently, that the large-frequency behaviour on both sides of Eq. (3.76a) is consistent in the MF.

B.3 Asymptotics in the KF

In the KF, the proof is complicated due to the Keldysh indices, but follows the same principle as in the MF. It is most compactly presented by defining

$$
\tilde{K}\!\left(\mathbf{\Omega}^{(j),[\lambda]}_p\right)=\prod_{i=1}^{j}\frac{1}{\omega^{[\lambda]}_{\overline{1\ldots i}}-\varepsilon_i'}, \tag{B.20}
$$

such that the spectral representation of the connected 4p KF correlator reads (following from the Fourier transformation of Eq. (2.38))

$$G^{\mathrm{con};\boldsymbol{k}}(\boldsymbol{\omega}) = \sum_{\lambda=1}^{4} \delta_{k_{\overline{\lambda}},2}\,(-1)^{\lambda-1}(-1)^{k_{\overline{1}\dots\overline{\lambda-1}}} \int \mathrm{d}^3\varepsilon'\, \tilde{K}\Big(\boldsymbol{\Omega}_p^{(3),[\overline{\lambda}]}\Big)\, S_p^{\mathrm{con}}(\boldsymbol{\varepsilon'}). \qquad (\mathrm{B.21})$$

The additional complexity due to the Keldysh indices is best investigated for the specific permutations $p = (\overline{1}234),(\overline{1}243)$. Then, an expansion to leading order in ω_3 yields

$$G^{\mathrm{con};\boldsymbol{k}}_{p=(\overline{1}234),(\overline{1}243)}(\mathrm{i}\omega_1, \mathrm{i}\omega_{12}-\mathrm{i}\omega_1, \mathrm{i}\omega_3, \mathrm{i}\omega_{34}-\mathrm{i}\omega_3)$$

$$= \frac{1}{\omega_3} \sum_{\overline{12}} \int \mathrm{d}^3\varepsilon' \Big[\delta_{k_{\overline{1}},2}\,\tilde{K}\Big(\boldsymbol{\Omega}^{(2),[\overline{1}]}_{(\overline{1}234)}\Big) - \delta_{k_{\overline{2}},2}\,(-1)^{k_{\overline{1}}}\tilde{K}\Big(\boldsymbol{\Omega}^{(2),[\overline{2}]}_{(\overline{1}234)}\Big) + \delta_{k_3,2}\,(-1)^{k_{\overline{12}}}\tilde{K}\Big(\boldsymbol{\Omega}^{(2),[3]}_{(\overline{1}234)}\Big)$$

$$- \delta_{k_4,2}\,(-1)^{k_{\overline{123}}}\tilde{K}\Big(\boldsymbol{\Omega}^{(2),[4]}_{(\overline{1}234)}\Big) \Big] S^{\mathrm{con}}_{(\overline{1}234)}(\boldsymbol{\varepsilon'})$$

$$- \frac{1}{\omega_3} \sum_{\overline{12}} \int \mathrm{d}^3\varepsilon' \Big[\delta_{k_{\overline{1}},2}\,\tilde{K}\Big(\boldsymbol{\Omega}^{(2),[\overline{1}]}_{(\overline{1}243)}\Big) - \delta_{k_{\overline{2}},2}\,(-1)^{k_{\overline{1}}}\tilde{K}\Big(\boldsymbol{\Omega}^{(2),[\overline{2}]}_{(\overline{1}243)}\Big) + \delta_{k_4,2}\,(-1)^{k_{\overline{12}}}\tilde{K}\Big(\boldsymbol{\Omega}^{(2),[4]}_{(\overline{1}243)}\Big)$$

$$- \delta_{k_3,2}\,(-1)^{k_{\overline{124}}}\tilde{K}\Big(\boldsymbol{\Omega}^{(2),[3]}_{(\overline{1}243)}\Big) \Big] S^{\mathrm{con}}_{(\overline{1}243)}(\boldsymbol{\varepsilon'})$$

$$+ \mathcal{O}\left(\frac{1}{(\omega_3)^2}\right). \qquad (\mathrm{B.22})$$

Since $\omega^{[3]}_{\overline{1}} = \omega^{[4]}_{\overline{1}}$ and $\omega^{[3]}_{\overline{12}} = \omega^{[4]}_{\overline{12}}$, it follows that

$$\tilde{K}\Big(\boldsymbol{\Omega}^{(2),[4]}_{(\overline{1}234)}\Big) = \frac{1}{\Big(\omega^{[4]}_{\overline{1}}-\varepsilon'_1\Big)\Big(\omega^{[4]}_{\overline{12}}-\varepsilon'_2\Big)} = \tilde{K}\Big(\boldsymbol{\Omega}^{(2),[3]}_{(\overline{1}234)}\Big) = \tilde{K}\Big(\boldsymbol{\Omega}^{(2),[4]}_{(\overline{1}243)}\Big) = \tilde{K}\Big(\boldsymbol{\Omega}^{(2),[3]}_{(\overline{1}243)}\Big). \quad (\mathrm{B.23})$$

Thus, the respective last two terms in both square brackets in Eq. (B.22) simplify to

$$\delta_{k_3,2}\,(-1)^{k_{\overline{12}}}\tilde{K}\Big(\boldsymbol{\Omega}^{(2),[3]}_{(\overline{1}234)}\Big) - \delta_{k_4,2}\,(-1)^{k_{\overline{123}}}\tilde{K}\Big(\boldsymbol{\Omega}^{(2),[4]}_{(\overline{1}234)}\Big)$$

$$= (-1)^{k_{\overline{12}}}\frac{1}{2}\Big[1 + (-1)^{k_3} - \Big(1 + (-1)^{k_4}\Big)(-1)^{k_3}\Big]\tilde{K}\Big(\boldsymbol{\Omega}^{(2),[3]}_{(\overline{1}234)}\Big)$$

$$= (-1)^{k_{\overline{12}}}\delta_{k_{34},3}\,\tilde{K}\Big(\boldsymbol{\Omega}^{(2),[3]}_{(\overline{1}234)}\Big)$$

$$= \delta_{k_4,2}\,(-1)^{k_{\overline{12}}}\tilde{K}\Big(\boldsymbol{\Omega}^{(2),[4]}_{(\overline{1}243)}\Big) - \delta_{k_3,2}\,(-1)^{k_{\overline{124}}}\tilde{K}\Big(\boldsymbol{\Omega}^{(2),[3]}_{(\overline{1}243)}\Big), \qquad (\mathrm{B.24})$$

where we used the Kronecker-delta representation $\delta_{k_i,2} = \frac{1}{2}\Big(1+(-1)^{k_i}\Big)$ for $k_i \in \{1,2\}$ and $\delta_{k_{34},2} = \frac{1}{2}\Big(1-(-1)^{k_{34}}\Big)$ for $k_{34} \in \{2,3,4\}$. Inserting Eq. (B.24) together with $\tilde{K}\Big(\boldsymbol{\Omega}^{(2),[\overline{1}]}_{(\overline{1}234)}\Big) = \tilde{K}\Big(\boldsymbol{\Omega}^{(2),[\overline{1}]}_{(\overline{1}243)}\Big)$ and $\tilde{K}\Big(\boldsymbol{\Omega}^{(2),[\overline{2}]}_{(\overline{1}234)}\Big) = \tilde{K}\Big(\boldsymbol{\Omega}^{(2),[\overline{2}]}_{(\overline{1}243)}\Big)$ into Eq. (B.22), we then obtain

$$G^{\mathrm{con};\boldsymbol{k}}_{p=(\overline{1}234),(\overline{1}243)}(\mathrm{i}\omega_1, \mathrm{i}\omega_{12}-\mathrm{i}\omega_1, \mathrm{i}\omega_3, \mathrm{i}\omega_{34}-\mathrm{i}\omega_3)$$

$$= \frac{1}{\omega_3} \sum_{\overline{12}} \int \mathrm{d}\varepsilon'_1 \mathrm{d}\varepsilon'_2 \Big[\delta_{k_{\overline{1}},2}\,\tilde{K}\Big(\boldsymbol{\Omega}^{(2),[\overline{1}]}_{(\overline{1}234)}\Big) - \delta_{k_{\overline{2}},2}\,(-1)^{k_{\overline{1}}}\tilde{K}\Big(\boldsymbol{\Omega}^{(2),[\overline{2}]}_{(\overline{1}234)}\Big) \Big]$$

$$\times \int \mathrm{d}\varepsilon'_3 \Big[S^{\mathrm{con}}_{(\overline{1}234)}(\boldsymbol{\varepsilon'}) - S^{\mathrm{con}}_{(\overline{1}243)}(\boldsymbol{\varepsilon'}) \Big]$$

$$+ \frac{1}{\omega_3} \sum_{\overline{12}} \int d\varepsilon_1' d\varepsilon_2' \, (-1)^{k_{\overline{12}}} \, \delta_{k_{34},3} \, \tilde{K}\left(\mathbf{\Omega}_{(\overline{12}34)}^{(2),[3]}\right) \int d\varepsilon_3' \left[S_{(\overline{12}34)}^{\mathrm{con}}(\boldsymbol{\varepsilon}') - S_{(\overline{12}43)}^{\mathrm{con}}(\boldsymbol{\varepsilon}') \right]$$

$$+ \mathcal{O}\left(\frac{1}{(\omega_3)^2}\right)$$

$$= \mathcal{O}\left(\frac{1}{(\omega_3)^2}\right). \tag{B.25}$$

In the last step, we again used Eq. (B.16). The same calculation can be repeated for the remaining permutations $p = (\overline{1}34\overline{2})$, $(\overline{1}34\overline{2})$, $(34\overline{12})$, and $(43\overline{12})$, yielding the final result

$$G^{\mathrm{con};\boldsymbol{k}}(\mathrm{i}\omega_1, \mathrm{i}\omega_{12} - \mathrm{i}\omega_1, \mathrm{i}\omega_3, \mathrm{i}\omega_{34} - \mathrm{i}\omega_3) = \mathcal{O}\left(\frac{1}{(\omega_3)^2}\right). \tag{B.26}$$

Thus, also in the KF, $G^{\mathrm{con};\boldsymbol{k}}$ shows the correct scaling behaviour for the consistency of Eq. (3.76a), concluding our proof.

C Calculations for the analytic continuation of multipoint correlators

This appendix reproduces Apps. A to G and parts of App. H of [P4] *with minor modifications to put these appendices into the context of this thesis.*

C.1 MF kernels

This appendix is devoted to a discussion of the full primary MF kernel K, including both regular and anomalous terms. It is defined via Eq. (3.59) for the MF kernel $\mathcal{K}(\boldsymbol{\Omega}_p)$. In Ref. [KLvD21], it was shown that it can be computed via

$$\mathcal{K}(\boldsymbol{\Omega}_p) = \int_0^\beta \mathrm{d}\tau'_{\bar\ell}\, e^{\Omega_{\bar 1\ldots\bar\ell}\tau'_{\bar\ell}} \prod_{i=\ell-1}^{1} \left[-\int_0^{\beta-\tau'_{\overline{i+1}\ldots\bar\ell}} \mathrm{d}\tau'_{\bar i}\, e^{\Omega_{\bar 1\ldots\bar i}\tau'_{\bar i}} \right] = \beta\delta_{\Omega_{\bar 1\ldots\bar\ell}}K(\boldsymbol{\Omega}_p) + \mathcal{R}(\boldsymbol{\Omega}_p). \quad \text{(C.1)}$$

The residual part $\mathcal{R}$ is not of interest, for reasons explained after Eq. (3.61). The primary part $K(\boldsymbol{\Omega}_p)$ is obtained[1] by collecting all contributions multiplying $\beta\delta_{\Omega_{\bar 1\ldots\bar\ell}}$, and its argument satisfies $\Omega_{\bar 1\ldots\bar\ell} = 0$ by definition. Before presenting explicit expressions for K, let us briefly recall where it is needed in the main part of this thesis.

The analytical continuation of MF to KF correlators, based on $\tilde G_p(\mathrm{i}\boldsymbol{\omega}_p \to \boldsymbol{\omega}^{[\eta_j]})$ (Eq. (5.1b)), utilizes regular partial MF correlators, $\tilde G_p(\mathrm{i}\boldsymbol{\omega}_p) = [\tilde K * S_p](\mathrm{i}\boldsymbol{\omega}_p)$ (Eq. (3.63b)). These are expressed through regular MF kernels $\tilde K(\boldsymbol{\Omega}_p)$ having a simple product form, $\prod_{i=1}^{\ell-1} \Omega_{\bar 1\ldots\bar i}^{-1}$, with $\Omega_{\bar 1\ldots\bar\ell} = 0$ understood. The more complicated primary kernel $K(\boldsymbol{\Omega}_p)$ is defined implicitly via Eq. (3.59). It includes both regular and anomalous parts, the latter involving vanishing partial frequency sums, $\Omega_{\bar 1\ldots\bar i} = 0$ with $i < \ell$. The primary kernel arises in two distinct contexts, involving either (i) imaginary-frequency convolutions $\star$ or (ii) real-frequency convolutions $*$, with different requirements for the bookkeeping of anomalous contributions. We discuss them in turn.

(i) For a specified permutation p, the regular partial $\tilde G_p(\mathrm{i}\boldsymbol{\omega}_p)$ can be extracted from the full MF correlator $G(\mathrm{i}\boldsymbol{\omega}')$ via a imaginary-frequency convolution, $[K \star G](\mathrm{i}\boldsymbol{\omega}_p)$ (Eq. (5.6)). There, the argument of $K(\boldsymbol{\Omega}_p)$ has the form $\boldsymbol{\Omega}_p = \mathrm{i}\boldsymbol{\omega}_p - \mathrm{i}\boldsymbol{\omega}'_p$. This is always bosonic, being the difference of two same-type Matsubara frequencies. The convolution $\star$ involves Matsubara sums $\sum_{\mathrm{i}\boldsymbol{\omega}'_p}$, generating many anomalous contributions with $\Omega_{\bar 1\ldots\bar i} = 0$. For these sums to be well-defined, the kernel $K(\boldsymbol{\Omega}_p)$ must thus be represented in a form that (in contrast to $\tilde K(\boldsymbol{\Omega}_p)$) is manifestly singularity-free for all values of $\Omega_{\bar 1\ldots\bar i}$, including 0.

(ii) In Eq. (5.6), $\tilde G_p$ is given by that part of $[K \star G]$ that is $\mathcal{O}(\beta^0)$; subleading powers of β are not needed. Therefore, we seek the MF $G(\mathrm{i}\boldsymbol{\omega}')$ in the form of an $\beta\delta$ expansion, i.e. an expansion in powers of $\beta\delta_{\omega'_{\bar 1\ldots\bar i}}$. Then each of them can collapse one Matsubara sum $1/(-\beta)\sum_{\omega'_{\bar 1\ldots\bar i}}$ while their β factors cancel. To obtain a $\beta\delta$ expansion for $G(\mathrm{i}\boldsymbol{\omega}')$, it is convenient to express it via a permutation sum of real-frequency convolutions, $\sum_p [K * S_p](\mathrm{i}\boldsymbol{\omega}'_p)$ (Eq. (3.60)), and represent the kernel $K(\boldsymbol{\Omega}_p)$, with argument $\boldsymbol{\Omega}_p = \mathrm{i}\boldsymbol{\omega}'_p - \boldsymbol{\varepsilon}_p$, as a $\beta\delta$ expansion in powers of $\beta\delta_{\Omega'_{\bar 1\ldots\bar i}}$.

Fortunately, suitable representations of K satisfying the respective requirements of either (i) or (ii) are available in the literature [Shv06, Shv16, KLvD21, P2]. We discuss them for $\ell \leq 4$ in Apps. C.1.1 and C.1.2, respectively.

---

[1] In Ref. [KLvD21], after Eq. (41), it was stated that the lower boundary terms yield K; that is incorrect—they yield only $\tilde K$.

C.1.1 Singularity-free representation of K

Consider case (i), involving $K \star G$, where the argument of $K(\boldsymbol{\Omega}_p)$ is a bosonic Matsubara frequency. We seek a singularity-free (sf) representation for K, to be denoted K^{sf} for the purpose of this appendix. That such a representation exists is obvious from the form of integrals in Eq. (C.1): inserting $\Omega_{\bar{1}...\bar{i}} = 0$ there reduces an exponential function to 1, so no contributions singular in $\Omega_{\bar{1}...\bar{i}}$ can arise. To find K^{sf}, one simply has to perform the integrals explicitly, treating the cases $\Omega_{\bar{1}...\bar{i}} \neq 0$ or $= 0$ separately and distinguish them using Kronecker symbols.

Such a direct computation of Eq. (C.1) has been performed in [P2] (see Ch. 4) for arbitrary ℓ and an arbitrary number of vanishing partial frequency sums, $\Omega_{\bar{1}...\bar{i}} = 0$. The following equations summarize the results for $\ell \leq 4$:

$$K^{\text{sf}}(\boldsymbol{\Omega}_p) \overset{\ell=2}{=} \Delta_{\Omega_{\bar{1}}} - \tfrac{\beta}{2}\delta_{\Omega_{\bar{1}}}, \tag{C.2a}$$

$$K^{\text{sf}}(\boldsymbol{\Omega}_p) \overset{\ell=3}{=} \Delta_{\Omega_{\overline{12}}}\Big(\Delta_{\Omega_{\bar{1}}} - \tfrac{\beta}{2}\delta_{\Omega_{\bar{1}}}\Big) - \delta_{\Omega_{\overline{12}}}\Big(\Delta_{\Omega_{\bar{1}}}^2 + \tfrac{\beta}{2}\Delta_{\Omega_{\bar{1}}} - \tfrac{\beta^2}{6}\delta_{\Omega_{\bar{1}}}\Big), \tag{C.2b}$$

$$K^{\text{sf}}(\boldsymbol{\Omega}_p) \overset{\ell=4}{=} \Delta_{\Omega_{\overline{123}}}\Big[\Delta_{\Omega_{\overline{12}}}\Big(\Delta_{\Omega_{\bar{1}}} - \tfrac{\beta}{2}\delta_{\Omega_{\bar{1}}}\Big) - \delta_{\Omega_{\overline{12}}}\Big(\Delta_{\Omega_{\bar{1}}}^2 + \tfrac{\beta}{2}\Delta_{\Omega_{\bar{1}}} - \tfrac{\beta^2}{6}\delta_{\Omega_{\bar{1}}}\Big)\Big]$$
$$- \delta_{\Omega_{\overline{123}}}\Big[\Delta_{\Omega_{\overline{12}}}\Delta_{\Omega_{\bar{1}}}\Big(\Delta_{\Omega_{\overline{12}}} + \Delta_{\Omega_{\bar{1}}} + \tfrac{\beta}{2}\Big) - \tfrac{\beta}{2}\Delta_{\Omega_{\overline{12}}}\delta_{\Omega_{\bar{1}}}\Big(\Delta_{\Omega_{\overline{12}}} + \tfrac{\beta}{3}\Big)$$
$$- \delta_{\Omega_{\overline{12}}}\Delta_{\Omega_{\bar{1}}}\Big(\Delta_{\Omega_{\bar{1}}}^2 + \tfrac{\beta}{2}\Delta_{\Omega_{\bar{1}}} + \tfrac{\beta^2}{6}\Big) + \tfrac{\beta^3}{24}\delta_{\Omega_{\overline{12}}}\delta_{\Omega_{\bar{1}}}\Big]. \tag{C.2c}$$

Equations (C.2) are manifestly singularity-free for all values of their frequency arguments—including those with $\Omega_{\bar{1}...\bar{i}} = 0$, for which $\Delta_{\Omega_{\bar{1}...\bar{i}}}$ terms vanish by definition (Eq. (3.15)).

C.1.2 $\beta\delta$ expansion for K

Next, consider case (ii), involving $G = \sum_p K * S_p$ (Eqs. (3.60) and (3.61)), where the argument of $K(\boldsymbol{\Omega}_p)$ has the form $\boldsymbol{\Omega}_p = i\boldsymbol{\omega}_p - \boldsymbol{\varepsilon}_p$, and we seek a $\beta\delta$ expansion for G. For this purpose, the kernels K^{sf} of Eqs. (C.2) are inconvenient, because they contain some δ factors not accompanied by β. Instead, G can be expressed through an alternative kernel, to be denoted K^{alt}, which constitutes a $\beta\delta$ expansion itself and hence differs from K^{sf}, but yields the same result for G when summed over all permutations, so that

$$G(i\boldsymbol{\omega}) = \sum_p [K^{\text{sf}} * S_p](i\boldsymbol{\omega}) = \sum_p [K^{\text{alt}} * S_p](i\boldsymbol{\omega}). \tag{C.3}$$

Explicit expressions for K^{alt} were given in Ref. [KLvD21] for up to one potentially vanishing frequency (general 2p correlators, 3p correlators with one bosonic operator, and fermionic 4p correlators). By also allowing general 3p correlators, these results are extended to

$$K^{\text{alt}}(\boldsymbol{\Omega}_p) \overset{\ell=2}{=} \frac{1}{\Omega_{\bar{1}}} - \frac{\beta}{2}\delta_{\Omega_{\bar{1}}}, \tag{C.4a}$$

$$K^{\text{alt}}(\boldsymbol{\Omega}_p) \overset{\ell=3}{=} \frac{1}{\Omega_{\bar{1}}\Omega_{\overline{12}}} - \frac{\beta}{2}\Big(\delta_{\Omega_{\overline{12}}}\Delta_{\Omega_{\bar{1}}} + \delta_{\Omega_{\bar{1}}}\Delta_{\Omega_{\overline{12}}}\Big) + \frac{\beta^2}{6}\delta_{\Omega_{\bar{1}}}\delta_{\Omega_{\overline{12}}}, \tag{C.4b}$$

$$K^{\text{alt}}(\boldsymbol{\Omega}_p) \overset{\ell=4}{=} \frac{1}{\Omega_{\bar{1}}\Omega_{\overline{12}}\Omega_{\overline{123}}} - \frac{\beta}{2}\delta_{\Omega_{\overline{12}}}\frac{1}{\Omega_{\bar{1}}\Omega_{\overline{123}}}. \tag{C.4c}$$

The kernels (C.4) have the form $K^{\text{alt}} = \tilde{K} + \hat{K}^{\text{alt}}$, with regular part $\tilde{K}$ as given in Eq. (3.62), while the anomalous part, $\hat{K}^{\text{alt}}$, comprises terms multiplied by one or multiple factors $\beta\delta_{\Omega_{\bar{1}...\bar{i}}}$. (We remark that the nomenclature *regular* and *anomalous* is used non-

uniformly in the literature and our usage here may differ from Refs. [Shv06, KLvD21, P2].)
Whether or not $\Omega_{\bar{1}...\bar{i}} = i\omega_{\bar{1}...\bar{i}} - \varepsilon_{\bar{1}...\bar{i}}$ can vanish at all depends on the fermionic or bosonic
nature of the Matsubara frequencies. Take, e.g., $\ell = 4$ and all operators fermionic. Then, in
Eq. (C.2c), all terms multiplied by $\delta_{\Omega_{\overline{123}}}$ evaluate to $\delta_{\Omega_{\overline{123}}} = 0$, since $i\omega_{\overline{123}} \neq 0$ is a fermionic
Matsubara frequency. For the computation of fermionic 4p correlators, all terms proportional
to $\delta_{\Omega_{\bar{1}}}$ and $\delta_{\Omega_{\overline{123}}}$ can thus be dropped. Even if $i\omega_{\bar{1}...\bar{i}}$ is bosonic and vanishes, $\Omega_{\bar{1}...\bar{i}} = 0$
additionally requires $\varepsilon_{\bar{1}...\bar{i}} = 0$, enforced by a Dirac $\delta(\varepsilon_{\bar{1}...\bar{i}})$ in the PSFs; see App. C.2.1 for
further discussion of this point.

For a specified permutation p, the kernels K^{alt} are not singularity-free. In particular, the
regular part $\tilde{K}$ diverges if one (or multiple) $\Omega_{\bar{1}...\bar{i}} \to 0$. However, that singularity is canceled
by $1/\Omega_{\overline{i+1}...\bar{\ell}} = -1/\Omega_{\bar{1}...\bar{i}}$ from a cyclically related permutation in the sum over permutations
in Eq. (C.3). This can be shown explicitly by treating nominally vanishing denominators as
infinitesimal and tracking the cancellation of divergent terms while exploiting the equilibrium
condition (2.47) (see App. B of Ref. [KLvD21]).

The kernels K^{alt}, inserted into Eq. (C.4), result in the general form for MF correlators
given in Eq. (3.63):

$$G(i\boldsymbol{\omega}) = \tilde{G}(i\boldsymbol{\omega}) + \hat{G}(i\boldsymbol{\omega}), \tag{C.5a}$$

$$\hat{G}(i\boldsymbol{\omega}) = \sum_{j=1}^{\ell-1} \beta\delta_{i\omega_j}\hat{G}_j(i\boldsymbol{\omega}) + \sum_{j=1}^{\ell-1}\sum_{k>j}^{\ell-1} \left(\beta\delta_{i\omega_{jk}}\hat{G}_{jk}(i\boldsymbol{\omega}) + \beta^2\delta_{i\omega_j}\delta_{i\omega_k}\hat{G}_{j,k}(i\boldsymbol{\omega}) \right). \tag{C.5b}$$

As for Eq. (C.4), this form of the anomalous part of the correlator applies to general 2p and
3p correlators as well as fermionic 4p correlators. The subscripts of $\hat{G}$ indicate the frequency
in which they are anomalous. Even though their arguments nominally include all frequencies
$i\boldsymbol{\omega}$, they are independent of their respective anomalous frequency; e.g., $\hat{G}_1(i\omega_1, i\omega_2) = \hat{G}_1(i\omega_2)$
for $\ell = 3$. Note that this decomposition of the correlator is convenient for the analytic
continuation because the components, such as $\tilde{G}$ and $\hat{G}_i$ have a functional form, that allows
their arguments to be analytically continued, $i\omega_i \to z_i$. In anomalous components this
functional form is obtained by symbolically replacing all $\Delta_{i\omega}$ by $\frac{1}{i\omega}$ (see, e.g., Eq. (5.54) and
the discussion thereafter).

C.2 Discussion of PSFs

In App. C.2.1, we clarify the functional structure of PSFs and motivate their decomposition
into regular and anomalous contributions, $S_p = \tilde{S}_p + \hat{S}_p$ (Eq. (2.49)), analogous to that for
MF correlators. This decomposition aids investigations in subsequent appendices. As an
immediate application of the decomposition, we present an analysis of the effect of fully
anomalous PSFs on 3p MF correlators in App. C.2.2.

C.2.1 Decomposition of PSFs

Interacting thermal systems typically have a continuum of energy levels. Ref. [KS69] argues
that, in general, PSFs may contain contributions which diverge as $\mathrm{P}(\frac{1}{\varepsilon})$ for vanishing bosonic
frequencies ε, with P the principal value (see discussion after Eq. (3.44), in particular the
footnote.). As our derivations do not make assumptions on the shape of continuous PSF
contributions, such terms require no further consideration. However, Dirac delta contributions
in S_p can arise for finite systems or in the presence of conserved quantities. When these are
present, MF partial correlators $G_p = K * S_p$ (Eq. (3.60)) can contain anomalous terms, $\hat{G}_p$,
containing at least one factor $\delta_{i\omega_{\bar{1}...\bar{i}}}$, with $i < \ell$. These arise from anomalous $\delta_{\Omega_{\bar{1}...\bar{i}}}$ terms
in the MF kernel $K(\boldsymbol{\Omega}_p)$, with argument $\boldsymbol{\Omega}_p = i\boldsymbol{\omega}_p - \boldsymbol{\varepsilon}_p$ (Eqs. (C.3), (C.4)). Such terms

can contribute if $\Omega_{\bar{1}\dots\bar{i}} = 0$, requiring $\mathrm{i}\omega_{\bar{1}\dots\bar{i}} = 0$ *and* $\varepsilon_{\bar{1}\dots\bar{i}} = 0$. The first condition requires that $\mathrm{i}\omega_{\bar{1}\dots\bar{i}}$ is bosonic. This is the case if the sign $\zeta^{\bar{1}\dots\bar{i}} = \zeta^{\bar{1}}\dots\zeta^{\bar{i}}$ equals $+1$ (with $\zeta^j = \pm 1$ for bosonic/fermionic operators O^j). Then, the associated $\varepsilon_{\bar{1}\dots\bar{i}}$ is bosonic, too, according to the nomenclature introduced after Eq. (2.46). The second condition is met if the PSF $S_p(\boldsymbol{\varepsilon}_p)$ contains a term proportional to a bosonic Dirac delta, i.e. one having a bosonic $\varepsilon_{\bar{1}\dots\bar{i}}$ as argument, e.g. $\delta(\varepsilon_{\bar{1}\dots\bar{i}})\check{S}_{\bar{1}\dots\bar{i}}$. Then, the ε_p integrals in the convolution $K * S_p$ receive a finite contribution from the point $\varepsilon_{\bar{1}\dots\bar{i}} = 0$. We summarize these conditions via the symbolic notation

$$\delta_{\Omega_{\bar{1}\dots\bar{i}}} = \delta_{\mathrm{i}\omega_{\bar{1}\dots\bar{i}}}\delta_{\varepsilon_{\bar{1}\dots\bar{i}}}, \tag{C.6}$$

needed only for bosonic $\Omega_{\bar{1}\dots\bar{i}}$. Here $\delta_{\varepsilon_{\bar{1}\dots\bar{i}}}$, carrying a continuous variable as subscript, is defined only for bosonic $\varepsilon_{\bar{1}\dots\bar{i}}$ and by definition "acts on" $S_p(\boldsymbol{\varepsilon}_p)$ by extracting only those parts (if present) containing *bosonic* Dirac $\delta(\varepsilon_{\bar{1}\dots\bar{i}})$ factors. For the example above, $\delta_{\varepsilon_{\bar{1}\dots\bar{i}}}$ acts on $S_p(\boldsymbol{\varepsilon}_p)$ as

$$\delta_{\varepsilon_{\bar{1}\dots\bar{i}}}S_p(\boldsymbol{\varepsilon}_p) = \delta_{\varepsilon_{\bar{1}\dots\bar{i}}}\hat{S}_p(\boldsymbol{\varepsilon}_p) \sim \delta(\varepsilon_{\bar{1}\dots\bar{i}}). \tag{C.7}$$

As we always assume an even number of fermionic operators, $\zeta^{1\dots\ell} = +1$ follows.

The motivation for splitting PSFs as $S_p = \tilde{S}_p + \hat{S}_p$ is now clear. The anomalous $\hat{S}_p$ comprises all terms containing bosonic Dirac $\delta(\varepsilon_{\bar{1}\dots\bar{i}})$ factors, the regular $\tilde{S}$ everything else. The regular part of the MF correlator, $\tilde{G}$, receives contributions from both $\tilde{S}_p$ and $\hat{S}_p$; the anomalous part, $\hat{G}$, receives contributions only from $\hat{S}_p$, i.e. if $\hat{S}_p = 0$ for all p, then $\hat{G} = 0$.

For $\ell = 2$, the anomalous contribution consists of one term,

$$\hat{S}_p(\boldsymbol{\varepsilon}_p) = \delta(\varepsilon_{\bar{1}})\check{S}_{p;\bar{1}}, \tag{C.8}$$

where $\check{S}_{p;\bar{1}}$ is a constant. Due to the equilibrium condition (2.47), we can further conclude $\check{S}_{(12);1} = \check{S}_{(21);2}$.

For $\ell = 3$, the anomalous $\hat{S}_p$ reads

$$\hat{S}_p(\boldsymbol{\varepsilon}_p) = \delta(\varepsilon_{\bar{1}})\check{S}_{p;\bar{1}}(\circ, \varepsilon_{\bar{2}}, \varepsilon_{\bar{3}}) + \delta(\varepsilon_{\bar{3}})\check{S}_{p;\bar{3}}(\varepsilon_{\bar{1}}, \varepsilon_{\bar{2}}, \circ) + \delta(\varepsilon_{\bar{1}})\delta(\varepsilon_{\bar{2}})\check{S}_{p;\bar{1},\bar{2}}. \tag{C.9}$$

Here, we inserted $\circ$'s to emphasize that functions do not depend on these arguments, and $\check{S}_{p;\bar{1},\bar{2}}$ is a constant. For bosonic 3p functions, $\check{S}_{p;\bar{1}}$ and $\check{S}_{p;\bar{3}}$ do not contain further δ–factors that lead to anomalous parts, e.g., $\delta_{\varepsilon_{\bar{3}}}\check{S}_{p;\bar{1}}(\circ, \varepsilon_{\bar{2}}, \varepsilon_{\bar{3}}) = 0$.

To further illustrate the symbolic $\delta_{\varepsilon_{\bar{1}\dots\bar{i}}}$ notation introduced in Eq. (C.6), it yields the following relations when applied to the above definitions, for bosonic $\varepsilon_{\bar{i}}$:

$$\delta_{\varepsilon_{\bar{1}}}S_p(\boldsymbol{\varepsilon}_p) = \delta(\varepsilon_{\bar{1}})\check{S}_{p;\bar{1}}(\boldsymbol{\varepsilon}_p) + \delta(\varepsilon_{\bar{1}})\delta(\varepsilon_{\bar{2}})\check{S}_{p;\bar{1},\bar{2}}, \tag{C.10a}$$

$$\delta_{\varepsilon_{\bar{1}}}\delta_{\varepsilon_{\bar{2}}}S_p(\boldsymbol{\varepsilon}_p) = \delta(\varepsilon_{\bar{1}})\delta(\varepsilon_{\bar{2}})\check{S}_{p;\bar{1},\bar{2}}. \tag{C.10b}$$

For fermionic $\ell = 4$, we only need

$$\hat{S}_p(\boldsymbol{\varepsilon}_p) = \delta(\varepsilon_{\overline{12}})\check{S}_{p;\overline{12}}(\boldsymbol{\varepsilon}_p), \tag{C.11}$$

since, e.g., terms in the kernel proportional to $\delta_{\mathrm{i}\omega_{\bar{1}}-\varepsilon_{\bar{1}}}$ do not lead to anomalous contributions by the fermionic nature of $\mathrm{i}\omega_{\bar{1}}$.

C.2.2 Effect of fully anomalous PSFs on 3p MF correlators

In App. C.3.1 below, we discuss the general structure of 3p MF correlators inferred by the decomposition of the PSFs. The regular PSFs, $\tilde{S}_p$, can only contribute to the regular part of the correlator. However, the effect of anomalous PSFs, $\hat{S}_p$, is more involved and is studied in detail in the following.

To this end, we consider PSFs with finite weight at vanishing frequency arguments. In particular, we assume the maximally anomalous form $S_p^{\mathrm{ma}}(\varepsilon_{\bar{1}}, \varepsilon_{\bar{2}}) = \delta(\varepsilon_{\bar{1}})\delta(\varepsilon_{\bar{2}})\check{S}_{p;\bar{1},\bar{2}}$ (see Eq. (C.10b)). Then, the equilibrium condition Eq. (2.47) implies $\check{S}_{(123);1,2} = \check{S}_{(231);2,3} = \check{S}_{(312);3,1}$ and $\check{S}_{(132);1,3} = \check{S}_{(321);3,2} = \check{S}_{(213);2,1}$, since $\zeta_p = \zeta_{p_\lambda} = 1$ for purely bosonic correlators. For such PSFs, the 3p correlator evaluates to

$$
\begin{aligned}
G^{\mathrm{ma}}(\mathrm{i}\boldsymbol{\omega}) &= \sum_p [K * S_p^{\mathrm{ma}}](\mathrm{i}\boldsymbol{\omega}_p) \\
&= \left[\frac{\beta}{2} \left(\delta_{\mathrm{i}\omega_1} \Delta_{\mathrm{i}\omega_{12}} + \Delta_{\mathrm{i}\omega_1} \delta_{\mathrm{i}\omega_{12}} \right) + \frac{\beta^2}{6} \delta_{\mathrm{i}\omega_1} \delta_{\mathrm{i}\omega_{12}} \right] \check{S}_{(123);1,2} \\
&\quad + \left[\frac{\beta}{2} \left(\delta_{\mathrm{i}\omega_2} \Delta_{\mathrm{i}\omega_{23}} + \Delta_{\mathrm{i}\omega_2} \delta_{\mathrm{i}\omega_{23}} \right) + \frac{\beta^2}{6} \delta_{\mathrm{i}\omega_2} \delta_{\mathrm{i}\omega_{23}} \right] \check{S}_{(231);2,3} \\
&\quad + \left[\frac{\beta}{2} \left(\delta_{\mathrm{i}\omega_3} \Delta_{\mathrm{i}\omega_{31}} + \Delta_{\mathrm{i}\omega_3} \delta_{\mathrm{i}\omega_{31}} \right) + \frac{\beta^2}{6} \delta_{\mathrm{i}\omega_3} \delta_{\mathrm{i}\omega_{31}} \right] \check{S}_{(312);3,1} \\
&\quad + (2 \leftrightarrow 3) \\
&= \beta \left(\delta_{\mathrm{i}\omega_1} \Delta_{\mathrm{i}\omega_2} + \delta_{\mathrm{i}\omega_2} \Delta_{\mathrm{i}\omega_3} + \delta_{\mathrm{i}\omega_3} \Delta_{\mathrm{i}\omega_1} \right) \left(\check{S}_{(123);1,2} - \check{S}_{(132);1,3} \right) \\
&\quad + \frac{\beta^2}{2} \delta_{\mathrm{i}\omega_1} \delta_{\mathrm{i}\omega_2} \left(\check{S}_{(123);1,2} + \check{S}_{(132);1,3} \right),
\end{aligned}
\tag{C.12}
$$

where $(2 \leftrightarrow 3)$ exchanges the indices of the frequencies and PSFs. The contribution of the regular kernel in Eq. (C.4b) vanishes due to $\frac{1}{\mathrm{i}\omega_1 \, \mathrm{i}\omega_{12}} + \frac{1}{\mathrm{i}\omega_2 \, \mathrm{i}\omega_{23}} + \frac{1}{\mathrm{i}\omega_3 \, \mathrm{i}\omega_{31}} = 0$ with $\mathrm{i}\omega_3 = -\mathrm{i}\omega_{12}$.

For later reference (see Apps. C.3.1 and C.5.2), we define the constants

$$
\hat{G}_{1,2} = \tfrac{1}{2} \left(\check{S}_{(123);1,2} + \check{S}_{(132);1,3} \right),
\tag{C.13a}
$$

$$
\hat{G}_{1;2}^{\Delta} = \hat{G}_{2;3}^{\Delta} = \hat{G}_{3;1}^{\Delta} = \check{S}_{(132);1,3} - \check{S}_{(123);1,2},
\tag{C.13b}
$$

such that G^{ma} reads

$$
\hat{G}^{\mathrm{ma}}(\mathrm{i}\boldsymbol{\omega}) = \beta \left(\delta_{\mathrm{i}\omega_1} \Delta_{\mathrm{i}\omega_2} \hat{G}_{1;2}^{\Delta} + \delta_{\mathrm{i}\omega_2} \Delta_{\mathrm{i}\omega_3} \hat{G}_{2;3}^{\Delta} + \delta_{\mathrm{i}\omega_3} \Delta_{\mathrm{i}\omega_1} \hat{G}_{3;1}^{\Delta} \right) + \beta^2 \delta_{\mathrm{i}\omega_1} \delta_{\mathrm{i}\omega_2} \hat{G}_{1,2}.
\tag{C.13c}
$$

We emphasize that $\hat{G}_{i;j}^{\Delta}$ and $\hat{G}_{1,2}$ are nonzero only if the full PSFs S_p contain fully anomalous contributions S_p^{ma}, which is only the case for all operators being bosonic. In the next section, the most general form of 3p correlators is discussed.

C.3 Calculations for 3p correlators

This appendix is devoted to computations for the analytic continuation of 3p correlators, complementing the discussions in Sec. 5.5. First, in App. C.3.1, we discuss the general structure of MF correlators, needed in App. C.3.2 for the derivation of an explicit formula for partial MF correlators and the subsequent extraction of PSFs. In App. C.3.3, we then present manipulations needed to construct KF correlators from analytically continued MF correlators.

C.3.1 Structure of 3p correlators

For 3p correlators, Eq. (C.5) implies the general form

$$
\begin{aligned}
G_{i\omega_1, i\omega_2} &= \tilde{G}_{i\omega_1, i\omega_2} + \hat{G}_{i\omega_1, i\omega_2}, \\
\hat{G}_{i\omega_1, i\omega_2} &= \beta\delta_{i\omega_1} \hat{G}_{1; i\omega_2} + \beta\delta_{i\omega_2} \hat{G}_{2; i\omega_1} + \beta\delta_{i\omega_3} \hat{G}_{3; i\omega_1} + \beta^2 \delta_{i\omega_1} \delta_{i\omega_2} \hat{G}_{1,2}.
\end{aligned}
\tag{C.14}
$$

Here, we used the subscript notation introduced in Sec. 5.4.

For the conversion of Matsubara sums to contour integrals we distinguish restricted from unrestricted sums (see e.g. Eq. (5.9b)). Therefore we explicitly distinguish terms with $\Delta_{i\omega}$ factors, writing (cf. Eq. (5.47))

$$
\hat{G}_{i; i\omega_j} = \hat{G}_{i; i\omega_j}^{\slashed{\Delta}} + \Delta_{i\omega_j}\hat{G}_{i;j}^{\Delta}.
\tag{C.15}
$$

In Eq. (C.13b), we have identified the constants $\hat{G}^{\Delta}$ with (maximally anomalous) PSFs. For alternative frequency parametrizations in Eqs. (C.13), the constants in Eq. (C.15) read

$$
\hat{G}_{1;2}^{\Delta} = -\hat{G}_{1;3}^{\Delta} = -\hat{G}_{2;1}^{\Delta} = \hat{G}_{2;3}^{\Delta} = \hat{G}_{3;1}^{\Delta} = -\hat{G}_{3;2}^{\Delta},
\tag{C.16}
$$

such that, e.g., $\delta_{i\omega_1}\Delta_{i\omega_2}\hat{G}_{1;2}^{\Delta} = -\delta_{i\omega_1}\Delta_{i\omega_3}\hat{G}_{1;2}^{\Delta} = \delta_{i\omega_1}\Delta_{i\omega_3}\hat{G}_{1;3}^{\Delta}$, which follows from frequency conservation, $i\omega_{1\ldots\ell} = 0$, and the $\delta_{i\omega_i}$ factor multiplying $\hat{G}_i$.

C.3.2 Partial MF 3p correlators

In this appendix, we present explicit calculations concerning Steps 1 and 2 of our 3-step strategy outlined in Sec. 5.2.2. First, we introduce two identities used for simplifications in Step 1.

Consider the restricted Matsubara sum of Eq. (5.9b) for $f(i\omega') = \tilde{f}(i\omega')/(i\omega - i\omega')$. Using Eq. (5.11) for the residue term, one obtains

$$
\frac{1}{(-\beta)}\sum_{i\omega'}\left(\Delta_{i\omega - i\omega'} - \tfrac{\beta}{2}\delta_{i\omega - i\omega'}\right)\tilde{f}(i\omega') = \oint_z \frac{n_z \tilde{f}(z)}{i\omega - z} + \mathcal{O}(\tfrac{1}{\beta}).
\tag{C.17}
$$

Here, the restriction of the sum is implicit in the Δ symbol (Eq. (3.15)), and the first term of Eq. (5.11) was incorporated into the sum using the Kronecker δ. We can identify the summand on the left of Eq. (C.17) as the singularity-free 2p kernel of Eq. (C.2a), and therefore this identity constitutes the convenient cancellation in Eqs. (5.12) already on the level of kernels. Following the same line of arguments, one can show that

$$
\frac{1}{(-\beta)^2}\sum_{i\omega'}\left(\Delta_{i\omega - i\omega'}^2 + \tfrac{\beta^2}{12}\delta_{i\omega - i\omega'}\right)\tilde{f}(i\omega') = \mathcal{O}(\tfrac{1}{\beta}).
\tag{C.18}
$$

In the following, we focus on evaluating

$$
\tilde{G}_{(123)}(i\boldsymbol{\omega}_{(123)}) + \mathcal{O}(\tfrac{1}{\beta}) = [K \star G](i\boldsymbol{\omega}_{(123)}),
\tag{C.19}
$$

using the 3p kernel given in Eq. (C.2b) (with $\boldsymbol{\Omega}_{(123)} = i\boldsymbol{\omega}_{(123)} - i\boldsymbol{\omega}'_{(123)}$), and the general form of the 3p correlator displayed in Eq. (C.14). For convencience, we focus on the identity permutation $p = (123)$; all other permutations can be obtained by replacing indices with their permuted ones, $i \to \bar{i}$. We split the calculation of Eq. (C.19) into regular (r) and anomalous

(a) contributions from G:

$$\tilde{G}^{\mathrm{r}}_{(123)}(\mathrm{i}\boldsymbol{\omega}_{(123)}) + \mathcal{O}(\tfrac{1}{\beta}) = \left[K \star \tilde{G}\right](\mathrm{i}\boldsymbol{\omega}_{(123)}), \tag{C.20a}$$

$$\tilde{G}^{\mathrm{a}}_{(123)}(\mathrm{i}\boldsymbol{\omega}_{(123)}) + \mathcal{O}(\tfrac{1}{\beta}) = \left[K \star \hat{G}\right](\mathrm{i}\boldsymbol{\omega}_{(123)}). \tag{C.20b}$$

The computations are presented in Apps. C.3.2.1 and C.3.2.2, respectively, with the final result $\tilde{G}_{(123)} = \tilde{G}^{\mathrm{r}}_{(123)} + \tilde{G}^{\mathrm{a}}_{(123)}$ discussed in App. C.3.2.3. Additionally, we will use the super- and subscript notation introduced in Sec. 5.4 and suppress the frequency argument of $\tilde{G}^{\mathrm{r}}_{(123)}$ and $\tilde{G}^{\mathrm{a}}_{(123)}$.

C.3.2.1 Contributions from regular part

Step 1. *Matsubara summation through contour integration:* First, we concentrate on evaluating Eq. (C.20a):

$$\begin{aligned}
\tilde{G}^{\mathrm{r}}_{(123)} + \mathcal{O}(\tfrac{1}{\beta}) &= K \star \tilde{G} \\
&= \frac{1}{(-\beta)^2} \sum_{\mathrm{i}\omega'_1,\mathrm{i}\omega'_{12}} \left[\Delta_{\Omega_{12}}\left(\Delta_{\Omega_1} - \frac{\beta}{2}\delta_{\Omega_1}\right) + \delta_{\Omega_{12}}\left(-\Delta^2_{\Omega_1} - \frac{\beta}{2}\Delta_{\Omega_1} + \frac{\beta^2}{6}\delta_{\Omega_1}\right)\right]\tilde{G}_{\mathrm{i}\omega'_1,\mathrm{i}\omega'_{12}} \\
&= \frac{1}{(-\beta)^2} \sum_{\mathrm{i}\omega'_1} \sum_{\mathrm{i}\omega'_{12}}^{\neq \mathrm{i}\omega_{12}} \frac{1}{\mathrm{i}\omega_{12} - \mathrm{i}\omega'_{12}} \left(\Delta_{\Omega_1} - \frac{\beta}{2}\delta_{\Omega_1}\right)\tilde{G}_{\mathrm{i}\omega'_1,\mathrm{i}\omega'_{12}} \\
&\quad + \frac{1}{(-\beta)^2} \sum_{\mathrm{i}\omega'_1} \sum_{\mathrm{i}\omega'_{12}} \delta_{\Omega_{12}}\left(-\Delta^2_{\Omega_1} - \frac{\beta}{2}\Delta_{\Omega_1} + \frac{\beta^2}{6}\delta_{\Omega_1}\right)\tilde{G}_{\mathrm{i}\omega'_1,\mathrm{i}\omega'_{12}}. \tag{C.21}
\end{aligned}$$

The restricted sum over $\mathrm{i}\omega'_{12}$ can be rewritten using Eq. (C.17), and collecting all resulting terms $\sim \delta_{\Omega_{12}}$ yields

$$\begin{aligned}
\tilde{G}^{\mathrm{r}}_{(123)} + \mathcal{O}(\tfrac{1}{\beta}) &= \frac{1}{(-\beta)} \sum_{\mathrm{i}\omega'_1} \left(\Delta_{\Omega_1} - \frac{\beta}{2}\delta_{\Omega_1}\right)\oint_{z_{12}} \frac{n_{z_{12}}\tilde{G}_{\mathrm{i}\omega'_1,z_{12}}}{\mathrm{i}\omega_{12} - z_{12}} \\
&\quad + \frac{1}{(-\beta)^2} \sum_{\mathrm{i}\omega'_1} \sum_{\mathrm{i}\omega'_{12}} \delta_{\Omega_{12}}\left(-\Delta^2_{\Omega_1} - \frac{\beta^2}{12}\delta_{\Omega_1}\right)\tilde{G}_{\mathrm{i}\omega'_1,\mathrm{i}\omega'_{12}}. \tag{C.22}
\end{aligned}$$

The $\mathrm{i}\omega'_1$ sums can be further simplified with the help of Eqs. (C.17) and (C.18) for the first and second line, respectively, reproducing Eq. (5.13) for $\ell = 3$,

$$\tilde{G}^{\mathrm{r}}_{(123)} + \mathcal{O}(\tfrac{1}{\beta}) = \oint_{z_1,z_{12}} \frac{n_{z_1} n_{z_{12}} \tilde{G}_{z_1,z_{12}}}{(\mathrm{i}\omega_1 - z_1)(\mathrm{i}\omega_{12} - z_{12})} + \mathcal{O}(\tfrac{1}{\beta}), \tag{C.23}$$

with $\oint_{z_1,z_{12}} = \oint_{z_1} \oint_{z_{12}}$.

Step 2. *Extraction of PSFs:* Next, we deform the contours away from the imaginary axis, beginning with the contour integral over z_{12}. During the contour deformation, we have to carefully track possible singularities of $\tilde{G}_{z_1,z_{12}} = \tilde{G}(z_1, z_{12} - z_1, -z_{12})$. As explained in Sec. 5.4, possible branch cuts in the complex z_{12} plane lie on the lines defined by $\mathrm{Im}(z_{12}) = 0$ or $\mathrm{Im}(z_{12} - z_1) = 0$, see Fig. C.1(a). The branch cut at $\mathrm{Im}(z_{12}) = 0$ is taken into account by integrating infinitesimally above and below the real z_{12} axis, denoted by $\varepsilon^{\pm}_{12}$ with $\mathrm{Re}(z_{12}) = \varepsilon_{12}$.

The second branch cut $\mathrm{Im}(z_{12} - z_1) = 0$ is included by substituting $z_{12} \to z_2 = z_{12} - z_1$, with z_2 being the new integration variable. Therefore, the contour is shifted onto the line
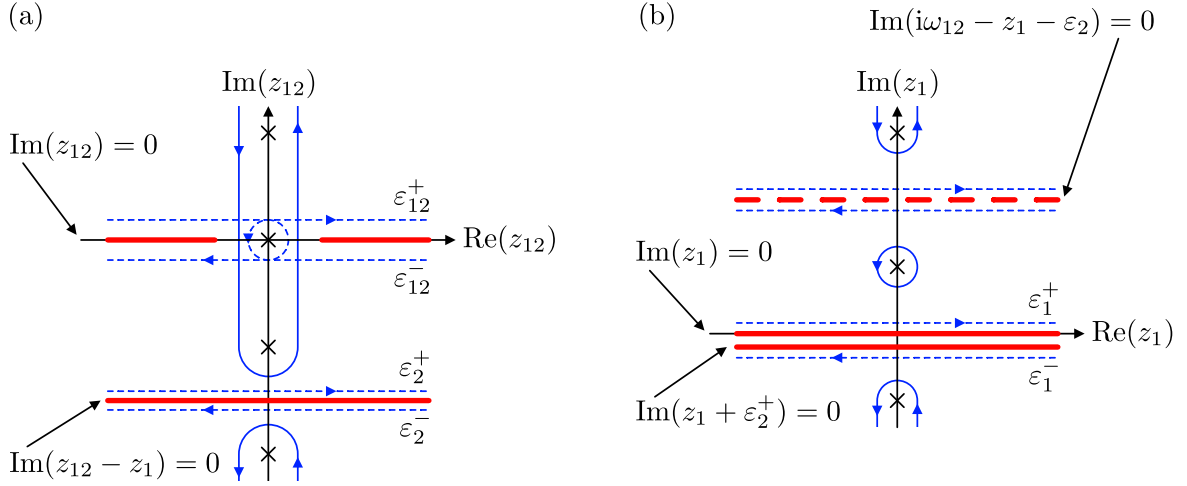
Figure C.1 (a) Contour deformation used in Eq. (C.25) for fermionic z_1 and z_2, therefore bosonic z_{12}. Black crosses denote the poles of $n_{z_{12}}$ on the imaginary axis given by bosonic Matsubara frequencies. The blue, solid contour encloses all the poles on the imaginary axis. It is deformed into the blue, dashed contour to integrate along the possible branch cuts of $\tilde{G}_{z_1,z_{12}}$ denoted by the red, thick lines, located at $\mathrm{Im}(z_{12}) = 0$ and $\mathrm{Im}(z_{12} - z_1) = 0$. (b) Contour deformation used to obtain Eq. (C.28). The branch cut at $\mathrm{Im}(z_1 + \varepsilon_2^+) = 0$ lies infinitesimally close to the branch cut $\mathrm{Im}(z_1) = 0$. Therefore, we integrate along the deformed blue, dashed contour, infinitesimally above and below the real axis, where the infinitesimal imaginary part of ε_1^-, with $\mathrm{Re}(z_1) = \varepsilon_1$, has to be larger than that of ε_2^+, i.e., $|\mathrm{Im}(\varepsilon_1^-)| > |\mathrm{Im}(\varepsilon_2^+)|$. The thick, red, dashed line denotes the pole at $\mathrm{Im}(\mathrm{i}\omega_{12} - z_1 - \varepsilon_2)$ coming from the kernel. However, these poles only contribute at $\mathcal{O}(\frac{1}{\beta})$ and can be neglected, see the discussion after Eq. (C.30).

$\mathrm{Im}(z_{12} - z_1) = 0 \rightarrow \mathrm{Im}(z_2) = 0$, i.e., onto the real axis of the complex z_2 plane, and integrating infinitesimally above and below the real axis of z_2, denoted by $\varepsilon_2^\pm$ with $\mathrm{Re}(z_2) = \varepsilon_2$. The substitution also affects the argument of the MWF in Eq. (C.23). However, since the z_1 contour encloses only the poles of n_{z_1}, z_1 can be treated as a Matsubara frequency, implying $e^{-\beta z_1} = \zeta^1$ and therefore

$$n_{z_{12}} = \frac{\zeta^{12}}{e^{-\beta z_{12}} - \zeta^{12}} \overset{z_{12} \rightarrow z_1 + z_2}{=} \frac{\zeta^1 \zeta^2}{e^{-\beta z_1} e^{-\beta z_2} - \zeta^1 \zeta^2} = \frac{\zeta^2}{e^{-\beta z_2} - \zeta^2} = n_{z_2}. \qquad (C.24)$$

Adding the contributions from both branch cuts, the z_{12} dependent terms in Eq. (C.23) evaluate to

$$\oint_{z_{12}} \frac{n_{z_{12}} \tilde{G}_{z_1,z_{12}}}{\mathrm{i}\omega_{12} - z_{12}} = \int_{\varepsilon_{12}} \frac{n_{\varepsilon_{12}} \tilde{G}_{z_1}^{\varepsilon_{12}}}{\mathrm{i}\omega_{12} - \varepsilon_{12}} + \int_{\varepsilon_2} \frac{n_{\varepsilon_2} \tilde{G}_{z_1}^{\varepsilon_2}}{\mathrm{i}\omega_{12} - z_1 - \varepsilon_2} + \mathcal{O}(\tfrac{1}{\beta}), \qquad (C.25)$$

see also Fig. C.1(a). The term $\mathcal{O}(\frac{1}{\beta})$ comes from the possible poles at $z_{12} = 0$ or $z_2 = 0$ (if z_{12} or z_2 are bosonic) which do not contribute at $\mathcal{O}(1)$, see Eq. (5.18).

Inserting Eq. (C.25) into Eq. (C.23) yields

$$\tilde{G}_{(123)}^{\mathrm{r}} + \mathcal{O}(\tfrac{1}{\beta}) = \oint_{z_1} \frac{n_{z_1}}{\mathrm{i}\omega_1 - z_1} \int_{\varepsilon_2} \frac{n_{\varepsilon_2} \tilde{G}_{z_1}^{\varepsilon_2}}{\mathrm{i}\omega_{12} - z_1 - \varepsilon_2} + \oint_{z_1} \frac{n_{z_1}}{\mathrm{i}\omega_1 - z_1} \int_{\varepsilon_{12}} \frac{n_{\varepsilon_{12}} \tilde{G}_{z_1}^{\varepsilon_{12}}}{\mathrm{i}\omega_{12} - \varepsilon_{12}}. \qquad (C.26)$$

Next we focus on the contour deformation of z_1. For the first term, we have illustrated possible branch cuts and the contours before and after the deformation in Fig. C.1(b). As the z_1 contour is deformed away from the Matsubara frequencies, we merely have to consider the singularities in the integrand of the ε_2 integral. After Eq. (C.30), we will show that the

singularities at $z_1 = i\omega_{12} - \varepsilon_2$ contribute at order $\mathcal{O}(\frac{1}{\beta})$. We can thus focus on the branch cut in $\tilde{G}^{\varepsilon_2}_{z_1}$. Previously we have taken the infinitesimal limit for the imaginary shifts of $\varepsilon_2^\pm$. Thus, during the z_1 contour deformation we have to ensure $|\text{Im}(\varepsilon_2^\pm)| < |\text{Im}(\varepsilon_1^\pm)|$, see Fig. C.1(b). The z_1 contours infinitesimally above and below $\text{Re}(z_1)$ are summarized in a discontinuity

$$\tilde{G}^{\varepsilon_2,\varepsilon_1} = \tilde{G}^{\varepsilon_2}_{\varepsilon_1^+} - \tilde{G}^{\varepsilon_2}_{\varepsilon_1^-}, \tag{C.27}$$

and we thus find for the first term in Eq. (C.26):

$$\oint_{z_1} \frac{n_{z_1}}{i\omega_1 - z_1} \int_{\varepsilon_2} \frac{n_{\varepsilon_2}\tilde{G}^{\varepsilon_2}_{z_1}}{i\omega_{12} - z_1 - \varepsilon_2} = \int_{\varepsilon_1}\int_{\varepsilon_2} \frac{n_{\varepsilon_1}n_{\varepsilon_2}\tilde{G}^{\varepsilon_2,\varepsilon_1}}{(i\omega_1 - \varepsilon_1)(i\omega_{12} - \varepsilon_{12})} + \mathcal{O}(\tfrac{1}{\beta}). \tag{C.28}$$

Repeating an analogous z_1 contour deformation for the second term in Eq. (C.26), we finally obtain

$$\tilde{G}^{\text{r}}_{(123)} = \int_{\varepsilon_1,\varepsilon_2} \frac{n_{\varepsilon_1}n_{\varepsilon_2}\tilde{G}^{\varepsilon_2,\varepsilon_1} + n_{\varepsilon_1}n_{\varepsilon_{12}}\tilde{G}^{\varepsilon_{12},\varepsilon_1}}{(i\omega_1 - \varepsilon_1)(i\omega_{12} - \varepsilon_{12})}, \tag{C.29}$$

which resembles the spectral representation in Eq. (3.63b) for $\ell = 3$.

The term $\mathcal{O}(\frac{1}{\beta})$ on the right of Eq. (C.28) originates from the pole at $z_1 = i\omega_{12} - \varepsilon_2$ in the denominator on the left, yielding

$$\mathcal{O}(\tfrac{1}{\beta}) = -\int_{\varepsilon_2} \frac{n_{\varepsilon_2}n_{-\varepsilon_2}\tilde{G}^{\varepsilon_2}_{i\omega_{12}}}{i\omega_2 - \varepsilon_2}, \tag{C.30}$$

with $\tilde{G}^{\varepsilon_2}_{i\omega_{12}} = \tilde{G}(i\omega_{12} - \varepsilon_2^+, \varepsilon_2^+, -i\omega_{12}) - \tilde{G}(i\omega_{12} - \varepsilon_2^-, \varepsilon_2^-, -i\omega_{12})$. That the integral on the right indeed is $\mathcal{O}(\frac{1}{\beta})$, although it lacks an explicit prefactor $1/\beta$, can be seen by the following argument: The product of two MWFs $n_{\varepsilon_2}n_{-\varepsilon_2}$ has finite support on an interval $\varepsilon_2 \in [-1/\beta, 1/\beta]$. Therefore, the integral scales as $1/\beta$.

To demonstrate this claim more explicitly, we proceed as follows. We note that we evaluated the imaginary-frequency convolution in Eq. (C.21) by evaluating first the ω'_{12} and then the ω'_1 sum. Due to frequency conservation, we could have also evaluated the convolution by first summing over, e.g., ω'_2 and then ω'_{12}, or ω'_1 and then ω'_2, yielding

$$\omega'_2, \text{ then } \omega'_{12}: \quad K \star \tilde{G} = \tilde{G}^{\text{r}}_{(123)} - \int_{\varepsilon_2} \frac{n_{\varepsilon_2}n_{-\varepsilon_2}\tilde{G}^{\varepsilon_2}_{i\omega_1}}{i\omega_2 - \varepsilon_2} + \mathcal{O}(\tfrac{1}{\beta})$$

$$\omega'_1, \text{ then } \omega'_2: \quad K \star \tilde{G} = \tilde{G}^{\text{r}}_{(123)} - \int_{\varepsilon_2} \frac{n_{\varepsilon_2}n_{-\varepsilon_2}\tilde{G}^{\varepsilon_2}_{i\omega_{12}}}{i\omega_2 - \varepsilon_2} + \int_{\varepsilon_{12}} \frac{n_{\varepsilon_{12}}n_{-\varepsilon_{12}}\tilde{G}^{\varepsilon_{12}}_{i\omega_1}}{i\omega_{12} - \varepsilon_{12}} + \mathcal{O}(\tfrac{1}{\beta}). \tag{C.31}$$

Equating the two expressions yields a proof for Eq. (C.30):

$$\begin{aligned}
\int_{\varepsilon_2} \frac{n_{\varepsilon_2}n_{-\varepsilon_2}\tilde{G}^{\varepsilon_2}_{i\omega_{12}}}{i\omega_2 - \varepsilon_2} &= \int_{\varepsilon_2} \frac{n_{\varepsilon_2}n_{-\varepsilon_2}\tilde{G}^{\varepsilon_2}_{i\omega_1}}{i\omega_2 - \varepsilon_2} + \int_{\varepsilon_{12}} \frac{n_{\varepsilon_{12}}n_{-\varepsilon_{12}}\tilde{G}^{\varepsilon_{12}}_{i\omega_1}}{i\omega_{12} - \varepsilon_{12}} + \mathcal{O}(\tfrac{1}{\beta}) \\
&= \oint_{z_2} \frac{n_{z_2}n_{-z_2}\tilde{G}_{i\omega_1,z_2}}{i\omega_2 - z_2} + \mathcal{O}(\tfrac{1}{\beta}) \\
&= -\frac{1}{(-\beta)^2} \sum_{i\omega'_2}^{\neq i\omega_2} \frac{\tilde{G}_{i\omega_1,i\omega'_2}}{(i\omega_2 - i\omega'_2)^2} - \frac{1}{12}\tilde{G}_{i\omega_1,i\omega_2} + \mathcal{O}(\tfrac{1}{\beta}) \\
&= \mathcal{O}(\tfrac{1}{\beta}). \tag{C.32}
\end{aligned}$$

We obtained the second line by a contour deformation in analogy to the derivation of Eq. (C.25). Here, the r.h.s. of the first line can be expressed as a contour integral along the branch cuts at $\mathrm{Im}(z_2) = 0$ and $\mathrm{Im}(z_{12}) = 0$ (blue dashed lines in Fig. C.1(a)) and the contour in the second line encloses the Matsubara frequencies (blue solid lines in Fig. C.1(a)). For the last step, we used Eq. (C.18).

C.3.2.2 Contributions from anomalous parts

Step 1. *Matsubara summation through contour integration:* To evaluate Eq. (C.20b), we first focus on $\beta\delta_{i\omega_3'}\hat{G}_{3;i\omega_1'}$, yielding $\tilde{G}_{3;(123)}^{\mathrm{a}}$ in a decomposition $\tilde{G}_{(123)}^{\mathrm{a}} = \sum_{i=1}^{3}\tilde{G}_{i;(123)}^{\mathrm{a}}$; the contributions from $\tilde{G}_{1;(123)}^{\mathrm{a}}$ and $\tilde{G}_{2;(123)}^{\mathrm{a}}$ follow from analogous calculations. Then, the imaginary-frequency convolution of the 3p kernel with $\beta\delta_{i\omega_3'}\hat{G}_{3;i\omega_1'}$ can be rewritten as

$$
\tilde{G}_{3;(123)}^{\mathrm{a}} + \mathcal{O}(\tfrac{1}{\beta}) = K \star \hat{G}_3
$$
$$
= \frac{1}{(-\beta)^2}\sum_{i\omega_1',i\omega_{12}'}\left[\Delta_{\Omega_{12}}\left(\Delta_{\Omega_1} - \frac{\beta}{2}\delta_{\Omega_1}\right) + \delta_{\Omega_{12}}\left(-\Delta_{\Omega_1}^2 - \frac{\beta}{2}\Delta_{\Omega_1} + \frac{\beta^2}{6}\delta_{\Omega_1}\right)\right]\beta\delta_{i\omega_{12}'}\hat{G}_{3;i\omega_1'}
$$
$$
= -\frac{1}{i\omega_{12}}\frac{1}{(-\beta)}\sum_{i\omega_1'}\left(\Delta_{\Omega_1} - \frac{\beta}{2}\delta_{\Omega_1}\right)\hat{G}_{3;i\omega_1'}
$$
$$
= -\frac{1}{i\omega_{12}}\frac{1}{(-\beta)}\sum_{i\omega_1'}\left(\Delta_{\Omega_1} - \frac{\beta}{2}\delta_{\Omega_1}\right)\hat{G}_{3;i\omega_1'}^{\slashed{\Delta}} - \frac{1}{i\omega_{12}}\frac{1}{(-\beta)}\sum_{i\omega_1'}^{\neq 0}\left(\Delta_{\Omega_1} - \frac{\beta}{2}\delta_{\Omega_1}\right)\frac{\hat{G}_{3;1}^{\Delta}}{i\omega_1'}. \tag{C.33}
$$

In the second step, we carried out the sum over $i\omega_{12}'$ and used $\delta_{\Omega_{12}}\delta_{i\omega_{12}'} = \delta_{i\omega_{12}}\delta_{i\omega_{12}'} = 0$, since we enforce the external Matsubara frequencies to be nonzero. In the third step, we further split the anomalous part according to Eq. (C.15).

The sums can be evaluated using Eq. (C.17) and yield

$$
\tilde{G}_{3;(123)}^{\mathrm{a}} + \mathcal{O}(\tfrac{1}{\beta}) = -\frac{1}{i\omega_{12}}\oint_{z_1}\frac{n_{z_1}\hat{G}_{3;z_1}^{\slashed{\Delta}}}{i\omega_1 - z_1} - \frac{1}{i\omega_{12}}\oint_{z_1}\frac{n_{z_1}}{(i\omega_1 - z_1)}\frac{\hat{G}_{3;1}^{\Delta}}{z_1}
$$
$$
+ \frac{1}{i\omega_{12}}\mathop{\mathrm{Res}}_{z_1=0}\left(\frac{n_{z_1}}{(i\omega_1 - z_1)}\frac{\hat{G}_{3;1}^{\Delta}}{z_1}\right) + \mathcal{O}(\tfrac{1}{\beta}), \tag{C.34}
$$

where we excluded the contribution from $i\omega_1' \to z_1 = 0$ by subtracting the residue.

Step 2. *Extraction of PSFs:* The first contour integral in Eq. (C.34) can be deformed analogously to the 2p case in Sec. 5.3.2. The integrand of the second contour integral only has poles on the imaginary axis since $\hat{G}_{3;1}^{\Delta}$ is a constant. Thus, the integral vanishes by closing the contour in the left and right half of the complex z_1 plane. Further evaluating the residue, we then obtain

$$
\tilde{G}_{3;(123)}^{\mathrm{a}} = -\frac{1}{i\omega_{12}}\int_{\varepsilon_1}\frac{n_{\varepsilon_1}\hat{G}_3^{\slashed{\Delta};\varepsilon_1}}{i\omega_1 - \varepsilon_1} - \frac{1}{2}\frac{\hat{G}_{3;1}^{\Delta}}{i\omega_1\,i\omega_{12}} = \int_{\varepsilon_1,\varepsilon_2}\frac{\hat{\delta}(\varepsilon_{12})n_{\varepsilon_1}\hat{G}_3^{\slashed{\Delta};\varepsilon_1} - \frac{1}{2}\hat{\delta}(\varepsilon_1)\hat{\delta}(\varepsilon_{12})\hat{G}_{3;1}^{\Delta}}{(i\omega_1 - \varepsilon_1)(i\omega_{12} - \varepsilon_{12})},
$$
$$
\tag{C.35}
$$

where we recovered the form of the spectral representation in Eq. (3.63b) by introducing Dirac delta functions.

Similarly, the contributions from $\hat{G}_1$, $\hat{G}_2$, and also $\hat{G}_{1,2}$ to Eq. (C.20b) can be derived, leading to the general result

$$\tilde{G}^{\mathrm{a}}_{(123)} = \int_{\varepsilon_1,\varepsilon_2} \frac{1}{(\mathrm{i}\omega_1 - \varepsilon_1)(\mathrm{i}\omega_{12} - \varepsilon_{12})}\left[\hat{\delta}(\varepsilon_1)n_{\varepsilon_2}\hat{G}^{\Delta;\varepsilon_2}_1 + \hat{\delta}(\varepsilon_2)n_{\varepsilon_1}\hat{G}^{\Delta;\varepsilon_1}_2 + \hat{\delta}(\varepsilon_{12})n_{\varepsilon_1}\hat{G}^{\Delta;\varepsilon_1}_3\right.$$
$$\left. + \hat{\delta}(\varepsilon_1)\hat{\delta}(\varepsilon_2)\left(\hat{G}_{1,2} - \tfrac{1}{2}\hat{G}^{\Delta}_{3;1}\right)\right]. \tag{C.36}$$

Here, only $\hat{G}^{\Delta}_{3;1}$ enters, since contributions from $\hat{G}^{\Delta}_{1;2}$ and $\hat{G}^{\Delta}_{2;1}$ cancel to due Eq. (C.16).

C.3.2.3 Final result

The main results of the previous sections are Eqs. (C.29) and (C.36), yielding the spectral representation for $\tilde{G}_{(123)} = \tilde{G}^{\mathrm{r}}_{(123)} + \tilde{G}^{\mathrm{a}}_{(123)}$. The partial MF correlator $\tilde{G}_p = \tilde{G}^{\mathrm{r}}_p + \tilde{G}^{\mathrm{a}}_p$ for a general permutation p is then obtained by replacing any index by its permuted counterpart, $i \to p(i) = \bar{i}$. Thus, we obtain our final result

$$\tilde{G}_p(\mathrm{i}\boldsymbol{\omega}_p) = \int_{\varepsilon_{\bar{1}},\varepsilon_{\bar{2}}} \frac{(2\pi\mathrm{i})^2 S_p(\varepsilon_{\bar{1}}, \varepsilon_{\bar{2}})}{(\mathrm{i}\omega_{\bar{1}} - \varepsilon_{\bar{1}})(\mathrm{i}\omega_{\overline{12}} - \varepsilon_{\overline{12}})}, \tag{C.37}$$

with the PSFs given by

$$(2\pi\mathrm{i})^2 S_p(\varepsilon_{\bar{1}}, \varepsilon_{\bar{2}}) = n_{\varepsilon_{\bar{1}}}n_{\varepsilon_{\bar{2}}}\tilde{G}^{\varepsilon_{\bar{2}},\varepsilon_{\bar{1}}} + n_{\varepsilon_{\bar{1}}}n_{\varepsilon_{\overline{12}}}\tilde{G}^{\varepsilon_{\overline{12}},\varepsilon_{\bar{1}}} + \hat{\delta}(\varepsilon_{\bar{1}})n_{\varepsilon_{\bar{2}}}\hat{G}^{\Delta;\varepsilon_{\bar{2}}}_{\bar{1}}$$
$$+ \hat{\delta}(\varepsilon_{\bar{2}})n_{\varepsilon_{\bar{1}}}\hat{G}^{\Delta;\varepsilon_{\bar{1}}}_{\bar{2}} + \hat{\delta}(\varepsilon_{\bar{3}})n_{\varepsilon_{\bar{1}}}\hat{G}^{\Delta;\varepsilon_{\bar{1}}}_{\bar{3}} + \hat{\delta}(\varepsilon_{\bar{1}})\hat{\delta}(\varepsilon_{\bar{2}})\left(\hat{G}_{\bar{1},\bar{2}} - \tfrac{1}{2}\hat{G}^{\Delta}_{3;\bar{1}}\right). \tag{C.38}$$

PSFs for all six permutations are recovered by inserting the respective $\bar{i}$ into above equation. They can be expressed in terms of analytic regions (cf. Fig. 5.3) using

$$\tilde{G}^{\varepsilon_2,\varepsilon_1} = -\tilde{G}^{\varepsilon_{13},\varepsilon_1} = -\tilde{G}^{\varepsilon_2,\varepsilon_3} = \tilde{G}^{\varepsilon_{13},\varepsilon_3} = \tilde{G}'^{[3]} - \tilde{G}^{[1]} - \tilde{G}'^{[1]} + \tilde{G}^{[3]}, \tag{C.39a}$$

$$\tilde{G}^{\varepsilon_1,\varepsilon_2} = -\tilde{G}^{\varepsilon_{23},\varepsilon_2} = -\tilde{G}^{\varepsilon_1,\varepsilon_3} = \tilde{G}^{\varepsilon_{23},\varepsilon_3} = \tilde{G}'^{[3]} - \tilde{G}^{[2]} - \tilde{G}'^{[2]} + \tilde{G}^{[3]}, \tag{C.39b}$$

$$\tilde{G}^{\varepsilon_3,\varepsilon_1} = -\tilde{G}^{\varepsilon_{12},\varepsilon_1} = -\tilde{G}^{\varepsilon_3,\varepsilon_2} = \tilde{G}^{\varepsilon_{12},\varepsilon_2} = \tilde{G}'^{[2]} - \tilde{G}^{[1]} - \tilde{G}'^{[1]} + \tilde{G}^{[2]}, \tag{C.39c}$$

$$\hat{G}^{\Delta;\varepsilon_2}_1 = -\hat{G}^{\Delta;\varepsilon_3}_1 = \hat{G}^{\Delta;[2]}_1 - \hat{G}^{\Delta;[3]}_1, \tag{C.39d}$$

$$\hat{G}^{\Delta;\varepsilon_1}_2 = -\hat{G}^{\Delta;\varepsilon_2}_2 = \hat{G}^{\Delta;[1]}_2 - \hat{G}^{\Delta;[3]}_2, \tag{C.39e}$$

$$\hat{G}^{\Delta;\varepsilon_1}_3 = -\hat{G}^{\Delta;\varepsilon_2}_3 = \hat{G}^{\Delta;[1]}_3 - \hat{G}^{\Delta;[2]}_3, \tag{C.39f}$$

$$\hat{G}^{\Delta}_{1;2} = -\hat{G}^{\Delta}_{1;3} = -\hat{G}^{\Delta}_{2;1} = \hat{G}^{\Delta}_{2;3} = \hat{G}^{\Delta}_{3;1} = -\hat{G}^{\Delta}_{3;2}, \tag{C.39g}$$

$$\hat{G}_{\bar{1},\bar{2}} = \hat{G}_{1,2}, \tag{C.39h}$$

with the definitions introduced in Sec. 5.5

$$G^{[1]} = \tilde{G}(\varepsilon_1^+, \varepsilon_2^-, \varepsilon_3^-), \quad G'^{[1]} = \tilde{G}(\varepsilon_1^-, \varepsilon_2^+, \varepsilon_3^+), \tag{C.40a}$$

$$G^{[2]} = \tilde{G}(\varepsilon_1^-, \varepsilon_2^+, \varepsilon_3^-), \quad G'^{[2]} = \tilde{G}(\varepsilon_1^+, \varepsilon_2^-, \varepsilon_3^+), \tag{C.40b}$$

$$G^{[3]} = \tilde{G}(\varepsilon_1^-, \varepsilon_2^-, \varepsilon_3^+), \quad G'^{[3]} = \tilde{G}(\varepsilon_1^+, \varepsilon_2^+, \varepsilon_3^-), \tag{C.40c}$$

$$\hat{G}^{\Delta;[2]}_1 = \hat{G}^{\Delta}_1(\circ, \varepsilon_2^+, \varepsilon_3^-), \quad \hat{G}^{\Delta;[3]}_1 = \hat{G}^{\Delta}_1(\circ, \varepsilon_2^-, \varepsilon_3^+), \tag{C.40d}$$

$$\hat{G}^{\Delta;[1]}_2 = \hat{G}^{\Delta}_1(\varepsilon_1^+, \circ, \varepsilon_3^-), \quad \hat{G}^{\Delta;[3]}_2 = \hat{G}^{\Delta}_1(\varepsilon_1^-, \circ, \varepsilon_3^+), \tag{C.40e}$$

$$\hat{G}^{\Delta;[1]}_3 = \hat{G}^{\Delta}_1(\varepsilon_1^+, \varepsilon_2^-, \circ), \quad \hat{G}^{\Delta;[2]}_3 = \hat{G}^{\Delta}_1(\varepsilon_1^-, \varepsilon_2^+, \circ). \tag{C.40f}$$

p	$\boldsymbol{k}_p$	$[\hat{\eta}_1\hat{\eta}_2]$	$[\overline{\hat{\eta}}_1\overline{\hat{\eta}}_2]$	$K^{[\hat{\eta}_1\hat{\eta}_2]}(\boldsymbol{\omega}_p) = \tilde{K}(\boldsymbol{\omega}_p^{[\overline{\hat{\eta}}_1]}) - \tilde{K}(\boldsymbol{\omega}_p^{[\overline{\hat{\eta}}_2]})$
(123)	212	[13]	[13]	$\tilde{K}(\boldsymbol{\omega}_{(123)}^{[1]}) - \tilde{K}(\boldsymbol{\omega}_{(123)}^{[3]}) = \hat{\delta}(\omega_1)\frac{1}{\omega_2^-} - \hat{\delta}(\omega_{12})\frac{1}{\omega_2^-}$
(132)	221	[12]	[13]	$\tilde{K}(\boldsymbol{\omega}_{(132)}^{[1]}) - \tilde{K}(\boldsymbol{\omega}_{(132)}^{[3]}) = -\hat{\delta}(\omega_1)\frac{1}{\omega_2^-}$
(213)	122	[23]	[13]	$\tilde{K}(\boldsymbol{\omega}_{(213)}^{[1]}) - \tilde{K}(\boldsymbol{\omega}_{(213)}^{[3]}) = \hat{\delta}(\omega_{12})\frac{1}{\omega_2^-}$
(231)	122	[23]	[31]	$\tilde{K}(\boldsymbol{\omega}_{(231)}^{[3]}) - \tilde{K}(\boldsymbol{\omega}_{(231)}^{[1]}) = \hat{\delta}(\omega_1)\frac{1}{\omega_2^-}$
(312)	221	[12]	[31]	$\tilde{K}(\boldsymbol{\omega}_{(312)}^{[3]}) - \tilde{K}(\boldsymbol{\omega}_{(312)}^{[1]}) = -\hat{\delta}(\omega_{12})\frac{1}{\omega_2^-}$
(321)	212	[13]	[31]	$\tilde{K}(\boldsymbol{\omega}_{(321)}^{[3]}) - \tilde{K}(\boldsymbol{\omega}_{(321)}^{[1]}) = -\hat{\delta}(\omega_1)\frac{1}{\omega_2^-} + \hat{\delta}(\omega_{12})\frac{1}{\omega_2^-}$

Table C.1 $\ell = 3$: Simplification of the Keldysh kernel (3.67c) for the KF correlator $G^{[13]}$ for all permutations by application of the identity (5.32). For permutations $p = (123)$ and $p = (321)$, manipulations presented in Eq. (C.43) were performed. Additionally, energy conservation and the constraints enforced by the δ-functions allow us to express all denominators through ω_2^-.

Here, we have inserted a $\circ$ at the position of the frequency arguments on which the function does not depend. Note that Eqs. (C.39a)–(C.39c) also imply, e.g., $\tilde{G}^{\varepsilon_2,\varepsilon_1} = \tilde{G}^{\varepsilon_1,\varepsilon_2} + \tilde{G}^{\varepsilon_3,\varepsilon_1}$. Relations of this form can be used to simply PSF (anti)commutators, which appear in Sec. 5.5.2.

One additional comment is in order for the regular contributions in Eq. (C.38). Consider, e.g., permutation $p = (123)$ and n_{ε_1} a bosonic MWF. Then, if the regular contributions $\tilde{G}^{\varepsilon_2,\varepsilon_1}$ and $\tilde{G}^{\varepsilon_{12},\varepsilon_1}$ contain terms proportional to Dirac $\delta(\varepsilon_1)$, the combination $n_{\varepsilon_1}\delta(\varepsilon_1)$ is ill-defined as the MWF diverges for vanishing frequencies. For their evaluation, however, we can use Eqs. (C.39a)–(C.39c) to rewrite

$$
(2\pi\mathrm{i})^2 \tilde{S}_{(123)}(\varepsilon_1, \varepsilon_2) = n_{\varepsilon_1} n_{\varepsilon_2} \tilde{G}^{\varepsilon_2,\varepsilon_1} + n_{\varepsilon_1} n_{\varepsilon_{12}} \left(\tilde{G}^{\varepsilon_1,\varepsilon_{12}} - \tilde{G}^{\varepsilon_2,\varepsilon_1} \right)
$$
$$
= -n_{-\varepsilon_2} n_{\varepsilon_{12}} \tilde{G}^{\varepsilon_2,\varepsilon_1} + n_{\varepsilon_1} n_{\varepsilon_{12}} \tilde{G}^{\varepsilon_1,\varepsilon_{12}}. \tag{C.41}
$$

Here, the first term does not include n_{ε_1}, and the discontinuity $\tilde{G}^{\varepsilon_1,\varepsilon_{12}}$ in the second term does not contain $\delta(\varepsilon_1)$ contributions (see, e.g., Eqs. (C.101) and discussion thereafter), circumventing the occurrence of bosonic $n_{\varepsilon_1}\delta(\varepsilon_1)$ contributions.

C.3.3 Simplifications for KF correlators for $\ell = 3$

The simplifications for the KF kernels performed in this appendix are based on results derived by Anxiang Ge in his Master's thesis [Ge20]. For completeness, they are included here, since they are crucial ingredients for the analytic continuation of 3p functions in Sec. 5.5.

In the following, we show that the spectral representation of Keldysh components can be recast into a form that is formally equivalent to Eqs. (3.67), but more convenient for the purpose of analytic continuation. The new representation enables us to insert the PSFs in Eq. (C.38) and obtain expressions for the Keldysh components in terms of analytic continuations of MF correlators. This constitutes Step 3 of our three-step strategy.

While the following calculations are demonstrated for explicit examples of 3p KF components, they can be generalized to arbitrary KF components and even to arbitrary ℓp functions (see App. C.6).

p	Kernel of $G^{[123]} - G^{[3]}$
(123)	$K^{[123]}(\boldsymbol{\omega}_{(123)}) - \tilde{K}(\boldsymbol{\omega}_{(123)}^{[3]}) = \hat{\delta}(\omega_1)\hat{\delta}(\omega_2) + \hat{\delta}(\omega_1)\frac{1}{\omega_2^-}$
(132)	$K^{[123]}(\boldsymbol{\omega}_{(132)}) - \tilde{K}(\boldsymbol{\omega}_{(132)}^{[3]}) = -\hat{\delta}(\omega_1)\frac{1}{\omega_2^-} - \hat{\delta}(\omega_2)\frac{1}{\omega_1^-}$
(213)	$K^{[123]}(\boldsymbol{\omega}_{(213)}) - \tilde{K}(\boldsymbol{\omega}_{(213)}^{[3]}) = \hat{\delta}(\omega_1)\hat{\delta}(\omega_2) + \hat{\delta}(\omega_2)\frac{1}{\omega_1^-}$
(231)	$K^{[123]}(\boldsymbol{\omega}_{(231)}) - \tilde{K}(\boldsymbol{\omega}_{(231)}^{[3]}) = -\hat{\delta}(\omega_2)\frac{1}{\omega_1^-} - \hat{\delta}(\omega_1)\frac{1}{\omega_2^-}$
(312)	$K^{[123]}(\boldsymbol{\omega}_{(312)}) - \tilde{K}(\boldsymbol{\omega}_{(312)}^{[3]}) = \hat{\delta}(\omega_1)\hat{\delta}(\omega_2) + \hat{\delta}(\omega_2)\frac{1}{\omega_1^-}$
(321)	$K^{[123]}(\boldsymbol{\omega}_{(321)}) - \tilde{K}(\boldsymbol{\omega}_{(321)}^{[3]}) = \hat{\delta}(\omega_1)\hat{\delta}(\omega_2) + \hat{\delta}(\omega_1)\frac{1}{\omega_2^-}$

Table C.2 $\ell = 3$: Keldysh kernel for $G^{[123]} - G^{[3]}$ in Eq. (C.45), evaluated for all permutations.

C.3.3.1 Simplifications for KF correlator $G^{[\eta_1\eta_2]}$

We begin with outlining the necessary steps to express the KF component $G^{[\eta_1\eta_2]}$ in terms of analytically continued MF correlators on the example $G^{[13]}$. The simplifcations rely on repeated application of identity (5.32).

The spectral representation in Eqs. (3.67) serves as our starting point. As a first step, we bring the Keldysh kernel $K^{[\hat{\eta}_1\hat{\eta}_2]}$ in a more convenient form, starting with permutation $p = (123)$, where $[\hat{\eta}_1\hat{\eta}_2] = [\eta_1\eta_2] = [13]$ and therefore

$$K^{[13]}(\boldsymbol{\omega}_{(123)}) = \tilde{K}(\boldsymbol{\omega}_{(123)}^{[1]}) - \tilde{K}(\boldsymbol{\omega}_{(123)}^{[3]}) = \frac{1}{\omega_1^{[1]}\omega_{12}^{[1]}} - \frac{1}{\omega_1^{[3]}\omega_{12}^{[3]}}. \tag{C.42}$$

In the first term, all frequency combinations in the denominator acquire a positive imaginary shift, whereas in the second term they obtain a negative imaginary shift. Adding and subtracting $1/(\omega_1^{[1]}\omega_{12}^{[3]})$, identity (5.32) leads to

$$K^{[13]}(\boldsymbol{\omega}_{(123)}) = \left(\frac{1}{\omega_1^{[1]}} - \frac{1}{\omega_1^{[3]}}\right)\frac{1}{\omega_{12}^{[3]}} + \left(\frac{1}{\omega_{12}^{[1]}} - \frac{1}{\omega_{12}^{[3]}}\right)\frac{1}{\omega_1^{[1]}} = \hat{\delta}(\omega_1)\frac{1}{\omega_2^-} + \hat{\delta}(\omega_{12})\frac{1}{\omega_1^+}. \tag{C.43}$$

The kernels for all other permutations can be simplified in a similar manner, and the results are summarized in Tab. C.1. Collecting all contributions proportional to either $\hat{\delta}(\omega_1)/\omega_2^-$ or $\hat{\delta}(\omega_{12})/\omega_2^-$ yields Eq. (5.49). The PSF (anti)commutators therein are evaluated using the relations in Eqs. (C.39) and result in

$$S_{[1,[2,3]_-]_+} = S_{(123)} - S_{(132)} + S_{(231)} - S_{(321)}, \tag{C.44a}$$
$$= N_{\varepsilon_1}\tilde{G}^{\varepsilon_1,\varepsilon_2} - 2\hat{\delta}(\varepsilon_1)\hat{G}_1^{\Delta;\varepsilon_2} - 2\hat{\delta}(\varepsilon_1)\hat{\delta}(\varepsilon_2)\hat{G}_{1;2}^{\Delta},$$
$$S_{[[1,2]_-,3]_+} = S_{(123)} - S_{(213)} + S_{(312)} - S_{(321)} \tag{C.44b}$$
$$= -N_{\varepsilon_{12}}\tilde{G}^{\varepsilon_{12},\varepsilon_2} + 2\hat{\delta}(\varepsilon_{12})\hat{G}_3^{\Delta;\varepsilon_2} + 2\hat{\delta}(\varepsilon_1)\hat{\delta}(\varepsilon_2)\hat{G}_{3;2}^{\Delta},$$

where we suppressed the frequency arguments of the PSFs.

C.3.3.2 Simplifications for KF correlator $G^{[\eta_1\eta_2\eta_3]}$

In Sec. 5.5.2.2 it was pointed out that the Keldysh component $G^{[123]}$ can be computed by subtracting a fully retarded correlator, e.g. $G^{[3]}$, in order to reuse identity (5.32).

The kernel of $G^{[3]}$ is simply given by $K^{[\hat{3}]}(\boldsymbol{\omega}_p) = K(\boldsymbol{\omega}_p^{[3]})$ and therefore permutation independent, as discussed before Eq. (3.70). Since $G^{[123]} = G^{222}$ implies $\boldsymbol{k}_p = 222$ and consequently $[\hat{\eta}_1\hat{\eta}_2\hat{\eta}_3] = [123]$ for any permutation, the kernel for $G^{[123]} - G^{[3]}$ reads

$$K^{[123]}(\boldsymbol{\omega}_p) - K^{[\hat{3}]}(\boldsymbol{\omega}_p) = \tilde{K}(\boldsymbol{\omega}_p^{[\overline{1}]}) - \tilde{K}(\boldsymbol{\omega}_p^{[\overline{2}]}) + \tilde{K}(\boldsymbol{\omega}_p^{[\overline{3}]}) - \tilde{K}(\boldsymbol{\omega}_p^{[3]}), \qquad (C.45)$$

and therefore the effect of subtracting $G^{[3]}$ is permutation dependent.

We first consider permutation $p = (123)$, for which the difference of kernels simplifies to

$$
\begin{aligned}
K^{[123]}(\boldsymbol{\omega}_{(123)}) - K^{[3]}(\boldsymbol{\omega}_{(123)}) &= \tilde{K}(\boldsymbol{\omega}_{(123)}^{[1]}) - \tilde{K}(\boldsymbol{\omega}_{(123)}^{[2]}) \\
&= \frac{1}{\omega_1^{[1]}\omega_{12}^{[1]}} - \frac{1}{\omega_1^{[2]}\omega_{12}^{[2]}} = \hat{\delta}(\omega_1)\frac{1}{\omega_2^+}.
\end{aligned} \qquad (C.46)
$$

In the last step, we were able to use Eq. (5.32) again, set $\omega_{12}^{[1]} = \omega_{12}^{[2]} = \omega_{12}^+$, and reduced $\omega_{12} = \omega_2$ due to the δ-function. For the comparison to kernels of other permutations, it is convenient to additionally add and subtract $\hat{\delta}(\omega_1)/\omega_2^-$ to obtain

$$K^{[123]}(\boldsymbol{\omega}_{(123)}) - K^{[3]}(\boldsymbol{\omega}_{(123)}) = \hat{\delta}(\omega_1)\hat{\delta}(\omega_2) + \hat{\delta}(\omega_1)\frac{1}{\omega_2^-}. \qquad (C.47)$$

For permutation $p = (132)$, Eq. (C.45) yields

$$\tilde{K}(\boldsymbol{\omega}_{(132)}^{[1]}) - \tilde{K}(\boldsymbol{\omega}_{(132)}^{[3]}) + \tilde{K}(\boldsymbol{\omega}_{(132)}^{[2]}) - \tilde{K}(\boldsymbol{\omega}_{(132)}^{[3]}) = \hat{\delta}(\omega_1)\frac{1}{\omega_3^+} - \hat{\delta}(\omega_{13})\frac{1}{\omega_1^-}. \qquad (C.48)$$

Using $\omega_3^+ = -\omega_2^-$ due to energy conservation and the δ–function, the first term matches the second term in Eq. (C.47). Therefore, PSFs of permutations $p = (123), (132)$ can be expressed through PSF (anti)commutators as in the previous section, motivating the manipulation from Eq. (C.46) to (C.47).

A summary of the kernels for all permutations is given in Tab. C.2. In these kernels, a total of three unique terms occur, given by $\hat{\delta}(\omega_1)\hat{\delta}(\omega_2)$, $\hat{\delta}(\omega_1)/\omega_2^-$, or $\hat{\delta}(\omega_2)/\omega_1^-$. Collecting all PSFs convoluted with the same expressions gives Eq. (5.55), with the PSF (anti)commutators evaluating to

$$
\begin{aligned}
S_{[[1,2]_+,3]_+}(\varepsilon_1, \varepsilon_2) &= (1 + N_{\varepsilon_1}N_{\varepsilon_2})\tilde{G}^{\varepsilon_2,\varepsilon_1} + N_{\varepsilon_{12}}N_{\varepsilon_1}\tilde{G}^{\varepsilon_{12},\varepsilon_1} - 2\hat{\delta}(\varepsilon_1)N_{\varepsilon_2}\hat{G}_1^{\Delta;\varepsilon_2} \\
&\quad - 2\hat{\delta}(\varepsilon_2)N_{\varepsilon_1}\hat{G}_2^{\Delta;\varepsilon_1} - 2\hat{\delta}(\varepsilon_{12})N_{\varepsilon_1}\hat{G}_3^{\Delta;\varepsilon_1} + 4\hat{\delta}(\varepsilon_1)\hat{\delta}(\varepsilon_2)\hat{G}_{1,2}, \\
S_{[1,[2,3]_-]_-}(\varepsilon_1, \varepsilon_2) &= \tilde{G}^{\varepsilon_1,\varepsilon_2}, \\
S_{[2,[1,3]_-]_-}(\varepsilon_2, \varepsilon_1) &= \tilde{G}^{\varepsilon_2,\varepsilon_1}.
\end{aligned} \qquad (C.49)
$$

This concludes our appendix on additional computations for the analytic continuation of 3p correlators.

C.4 Partial MF 4p correlators

In this appendix, we discuss purely fermionic partial MF 4p correlators. However, we do not display explicit calculations here. Rather, we introduce an iterative procedure to derive the

structure of 4p PSFs from 3p PSFs, based on our insights from 2p and 3p calculations. For a general fermionic MF 4p correlator, only the sums of two fermionic frequencies result in bosonic frequencies, which, in turn, might lead to anomalous terms. According to Eq. (C.5), the general form of the correlator thus reads

$$G_{i\omega_1,i\omega_2,i\omega_3} = \tilde{G}_{i\omega_1,i\omega_2,i\omega_3} + \beta\delta_{i\omega_{12}}\hat{G}_{12;i\omega_1,i\omega_3} + \beta\delta_{i\omega_{13}}\hat{G}_{13;i\omega_1,i\omega_2} + \beta\delta_{i\omega_{23}}\hat{G}_{23;i\omega_1,i\omega_2}. \quad \text{(C.50)}$$

C.4.1 Regular contributions

Step 1. *Matsubara summation through contour integration:* To derive partial MF 4p correlators, we insert Eq. (C.50) and the singularity-free 4p kernel (Eq. (C.2c)) into Eq. (5.6):

$$\tilde{G}_{(1234)}(i\boldsymbol{\omega}_{(1234)}) + \mathcal{O}(\tfrac{1}{\beta}) = [K \star G](i\boldsymbol{\omega}_{(1234)}). \quad \text{(C.51)}$$

Here, we again consider the permutation $p = (1234)$ first, before obtaining the general result by replacing all indices $i \to \bar{i}$. By repeated use of the identities in Eqs. (C.17) and (C.18), together with the analogously proven new identity

$$\frac{1}{(-\beta)^3}\sum_{i\omega'}\Delta^3_{i\omega-i\omega'}\tilde{f}(i\omega') = \mathcal{O}(\tfrac{1}{\beta}), \quad \text{(C.52)}$$

the imaginary-frequency convolution can again be expressed through contour integrals. Focusing on the regular contribution to the correlator, $\tilde{G}$, first, we indeed recover Eq. (5.13) for $\ell = 4$:

$$\tilde{G}^r_{(1234)}(i\boldsymbol{\omega}_{(1234)}) + \mathcal{O}(\tfrac{1}{\beta}) = \left[K \star \tilde{G}\right](i\boldsymbol{\omega}_{(1234)})$$
$$= \oint_{z_1}\oint_{z_{12}}\oint_{z_{123}} \frac{n_{z_1}n_{z_{12}}n_{z_{123}}\tilde{G}_{z_1,z_{12},z_{123}}}{(i\omega_1 - z_1)(i\omega_{12} - z_{12})(i\omega_{123} - z_{123})}. \quad \text{(C.53)}$$

Step 2. *Extraction of PSFs:* For the deformation of the contour, it is instructive to recapitulate the 2p and 3p results for the regular contributions to the PSFs. As a function of complex frequencies, a general 2p MF correlator $\tilde{G}_{z_1} = \tilde{G}(z_1, -z_1)$ has one possible branch cut defined by $\text{Im}(z_1) = 0$, resulting in

$$(2\pi i)S^r_{(12)}(\varepsilon_1) = n_{\varepsilon_1}\tilde{G}^{\varepsilon_1}. \quad \text{(C.54)}$$

In the 3p case, the additional frequency dependence of $\tilde{G}_{z_1,z_{12}} = \tilde{G}(z_1, z_{12} - z_1, -z_{12})$ introduces two further branch cuts at $\text{Im}(z_{12}) = 0$ and $\text{Im}(z_{12} - z_1) = \text{Im}(z_2) = 0$, additionally to $\text{Im}(z_1) = 0$. According to Eq. (C.23), the contour of $\oint_{z_{12}}$ is deformed first, taking account of the latter two out of the three branch cuts. This yields a sum of the discontinuities $\tilde{G}^{\varepsilon_{12}}_{z_1}$ and $\tilde{G}^{\varepsilon_2}_{z_1}$, multiplied with the respective MWFs (Eq. (C.25)). The subsequent contour deformation of $\oint_{z_1}$ reduces to an effective 2p calculation, i.e., only the branch cut at $\text{Im}(z_1) = 0$ remains, resulting in

$$(2\pi i)^2 S^r_{(123)}(\varepsilon_1, \varepsilon_2) = n_{\varepsilon_2}n_{\varepsilon_1}\tilde{G}^{\varepsilon_2,\varepsilon_1} + n_{\varepsilon_{12}}n_{\varepsilon_1}\tilde{G}^{\varepsilon_{12},\varepsilon_1}, \quad \text{(C.55)}$$

with the discontinuity in ε_1 to the right of ε_2 and ε_{12}.

In the 4p case, the new frequency z_{123} generates four additional branch cuts (see discussion in Sec. 5.4.1), defined by vanishing $\text{Im}(z_{123})$, $\text{Im}(z_{123} - z_1)$, $\text{Im}(z_{123} - z_{12})$ or $\text{Im}(z_{123} - z_{12} + z_1)$, yielding a total of seven possible branch cuts together with $\text{Im}(z_{12}) = 0$, $\text{Im}(z_{12} - z_1) = 0$, and $\text{Im}(z_1) = 0$ from the 3p case. Since $\oint_{z_{123}}$ is deformed first according to Eq. (C.53), the

four new branch cuts are taken into account via a sum of the discontinuities $\tilde{G}^{\varepsilon_3}_{z_{12},z_1}$, $\tilde{G}^{\varepsilon_{123}}_{z_{12},z_1}$, $\tilde{G}^{\varepsilon_{13}}_{z_{12},z_1}$, and $\tilde{G}^{\varepsilon_{23}}_{z_{12},z_1}$, multiplied with the respective MWFs. For each of these discontinuities, the subsequent contour deformations of $\oint_{z_{12}}$ and $\oint_{z_1}$ reduces to an effective 3p calculation. Consequently, we obtain

$$
\begin{aligned}
(2\pi\mathrm{i})^3 S^{\mathrm{r}}_{(1234)}(\varepsilon_1,\varepsilon_2,\varepsilon_3) &= n_{\varepsilon_3}n_{\varepsilon_2}n_{\varepsilon_1}\tilde{G}^{\varepsilon_3,\varepsilon_2,\varepsilon_1} + n_{\varepsilon_{123}}n_{\varepsilon_2}n_{\varepsilon_1}\tilde{G}^{\varepsilon_{123},\varepsilon_2,\varepsilon_1} + n_{\varepsilon_{13}}n_{\varepsilon_2}n_{\varepsilon_1}\tilde{G}^{\varepsilon_{13},\varepsilon_2,\varepsilon_1} \\
&+ n_{\varepsilon_{23}}n_{\varepsilon_2}n_{\varepsilon_1}\tilde{G}^{\varepsilon_{23},\varepsilon_2,\varepsilon_1} + n_{\varepsilon_3}n_{\varepsilon_{12}}n_{\varepsilon_1}\tilde{G}^{\varepsilon_3,\varepsilon_{12},\varepsilon_1} + n_{\varepsilon_{123}}n_{\varepsilon_{12}}n_{\varepsilon_1}\tilde{G}^{\varepsilon_{123},\varepsilon_{12},\varepsilon_1} \\
&+ n_{\varepsilon_{13}}n_{\varepsilon_{12}}n_{\varepsilon_1}\tilde{G}^{\varepsilon_{13},\varepsilon_{12},\varepsilon_1} + n_{\varepsilon_{23}}n_{\varepsilon_{12}}n_{\varepsilon_1}\tilde{G}^{\varepsilon_{23},\varepsilon_{12},\varepsilon_1}.
\end{aligned}
\tag{C.56}
$$

We have also checked this result by explicit contour deformations in Eq. (C.53). There, the poles of the denominators can be ignored since they only contribute at order $\mathcal{O}\left(\frac{1}{\beta}\right)$, similarly to Eq. (C.30) in the 3p case. To further simplify Eq. (C.56), we note that, for fermionic 4p correlators, two consecutive bosonic discontinuities have to vanish, i.e., $\tilde{G}^{\varepsilon_{13},\varepsilon_{12},\varepsilon_1} = \tilde{G}^{\varepsilon_{23},\varepsilon_{12},\varepsilon_1} = 0$, since their kernels carry one bosonic argument only (see App. C.5.1 for further details).

C.4.2 Anomalous contributions

We do not present the derivations of the anomalous contributions of G to Eq. (C.51) explicitly here, as these correspond to 3p calculations. There is one crucial difference, however. The anomalous kernel in Eq. (C.4c) for the fermionic 4p case reduces to

$$
\hat{K}^{\mathrm{alt}}(\boldsymbol{\Omega}_p) = -\frac{\beta}{2}\delta_{\mathrm{i}\omega_{\overline{12}}-\varepsilon_{\overline{12}}}\frac{1}{\left(\mathrm{i}\omega_{\overline{1}}-\varepsilon_{\overline{1}}\right)\left(\mathrm{i}\omega_{\overline{3}}-\varepsilon_{\overline{3}}\right)},
\tag{C.57}
$$

and thus only depends on fermionic Matsubara frequencies. Therefore, anomalous terms such as $\hat{G}_{13;\mathrm{i}\omega_1,\mathrm{i}\omega_2}$ only depend on the frequencies $\mathrm{i}\omega_1$ and $\mathrm{i}\omega_2$ separately, but not on their sum $\mathrm{i}\omega_{12}$. In the complex frequency plain, this implies that $\hat{G}_{13;z_1,z_2}$ has branch cuts only for $\mathrm{Im}(z_1) = 0$ and $\mathrm{Im}(z_2) = 0$, but not for $\mathrm{Im}(z_{12}) = 0$, in contrast to the regular 3p case. Additionally, since the denominators in Eq. (C.57) are non-singular due to the fermionic Matsubara frequencies, we need not distinguish the anomalous contributions by factors of $\Delta_{\mathrm{i}\omega}$, e.g., splitting $\hat{G}_{13}$, into $\hat{G}_{13}^{\underline{\Delta}}$ and $\hat{G}_{13}^{\Delta}$ terms, as was the case for 3p functions (Eq. (C.15)).

C.4.3 Final result

Finally, the fermionic partial 4p correlators for general permutations p is obtained from the full correlator via

$$
\tilde{G}_p(\mathrm{i}\boldsymbol{\omega}_p) = \int_{\varepsilon_{\overline{1}},\varepsilon_{\overline{2}},\varepsilon_{\overline{3}}} \frac{(2\pi\mathrm{i})^3 S_p(\varepsilon_{\overline{1}},\varepsilon_{\overline{2}},\varepsilon_{\overline{3}})}{(\mathrm{i}\omega_{\overline{1}}-\varepsilon_{\overline{1}})(\mathrm{i}\omega_{\overline{12}}-\varepsilon_{\overline{12}})(\mathrm{i}\omega_{\overline{123}}-\varepsilon_{\overline{123}})},
\tag{C.58}
$$

with the PSFs given by

$$
\begin{aligned}
(2\pi\mathrm{i})^3 S_p(\varepsilon_{\overline{1}},\varepsilon_{\overline{2}},\varepsilon_{\overline{3}}) &= n_{\varepsilon_{\overline{3}}}n_{\varepsilon_{\overline{2}}}n_{\varepsilon_{\overline{1}}}\tilde{G}^{\varepsilon_{\overline{3}},\varepsilon_{\overline{2}},\varepsilon_{\overline{1}}} + n_{\varepsilon_{\overline{123}}}n_{\varepsilon_{\overline{2}}}n_{\varepsilon_{\overline{1}}}\tilde{G}^{\varepsilon_{\overline{123}},\varepsilon_{\overline{2}},\varepsilon_{\overline{1}}} + n_{\varepsilon_{\overline{13}}}n_{\varepsilon_{\overline{2}}}n_{\varepsilon_{\overline{1}}}\tilde{G}^{\varepsilon_{\overline{13}},\varepsilon_{\overline{2}},\varepsilon_{\overline{1}}} \\
&+ n_{\varepsilon_{\overline{23}}}n_{\varepsilon_{\overline{2}}}n_{\varepsilon_{\overline{1}}}\tilde{G}^{\varepsilon_{\overline{23}},\varepsilon_{\overline{2}},\varepsilon_{\overline{1}}} + n_{\varepsilon_{\overline{3}}}n_{\varepsilon_{\overline{12}}}n_{\varepsilon_{\overline{1}}}\tilde{G}^{\varepsilon_{\overline{3}},\varepsilon_{\overline{12}},\varepsilon_{\overline{1}}} + n_{\varepsilon_{\overline{123}}}n_{\varepsilon_{\overline{12}}}n_{\varepsilon_{\overline{1}}}\tilde{G}^{\varepsilon_{\overline{123}},\varepsilon_{\overline{12}},\varepsilon_{\overline{1}}} \\
&+ n_{\varepsilon_{\overline{3}}}n_{\varepsilon_{\overline{1}}}\hat{\delta}(\varepsilon_{\overline{12}})\,\hat{G}^{\varepsilon_{\overline{3}},\varepsilon_{\overline{1}}}_{\overline{12}} + n_{\varepsilon_{\overline{2}}}n_{\varepsilon_{\overline{1}}}\hat{\delta}(\varepsilon_{\overline{13}})\,\hat{G}^{\varepsilon_{\overline{2}},\varepsilon_{\overline{1}}}_{\overline{13}} + n_{\varepsilon_{\overline{2}}}n_{\varepsilon_{\overline{1}}}\hat{\delta}(\varepsilon_{\overline{23}})\,\hat{G}^{\varepsilon_{\overline{2}},\varepsilon_{\overline{1}}}_{\overline{23}}.
\end{aligned}
\tag{C.59}
$$

For the anomalous parts, the order of discontinuities does not matter, as, e.g., $\hat{G}^{\varepsilon_{\overline{3}},\varepsilon_{\overline{1}}}_{\overline{12}} = \hat{G}^{\varepsilon_{\overline{1}},\varepsilon_{\overline{3}}}_{\overline{12}}$.

For completeness, we express the discontinuities in Eq. (C.59) in terms of analytic regions according to their definition in Sec. 5.6.1. This gives

$$\tilde{G}^{\varepsilon_1,\varepsilon_2,\varepsilon_3} = -\tilde{G}^{\varepsilon_{234},\varepsilon_2,\varepsilon_3} = -\tilde{G}^{\varepsilon_1,\varepsilon_2,\varepsilon_4} = \tilde{G}^{\varepsilon_{234},\varepsilon_2,\varepsilon_4} = -\tilde{G}^{\varepsilon_1,\varepsilon_{34},\varepsilon_3} = \tilde{G}^{\varepsilon_{234},\varepsilon_{34},\varepsilon_3} = \tilde{G}^{\varepsilon_1,\varepsilon_{34},\varepsilon_4}$$
$$= -\tilde{G}^{\varepsilon_{234},\varepsilon_{34},\varepsilon_4} = C^{(3)} - C^{(4)} + C^{(123)} - C^{(124)} - C^{(13)}_{\mathrm{III}} + C^{(14)}_{\mathrm{III}} - C^{(23)}_{\mathrm{III}} + C^{(24)}_{\mathrm{III}}, \quad \text{(C.60a)}$$

$$\tilde{G}^{\varepsilon_1,\varepsilon_3,\varepsilon_2} = -\tilde{G}^{\varepsilon_{234},\varepsilon_3,\varepsilon_2} = -\tilde{G}^{\varepsilon_1,\varepsilon_3,\varepsilon_4} = \tilde{G}^{\varepsilon_{234},\varepsilon_3,\varepsilon_4} = -\tilde{G}^{\varepsilon_1,\varepsilon_{24},\varepsilon_2} = \tilde{G}^{\varepsilon_{234},\varepsilon_{24},\varepsilon_2} = \tilde{G}^{\varepsilon_1,\varepsilon_{24},\varepsilon_4}$$
$$= -\tilde{G}^{\varepsilon_{234},\varepsilon_{24},\varepsilon_4} = C^{(2)} - C^{(4)} + C^{(123)} - C^{(134)} - C^{(12)}_{\mathrm{III}} + C^{(14)}_{\mathrm{III}} - C^{(23)}_{\mathrm{III}} + C^{(34)}_{\mathrm{III}}, \quad \text{(C.60b)}$$

$$\tilde{G}^{\varepsilon_1,\varepsilon_4,\varepsilon_2} = -\tilde{G}^{\varepsilon_{234},\varepsilon_4,\varepsilon_2} = -\tilde{G}^{\varepsilon_1,\varepsilon_4,\varepsilon_3} = \tilde{G}^{\varepsilon_{234},\varepsilon_4,\varepsilon_3} = -\tilde{G}^{\varepsilon_1,\varepsilon_{23},\varepsilon_2} = \tilde{G}^{\varepsilon_{234},\varepsilon_{23},\varepsilon_2} = \tilde{G}^{\varepsilon_1,\varepsilon_{23},\varepsilon_3}$$
$$= -\tilde{G}^{\varepsilon_{234},\varepsilon_{23},\varepsilon_3} = C^{(2)} - C^{(3)} + C^{(124)} - C^{(134)} - C^{(12)}_{\mathrm{III}} + C^{(13)}_{\mathrm{III}} - C^{(24)}_{\mathrm{III}} + C^{(34)}_{\mathrm{III}}, \quad \text{(C.60c)}$$

$$\tilde{G}^{\varepsilon_2,\varepsilon_1,\varepsilon_3} = -\tilde{G}^{\varepsilon_{134},\varepsilon_1,\varepsilon_3} = -\tilde{G}^{\varepsilon_2,\varepsilon_1,\varepsilon_4} = \tilde{G}^{\varepsilon_{134},\varepsilon_1,\varepsilon_4} = -\tilde{G}^{\varepsilon_2,\varepsilon_{34},\varepsilon_3} = \tilde{G}^{\varepsilon_{134},\varepsilon_{34},\varepsilon_3} = \tilde{G}^{\varepsilon_2,\varepsilon_{34},\varepsilon_4}$$
$$= -\tilde{G}^{\varepsilon_{134},\varepsilon_{34},\varepsilon_4} = C^{(3)} - C^{(4)} + C^{(123)} - C^{(124)} - C^{(13)}_{\mathrm{II}} + C^{(14)}_{\mathrm{II}} - C^{(23)}_{\mathrm{II}} + C^{(24)}_{\mathrm{II}}, \quad \text{(C.60d)}$$

$$\tilde{G}^{\varepsilon_3,\varepsilon_1,\varepsilon_2} = -\tilde{G}^{\varepsilon_{124},\varepsilon_1,\varepsilon_2} = -\tilde{G}^{\varepsilon_3,\varepsilon_1,\varepsilon_4} = \tilde{G}^{\varepsilon_{124},\varepsilon_1,\varepsilon_4} = -\tilde{G}^{\varepsilon_3,\varepsilon_{24},\varepsilon_2} = \tilde{G}^{\varepsilon_{124},\varepsilon_{24},\varepsilon_2} = \tilde{G}^{\varepsilon_3,\varepsilon_{24},\varepsilon_4}$$
$$= -\tilde{G}^{\varepsilon_{124},\varepsilon_{24},\varepsilon_4} = C^{(2)} - C^{(4)} + C^{(123)} - C^{(134)} - C^{(12)}_{\mathrm{II}} + C^{(34)}_{\mathrm{II}} + C^{(14)}_{\mathrm{IV}} - C^{(23)}_{\mathrm{IV}}, \quad \text{(C.60e)}$$

$$\tilde{G}^{\varepsilon_4,\varepsilon_1,\varepsilon_2} = -\tilde{G}^{\varepsilon_{123},\varepsilon_1,\varepsilon_2} = -\tilde{G}^{\varepsilon_4,\varepsilon_1,\varepsilon_3} = \tilde{G}^{\varepsilon_{123},\varepsilon_1,\varepsilon_3} = -\tilde{G}^{\varepsilon_4,\varepsilon_{23},\varepsilon_2} = \tilde{G}^{\varepsilon_{123},\varepsilon_{23},\varepsilon_2} = \tilde{G}^{\varepsilon_4,\varepsilon_{23},\varepsilon_3}$$
$$= -\tilde{G}^{\varepsilon_{123},\varepsilon_{23},\varepsilon_3} = C^{(2)} - C^{(3)} + C^{(124)} - C^{(134)} - C^{(12)}_{\mathrm{IV}} + C^{(13)}_{\mathrm{IV}} - C^{(24)}_{\mathrm{IV}} + C^{(34)}_{\mathrm{IV}}, \quad \text{(C.60f)}$$

$$\tilde{G}^{\varepsilon_2,\varepsilon_3,\varepsilon_1} = -\tilde{G}^{\varepsilon_{134},\varepsilon_3,\varepsilon_1} = -\tilde{G}^{\varepsilon_2,\varepsilon_3,\varepsilon_4} = \tilde{G}^{\varepsilon_{134},\varepsilon_3,\varepsilon_4} = -\tilde{G}^{\varepsilon_2,\varepsilon_{14},\varepsilon_1} = \tilde{G}^{\varepsilon_{134},\varepsilon_{14},\varepsilon_1} = \tilde{G}^{\varepsilon_2,\varepsilon_{14},\varepsilon_4}$$
$$= -\tilde{G}^{\varepsilon_{134},\varepsilon_{14},\varepsilon_4} = C^{(1)} - C^{(4)} + C^{(123)} - C^{(234)} - C^{(12)}_{\mathrm{I}} + C^{(34)}_{\mathrm{I}} - C^{(13)}_{\mathrm{II}} + C^{(24)}_{\mathrm{II}}, \quad \text{(C.60g)}$$

$$\tilde{G}^{\varepsilon_3,\varepsilon_2,\varepsilon_1} = -\tilde{G}^{\varepsilon_{124},\varepsilon_2,\varepsilon_1} = -\tilde{G}^{\varepsilon_3,\varepsilon_2,\varepsilon_4} = \tilde{G}^{\varepsilon_{124},\varepsilon_2,\varepsilon_4} = -\tilde{G}^{\varepsilon_3,\varepsilon_{14},\varepsilon_1} = \tilde{G}^{\varepsilon_{124},\varepsilon_{14},\varepsilon_1} = \tilde{G}^{\varepsilon_3,\varepsilon_{14},\varepsilon_4}$$
$$= -\tilde{G}^{\varepsilon_{124},\varepsilon_{14},\varepsilon_4} = C^{(1)} - C^{(4)} + C^{(123)} - C^{(234)} - C^{(12)}_{\mathrm{II}} + C^{(34)}_{\mathrm{II}} - C^{(13)}_{\mathrm{I}} + C^{(24)}_{\mathrm{I}}, \quad \text{(C.60h)}$$

$$\tilde{G}^{\varepsilon_2,\varepsilon_4,\varepsilon_1} = -\tilde{G}^{\varepsilon_{134},\varepsilon_4,\varepsilon_1} = -\tilde{G}^{\varepsilon_2,\varepsilon_4,\varepsilon_3} = \tilde{G}^{\varepsilon_{134},\varepsilon_4,\varepsilon_3} = -\tilde{G}^{\varepsilon_2,\varepsilon_{13},\varepsilon_1} = \tilde{G}^{\varepsilon_{134},\varepsilon_{13},\varepsilon_1} = \tilde{G}^{\varepsilon_2,\varepsilon_{13},\varepsilon_3}$$
$$= -\tilde{G}^{\varepsilon_{134},\varepsilon_{13},\varepsilon_3} = C^{(1)} - C^{(3)} + C^{(124)} - C^{(234)} - C^{(12)}_{\mathrm{I}} + C^{(34)}_{\mathrm{I}} - C^{(14)}_{\mathrm{II}} + C^{(23)}_{\mathrm{II}}, \quad \text{(C.60i)}$$

$$\tilde{G}^{\varepsilon_4,\varepsilon_2,\varepsilon_1} = -\tilde{G}^{\varepsilon_{123},\varepsilon_2,\varepsilon_1} = -\tilde{G}^{\varepsilon_4,\varepsilon_2,\varepsilon_3} = \tilde{G}^{\varepsilon_{123},\varepsilon_2,\varepsilon_3} = -\tilde{G}^{\varepsilon_4,\varepsilon_{13},\varepsilon_1} = \tilde{G}^{\varepsilon_{123},\varepsilon_{13},\varepsilon_1} = \tilde{G}^{\varepsilon_4,\varepsilon_{13},\varepsilon_3}$$
$$= -\tilde{G}^{\varepsilon_{123},\varepsilon_{13},\varepsilon_3} = C^{(1)} - C^{(3)} + C^{(124)} - C^{(234)} - C^{(12)}_{\mathrm{IV}} + C^{(34)}_{\mathrm{IV}} - C^{(14)}_{\mathrm{I}} + C^{(23)}_{\mathrm{I}}, \quad \text{(C.60j)}$$

$$\tilde{G}^{\varepsilon_3,\varepsilon_4,\varepsilon_1} = -\tilde{G}^{\varepsilon_{124},\varepsilon_4,\varepsilon_1} = -\tilde{G}^{\varepsilon_3,\varepsilon_4,\varepsilon_2} = \tilde{G}^{\varepsilon_{124},\varepsilon_4,\varepsilon_2} = -\tilde{G}^{\varepsilon_3,\varepsilon_{12},\varepsilon_1} = \tilde{G}^{\varepsilon_{124},\varepsilon_{12},\varepsilon_1} = \tilde{G}^{\varepsilon_3,\varepsilon_{12},\varepsilon_2}$$
$$= -\tilde{G}^{\varepsilon_{124},\varepsilon_{12},\varepsilon_2} = C^{(1)} - C^{(2)} + C^{(134)} - C^{(234)} - C^{(14)}_{\mathrm{IV}} + C^{(23)}_{\mathrm{IV}} - C^{(13)}_{\mathrm{I}} + C^{(24)}_{\mathrm{I}}, \quad \text{(C.60k)}$$

$$\tilde{G}^{\varepsilon_4,\varepsilon_3,\varepsilon_1} = -\tilde{G}^{\varepsilon_{123},\varepsilon_3,\varepsilon_1} = -\tilde{G}^{\varepsilon_4,\varepsilon_3,\varepsilon_2} = \tilde{G}^{\varepsilon_{123},\varepsilon_3,\varepsilon_2} = -\tilde{G}^{\varepsilon_4,\varepsilon_{12},\varepsilon_1} = \tilde{G}^{\varepsilon_{123},\varepsilon_{12},\varepsilon_1} = \tilde{G}^{\varepsilon_4,\varepsilon_{12},\varepsilon_2}$$
$$= -\tilde{G}^{\varepsilon_{123},\varepsilon_{12},\varepsilon_2} = C^{(1)} - C^{(2)} + C^{(134)} - C^{(234)} - C^{(14)}_{\mathrm{I}} + C^{(23)}_{\mathrm{I}} - C^{(13)}_{\mathrm{IV}} + C^{(24)}_{\mathrm{IV}}, \quad \text{(C.60l)}$$

$$\tilde{G}^{\varepsilon_{12},\varepsilon_1,\varepsilon_3} = -\tilde{G}^{\varepsilon_{34},\varepsilon_1,\varepsilon_3} = \tilde{G}^{\varepsilon_{12},\varepsilon_3,\varepsilon_1} = -\tilde{G}^{\varepsilon_{34},\varepsilon_3,\varepsilon_1} = -\tilde{G}^{\varepsilon_{12},\varepsilon_2,\varepsilon_3} = \tilde{G}^{\varepsilon_{34},\varepsilon_2,\varepsilon_3}$$
$$= -\tilde{G}^{\varepsilon_{12},\varepsilon_3,\varepsilon_2} = \tilde{G}^{\varepsilon_{34},\varepsilon_3,\varepsilon_2} = -\tilde{G}^{\varepsilon_{12},\varepsilon_1,\varepsilon_4} = \tilde{G}^{\varepsilon_{34},\varepsilon_1,\varepsilon_4} = -\tilde{G}^{\varepsilon_{12},\varepsilon_4,\varepsilon_1} = \tilde{G}^{\varepsilon_{34},\varepsilon_4,\varepsilon_1}$$
$$= \tilde{G}^{\varepsilon_{12},\varepsilon_2,\varepsilon_4} = -\tilde{G}^{\varepsilon_{34},\varepsilon_2,\varepsilon_4} = \tilde{G}^{\varepsilon_{12},\varepsilon_4,\varepsilon_2} = -\tilde{G}^{\varepsilon_{34},\varepsilon_4,\varepsilon_2}$$

$$= C_{\text{II}}^{(13)} - C_{\text{III}}^{(13)} - C_{\text{II}}^{(14)} + C_{\text{III}}^{(14)} + C_{\text{II}}^{(23)} - C_{\text{III}}^{(23)} - C_{\text{II}}^{(24)} + C_{\text{III}}^{(24)}, \tag{C.60m}$$

$$\tilde{G}^{\varepsilon_{13},\varepsilon_1,\varepsilon_2} = -\tilde{G}^{\varepsilon_{24},\varepsilon_1,\varepsilon_2} = \tilde{G}^{\varepsilon_{13},\varepsilon_2,\varepsilon_1} = -\tilde{G}^{\varepsilon_{24},\varepsilon_2,\varepsilon_1} = -\tilde{G}^{\varepsilon_{13},\varepsilon_3,\varepsilon_2} = \tilde{G}^{\varepsilon_{24},\varepsilon_3,\varepsilon_2}$$

$$= -\tilde{G}^{\varepsilon_{13},\varepsilon_2,\varepsilon_3} = \tilde{G}^{\varepsilon_{24},\varepsilon_2,\varepsilon_3} = -\tilde{G}^{\varepsilon_{13},\varepsilon_1,\varepsilon_4} = \tilde{G}^{\varepsilon_{24},\varepsilon_1,\varepsilon_4} = -\tilde{G}^{\varepsilon_{13},\varepsilon_4,\varepsilon_1}$$

$$= \tilde{G}^{\varepsilon_{24},\varepsilon_4,\varepsilon_1} = \tilde{G}^{\varepsilon_{13},\varepsilon_3,\varepsilon_4} = -\tilde{G}^{\varepsilon_{24},\varepsilon_3,\varepsilon_4} = \tilde{G}^{\varepsilon_{13},\varepsilon_4,\varepsilon_3} = -\tilde{G}^{\varepsilon_{24},\varepsilon_4,\varepsilon_3}$$

$$= C_{\text{II}}^{(12)} - C_{\text{III}}^{(12)} + C_{\text{III}}^{(14)} - C_{\text{IV}}^{(14)} - C_{\text{III}}^{(23)} + C_{\text{IV}}^{(23)} - C_{\text{II}}^{(34)} + C_{\text{III}}^{(34)}, \tag{C.60n}$$

$$\tilde{G}^{\varepsilon_{14},\varepsilon_1,\varepsilon_2} = -\tilde{G}^{\varepsilon_{23},\varepsilon_1,\varepsilon_2} = \tilde{G}^{\varepsilon_{14},\varepsilon_2,\varepsilon_1} = -\tilde{G}^{\varepsilon_{23},\varepsilon_2,\varepsilon_1} = -\tilde{G}^{\varepsilon_{14},\varepsilon_4,\varepsilon_2} = \tilde{G}^{\varepsilon_{23},\varepsilon_4,\varepsilon_2}$$

$$= -\tilde{G}^{\varepsilon_{14},\varepsilon_2,\varepsilon_4} = \tilde{G}^{\varepsilon_{23},\varepsilon_2,\varepsilon_4} = -\tilde{G}^{\varepsilon_{14},\varepsilon_1,\varepsilon_3} = \tilde{G}^{\varepsilon_{23},\varepsilon_1,\varepsilon_3} = -\tilde{G}^{\varepsilon_{14},\varepsilon_3,\varepsilon_1}$$

$$= \tilde{G}^{\varepsilon_{23},\varepsilon_3,\varepsilon_1} = \tilde{G}^{\varepsilon_{14},\varepsilon_4,\varepsilon_3} = -\tilde{G}^{\varepsilon_{23},\varepsilon_4,\varepsilon_3} = \tilde{G}^{\varepsilon_{14},\varepsilon_3,\varepsilon_4} = -\tilde{G}^{\varepsilon_{23},\varepsilon_3,\varepsilon_4}$$

$$= -C_{\text{III}}^{(12)} + C_{\text{IV}}^{(12)} + C_{\text{III}}^{(13)} - C_{\text{IV}}^{(13)} - C_{\text{III}}^{(24)} + C_{\text{IV}}^{(24)} + C_{\text{III}}^{(34)} - C_{\text{IV}}^{(34)}. \tag{C.60o}$$

Here, the analytic continuations of $\tilde{G}$ are labeled according to the analytic regions in Fig. 5.4

$$C^{(1)} = \tilde{G}(\varepsilon_1^+, \varepsilon_2^-, \varepsilon_3^-, \varepsilon_4^-; \varepsilon_{12}^+, \varepsilon_{13}^+, \varepsilon_{14}^+), \qquad C^{(2)} = \tilde{G}(\varepsilon_1^-, \varepsilon_2^+, \varepsilon_3^-, \varepsilon_4^-; \varepsilon_{12}^+, \varepsilon_{13}^-, \varepsilon_{14}^-),$$

$$C^{(3)} = \tilde{G}(\varepsilon_1^-, \varepsilon_2^-, \varepsilon_3^+, \varepsilon_4^-; \varepsilon_{12}^-, \varepsilon_{13}^+, \varepsilon_{14}^-), \qquad C^{(4)} = \tilde{G}(\varepsilon_1^-, \varepsilon_2^-, \varepsilon_3^-, \varepsilon_4^+; \varepsilon_{12}^-, \varepsilon_{13}^-, \varepsilon_{14}^+),$$

$$C_{\text{I}}^{(12)} = \tilde{G}(\varepsilon_1^+, \varepsilon_2^+, \varepsilon_3^-, \varepsilon_4^-; \varepsilon_{12}^+, \varepsilon_{13}^+, \varepsilon_{14}^+), \qquad C_{\text{II}}^{(12)} = \tilde{G}(\varepsilon_1^+, \varepsilon_2^+, \varepsilon_3^-, \varepsilon_4^-; \varepsilon_{12}^+, \varepsilon_{13}^+, \varepsilon_{14}^-),$$

$$C_{\text{III}}^{(12)} = \tilde{G}(\varepsilon_1^+, \varepsilon_2^+, \varepsilon_3^-, \varepsilon_4^-; \varepsilon_{12}^+, \varepsilon_{13}^-, \varepsilon_{14}^+), \qquad C_{\text{IV}}^{(12)} = \tilde{G}(\varepsilon_1^+, \varepsilon_2^+, \varepsilon_3^-, \varepsilon_4^-; \varepsilon_{12}^+, \varepsilon_{13}^-, \varepsilon_{14}^+),$$

$$C_{\text{I}}^{(13)} = \tilde{G}(\varepsilon_1^+, \varepsilon_2^-, \varepsilon_3^+, \varepsilon_4^-; \varepsilon_{12}^+, \varepsilon_{13}^+, \varepsilon_{14}^+), \qquad C_{\text{II}}^{(13)} = \tilde{G}(\varepsilon_1^+, \varepsilon_2^-, \varepsilon_3^+, \varepsilon_4^-; \varepsilon_{12}^+, \varepsilon_{13}^+, \varepsilon_{14}^-),$$

$$C_{\text{III}}^{(13)} = \tilde{G}(\varepsilon_1^+, \varepsilon_2^-, \varepsilon_3^+, \varepsilon_4^-; \varepsilon_{12}^+, \varepsilon_{13}^+, \varepsilon_{14}^-), \qquad C_{\text{IV}}^{(13)} = \tilde{G}(\varepsilon_1^+, \varepsilon_2^-, \varepsilon_3^+, \varepsilon_4^-; \varepsilon_{12}^-, \varepsilon_{13}^+, \varepsilon_{14}^+),$$

$$C_{\text{I}}^{(14)} = \tilde{G}(\varepsilon_1^+, \varepsilon_2^-, \varepsilon_3^-, \varepsilon_4^+; \varepsilon_{12}^+, \varepsilon_{13}^+, \varepsilon_{14}^+), \qquad C_{\text{II}}^{(14)} = \tilde{G}(\varepsilon_1^+, \varepsilon_2^-, \varepsilon_3^-, \varepsilon_4^+; \varepsilon_{12}^+, \varepsilon_{13}^-, \varepsilon_{14}^+),$$

$$C_{\text{III}}^{(14)} = \tilde{G}(\varepsilon_1^+, \varepsilon_2^-, \varepsilon_3^-, \varepsilon_4^+; \varepsilon_{12}^-, \varepsilon_{13}^-, \varepsilon_{14}^+), \qquad C_{\text{IV}}^{(14)} = \tilde{G}(\varepsilon_1^+, \varepsilon_2^-, \varepsilon_3^-, \varepsilon_4^+; \varepsilon_{12}^-, \varepsilon_{13}^+, \varepsilon_{14}^+),$$

$$C_{\text{I}}^{(23)} = \tilde{G}(\varepsilon_1^-, \varepsilon_2^+, \varepsilon_3^+, \varepsilon_4^-; \varepsilon_{12}^-, \varepsilon_{13}^-, \varepsilon_{14}^-), \qquad C_{\text{II}}^{(23)} = \tilde{G}(\varepsilon_1^-, \varepsilon_2^+, \varepsilon_3^+, \varepsilon_4^-; \varepsilon_{12}^-, \varepsilon_{13}^+, \varepsilon_{14}^-),$$

$$C_{\text{III}}^{(23)} = \tilde{G}(\varepsilon_1^-, \varepsilon_2^+, \varepsilon_3^+, \varepsilon_4^-; \varepsilon_{12}^+, \varepsilon_{13}^+, \varepsilon_{14}^-), \qquad C_{\text{IV}}^{(23)} = \tilde{G}(\varepsilon_1^-, \varepsilon_2^+, \varepsilon_3^+, \varepsilon_4^-; \varepsilon_{12}^+, \varepsilon_{13}^-, \varepsilon_{14}^-),$$

$$C_{\text{I}}^{(24)} = \tilde{G}(\varepsilon_1^-, \varepsilon_2^+, \varepsilon_3^-, \varepsilon_4^+; \varepsilon_{12}^-, \varepsilon_{13}^-, \varepsilon_{14}^-), \qquad C_{\text{II}}^{(24)} = \tilde{G}(\varepsilon_1^-, \varepsilon_2^+, \varepsilon_3^-, \varepsilon_4^+; \varepsilon_{12}^-, \varepsilon_{13}^-, \varepsilon_{14}^+),$$

$$C_{\text{III}}^{(24)} = \tilde{G}(\varepsilon_1^-, \varepsilon_2^+, \varepsilon_3^-, \varepsilon_4^+; \varepsilon_{12}^+, \varepsilon_{13}^-, \varepsilon_{14}^+), \qquad C_{\text{IV}}^{(24)} = \tilde{G}(\varepsilon_1^-, \varepsilon_2^+, \varepsilon_3^-, \varepsilon_4^+; \varepsilon_{12}^+, \varepsilon_{13}^-, \varepsilon_{14}^-),$$

$$C_{\text{I}}^{(34)} = \tilde{G}(\varepsilon_1^-, \varepsilon_2^-, \varepsilon_3^+, \varepsilon_4^+; \varepsilon_{12}^-, \varepsilon_{13}^-, \varepsilon_{14}^-), \qquad C_{\text{II}}^{(34)} = \tilde{G}(\varepsilon_1^-, \varepsilon_2^-, \varepsilon_3^+, \varepsilon_4^+; \varepsilon_{12}^-, \varepsilon_{13}^-, \varepsilon_{14}^+),$$

$$C_{\text{III}}^{(34)} = \tilde{G}(\varepsilon_1^-, \varepsilon_2^-, \varepsilon_3^+, \varepsilon_4^+; \varepsilon_{12}^-, \varepsilon_{13}^+, \varepsilon_{14}^+), \qquad C_{\text{IV}}^{(34)} = \tilde{G}(\varepsilon_1^-, \varepsilon_2^-, \varepsilon_3^+, \varepsilon_4^+; \varepsilon_{12}^-, \varepsilon_{13}^+, \varepsilon_{14}^-),$$

$$C^{(123)} = \tilde{G}(\varepsilon_1^+, \varepsilon_2^+, \varepsilon_3^+, \varepsilon_4^-; \varepsilon_{12}^+, \varepsilon_{13}^+, \varepsilon_{14}^-), \qquad C^{(124)} = \tilde{G}(\varepsilon_1^+, \varepsilon_2^+, \varepsilon_3^-, \varepsilon_4^+; \varepsilon_{12}^+, \varepsilon_{13}^-, \varepsilon_{14}^+),$$

$$C^{(134)} = \tilde{G}(\varepsilon_1^+, \varepsilon_2^-, \varepsilon_3^+, \varepsilon_4^+; \varepsilon_{12}^-, \varepsilon_{13}^+, \varepsilon_{14}^+), \qquad C^{(234)} = \tilde{G}(\varepsilon_1^-, \varepsilon_2^+, \varepsilon_3^+, \varepsilon_4^+; \varepsilon_{12}^-, \varepsilon_{13}^-, \varepsilon_{14}^-). \tag{C.61}$$

The discontinuities in the anomalous parts Eq. (C.59) read

$$\hat{G}_{12}^{\varepsilon_1,\varepsilon_3} = -\hat{G}_{12}^{\varepsilon_2,\varepsilon_3} = -\hat{G}_{12}^{\varepsilon_1,\varepsilon_4} = \hat{G}_{12}^{\varepsilon_2,\varepsilon_4} = \hat{C}_{12}^{(13)} - \hat{C}_{12}^{(14)} - \hat{C}_{12}^{(23)} + \hat{C}_{12}^{(24)}, \tag{C.62a}$$

$$\hat{G}_{13}^{\varepsilon_1,\varepsilon_2} = -\hat{G}_{13}^{\varepsilon_3,\varepsilon_2} = -\hat{G}_{13}^{\varepsilon_1,\varepsilon_4} = \hat{G}_{13}^{\varepsilon_3,\varepsilon_4} = \hat{C}_{13}^{(12)} - \hat{C}_{13}^{(14)} - \hat{C}_{13}^{(23)} + \hat{C}_{13}^{(34)}, \tag{C.62b}$$

$$\hat{G}_{14}^{\varepsilon_1,\varepsilon_2} = -\hat{G}_{14}^{\varepsilon_4,\varepsilon_2} = -\hat{G}_{14}^{\varepsilon_1,\varepsilon_3} = \hat{G}_{14}^{\varepsilon_4,\varepsilon_3} = \hat{C}_{14}^{(12)} - \hat{C}_{14}^{(13)} - \hat{C}_{14}^{(24)} + \hat{C}_{14}^{(34)}, \tag{C.62c}$$

with

$$\hat{C}_{12}^{(13)} = \hat{G}_{12}(\varepsilon_1^+, \varepsilon_2^-, \varepsilon_3^+, \varepsilon_4^-), \qquad \hat{C}_{12}^{(24)} = \hat{G}_{12}(\varepsilon_1^-, \varepsilon_2^+, \varepsilon_3^-, \varepsilon_4^+),$$

$$\hat{C}_{12}^{(14)} = \hat{G}_{12}(\varepsilon_1^+, \varepsilon_2^-, \varepsilon_3^-, \varepsilon_4^+), \qquad \hat{C}_{12}^{(23)} = \hat{G}_{12}(\varepsilon_1^-, \varepsilon_2^+, \varepsilon_3^+, \varepsilon_4^-),$$

$$\hat{C}_{13}^{(12)} = \hat{G}_{13}(\varepsilon_1^+, \varepsilon_2^+, \varepsilon_3^-, \varepsilon_4^-), \qquad \hat{C}_{13}^{(34)} = \hat{G}_{13}(\varepsilon_1^-, \varepsilon_2^-, \varepsilon_3^+, \varepsilon_4^+),$$

$$\hat{C}_{13}^{(14)} = \hat{G}_{13}(\varepsilon_1^+, \varepsilon_2^-, \varepsilon_3^-, \varepsilon_4^+), \qquad \hat{C}_{13}^{(23)} = \hat{G}_{13}(\varepsilon_1^-, \varepsilon_2^+, \varepsilon_3^+, \varepsilon_4^-),$$

$$\hat{C}_{14}^{(12)} = \hat{G}_{14}(\varepsilon_1^+, \varepsilon_2^+, \varepsilon_3^-, \varepsilon_4^-), \qquad \hat{C}_{14}^{(34)} = \hat{G}_{14}(\varepsilon_1^-, \varepsilon_2^-, \varepsilon_3^+, \varepsilon_4^+),$$

$$\hat{C}_{14}^{(13)} = \hat{G}_{14}(\varepsilon_1^+, \varepsilon_2^-, \varepsilon_3^+, \varepsilon_4^-), \qquad \hat{C}_{14}^{(24)} = \hat{G}_{14}(\varepsilon_1^-, \varepsilon_2^+, \varepsilon_3^-, \varepsilon_4^+). \qquad \text{(C.63)}$$

The remaining terms follow from $\hat{G}_{34} = \hat{G}_{12}$, $\hat{G}_{24} = \hat{G}_{13}$, and $\hat{G}_{23} = \hat{G}_{14}$.

C.5 Additional spectral representations

This appendix is based on results derived by Anxiang Ge in his Master's thesis [Ge20]. For completeness, they are included here, since they are crucial ingredients for the analytic continuation of general multipoint correlators in Sec. 5.6.2.1.

In this appendix, we derive spectral representations for discontinuities (App. C.5.1) and for anomalous parts (App. C.5.2) for general ℓ. These are used in App. C.6.2 to relate Keldysh components $G^{[\eta_1 \eta_2]}$ to discontinuities of regular parts and analytic continuations of anomalous parts, resulting in Eq. (5.69) in Sec. 5.6.2.1. Additionally, they serve as a key ingredient in App. C.7 for consistency checks performed on our results for the 2p, 3p, and 4p PSFs, where we express all occurring discontinuities through PSF (anti)commutators. We use the notation introduced in the beginning of Sec. 5.6.2 throughout this appendix.

C.5.1 Spectral representation of discontinuities

Here, we focus on the discontinuities of the regular MF correlator $\tilde{G}$, as introduced in Sec. 5.4. The results carry over to anomalous contributions $\hat{G}$, as presented in App. C.5.2. We first consider discontinuities of 3p correlators (App. C.5.1.1) and then their generalization to arbitrary ℓ (App. C.5.1.2).

C.5.1.1 Example for $\ell = 3$

Let us consider the discontinuity in Eq. (5.43) as an example for $\ell = 3$. Inserting the spectral representation in Eqs. (3.63) yields

$$\frac{1}{(2\pi i)^2} \tilde{G}_{\omega_1^+}^{\omega_2} = \frac{1}{(2\pi i)^2} \left(\tilde{G}_{\omega_2^+, \omega_1^+} - \tilde{G}_{\omega_2^-, \omega_1^+} \right)$$

$$= \int_{\varepsilon_1} \int_{\varepsilon_2} \int_{\varepsilon_3} \delta(\varepsilon_{123})$$

$$\times \left[\left(\frac{1}{\omega_{13}^- - \varepsilon_{13}} - \frac{1}{\omega_{13}^+ - \varepsilon_{13}} \right) \frac{S_{(132)}(\varepsilon_1, \varepsilon_3)}{\omega_1^+ - \varepsilon_1} + \left(\frac{1}{\omega_2^+ - \varepsilon_2} - \frac{1}{\omega_2^- - \varepsilon_2} \right) \frac{S_{(213)}(\varepsilon_2, \varepsilon_1)}{\omega_{12}^+ - \varepsilon_{12}} \right.$$

$$\left. + \left(\frac{1}{\omega_2^+ - \varepsilon_2} - \frac{1}{\omega_2^- - \varepsilon_2} \right) \frac{S_{(231)}(\varepsilon_2, \varepsilon_3)}{\omega_{23}^- - \varepsilon_{23}} + \left(\frac{1}{\omega_{13}^- - \varepsilon_{13}} - \frac{1}{\omega_{13}^+ - \varepsilon_{13}} \right) \frac{S_{(312)}(\varepsilon_3, \varepsilon_1)}{\omega_3^- - \varepsilon_3} \right]$$

$$= \int_{\varepsilon_1} \int_{\varepsilon_2} \int_{\varepsilon_3} \delta(\varepsilon_{123}) \left[\hat{\delta}(\omega_2 - \varepsilon_2) \frac{S_{[2,13]_-}(\varepsilon_1, \varepsilon_2, \varepsilon_3)}{\omega_1^+ - \varepsilon_1} + \hat{\delta}(\omega_2 - \varepsilon_2) \frac{S_{[2,31]_-}(\varepsilon_1, \varepsilon_2, \varepsilon_3)}{\omega_3^- - \varepsilon_3} \right]$$

$$= - \int_{\varepsilon_1} \frac{1}{\omega_1^+ - \varepsilon_1} S_{[2,[1,3]_-]_-} (\varepsilon_1, \omega_2, -\varepsilon_1 - \omega_2) \,, \tag{C.64}$$

where we used the identity (5.32) and energy conservation. The permutations $p = (123), (321)$ do not contribute to the discontinuity as their kernels only depend on the external frequencies ω_1^+ and ω_3^- with imaginary parts independent of $\omega_2^\pm$.

For the discontinuity $\tilde{G}^{\omega_2, \omega_1} = \tilde{G}^{\omega_2}_{\omega_1^+} - \tilde{G}^{\omega_2}_{\omega_1^-}$, Eq. (C.64) yields

$$\tilde{G}^{\omega_2, \omega_1} = (2\pi i)^2 S_{[2,[1,3]_-]_-}(\boldsymbol{\omega}) \,, \qquad \tilde{G}^{\omega_{12}, \omega_1} = (2\pi i)^2 S_{[[1,2]_-,3]_-}(\boldsymbol{\omega}) \,. \tag{C.65}$$

The second identity for $\tilde{G}^{\omega_{12}, \omega_1}$ follows from a similar derivation as for $\tilde{G}^{\omega_2, \omega_1}$. Note that the above relations hold for permuted indices as well (see Eq. (C.102)). Thus, consecutive discontinuities eventually give a (nested) commutator of PSFs. For $\ell = 2$, this corresponds to the standard spectral function, $-\tilde{G}^{\omega_1} = (2\pi i) S_{[1,2]_-} = (2\pi i) S^{\text{std}}$.

C.5.1.2 Generalization to arbitrary ℓ

For general ℓp functions, the discontinuity in Eq. (5.41) can be computed analogously by inserting the spectral representation. Then, only those permutations survive the difference for which the frequency combinations ω_I or ω_{I^c} appear in the kernel $\tilde{K}(\boldsymbol{z}_p)$, leading to

$$\tilde{G}^{\omega_I}_{\check{\boldsymbol{z}}^{\mathrm{r}}} = \tilde{G}_{\omega_I^+, \check{\boldsymbol{z}}^{\mathrm{r}}} - \tilde{G}_{\omega_I^-, \check{\boldsymbol{z}}^{\mathrm{r}}} = \sum_{\overline{I}|\overline{I}^c} [\tilde{K}_{\overline{I}|\overline{I}^c} \diamond S_{[\overline{I}, \overline{I}^c]_-}](\boldsymbol{z}_{\overline{I}|\overline{I}^c}(\omega_I, \check{\boldsymbol{z}}^{\mathrm{r}})) \,, \tag{C.66a}$$

$$\tilde{K}_{\overline{I}|\overline{I}^c}(\boldsymbol{z}_{\overline{I}|\overline{I}^c}(\omega_I, \check{\boldsymbol{z}}^{\mathrm{r}})) = \tilde{K}(\boldsymbol{z}_{\overline{I}|\overline{I}^c}(\omega_I^+, \check{\boldsymbol{z}}^{\mathrm{r}})) - \tilde{K}(\boldsymbol{z}_{\overline{I}|\overline{I}^c}(\omega_I^-, \check{\boldsymbol{z}}^{\mathrm{r}}))$$

$$= \hat{\delta}(\omega_I) \tilde{K}(\boldsymbol{z}_{\overline{I}}(\check{\boldsymbol{z}}^{\mathrm{r}})) \tilde{K}(\boldsymbol{z}_{\overline{I}^c}(\check{\boldsymbol{z}}^{\mathrm{r}})) \tag{C.66b}$$

$$\tilde{K}(\boldsymbol{z}_{\overline{I}}) = \prod_{i=1}^{|I|-1} \frac{1}{\omega_{\overline{I}_1 \ldots \overline{I}_i \ldots}} \,. \tag{C.66c}$$

The set $I^c = L \backslash I$ is complementary to I. Here, $\boldsymbol{z}_p(\omega_I, \check{\boldsymbol{z}}^{\mathrm{r}})$ expresses the permuted vector $\boldsymbol{z}_p$ in terms of ω_I and the remaining $\ell - 2$ independent frequencies $\check{\boldsymbol{z}}^{\mathrm{r}}$, and similarly $\boldsymbol{z}_{\overline{I}}(\check{\boldsymbol{z}}^{\mathrm{r}})$ for the subtuple $\boldsymbol{z}_{\overline{I}}$. Equation (C.66c) defines a regular kernel for the subtuple $\boldsymbol{z}_{\overline{I}}$. In Eq. (C.66b), the difference of regular kernels leads to the Dirac delta factor due to $1/\omega_I^+ - 1/\omega_I^- = \hat{\delta}(\omega_I)$ and $1/\omega_{I^c}^+ - 1/\omega_{I^c}^- = -\hat{\delta}(\omega_I)$ (using Eq. (5.32)). The definition of the regular product kernel in Eq. (C.66b) implies $\tilde{K}_{\overline{I}|\overline{I}^c} = \tilde{K}_{\overline{I}^c|\overline{I}}$; thus, the corresponding PSFs from permutations $\overline{I}|\overline{I}^c$ and $\overline{I}^c|\overline{I}$ have been combined in an PSF commutator in Eq. (C.66a).

Consider, e.g., the 3p discontinuity $\tilde{G}^{\omega_2}_{\omega_1^+}$ from App. C.5.1.1, where the sets in Eq. (C.66) are given by $I = \{2\}$, $I^c = \{1, 3\}$, and $\check{\boldsymbol{z}}^{\mathrm{r}} = \omega_1^+$. Then, the sum over permutations $p = \overline{I}|\overline{I}^c$ includes $\overline{I}|\overline{I}^c \in \{2|13, 2|31\}$, and we obtain the PSF commutator contribution $S_{[2,13]_-}$ in Eq. (C.64) from Eq. (C.66).

For $\ell = 4$, let us consider $\tilde{G}^{\omega_{13}}_{z_1, z_2}$ as an example. Then, the sets $I = \{1, 3\}$ and $I^c = \{2, 4\}$ yield the permutations $\{13|24, 13|42, 31|24, 31|42\}$, resulting in

$$\tilde{G}^{\omega_{13}}_{z_1, z_2} = \int \mathrm{d}^4 \varepsilon \, \frac{\delta(\varepsilon_{1234}) \hat{\delta}(\varepsilon_{13})}{(z_1 - \varepsilon_1)(z_2 - \varepsilon_2)} S_{[[1,3]_-, [2,4]_-]_-}(\boldsymbol{\varepsilon}) \,, \tag{C.67}$$

where we summarized all terms with the same kernels.

To compute consecutive discontinuities, such as $\tilde{G}^{\omega_2, \omega_1}$ (see Eq. (C.65)), we can iterate the above procedure: By analyzing the spectral representation of the first discontinuity, we determine the branch cuts which lead to non-vanishing second discontinuities, and then

compute these second discontinuities by use of identity (5.32). For fermionic 4p correlators, this iterative procedure implies that double bosonic discontinuities must vanish, e.g., $\tilde{G}^{\omega_{13},\omega_{14}}_{\omega_1^+} = 0$. This follows from the spectral representation of $\tilde{G}^{\omega_{13}}_{z_1,z_2}$ in Eq. (C.67), where the kernels only depend on fermionic frequencies z_1, z_2 in the denominators. Hence, there is no $\mathrm{Im}z_{14} = 0$ branch cut, and therefore $\tilde{G}^{\omega_{13},\omega_{14}}_{\omega_1^+}$ must vanish.

C.5.2 Spectral representation of anomalous parts

In this appendix, we focus on the spectral representation for contributions to the MF correlator anomalous w.r.t. one frequency. We again start with an example for $\ell = 3$ (App. C.5.2.1), before generalizing to arbitrary ℓ (App. C.5.2.2).

C.5.2.1 Example for $\ell = 3$

Consider $\beta\delta_{\mathrm{i}\omega_1}\hat{G}_1(\mathrm{i}\boldsymbol{\omega})$ for $\ell = 3$. Only those terms in the 3p kernel Eq. (C.4b) proportional to $\delta_{\Omega_1} = \delta_{\mathrm{i}\omega_1}\delta_{\varepsilon_1}$ and $\delta_{\Omega_{23}} = \delta_{\mathrm{i}\omega_{23}}\delta_{\varepsilon_{23}} = \delta_{\mathrm{i}\omega_1}\delta_{\varepsilon_1}$ can contribute to $\hat{G}_1$. Hence, the anomalous PSFs S_p must contain factors $\delta(\varepsilon_1)$, i.e.,

$$\beta\delta_{\mathrm{i}\omega_1}\hat{G}_1(\mathrm{i}\boldsymbol{\omega})$$

$$= -\tfrac{1}{2}\beta\delta_{\mathrm{i}\omega_1}\int \mathrm{d}^3\varepsilon\,\delta(\varepsilon_{123})\Bigg[\delta_{\varepsilon_1}S_{(123)}(\varepsilon_1,\varepsilon_2)\Delta_{\mathrm{i}\omega_{12}-\varepsilon_{12}} + \delta_{\varepsilon_1}S_{(132)}(\varepsilon_1,\varepsilon_3)\Delta_{\mathrm{i}\omega_{13}-\varepsilon_{13}}$$

$$+ \delta_{\varepsilon_{23}}S_{(231)}(\varepsilon_2,\varepsilon_3)\Delta_{\mathrm{i}\omega_2-\varepsilon_2} + \delta_{\varepsilon_{23}}S_{(321)}(\varepsilon_3,\varepsilon_2)\Delta_{\mathrm{i}\omega_3-\varepsilon_3}\Bigg]$$

$$= -\tfrac{1}{2}\beta\delta_{\mathrm{i}\omega_1}\int \mathrm{d}^3\varepsilon\,\delta(\varepsilon_{123})\Bigg[\delta_{\varepsilon_1}S_{[1,23]_+}(\varepsilon_1,\varepsilon_2,\varepsilon_3)\Delta_{\mathrm{i}\omega_2-\varepsilon_2} + \delta_{\varepsilon_1}S_{[1,32]_+}(\varepsilon_1,\varepsilon_2,\varepsilon_3)\Delta_{\mathrm{i}\omega_3-\varepsilon_3}\Bigg]$$

$$= -\tfrac{1}{2}\beta\delta_{\mathrm{i}\omega_1}\int \mathrm{d}^3\varepsilon\,\delta(\varepsilon_{123})\,\delta_{\varepsilon_1}S_{[1,[2,3]_-]_+}(\varepsilon_1,\varepsilon_2,\varepsilon_3)\Delta_{\mathrm{i}\omega_2-\varepsilon_2}, \tag{C.68}$$

where we used the symbolic Kronecker notation from App. C.2.1. The remaining contributions $p = (213), (312)$ can only contribute to the anomalous terms $\hat{G}_2$ and $\hat{G}_3$, as they are not proportional to $\delta_{\mathrm{i}\omega_1}$.

Note that, in the spectral representation (C.68), the decomposition of $\hat{G}_{1;\mathrm{i}\omega_2} = \hat{G}^{\Delta}_{1;\mathrm{i}\omega_2} + \Delta_{\mathrm{i}\omega_2}\hat{G}^{\Delta}_{1;2}$ follows from the PSF decomposition. Only PSF terms proportional to $\delta(\varepsilon_2)$, $\delta_{\varepsilon_1}\delta_{\varepsilon_2}S_{[1,[2,3]_-]_+}$, contribute to $\hat{G}^{\Delta}_{1;2}$. In the absence of such $\delta(\varepsilon_2)$ contributions, we can evaluate $\Delta_{\mathrm{i}\omega_2-\varepsilon_2} \to 1/(\mathrm{i}\omega_2 - \varepsilon_2)$ and compute the discontinuity $\hat{G}^{\Delta;\omega_2}_1 = \hat{G}^{\Delta}_{1;\omega_2^+} - \hat{G}^{\Delta}_{1;\omega_2^-}$:

$$\delta(\omega_1)\delta(\omega_2)\hat{G}^{\Delta}_{1;2} = -\delta_{\omega_1}\delta_{\omega_2}S_{1[2,3]_-}(\omega_1,\omega_2,-\omega_{12}),$$
$$\delta(\omega_1)\hat{G}^{\Delta;\omega_2}_1 = (2\pi\mathrm{i})\delta_{\omega_1}(1-\delta_{\omega_2})S_{1[2,3]_-}(\omega_1,\omega_2,-\omega_{12}). \tag{C.69}$$

Here, we used $\delta_{\omega_1}S_{[1,[2,3]_-]_+} = 2\delta_{\omega_1}S_{1[2,3]_-}$ due to the equilibrium condition (2.47). These commutator representations will be used for the 3p consistency check in App. C.7.2.2.

C.5.2.2 Generalization to arbitrary ℓ

Now, we generalize the insights from the $\ell = 3$ example to arbitrary ℓ. The result will be used in App. C.6 to provide a general formula for the construction of KF components $G^{[\eta_1\eta_2]}$ from MF functions.

In the $\beta\delta$ expansion of the MF kernel $K = \tilde{K} + \hat{K}^{\beta\delta} + \mathcal{O}(\delta^2)$, the $\beta\delta$ term reads (see Eq. (45) in Ref. [KLvD21])

$$\beta\hat{K}^\beta(\mathbf{\Omega}_p) = -\tfrac{\beta}{2}\sum_{i=1}^{\ell-1}\delta_{\Omega_{\overline{1}\ldots\overline{i}}}\prod_{\substack{j=1\\j\neq i}}^{\ell-1}\Delta_{\Omega_{\overline{1}\ldots\overline{j}}}, \tag{C.70}$$

which was originally derived for $\ell \leq 4$, but can be extended to arbitrary ℓ with the same line of arguments, starting from the results in [P2]. For general ℓp functions and terms anomalous w.r.t. the frequency $\mathrm{i}\omega_I = 0$, with $I \subset L = \{1,\ldots,\ell\}$, only permutations of the form $p = \overline{I}|\overline{I}^c$ and $p = \overline{I}^c|\overline{I}$, with $I^c = L\backslash I$ again the complementary set to I, can lead to the $\beta\delta_{\mathrm{i}\omega_I}$ factor coming from the anomalous kernel in Eq. (C.70), yielding

$$\beta\delta_{\mathrm{i}\omega_I}\hat{G}_I(\mathrm{i}\boldsymbol{\omega})$$
$$= -\tfrac{1}{2}\beta\delta_{\mathrm{i}\omega_I}\sum_{\overline{I}|\overline{I}^c}\int \mathrm{d}^\ell\varepsilon_p\,\delta(\varepsilon_{1\ldots\ell})\prod_{i=1}^{|I|-1}\Delta_{\Omega_{I_{\overline{1}}\ldots I_{\overline{i}}}}\prod_{i=1}^{|I^c|-1}\Delta_{\Omega_{I^c_{\overline{1}}\ldots I^c_{\overline{i}}}}\delta_{\varepsilon_{\overline{I}}}S_{[\overline{I},\overline{I}^c]_+}(\boldsymbol{\varepsilon}(\boldsymbol{\varepsilon}_{\overline{I}|\overline{I}^c})). \tag{C.71}$$

Equation (C.68) is a direct application of this formula for $\ell = 3$, $I = \{1\}$, and $I^c = \{2,3\}$, where the permutations $p = \overline{I}|\overline{I}^c$ run over $\overline{I}|\overline{I}^c \in \{1|23, 1|32\}$.

To make the connection to Keldysh correlators in the next appendix, we replace any $\Delta_{\mathrm{i}\omega} \to 1/(\mathrm{i}\omega)$ in the final expression for $\hat{G}_I$, which amounts to replacing $\Delta_\Omega \to 1/\Omega$ in the kernels, such that

$$\hat{G}_{I;\check{z}^{\mathrm{r}}} \equiv \left[\hat{G}_I(\mathrm{i}\boldsymbol{\omega})\right]_{\Delta_{\mathrm{i}\omega}\to\frac{1}{\mathrm{i}\omega},\,\mathrm{i}\boldsymbol{\omega}\to z(\check{z}^{\mathrm{r}})}$$
$$= -\tfrac{1}{2}\sum_{\overline{I}|\overline{I}^c}\int \mathrm{d}^\ell\varepsilon_p\,\delta(\varepsilon_{1\ldots\ell})\tilde{K}(\boldsymbol{z}_{\overline{I}}(\check{z}^{\mathrm{r}}) - \boldsymbol{\varepsilon}_{\overline{I}})\tilde{K}(\boldsymbol{z}_{\overline{I}^c}(\check{z}^{\mathrm{r}}) - \boldsymbol{\varepsilon}_{\overline{I}^c})\,\delta_{\varepsilon_{\overline{I}}}S_{[\overline{I},\overline{I}^c]_+}(\boldsymbol{\varepsilon}(\boldsymbol{\varepsilon}_{\overline{I}|\overline{I}^c})), \tag{C.72}$$

where we identified a product of regular kernels (see Eq. (C.66c)). The subscript $\check{z}^{\mathrm{r}}$ again denotes $\ell-2$ independent frequencies parametrizing the $\ell-1$ arguments $\boldsymbol{z}$ of $\hat{G}_I(\boldsymbol{z}(\check{z})) = \hat{G}_{I;\check{z}}$, with $\boldsymbol{z}$ independent of the anomalous frequency ω_I.

The anomalous parts $\hat{G}_I$ typically enter the Keldysh components with prefactors depending on $4\pi\mathrm{i}\,\delta(\omega_I)$. Including this factor, the spectral representation turns out to be particularly convenient, as we can make use of the definition in Eq. (5.64a), leading to

$$4\pi\mathrm{i}\,\delta(\omega_I)\hat{G}_{I;\check{z}^{\mathrm{r}}} = -2\,\hat{\delta}(\omega_I)\hat{G}_{I;\check{z}^{\mathrm{r}}}$$
$$= \sum_{\overline{I}|\overline{I}^c}\int \mathrm{d}^\ell\varepsilon_p\,\delta(\varepsilon_{\overline{1}\ldots\overline{\ell}})\hat{\delta}(\omega_{\overline{I}} - \varepsilon_{\overline{I}})\tilde{K}(\boldsymbol{z}_{\overline{I}}(\check{z}^{\mathrm{r}}) - \boldsymbol{\varepsilon}_{\overline{I}})\tilde{K}(\boldsymbol{z}_{\overline{I}^c}(\check{z}^{\mathrm{r}}) - \boldsymbol{\varepsilon}_{\overline{I}^c})\,\delta_{\varepsilon_{\overline{I}}}S_{[\overline{I},\overline{I}^c]_+}(\boldsymbol{\varepsilon}(\boldsymbol{\varepsilon}_{\overline{I}|\overline{I}^c}))$$
$$= \sum_{\overline{I}|\overline{I}^c}\int \mathrm{d}^\ell\varepsilon_p\,\delta(\varepsilon_{\overline{1}\ldots\overline{\ell}})\tilde{K}_{\overline{I}|\overline{I}^c}(\boldsymbol{z}_{\overline{I}|\overline{I}^c}(\omega_I,\check{z}^{\mathrm{r}}) - \boldsymbol{\varepsilon}_{\overline{I}|\overline{I}^c})\,\delta_{\varepsilon_{\overline{I}}}S_{[\overline{I},\overline{I}^c]_+}(\boldsymbol{\varepsilon}(\boldsymbol{\varepsilon}_{\overline{I}|\overline{I}^c})). \tag{C.73}$$

In the second step, we used $\omega_I = \omega_{\overline{I}}$ and

$$\delta_{\varepsilon_{\overline{I}}}S_{[\overline{I},\overline{I}^c]_+}(\boldsymbol{\varepsilon}_{\overline{I}|\overline{I}^c})\hat{\delta}(\omega_I) = \delta_{\varepsilon_{\overline{I}}}S_{[\overline{I},\overline{I}^c]_+}(\boldsymbol{\varepsilon}_{\overline{I}|\overline{I}^c})\hat{\delta}(\omega_{\overline{I}} - \varepsilon_{\overline{I}}). \tag{C.74}$$

In the last line, we inserted the definition of the regular product kernel (C.66b). Equation (C.73) is the representation needed in Eq. (C.84) to express Keldysh components $G^{[\eta_1\eta_2]}$ in terms of analytically continued anomalous parts of MF correlators.

C.6 Simplifications for KF correlators

This appendix is based on results derived by Anxiang Ge in his Master's thesis [Ge20]. For completeness, they are included here, since they are crucial ingredients for the analytic continuation of general multipoint correlators in Sec. 5.6.2.

In this appendix, we derive reformulations of the spectral representation of KF components, presented in Secs. 5.6.2.1 and 5.6.2.2, which are amenable to finding relations between KF correlators and analytically continued MF correlators. First, we derive a convenient identity for particular KF kernels for general ℓp correlators in App. C.6.1. This identity is then applied in App. C.6.2 to obtain an alternative representation of KF components $G^{[\eta_1\eta_2]}$, yielding a general analytic continuation formula (Eq. (C.84)) for these components (using the results from App. C.5). This constitutes a generalization of Eq. (3.71) for $G^{[\eta_1]}$ ($\alpha = 1$) to $\alpha = 2$. An analogous procedure is then applied to KF components $G^{[\eta_1\cdots\eta_\alpha]}$ for $\alpha = 3$ and $\alpha = 4$ in Apps. C.6.3 and C.6.4, respectively (see Eqs. (5.72) and (C.90)). In the following, we will use the notation introduced in the beginning of Sec. 5.6.2 repeatedly.

C.6.1 Identity for $K^{[\hat{\eta}_1\hat{\eta}_2]}$ for general ℓp correlators

For $\alpha = 2$, Keldysh correlators $G^{[\eta_1\eta_2]}$ are determined by the KF kernel $K^{[\hat{\eta}_1\hat{\eta}_2]} = K^{[\hat{\eta}_1]} - K^{[\hat{\eta}_2]}$ in Eq. (3.67d). For $\alpha \geq 2$, such differences of fully retarded kernels occur repeatedly in the spectral representation. In the following, we therefore derive a convenient identity for the kernel $K^{[\hat{\eta}_1\hat{\eta}_2]}$.

According to Eqs. (3.67c) and (3.69), the kernel $K^{[\hat{\eta}_1\hat{\eta}_2]}$ takes the form

$$K^{[\hat{\eta}_1\hat{\eta}_2]}(\boldsymbol{\omega}_p) = K^{[\hat{\eta}_1]}(\boldsymbol{\omega}_p) - K^{[\hat{\eta}_2]}(\boldsymbol{\omega}_p) = \tilde{K}(\boldsymbol{\omega}_p^{[\bar{\hat{\eta}}_1]}) - \tilde{K}(\boldsymbol{\omega}_p^{[\bar{\hat{\eta}}_2]}). \tag{C.75}$$

Note that $\hat{\eta}_1 < \hat{\eta}_2$, which holds by definition, does not imply $\bar{\hat{\eta}}_1 < \bar{\hat{\eta}}_2$.

For simplicity, we rename $\mu = \hat{\eta}_1$ and $\nu = \hat{\eta}_2$. Using Eqs. (3.67d) and (3.68), the retarded kernels generally read

$$K^{[\mu]}(\boldsymbol{\omega}_p) = \left(\prod_{i=1}^{\mu-1} \frac{1}{\omega_{\bar{1}\dots\bar{i}}^-}\right)\left(\prod_{i=\mu}^{\ell-1} \frac{1}{\omega_{\bar{1}\dots\bar{i}}^+}\right) = K_{1\mu}^- K_{\mu\ell}^+, \qquad K_{xy}^\pm = \prod_{i=x}^{y-1} \frac{1}{\omega_{\bar{1}\dots\bar{i}}^\pm}. \tag{C.76}$$

From this definition of $K_{xy}^\pm$, the identities

$$K_{xy}^\pm K_{yz}^\pm = K_{xz}^\pm, \qquad K_{xx}^\pm = 1, \qquad K^{[\mu]} = K_{1\mu}^- K_{\mu\ell}^+ \tag{C.77}$$

directly follow, which allow us to rewrite $K^{[\mu\nu]}(\boldsymbol{\omega}_p)$ as

$$\begin{aligned} K^{[\mu\nu]} = K^{[\mu]} - K^{[\nu]} &= K_{1\mu}^- \left(K_{\mu\nu}^+ - K_{\mu\nu}^-\right) K_{\nu\ell}^+ \\ &= \sum_{y=\mu}^{\nu-1} K_{1\mu}^- \left(K_{\mu y+1}^+ K_{y+1\nu}^- - K_{\mu y}^+ K_{y\nu}^-\right) K_{\nu\ell}^+ \\ &= \sum_{y=\mu}^{\nu-1} K_{1\mu}^- K_{\mu y}^+ \underbrace{\left(\frac{1}{\omega_{\bar{1}\dots\bar{y}}^+} - \frac{1}{\omega_{\bar{1}\dots\bar{y}}^-}\right)}_{=\hat{\delta}(\omega_{\bar{1}\dots\bar{y}})} K_{y+1\nu}^- K_{\nu\ell}^+. \end{aligned} \tag{C.78}$$

In the second line, the terms $y = \mu$ and $y = \nu - 1$ represent the first line, the remaining contributions $\mu < y < \nu - 1$ cancel pairwise. In the last line, we used identity (5.32) to obtain

$\hat{\delta}(\omega_{\overline{1}...\overline{y}})$, enforcing $\omega^{\pm}_{\overline{1}...\overline{i}} = \omega^{\pm}_{\overline{y+1}...\overline{i}}$ for $i > y$. Inserting this identity into the arguments of $K^{-}_{y+1\nu}K^{+}_{\nu\ell}$ yields

$$
\begin{aligned}
K^{[\mu\nu]}(\boldsymbol{\omega}_p) &= \sum_{y=\mu}^{\nu-1} K^{[\mu]}(\boldsymbol{\omega}_{\overline{1}...\overline{y}})\hat{\delta}(\omega_{\overline{1}...\overline{y}})K^{[\nu]}(\boldsymbol{\omega}_{\overline{y+1}...\overline{\ell}}) = \sum_{y=\mu}^{\nu-1} \tilde{K}(\boldsymbol{\omega}^{[\overline{\mu}]}_{\overline{1}...\overline{y}})\hat{\delta}(\omega_{\overline{1}...\overline{y}})\tilde{K}(\boldsymbol{\omega}^{[\overline{\nu}]}_{\overline{y+1}...\overline{\ell}}) \\
&= \sum_{y=\mu}^{\nu-1} \tilde{K}_{\overline{1}...\overline{y}|\overline{y+1}...\overline{\ell}}(\boldsymbol{\omega}^{[\overline{\mu}][\overline{\nu}]}_{\overline{1}...\overline{y}|\overline{y+1}...\overline{\ell}}).
\end{aligned}
\tag{C.79}
$$

The last equality follows from the definition (5.64a), with $\alpha = 2$, $\eta_1 = \overline{\mu}$, $\eta_2 = \overline{\nu}$, $\overline{I}^1 = \overline{1}...\overline{y}$, and $\overline{I}^2 = \overline{y+1}...\overline{\ell}$. Note that, for $\ell = 3$, Eq. (C.79) readily yields the results of Tab. C.1.

C.6.2 Simplifications for $G^{[\eta_1\eta_2]}$ for ℓp correlators

After the preparations in Apps. C.5 and C.6.1, we can now derive an alternative representation of the Keldysh correlators $G^{[\eta_1\eta_2]}$, equivalent to the spectral representation in Eqs. (3.67) but more convenient for the analytic continuation. This generalizes the concepts of Sec. C.3.3.1 from $\ell = 3$ to arbitrary ℓ.

We start by inserting Eq. (C.79) into the spectral representation in Eqs. (3.67),

$$
G^{[\eta_1\eta_2]}(\boldsymbol{\omega}) = \sum_p [K^{[\hat{\eta}_1\hat{\eta}_2]} * S_p](\boldsymbol{\omega}_p) = \sum_p \sum_{y=\hat{\eta}_1}^{\hat{\eta}_2-1} \left(\tilde{K}_{\overline{1}...\overline{y}|\overline{y+1}...\overline{\ell}} * S_p \right)(\boldsymbol{\omega}^{[\overline{\hat{\eta}}_1][\overline{\hat{\eta}}_2]}_{\overline{1}...\overline{y}|\overline{y+1}...\overline{\ell}}).
\tag{C.80}
$$

Since $\hat{\eta}_1 \le y < \hat{\eta}_2$, the subtuples $\overline{I} = (\overline{1}...\overline{y})$ and $\overline{I}^c = (\overline{y+1}...\overline{\ell})$ always contain $\overline{\hat{\eta}}_1$ and $\overline{\hat{\eta}}_2$, respectively. Each of these in turn equals either η_1 or η_2, since $\hat{\eta}_i \in \{p^{-1}(\eta_1), p^{-1}(\eta_2)\}$, hence $\overline{\hat{\eta}}_i \in \{\eta_1, \eta_2\}$. Correspondingly, we will denote the subtuple containing η_1 as $\overline{I}^1$, and that containing η_2 as $\overline{I}^2$. The sum over y can then be interpreted as a sum over all possible partitions of $(\overline{1}, \dots, \overline{\ell})$ for which each of the two subtuples contains either η_1 or η_2. Defining $\mathcal{I}^{12} = \{(I^1, I^2)|\eta_1 \in I^1, \eta_2 \in I^2, I^1 \cup I^2 = L, I^1 \cap I^2 = \emptyset\}$ as the set of all possibilities to partition $L = \{1, \dots, \ell\}$ into subsets I^1 and I^2 containing η_1 and η_2, respectively, we find

$$
G^{[\eta_1\eta_2]}(\boldsymbol{\omega}) = \sum_{(I^1,I^2)\in\mathcal{I}^{12}} \Big[\sum_{\overline{I}^1|\overline{I}^2} \left(\tilde{K}_{\overline{I}^1|\overline{I}^2} \diamond S_{\overline{I}^1|\overline{I}^2} \right)(\boldsymbol{\omega}^{[\eta_1][\eta_2]}_{\overline{I}^1|\overline{I}^2}) + \sum_{\overline{I}^2|\overline{I}^1} \left(\tilde{K}_{\overline{I}^2|\overline{I}^1} \diamond S_{\overline{I}^2|\overline{I}^1} \right)(\boldsymbol{\omega}^{[\eta_2][\eta_1]}_{\overline{I}^2|\overline{I}^1}) \Big].
\tag{C.81}
$$

Here, we collected all terms in Eq. (C.80) proportional to $\hat{\delta}(\omega_{\overline{I}^1})$ and summed over all allowed partitions. Using the symmetry of the kernels (5.64a) and the (anti)commutator notation from Eq. (5.66), we finally obtain

$$
G^{[\eta_1\eta_2]}(\boldsymbol{\omega}) = \sum_{(I^1,I^2)\in\mathcal{I}^{12}} \sum_{\overline{I}^1|\overline{I}^2} \left(\tilde{K}_{\overline{I}^1|\overline{I}^2} \diamond S_{[\overline{I}^1,\overline{I}^2]_+} \right)(\boldsymbol{\omega}^{[\eta_1][\eta_2]}_{\overline{I}^1|\overline{I}^2}).
\tag{C.82}
$$

Building on this expression, the KF component can be related to MF functions for arbitrary ℓ. For this purpose, we use the equilibrium condition to replace PSF commutators with anticommutators,

$$
S_{[\overline{I},\overline{I}^c]_+}(\boldsymbol{\varepsilon}_{\overline{I}|\overline{I}^c}) = N_{\varepsilon_{\overline{I}}} S_{[\overline{I},\overline{I}^c]_-}(\boldsymbol{\varepsilon}_{\overline{I}|\overline{I}^c}) + \delta_{\varepsilon_{\overline{I}}} S_{[\overline{I},\overline{I}^c]_+}(\boldsymbol{\varepsilon}_{\overline{I}|\overline{I}^c}),
\tag{C.83}
$$

$$
N_{\varepsilon_{\overline{I}}} = \frac{\zeta^{\overline{I}} e^{\beta\varepsilon_{\overline{I}}} + 1}{\zeta^{\overline{I}} e^{\beta\varepsilon_{\overline{I}}} - 1} = \coth(\beta\varepsilon_{\overline{I}}/2)^{\zeta^{\overline{I}}},
$$

where $N_{\varepsilon_{\overline{I}}}$ is identical to the statistical factor in Eq. (5.34), and we used the symbolic Kronecker notation from App. C.2.1. The sign factor is given by $\zeta^{\overline{I}} = \pm 1$ for an even/odd number of fermionic operators in the set $\overline{I}$. Inserting Eq. (C.83) into the representation (C.82), we thus obtain

$$
G^{[\eta_1\eta_2]}(\boldsymbol{\omega})
$$

$$
= \sum_{(I^1,I^2)\in\mathcal{I}^{12}} \sum_{\overline{I}^1|\overline{I}^2} \int \mathrm{d}^\ell\varepsilon\,\delta(\varepsilon_{1\ldots\ell})\,\tilde{K}_{\overline{I}^1|\overline{I}^2}(\boldsymbol{\omega}^{[\eta_1][\eta_2]}_{\overline{I}^1|\overline{I}^2} - \boldsymbol{\varepsilon}_{\overline{I}^1|\overline{I}^2})
$$

$$
\times \left(N_{\varepsilon_{\overline{I}^1}} S_{[\overline{I}^1,\overline{I}^2]_-}(\boldsymbol{\varepsilon}_{\overline{I}^1|\overline{I}^2}) + \delta_{\varepsilon_{\overline{I}^1}} S_{[\overline{I}^1,\overline{I}^2]_+}(\boldsymbol{\varepsilon}_{\overline{I}^1|\overline{I}^2}) \right)
$$

$$
= \sum_{(I^1,I^2)\in\mathcal{I}^{12}} \left(N_{\omega_{I^1}} \tilde{G}^{\omega_{I^1}}_{\check{\boldsymbol{z}}} + 4\pi\mathrm{i}\,\delta(\omega_{I^1})\,\hat{G}_{I^1;\check{\boldsymbol{z}}} \right) \qquad \text{with } \check{\boldsymbol{z}} = \{\omega_i^-\,|\,i\neq\eta_1, i\neq\eta_2\}. \qquad (\text{C.84})
$$

This remarkable formula generalizes Eq. (3.71) for $G^{[\eta_1]}$, i.e. for $\alpha = 1$ and arbitrary ℓ, to $G^{[\eta_1\eta_2]}$ ($\alpha = 2$). To obtain its final form, we used that the retarded product kernel (Eq. (5.64a)) in the second line is proportional to $\hat{\delta}(\omega_{\overline{I}^1} - \varepsilon_{\overline{I}^1})$ and thereby sets $N_{\varepsilon_{\overline{I}^1}} = N_{\omega_{\overline{I}^1}} = N_{\omega_{I^1}}$ independent of the integration variables. In the second step, we then identified the spectral representations of discontinuities of the regular MF correlator $\tilde{G}^{\omega_{I^1}}_{\check{\boldsymbol{z}}}$ (Eq. (C.66)) and of the anomalous contribution $\hat{G}_{I^1;\check{\boldsymbol{z}}}$ (Eq. (C.73)). Note that the retarded product kernel coincides with the kernel (C.66b) with a suitably continued $\check{\boldsymbol{z}}$. In Eq. (C.84), the $\ell - 2$ frequencies in $\check{\boldsymbol{z}}$ carry negative imaginary shifts, in accordance with the definition of $\boldsymbol{\omega}^{[\eta_1][\eta_2]}_{\overline{I}^1|\overline{I}^2}$.

C.6.3 Simplifications for $G^{[\eta_1\eta_2\eta_3]}$ for $\ell\mathbf{p}$ correlators

The calculation in App. C.3.3.2, too, can be generalized to arbitrary ℓp correlators, in particular for the spectral representation of $G^{[\eta_1\eta_2\eta_3]} - G^{[\eta_3]}$. The Keldysh kernel for $G^{[3]}$ is given by $\tilde{K}(\boldsymbol{\omega}^{[\eta_3]}_p) = K^{[\mu_3]}(\boldsymbol{\omega}_p)$ for arbitrary permutations p, with $\mu_3 = p^{-1}(\eta_3)$. Then, the corresponding Keldysh kernel for $G^{[\eta_1\eta_2\eta_3]} - G^{[\eta_3]}$ reads

$$
K^{[\hat{\eta}_1\hat{\eta}_2\hat{\eta}_3]} - K^{[\mu_3]} = K^{[\hat{\eta}_1]} - K^{[\hat{\eta}_2]} + K^{[\hat{\eta}_3]} - K^{[\mu_3]}, \qquad (\text{C.85})
$$

such that the effect of subtracting $K^{[\mu_3]}$ depends on the permutation. The permutations can be divided into six categories, depending on the order in which the $\mu_j = p^{-1}(\eta_j)$ occur, see Tab. C.3. This is important since placing the μ_j in increasing order yields $[\hat{\eta}_1\hat{\eta}_2\hat{\eta}_3]$, see discussion before Eqs. (3.67).

Here, we focus on the key steps in rewriting permutations with $\mu_1 < \mu_2 < \mu_3$, denoted by $\sum_{p|\mu_1<\mu_2<\mu_3}$. Defining $\mathcal{I}^{123} = \{(I^1,I^2,I^3)\,|\,\eta_1 \in I^1, \eta_2 \in I^2, \eta_3 \in I^3, I^b \cap I^{b'} = \emptyset \text{ for } b \neq b'\}$ as the set of all possibilities to partition $L = \{1,...,\ell\}$ into three blocks, each of which contains one of the indices $\eta_j \in I^j$, we have

$$
\sum_{p|\mu_1<\mu_2<\mu_3} \left[\left(K^{[\hat{\eta}_1\hat{\eta}_2\hat{\eta}_3]} - K^{[\mu_3]} \right) * S_p \right](\boldsymbol{\omega}_p)
$$

$$
= \sum_{p|\mu_1<\mu_2<\mu_3} \left(K^{[\mu_1\mu_2]} * S_p \right)(\boldsymbol{\omega}_p) = \sum_{p|\mu_1<\mu_2<\mu_3} \sum_{y=\mu_1}^{\mu_2-1} \left(\tilde{K}_{\overline{1\ldots y}|\overline{y+1\ldots\ell}} * S_p \right)(\boldsymbol{\omega}^{[\eta_1][\eta_2]}_{\overline{1\ldots y}|\overline{y+1\ldots\ell}})
$$

$$
= \sum_{(I^1,I^2,I^3)\in\mathcal{I}^{123}} \sum_{\overline{I}^1|\overline{I}^{2|3}} \left(\tilde{K}_{\overline{I}^1|\overline{I}^{2|3}} \diamond S_{\overline{I}^1|\overline{I}^{2|3}} \right)(\boldsymbol{\omega}^{[\eta_1][\eta_2]}_{\overline{I}^1|\overline{I}^{2|3}}). \qquad (\text{C.86})
$$

p	$K^{[\hat\eta_1\hat\eta_2\hat\eta_3]} - K^{[\mu_3]}$	$G^{[\eta_1\eta_2\eta_3]} - G^{[\eta_3]} = \sum_p \left[\left(K^{[\hat\eta_1\hat\eta_2\hat\eta_3]} - K^{[\mu_3]} \right) * S_p \right] (\boldsymbol\omega_p)$
		$= \sum_{(I^1,I^2,I^3)\in\mathcal{I}^{123}}$
$\mu_1 < \mu_2 < \mu_3$	$K^{[\mu_1\mu_2]}$	$\left\{ \sum_{\overline{I}^1\mid\overline{I}^2\mid\overline{I}^3} \left[\left(\tilde{K}_{\overline{I}^1\mid\overline{I}^2\mid\overline{I}^3} \diamond S_{\overline{I}^1\mid\overline{I}^2\mid\overline{I}^3} \right) (\boldsymbol\omega^{[\eta_1][\eta_2][\eta_3]}_{\overline{I}^1\mid\overline{I}^2\mid\overline{I}^3}) \right.\right.$
		$\left. + \left(\tilde{K}_{\overline{I}^1\mid\overline{I}^{2\mid3}} \diamond S_{\overline{I}^1\mid\overline{I}^{2\mid3}} \right) (\boldsymbol\omega^{[\eta_1][\eta_3]}_{\overline{I}^1\mid\overline{I}^{2\mid3}}) \right]$
$\mu_1 < \mu_3 < \mu_2$	$K^{[\mu_1\mu_3]} - K^{[\mu_3\mu_2]}$	$+ \sum_{\overline{I}^1\mid\overline{I}^3\mid\overline{I}^2} \left[\left(\tilde{K}_{\overline{I}^1\mid\overline{I}^{3\mid2}} \diamond S_{\overline{I}^1\mid\overline{I}^{3\mid2}} \right) (\boldsymbol\omega^{[\eta_1][\eta_3]}_{\overline{I}^1\mid\overline{I}^{3\mid2}}) \right.$
		$\left. + \left(\tilde{K}_{\overline{I}^{1\mid3}\mid\overline{I}^2} \diamond S_{\overline{I}^{1\mid3}\mid\overline{I}^2} \right) (\boldsymbol\omega^{[\eta_3][\eta_2]}_{\overline{I}^{1\mid3}\mid\overline{I}^2}) \right]$
$\mu_2 < \mu_1 < \mu_3$	$K^{[\mu_2\mu_1]}$	$+ \sum_{\overline{I}^2\mid\overline{I}^1\mid\overline{I}^3} \left[\left(\tilde{K}_{\overline{I}^2\mid\overline{I}^1\mid\overline{I}^3} \diamond S_{\overline{I}^2\mid\overline{I}^1\mid\overline{I}^3} \right) (\boldsymbol\omega^{[\eta_2][\eta_1][\eta_3]}_{\overline{I}^2\mid\overline{I}^1\mid\overline{I}^3}) \right.$
		$\left. + \left(\tilde{K}_{\overline{I}^2\mid\overline{I}^{1\mid3}} \diamond S_{\overline{I}^2\mid\overline{I}^{1\mid3}} \right) (\boldsymbol\omega^{[\eta_2][\eta_3]}_{\overline{I}^2\mid\overline{I}^{1\mid3}}) \right]$
$\mu_2 < \mu_3 < \mu_1$	$K^{[\mu_2\mu_3]} - K^{[\mu_3\mu_1]}$	$+ \sum_{\overline{I}^2\mid\overline{I}^3\mid\overline{I}^1} \left[\left(\tilde{K}_{\overline{I}^2\mid\overline{I}^{3\mid1}} \diamond S_{\overline{I}^2\mid\overline{I}^{3\mid1}} \right) (\boldsymbol\omega^{[\eta_2][\eta_3]}_{\overline{I}^2\mid\overline{I}^{3\mid1}}) \right.$
		$\left. + \left(\tilde{K}_{\overline{I}^{2\mid3}\mid\overline{I}^1} \diamond S_{\overline{I}^{2\mid3}\mid\overline{I}^1} \right) (\boldsymbol\omega^{[\eta_3][\eta_1]}_{\overline{I}^{2\mid3}\mid\overline{I}^1}) \right]$
$\mu_3 < \mu_1 < \mu_2$	$-K^{[\mu_1\mu_2]}$	$+ \sum_{\overline{I}^3\mid\overline{I}^1\mid\overline{I}^2} \left[\left(\tilde{K}_{\overline{I}^3\mid\overline{I}^1\mid\overline{I}^2} \diamond S_{\overline{I}^3\mid\overline{I}^1\mid\overline{I}^2} \right) (\boldsymbol\omega^{[\eta_3][\eta_1][\eta_2]}_{\overline{I}^3\mid\overline{I}^1\mid\overline{I}^2}) \right.$
		$\left. - \left(\tilde{K}_{\overline{I}^{3\mid1}\mid\overline{I}^2} \diamond S_{\overline{I}^{3\mid1}\mid\overline{I}^2} \right) (\boldsymbol\omega^{[\eta_3][\eta_2]}_{\overline{I}^{3\mid1}\mid\overline{I}^2}) \right]$
$\mu_3 < \mu_2 < \mu_1$	$-K^{[\mu_2\mu_1]}$	$+ \sum_{\overline{I}^3\mid\overline{I}^2\mid\overline{I}^1} \left[\left(\tilde{K}_{\overline{I}^3\mid\overline{I}^2\mid\overline{I}^1} \diamond S_{\overline{I}^3\mid\overline{I}^2\mid\overline{I}^1} \right) (\boldsymbol\omega^{[\eta_3][\eta_2][\eta_1]}_{\overline{I}^3\mid\overline{I}^2\mid\overline{I}^1}) \right.$
		$\left.\left. - \left(\tilde{K}_{\overline{I}^{3\mid2}\mid\overline{I}^1} \diamond S_{\overline{I}^{3\mid2}\mid\overline{I}^1} \right) (\boldsymbol\omega^{[\eta_3][\eta_1]}_{\overline{I}^{3\mid2}\mid\overline{I}^1}) \right] \right\}$

Table C.3 Keldysh kernel of $G^{[\eta_1\eta_2\eta_3]} - G^{[\eta_3]}$ (Eq. (C.85)) for different permutation classes depending on the order of the $\mu_i = p^{-1}(\eta_i)$. Manipulations similar to Eqs. (C.86) and (C.87) result in the alternative spectral representation in the third column, which can be further rewritten as Eq. (5.72) using Eq. (C.88) (and equivalent identities).

In the first step, we used that $[\hat\eta_1\hat\eta_2\hat\eta_3] = [\mu_1\mu_2\mu_3]$. In the second step, we inserted the kernel expansion Eq. (C.79) with $\overline{\mu}_j = \eta_j$. In the third step, we identified the sum over y as a sum over all possibilities to subdivide the permutations into the form $p = \overline{I}^1\mid\overline{I}^2\mid\overline{I}^3$ (which guarantees $\mu_1 < \mu_2 < \mu_3$), with the concatenation of $\overline{I}^2$ and $\overline{I}^3$ denoted by $\overline{I}^{2\mid3} = \overline{I}^2_1 \ldots \overline{I}^2_{\mid I^2\mid}\overline{I}^3_1 \ldots \overline{I}^3_{\mid I^3\mid}$.

Further, we use

$$\sum_{(I^1,I^2,I^3)\in\mathcal{I}^{123}} \sum_{\overline{I}^1\mid\overline{I}^2\mid\overline{I}^3} \left(\tilde{K}_{\overline{I}^1\mid\overline{I}^{2\mid3}} \diamond S_{\overline{I}^1\mid\overline{I}^{2\mid3}} \right) (\boldsymbol\omega^{[\eta_1][\eta_2]}_{\overline{I}^1\mid\overline{I}^{2\mid3}})$$

$$- \sum_{(I^1,I^2,I^3)\in\mathcal{I}^{123}} \sum_{\overline{I}^1\mid\overline{I}^2\mid\overline{I}^3} \left(\tilde{K}_{\overline{I}^1\mid\overline{I}^{2\mid3}} \diamond S_{\overline{I}^1\mid\overline{I}^{2\mid3}} \right) (\boldsymbol\omega^{[\eta_1][\eta_3]}_{\overline{I}^1\mid\overline{I}^{2\mid3}})$$

$$= \sum_{(I^1, I^2, I^3) \in \mathcal{I}^{123}} \sum_{\overline{I}^1 | \overline{I}^2 | \overline{I}^3} \left(\tilde{K}_{\overline{I}^1 | \overline{I}^2 | \overline{I}^3} \diamond S_{\overline{I}^1 | \overline{I}^2 | \overline{I}^3} \right) (\boldsymbol{\omega}_{\overline{I}^1 | \overline{I}^2 | \overline{I}^3}^{[\eta_1][\eta_2][\eta_3]}), \tag{C.87}$$

which again follows by inserting Eq. (C.79), to arrive at the result in Tab. C.3.

Contributions of different permutations can be further simplified, e.g., the second term of $p|\mu_1 < \mu_2 < \mu_3$ and the first term of $p|\mu_1 < \mu_3 < \mu_2$ can be collected, yielding

$$\sum_{(I^1, I^2, I^3) \in \mathcal{I}^{123}} \sum_{\overline{I}^1 | \overline{I}^2 | \overline{I}^3} \left(\tilde{K}_{\overline{I}^1 | \overline{I}^{2|3}} \diamond S_{\overline{I}^1 | \overline{I}^{2|3}} \right) (\boldsymbol{\omega}_{\overline{I}^1 | \overline{I}^{2|3}}^{[\eta_1][\eta_3]})$$

$$+ \sum_{(I^1, I^2, I^3) \in \mathcal{I}^{123}} \sum_{\overline{I}^1 | \overline{I}^3 | \overline{I}^2} \left(\tilde{K}_{\overline{I}^1 | \overline{I}^{3|2}} \diamond S_{\overline{I}^1 | \overline{I}^{3|2}} \right) (\boldsymbol{\omega}_{\overline{I}^1 | \overline{I}^{3|2}}^{[\eta_1][\eta_3]})$$

$$= \sum_{(I^1, I^{23}) \in \mathcal{I}^{1|23}} \sum_{\overline{I}^1 | \overline{I}^{23}} \left[\tilde{K}_{\overline{I}^1 | \overline{I}^{23}} \diamond S_{\overline{I}^1 | \overline{I}^{23}} \right] (\boldsymbol{\omega}_{\overline{I}^1 | \overline{I}^{23}}^{[\eta_1][\eta_3]}), \tag{C.88}$$

with $\mathcal{I}^{1|23}$ defined in Eq. (5.73a). Using the symmetry of retarded product kernels, e.g., $\tilde{K}_{\overline{I}^1 | \overline{I}^{23}} = \tilde{K}_{\overline{I}^{23} | \overline{I}^1}$, the spectral representation of $G^{[\eta_1 \eta_2 \eta_3]} - G^{[\eta_3]}$ finally results in Eq. (5.72). Unlike for $\alpha = 2$ we don't have a general formula for the analytic continuation to $G^{[\eta_1 \eta_2 \eta_3]}$.

Equation (5.74) shows an example for $\ell = 4$. Inserting Eq. (5.62) into the PSF (anti)commutators and abbreviating $S_p' = (2\pi i)^3 S_p$, we obtain the following relations:

$$S'_{[[[\overline{1},\overline{2}]_-,\overline{3}]_+,\overline{4}]_+} = -N_{\overline{4}} \Big(N_{\overline{3}} \tilde{G}^{\varepsilon_{\overline{3}}, \varepsilon_{\overline{12}}, \varepsilon_{\overline{1}}} + N_{\overline{12}} \tilde{G}^{\varepsilon_{\overline{12}}, \varepsilon_{\overline{3}}, \varepsilon_{\overline{1}}} - 2\hat{\delta}(\varepsilon_{\overline{12}}) \hat{G}_{\overline{12}}^{\varepsilon_{\overline{3}}, \varepsilon_{\overline{1}}} \Big),$$

$$S'_{[[\overline{1},\overline{2}]_-,[\overline{3},\overline{4}]_+]_+} = N_{\overline{12}} \Big(N_{\overline{4}} \tilde{G}^{\varepsilon_{\overline{4}}, \varepsilon_{\overline{3}}, \varepsilon_{\overline{2}}} + N_{\overline{3}} \tilde{G}^{\varepsilon_{\overline{3}}, \varepsilon_{\overline{4}}, \varepsilon_{\overline{2}}} \Big) - 2\hat{\delta}(\varepsilon_{\overline{12}}) N_{\overline{3}} \hat{G}_{\overline{12}}^{\varepsilon_{\overline{1}}, \varepsilon_{\overline{3}}}. \tag{C.89}$$

Inserting these into the alternative spectral representation (5.72), we can evaluate the convolution integrals and obtain the relations in Eqs. (5.75g)–(5.75j), which express KF components in terms of MF functions and MWFs.

C.6.4 Simplifications for $G^{[1234]}$ for $\ell = 4$

For $\alpha = 4$, we can directly apply Eq. (C.79) on the Keldysh kernel, and a straightforward calculation gives

$$G^{[1234]}(\boldsymbol{\omega}) = \sum_{\overline{234}} [\tilde{K}_{\overline{234}|1} \diamond S_{[\overline{234},1]_+}](\boldsymbol{\omega}_{\overline{234}|1}^{[4][1]}) + \sum_{\overline{134}} [\tilde{K}_{\overline{134}|2} \diamond S_{[\overline{134},2]_+}](\boldsymbol{\omega}_{\overline{134}|2}^{[4][2]})$$

$$+ \sum_{\overline{124}} [\tilde{K}_{\overline{124}|3} \diamond S_{[\overline{124},3]_+}](\boldsymbol{\omega}_{\overline{124}|3}^{[2][3]}) + \sum_{\overline{123}} [\tilde{K}_{\overline{123}|4} \diamond S_{[\overline{123},4]_+}](\boldsymbol{\omega}_{\overline{123}|4}^{[3][4]})$$

$$+ [\tilde{K}_{4|12|3} \diamond S_{[[4,[1,2]_-]_-,3]_+}](\boldsymbol{\omega}_{4|12|3}^{[4][2][3]}) + [\tilde{K}_{3|14|2} \diamond S_{[[3,[1,4]_-]_-,2]_+}](\boldsymbol{\omega}_{3|14|2}^{[3][1][2]})$$

$$+ [\tilde{K}_{1|23|4} \diamond S_{[[1,[2,3]_-]_-,4]_+}](\boldsymbol{\omega}_{1|23|4}^{[1][3][4]}) + [\tilde{K}_{2|34|1} \diamond S_{[[2,[3,4]_-]_-,1]_+}](\boldsymbol{\omega}_{2|34|1}^{[2][4][1]})$$

$$+ [\tilde{K}_{4|2|13} \diamond S_{[[4,2]_+,[1,3]_-]_-}](\boldsymbol{\omega}_{4|2|13}^{[4][2][3]}) + [\tilde{K}_{1|3|24} \diamond S_{[[1,3]_+,[2,4]_-]_-}](\boldsymbol{\omega}_{1|3|24}^{[1][3][4]})$$

$$+ (-2\pi i)^3 \Big(S_{[[[2,3]_+,1]_-,4]_-} + S_{[[[3,4]_+,2]_-,1]_-} - S_{[[[3,4]_-,2]_-,1]_+}$$

$$- S_{[[[4,1]_-,3]_-,2]_+} + S_{[[4,2]_+,[1,3]_+]_+} \Big)(\boldsymbol{\omega}), \tag{C.90}$$

where $\sum_{\overline{I}}$ denotes a sum over permutations of the subset $I \subset \{1, \dots, \ell\}$. All occuring PSF (anti)commutators can be identified with one of the following four forms,

$$S'_{[[[\overline{1},\overline{2}]_-,\overline{3}]_-,\overline{4}]_+} = N_{\overline{4}}\tilde{G}^{\varepsilon_{\overline{4}},\varepsilon_{\overline{3}},\varepsilon_{\overline{2}}}, \tag{C.91a}$$

$$S'_{[[\overline{1},\overline{2}]_-,[\overline{3},\overline{4}]_+]_-} = N_{\overline{4}}\tilde{G}^{\varepsilon_{\overline{4}},\varepsilon_{\overline{3}},\varepsilon_{\overline{2}}} + N_{\overline{3}}\tilde{G}^{\varepsilon_{\overline{3}},\varepsilon_{\overline{4}},\varepsilon_{\overline{2}}}, \tag{C.91b}$$

$$S'_{[[[\overline{1},\overline{2}]_+,\overline{3}]_-\overline{4}]_-} = N_{\overline{1}}\tilde{G}^{\varepsilon_{\overline{2}},\varepsilon_{\overline{4}},\varepsilon_{\overline{3}}} + N_{\overline{2}}\tilde{G}^{\varepsilon_{\overline{1}},\varepsilon_{\overline{4}},\varepsilon_{\overline{3}}} + N_{\overline{13}}\tilde{G}^{\varepsilon_{\overline{13}},\varepsilon_{\overline{1}},\varepsilon_{\overline{2}}} + N_{\overline{14}}\tilde{G}^{\varepsilon_{\overline{14}},\varepsilon_{\overline{1}},\varepsilon_{\overline{2}}}$$
$$\qquad\qquad - 2\hat{\delta}(\varepsilon_{\overline{13}})\hat{G}^{\varepsilon_{\overline{1}},\varepsilon_{\overline{2}}}_{\overline{13}} - 2\hat{\delta}(\varepsilon_{\overline{14}})\hat{G}^{\varepsilon_{\overline{1}},\varepsilon_{\overline{2}}}_{\overline{14}}, \tag{C.91c}$$

$$S'_{[[\overline{1},\overline{2}]_+,[\overline{3},\overline{4}]_+]_+} = N_{\overline{1}}N_{\overline{3}}\hat{G}^{\varepsilon_{\overline{1}},\varepsilon_{\overline{3}}}_{\overline{12}} - (1 + N_{\overline{1}}N_{\overline{2}})(\hat{G}^{\varepsilon_{\overline{1}},\varepsilon_{\overline{2}}}_{\overline{13}} + \hat{G}^{\varepsilon_{\overline{1}},\varepsilon_{\overline{2}}}_{\overline{14}})$$
$$\qquad - (1 + N_{\overline{1}}N_{\overline{2}})(N_{\overline{3}}\tilde{G}^{\varepsilon_{\overline{3}},\varepsilon_{\overline{2}},\varepsilon_{\overline{1}}} + N_{\overline{4}}\tilde{G}^{\varepsilon_{\overline{4}},\varepsilon_{\overline{2}},\varepsilon_{\overline{1}}} + N_{\overline{13}}\tilde{G}^{\varepsilon_{\overline{13}},\varepsilon_{\overline{2}},\varepsilon_{\overline{1}}} + N_{\overline{23}}\tilde{G}^{\varepsilon_{\overline{23}},\varepsilon_{\overline{2}},\varepsilon_{\overline{1}}})$$
$$\qquad - N_{\overline{1}}N_{\overline{12}}(N_{\overline{3}}\tilde{G}^{\varepsilon_{\overline{3}},\varepsilon_{\overline{12}},\varepsilon_{\overline{1}}} + N_{\overline{4}}\tilde{G}^{\varepsilon_{\overline{4}},\varepsilon_{\overline{2}},\varepsilon_{\overline{1}}}), \tag{C.91d}$$

where we abbreviated $S'_p = (2\pi\mathrm{i})^3 S_p$ and $N_i = N_{\varepsilon_i}$, and we used Eq. (5.62) to evaluated above expressions. Inserting these into Eq. (C.90) and after application of Cauchy's integral formula, one obtains Eq. (5.75k).

C.7 Consistency checks

In Eqs. (5.21), (5.48), and (5.62), we expressed the 2p, 3p and 4p PSFs in terms of analytically continued MF functions. While the derivation of these important results extends over several pages, some consistency checks can be presented compactly. In App. C.7.1, we first show that our formulas fulfill the equilibrium condition (2.47). Since this was not explicitly imposed during the derivations, it serves as a strong test for our results. In App. C.7.2, we further show, for $\ell = 2, 3, 4$, that our formulas for $S_p[G]$, when expressing that G through PSFs, recover the input PSFs.

C.7.1 Fulfillment of the equilibrium condition

Here, we show that the results in (5.48) and (5.62) fulfill the equilibrium condition (2.47) (for the 2p case, this was already demonstrated in (5.24)). It suffices to show that they are fulfilled for p_λ with $\lambda = 2$, i.e., that for $p = (\overline{1} \dots \overline{\ell})$ we have

$$S_{(\overline{1}\dots\overline{\ell})}(\boldsymbol{\varepsilon}_{(\overline{1}\dots\overline{\ell})}) = \zeta^{\overline{1}}e^{\beta\varepsilon_{\overline{1}}}S_{(\overline{2}\dots\overline{\ell1})}(\boldsymbol{\varepsilon}_{(\overline{2}\dots\overline{\ell1})}). \tag{C.92}$$

The result for general λ follows by induction.

We start with $\ell = 3$ and separate the contributions to the PSFs in Eq. (5.48) from the regular $\tilde{G}$ (denoted by S^{r}_p) and the anomalous $\hat{G}$ terms (denoted by S^{a}_p), $S_p = S^{\mathrm{r}}_p + S^{\mathrm{a}}_p$. Inserting Eq. (5.48) into Eq. (C.92) first yields

$$\zeta^{\overline{1}}e^{\beta\varepsilon_{\overline{1}}}(2\pi\mathrm{i})^2 S^{\mathrm{r}}_{(\overline{231})} = \zeta^{\overline{1}}e^{\beta\varepsilon_{\overline{1}}}\left[n_{\varepsilon_{\overline{2}}}n_{\varepsilon_{\overline{3}}}\tilde{G}^{\varepsilon_{\overline{3}},\varepsilon_{\overline{2}}} + n_{\varepsilon_{\overline{2}}}n_{\varepsilon_{\overline{23}}}\tilde{G}^{\varepsilon_{\overline{23}},\varepsilon_{\overline{2}}}\right]$$

$$= \zeta^{\overline{1}}e^{\beta\varepsilon_{\overline{1}}}\left[n_{\varepsilon_{\overline{2}}}(n_{\varepsilon_{\overline{3}}} - n_{\varepsilon_{\overline{23}}})\tilde{G}^{\varepsilon_{\overline{3}},\varepsilon_{\overline{2}}} - n_{\varepsilon_{\overline{2}}}n_{\varepsilon_{\overline{23}}}\tilde{G}^{\varepsilon_{\overline{2}},\varepsilon_{\overline{1}}}\right]$$

$$= \zeta^{\overline{1}}e^{\beta\varepsilon_{\overline{1}}}\left[-n_{\varepsilon_{\overline{12}}}n_{-\varepsilon_{\overline{1}}}\tilde{G}^{\varepsilon_{\overline{12}},\varepsilon_{\overline{1}}} - n_{\varepsilon_{\overline{2}}}n_{-\varepsilon_{\overline{1}}}\tilde{G}^{\varepsilon_{\overline{2}},\varepsilon_{\overline{1}}}\right]$$

$$= (2\pi\mathrm{i})^2 S^{\mathrm{r}}_{(\overline{123})}, \tag{C.93}$$

where we used in the first line $\tilde{G}^{\varepsilon_{\overline{23}},\varepsilon_{\overline{2}}} = -\tilde{G}^{\varepsilon_{\overline{3}},\varepsilon_{\overline{2}}} - \tilde{G}^{\varepsilon_{\overline{2}},\varepsilon_{\overline{1}}}$ (following from Eqs. (C.39)), in the second line $n_{\varepsilon_{\overline{2}}}(n_{\varepsilon_{\overline{3}}} - n_{\varepsilon_{\overline{23}}}) = -n_{\varepsilon_{\overline{12}}}n_{-\varepsilon_{\overline{1}}}$, and in the third line

$$\zeta^{\overline{1}}e^{\beta\varepsilon_{\overline{1}}}n_{-\varepsilon_{\overline{1}}} = \frac{\zeta^{\overline{1}}e^{\beta\varepsilon_{\overline{1}}}}{\zeta^{\overline{1}}e^{\beta\varepsilon_{\overline{1}}} - 1} = -n_{\varepsilon_{\overline{1}}}. \tag{C.94}$$

For the $\hat{G}$ terms, we similarly obtain

$$\zeta^{\overline{1}}e^{\beta\varepsilon_{\overline{1}}}(2\pi\mathrm{i})^2 S^{\mathrm{a}}_{(\overline{231})}$$

$$= \zeta^{\overline{1}}e^{\beta\varepsilon_{\overline{1}}}\left[\hat{\delta}(\varepsilon_{\overline{2}})n_{\varepsilon_{\overline{3}}}\hat{G}^{\Delta;\varepsilon_{\overline{3}}}_{\overline{2}} + \hat{\delta}(\varepsilon_{\overline{3}})n_{\varepsilon_{\overline{2}}}\hat{G}^{\Delta;\varepsilon_{\overline{2}}}_{\overline{3}} + \hat{\delta}(\varepsilon_{\overline{1}})n_{\varepsilon_{\overline{2}}}\hat{G}^{\Delta;\varepsilon_{\overline{2}}}_{\overline{1}} + \hat{\delta}(\varepsilon_{\overline{2}})\hat{\delta}(\varepsilon_{\overline{3}})\left(\hat{G}_{\overline{2},\overline{3}} - \tfrac{1}{2}\hat{G}^{\Delta}_{\overline{1};\overline{2}}\right)\right]$$

$$= \zeta^{\overline{1}}e^{\beta\varepsilon_{\overline{1}}}\left[-\hat{\delta}(\varepsilon_{\overline{2}})n_{-\varepsilon_{\overline{1}}}\hat{G}^{\Delta;\varepsilon_{\overline{1}}}_{\overline{2}} - \hat{\delta}(\varepsilon_{\overline{3}})n_{-\varepsilon_{\overline{1}}}\hat{G}^{\Delta;\varepsilon_{\overline{1}}}_{\overline{3}} + \hat{\delta}(\varepsilon_{\overline{1}})n_{\varepsilon_{\overline{2}}}\hat{G}^{\Delta;\varepsilon_{\overline{2}}}_{\overline{1}} + \hat{\delta}(\varepsilon_{\overline{1}})\hat{\delta}(\varepsilon_{\overline{2}})\left(\hat{G}_{\overline{1},\overline{2}} - \tfrac{1}{2}\hat{G}^{\Delta}_{\overline{3};\overline{1}}\right)\right]$$

$$= (2\pi\mathrm{i})^2 S^{\mathrm{a}}_{(\overline{123})}. \tag{C.95}$$

In the last step, we used that $\hat{G}_{\overline{1}} \neq 0$ and $\hat{G}_{\overline{1},\overline{2}} \neq 0$ imply $\zeta^{\overline{1}} = +1$. Thus, we find that our 3p formula (5.48) indeed fulfills the equilibrium condition.

For 4p PSFs, we confirmed the fulfillment of the equilibrium condition by inserting the analytic regions (C.60) for the discontinuities and by comparing the coefficients.

C.7.2 Full recovery of spectral information

Equations (5.21), (5.48), and (5.62) contain formulas for PSFs, $S_p[G]$, as functionals of the MF correlator G for $\ell = 2, 3, 4$. In this section, we explicitly perform the following consistency check: given an arbitrary set of PSFs S_p as input, compute the MF correlator $G = \sum_p K * S_p$ and verify that $S_p[G]$ correctly recovers the input PSFs. To this end, we insert results from App. C.5 to express the discontinuities in the formulas via PSF (anti)commutators. From the resulting expressions, we then show $S_p[G] = S_p$ by use of the equilibrium condition (2.47).

C.7.2.1 For $\ell = 2$

We first examine the relations between the MF correlator and the PSF contributions. Using the decomposition of PSFs from App. C.2.1, the standard spectral function reads

$$S_{\mathrm{std}}(\varepsilon_1) = S_{[1,2]_-}(\varepsilon_1, -\varepsilon_1) = \tilde{S}_{[1,2]_-}(\varepsilon_1, -\varepsilon_1). \tag{C.96}$$

For bosonic functions, $\zeta = +1$, there may be anomalous contributions $\delta(\epsilon_{\overline{1}})\check{S}_{p;\overline{1}}$. However, the equilibrium condition implies $\check{S}_{(12);1} = \check{S}_{(21);2}$, so that the anomalous contributions cancel in the PSF commutator. Instead, they solely enter the anomalous correlator, $\hat{G}(\mathrm{i}\omega_1) = \beta\delta_{\mathrm{i}\omega_1}\hat{G}_1$, via the spectral representation with kernel (C.4a), yielding

$$\hat{G}_1 = -\check{S}_{(12);1}. \tag{C.97}$$

Now, we can show that Eq. (5.21) recovers the input PSFs from the MF correlator. Inserting $\tilde{G}^{\varepsilon_1} = -\tilde{G}^{\varepsilon_2} = (-2\pi\mathrm{i})S^{\mathrm{std}}(\varepsilon_1)$ (Eq. (5.25)) and Eq. (C.97) into Eq. (5.21) yields

$$S_p[G] = \frac{1}{2\pi\mathrm{i}}\left[n_{\varepsilon_{\overline{1}}}\tilde{G}^{\varepsilon_{\overline{1}}} + \hat{\delta}(\varepsilon_{\overline{1}})\hat{G}_{\overline{1}}\right] = -n_{\varepsilon_{\overline{1}}}\tilde{S}_{[\overline{1},\overline{2}]_-} + \delta_{\varepsilon_{\overline{1}}}S_{(\overline{12})}. \tag{C.98}$$

(Here and in the following, we suppress frequency arguments of PSFs.) To simplify the PSF commutator, we can use the equilibrium condition (2.47) to obtain

$$-n_{\varepsilon_{\bar{1}}}\tilde{S}_{[\bar{1},\bar{2}]_-} = \frac{-1}{\zeta^{\bar{1}}e^{-\beta\varepsilon_{\bar{1}}}-1}[\tilde{S}_{(\overline{12})} - \zeta^{\bar{1}}e^{-\beta\varepsilon_{\bar{1}}}\tilde{S}_{(\overline{12})}] = \tilde{S}_{(\overline{12})} = (1-\delta_{\varepsilon_{\bar{1}}})S_{(\overline{12})}. \tag{C.99}$$

For bosonic 2p functions, the MWF $n_{\varepsilon_{\bar{1}}}$ is undefined for $\varepsilon_{\bar{1}} = 0$. But since $\tilde{S}_p$ then has no $\delta(\varepsilon_{\bar{1}})$ contribution, the left and right side of Eq. (5.21) can only differ by zero spectral weight. We can nevertheless recover the correct value for $\tilde{S}_p(\varepsilon_{\bar{1}})$ at $\varepsilon_{\bar{1}} = 0$ if we demand that continuum contributions are (piece-wise) continuous. Then, the correct value at $\varepsilon_{\bar{1}} = 0$ is obtained from the formula in Eq. (5.21) by taking the appropriate limit.

Inserting Eq. (C.99) into Eq. (C.98) results in

$$S_p[G] = (1-\delta_{\varepsilon_{\bar{1}}})S_{(\overline{12})} + \delta_{\varepsilon_{\bar{1}}}S_{(\overline{12})} = S_{(\overline{12})}, \tag{C.100}$$

concluding our proof.

C.7.2.2 For $\ell = 3$

Following the line of argument for $\ell = 2$ from the previous section, we now check that the formula $S_p[G]$ recovers the input PSF S_p also for $\ell = 3$. Analogously to Eq. (C.99), the MWFs can be eliminated using the identity (suppressing frequency arguments)

$$S_{(\overline{123})} = -n_{\varepsilon_{\bar{1}}}S_{[\bar{1},\overline{23}]_-} + \delta_{\varepsilon_{\bar{1}}}S_{(\overline{123})}, \tag{C.101a}$$

$$S_{(\overline{231})} = n_{-\varepsilon_{\bar{1}}}S_{[\bar{1},\overline{23}]_-} + \delta_{\varepsilon_{\bar{1}}}S_{(\overline{231})}. \tag{C.101b}$$

Note that $\delta(\varepsilon_{\bar{1}})$ contributions cancel in $S_{[\bar{1},\overline{23}]_-}$ for $\zeta^{\bar{1}} = +$ due to the equilibrium condition (as before), i.e., $S_{[\bar{1},\overline{23}]_-} = (1-\delta_{\varepsilon_{\bar{1}}})S_{[\bar{1},\overline{23}]_-}$. Hence, such terms must be treated separately to obtain the PSF on the left.

In App. C.5.1, we have already shown that the discontinuities in the 3p PSF are proportional to nested PSF commutators. Analogously to the derivations for Eqs. (C.13a), (C.69), and (C.65), we obtain the following relations:

$$\hat{\delta}(\varepsilon_{\bar{1}})\hat{\delta}(\varepsilon_{\bar{2}})\hat{G}_{\bar{1},\bar{2}} = (2\pi i)^2\tfrac{1}{2}\delta_{\varepsilon_{\bar{1}}}\delta_{\varepsilon_{\bar{2}}}S_{\bar{1}[\bar{2},\bar{3}]_+},$$

$$\hat{\delta}(\varepsilon_{\bar{1}})\hat{\delta}(\varepsilon_{\bar{2}})\hat{G}^{\Delta}_{\bar{3};\bar{1}} = -(2\pi i)^2\delta_{\varepsilon_{\bar{1}}}\delta_{\varepsilon_{\bar{2}}}S_{\bar{1}[\bar{2},\bar{3}]_-},$$

$$\hat{\delta}(\varepsilon_{\bar{1}})\hat{G}^{\Delta;\varepsilon_{\bar{2}}}_{\bar{1}} = -(2\pi i)^2\delta_{\varepsilon_{\bar{1}}}(1-\delta_{\varepsilon_{\bar{2}}})S_{\bar{1}[\bar{2},\bar{3}]_-},$$

$$\hat{\delta}(\varepsilon_{\bar{2}})\hat{G}^{\Delta;\varepsilon_{\bar{1}}}_{\bar{2}} = -(2\pi i)^2\delta_{\varepsilon_{\bar{2}}}(1-\delta_{\varepsilon_{\bar{1}}})S_{\bar{2}[\bar{1},\bar{3}]_-},$$

$$\hat{\delta}(\varepsilon_{\bar{3}})\hat{G}^{\Delta;\varepsilon_{\bar{1}}}_{\bar{3}} = -(2\pi i)^2\delta_{\varepsilon_{\bar{3}}}(1-\delta_{\varepsilon_{\bar{1}}})S_{[\bar{1},\bar{2}]_-\bar{3}},$$

$$\tilde{G}^{\varepsilon_{\bar{2}},\varepsilon_{\bar{1}}} = (2\pi i)^2 S_{[\bar{2},[\bar{1},\bar{3}]_-]_-},$$

$$\tilde{G}^{\varepsilon_{\overline{12}},\varepsilon_{\bar{1}}} = -(2\pi i)^2 S_{[\bar{3},[\bar{1},\bar{2}]_-]_-}. \tag{C.102}$$

Inserting these into Eq. (5.48) yields

$$S_p[G] = \frac{1}{(2\pi i)^2}\left[n_{\varepsilon_{\bar{1}}}\left(n_{\varepsilon_{\bar{2}}}\tilde{G}^{\varepsilon_{\bar{2}},\varepsilon_{\bar{1}}} + \hat{\delta}(\varepsilon_{\bar{2}})\hat{G}^{\Delta;\varepsilon_{\bar{1}}}_{\bar{2}} + n_{\varepsilon_{\overline{12}}}\tilde{G}^{\varepsilon_{\overline{12}},\varepsilon_{\bar{1}}} + \hat{\delta}(\varepsilon_{\bar{3}})\hat{G}^{\Delta;\varepsilon_{\bar{1}}}_{\bar{3}}\right)\right.$$

$$\left. + \hat{\delta}(\varepsilon_{\bar{1}})n_{\varepsilon_{\bar{2}}}\hat{G}^{\Delta;\varepsilon_{\bar{2}}}_{\bar{1}} - \tfrac{1}{2}\hat{\delta}(\varepsilon_{\bar{1}})\hat{\delta}(\varepsilon_{\bar{2}})\left(\hat{G}^{\Delta}_{\bar{3};\bar{1}} - 2\hat{G}_{\bar{1},\bar{2}}\right)\right]$$

$$= n_{\varepsilon_{\bar{1}}} \left(n_{\varepsilon_{\bar{2}}} S_{[\bar{2},[\bar{1},\bar{3}]-]-} - \delta_{\varepsilon_{\bar{2}}}(1 - \delta_{\varepsilon_{\bar{1}}}) S_{\bar{2}[\bar{1},\bar{3}]-} - n_{\varepsilon_{\overline{12}}} S_{[\bar{3},[\bar{1},\bar{2}]-]-} - \delta_{\varepsilon_{\bar{3}}}(1 - \delta_{\varepsilon_{\bar{1}}}) S_{[\bar{1},\bar{2}]-\bar{3}} \right)$$
$$- n_{\varepsilon_{\bar{2}}} \delta_{\varepsilon_{\bar{1}}}(1 - \delta_{\varepsilon_{\bar{2}}}) S_{\bar{1}[\bar{2},\bar{3}]-} + \delta_{\varepsilon_{\bar{1}}} \delta_{\varepsilon_{\bar{2}}} S_{(\overline{123})}. \tag{C.103}$$

We can now check whether Eq. (C.103) reproduces the full PSF, $S_{(\overline{123})}$, by repeated application of Eqs. (C.101). For this purpose, we use the PSF decomposition in App. C.2.1 to separately consider the contributions in the PSF proportional to $\delta(\varepsilon_{\bar{1}})$, and those which are not. Note that $S_{[\bar{2},[\bar{1},\bar{3}]-]-}$ and $S_{[[\bar{1},\bar{2}]-,\bar{3}]-}$ in the third line of Eq. (C.103) contribute to both of these cases.

For PSF contributions not proportional to $\delta(\varepsilon_{\bar{1}})$, the last line of Eq. (C.103) can be omitted (due to $\delta_{\varepsilon_{\bar{1}}}$), so that

$$(1 - \delta_{\varepsilon_{\bar{1}}}) S_p[G] = -(1 - \delta_{\varepsilon_{\bar{1}}}) n_{\varepsilon_{\bar{1}}} \left(-n_{\varepsilon_{\bar{2}}} S_{[\bar{2},[\bar{1},\bar{3}]-]-} + \delta_{\varepsilon_{\bar{2}}} S_{\bar{2}[\bar{1},\bar{3}]-} + n_{-\varepsilon_{\bar{3}}} S_{[\bar{3},[\bar{1},\bar{2}]-]-} + \delta_{\varepsilon_{\bar{3}}} S_{[\bar{1},\bar{2}]-\bar{3}} \right)$$
$$= -(1 - \delta_{\varepsilon_{\bar{1}}}) n_{\varepsilon_{\bar{1}}} \left(S_{\bar{2}[\bar{1},\bar{3}]-} + S_{[\bar{1},\bar{2}]-\bar{3}} \right) = -(1 - \delta_{\varepsilon_{\bar{1}}}) n_{\varepsilon_{\bar{1}}} S_{[\bar{1},\overline{23}]-}$$
$$= (1 - \delta_{\varepsilon_{\bar{1}}}) S_{(\overline{123})}. \tag{C.104}$$

Here, we used Eqs. (C.101) in the first and third step.

For PSF contributions proportional to $\delta(\varepsilon_{\bar{1}})$, the MWF $n_{\varepsilon_{\bar{1}}}$ multiplying $S_{[\bar{2},[\bar{1},\bar{3}]-]-}$ and $S_{[[\bar{1},\bar{2}]-,\bar{3}]-}$ in Eq. (C.103) seems to diverge in the bosonic case. This issue was already discussed in Eq. (C.41) (for unpermuted indices): There, $\tilde{G}^{\varepsilon_{\bar{1}},\varepsilon_{\overline{12}}} = (2\pi i)^2 S_{[\bar{1},[\bar{2},\bar{3}]-]-}$ does not contain factors $\delta(\varepsilon_{\bar{1}})$ due to the equilibrium condition, and therefore only the first term, expressed as $-n_{\varepsilon_{\overline{12}}} n_{-\varepsilon_{\bar{2}}} S_{[\bar{2},[\bar{1},\bar{3}]-]-}$, needs to be considered. As this PSF commutator does not contain factors $\delta(\varepsilon_{\bar{2}})$ due to the equilibrium condition, we obtain (using $n_{\varepsilon_{\bar{2}}} = n_{\varepsilon_{\overline{12}}} = n_{-\varepsilon_{\bar{3}}}$ and $\delta_{\varepsilon_{\bar{2}}} = \delta_{\varepsilon_{\overline{12}}} = \delta_{\varepsilon_{\bar{3}}}$ due to $\delta_{\varepsilon_{\bar{1}}}$)

$$\delta_{\varepsilon_{\bar{1}}} S_p[G] = \delta_{\varepsilon_{\bar{1}}} \left(-n_{\varepsilon_{\bar{2}}} n_{-\varepsilon_{\bar{2}}} S_{[\bar{2},[\bar{1},\bar{3}]-]-} - n_{\varepsilon_{\overline{12}}}(1 - \delta_{\varepsilon_{\bar{2}}}) S_{\bar{1}[\bar{2},\bar{3}]-} + \delta_{\varepsilon_{\bar{2}}} S_{(\overline{123})} \right)$$
$$= \delta_{\varepsilon_{\bar{1}}} \left(-n_{\varepsilon_{\bar{2}}}(1 - \delta_{\varepsilon_{\bar{2}}}) S_{[\bar{1},\bar{3}]-\bar{2}} - n_{\varepsilon_{\overline{12}}}(1 - \delta_{\varepsilon_{\bar{2}}}) S_{\bar{1}[\bar{2},\bar{3}]-} + \delta_{\varepsilon_{\bar{2}}} S_{(\overline{123})} \right)$$
$$= \delta_{\varepsilon_{\bar{1}}} \left(n_{-\varepsilon_{\bar{3}}}(1 - \delta_{\varepsilon_{\bar{3}}}) S_{[\bar{3},\overline{12}]-} + \delta_{\varepsilon_{\bar{3}}} S_{(\overline{123})} \right) = \delta_{\varepsilon_{\bar{1}}} \left((1 - \delta_{\varepsilon_{\bar{3}}}) S_{(\overline{123})} + \delta_{\varepsilon_{\bar{3}}} S_{(\overline{123})} \right)$$
$$= \delta_{\varepsilon_{\bar{1}}} S_{(\overline{123})}. \tag{C.105}$$

Here, Eq. (C.101b) was applied in the first and the third step.

Therefore, we conclude that Eq. (C.103) indeed recovers the input PSF $S_{(\overline{123})}$, including terms proportional to $\delta(\varepsilon_{\bar{1}})$ in Eq. (C.105) and those which are not in Eq. (C.104).

C.7.2.3 For $\ell = 4$

Now, the same consistency check can be performed for fermionic 4p correlators. Similarly to Eq. (C.101), for 4p PSFs, we have

$$S_{(\overline{1234})} = -n_{\varepsilon_{\bar{1}}} S_{[\bar{1},\overline{234}]-} \tag{C.106a}$$
$$S_{(\overline{1234})} = -n_{\varepsilon_{\overline{12}}} S_{[\overline{12},\overline{34}]-} + \delta_{\varepsilon_{\overline{12}}} S_{(\overline{1234})}. \tag{C.106b}$$

Here, the symbolic Kronecker δ only arises in the latter case, since $\varepsilon_{\bar{1}}$ is the energy difference for a fermionic operator. Starting from the formula in Eq. (5.62), we obtain

$$
S_p[G] = \frac{n_{\varepsilon_{\bar{1}}}}{(2\pi i)^3}\left[n_{\varepsilon_{\bar{2}}}\left(n_{\varepsilon_{\bar{3}}}\tilde{G}^{\varepsilon_{\bar{3}},\varepsilon_{\bar{2}},\varepsilon_{\bar{1}}} + n_{\varepsilon_{\overline{123}}}\tilde{G}^{\varepsilon_{\overline{123}},\varepsilon_{\bar{2}},\varepsilon_{\bar{1}}} + n_{\varepsilon_{\overline{13}}}\tilde{G}^{\varepsilon_{\overline{13}},\varepsilon_{\bar{2}},\varepsilon_{\bar{1}}} + n_{\varepsilon_{\overline{23}}}\tilde{G}^{\varepsilon_{\overline{23}},\varepsilon_{\bar{2}},\varepsilon_{\bar{1}}} \right) \right.
$$

$$
+ n_{\varepsilon_{\overline{12}}}\left(n_{\varepsilon_{\bar{3}}}\tilde{G}^{\varepsilon_{\bar{3}},\varepsilon_{\overline{12}},\varepsilon_{\bar{1}}} + n_{\varepsilon_{\overline{123}}}\tilde{G}^{\varepsilon_{\overline{123}},\varepsilon_{\overline{12}},\varepsilon_{\bar{1}}} \right) + n_{\varepsilon_{\bar{3}}}\hat{\delta}(\varepsilon_{\overline{12}})\,\hat{G}^{\varepsilon_{\bar{3}},\varepsilon_{\bar{1}}}_{\overline{12}}
$$

$$
\left. + n_{\varepsilon_{\bar{2}}}\hat{\delta}(\varepsilon_{\overline{13}})\,\hat{G}^{\varepsilon_{\bar{2}},\varepsilon_{\bar{1}}}_{\overline{13}} + n_{\varepsilon_{\bar{2}}}\hat{\delta}(\varepsilon_{\overline{23}})\,\hat{G}^{\varepsilon_{\bar{2}},\varepsilon_{\bar{1}}}_{\overline{23}} \right]
$$

$$
= -n_{\varepsilon_{\bar{1}}}\left[n_{\varepsilon_{\bar{2}}}\left(n_{\varepsilon_{\bar{3}}}S_{[\bar{3},[\bar{2},[\bar{1},\bar{4}]_-]_-]_-} + n_{\varepsilon_{\overline{123}}}S_{[[\bar{2},[\bar{1},\bar{3}]_-]_-,\bar{4}]_-} + n_{\varepsilon_{\overline{13}}}S_{[[\bar{1},\bar{3}]_-,[\bar{2},\bar{4}]_-]_-} \right.\right.
$$

$$
\left. - \delta_{\varepsilon_{\overline{13}}}S_{[\bar{1},\bar{3}]_--[\bar{2},\bar{4}]_-} + n_{\varepsilon_{\overline{23}}}S_{[[\bar{2},\bar{3}]_-,[\bar{1},\bar{4}]_-]_-} - \delta_{\varepsilon_{\overline{23}}}S_{[\bar{1},\bar{4}]_--[\bar{2},\bar{3}]_-} \right)
$$

$$
\left. + n_{\varepsilon_{\overline{12}}}\left(n_{\varepsilon_{\bar{3}}}S_{[\bar{3},[[\bar{1},\bar{2}]_-,\bar{4}]_-]_-} + n_{\varepsilon_{\overline{123}}}S_{[[[\bar{1},\bar{2}]_-,\bar{3}]_-,\bar{4}]_-} \right) - n_{\varepsilon_{\bar{3}}}\delta_{\varepsilon_{\overline{12}}}S_{[\bar{1},\bar{2}]_--[\bar{3},\bar{4}]_-} \right]
$$

$$\tag{C.107a}$$

$$
= n_{\varepsilon_{\bar{1}}}\left[n_{\varepsilon_{\bar{2}}}\left(S_{\bar{3}[\bar{2},[\bar{1},\bar{4}]_-]_-} + S_{[\bar{2},[\bar{1},\bar{3}]_-]_-\bar{4}} + S_{[\bar{1},\bar{3}]_--[\bar{2},\bar{4}]_-} + S_{[\bar{2},\bar{3}]_--[\bar{1},\bar{4}]_-} \right) \right.
$$

$$
+ n_{\varepsilon_{\overline{12}}}(1 - \delta_{\varepsilon_{\overline{12}}})\left(S_{\bar{3}[[\bar{1},\bar{2}]_-,\bar{4}]_-]_-} + S_{[[\bar{1},\bar{2}]_-,\bar{3}]_-\bar{4}} \right)
$$

$$
\left. - n_{\varepsilon_{\bar{3}}}\delta_{\varepsilon_{\overline{12}}}\left(S_{\bar{4}[[\bar{1},\bar{2}]_-,\bar{3}]_-} - S_{[\bar{1},\bar{2}]_--[\bar{3},\bar{4}]_-} \right) \right]
$$

$$
= n_{\varepsilon_{\bar{1}}}\left[n_{\varepsilon_{\bar{2}}}S_{[[\overline{34},\bar{1}]_-,\bar{2}]_-} + n_{\varepsilon_{\overline{12}}}S_{[[\bar{1},\bar{2}]_-,\overline{34}]_-} - \delta_{\varepsilon_{\overline{12}}}S_{[\bar{1},\bar{2}]_--\overline{34}} \right]
$$

$$
= -n_{\varepsilon_{\bar{1}}}S_{[\bar{1},\overline{234}]} = S_{(\overline{1234})}. \tag{C.107b}
$$

In the first step, we inserted expressions for the discontinuities, derived analogously to Eqs. (C.13a), (C.65), and (C.69). We applied relations (C.106) to eliminate the MWFs in the remaining steps. For the second step, we note that $S_{[\bar{3},[[\bar{1},\bar{2}]_-,\bar{4}]_-]_-}$ and $S_{[[[\bar{1},\bar{2}]_-,\bar{3}]_-,\bar{4}]_-}$ contain terms with and without $\delta(\varepsilon_{\overline{12}})$ factor. For the $\delta(\varepsilon_{\overline{12}})$ terms, the prefactor of $n_{\varepsilon_{\overline{12}}}$ is undefined at $\varepsilon_{\overline{12}}$. Analogously to the 3p calculation, we evaluate Eq. (C.107a) using $\delta_{\varepsilon_{\overline{12}}}(S_{[\bar{3},[[\bar{1},\bar{2}]_-,\bar{4}]_-]_-} + S_{[[[\bar{1},\bar{2}]_-,\bar{3}]_-,\bar{4}]_-}) = 0$ and $n_{-\varepsilon_{\overline{34}}}(-n_{\varepsilon_{\bar{3}}} + n_{-\varepsilon_{\bar{4}}}) = n_{-\varepsilon_{\bar{3}}}n_{-\varepsilon_{\bar{4}}}$:

$$
n_{\varepsilon_{\overline{12}}}\left(n_{\varepsilon_{\bar{3}}}S_{[\bar{3},[[\bar{1},\bar{2}]_-,\bar{4}]_-]_-} + n_{\varepsilon_{\overline{123}}}S_{[[[\bar{1},\bar{2}]_-,\bar{3}]_-,\bar{4}]_-} \right) \tag{C.108}
$$

$$
= n_{\varepsilon_{\overline{12}}}(1 - \delta_{\varepsilon_{\overline{12}}})\left(n_{\varepsilon_{\bar{3}}}S_{[\bar{3},[[\bar{1},\bar{2}]_-,\bar{4}]_-]_-} + n_{\varepsilon_{\overline{123}}}S_{[[[\bar{1},\bar{2}]_-,\bar{3}]_-,\bar{4}]_-} \right) + \delta_{\varepsilon_{\overline{12}}}n_{-\varepsilon_{\bar{3}}}n_{-\varepsilon_4}S_{[[[\bar{1},\bar{2}]_-,\bar{3}]_-,\bar{4}]_-}.
$$

To simplify the $\delta_{\varepsilon_{12}}$ terms in the third step, remember that the Kronecker symbol extracts those PSF contributions proportional to a $\delta(\varepsilon_{12})$, such that the equilibrium condition allows for manipulations like $\delta_{\varepsilon_{12}}S_{1234} = \delta_{\varepsilon_{12}}S_{3412}$. Finally, Eq. (C.107b) shows that the formula in Eq. (5.62) fully recovers the input PSFs from 4p MF correlators.

C.8 Additional Hubbard atom material

C.8.1 Useful identities

In this section, we prove the identities given in Eqs. (5.81a) and (5.81b). The first identity follows from

$$\lim_{\gamma_0 \to 0^+} \left(\frac{\omega + \mathrm{i}\gamma_0}{(\omega + \mathrm{i}\gamma_0)^2 - u^2} - \frac{\omega - \mathrm{i}\gamma_0}{(\omega - \mathrm{i}\gamma_0)^2 - u^2} \right) = -\mathrm{i} \lim_{\gamma_0 \to 0^+} \left(\frac{\gamma_0}{(\omega + u)^2 + \gamma_0^2} + \frac{\gamma_0}{(\omega - u)^2 + \gamma_0^2} \right)$$
$$= -\mathrm{i}\pi \left[\delta(\omega + u) + \delta(\omega - u) \right], \qquad (C.109)$$

where we used Eq. (5.32). Identity (5.81b) is derived via

$$\lim_{\gamma_0 \to 0^+} \left(\frac{1}{(\omega + \mathrm{i}\gamma_0)^2 - u^2} - \frac{1}{(\omega - \mathrm{i}\gamma_0)^2 - u^2} \right) = \frac{\mathrm{i}}{u} \lim_{\gamma_0 \to 0^+} \left(\frac{\gamma_0}{(\omega + u)^2 + \gamma_0^2} - \frac{\gamma_0}{(\omega - u)^2 + \gamma_0^2} \right)$$
$$= \frac{\mathrm{i}\pi}{u} \left[\delta(\omega + u) - \delta(\omega - u) \right]. \qquad (C.110)$$

C.8.2 Simplifications for 3p electron-density correlator

In Sec. 5.7.2.1, we introduced the 3p electron-density correlator with regular and anomalous parts

$$\tilde{G}(\mathrm{i}\omega_1, \mathrm{i}\omega_2) = \frac{u^2 - \mathrm{i}\omega_1 \, \mathrm{i}\omega_2}{\left[(\mathrm{i}\omega_1)^2 - u^2 \right] \left[(\mathrm{i}\omega_2)^2 - u^2 \right]},$$
$$\hat{G}_3(\mathrm{i}\omega_1) = \frac{u \, \mathrm{t}}{2} \frac{1}{(\mathrm{i}\omega_1)^2 - u^2}. \qquad (C.111)$$

Here, we derive the explicit expression $G'^{[2]} - G^{[3]}$ given in Eq. (5.88),

$$G'^{[2]} - G^{[3]} = \tilde{G}(\omega_1^+, \omega_2^-) - \tilde{G}(\omega_1^-, \omega_2^-) \qquad (C.112)$$
$$= \frac{u^2}{(\omega_2^-)^2 - u^2} \left(\frac{1}{(\omega_1^+)^2 - u^2} - \frac{1}{(\omega_1^-)^2 - u^2} \right) - \frac{\omega_2^-}{(\omega_2^-)^2 - u^2} \left(\frac{\omega_1^+}{(\omega_1^+)^2 - u^2} - \frac{\omega_1^-}{(\omega_1^-)^2 - u^2} \right).$$

Using both identities (C.109) and (C.110), this expression can be further simplified to

$$G'^{[2]} - G^{[3]} = \pi \mathrm{i} \frac{u + \omega_2^-}{(\omega_2^-)^2 - u^2} \delta(\omega_1 + u) + \pi \mathrm{i} \frac{\omega_2^- - u}{(\omega_2^-)^2 - u^2} \delta(\omega_1 - u). \qquad (C.113)$$

Additionally multiplying both sides with $N_1 = N_{\omega_1}$ and using $N_{-\omega_1} = -N_{\omega_1}$, we recover the first term in the second line of Eq. (5.88),

$$N_1 \left(G'^{[2]} - G^{[3]} \right) = \pi \mathrm{i} \, \mathrm{t} \left[\frac{\delta(\omega_1 - u)}{\omega_2^- + u} - \frac{\delta(\omega_1 + u)}{\omega_2^- - u} \right]. \qquad (C.114)$$

Next, we consider the Keldysh component $G^{[123]}_{d_\uparrow d_\uparrow^\dagger n_\uparrow}$. Since the regular part in Eq. (C.111) is independent of $\mathrm{i}\omega_3$, we can set $G'^{[1]} = G^{[2]}$ and $G'^{[2]} = G^{[1]}$ (see Fig. 5.5(b)). Additionally using Eq. (5.57) as well as $\hat{G}_1 = \hat{G}_2$ for the 3p electron-density correlator, the last FDR in Eq. (5.58) reduces to

$$G^{[123]}_{d_\uparrow d_\uparrow^\dagger n_\uparrow} = G'^{[3]} + N_1 N_2 \left(G'^{[3]} - G^{[2]} - G^{[1]} + G^{[3]} \right) + 4\pi \mathrm{i} \, \delta(\omega_{12}) N_1 \left(\hat{G}_3^{[1]} - \hat{G}_3^{[2]} \right). \qquad (C.115)$$

Here, we show that all terms except $G'^{[3]}$ cancel out. To this end, we can reuse Eq. (C.113) to obtain

$$
\begin{aligned}
&G'^{[3]} - G^{[2]} - G^{[1]} + G^{[3]} \\
&= \tilde{G}(\omega_1^+, \omega_2^+, \omega_3^-) - \tilde{G}(\omega_1^-, \omega_2^+, \omega_3^-) - \tilde{G}(\omega_1^+, \omega_2^-, \omega_3^-) + \tilde{G}(\omega_1^-, \omega_2^-, \omega_3^+) \\
&= \pi i\, \delta(\omega_1 + u) \left(\frac{1}{\omega_2^+ - u} - \frac{1}{\omega_2^- - u} \right) + \pi i\, \delta(\omega_1 - u) \left(\frac{1}{\omega_2^+ + u} - \frac{1}{\omega_2^- + u} \right) \\
&= 2\pi^2 \left[\delta(\omega_1 + u)\delta(\omega_2 - u) + \delta(\omega_1 - u)\delta(\omega_2 + u) \right] \\
&= 2\pi^2 \delta(\omega_{12}) \left[\delta(\omega_1 + u) + \delta(\omega_1 - u) \right].
\end{aligned}
\tag{C.116}
$$

The discontinuity of $\hat{G}_3$ is easily evaluated with identity (C.110)

$$
\hat{G}_3^{[1]} - \hat{G}_3^{[2]} = \frac{u\, t}{2} \left(\frac{1}{(\omega_1^+)^2 - u^2} - \frac{1}{(\omega_1^-)^2 - u^2} \right) = \pi i \frac{t}{2} \left[\delta(\omega_1 + u) - \delta(\omega_1 - u) \right].
\tag{C.117}
$$

Inserting all terms (except $G'^{[3]}$) in Eq. (C.115) and using again $N_i = N_{\omega_i} = -N_{-\omega_i}$, we find

$$
\begin{aligned}
&N_1 N_2 \left(G'^{[3]} - G^{[2]} - G^{[1]} + G^{[3]} \right) + 4\pi i\, \delta(\omega_{12}) N_1 \sqrt{2} \left(\hat{G}_3^{[1]} - \hat{G}_3^{[2]} \right) \\
&= -2\pi^2 t^2 \delta(\omega_{12}) \left[\delta(\omega_1 + u) + \delta(\omega_1 - u) \right] + 2\pi^2 t^2 \delta(\omega_{12}) \left[\delta(\omega_1 + u) + \delta(\omega_1 - u) \right] = 0.
\end{aligned}
\tag{C.118}
$$

Thus, Eq. (C.115) reduces to

$$
G^{[123]}_{d_\uparrow d_\uparrow^\dagger n_\uparrow} = G'^{[3]},
\tag{C.119}
$$

corresponding to the last equality in Eq. (5.89).

Bibliography

[P1] J. Halbinger and M. Punk, *Quenched disorder at antiferromagnetic quantum critical points in two-dimensional metals*, Phys. Rev. B **103** (2021), 235157. See pages: ix, 3, 133, 134, 138, 139, and 161

[P2] J. Halbinger, B. Schneider, and B. Sbierski, *Spectral representation of Matsubara n-point functions: Exact kernel functions and applications*, SciPost Phys. **15** (2023), 183. See pages: ix, 2, 5, 11, 19, 22, 24, 32, 39, 40, 64, 65, 90, 91, 161, 173, 174, 175, and 194

[P3] J.-M. Lihm, J. Halbinger, J. Shim, J. von Delft, F. B. Kugler, and S.-S. B. Lee, *Symmetric improved estimators for multipoint vertex functions*, arXiv preprint arXiv:2310.12098 (2023). See pages: ix, 3, 5, 14, 35, 36, 88, 93, 94, 95, 161, and 165

[P4] A. Ge, J. Halbinger, S.-S. B. Lee, J. von Delft, and F. B. Kugler, *Analytic continuation of multipoint correlation functions*, arXiv preprint arXiv:2311.11389 (2023). See pages: ix, 2, 11, 13, 14, 15, 19, 22, 23, 24, 27, 28, 30, 31, 33, 40, 61, 91, 161, and 173

[AC00] A. Abanov and A. V. Chubukov, *Spin-Fermion Model near the Quantum Critical Point: One-Loop Renormalization Group Results*, Phys. Rev. Lett. **84** (2000), 5608–5611. See pages: 1 and 134

[AC04] A. Abanov and A. Chubukov, *Anomalous Scaling at the Quantum Critical Point in Itinerant Antiferromagnets*, Phys. Rev. Lett. **93** (2004), 255702. See pages: 134 and 137

[ACS03] A. Abanov, A. V. Chubukov, and J. Schmalian, *Quantum-critical theory of the spin-fermion model and its application to cuprates: Normal state analysis*, Adv. Phys. **52** (2003), no. 3, 119–218. See pages: 1, 134, 136, 137, and 138

[ADG75] A. A. Abrikosov, I. Dzyaloshinskii, and L. P. Gorkov, *Methods of Quantum Field Theory in Statistical Physics*, Dover Publ., 1975. See page: 1

[AKC+22] S. Adler, F. Krien, P. Chalupa-Gantner, G. Sangiovanni, and A. Toschi, *Non-perturbative intertwining between spin and charge correlations: A "smoking gun" single-boson-exchange result*, arXiv preprint arXiv:2212.09693 (2022). See pages: 88 and 161

[And61] P. W. Anderson, *Localized Magnetic States in Metals*, Phys. Rev. **124** (1961), 41–53. See page: 3

[AP15] T. Ayral and O. Parcollet, *Mott physics and spin fluctuations: A unified framework*, Phys. Rev. B **92** (2015), 115109. See pages: 39 and 40

[AP16] T. Ayral and O. Parcollet, *Mott physics and spin fluctuations: A functional viewpoint*, Phys. Rev. B **93** (2016), 235124. See pages: 39 and 40

[AS10] A. Altland and B. D. Simons, *Condensed Matter Field Theory*, 2nd ed., Cambridge University Press, 2010. See pages: 1, 2, 25, and 133

[ATL12]   ATLAS Collaboration, *Observation of a new particle in the search for the Standard Model Higgs boson with the ATLAS detector at the LHC*, Phys. Lett. B **716** (2012), no. 1, 1–29. See page: 1

[BCP08]   R. Bulla, T. A. Costi, and T. Pruschke, *Numerical renormalization group method for quantum impurity systems*, Rev. Mod. Phys. **80** (2008), 395–450. See pages: 17 and 93

[BCS57a] J. Bardeen, L. N. Cooper, and J. R. Schrieffer, *Microscopic Theory of Superconductivity*, Phys. Rev. **106** (1957), 162–164. See page: 1

[BCS57b] J. Bardeen, L. N. Cooper, and J. R. Schrieffer, *Theory of Superconductivity*, Phys. Rev. **108** (1957), 1175–1204. See page: 1

[BF04]   H. Bruus and K. Flensberg, *Many-Body Quantum Theory in Condensed Matter Physics*, Oxford Graduate Texts, 2004. See pages: 12, 20, and 21

[BFK+15] M. Bartelmann, B. Feuerbacher, T. Krüger, D. Lüst, A. Rebhan, and A. Wipf, *Theoretische Physik*, Springer-Verlag, 2015. See page: 10

[BHP98]   R. Bulla, A. C. Hewson, and T. Pruschke, *Numerical renormalization group calculations for the self-energy of the impurity Anderson model*, J. Phys.: Condens. Matter **10** (1998), no. 37, 8365. See pages: 3 and 93

[BLST19] E. Berg, S. Lederer, Y. Schattner, and S. Trebst, *Monte Carlo Studies of Quantum Critical Metals*, Ann. Rev. of Cond. Mat. Phys. **10** (2019), no. 1, 63–84. See page: 1

[BM61]   G. Baym and N. D. Mermin, *Determination of Thermodynamic Green's Functions*, J. Math. Phys. **2** (1961), no. 2, 232–234. See page: 2

[BM86]   J. G. Bednorz and K. A. Müller, *Possible High Tc Superconductivity in the Ba-La-Cu-O System*, Z. Phys. B **64** (1986), no. 2, 189–193. See page: 1

[CdCL+84] C. Castellani, C. di Castro, P. A. Lee, M. Ma, S. Sorella, and E. Tabet, *Spin fluctuations in disordered interacting electrons*, Phys. Rev. B **30** (1984), 1596–1598. See page: 139

[CGS+18] P. Chalupa, P. Gunacker, T. Schäfer, K. Held, and A. Toschi, *Divergences of the irreducible vertex functions in correlated metallic systems: Insights from the Anderson impurity model*, Phys. Rev. B **97** (2018), no. 24, 245136. See page: 88

[CMS12]   CMS Collaboration, *Observation of a new boson at a mass of 125 GeV with the CMS experiment at the LHC*, Phys. Lett. B **716** (2012), no. 1, 30–61. See page: 1

[CSR+21] P. Chalupa, T. Schäfer, M. Reitner, D. Springer, S. Andergassen, and A. Toschi, *Fingerprints of the Local Moment Formation and its Kondo Screening in the Generalized Susceptibilities of Many-Electron Problems*, Phys. Rev. Lett. **126** (2021), 056403. See pages: 88 and 161

[DL13]   D. Dalidovich and S.-S. Lee, *Perturbative non-Fermi liquids from dimensional regularization*, Phys. Rev. B **88** (2013), 245106. See page: 138

[Dot00]   V. Dotsenko, *Introduction to the Replica Theory of Disordered Statistical Systems*, Cambridge University Press, 2000. See page: 140

[Dot10] V. Dotsenko, *One more discussion of the replica trick: the examples of exact solutions*, arXiv preprint arXiv:1010.3913 (2010). See page: 140

[EB64] F. Englert and R. Brout, *Broken Symmetry and the Mass of Gauge Vector Mesons*, Phys. Rev. Lett. **13** (1964), 321–323. See page: 1

[EGPS21] I. Esterlis, H. Guo, A. A. Patel, and S. Sachdev, *Large-N theory of critical Fermi surfaces*, Phys. Rev. B **103** (2021), 235129. See page: 162

[EK95] V. J. Emery and S. A. Kivelson, *Superconductivity in Bad Metals*, Phys. Rev. Lett. **74** (1995), 3253–3256. See page: 134

[Eli62] G. M. Eliashberg, *Transport equation for a degenerate system of Fermi particles*, Sov. Phys. JETP **14** (1962), 886. See pages: 2, 39, 40, 61, and 80

[Eva90] T. S. Evans, *Spectral representation of three-point functions at finite temperature*, Phys. Lett. B **252** (1990), no. 1, 108–112. See pages: 2 and 61

[Eva92] T. S. Evans, *N-point finite temperature expectation values at real times*, Nucl. Phys. B **374** (1992), no. 2, 340–370. See pages: 2, 15, 16, 61, and 76

[Fin83] A. M. Finkel'shtein, *Influence of Coulomb interaction on the properties of disordered metals*, Sov. Phys. JETP **57** (1983), 97. See page: 139

[Fra13] E. Fradkin, *Field Theories of Condensed Matter Physics*, 2nd ed., Cambridge University Press, 2013. See pages: 135 and 136

[FYG21] J. Fei, C.-N. Yeh, and E. Gull, *Nevanlinna Analytical Continuation*, Phys. Rev. Lett. **126** (2021), 056402. See page: 161

[FYZG21] J. Fei, C.-N. Yeh, D. Zgid, and E. Gull, *Analytical continuation of matrix-valued functions: Carathéodory formalism*, Phys. Rev. B **104** (2021), 165111. See page: 161

[GCH03] O. Gunnarsson, M. Calandra, and J. E. Han, *Colloquium: Saturation of electrical resistivity*, Rev. Mod. Phys. **75** (2003), 1085–1099. See page: 134

[Ge20] A. Ge, *Analytic Continuation of Correlators from the Matsubara to the Keldysh Formalism*, Master's thesis, Ludwig-Maximilians-Universität München, 2020. See pages: v, 79, 184, 191, and 195

[Ger17] M. H. Gerlach, *Quantum Monte Carlo studies of a metallic spin-density wave transition*, Ph.d. thesis, Universität zu Köln, 2017. See pages: 133, 135, and 136

[GJSS91] J. E. Gubernatis, M. Jarrell, R. N. Silver, and D. S. Sivia, *Quantum Monte Carlo simulations and maximum entropy: Dynamics from imaginary-time data*, Phys. Rev. B **44** (1991), 6011–6029. See page: 2

[GKKR96] A. Georges, G. Kotliar, W. Krauth, and M. J. Rozenberg, *Dynamical mean-field theory of strongly correlated fermion systems and the limit of infinite dimensions*, Rev. Mod. Phys. **68** (1996), 13–125. See page: 93

[GMDSV95] J. González, M. A. Martín-Delgado, G. Sierra, and A. H. Vozmediano, *Quantum Electron Liquids and High-Tc Superconductivity*, Springer-Verlag, 1995. See page: 135

[GMPS20] R. L. Greene, P. R. Mandal, N. R. Poniatowski, and T. Sarkar, *The Strange Metal State of the Electron-Doped Cuprates*, Ann. Rev. of Cond. Mat. Phys. **11** (2020), no. 1, 213–229. See pages: 1 and 134

[GPES22] H. Guo, A. A. Patel, I. Esterlis, and S. Sachdev, *Large-N theory of critical Fermi surfaces. II. Conductivity*, Phys. Rev. B **106** (2022), 115151. See page: 162

[Gri69] R. B. Griffiths, *Nonanalytic Behavior Above the Critical Point in a Random Ising Ferromagnet*, Phys. Rev. Lett. **23** (1969), 17–19. See page: 139

[GRK20] R. Goll, A. Rückriegel, and P. Kopietz, *Zero-magnon sound in quantum Heisenberg ferromagnets*, Phys. Rev. B **102** (2020), 224437. See page: 40

[GRS+17] O. Gunnarsson, G. Rohringer, T. Schäfer, G. Sangiovanni, and A. Toschi, *Breakdown of Traditional Many-Body Theories for Correlated Electrons*, Phys. Rev. Lett. **119** (2017), 056402. See page: 88

[GRW+23] A. Ge, N. Ritz, E. Walter, S. Aguirre, J. von Delft, and F. B. Kugler, *Real-frequency quantum field theory applied to the single-impurity Anderson model*, arXiv preprint arXiv:2307.10791 (2023). See pages: 2, 26, 88, and 162

[GTKK19] R. Goll, D. Tarasevych, J. Krieg, and P. Kopietz, *Spin functional renormalization group for quantum Heisenberg ferromagnets: Magnetization and magnon damping in two dimensions*, Phys. Rev. B **100** (2019), 174424. See page: 40

[Gue94a] F. Guerin, *Rules for diagrams in thermal field theories*, Phys. Rev. D **49** (1994), 4182–4195. See pages: 2 and 61

[Gue94b] F. Guerin, *Retarded-advanced N-point Green functions in thermal field theories*, Nucl. Phys. B **432** (1994), no. 1-2, 281–311. See pages: 2 and 61

[GWG+22] M. Gievers, E. Walter, A. Ge, J. von Delft, and F. B. Kugler, *Multiloop flow equations for single-boson exchange fRG*, Eur. Phys. J. B **95** (2022), no. 7, 108. See pages: 88 and 161

[Her76] J. A. Hertz, *Quantum critical phenomena*, Phys. Rev. B **14** (1976), 1165–1184. See pages: 134 and 137

[HGL23] Z. Huang, E. Gull, and L. Lin, *Robust analytic continuation of Green's functions via projection, pole estimation, and semidefinite relaxation*, Phys. Rev. B **107** (2023), 075151. See page: 161

[Hig64a] P. W. Higgs, *Broken Symmetries and the Masses of Gauge Bosons*, Phys. Rev. Lett. **13** (1964), 508–509. See page: 1

[Hig64b] P. W. Higgs, *Broken symmetries, massless particles and gauge fields*, Phys. Lett. **12** (1964), no. 2, 132–133. See page: 1

[HJB+09] H. Hafermann, C. Jung, S. Brener, M. I. Katsnelson, A. N. Rubtsov, and A. I. Lichtenstein, *Superperturbation solver for quantum impurity models*, EPL **85** (2009), no. 2, 27007. See pages: 2, 39, 40, 88, and 93

[HKV07] J. A. Hoyos, C. Kotabage, and T. Vojta, *Effects of Dissipation on a Quantum Critical Point with Disorder*, Phys. Rev. Lett. **99** (2007), 230601. See page: 140

[HOM04] A. C. Hewson, A. Oguri, and D. Meyer, *Renormalized parameters for impurity models*, Eur. Phys. J. B **40** (2004), no. 2, 177–189. See page: 95

[HPW12] H. Hafermann, K. R. Patton, and P. Werner, *Improved estimators for the self-energy and vertex function in hybridization-expansion continuous-time quantum monte carlo simulations*, Phys. Rev. B **85** (2012), 205106. See pages: 3, 93, 94, and 162

[JK23] I. Jang and K.-S. Kim, *Effects of general non-magnetic quenched disorder on a spin-density-wave quantum critical metallic system in two spatial dimension*, Ann. Phys. **448** (2023), 169164. See page: 162

[JPS10] S. G. Jakobs, M. Pletyukhov, and H. Schoeller, *Properties of multi-particle Green's and vertex functions within Keldysh formalism*, J. Phys. A **43** (2010), no. 10, 103001. See pages: 61 and 91

[KA99] A. Kamenev and A. Andreev, *Electron-electron interactions in disordered metals: Keldysh formalism*, Phys. Rev. B **60** (1999), 2218–2238. See page: 139

[Kam23] A. Kamenev, *Field Theory of Non-Equilibrium Systems*, 2nd ed., Cambridge University Press, 2023. See pages: 1, 8, 13, 25, 26, 30, 133, 139, and 140

[Kau21] J. Kaufmann, *Local and Nonlocal Correlations in Interacting Electron Systems*, Ph.d. thesis, Technische Universität Wien, 2021. See page: 2

[KB96a] T. R. Kirkpatrick and D. Belitz, *Quantum critical behavior of disordered itinerant ferromagnets*, Phys. Rev. B **53** (1996), 14364–14376. See page: 140

[KB96b] T. R. Kirkpatrick and D. Belitz, *Long-Range Order versus Random-Singlet Phases in Quantum Antiferromagnetic Systems with Quenched Disorder*, Phys. Rev. Lett. **76** (1996), 2571–2574. See page: 140

[KBS10] P. Kopietz, L. Bartosch, and F. Schütz, *Introduction to the Functional Renormalization Group*, Springer, 2010. See page: 36

[KCP22] J. Kaye, K. Chen, and O. Parcollet, *Discrete Lehmann representation of imaginary time Green's functions*, Phys. Rev. B **105** (2022), 235115. See page: 161

[Kel65] L. V. Keldysh, *Diagram technique for nonequilibrium processes*, Sov. Phys. JETP **20** (1965), 1018. See pages: 1, 13, 14, and 26

[KFG15] E. Kozik, M. Ferrero, and A. Georges, *Nonexistence of the Luttinger-Ward Functional and Misleading Convergence of Skeleton Diagrammatic Series for Hubbard-Like Models*, Phys. Rev. Lett. **114** (2015), 156402. See page: 88

[KGK+19] J. Kaufmann, P. Gunacker, A. Kowalski, G. Sangiovanni, and K. Held, *Symmetric improved estimators for continuous-time quantum Monte Carlo*, Phys. Rev. B **100** (2019), 075119. See pages: 3, 93, 94, and 162

[KK19] J. Krieg and P. Kopietz, *Exact renormalization group for quantum spin systems*, Phys. Rev. B **99** (2019), 060403. See page: 40

[KKH21] F. Krien, A. Kauch, and K. Held, *Tiling with triangles: parquet and $GW\gamma$ methods unified*, Phys. Rev. Res. **3** (2021), no. 1, 013149. See page: 88

[KKWH23] P. Kappl, F. Krien, C. Watzenböck, and K. Held, *Non-linear responses and three-particle correlators in correlated electron systems exemplified by the Anderson impurity model*, Phys. Rev. B **107** (2023), no. 20, 205108. See pages: 40 and 88

[KLvD21] F. B. Kugler, S.-S. B. Lee, and J. von Delft, *Multipoint Correlation Functions: Spectral Representation and Numerical Evaluation*, Phys. Rev. X **11** (2021), 041006. See pages: ix, 2, 3, 5, 11, 12, 13, 14, 15, 16, 17, 19, 21, 22, 24, 26, 27, 28, 30, 31, 32, 33, 34, 35, 37, 39, 40, 62, 88, 91, 93, 166, 168, 173, 174, 175, and 194

[Kob90] R. Kobes, *Correspondence between imaginary-time and real-time finite-temperature field theory*, Phys. Rev. D **42** (1990), no. 2, 562. See pages: 2 and 61

[Kob91] R. Kobes, *Retarded functions, dispersion relations, and Cutkosky rules at zero and finite temperature*, Phys. Rev. D **43** (1991), no. 4, 1269. See pages: 2 and 61

[KOBH13] M. Kinza, J. Ortloff, J. Bauer, and C. Honerkamp, *Alternative functional renormalization group approach to the single impurity Anderson model*, Phys. Rev. B **87** (2013), 035111. See page: 88

[KS69] P. C. Kwok and T. D. Schultz, *Correlation functions and Green functions: zero-frequency anomalies*, J. Phys. C: Solid State Phys. **2** (1969), no. 7, 1196. See pages: 24, 25, 28, and 175

[KSF01] H. Kleinert and V. Schulte-Frohlinde, *Critical Properties of ϕ^4-Theories*, World Scientific, 2001. See page: 138

[Kub57] R. Kubo, *Statistical-Mechanical Theory of Irreversible Processes. I. General Theory and Simple Applications to Magnetic and Conduction Problems*, J. Phys. Soc. Jpn. **12** (1957), no. 6, 570–586. See pages: 1, 28, and 88

[Kug22] F. B. Kugler, *Improved estimator for numerical renormalization group calculations of the self-energy*, Phys. Rev. B **105** (2022), 245132. See pages: 3, 93, and 94

[KV19] F. Krien and A. Valli, *Parquetlike equations for the Hedin three-leg vertex*, Phys. Rev. B **100** (2019), no. 24, 245147. See page: 88

[KVC19] F. Krien, A. Valli, and M. Capone, *Single-boson exchange decomposition of the vertex function*, Phys. Rev. B **100** (2019), no. 15, 155149. See pages: 88 and 161

[Lee09] S.-S. Lee, *Low-energy effective theory of Fermi surface coupled with U(1) gauge field in $2+1$ dimensions*, Phys. Rev. B **80** (2009), 165102. See page: 138

[Lee18] S.-S. Lee, *Recent Developments in Non-Fermi Liquid Theory*, Ann. Rev. of Cond. Mat. Phys. **9** (2018), no. 1, 227–244. See pages: 1, 3, and 137

[LKvD21] S.-S. B. Lee, F. B. Kugler, and J. von Delft, *Computing Local Multipoint Correlators Using the Numerical Renormalization Group*, Phys. Rev. X **11** (2021), 041007. See pages: 2, 3, 17, 88, 93, 94, 161, 162, 165, and 166

[LRVW07] H. v. Löhneysen, A. Rosch, M. Vojta, and P. Wölfle, *Fermi-liquid instabilities at magnetic quantum phase transitions*, Rev. Mod. Phys. **79** (2007), 1015–1075. See pages: 1 and 134

[LSL17] P. Lunts, A. Schlief, and S.-S. Lee, *Emergence of a control parameter for the antiferromagnetic quantum critical metal*, Phys. Rev. B **95** (2017), 245109. See page: 134

[Mah00] G. D. Mahan, *Many-Particle Physics*, 3rd ed., Kluwer Academic/Plenum Publisher, 2000. See pages: 93 and 134

[Mat55] T. Matsubara, *A New Approach to Quantum-Statistical Mechanics*, Prog. Theor. Phys. **14** (1955), no. 4, 351–378. See pages: 1, 10, and 11

[Met91] W. Metzner, *Linked-cluster expansion around the atomic limit of the Hubbard model*, Phys. Rev. B **43** (1991), 8549–8563. See page: 88

[Mil93] A. J. Millis, *Effect of a nonzero temperature on quantum critical points in itinerant fermion systems*, Phys. Rev. B **48** (1993), 7183–7196. See pages: 134 and 137

[MMS02] A. J. Millis, D. K. Morr, and J. Schmalian, *Quantum Griffiths effects in metallic systems*, Phys. Rev. B **66** (2002), 174433. See page: 140

[MS10a] M. A. Metlitski and S. Sachdev, *Quantum phase transitions of metals in two spatial dimensions. I. Ising-nematic order*, Phys. Rev. B **82** (2010), 075127. See page: 138

[MS10b] M. A. Metlitski and S. Sachdev, *Quantum phase transitions of metals in two spatial dimensions. II. Spin density wave order*, Phys. Rev. B **82** (2010), 075128. See pages: 134, 136, and 138

[NO98] J. W. Negele and H. Orland, *Quantum Many-Particle Systems*, Perseus Books, 1998. See pages: 2 and 25

[NVBK99] R. Narayanan, T. Vojta, D. Belitz, and T. R. Kirkpatrick, *Influence of Rare Regions on Magnetic Quantum Phase Transitions*, Phys. Rev. Lett. **82** (1999), 5132–5135. See page: 140

[Ogu01] A. Oguri, *Transmission Probability for Interacting Electrons Connected to Reservoirs*, J. Phys. Soc. Japan **70** (2001), no. 9, 2666–2681. See pages: 39 and 40

[OH18a] A. Oguri and A. C. Hewson, *Higher-Order Fermi-Liquid Corrections for an Anderson Impurity Away from Half Filling*, Phys. Rev. Lett. **120** (2018), 126802. See page: 95

[OH18b] A. Oguri and A. C. Hewson, *Higher-order Fermi-liquid corrections for an Anderson impurity away from half filling : Equilibrium properties*, Phys. Rev. B **97** (2018), 045406. See page: 95

[Onn11] H. K. Onnes, Commun. Phys. Lab. Univ. Leiden **120b, 122b, 124c** (1911). See page: 1

[OTTS22] A. Oguri, Y. Teratani, K. Tsutsumi, and R. Sakano, *Current noise and Keldysh vertex function of an Anderson impurity in the Fermi-liquid regime*, Phys. Rev. B **105** (2022), 115409. See page: 95

[PART23] M. Pelz, S. Adler, M. Reitner, and A. Toschi, *Highly nonperturbative nature of the Mott metal-insulator transition: Two-particle vertex divergences in the coexistence region*, Phys. Rev. B **108** (2023), 155101. See page: 88

[PGES23] A. A. Patel, H. Guo, I. Esterlis, and S. Sachdev, *Universal theory of strange metals from spatially random interactions*, Science **381** (2023), no. 6659, 790–793. See page: 162

[Pim19] D. Pimenov, *Beyond the Landau-Ginzburg-Wilson paradigm: Analytical studies of non-standard quantum criticality*, Ph.D. thesis, Ludwig-Maximilians-Universität München, Oktober 2019. See pages: 134, 135, and 137

[PS16]   M. E. Peskin and D. V. Schroeder, *An Introduction to Quantum Field Theory*, Westview Press, 2016. See page: 1

[PST00] S. Pairault, D. Sénéchal, and A.-M.S. Tremblay, *Strong-coupling perturbation theory of the Hubbard model*, Eur. Phys. J. B **16** (2000), no. 1, 85–105. See page: 88

[RHT+18] G. Rohringer, H. Hafermann, A. Toschi, A. A. Katanin, A. E. Antipov, M. I. Katsnelson, A. I. Lichtenstein, A. N. Rubtsov, and K. Held, *Diagrammatic routes to nonlocal correlations beyond dynamical mean field theory*, Rev. Mod. Phys. **90** (2018), 025003. See page: 93

[RNFW+24] M. K. Ritter, Y. Núñez Fernández, M. Wallerberger, J. von Delft, H. Shinaoka, and X. Waintal, *Quantics Tensor Cross Interpolation for High-Resolution Parsimonious Representations of Multivariate Functions*, Phys. Rev. Lett. **132** (2024), 056501. See page: 162

[Roh13] G. Rohringer, *New routes towards a theoretical treatment of nonlocal electronic correlations*, Ph.d. thesis, Technische Universität Wien, 2013. See pages: 15, 16, 19, 20, 21, 31, 39, and 88

[RVT12] G. Rohringer, A. Valli, and A. Toschi, *Local electronic correlation at the two-particle level*, Phys. Rev. B **86** (2012), 125114. See page: 88

[Sac11] S. Sachdev, *Quantum Phase Transitions*, 2nd ed., Cambridge University Press, 2011. See pages: 1, 134, and 137

[Sch61] J. S. Schwinger, *Brownian Motion of a Quantum Oscillator*, J. Math. Phys. **2** (1961), 407–432. See pages: 1 and 13

[SCM14] T. Shibauchi, A. Carrington, and Y. Matsuda, *A Quantum Critical Point Lying Beneath the Superconducting Dome in Iron Pnictides*, Ann. Rev. of Cond. Mat. Phys. **5** (2014), no. 1, 113–135. See pages: 1 and 134

[SCW+16] T. Schäfer, S. Ciuchi, M. Wallerberger, P. Thunström, O. Gunnarsson, G. Sangiovanni, G. Rohringer, and A. Toschi, *Nonperturbative landscape of the Mott-Hubbard transition: Multiple divergence lines around the critical endpoint*, Phys. Rev. B **94** (2016), 235108. See page: 88

[SHS21] J. A. Sobota, Y. He, and Z.-X. Shen, *Angle-resolved photoemission studies of quantum materials*, Rev. Mod. Phys. **93** (2021), 025006. See page: 1

[Shv06] A. M. Shvaika, *On the spectral relations for multitime correlation functions*, Condens. Matter Phys. **9** (2006), no. 3, 447. See pages: 2, 24, 32, 39, 40, 173, and 175

[Shv16] A. M. Shvaika, *Spectral properties of four-time fermionic Green's functions*, Condens. Matter Phys. **19** (2016), no. 3, 33004. See pages: 32, 39, 40, and 173

[SL15]   S. Sur and S.-S. Lee, *Quasilocal strange metal*, Phys. Rev. B **91** (2015), 125136. See pages: 134, 135, 136, 138, and 140

[SLL17]   A. Schlief, P. Lunts, and S.-S. Lee, *Exact Critical Exponents for the Antiferromagnetic Quantum Critical Metal in Two Dimensions*, Phys. Rev. X **7** (2017), 021010. See pages: 134 and 138

[SLL18]   A. Schlief, P. Lunts, and S.-S. Lee, *Noncommutativity between the low-energy limit and integer dimension limits in the ϵ expansion: A case study of the antiferromagnetic quantum critical metal*, Phys. Rev. B **98** (2018), 075140. See page: 134

[SOOY17] H. Shinaoka, J. Otsuki, M. Ohzeki, and K. Yoshimi, *Compressing Green's function using intermediate representation between imaginary-time and real-frequency domains*, Phys. Rev. B **96** (2017), 035147. See pages: 2, 161, and 162

[ST65]   K. W. H. Stevens and G. A. Toombs, *Green functions in solid state physics*, Proc. Phys. Soc. **85** (1965), no. 6, 1307. See page: 25

[Suz71]   M. Suzuki, *Ergodicity, constants of motion, and bounds for susceptibilities*, Physica **51** (1971), no. 2, 277–291. See page: 28

[SvL13]   G. Stefanucci and R. van Leeuwen, *Nonequilibrium Many-Body Theory of Quantum Systems: A Modern Introduction*, Cambridge University Press, 2013. See pages: 2, 5, 10, 11, and 13

[TAB$^+$14] C. Taranto, S. Andergassen, J. Bauer, K. Held, A. Katanin, W. Metzner, G. Rohringer, and A. Toschi, *From infinite to two dimensions through the functional renormalization group*, Phys. Rev. Lett. **112** (2014), 196402. See page: 162

[Tay93]   J. C. Taylor, *Real- and imaginary-time thermal field theory*, Phys. Rev. D **47** (1993), 725–726. See pages: 2 and 61

[TCL19]   A. Taheridehkordi, S. H. Curnoe, and J. P. F. LeBlanc, *Algorithmic Matsubara integration for Hubbard-like models*, Phys. Rev. B **99** (2019), 035120. See pages: 2, 88, and 161

[TGCR18] P. Thunström, O. Gunnarsson, S. Ciuchi, and G. Rohringer, *Analytical investigation of singularities in two-particle irreducible vertex functions of the Hubbard atom*, Phys. Rev. B **98** (2018), 235107. See page: 88

[Tho13]   M. Thomson, *Modern Particle Physics*, Cambridge University Press, 2013. See page: 1

[TK21]   D. Tarasevych and P. Kopietz, *Dissipative spin dynamics in hot quantum paramagnets*, Phys. Rev. B **104** (2021), 024423. See page: 40

[TKH07]   A. Toschi, A. A. Katanin, and K. Held, *Dynamical vertex approximation: A step beyond dynamical mean-field theory*, Phys. Rev. B **75** (2007), 045118. See pages: 39 and 40

[TRK$^+$22] D. Tarasevych, A. Rückriegel, S. Keupert, V. Mitsiioannou, and P. Kopietz, *Spin-functional renormalization group for the $J_1 J_2 J_3$ quantum Heisenberg model*, Phys. Rev. B **106** (2022), 174412. See page: 40

[Voj03a] M. Vojta, *Quantum phase transitions*, Rep. Prog. Phys. **66** (2003), no. 12, 2069. See pages: 133, 135, and 139

[Voj03b] T. Vojta, *Disorder-Induced Rounding of Certain Quantum Phase Transitions*, Phys. Rev. Lett. **90** (2003), 107202. See page: 140

[Voj13]   T. Vojta, *Phases and phase transitions in disordered quantum systems*, AIP Conf. Proc. **1550** (2013), no. 1, 188–247. See page: 139

[VWFP18] J. Vučičević, N. Wentzell, M. Ferrero, and O. Parcollet, *Practical consequences of the Luttinger-Ward functional multivaluedness for cluster DMFT methods*, Phys. Rev. B **97** (2018), 125141. See page: 88

[VZ85]   J. J. M. Verbaarschot and M. R. Zirnbauer, *Critique of the replica trick*, J. Phys. A: Math. Gen. **18** (1985), no. 7, 1093. See page: 140

[Wel05a] H. A. Weldon, *Search for combinations of thermal* n-*point functions with analytic extensions*, Phys. Rev. D **71** (2005), 036002. See pages: 2 and 61

[Wel05b] H. A. Weldon, *Thermal four-point functions with analytic extensions*, Phys. Rev. D **72** (2005), 096005. See pages: 2 and 61

[Wen04]   X.-G. Wen, *Quantum Field Theory of Many-Body Systems: From the Origin of Sound to an Origin of Light and Electrons*, Oxford University Press, 2004. See page: 67

[WFHT22] C. Watzenböck, M. Fellinger, K. Held, and A. Toschi, *Long-term memory magnetic correlations in the Hubbard model: A dynamical mean-field theory analysis*, SciPost Phys. **12** (2022), 184. See pages: 2, 24, 25, 28, 29, 30, 37, 39, and 40

[WH02]   E. Wang and U. Heinz, *Generalized fluctuation-dissipation theorem for nonlinear response functions*, Phys. Rev. D **66** (2002), 025008. See pages: 61, 79, 87, and 91

[Wil68]   R. M. Wilcox, *Bounds for the Isothermal, Adiabatic, and Isolated Static Susceptibility Tensors*, Phys. Rev. **174** (1968), 624–629. See page: 28

[WLT+20] N. Wentzell, G. Li, A. Tagliavini, C. Taranto, G. Rohringer, K. Held, A. Toschi, and S. Andergassen, *High-frequency asymptotics of the vertex function: Diagrammatic parametrization and algorithmic implementation*, Phys. Rev. B **102** (2020), 085106. See pages: 88, 94, 161, and 165

[WSK21]   M. Wallerberger, H. Shinaoka, and A. Kauch, *Solving the Bethe-Salpeter equation with exponential convergence*, Phys. Rev. Res. **3** (2021), 033168. See pages: 88, 161, and 162

[Zir99]   M. R. Zirnbauer, *Another critique of the replica trick*, arXiv preprint arXiv:cond-mat/9903338 (1999). See page: 140